

Appendix 1

Terminology

Event tree analysis is an inductive analysis that depicts the sequence of occurrences that shows the logical sequence of the occurrence of events in, or states of, a system following an initiating event.

A *failure mode* is a way that failure can occur, described by the means by which element or component failures must occur to cause loss of the sub-system or system function.

Fault tree analysis is a systems engineering method for representing the logical combinations of various component states and possible causes that can result in a specific system state (called the top event).

A *fragility curve* is a function that defines the probability of failure, conditioned on some appropriately defined intensity such as an applied load, a velocity, flood elevation, or other parameter.

A *hazard* is a threat, which may result from either an external cause (e.g. earthquake, flood, or human agency) or an internal vulnerability, with the potential to initiate a failure mode. It is a source of potential harm or a situation with a potential to cause loss.

The *performance* of a system or component is its ability to meet functional requirements. The performance of an item was described by various elements, such as flood protection, reliability, capability, efficiency, and maintainability. The design and operation of the system affects this performance.

A *system* is an entity comprising an interacting collection of discrete elements and commonly defined using deterministic models. The word *deterministic* implies that the system is identifiable and not uncertain in its architecture. The definition of the system is based on analyzing its functional and/or performance requirements. A description of a system may be a combination of functional and physical elements. A system was divided into subsystems that interact. Additional details in the definition of the system lead to a description of the physical elements, components, and various aspects of the system. Methods to address uncertainty in systems architecture are available and were employed as provided by Ayyub and Klir (1996).

Reliability is the ability of a system or a component to fulfill its design functions under designated operating and/or environmental conditions for a specified time period. This ability is commonly measured using probabilities. Reliability is, therefore, the probability that the failure event, however defined, does not occur.

Consequences are damages or losses from some failure event. Each failure of a system has some consequence(s). A failure could cause economic damage, environmental damage, injury or loss of human life, or other possible events. Consequences need to be quantified in terms of failure-consequence severities using relative or absolute measures for various consequence types to facilitate risk analysis.

Risk is the potential of losses for a system resulting from an uncertain exposure to a hazard or as a result of an uncertain event. Risk should be based on identified risk events or event scenarios. Risk is a multi-dimensional quantity that includes event-occurrence probability, event-occurrence consequences, consequence significance, and the exposed population; however, it is commonly measured as a pair of the probability of occurrence of an event, and the outcomes or consequences associated with the event's occurrence. Another common representation of risk is in the form of a curve depicting specified losses and the probability of exceeding those losses.

Probability is a measure of the likelihood, chance, odds, or degree of belief that a particular outcome will occur. A conditional probability is the probability of event occurrence based on the assumption that another event (or multiple events) has occurred.

Safety was defined as the judgment of risk tolerance (or acceptability in the case of decision making) for the system. Safety is a relative term since the decision of risk acceptance may vary depending on the individual or the group of people making the judgment.

Risk analysis is the technical and scientific process to breakdown risk into its underlying components. Risk analysis provides the processes for identifying hazards, event-probability assessment, and consequence assessment. The risk analysis process answers three basic questions: (1) What can go wrong? (2) What is the likelihood that it will go wrong? (3) What are the consequences if it does go wrong? Also, risk analysis can include the impact of making any changes to a system to control risks.

Risk Assessment is an examining of the tradeoffs that must take in any effort directed toward risk mitigation or risk reduction.

Risk communication was defined as an interactive process of exchange of information and opinion among stakeholders such as individuals, groups, and institutions. It often involves multiple messages about the nature of risk or expressing concerns, opinions, or reactions to risk managers or to legal and institutional arrangements for risk management. Risk communication greatly affects risk acceptance and defines the acceptance criteria for safety.

A *scenario* is a unique combination of circumstances that lead to an outcome of interest. Thus there may be loading scenarios, failure scenarios or downstream flooding scenarios.

Appendix 2

New Orleans East Basin

NOE – Background

The New Orleans East hurricane protection system was designed as part of the Lake Pontchartrain, LA, and Vicinity Hurricane Protection Project. The New Orleans East (NOE) portion of the project protects 45,000 acres of urban, industrial, commercial, and ecological lands. As designed, the levees were generally constructed with a 10-foot crown width with side slopes of 1 on 3. The height of the levees varies but was in the range of 12–19 feet, depending upon location. There are also various types of floodwall segments along the line of protection. As designed, there is a total of approximately 206,000 linear feet of levees and floodwalls, eight pump stations, three U.S. Fish and Wildlife Service (USFWS) pump stations, a multitude of culverts through/over the levee/floodwall, and multiple gate closures for road and rail crossings. The NOE basin is essentially broken into two major sections, as shown in Figure NOE 1. The west side of the basin is primarily residential and the east side is essentially a wetlands area. These two areas are separated by a small levee. The west side of the basin is further divided into residential and industrial areas. The area along the GIWW and IHNC is primarily industrial while the remainder of the western portion is residential in nature.



Figure NOE 1. New Orleans East Basin – Major Stretches by DM

NOE – Design Memorandums

For the purposes of the IPET Task 10 risk assessment, each basin must be broken into “reaches” that are defined by a combination of physical characteristics, major elevation changes, and potential consequences. Many of the basic reaches were defined by when individual design memorandums (DM) were completed and then constructed since different stretches of the levee/floodwall were raised at different times throughout the life of the NOE protection system. There are a total of 7 levee/floodwall major stretches separated by different DM’s within NOE. These 7 are defined below and illustrated in Figure 1.

- **Lakefront Airport Floodwall**
 - Beginning Point: Northwest corner of basin below Ted Hickey Bridge
 - Ending Point: End of floodwall just south of Hayne Blvd closure gate
- **Citrus Lakefront Levee/Floodwall**
 - Beginning Point: Begin transition levee just south of Hayne Blvd closure
 - Ending Point: Levee height transition at Paris Road and USFWS levee
- **Lakefront Levee**
 - Beginning Point: Levee transition at Paris Road and USFWS interior levee

- Ending Point: South Point at northeast end of basin
- **East Levee**
 - Beginning Point: South Point at northeast corner of basin
 - Ending Point: GIWW at southeast corner of basin
- **East Back Levee**
 - Beginning Point: GIWW at southeast corner of basin
 - Ending Point: Northeast end of Michoud Canal floodwall
- **Citrus Back Levee/Floodwall**
 - Beginning Point: Northeast end of Michoud Canal floodwall
 - Ending Point: Southwest corner of basin at IHNC
- **IHNC East Levee/Floodwall**
 - Beginning Point: Southwest corner of basin at IHNC
 - Ending Point: Northwest corner of basin under Ted Hickey Bridge

NOE Basin – Layout of Reaches for Risk Model (Pre-Katrina)

Within these major stretches defined by the DM's there are reaches, which are defined by physical changes in the protection system, i.e. switching from floodwall to levee, etc..., or by changes in geotechnical parameters. Within each reach, there are specific "key points" whose reliability needs to be determined in order to calculate the effect on the overall reach being evaluated. An example of a "key point" would be a closure gate at a road or rail line crossing along a floodwall. In addition, there are transition points between walls and levees that are also a critical part of the risk analysis, particularly since several of these transition points were locations where significant scour damage occurred during Katrina. Task 10 engineers reviewed existing plans, damage survey reports, and conducted field verification inspections to ensure each basin was accurately defined within the system. As a part of the field verification inspections, GPS coordinates were obtained and stationing from DM's and "as-built" plans were verified. For each basin, this information was transformed into a spread sheet and then a system map for each basin, as shown in Figure NOE 2 and further clarified in Figure NOE 3 for "congested" areas where several shorter reaches are close together. Finally, digital photographs with incorporated notes were developed to compliment the spread sheets and system map for further clarification. This collection of information was then categorized to get a clear picture of how the basin should be defined for risk assessment purposes. There are a couple of interior, local levees, but these are not considered substantial hurricane protection systems and are only used to define the interior drainage within the basin itself. Therefore, they are not shown and defined within the context of the risk model other than for flow characteristics.

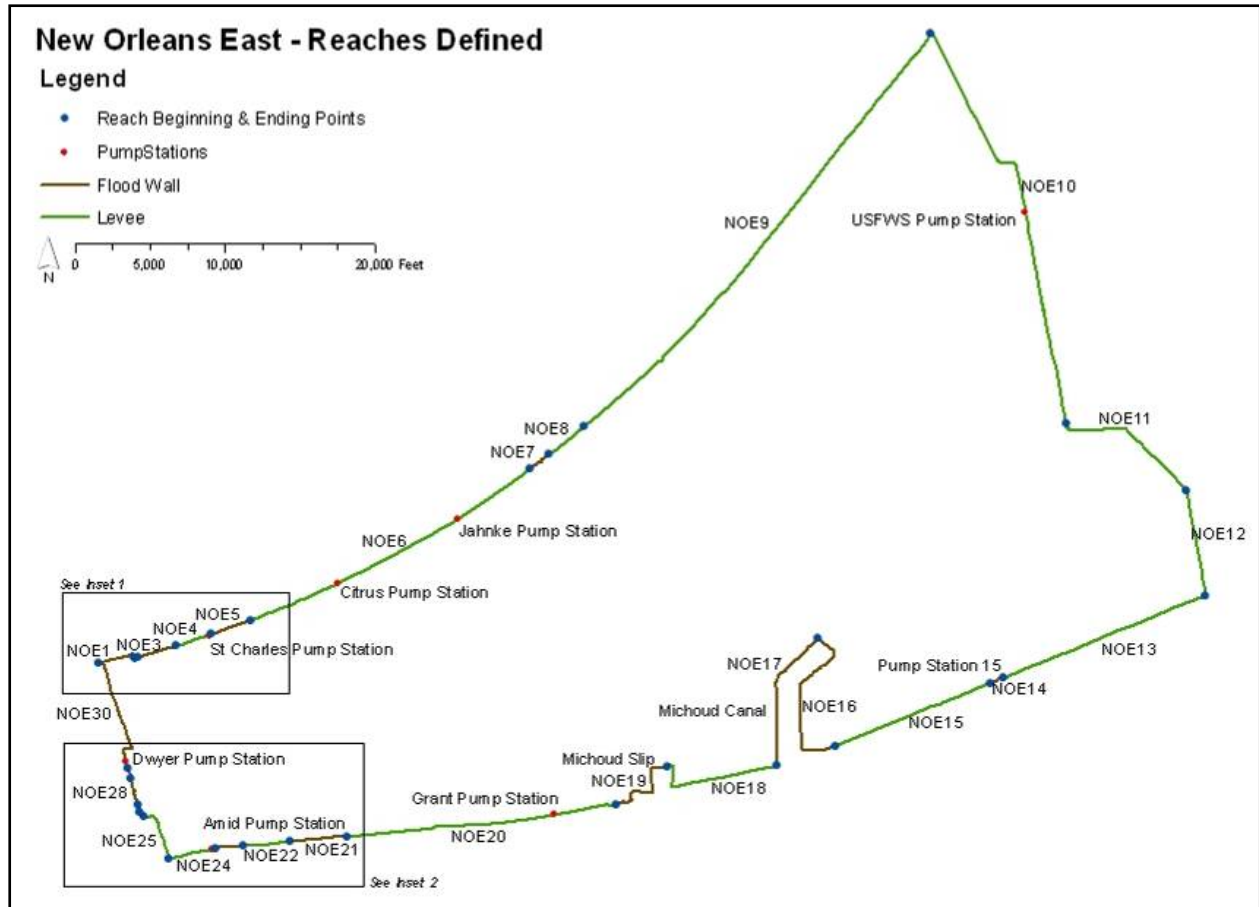


Figure NOE 2. New Orleans East Basin – Reaches Defined

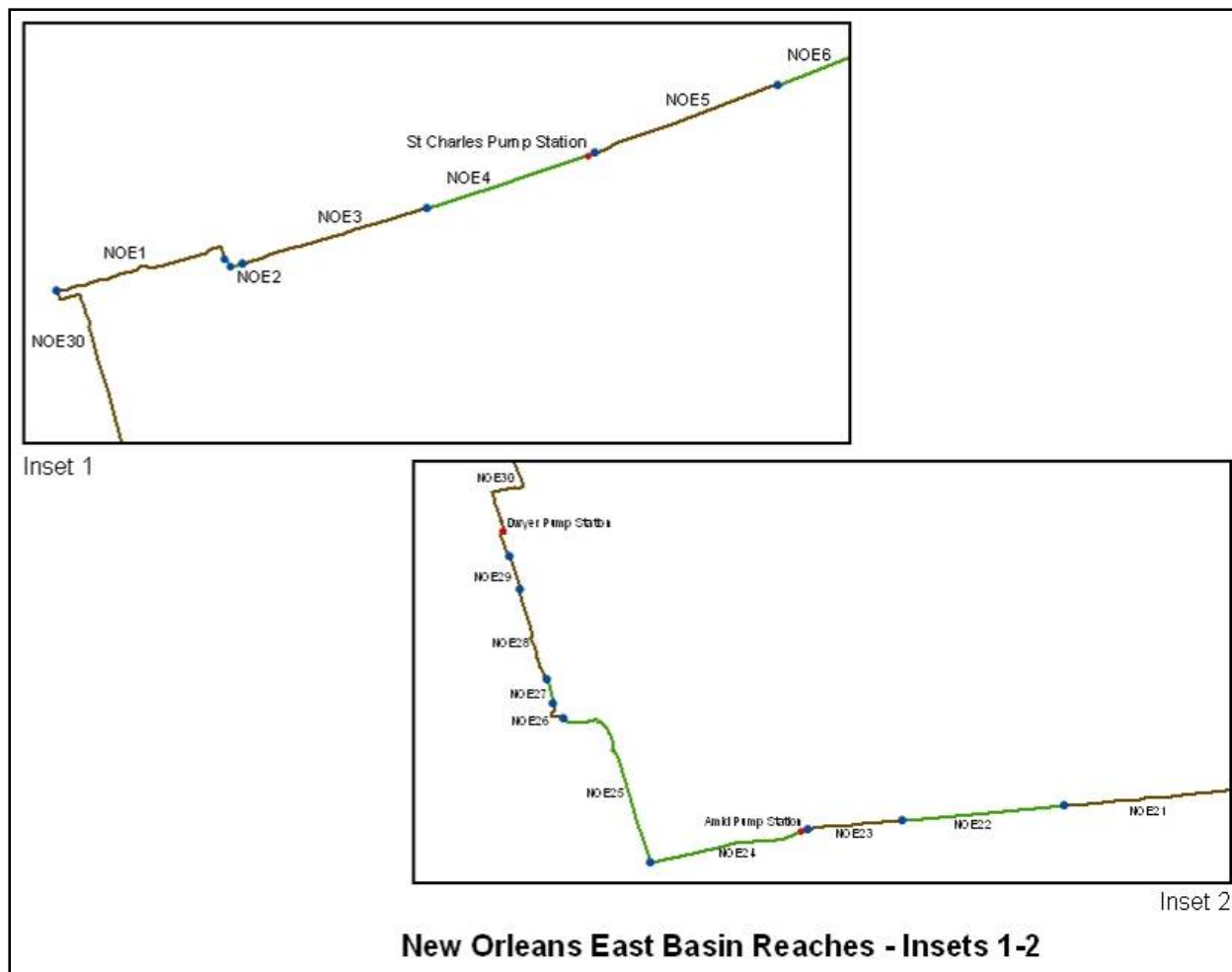


Figure NOE 3. New Orleans East Basin – Insets 1 & 2 (Refer to Figure NOE 2)

Task 10 basin definition starts at the northwest corner of the basin where the floodwall along the IHNC intersects the floodwall along the Lakefront Airport (Reach NOE1). This occurs at Sta. 4+02 B/L, which is equal to the DM stationing of 10+13 W/L. The end of the physical definition of the NOE basin occurs at the same point since it is self enclosed. Refer to Figures NOE 2 and NOE 3 for the general location of the reach as the basic characteristics are detailed within this narrative.

Reach NOE1 (Lakefront Airport DM)

This reach is defined by 2,326 linear feet of concrete I-wall along the Lakefront Airport. It is located at the northwest end of the basin. There are two key points (NOE1a and NOE1b) within this reach, both closure gates, located near the end of this reach. Relatively short T-wall sections surround the gate closures. The reach ends just after the second closure gate for Hayne Boulevard. The weighted average elevation of the top of this wall was approximately elevation 11.6 (NAVD88 2004.65) based upon a physical survey taken November 2005. It had an average free standing height of approximately 8.2 feet based upon field measurements following Katrina. There was significant scour from limited overtopping and/or wave splash along this section of

I-wall, as shown in Figure NOE 4, but there was no permanent deformation of the wall. Refer to the “Post Katrina NOE System Definition” section of this narrative for a detailed description of changes to this reach made by Task Force Guardian (TFG).



Figure NOE 4. Scour Behind Lakefront Airport FW from Overtopping

Reach NOE2 (Citrus Lakefront DM)

This reach is defined by a short 97-ft transition levee between the end of the Lakefront Airport floodwall and the beginning of the west Stars & Stripes floodwall. There are no key points within this reach; however, there are two transition features where the levee ties into the concrete capped I-walls on both ends of the reach. One of these transition points (between Reach NOE 1 and NOE 2) is shown in Figure NOE 5 where the scour occurred during Katrina. The weighted average height of this reach was 13.3 (NAVD88 2004.65) based upon an adjusted LIDAR done prior to Katrina, although at the transition between NOE1 and NOE2 the reach is significantly lower until the railroad embankment is encountered.

Reach NOE3 (Citrus Lakefront DM)

This reach is defined by 2,325 linear feet of concrete capped I-wall. This reach is commonly referred to as the west Stars & Stripes floodwall. There are two basic types of floodwall along this reach each consisting of about ½ the length of this reach. The first type is a concrete capped I-wall with levee on both sides and the second is a concrete I-wall section where the protected side has a concrete sidewalk adjacent to a road. The risk assessment model focused on both of these with an emphasis on the I-wall section without the concrete sidewalk which helps to serve as erosion protection when the wall is overtopped. There are no key or transition points within this reach. The weighted average top of wall elevation along this reach is elevation 13.5 (NAVD88 2004.65) based upon a physical survey taken in March 2006.

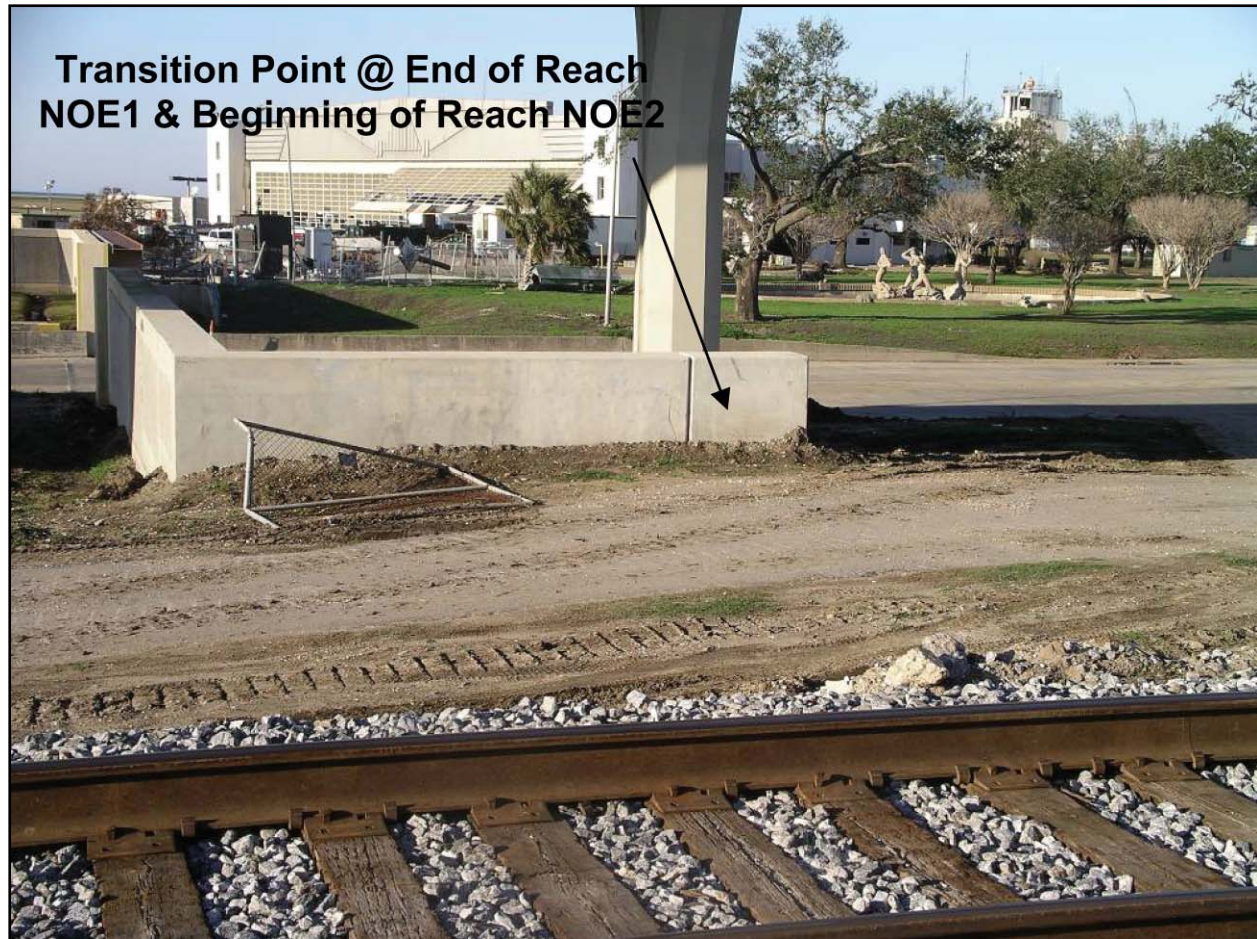


Figure NOE 5. Transition Point Between Reaches (NOE 1 & NOE 2) (Viewed from Reach NOE2 looking north towards Lakefront Airport)

Reach NOE4 (Citrus Lakefront DM)

This reach is defined by 2,330 linear feet of the Stars and Stripes levee. It is located between the west and east Stars and Stripes floodwalls. A small concrete I-wall for the discharge pipes at the St. Charles Pump Station is located near the east end of this reach. There are no key points within this reach, but there are two transition points where the levee abuts both Stars and Stripes floodwalls. The ends of the St. Charles Pump Station floodwall are not considered transition points since they are essentially flush with the top of the levee. The weighted average top elevation of this reach was 13.3 (NAVD88 2004.65) based upon an adjusted LIDAR survey taken prior to Katrina. The transition between the levee and the east Stars & Strips floodwall is shown in Figure NOE 6.

Reach NOE5 (Citrus Lakefront DM)

This reach is defined by 2,270 linear feet of concrete I-wall. It is commonly referred to as the east Stars and Stripes floodwall. There are no key or transition points within this reach. The weighted average top of wall elevation for this reach is 13.7 (NAVD88 2004.65) based upon a physical survey done in November 2005. This wall was not damaged during Katrina.



Figure NOE 6. Transition between Reaches NOE4 (Levee) and NOE5 (FW)

Reach NOE6 (Citrus Lakefront DM)

This reach is defined by a 19,112 linear feet segment of levee. It begins at the end of the east Stars & Stripes floodwall and ends at the west side of the Lincoln Beach floodwall. There are a couple of short, small floodwall sections within this reach located at the Citrus and Jahncke Pump Stations; however, these are very short walls that are not considered significant within the overall characteristics of the reach. There are three transition points assigned to this reach. These are for the levee/concrete I-wall interface points where the east Stars & Stripes floodwall ends, the Jahncke Pump Station floodwall, and where the levee ties into the west side of the Lincoln Beach floodwall. The floodwall at the Citrus Pump Station was not considered as a transition point since the top of the wall was essentially flush with the top of the levee. The weighted average elevation for the top of this reach was 12.9 (NAVD88 2004.65) based upon an adjusted LIDAR survey taken prior to Katrina. There was some minor overtopping and/or wave splash over this levee at various locations, as indicated in Figure NOE 7, but no significant damage.

Reach NOE7 (Citrus Lakefront DM)

This reach is defined by a 1,474 linear feet of concrete I-wall located at Lincoln Beach. There is one “key point” located in the flood wall, which is a closure gate that is approximately

100 feet wide. Short concrete T-walls surround the gate. The weighted average top of wall elevation for this reach is 12.1 (NAVD88 2004.65) based upon a physical survey taken in November 2005. The wall was overtopped during Katrina and performed very well. The Lincoln Beach floodwall is shown in Figure NOE 8 for reference.



Figure NOE 7. Minor Scour from Overtopping at Jahncke Pump Station



Figure NOE 8. Lincoln Beach Floodwall (Reach NOE7) (Looking west from Reach NOE8)

Reach NOE8 (Citrus Lakefront DM)

This reach of levee, 2,724 linear feet, ends the Citrus Lakefront section at the intersection of Paris Road, the interior local levee, and the west side of the Lakefront Levee. There are no key points within this reach, although the levee height is considerably different as it proceeds to the Lakefront Levee section, as shown in Figure NOE 9. The weighted average top elevation of this levee was 12.6 (NAVD 88 2004.65) based upon an adjusted LIDAR survey taken prior to Katrina. This section was overtopped and damaged during Katrina, primarily in the area where the lower Citrus Lakefront levee section transitions to the higher East Lakefront Levee section as shown in Figure NOE 9. This represents the only transition point within this reach.



Figure NOE 9. Begin Lakefront Levee at Citrus Lakefront and Paris Road (Lakefront Levee @ El. 18.6 +/- and Citrus Lakefront Levee @ 12.6+/-)

Reach NOE9 (Lakefront Levee DM)

This reach covers 33,165 feet of levee along Lake Pontchartrain from Paris Road to South Point, which is the extreme northeast corner of the basin. There is 368-ft-long I-wall around the Exxon/Mobil pipeline crossing that provides the only transition point within the reach. The weighted average top elevation of this reach was 18.6 (NAVD88 2004.65) based upon an adjusted LIDAR survey taken before Katrina. This reach was not overtopped or damaged to any significant extent during the storm.

Reach NOE10 (East Levee DM)

This reach is defined by a 27,665-linear-ft segment of levee from South Point to where Highway 90 crosses the levee. There are four transition points within this stretch, including three different drainage culvert headwalls on the levee toe. The other remaining transition point is for the floodwall surrounding the gated closure at Highway 11. The gated closure at Highway 11 represents the only “key point” within the reach as well. The weighted average top elevation of this levee is 15.1 (NAVD88 2004.65) based upon an adjusted LIDAR survey done prior to

Katrina. This section was slightly overtopped or subject to wave splash during Katrina, but suffered minimal damage other than at transition points.

Reach NOE11 (East Levee DM)

This levee is 8,942' long and extends southeast from Highway 11 and serves as the section where the levee design was modified to account for wave action. There are no "key points" located within this reach. The weighted average top elevation of this reach was 16.7 (NAVD88 2004.65) based upon an adjusted LIDAR survey taken prior to Katrina. It is believed that this section of levee suffered minor overtopping and/or wave splash, but overall it performed well.

Reach NOE12 (East Levee DM)

The final reach of levee along the East section is 7,190 ft long and extends to the GIWW with a weighted average top elevation of 15.0 (NAVD88 2004.65) based upon an adjusted LIDAR survey taken prior to Katrina. There are two transition points within this reach including a short sheet pile wall around a drainage structure and transition concrete I-walls around a railroad crossing. There is one key point, the railroad gated closure, which is included in this reach. At the time of Katrina, the railroad closure gate and transition walls were roughly 4 feet lower than the adjacent levee and was overtopped and heavily damaged during the storm. An aerial view of this damage is shown in Figure NOE 10.



Figure NOE 10. Aerial View of Damage at RR Closure Along East Levee

Reach NOE13 (East Back Levee DM)

This section of levee, measuring 22,257 linear feet, was heavily damaged during Katrina from overtopping. Prior to Katrina, it had a weighted average top elevation of 15.5 (NAVD88 2004.65) based upon an adjusted LIDAR survey that was taken before the storm. It begins at the east end where it ties into the southern edge of the East Levee and continues to the east end of the floodwall around the Orleans Parish Pump Station #15. There are no key points within this reach. There is one transition point assigned to this reach for the floodwall/levee interface at the very western edge of this reach where it ties into the Pump Station #15 floodwall. Much of this levee was destroyed, as shown in Figure NOE 11, and was rebuilt by TFG.



Figure NOE 11. Failure of Levee by Overtopping East of Pump Station #15 (East Back Levee)

Reach NOE14 (East Back DM)

This reach is defined by the floodwall around Orleans Parish Pump Station #15. There were two types of walls within this reach prior to Katrina, two 120-ft transition sheet pile walls at elevation 17.5 (NAVD88 2004.65) at the both ends of a middle 253-ft T-wall section with a top elevation of 22.2 (NAVD88 2004.65). The total length of this reach is 493 feet. Portions of the transition sheet pile sections were heavily damaged during Katrina as shown in Figure NOE 12. There are no key or transition points assigned to this reach.



Figure NOE 12. Floodwall Failure Near Orleans Pump Station #15

Reach NOE15 (East Back DM)

This 10,120-ft section of levee extends from the west end of the Orleans Parish Pump Station #15 floodwall to the start of the floodwall on the east side of the Michoud Canal at the GIWW. This levee section had a weighted average top elevation of 16.8 (NAVD88 2004.65) at the time of Katrina based upon an adjusted LIDAR survey taken prior to the storm. There are no key points, but two transition points assigned to this reach. Both transition points are for levee/floodwall interfaces at both ends of this reach. This reach was heavily damaged during Katrina and was rebuilt under TFG.

Reach NOE16 (East Back DM)

This reach consists of the east floodwall around the Michoud Canal. It is primarily concrete capped I-wall, but has a short transition sheet pile wall at the beginning of the reach. It is approximately 10,757 feet long and had a weighted average top elevation of 17.9 (NAVD88 2004.65) based upon a physical survey taken in November 2005. The reach starts at the GIWW and continues along the Michoud Canal where it joins with the Citrus Back floodwall. There are 18 key points along this reach for gated closures at industry and road crossings. However, from site inspections, it appears as if five of these gates are placed in the permanently closed position.

As shown in Figure NOE 13, the transition sheet pile floodwall at the beginning of this reach failed during Katrina; this section was rebuilt under TFG. The concrete capped I-wall section was overtopped and suffered significant scour as shown in Figure NOE 14, but performed well. There are no transition points assigned to this reach.

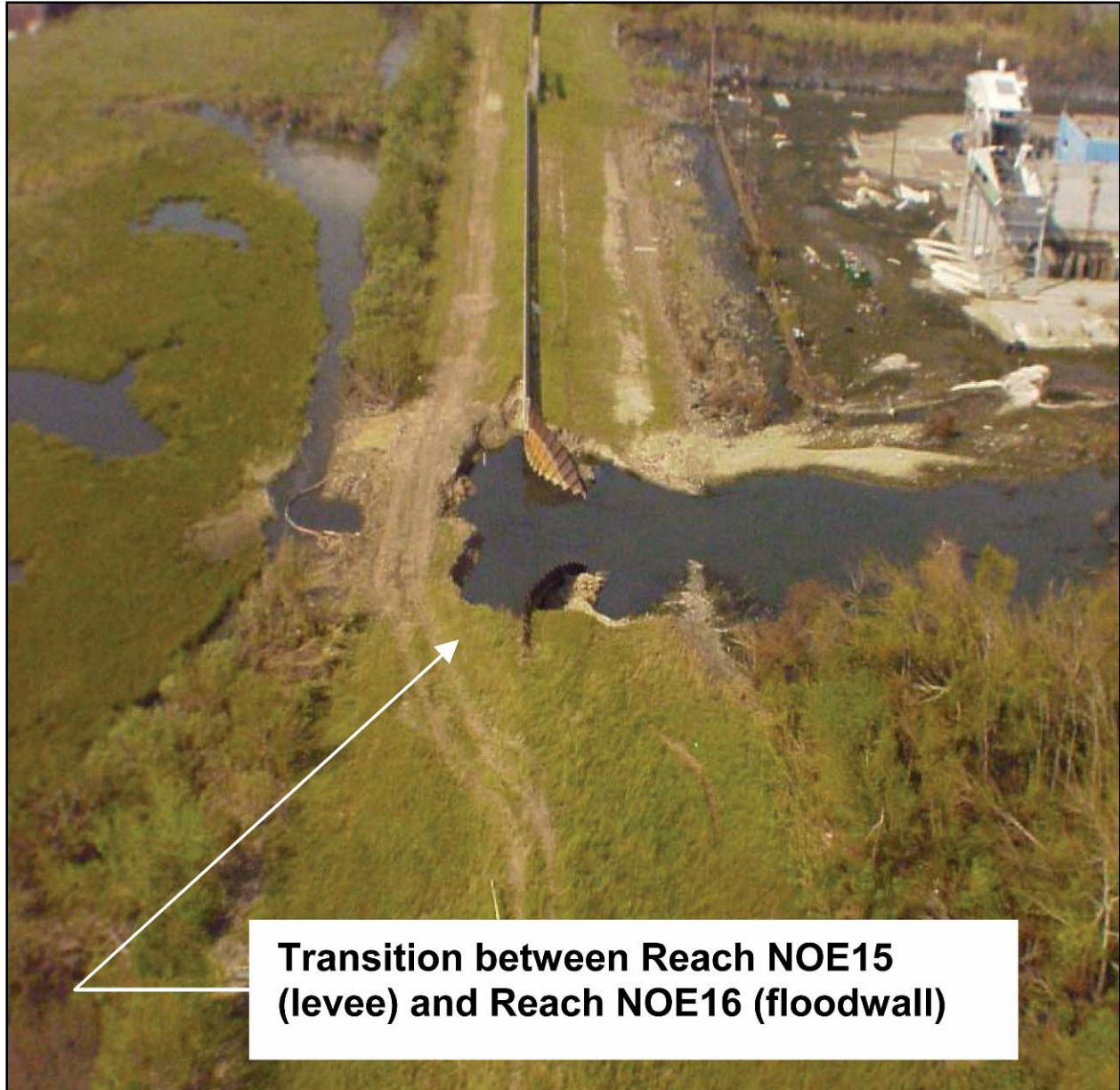


Figure NOE 13. Floodwall Failure at East End of Michoud Canal FW



Figure NOE 14. Scour Damage Behind Michoud Canal Floodwall

Reach NOE17 (Citrus Back DM)

The beginning of this reach starts at the northwest end of the Michoud Canal and ends at the southwest side of the Michoud Canal at the GIWW. This reach consists of 9,318 feet of floodwall with an average weighted top elevation of 20.8 (NAVD88 2004.65) based upon a physical survey taken in November 2005. This section was overtopped during Katrina but suffered only minor scour problems. There are no key or transition points assigned to this reach.

Reach NOE18 (Citrus Back DM)

This reach represents the 7,905 ft segment of levee between the Michoud Canal and Michoud Slip. There are no key points within this reach of levee, but there are two transition points where the levee ties into floodwalls on both ends. This reach had a weighted average top elevation of 17.2 (NAVD88 2004.65) at the time of Katrina based upon an adjusted LIDAR survey taken prior to the storm.

Reach NOE19 (Citrus Back DM)

The reach represents the 6,155 ft of floodwall around the Michoud Slip. There are two key points (gated closure) within this reach, but no transition points assigned to this reach. This reach has a weighted average top elevation of 16.7 (NAVD88 2004.65) based upon a physical survey taken in November 2005. This section of wall suffered minimal scour damage during Katrina.

Reach NOE20 (Citrus Back DM)

This reach contains 15,940 feet of levee between the west end of the Michoud Slip and the east end of the combination floodwall for the bulk loading facility. There are two transition points assigned to this reach where the levee ties into floodwalls at both ends. There are no key points within this reach. This reach has a weighted average top elevation of elevation 14.0 (NAVD88 2004.65) based upon an adjusted LIDAR survey taken before the storm. Portions of this levee were overtopped during Katrina with moderate areas of scour damage, as shown in Figure NOE 15, but there were no major breaches in this reach.



Figure NOE 15. Scour Damage Along Citrus Back Levee

Reach NOE21 (Citrus Back DM)

This reach is defined by the 1,820-ft combination floodwall built for the Bulk Loading Facility and Elaine Pump Station. This wall was heavily damaged during Katrina, as shown in Figure NOE 16, and was repaired under TFG. Prior to Katrina, it had a top elevation of 12.1 (NAVD88 2004.65) based upon both physical survey and LIDAR information. There is one key point, gate N1 for the Bulk Loading Facility, within this reach. There are no transition points assigned to this reach.



Figure NOE 16. Floodwall Failure at Bulk Loading Facility/Elaine PS

Reach NOE22 (Citrus Back DM)

This reach is for the levee (3,453 ft long) between the floodwall at the Bulk Loading Facility/Elaine PS (east side of reach) and the floodwall that is just east of the Amid Pump Station (west side of reach). There are no key points within this reach, but there are two transition points where the levee ties into the adjacent floodwalls on both ends. It had a weighted average top elevation of 13.4 (NAVD88 2004.65) prior to Katrina based upon an adjusted LIDAR survey taken before the storm. There was minor overtopping of this reach during Katrina with no significant damage.

Reach NOE23 (Citrus Back DM)

This reach is the 1,587 ft section of floodwall located just east of the Amid Pump Station. This wall did suffer minor overtopping, but no major damage. It had a weighted average top elevation of 14.5 (NAVD88 2004.65) based upon a physical survey taken in November 2005. There are no key or transition points assigned to this reach.

Reach NOE24 (Citrus Back DM)

The final reach of the Citrus Back Levee stretch is 2,348 feet of levee extending from the end of the floodwall just east of the Amid Pump Station to its tie in with the Inner Harbor Navigation Canal (IHNC) east levee. There is one key point (railroad closure gate) located within this reach and two transition points (railroad closure transition I-walls and the end of the I-wall near the Amid Pump Station). The transition around the railroad closure structure was overtopped and sustained significant scour damage, as shown in Figure NOE 17. This reach had a weighted average top elevation of 13.8 (NAVD88 2004.65) based upon an adjusted LIDAR survey taken prior to Katrina.



Figure NOE 17. Erosion Damage Around RR Closure (Near GIWW and IHNC Intersection)

Reach NOE25 (IHNC DM)

This reach is 3,803 feet long and consists primarily of levee with several gated closures. The weighted average top elevation of this reach was 12.2 (NAVD88 2004.65) based upon an adjusted LIDAR survey taken prior to Katrina. There are four closure gates, each a key point, within this reach; all of which suffered erosion damage from overtopping during Katrina. Each of these four closure structures has short adjoining I-walls which represent four transition points that are assigned to this reach. There is one additional transition point assigned to this reach

where the end of the levee ties into the beginning of the floodwall, as shown in Figure NOE 19. A typical example of the scour damage around these closure structures is shown in Figure NOE 18. Structural damage was minimal to these closure structures. The very end of this reach suffered a major washout area where the levee serves as a ramp just near the I-10 overpass. A photograph of this washout damage is shown in Figure NOE 19.

Reach NOE26 (IHNC DM)

This short reach of floodwall (537 ft) starts near the end of the washout area and extends just under the I-10 overpass. This section is considered a reach because it faces several different directions and contains two key points, both closure gates. There are no transition points assigned to this reach. The weighted average top elevation of this wall was 12.4 (NAVD88 2004.65) based upon a physical survey of the wall completed in November 2005. This section was overtopped but received minimal scour damage behind the wall.

Reach NOE27 (IHNC DM)

This reach consists of a short transition levee (526 ft) between floodwalls. There are no key points within this short reach, but there are two transitions assigned to this reach where the floodwall interfaces with the levee. The weighted average top elevation of the levee was 12.6 (NAVD88 2004.65) based upon a physical survey taken of this reach in November 2005. This reach was overtopped during Katrina, but suffered no significant damage.



Figure NOE 18. Scour Damage around Gated Closure Along IHNC



Figure NOE 19. Major Washout Area from Overtopping Near I-10 Overpass (Note: Located Along IHNC East Side)

Reach NOE28 (IHNC DM)

This section of floodwall (1,876 ft) starts between the I-10 and Highway 90 overpasses and ends where it serves as the foundation for the Dupuy Storage Facility (see Figure NOE 20). There are no key points, but there is one transition point in this section, which is the old Highway 90 overpass location. It does not appear as if remedial repairs were made to this transition section when the overpass was relocated. The weighted average top elevation of this reach is 12.9 (NAVD88 2004.65) based upon a physical survey taken during November 2005. This reach was overtopped with minimal damage during Katrina.



Figure NOE 20. Floodwall Serves as Building Foundation (Dupuy Storage Facility – IHNC East)

Reach NOE29 (IHNC DM)

This short section of floodwall (643 ft) serves as the Dupuy Storage Building foundation as shown in Figure NOE 20. This section was deemed an individual reach because overtopping issues along this short reach warranted its treatment as a separate structure. The weighted average top elevation is 13.5 (NAVD88 2004.65) based upon a physical survey taken during November 2005.

Reach NOE30 (IHNC DM)

The last reach of the basin consists of 8,168 ft of floodwall. There are several key points (closure gates) within this reach. There is one transition within this reach at the Jourdan Road crossing. The weighted average top elevation of this reach is 12.2 (NAVD88 2004.65) based upon a physical survey taken in November 2005. This includes the shorter sections of T-walls located around closure gates. Portions of this wall were overtopped as indicated by the erosion behind the floodwall adjacent to closure gate E-13 and shown in Figure NOE 21. This erosion, which measures approximately 8-ft wide by 2.5-ft deep, did not cause major structural problems for the wall at this location.



Figure NOE 21. Erosion Behind Floodwall Adjacent to Gate E-13 (IHNC East)

NOE – Post-Katrina Layout of Reaches for Risk Model

Reach NOE1 (Lakefront Airport DM)

The only significant change made by TFG to this reach was to repair the scour damage along the wall and placement of a concrete scour pad on the protected side of the wall shown in Figure NOE 22. Refer back to Figure NOE 4 for a photograph of the wall following Katrina without the scour pad, which was taken from the same general location as Figure NOE 22, as noted by the road ramp on the right hand side of both photographs.



Figure NOE 22. Scour Protection Pad Behind Lakefront Airport FW

Reach NOE2 (Citrus Lakefront DM)

The only significant change made to this reach was improved scour protection around the transition points at both ends where the levees tie into floodwalls. An example of this improved protection is shown in Figure NOE 23, where the transition between Reach NOE 1 (floodwall) and NOE 2 (levee) has been raised and protected with a concrete pad. Figure NOE 23 is taken from the same general location as Figure NOE 5 which shows the transition before the improvement.



Figure NOE 23. Transition Improvements Between Reaches NOE 1&2 (Note: refer back to Figure NOE 5 taken from same location)

Reach NOE3 (Citrus Lakefront DM)

The major improvement to this reach was the installation of a concrete scour pad on the protected side along the entire reach. There were no changes made to free standing wall heights in this reach from the pre-Katrina condition.

Reach NOE4 (Citrus Lakefront DM)

The only significant improvement to this reach, known as the Stars & Strips Levee, made by TFG was improved scour protection around the transitions located at both the east and west ends of this reach. Figure NOE 24 depicts the improved scour protection at the interface of Reaches NOE4 (Stars & Stripes Levee) and NOE5 (East Stars & Stripes Floodwall). Refer back to Figure NOE 6 for a photograph of this transition taken after Katrina but prior to TFG repairs.

Reach NOE5 (Citrus Lakefront DM)

There have been two major improvements to this reach. The first is the free standing height of this I-wall has been reduced from approximately 7.5 feet (pre-Katrina) to 6.0 feet (TFG

improvements). Secondly, a concrete scour protection pad has been added on the protected side of the wall for its entire length.

Reach NOE6 (Citrus Lakefront DM)

The only significant improvements to this reach were scour protection that was placed around all three transition points. An example of the scour protection around the Jahncke Pump Station Floodwall is shown in Figure NOE 25 at the same general location where the damage photo (Figure NOE 7) was taken following Katrina.



Figure NOE 24. Transition Improvements Between Reaches NOE 4&5 (Note: refer back to Figure NOE 6 taken from same location)



Figure NOE 25. Transition Improvements at Jahncke Pump Station (Note: refer back to Figure NOE 7 taken from same location)

Reach NOE7 (Citrus Lakefront DM)

The major improvements to the Lincoln Beach floodwall were a reduction in the free standing height of the I-wall sections and scour protection. The free standing height has been reduced from approximately 10 feet (pre-Katrina) to 5.5 feet (post Katrina repairs under TFG). A concrete scour protection pad was added at the base of the wall on the protected side. A view of the improvements (under construction) to the Lincoln Beach floodwall is shown in Figure NOE 26, taken from roughly the same vantage point as Figure NOE 8, which is at the east edge of the wall looking west from Reach NOE8.



Figure NOE 26. Lincoln Beach Floodwall Repairs (Note: refer back to Figure NOE 8 taken from same location)

Reach NOE8 (Citrus Lakefront DM)

The only improvement made to the last reach associated with this DM was improved scour protection around the east end of the Lincoln Beach floodwall transition into this reach. This transition point is assigned to Reach NOE8 and scour protection at this interface, as shown in Figure NOE 26, was provided by TFG. The transition between the end of this DM and the beginning of the higher Lakefront Levee section has not been significantly changed from pre-Katrina conditions.

Reach NOE9 (Lakefront Levee DM)

This reach was not damaged during Katrina and no major changes were made under TFG with the exception of transition point scour improvements around the Exxon/Mobil floodwall pipeline crossing.

Reach NOE10 (East Levee DM)

This reach suffered minimal damage during Katrina and there are no major changes to the characteristics of this reach itself. However, scour protection improvements were made to three of the four transition points within this reach. These repairs were made at the drainage structure headwalls, as typically shown in Figure NOE 27. The other transition point, the floodwall at the Highway 11 gated closure, had no changes made to it under TFG.

Reach NOE11 (East Levee DM)

There were no improvements made to this reach or any of the transitions within this reach.



Figure NOE 27. Scour Repairs to Drainage Structure Headwalls (Note: Reach NOE10 drainage structure repairs – typical)

Reach NOE12 (East Levee DM)

There were significant repairs made to select areas of this reach that were heavily damaged during Katrina. The first major repair was the entire levee was rebuilt from the CSX railroad closure structure southward to where the levee ties into the East Back Levee at the GIWW. Therefore, the pre-Katrina weighted average elevation of 15.0 was restored under TFG

(NAVD88 2004.65). The second major improvement was the reconstruction of the CSX railroad closure gates and adjoining floodwalls. At the time Katrina hit, this gated closure and supporting floodwall structure was roughly 4 feet lower than the adjoining levees and it was heavily damaged, as shown in Figure NOE 10. A new gate and supporting floodwall was installed, as shown in Figure NOE 28. Note that the new gate and supporting walls were constructed such that it is no longer 4 feet lower than the adjacent levees.



Figure NOE 28. Reconstruction of CSX Railroad Closure Structure

Reach NOE13 (East Back Levee DM)

This section of levee suffered heavy damage from overtopping during Katrina, and it was totally rebuilt under TFG. The new levee was constructed to elevation 19.5 (NAVD88 2004.65) with a final design grade of elevation 17.5 to account for 2 feet of long-term settlement. Thus, this reach will be approximately 4 feet higher than the pre-Katrina condition as constructed and 2 feet higher once the long-term settlement occurs, and it reaches its design elevation. Not only was the levee raised but it was also built with better materials and with improved methods. Prior to the Katrina, this reach had been constructed with hydraulic fill taken from the MRGO/GIWW, which included a mix of sand and silt materials. Within the context of this analysis, the pre-Katrina soil properties for this reach were classified as “high to very highly erodible” in terms of resistance to overtopping damage. Since the new levee was constructed with better material and

better methods (not hydraulically filled), the erodibility classification was improved to the “moderate” category. Figure NOE 29 shows the newly constructed levee. It can be compared back to the failed levee along this reach shown in Figure NOE 11.



Figure NOE 29. New Levee Along the GIWW (East Back Levee)

Reach NOE14 (East Back Levee DM)

This 493-ft reach of combination floodwall was also heavily damaged during Katrina and was the focus of major repairs by TFG. The surrounding sheet pile I-walls failed during Katrina (see Figure NOE 12) and were replaced primarily with a concrete T-wall at elevation 22.2 (NAVD88 2004.65). There is a very short (18 feet) transition of shorter concrete I-wall at elevation 20.2 on the west end of the repaired section. Thus, the weighted average elevation of this overall reach has been raised from 19.9 (pre-Katrina) to 22.1 (post-Katrina repairs under TFG). The newly repaired wall is shown in Figure NOE 30.

Reach NOE15 (East Back Levee DM)

This reach of levee failed by overtopping during Katrina and was rebuilt by TFG. The new levee was built to elevation 19.5 with a final design grade of elevation 17.5 (NAVD88 2004.65) to account for 2 feet of long-term settlement. The pre-Katrina elevation of this reach was

approximately 16.8. Thus, as constructed, the new levee is roughly 2.7 feet higher with a final height 0.7 feet higher once it settles to its final grade. Like the Reach NOE13 repairs, this new levee was also constructed with more erosion resistant material and with improved construction methods when compared to the pre-Katrina condition.



Figure NOE 30. Repaired Floodwalls Around Pump Station #15

Reach NOE16 (East Back Levee DM)

Many parts of this reach of floodwall were significantly overtopped during Katrina, including a failed section of transition sheet pile near the beginning of the reach, as shown in Figure NOE 13. This short section of transition sheet pile I-wall has been replaced with a concrete I-wall by TFG. In addition, the free standing height of the non-failed concrete I-wall sections was reduced from approximately 7.5 feet (pre-Katrina) to 4.5 feet (post-Katrina). Also, a concrete scour pad, as shown in Figure NOE 31, has been provided on the protected side of the concrete I-wall sections. Both the shortened free standing height and scour protection pad are evident in the figure.



Figure NOE 31. Michoud Canal Floodwall Improvements

Reach NOE17 (Citrus Back Levee DM)

Consistent with the east side of the Michoud Canal, the west side also had its free standing height reduced and scour protection provided on the back side. During a visual inspection held during June 2006, TFG construction crews were making the noted improvements as evident in Figure NOE 32. The free standing height was reduced to 7.0 feet (post-Katrina) from 9.3 feet (pre-Katrina). A scour protection pad was provided on the back side.



Figure NOE 32. West Floodwall Repairs around Michoud Canal (Note scour pad at base of wall and increased stability berm)

Reach NOE18 (Citrus Back Levee DM)

This reach of levee is located between the floodwalls surrounding the Michoud Canal and Michoud Slip. There were no major renovations made to this reach or transition points.

Reach NOE19 (Citrus Back Levee DM)

This reach of floodwall is located around the Michoud Slip. The free standing height was reduced to approximately 6.0 feet (post-Katrina) from an average of 8.1 feet (pre-Katrina). A scour protection pad similar to those found in other figures was also placed at the base of the wall on the protected side.

Reach NOE20 (Citrus Back Levee DM)

This reach of levee is located between the floodwalls around the Michoud Slip and Bulk Loading Facility. There was some moderate scour damage to the levee, as shown in Figure NOE 15, but no breaching. The only repairs made to this reach were for scour repair, as shown in Figure NOE 33. For the purposes of this risk assessment, it was assumed that the pre-Katrina and

post-Katrina conditions were the same. There were no scour protection improvements made to the levee/wall interfaces at the ends of this reach.



Figure NOE 33. Scour Damage Repairs Along Citrus Back Levee (Note: reference Figure NOE 15 which shows damage following Katrina)

Reach NOE21 (Citrus Back Levee DM)

This reach of floodwall failed during Katrina as shown in Figure NOE 16. It was replaced by an “L-wall,” which is assumed to have the same reliability as a “T-wall” within the context of this risk analysis. This new L-wall is shown in Figure NOE 34. Prior to Katrina, the previous I-wall had a weighted average top elevation of 12.1 (NAVD88 2004.65) and it is believed the failure was due to massive overtopping. The new L-wall was constructed to a top elevation of 14.5 (NAVD88 2004.65).



Figure NOE 35. New L-Wall at Bulk Loading Facility

Reach NOE22 (Citrus Back Levee DM)

This reach of levee is between the floodwalls that are east of the Amid Pump Station and the Bulk Loading Facility. There was minimal damage to this reach during Katrina and no major renovations were made by TFG, including no scour protection at the levee/floodwall interfaces.

Reach NOE23 (Citrus Back Levee DM)

This reach of I-wall is located just east of the Amid Pump Station. It was overtopped during Katrina and received minor scour damage. The free standing height of the wall was reduced to 4.5 feet (post-Katrina) from 6.0 feet (pre-Katrina). A scour protection pad was also added at the base of the back side of the wall similar to those already shown in other areas.

Reach NOE24 (Citrus Back Levee DM)

This last reach of levee along the GIWW was damaged in a few spots during Katrina but had no major breaches. Major repairs undertaken by TFG within this reach included scour repairs around the Amid Pump Station discharge pipes along with scour protection improvements at the transition of levee/wall interfaces, including the heavily damaged area around the railroad

crossing closure near the GIWW/IHNC intersection. This area was heavily damaged during Katrina, as shown in Figure NOE 17. The scour protection repairs to this area are shown in Figure NOE 36, which illustrates a new transition wall on the east side of the closure and grouted rock at the end of the west transition wall to this closure.



Figure NOE 36. TFG Repairs to RR Closure at the GIWW/IHNC Intersection (Note: repairs include new transition wall and grouted rock)

Reach NOE25 (IHNC East)

This reach of levee was overtopped and damaged primarily at closure gate floodwall/levee interface transition points as shown in Figures NOE 18 and 19. Improvements made by TFG to this reach include providing grouted rock scour protection at levee/floodwall interfaces and repair of the major washout section that was damaged during Katrina. A typical scour improvement around a levee/floodwall interface along the IHNC is shown in Figure NOE 37.



Figure NOE 37. Transition Improvements along IHNC Levee/FW Interfaces

Reach NOE26 (IHNC East)

There were no major repairs made to this section of floodwall since the transition points are assigned to the adjoining levee reaches.

Reach NOE27 (IHNC East)

This relatively short reach of levee located between the I-10 and Highway 90 bridges was overtopped during Katrina with minimal damage. The only significant improvement to this reach was the placement of grouted rock at the levee/floodwall interfaces.

Reach NOE28 (IHNC East)

This section of floodwall is located behind the Folger's Coffee Plant and continues to where it serves as the Dupuy Storage Building foundation. Scour protection, in the way of grouted rock, was provided at the base of the wall on the protected side. There is no significant change to the free standing height of the wall along this section as it was roughly 5.0 feet prior to Katrina. It is noted that the lower, unprotected old Highway 90 crossing was not significantly changed by TFG.

Reach NOE29 (IHNC East)

This relatively short section of floodwall was placed as a separate reach since it serves as the building foundation (Dupuy Storage Facility), as shown in Figure NOE 20. It was made a separate reach since the building itself provided significant scour protection for this reach, but could also cause increased load without allowing overtopping. It was not damaged during Katrina and no major changes were made to this reach.

Reach NOE30 (IHNC East)

This last reach of the New Orleans East Basin consists primarily of concrete I-wall that was overtopped during Katrina. Several areas of the wall suffered significant scour on the protected side, see Figure NOE 21 for reference, and have been repaired by placing a scour pad at the base of the back side in the form of grouted rock. The free standing height of the I-walls along this reach has not been significantly changed from pre-Katrina condition since they averaged roughly 6 feet at the time of the storm.

Summary of Improvements - New Orleans East Basin

There are a variety of improvements to the NOE Basin made by TFG. These primarily fall into two major categories: new walls/levees and scour protection. Scour protection improvements are primarily limited to the back side of floodwalls and transitions around levee/wall interfaces. However, where new levees were built along the southern portion of the East Levee and along the GIWW, improved materials and construction methods were used such that improved resistance to erosion from overtopping can also be expected when compared to the pre-Katrina condition.

For the new floodwall sections, generally more reliable, stable walls replaced less reliable I-wall sections. This includes both T-wall and L-wall sections, which in the context of this analysis, are considered to be very reliable in terms of stability. In addition, these were built to an elevation considerably higher than the wall sections that failed, providing a higher level of protection for that reach.

In an effort to make a relatively easy comparison of the physical changes to an individual NOE Basin reach from pre-Katrina to post-Katrina, Table NOE 1 was created. A general description of the reach location and number is provided along the left hand side of the table. For each reach, the type of protection, weighted average top elevation, wall free standing height (stick-up), and scour protection measures are shown in red for pre-Katrina conditions. The changes implemented by TFG to the reach characteristics are then shown in blue on the right hand side of the table. If there was no significant change to the reach for a particular characteristic(s), then the post-Katrina box is shaded gray.

Table NOE 1. Summary of Reach Changes for NOE Basin

Reach	Reach Description	Pre-K Protect	Pre-K Elev.	Pre-K Stick-up	Pre-K Scour Protect	Post K Protect	Post K Elev.	Post-K Stick-up	Post K Scour Protection
NOE1	LF Airport	I-wall	11.6	8.2	None				Conc. Pad
NOE2	Citrus LF	Levee	13.3	n/a	None				
NOE3	Stars/Stripes West FW	I-wall	13.5	10.0	None				Conc. Pad
NOE4	Stars/Stripes Levee	Levee	13.3	n/a	None				
NOE5	Stars/Stripes East FW	I-wall	13.7	7.5	None			6.0	Conc. Pad
NOE6	Citrus LF	Levee	12.9	n/a	None				
NOE7	Lincoln Beach Flood Wall	I-wall	12.1	10.0	None			5.5	Conc. Pad
NOE8	Citrus LF	Levee	12.6	n/a	None				
NOE9	East Lakefront	Levee	18.6	n/a	None				
NOE10	East Levee	Levee	15.1	n/a	None				
NOE11	East Levee	Levee	16.7	n/a	None				
NOE12	East Levee	Levee	17.7	n/a	None				
NOE13	East Back	Levee	15.5	n/a	None	New Levee	19.5		Better Soils
NOE14	PS #15 FW	I-wall	17.5	7.5	None	T-wall	22.1	n/a	n/a
NOE15	East Back	Levee	16.8	n/a	None	New Levee	19.5		Better Soils
NOE16	Mich. Canal East FW	I-wall	17.9	7.5	None			4.5	Conc. Pad
NOE17	Mich. Canal West FW	I-wall	20.8	9.3	None			7.0	Conc. Pad
NOE18	Between Mich Canal and Slip	Levee	17.2	n/a	None				
NOE19	Michoud Slip	I-wall	16.7	8.1	None			6.0	Conc. Pad
NOE20	Between Slip and Bulk Facility	Levee	14.0	n/a	None				
NOE21	Bulk Load FW	I-wall	12.1	6.0	None	L-wall	14.5	n/a	n/a
NOE22	Levee Just West of Bulk Load FW	Levee	13.4	n/a	None				
NOE23	FW East of Amid	I-wall	14.5	6.0	None			4.5	Conc. Pad
NOE24	Amid to IHNC	Levee	13.8	n/a	None				
NOE25	GIWW to I-10	Levee	12.2	n/a	None				
NOE26	Under I-10	I-wall	12.4	6.0	None			5.0	Grout Rock
NOE27	I-10 to Hwy 90	Levee	12.6	n/a	None				
NOE28	Hwy 90 to Dupuy Bldg	I-wall	12.9	5.0	None				Grouted Rock
NOE29	Dupuy Bldg	I-wall	13.5	6.0	Yes				
NOE30	Dupuy Bldg to Lakefront FW	I-wall	12.2	5.5	None			5.0	Grouted Rock

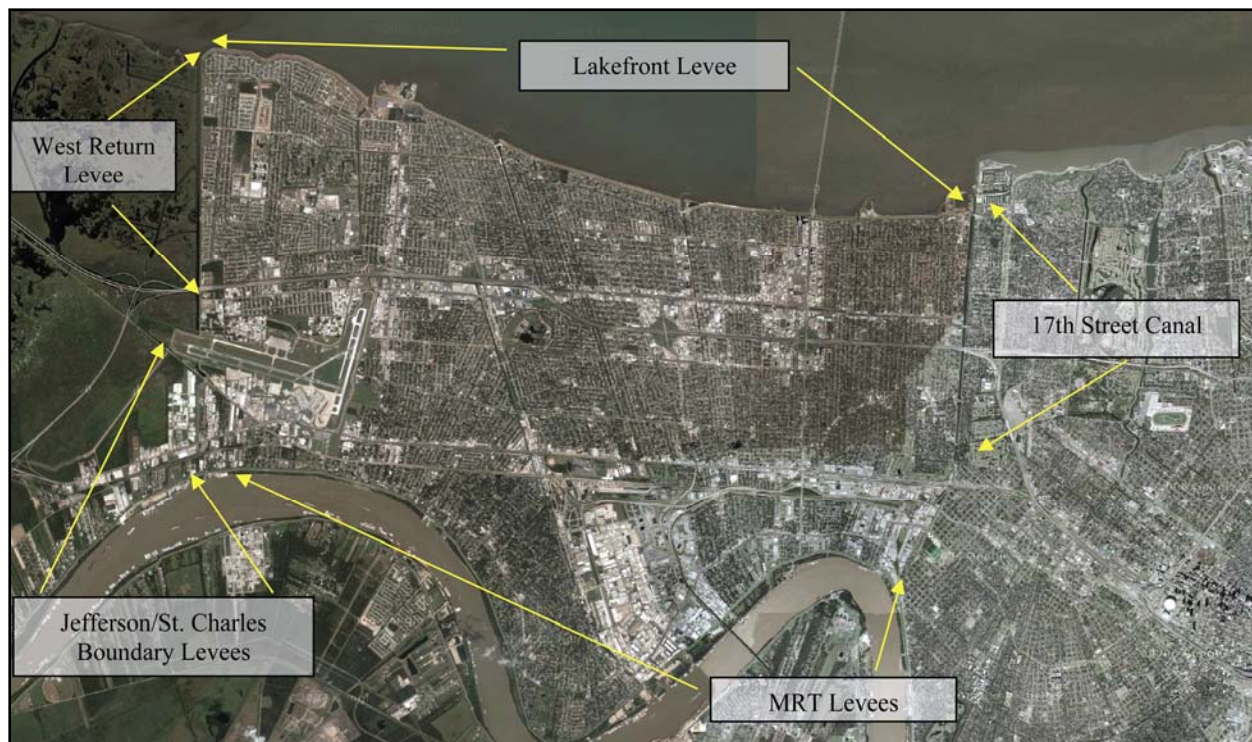
Appendix 3

Jefferson Basin

Field Reconnaissance and Definition of Reaches in Jefferson East Bank Basin

The basin for Jefferson East Bank has been broken down into five distinct sections to develop both reaches and features definitions for the risk model. These sections are based on General Design Memorandum (GDMs) published by the New Orleans District, USACE and updated by field reconnaissance by IPET Team 10. The Jefferson East Bank Basin has been defined by the following sections shown in the figure below:

1. West Return Levee
2. Lakefront Levee
3. 17th Street Canal
4. Mississippi River Levees
5. Jefferson/St. Charles Boundary Levees



Overview of Jefferson Parish Basins

Elevations

All vertical elevations in this report are defined in **NAVD88 2004.65** datum unless otherwise noted within the text. All horizontal datums are defined in State Plane Coordinates NAD83 – 1702 Louisiana South, UTM NAD83 Zone 15, and GCS NAD83.

Section 1: Kenner (West) Return Levee

References

The descriptions of the levees/floodwalls, stationing around the circumference of the polder, and terminology for associated features are referenced to the following document:

DEPARTMENT OF THE ARMY, NEW ORLEANS DISTRICT, CORPS OF ENGINEERS, “Jefferson / St. Charles Parish Return Levee”, Design Memorandum No. 17a – General Design, New Orleans, LA, July 1987.

Narrative

The Kenner (West) Return Levee has a T-wall structure for the entire length along the St. Charles Parish border. This section begins at the northerly end of the runway for the New Orleans International Airport and ends at the Lake Ponchartrain levee. This section has been broken down into four subsections of incrementally increasing wall height. Reach 1 is from

station 0+00 W/L to 29+50 W/L is a T-wall section with an design elevation of 12.8. The elevation changes from station 29+50 W/L to 31+75 W/L, where the T-Wall crosses under I-10 and the design elevation changes to 12.3 feet. The elevation of the T-wall changes back to design elevation 12.8 feet from station 31+75 W/L to 65+20.40 W/L. Reach 2 has a transition zone in the wall from station 65+20.40 W/L to 66+02.90 W/L where the T-wall design elevation increases to 13.3 feet. Reach 2 remains at the same elevation until station 130+70.00 W/L. At station 130+70.00 W/L, Reach 4 starts with another transition in the wall up to design elevation 13.8 feet. The T-wall remains at elevation 13.8 feet until station 173+04.70 W/L. At station 173+04.70 W/L, Reach 4 has a transition to design elevation 19.3 feet and continues until it connects with the Jefferson Lakefront Levee.

The major damage in this section from Hurricane Katrina was scour at the base of the floodwalls and flood side slope protection, displacement of stone protection and slight movement and rotation of the T-walls. There were no failure in this section during the hurricane. The minor repairs to this section should be completed prior to 1 June 2006 however the repairs are not under the direction of Task Force Guardian.



Typical T-Wall Transition in the Floodwall in Kenner Return Levee

Section 1 – West return Levee – Summary of Reaches and Features								
Section	Start	End	Structure	EL	Section / Point	Length (feet)	GDM Average Height (NVGD)	
1	00+00	0+55.0	T-Wall Transition	El 13 – El 13.5	S	55	13.25	↓
2	0+55.0	29+50.0	T-Wall	El 13.5	S	2895	13.5	
3	29+50.0	31+75.0	Interstate 10 Crossing	El 11.5	P	225	11.5	
4	31+75.0	46+73.20	T-Wall	El 13.5	S	1498	13.5	
5	46+73.20	47+09.20	T-Wall Transition	El 13.5 – El 14.0	P	36	13.75	
6	47+09.20	47+51.20	T-Wall at Pump Station	El 14.0	P	42	14	
7	47+51.20	47+87.20	T-Wall Transition	El 14.0 – El 13.5	P	36	13.75	
8	47+87.20	65+20.40	T-Wall	El 13.5	S	1733	13.5	Reach 1
9	65+20.40	66+02.90	T-Wall Transition	El 13.5 – El 14.0	P	83	13.75	↓
10	66+02.90	130+70.00	T-Wall	El 14.0	S	6467	14	Reach 2
11	130+70.00	131+20.00	T-Wall Transition	El 14.0 – El 14.5	S	50	14.25	↓
12	131+20.00	173+04.70	T-Wall	El 14.5	S	4235	14.5	Reach 3
13	173+04.70	178+54.70	T-Wall Transition	El 14.5 – El 20	P	549	17.25	↓
14	178+54.70	180+69.70	T-Wall	El 20	S	215	20	↓
15	180+69.70	180+74.70	T-Wall	El 20.5	S	5	20.5	Reach 4
Points				Width	Elevation			
1		I-10 Crossing		147	11.5			
2		Parish Line Pump Station		114	14			
3		Gate W-7 West Esplanade		6	14			
4		Gate W8 Vintage Street		6	14			

Section 1 – West Return Levee - Summary Coordinates for Defined Reaches							
		State Plane NAD83 1702 - LA South		Graphical Latitude	Longitude	UTM NAD 83	
		Northing	Easting			Zone 15 Northing	Easting
Return Levee							
Reach 1	START	546407.659	3614397.566	29 59 53.87687	90 16 46.29803	2501430.19	10897988.09
Reach 1	END	552907.875	3614407.909	30 00 58.22085	90 16 45.50041	2501345.82	10904491.17
Reach 2	START	558810.683	3614388.995	30 01 56.65366	90 16 45.09787	2501240.83	10910396.17
Reach 2	END						
Reach 3	START	563727.833	3614373.814	30 02 45.32911	90 16 44.75590	2501153.88	10915315.15
Reach 3	END						
Reach 4	START	564277.527	3614378.32	30 02 50.77003	90 16 44.64708	2501150.37	10915865.14
Reach 4	END						

Definition of reaches

Reach 1 – This reach consists of T-wall at average elevation 10.9 feet with a length of approximately 6,520 feet. There are two features in this reach. The features are the I-10 floodwall at elevation 10.4 feet and the Parish Line Pumping Station at elevation 11.75 feet.





I-10 Floodwall



Parish Line Pump Station (Note: Pump discharge through T-wall)

Reach 2 – This reach consists of T-wall at average elevation 11.0 feet with a length of approximately 6,550 feet. The only feature in this reach is Gate W7, West Esplanade Ave. The swing gate is 6 feet wide and 8 feet high with a sill elevation of 4.3 feet.



Gate W-7 West Esplanade

Reach 3 – This reach consists of T-wall at average elevation 12.6 feet with a length of approximately 4,285 feet. There is only one feature in this reach is Gate W8, Vintage Ave. The swing gate is 6 feet wide and 8 feet high with a sill elevation of 4.3 feet.



Gate W8 Vintage Street



Typical T-wall and slope protection on floodside in Reach 3

Reach 4 – This reach consists of T-wall at average elevation 15.7 feet with a length of approximately 769 feet. There are no features in this reach but there is a sheet pile transition into the Lakefront levee.



Section 2: Jefferson Parish Lakefront Levee

References

Descriptions of the levees/floodwalls, stationing around the circumference of the polder, and terminology for associated features are referenced to the following documents:

DEPARTMENT OF THE ARMY, NEW ORLEANS DISTRICT, CORPS OF ENGINEERS, “Jefferson Parish Lakefront Levee”, Design Memorandum No. 17 – General Design, Volumes I and II, New Orleans, LA, November 1987.

Narrative

The Jefferson Parish Lakefront Levee consists primarily of levee sections intermingled with four pump stations, two boat launch facilities and the Pontchartrain Causeway. This section has been broken down into four subsection (Reaches 5 to 8) defined on changes in levee elevation and the location of the pumping stations. Reach 5 is an earthen levee from station 0+00 B/L to 128+00.00 B/L with a crest elevation originally constructed at 17.3 feet, a 10-foot crest width, and 1 on 3 vegetated side slopes. Pump Station 4 (Duncan Canal PS) is located between stations 115+00.00 B/L and station 128+00.00 B/L. The original pump station has been taken out of service and replaced by a new pump station that is situated just westerly of the old station. T-walls have been reconfigured around the old and new pump stations and transition into the levee sections on both sides. The design elevation of the original Pump Station 4 is at elevation 21.7 feet. It appears that the walls surrounding the new pump station are at the same elevation of the old pump station.

There was no visible damage from Hurricane Katrina in this reach. Most damage was to the foreshore protection but little or no damage occurred to the levee or at the pump station walls. There will be only minor repairs that need to be completed prior to 1 June 2006.



Foreground: Original Pump Station and old masonry wall (not in Service)
Background: Duncan Pump Station with new T-walls

Reach 6 runs from Pumping Station No. 4 at station 128+00 B/L to Pumping Station No. 3 at station 210+00 B/L. The earthen levee cross section is similar to that in Reach 5 from station 128+00 to 141+00 B/L. From station 141+50 B/L to 145+50 B/L, the crest changes to design elevation of 15.8 to provide access to the Williams Boulevard Boat Launch. The elevation of the ramp over the levee is at elevation 13.8. From station 146+00 B/L to 184+50 B/L, the levee cross section is again typical to that on the other side of the boat launch. From station 185+50 B/L to Pumping Station No. 3 (Elmwood Canal) at station 210+00 B/L, the levee crest was originally designed to elevation 15.3 feet. Cantilever sheeting forms the transition from the levee to both sides of the pumping station. Along the lakefront, damage to the foreshore concrete slab protection was evident. It is noted that Pumping Station No. 3 consists of original construction on the western side and a later expansion on the eastern side that appears to have been built in the 2001 time frame.

There was no visible damage from Hurricane Katrina in this reach. Most damage was to the foreshore protection but little or no damage occurred to the levee or at the pump station walls. There will be only minor repairs that need to be completed prior to 1 June 2006.

Reach 7 runs from Pumping Station No.3 at station 221+45 to Pumping Station No.1 at station 464+50 B/L. The levee cross section is typical throughout the reach with a crest elevation originally constructed to elevation 15.3 feet and vegetated side slopes. Cantilever sheeting forms the transition from the levee to Pumping Station No. 2. It is noted that Pumping Station No. 2 consists of original construction on the western side and a later expansion on the eastern side that appears to have been built in the 2001 time frame. On the west side of this pumping station, the crest at the access road is approximately two feet low to facilitate passage of vehicles and the top elevation of the transition sheeting is lower than the crest of the levee. A portion of this reach was being re-constructed at the time of this reconnaissance inspection. Reference contract number W912P8-05-C-0014 for specific details. At the time of the inspection, there was a 200-foot gap in the levee near Pumping Station No. 2 that the contractor was using for access. This gap needs to be filled and vegetation needs to be established in order to restore the integrity of this reach. It is noted that the Lake Pontchartrain Causeway Boulevard intersects Reach 7 between station 434+80 B/L to 438+40 B/L. Existing details at the causeway are shown on the original design memorandum, which indicates two bottom roller gates to close the line of protection with the causeway below the crest of the levee. This section has changed and the causeway now passes over the protection structures, and the floodwalls form the transition from the causeway to the levee.

There was no visible damage from Hurricane Katrina in this reach. Most damage was to the foreshore protection but little or no damage occurred to the levee or at the pump station or Causeway walls. There will be only minor repairs that need to be completed prior to 1 June 2006.



Reconstruction of a Portion of Reach 7 Lakefront Levee

Reach 8 runs from Pumping Station No. 1 at station 479+95 B/L to its junction with the 17th Street Outfall Canal at station 550+22 B/L. From station 479+95 B/L to 485+00 B/L, the levee was originally constructed to elevation 15.7 feet. The access road to the Bonnabel Boat

Launch Area intersects the levee between stations 485+00 B/L to 486+50 B/L. The net grade for the access road is elevation 13.8 feet, and two swing gates are installed to maintain the level of protection. The top of the swing gates appears to be six inches lower than the top of the levee. After the access road to the boat launch, the levee transition from elevation 15.7 feet at station 486+50 to elevation 15.3 feet at station 487+50 and continues at this elevation to the limit of work at station 550+22.

There was no visible damage from Hurricane Katrina in this reach. Most damage was to the foreshore protection but little or no damage occurred to the levee or at the pump station walls. There will be only minor repairs that need to be completed prior to 1 June 2006.

Section 2 – Jefferson lakefront levee - Summary of Reaches and Features								
Section	Start	End	Structure	EL	Section/ Point	Length	GDM Average Height	
1	0+85	1+45	Levee Transition	EI 13.0 - EI 16.0	S	60	15.5	
2	1+45	115+00	Levee	EI 16	S	11005	16	↓
3	115+00	128+00	I-Wall/T-Wall for Pump Station #4	EI 17.0 - EI 22.5	P	1300	18.25	Reach 5
4	128+00	141+00	Levee	EI 16	S	1300	16	↓
5	141+00	141+50	Levee Transition	EI 16 - EI 14.5	P	50	17.25	
6	141+50	145+50	Levee - William Blvd Boat Launch	EI 14.5	P	400	14.5	↓
7	145+50	146+00	Levee Transition	EI 14.5 - EI 16.0	P	50	15.25	
8	146+00	208+00	Levee	EI 16	S	6200	16	Reach 6
9	208+00	223+00	I-Wall for Pump Station #3	EI 16.5	P	1500	16.5	↓
10	223+00	343+00	Levee	EI 16	S	12000	16	
11	343+00	355+00	I-Wall for Pump Station #2	EL 16.5	P	1200	16.5	↓
12	355+00	434+80	Levee	EL 16	S	7980	16	
13	434+80	438+40	Causeway Blvd	EI 16.5	P	360	16.5	↓
14	438+40	464+50	Levee	EI 16	S	2610	16	Reach 7
15	464+50	479+95	I-Wall/T-Wall for Pump Station #1	EI 16.5 - EI 22.5	P	1540	19.5	↓
16	479+95	487+50	Levee - Bonnabel Boat Launch	EI 14.5	P	760	14.5	
17	487+50	550+22	Levee	EI 16	S	6270	16	Reach 8

Points			Width	Elevation
1	1+00	Gate L1 Floodwall	20	17
2	104+22	Gate L3 Duncan Canal	22	17
3	145+13	Gate L4 Williams Blvd	60	14.5
4	402+04	Gate 2 - Causeway SB (no longer used)	45	14.5
5	402+45	Gate 3 - Causeway NB (no longer used)	45	14.5
6	475+54	Gate L9A Bonnabel Blvd South	22	16
7	475+54	Gate L9B Bonnabel Blvd North	22	16

Section 2 – Jefferson Lakefront Levee - Summary Coordinates for Defined Reaches

		State Plane NAD83 1702 - LA South		Graphical Latitude	Longitude	UTM NAD 83	
		Northing	Easting			Zone 15 Northing	Easting
Lakefront Levee							
Reach 5	START	564277.527	3614378.32	30 02 50.77003	90 16 44.64708	2501150.37	10915865.14
Reach 5	END	561991.187	3625823.549	30 02 27.07773	90 14 34.66901	2512633.87	10913744.89
Reach 6	START						
Reach 6	END	559141.211	3633246.774	30 01 58.15966	90 13 10.52729	2520102.00	10911001.96
Reach 7	START						
Reach 7	END	554468.982	3656812.867	30 01 09.56725	90 08 42.98123	2543747.54	10906671.25
Reach 8	START						
Reach 8	END	555079.333	3664232.118	30 01 14.83996	90 07 18.51511	2551161.68	10907390.11

Definition of Reaches

Reach 5 – This reach consists of a levee at average elevation 15.8 feet with a length of approximately 12,365 feet. There are two features in this reach. The first is Gate L1 at the start of the Lakefront Levee near the West Return Levee. Gate L1 is 20 feet in width and has a sill elevation of 10.0 feet. The second feature is the Duncan Canal Pumping Station at wall elevation 20.0 feet. There is a T-wall section around the new pump station which is approximately 2,236 feet in length. There is a swing gate at station 104+22 near the pump station, Gate L3, which is 22 feet wide and has a sill elevation at 10.0 feet.





Gate L1 – Lakefront Levee



Gate L3 – Duncan Canal Pump Station



Duncan Canal Pump Station

Reach 6 – This reach consists of Levee at average elevation 14.1 feet with a length of approximately 8,000 feet. There one feature in this reach which is the William Blvd Boat Launch at with a ramp at elevation 13.8 feet. The ramp also has a gate at station 145+13 which is 60 feet in width and a sill elevation at 9.25 feet.



Reach 7 – This reach consists of a levee at an average elevation 14.3 feet and length of approximately 25,650 feet. There two features contained in this reach. The first feature is Pump

Station #3 - Elmwood Canal at elevation 18.0 feet. The pump station has an uncapped sheet pile wall of about 750 feet in total length. The second feature in this reach is Pump Station #2 - Suburban Canal at elevation 18.0 feet. This pump station has an uncapped sheet pile wall of about 864 feet in total length. The Pontchartrain Causeway Boulevard is not considered a feature since the lanes have been raised above the protection walls and levees.





Pump Station #3 – Elmwood Canal Pump Station



Pump Station #2 – Suburban Canal Pump Station

Reach 8 – This reach consists of levee at average elevation 14.4 feet with a length of approximately 8,570 feet. There two features contained in this reach. The first is the Pump Station #1- Bonnabel Canal at elevation of 18.0 feet. This pump station has a sheet pile transition wall into a I-wall/T-wall of about 1,052 feet in total length. The second feature is Bonnabel Boat Launch which has a elevation 15.3 feet. The boat launch has two gates, L9A and L9B, which have a width of 22 feet and a sill elevation of 11.8 feet.



Pump Station #1 – Bonnabel Canal Pump Station



Bonnabel Boat Launch Ramp and Gate

Section 3: 17th Street Outfall Canal

References

Descriptions of the levees/floodwalls, stationing around the circumference of the polder, and terminology for associated features are referenced to the following documents:

DEPARTMENT OF THE ARMY, NEW ORLEANS DISTRICT, CORPS OF ENGINEERS, "Orleans Parish, Jefferson Parish, 17th Street Outfall Canal (Metairie Relief) Design Memorandum No. 20 – General Design, Volumes I and II, New Orleans, LA, March 1990.

Narrative

The west line of the 17th Street Outfall Canal runs from station 0+00 at its junction with the Lakefront Levee to station 119+95 at Pumping Station No. 6. This section is constructed primarily of I-wall sections on top of earthen levees. The west line of the 17th Street Canal has been broken out into three reaches based on elevation changes along the canal. Reach 9 has a design elevation 13.3 feet from stations 0+00 to 75+70 at the Veterans Highway Bridge. Reach 10 has a design elevation 13.8 feet from stations 77+70 to 92+50. Reach 11 has a design

elevation of 14.3 feet from stations 93+50 to 119+95. At the junction of the Lakefront Levee and the west wall of the 17th Street Outfall Canal north of Hammond Highway, construction work was ongoing under contract number W912P8-06-C-0008, titled “17th Street Canal Interim Closure Structure.” Interstate Highway 10, which passes over the I-wall in the vicinity of stations 90+00 to 92+50, has no effect on the integrity of the hurricane protection. There is a gate structure in the west wall just to the north of Pumping Station No.6 through which the CSX railroad line passes. The area was littered with sandbags indicating that the swing gate may not seal tightly. No storm related damage was observed along the west wall.

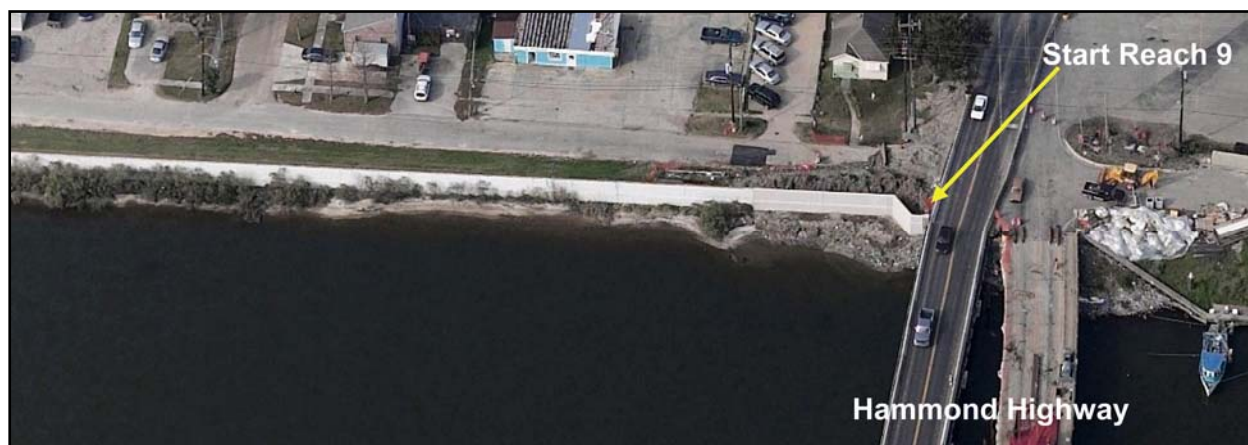
Section 3 – 17th Street Outfall Canal - Summary of Reaches and Features									
Section	Start	End	Structure	EL	Section / Point	Length	GDM Average Height		
1	0+00	0+10	Floodwall	16.5	P	10	16.5		
2	0+10	0+43.60	Floodwall Transition	EI 16.5 – EI 14.0	S	34	15.25		
3	0+43.60	2+75.10	I-Wall	EI 14.0	S	231	14		
4	2+75.10	2+81.0	T-Wall	EI 14.0	P	6	14		
5	2+81.0	3+05.10	Gate No. 1	EI 14.0	P	24	14		
6	3+05.10	3+11.0	T-Wall	EI 14.0	P	6	14		
7	3+11.0	3+40.50	I-Wall	EI 14.0	S	29	14		
8	3+40.50	3+47.00	T-Wall	EI 14.0	P	7	14		
9	3+47.00	4+09.00	Gate No. 2	EI 14.0	P	62	14		↓
10	4+09.00	4+15.50	T-Wall	EI 14.0	P	7	14		
11	4+15.50	75+70.00	I-Wall	EI 14.0	S	7154	14		Reach 9
12	75+70.00	76+00.00	I-Wall Transition	EI 14.0 – EI 14.5	S	30	14.25		↓
13	76+00.00	76+10.04	I-Wall	EI 14.5	P	10	14.5		
14	76+10.04	77+22.04	Veterans Hwy	EI 14.5	S	112	14.5		↓
15	77+22.04	92+50.0	I-Wall	EI 14.5	S	1528	14.5		Reach 10
16	92+50.0	93+50.0	I-Wall Transition	EI 14.5 – EI 15.0	S	100	14.75		↓
17	93+50.0	119+95.49	I-Wall	EI 15.0	S	2645	15		Reach 11

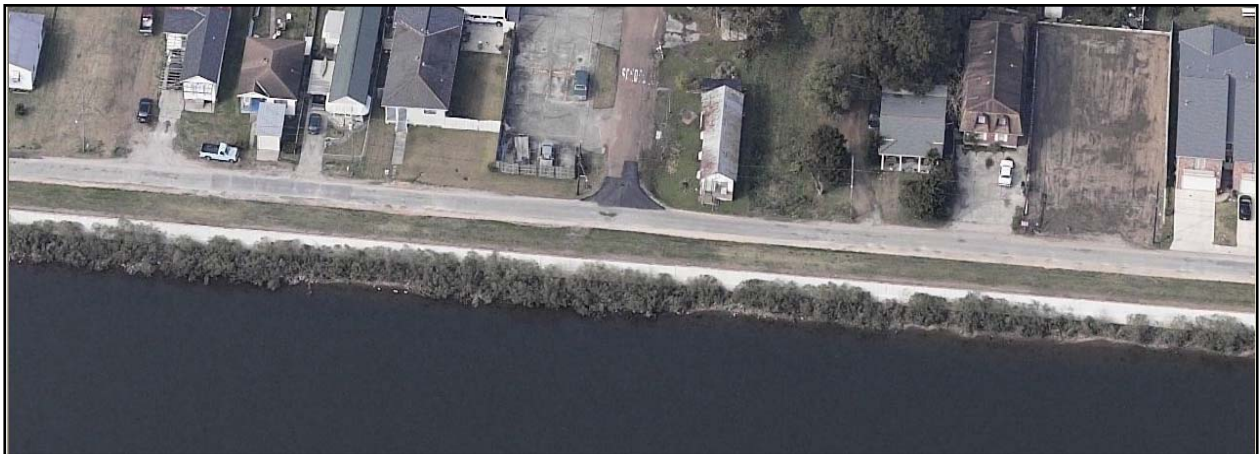
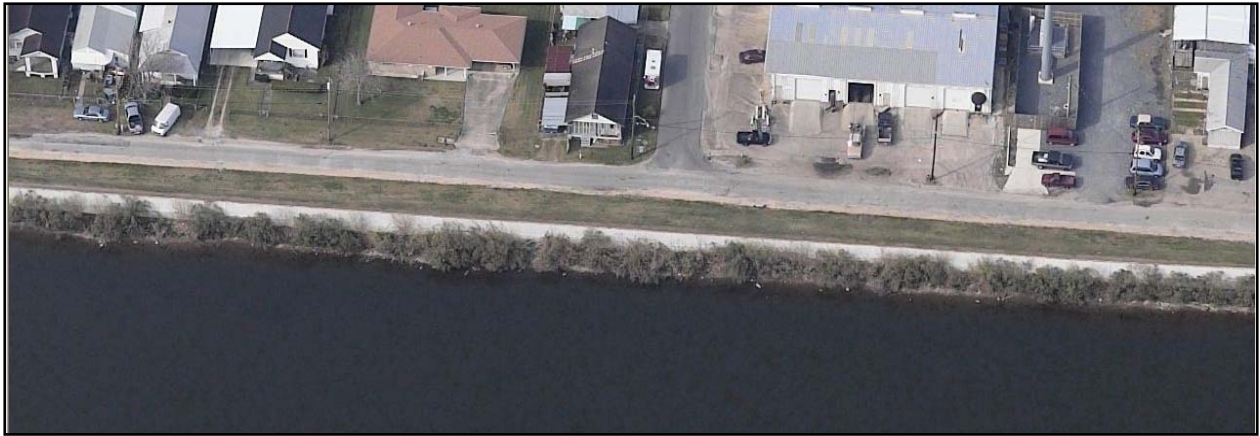
Points		Width	Elevation
1	Gate L 10 Orpheum Ave - 58 ft gap (under construction)	58	9.5
2	Old Hammond Hwy Bridge - 47 ft gap (under construction)	47	10
3	Gate E4 - Veterans Blvd.	8	14.5
4	Gate E5 - Veterans Blvd	8	14.5
5	Gate E8 - Canal Street	10	15
6	Gate E9 - Southern RR	22	15
7	Pump Station #6	150	14.5

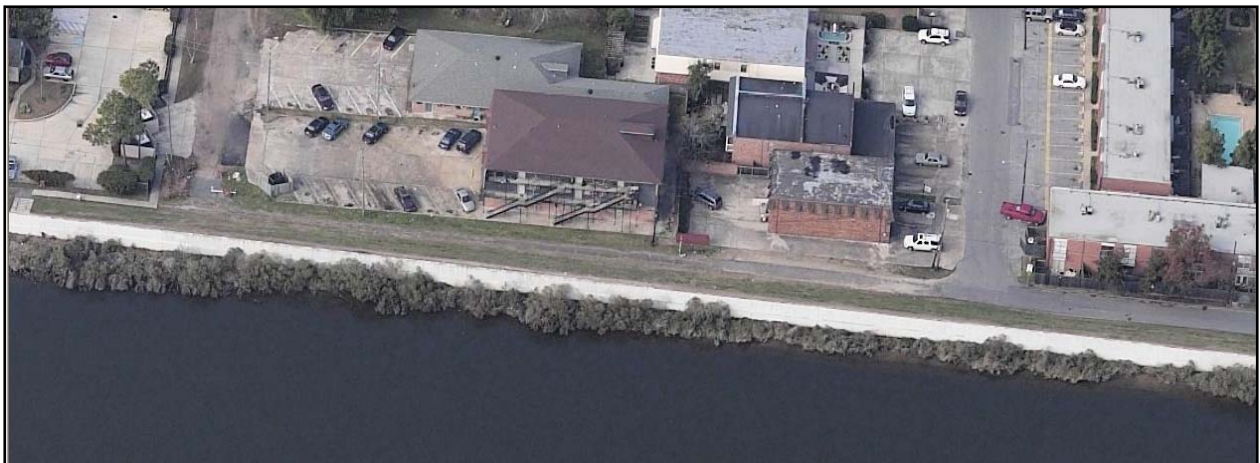
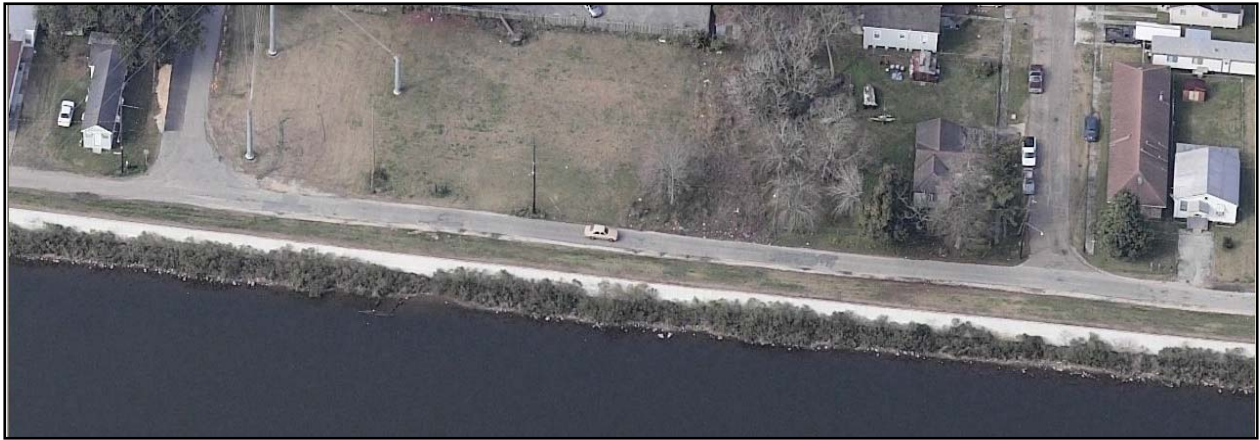
Section 3 – 17th Street Outfall Canal - Summary of Coordinates for Defined Reaches								
		State Plane NAD83 1702 - LA South		Graphical Latitude	Longitude	UTM NAD 83		
		Northing	Easting			Zone 15 Northing	Easting	
17th St. Canal Levee								
Reach 9	START	555079.333	3664232.118	30 01 14.83996	90 07 18.51511	2551161.68	10907390.11	
Reach 9	END	547700.195	3663758.46	30 00 01.84526	90 07 24.78918	2550795.34	10900000.24	
Reach 10	START							
Reach 10	END	545946.804	3663664.746	29 59 44.49864	90 07 26.06543	2550727.12	10898244.58	
Reach 11	START							
Reach 11	END	542850.391	3663595.224	29 59 13.85519	90 07 27.22762	2550702.65	10895145.55	

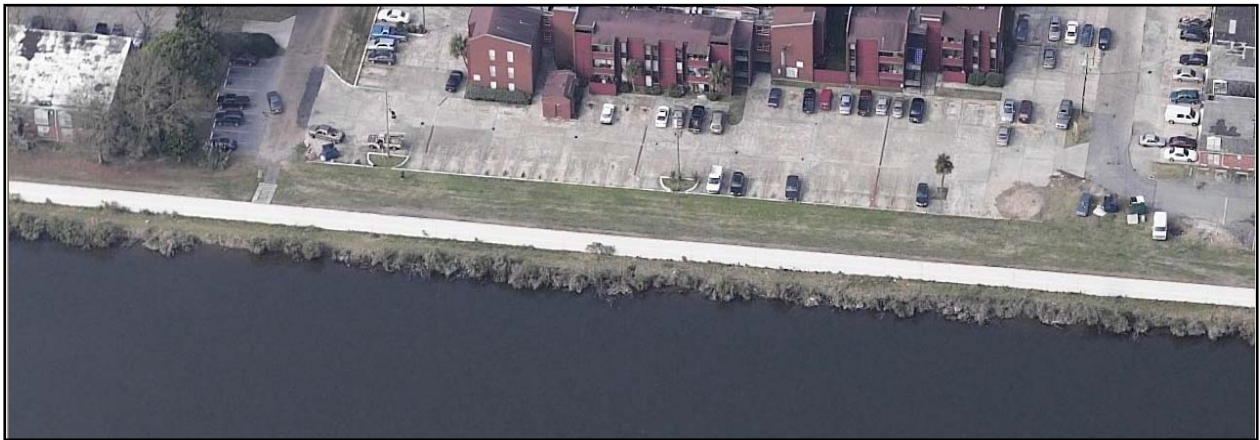
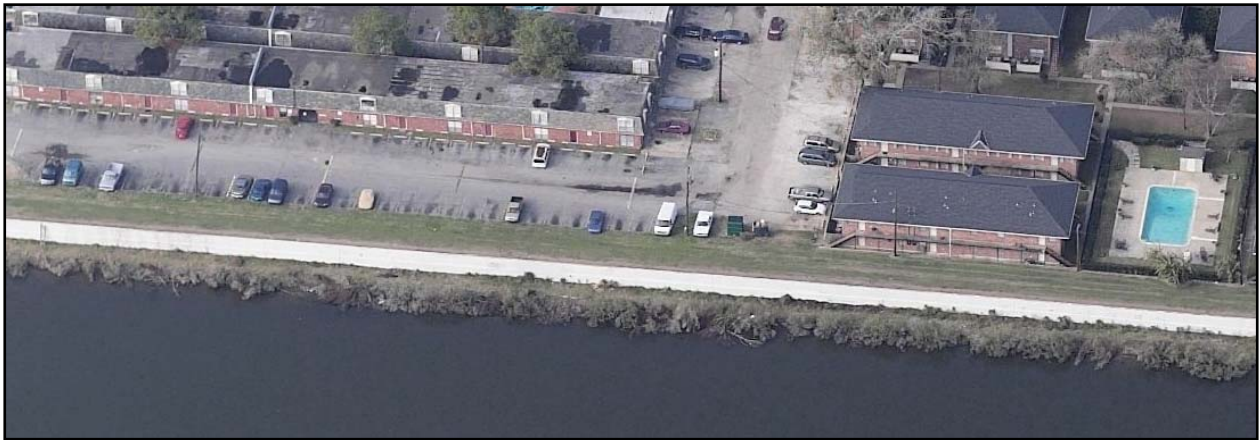
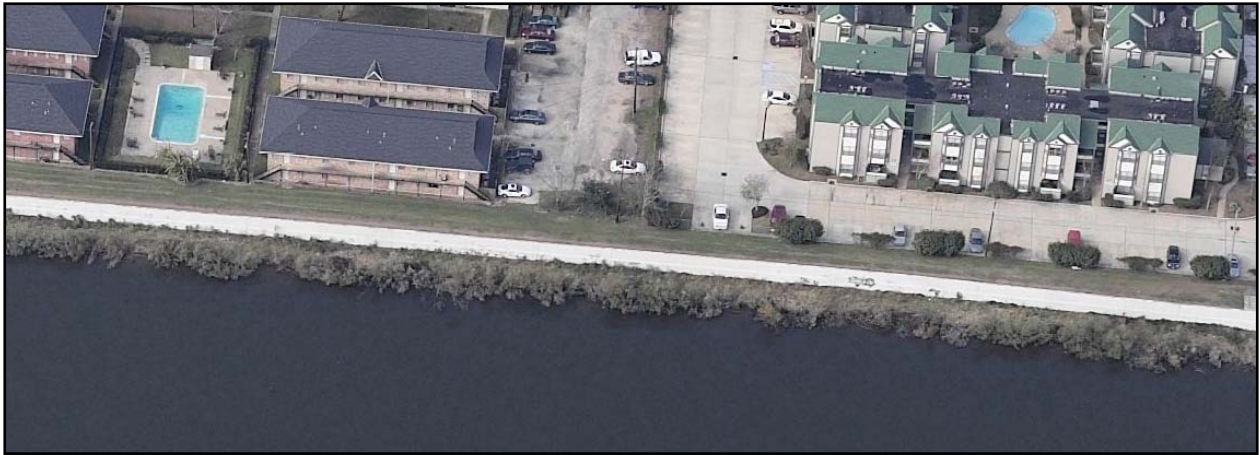
Definition of Reaches

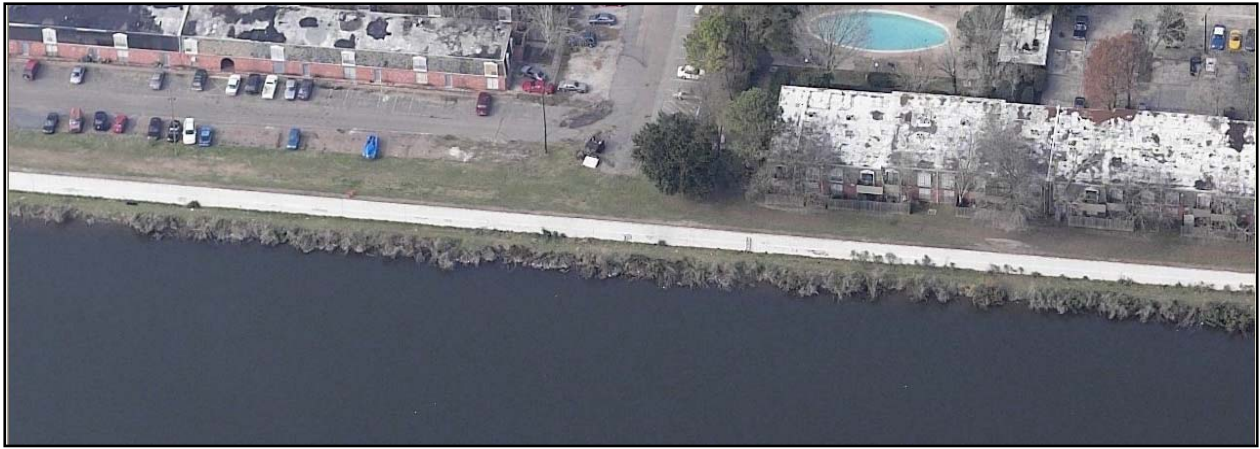
Reach 9 – This reach consists of an I-wall in levee section at an average elevation of 12.5 feet with a length of approximately 7,570 feet. The reach actually starts at the Lakefront levee however this area was under construction for flood proofing of the Hammond Highway bridge and was not accessible for inspection. There are two main features in this reach, Gate 1 at elevation 14.0 feet and Gate 2 is at elevation 14.0 feet. However, these gates have been removed for the construction work at the Hammond Highway. The sequence of pictures below defines the linear west line of Reach 9 (Note: These pictures are pre-Katrina).





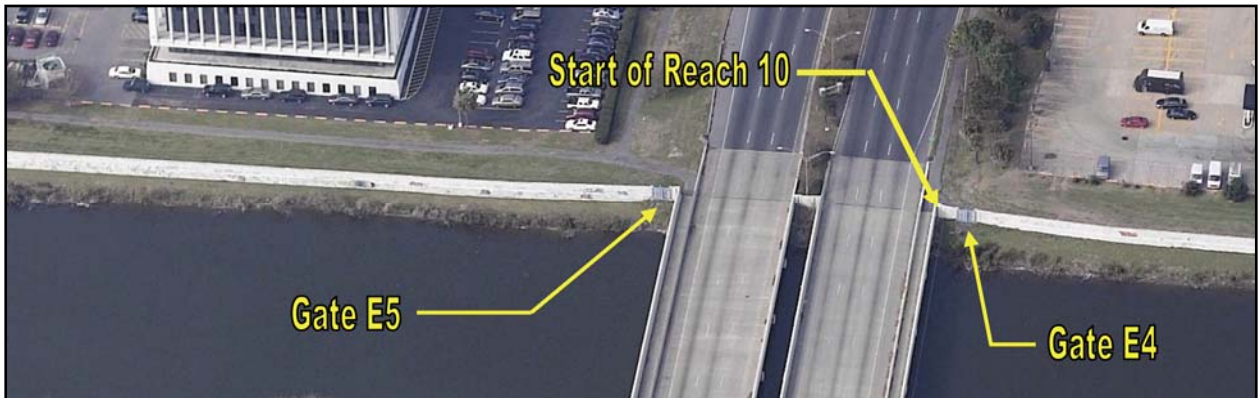






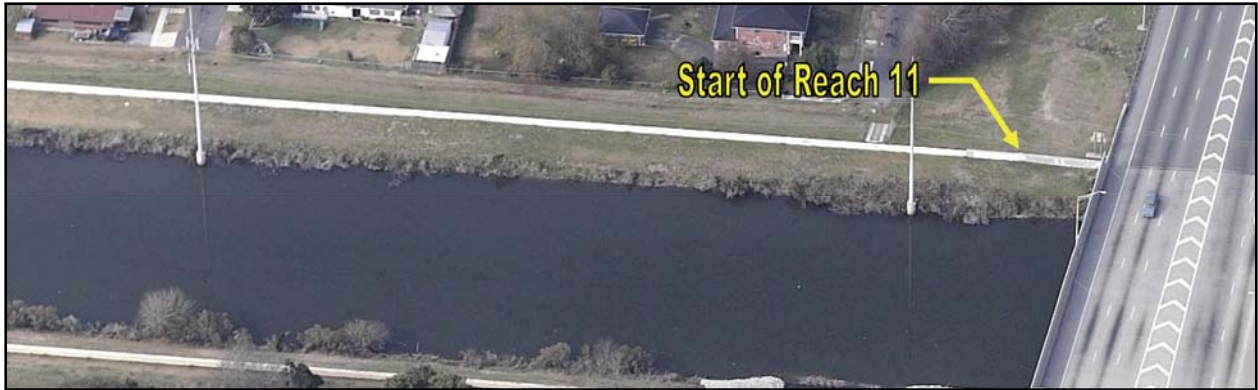


Reach 10 – This reach consists of an I-wall in a levee at an average elevation of 12.9 feet with a length of approximately 1,680 feet. This reach goes from Veterans Boulevard to just south of the I-10 overpass. There are two features in this reach, Gate E4 and Gate E5 with a elevation of 12.9 feet and a sill elevation of 6.5 feet. The Veterans Boulevard and I-10 overpass bridges have been floodproofed with tie-in parapet walls higher than the canal I-walls and are not considered features.

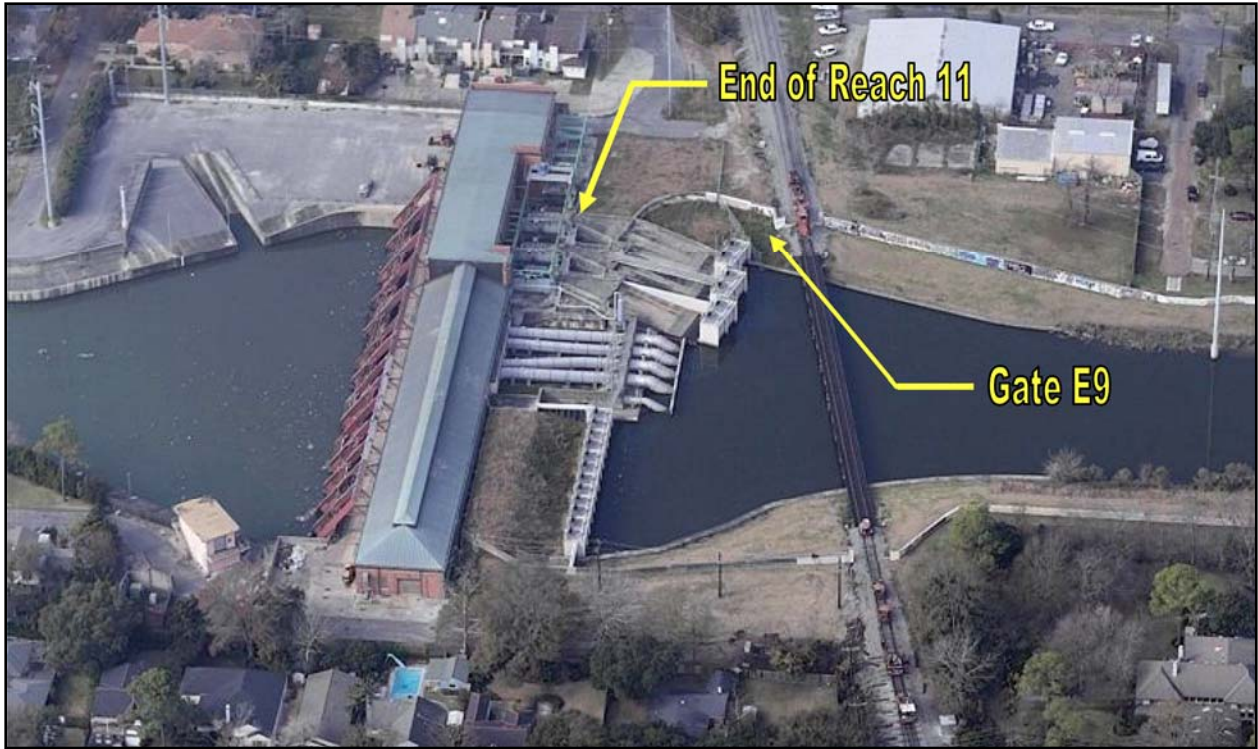




Reach 11 – This reach consists of I-wall in a levee at an average elevation of 13.4 feet with a length of approximately 2,745 feet. This reach goes from the I-10 overpass to Pump Station #6. There three features in this reach. The first is Canal Street Gate E8 which is at elevation of 12.0 feet. The second feature is the Canal Street Pump Station at elevation 13.5 feet. The final feature is the Southern Railroad Swing Gate E9 at elevation 10.3 feet.







Pump Station #6



Gate E9 CSX Railroad

Section 4: Mississippi River Levees

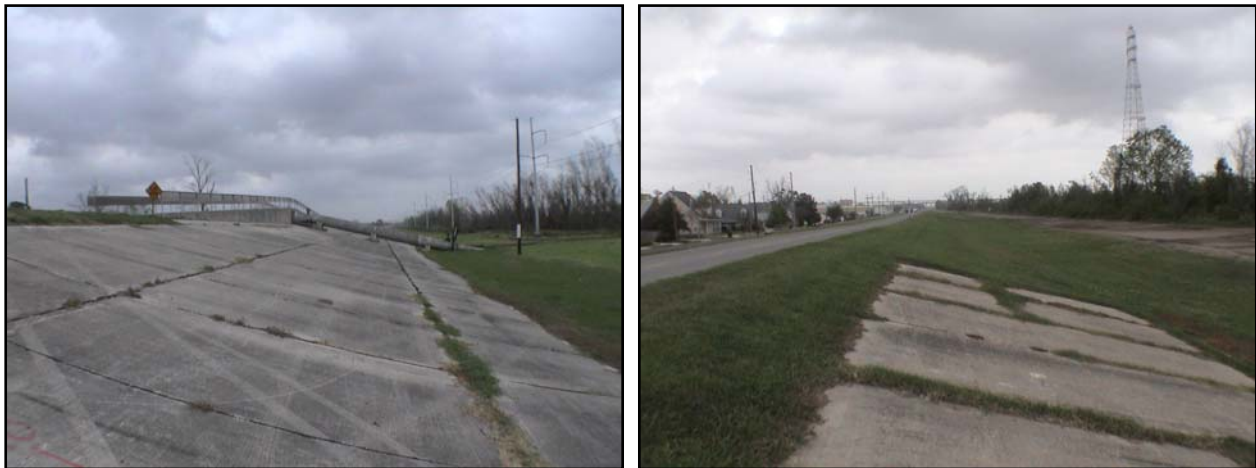
References

General design information was not available for the MRT levees within Jefferson Parish at the time of the report. Information was gathered from discussion with the East Jefferson Parish Levee Board and from the field recon.

Narrative

The MRT levees are earth structures with a 10-foot crown and side slopes of varying grades. About half of the levees along this section of the river have concrete scour protection on the flood side. There is no scour protection on the protected side of the levees. The levees are also well maintained with both an asphalt road and mowed grass slopes on both sides. The crown of the levee is extensively used by the public as a bike and walking path. There are a number of pipeline crossings and access ramps that were defined for this section. However none of these structures greatly interfered with the integrity of the levees so they were not included into the risk assessment.

This section has been broken down into three reaches defined on the change in elevation of the levees. Reach 12 starts at the Orleans East Parish line and goes along the river from station 0+00 to 388+17.51. Most of this reach was unprotected by the concrete scour protection. Reach 13 starts at station 388+17.51 and continues to station 538+17.51. This reach has concrete scour protection on about two-thirds of the flood side banks. Reach 14 starts at station 538+17.51 and runs to the St. Charles Parish border just southwest of the international airport. Most of this reach has concrete scour protection on the flood side banks.



Flood side of MRT in East Jefferson Parish
(Note: Concrete scour protection and asphalt roadway on crown)

Section 4 – Mississippi River Levees - Summary of Reaches and Features

MRT Levees								
1	0+00	388+17.51	Levee	26.6	S	38818	26.6	Reach 12
2	388+17.51	538+17.51	Levee	25	S	15000	25	Reach 13
3	538+17.51	608+12.06	Levee	24	S	6995	24	Reach 14

Section 4 – Mississippi River Levees - Summary of Coordinates for Defined Reaches

		State Plane NAD83 1702 - LA South		Graphical Latitude	Longitude	UTM NAD 83		
		Northing	Easting			Zone 15 Northing	Easting	
Mississippi Levee								
Reach 12	START	530021.436	3659583.755	29 57 07.28044	90 08 14.36542	2546875.73	10882251.64	
Reach 12	END	532634.821	3653607.193	29 57 33.76261	90 09 21.99695	2540858.17	10884779.48	
Reach 13	START							
Reach 13	END	523758.1	3642759.654	29 56 06.97997	90 11 26.31882	2530134.31	10875740.84	
Reach 14	START							
Reach 14	END	537504.405	3614269.527	29 58 25.75591	90 16 48.68478	2501431.68	10889079.25	

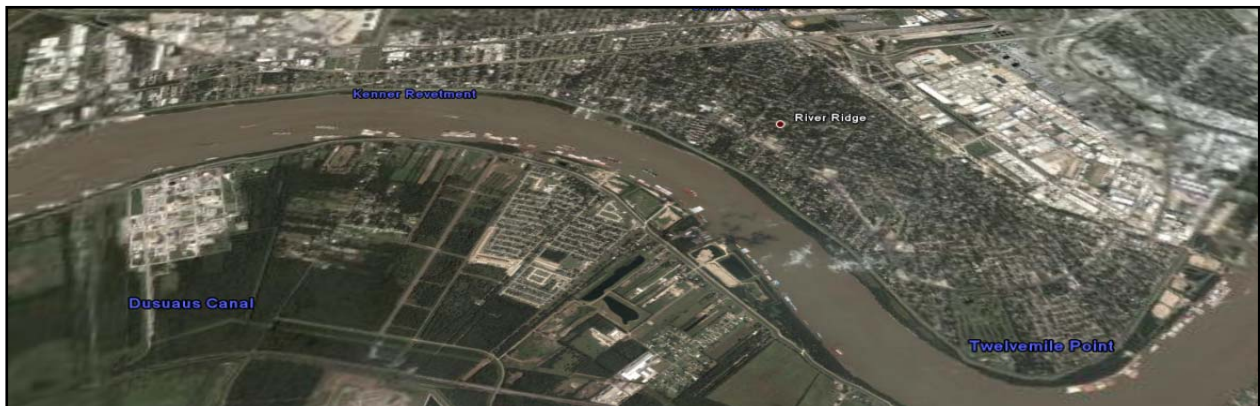
Reach 12



Reach 13



Reach 14



Section 5: Jefferson/St. Charles Parish Border Interior Levees

References

General design information was not available for the MRT levees within Jefferson Parish at the time of the report. Information was gathered from discussion with the East Jefferson Parish Levee Board and from the field recon.

Narrative

The MRT levees are earth structures with a 10-foot crown and side slopes of varying grades. About half of the levees along this section of the river have concrete scour protection on the flood side. There is no scour protection on the protected side of the levees. The levees are also well maintained with both an asphalt road and mowed grass slopes on both sides. The crown of the levee is extensively used by the public as a bike and walking path. There are a number of pipeline crossings and access ramps that were defined for this section. However none of these structures greatly interfered with the integrity of the levees so they were not included in the risk assessment.

This section has been broken down into three reaches defined on the change in elevation of the levees. Reach 12 starts at the Orleans East Parish line and goes along the river from station 0+00 to 388+17.51. Most of this reach was unprotected by the concrete scour protection. Reach 13 starts at station 388+17.51 and continues to station 538+17.51. This reach has concrete scour protection on about two-thirds of the flood side banks. Reach 14 starts at station 538+17.51 and runs to the St. Charles Parish border just southwest of the international airport. Most of this reach has concrete scour protection on the flood side banks.



Section 5 – Jefferson/St. Charles Parish Border Interior Levee - Summary of Reaches and Features								
Levee from Airport to MRT			Not Needed Since St Charles Has New Levee To Tie To Airport Runway Extension					
1	0	1000	Gap in levee	5	S	1000	5	
2	1000	1485	Sheet pile wall	10	S	485	10	
3	1485	1735	Gap in levee	3.5	S	250	3.5	Reach 15
4	0+00	32+89	Levee	10	S	3289	10	
5	32+89	42+69.9	Sheet pile wall - 42 ft gap @ 5.9 ft at RR	10.8	S	980	10.8	Reach 16
6	42+69.9	57+00	Sheet pile wall	10.5	S	1431	10.5	Reach 17
7	57+00	74+00	Levee	13	S	1700	13	Reach 18

Section 5 – Jefferson/St. Charles Parish Border Interior Levee - Summary of Coordinates for Defined Reaches

		State Plane NAD83 1702 - LA South		Graphical		UTM NAD 83 Zone 15	
		Northing	Easting	Latitude	Longitude	Northing	Easting
Return Levee							
Reach 15	START	537504.405	3614269.527	29 58 25.75591	90 16 48.68478	2501431.68	10889079.25
Reach 15	END	539488.473	3614278.54	29 58 45.39526	90 16 48.37495	2501411.83	10891064.28
Reach 16	START	543565.735	3614781.939	29 59 25.70992	90 16 42.22427	2501856.10	10895150.57
Reach 16	END						
Reach 17	START	544766.352	3614391.643	29 59 37.63026	90 16 46.53705	2501448.16	10896346.01
Reach 17	END						
Reach 18	START	546407.659	3614397.566	29 59 53.87687	90 16 46.29803	2501430.19	10897988.09
Reach 18	END						



Reach 15



Reach 16



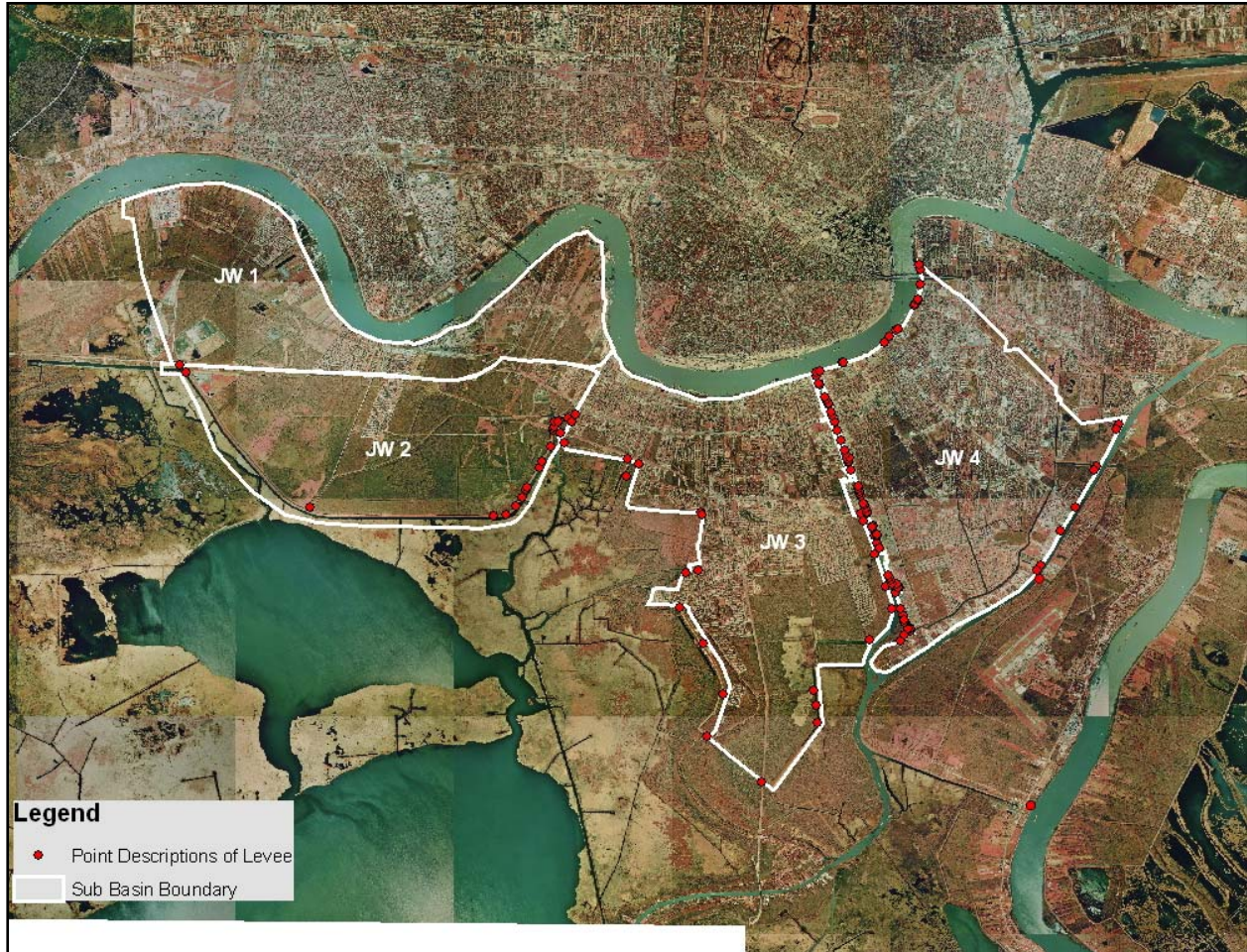
Reach 17



Reach 18

Jefferson West Bank Area

The West Bank Basin is composed of four sub-basins that are designed as three projects. These are 1) Cataouatche, 2) Westwego to Harvey Canal, and 3) Harvey Canal to Algiers Canal.



Cataouatche – JW1 and JW2

This area is located in Jefferson Parish and is generally bounded by the Mississippi River and its alluvial ridge to the north and the Lake Cataouatche levee to the west, south and east. The topography is flat with ground elevations ranging from +7.5 feet NGVD on the alluvial ridges along the Mississippi River to -5 feet NGVD in the interior of the area. Approximately 40 percent of the area is below sea level. The surface area is 22.6 square miles. The area is protected by 25.4 miles of levees, natural ridges and floodwalls.

Segment 1 extends from the main line Mississippi River levee (MRL) at the Jefferson Parrish boundary southward to the Texas and Pacific railroad tracks. There are no levees or dikes in this area. The natural contour of the area provides the protection, but this segment is listed since it is possible for storm surges to flank the Segment 2 levee reach and cause flooding.

Segment 2 is the proposed levee that follows the crushed stone roadway southward from the Texas and Pacific railroad tracks (that becomes an asphalt roadway which is used by the land fill operators in the area) to US 90.



Texas and Pacific railroad



Local levee along site of proposed HPS levee

Segment 3 is a short, small dike built parallel to Hwy 90. Hwy 90 is a 4-lane road with a raised median in the center. The median provides the higher level of protection. The road rises as a low relief ramp at the beginning of Segment 4.

Segment 4 is an earthen levee extending southward from Hwy 90 to the Cataouatche Pumping Station. The discharge lines of the first pumping station pass over the levee. The discharge lines of the second pump station (immediately adjacent to the first station) pass through a sheetpile wall.



Levee begins at Hwy 90



Typical levee in this area



Pump station near Hwy 90 with pipe crossing over levee

Segment 5 is an all clay levee that extends eastward from the Cataouatche Pumping Station to the I-Wall in the Segnette State Park.



Cataouatche Pump Station



Sheetpile wall transition to concrete capped I-wall at the Segnette State Park

Segment 6 is a concrete I-Wall atop a clay levee. The controlling grade listed for this area is the preconstruction levee grade. The area has two vehicular gates.



Concrete capped I-wall at the Segnette State Park



Swing in the concrete capped I-wall at the Segnette State Park where wall ends at the Segnette Pump Station

Segment 7 is completed floodwalls that lie between the Segnette Pump Station and the Old Westwego Pump Station.



Segnette Pump Station

Segment 8 extends from the floodwall at the head of Company Canal (closest line of flood protection to the Mississippi River) to the MRL. The natural contour of the area provides the protection.

Segment 9 is the West Jefferson Levee District Mississippi River levee. This all clay levee closes the north end of the sub-basin and extends from Westwego to the St. Charles Parish line.

Segment 10 is the interior drainage separator, which begins at the end of Segment 3. It proceeds along US 90 to the east until it intersects the Texas and Pacific railroad tracks just north of the Westbank Expressway. It then continues to the east along the railroad until it intersects Segment 8 and then turns north to the MRL. JW1 is to the north of the Segment 10 interior levee and JW2 is to the south.

There are a total of five vehicular floodgates (double swing) and two pedestrian (single swing) floodgates in the protection system. The sill elevations of these floodgates are at or above the current controlling elevation so these gates are not a factor in draining the area.

There are four pumping stations that drain the protected area.

Westwego to Harvey Canal – JW3

This area is located in Jefferson Parish and is generally bounded by the Mississippi River and its alluvial ridges on the north, the Harvey Canal on the east and marshes/wetlands on the south and west. The topography is flat with ground elevations ranging from +7.5 feet NGVD on the alluvial ridges along the Mississippi River to –4 feet NGVD in the interior of the area. Approximately 40 percent of the area is below sea level. The surface area is 21.4 square miles. The area is protected by 27.5 miles of levees and floodwalls.

Segment 1 is a floodwall stretching between the Old and New Westwego Pumping Stations and connects the Cataouatche sub-basin to Westwego to Harvey Canal sub-basin. The segregation of these two sub-basins is not very pronounced. The general contour tie to the Mississippi River levee is described in Segment 8 the JW1 Cataouatche sub-basin.

Segment 2 is the Westwego Levee that is a geosynthetic reinforced, clay levee running parallel to Mayronne Canal between the New Westwego Pumping Station and Dugues Canal-Westwego Seaplane Airport. A 400-ft canal closure was constructed at the head of the Dugues Canal.

Segment 3 runs between Dugues Canal and the New Westminster Pump Station and the North-South Levee. This levee is all clay.

Segment 4 is the Westminster Levee, which parallels the Grand Cross Canal, stretches between New Westminster Pumping Station and Orleans Village Pumping Station (out of service). This clay levee is geosynthetically reinforced.



New Westminster Pump Station

Segment 5 is the Orleans Village levee, which is all clay and paralleling Glasco Canal, between Orleans Village Pumping Station (out of service) and Oak Cove Pumping Station. Along this reach is the Ames and Mount Kennedy Pumping Stations connected by floodwall.



Ames Pump Station

Segment 6 consists of the Oak Cove and Hwy 45 clay levees running between Oak Cove Pumping Station and the Hwy 45 crossing. Also found along this length are areas of T-wall, I-wall, and one vehicular floodgate at Hwy 45.



Sheet pile transition at the LA Hwy 45



Double Swing gate at the LA Hwy 45 closure in the V-Line levee

Segment 7 is the V-Line Levee which is an I-wall between LA Hwy 45 and Hwy 3134.



V-line levee continues south of LA Hwy 45 closure



Southern tip of V-line levee

Segment 8 stretches from the V-Line Levee floodwall to the Old Estelle Pumping Station and is an all clay levee with one main road crossing.

Segment 9 is an all clay levee running parallel along the North bank of the Old Estelle Pumping Station Outfall Canal. It runs to the Harvey Canal.

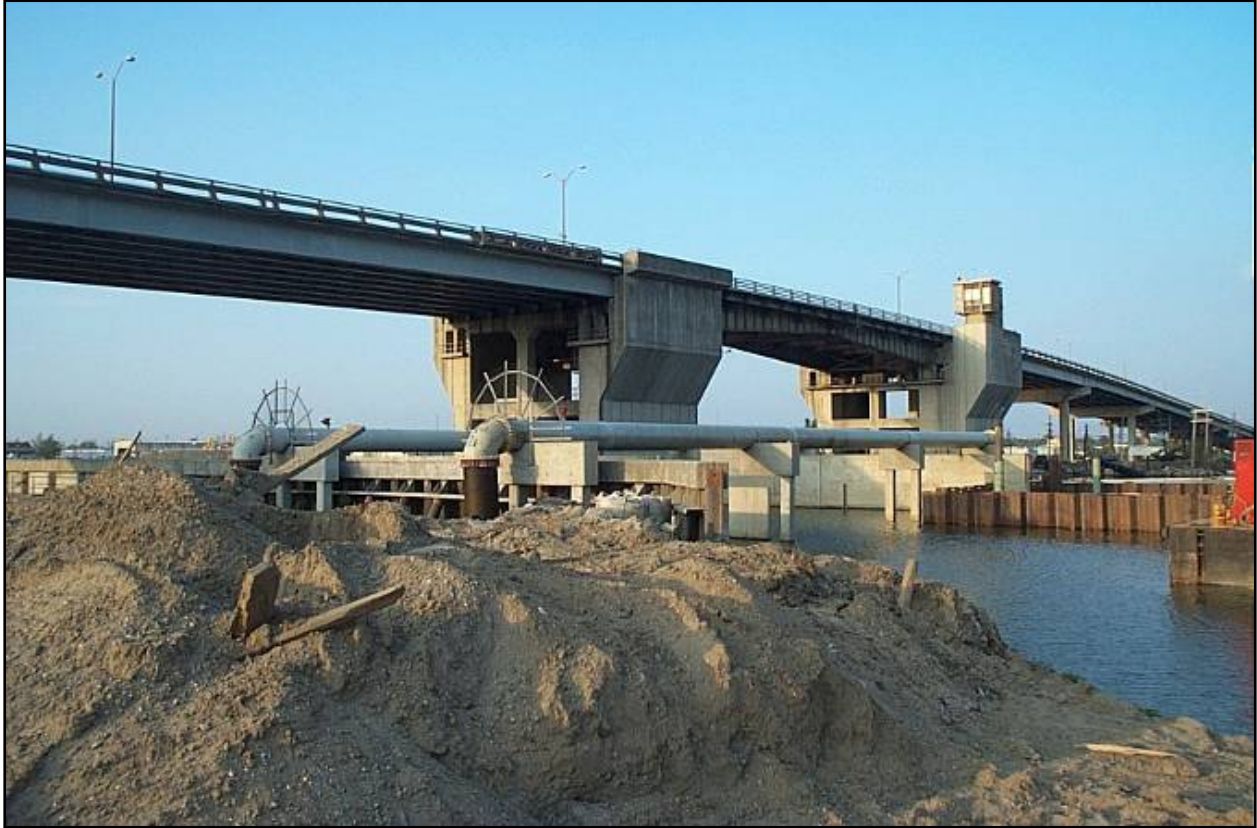
Segment 10 is the West Bank Harvey Canal Levee. It consists of a clay levee running from the mouth of the Harvey Canal to the LaPalco bridge. Along this segment is the New Estelle Pumping Station, a floodwall at the Bridgeline pipeline, and three areas of sheetpile closure required because of unstable earthen levee sections.



Sheetpile closures



New Estelle Pump Station



Lapalo Bridge Overpass construction of sector gate under way

Segment 11 stretches from LaPalco Bridge to the Harvey Lock, paralleling the Harvey Canal. This floodwall includes the Harvey and Cousins Pumping Stations, a vehicular gate and ties the Westwego and Harvey Canal sub-basin back into the Mississippi River Main Line levee.



Industrial area along Harvey Canal



US 90 Bridge over Harvey Canal near Harvey Lock



Looking south down Harvey Canal from Hwy 45 Bridge near Harvey Lock



Harvey Lock



Harvey Lock exit toward MS River



MS River Levee at exit of Harvey Canal



Harvey Pump Station and surrounding walls

Segment 12 is the West Jefferson Levee District Mississippi River levee. It encloses the north side of the sub-basin between Westwego and Harvey Canal and is an all clay levee.



Typical MRL. Paved 10 foot crown. Armor on flood side



MRL in vicinity of Northrup-Grumman Plant



Typical closure gate (vehicle and pedestrian) along MRL





There are 10 pedestrian floodgates (swing) and two roadway floodgates (one swing and one miter).

There are 11 pumping stations that drain the protected area. The location of the pumping stations.

Harvey Canal to Algiers Canal – JW4

This area is located in Jefferson and Plaquemines Parish and is generally bounded by the Mississippi River on the north, the Jefferson, Plaquemines & Orleans Parish lines on the east, the Algiers Canal on the south, and the Harvey Canal on the west. The topography is flat with ground elevations ranging from +15 feet NGVD on the alluvial ridges along the Mississippi River to -5 feet NGVD in the interior of the area. Approximately 40 percent of the area is below sea level. The surface area is 18.8 square miles. The area is protected by 21.3 miles of levees and floodwalls.

Segment 1 extends from the Harvey Canal Lock at the Mississippi River down the East bank of the Harvey Canal to the Hero Pumping Station where the pumping station discharge lines pass through a T-wall. This clay levee is a local levee in a heavily industrialized area.

Segment 2 extends from the South end of the Hero Pumping Station around the bend where it ties into the Algiers Canal levee. The clay levee is also a local levee in a heavily industrialized area.

Segment 3 picks up where segment 2 ended and continues along the West bank of the Algiers Canal. The clay levee is interrupted by floodwall segments that cross over the Belle Chasse tunnel and in front of Planters Pumping Station. It ends at the tie-in of the local levee separating Plaquemines and Orleans Parishes. A railroad track crosses over the top of the existing levee. A future floodgate is planned for the area.

Segment 4 is an all clay levee that runs along the length of the Orleans Parish line between Algiers Canal and the Mississippi River levee at the Greater New Orleans Bridge.

Segment 5 is the West Jefferson Levee District Mississippi River Levee stretching between the Harvey Canal and the Orleans Parish line beneath the Greater New Orleans Bridge. This levee consists of all clay levees with short reaches of concrete I-Wall atop clay levees with railroad and vehicular gates.

There are no floodgates, control structures, or drainage structures in the protection system.

There are two pumping stations that drain the protected area.

Appendix 4

St. Charles Basin

The St. Charles hurricane protection system (HPS), shown in Figure 1, was designed as part of the Lake Pontchartrain, LA, and Vicinity Hurricane Protection Project. The St. Charles HPS protects 17.2 square miles of urban, industrial, commercial, and ecological lands that is essentially a low density residential community with a small business district along U.S. Highway 61. The St. Charles Basin is generally bounded on the north by the St. Charles HPS, on the south by the Mississippi River Levee (MRL) and on the west by the Bonnet Carre guide levee. As designed, the HPS levees were generally constructed with a 10-foot crown width with side slopes of 1V on 3H for both the flood side and protected side. Topography is flat with ground elevations ranging from +12 feet NGVD on the alluvial ridges along the Mississippi River to -2 feet NGVD near the locally maintained levee south of Lake Pontchartrain. Approximately 25 percent of the developed area is below sea level. The design elevation of the HPS levees varies from 13 feet on the west to 12 feet on the east. There are also floodwall segments along the line of protection that consists of sheet-pile walls or concrete capped sheetpile walls constructed on the top of the levee. The line of protection was designed to provide protection from the Standard Project Hurricane. As designed, there is a total of approximately 9.5 miles of earthen levees, 1 mile of floodwall, one pump station, and five drainage structures, three swing gate closures for road and rail crossings, and one open gap for a rail crossing. The MRL is generally designed to elevation 26 feet with a 10 foot crown and a 1 V on 3 H slope on the land side and a 1 V on 4 H on the flood side. Similarly, the Bonnet Carre guide levee is generally designed to elevation 20.3 feet with a 10 foot crown and a 1 V on 3 H slope on the land side and a 1 V on 4 H on the flood side.

The basin is a mix of industrial and residential areas. The area between the HPS and Lake Pontchartrain is essentially a wetlands area. There are two sub-basins in the basin as shown in Figure 1.

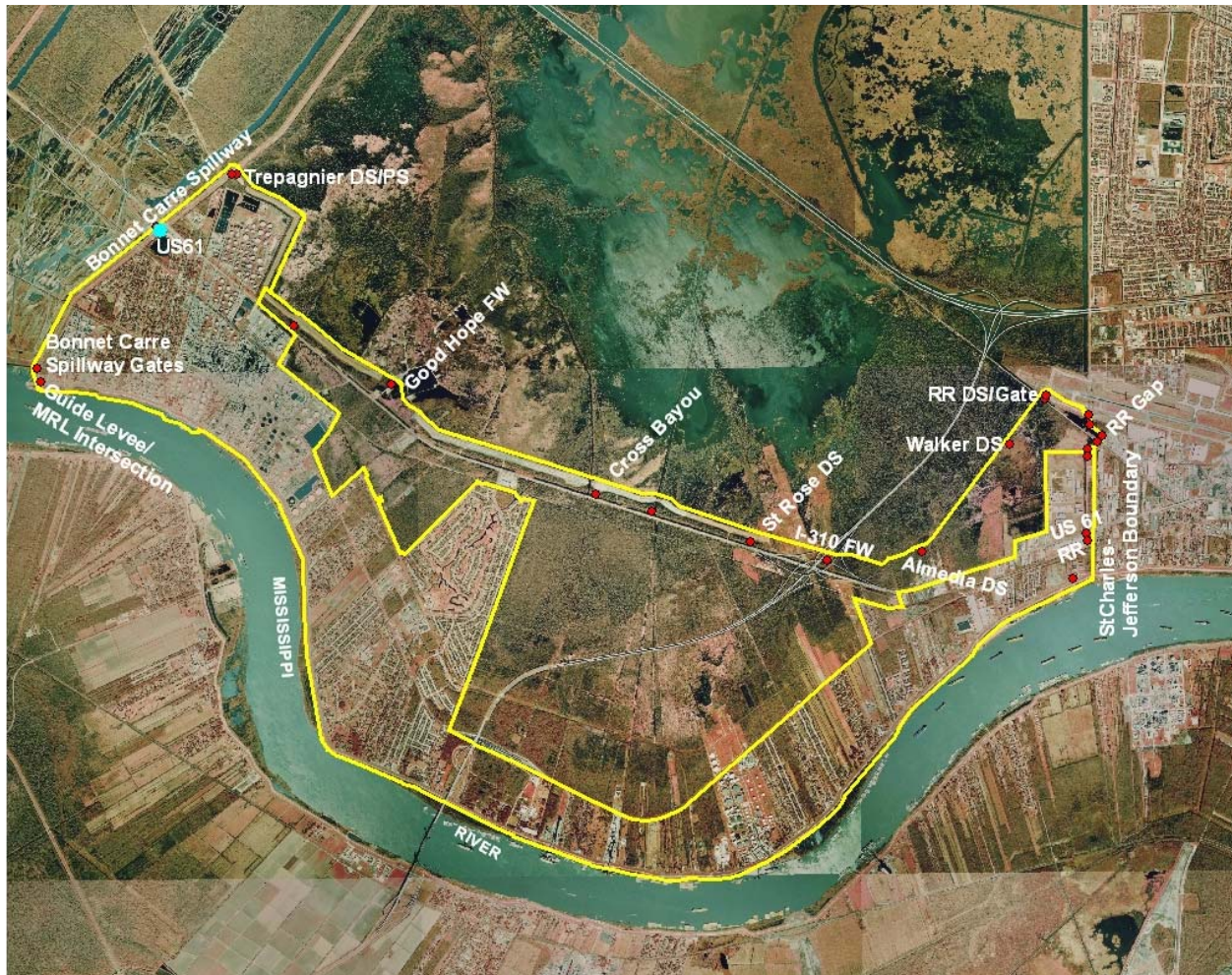
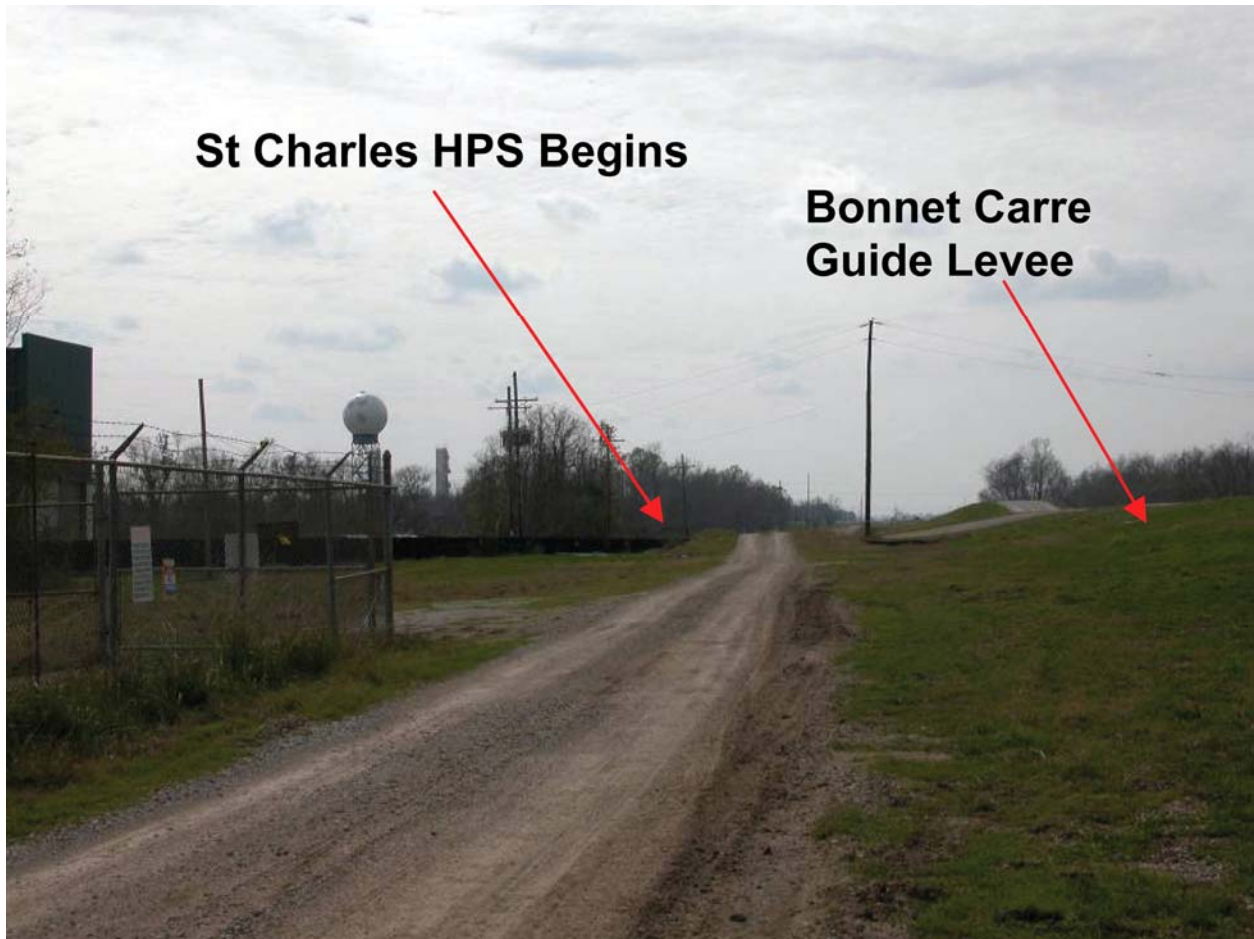


Figure 1. St. Charles Basin with sub-basins and annotations for significant features

The St. Charles HPS is made up of Reach SC1 – SC4 which begins at the Bonnet Carre Guide levee and extends eastward to the St. Charles – Jefferson Parrish border.

Reach SC1 is approximately 17,000-ft-long earthen levee (with a geotextile blanket) and contains (1) the Bayou Trepagnier Pump Station and Drainage Structure with a transition sheetpile wall, (2) a pipeline crossing and (3) the Good Hope floodwall. It was designed to a net grade of 13 ft MSL.



Intersection of St. Charles HPS and the Bonnet Carre Guide Levee



Trepagnier Drainage Structure



Trepagnier Pump Station

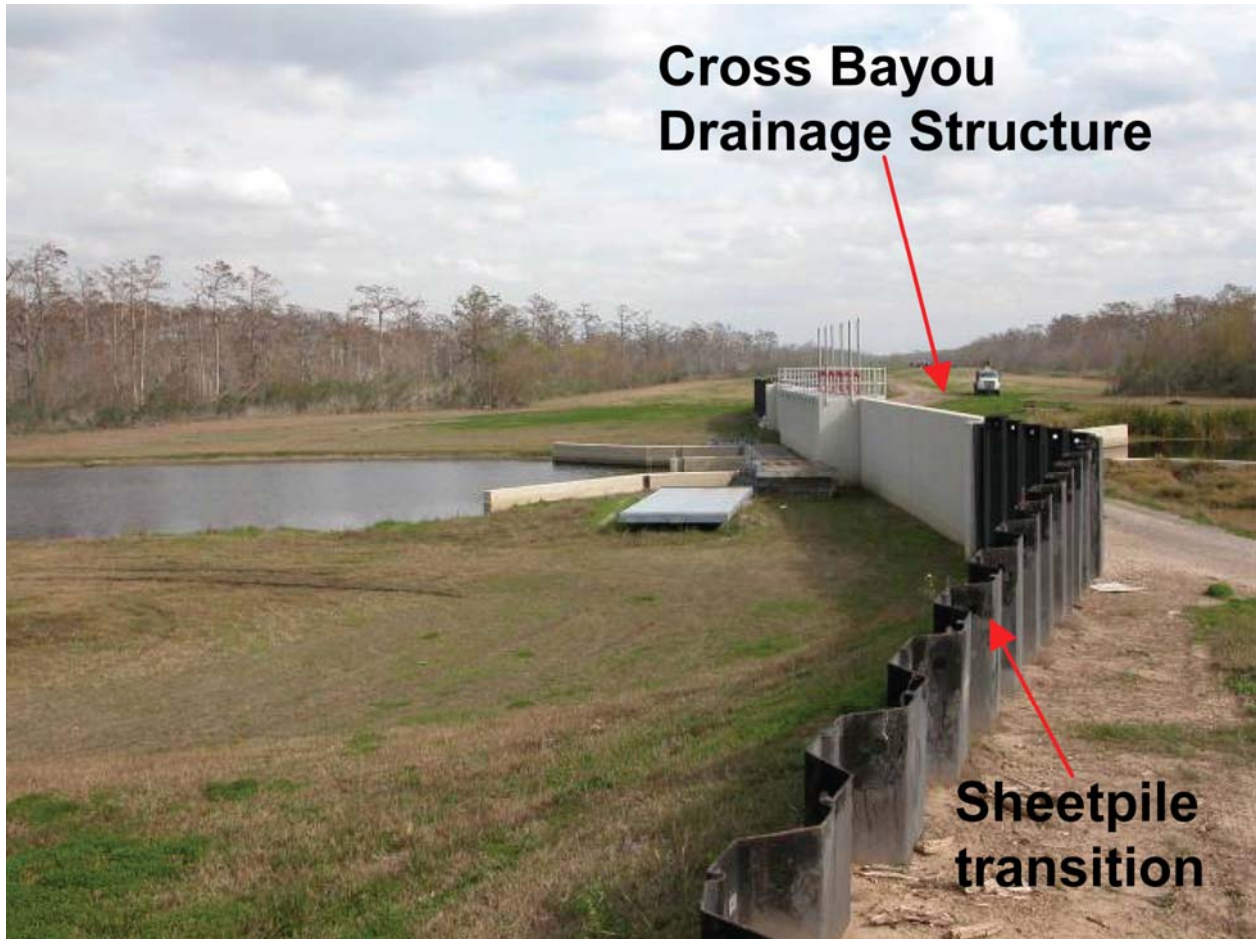


Pipeline Crossing with sheetpile transition to levee



Industrial access road closure gate

Reach SC2 is approximately 12,000-ft-long earthen levee (with a geotextile blanket) and contains (1) the Cross Bayou Drainage structure and the Gulf South Pipeline crossing. It is designed to an elevation of 12.5 ft. There is a 500-ft transition from 12.5 to 12 ft where SC3 begins.



Cross Bayou Drainage Structure



Gulf South Pipeline Crossing

Reach SC3 is approximately 24,000-ft-long earthen levee (with a geotextile blanket) and contains (1) The St.Rose, Almedia, and Walker Drainage structures, (2) the I310 Floodwall with one access gate, and (3) the railroad crossing near the airport runway extension. The RR crossing closure gate was not in place during Hurricane Katrina, but has since been completed. It was closed by sandbags for Katrina.



**St. Rose
Drainage
Structure**

**Sheetpile
Transition**

St. Rose Drainage Structure



I-310 Floodwall



I-310 Floodwall access closure gate (normally closed) with 24-ft closure gate



Alemedia Drainage Structure



Walker Drainage Structure with sheetpile transition



Railway Gated Crossing at Airport Levee (not constructed during Katrina)



Railway Gated Crossing at Airport Levee (not constructed during Katrina). HPS joins Airport Levee just north of the Railway Gated Crossing

Reach SC4 is approximately 8,048-ft-long earthen levee with most of it having an embedded sheetpile wall in its crown. It is designed to an elevation of 27.9 ft. It extends from where the HPS intersects the airport runway extension levee to the St. Charles – Jefferson Parish boundary, then proceeds southward to US 61, and on to the railroad crossing. Significant features are (1) an abrupt 3-ft drop in elevation at one 90 deg turn in the wall, (2) the 24-ft gap at the railroad crossing, (3) the US 61 crossing has no closure gate, and (4) the HPS ends at the railroad crossing, with the remainder of the parish boundary line at the same elevation as the RR until it intersects the MRL. The RR crossing gap was sandbagged during Katrina.



Floodwall as it turns east by the Airport runway extension



Corner of sheetpile floodwall as it turns south by the Airport runway extension (3 ft drop in elevation)



Floodwall as it turns south just north of the railroad crossing



Railroad crossing has no closure gate. During Katrina it was sandbagged.



St. Charles – Jefferson Parish Boundary Levee ends North of US 61 Highway – gap at this crossing



St. Charles – Jefferson Parish Boundary Levee South of US 61 Highway – no closure at this crossing



Short Transition Section of HPS from South of US 61 toward railroad



St. Charles –Jefferson Levee at South side of US 61



The basin protection then continues westward as the MRL at a design elevation of 26 ft. The MRL is an earthen levee with a 10-ft crown. No major structure or pipeline passes through the MRL.



Mississippi River Levee at the St. Charles-Jefferson boundary at Hwy 48



Top of Mississippi River Levee at the St. Charles-Jefferson boundary



I-310 passing over the Mississippi River Levee

At the east extend of the basin, the MRL intersects the Bonnet Carre guide levee, which continues the protection northward on the west side of the basin until it reached the HPS. This stretch contains the intersection with the spillway and US 61.



Mississippi River Levee intersection with Bonnet Carre Guide Levee



Bonnet Carre Spillway intersection with guide levee



Bonnet Carre Guide Levee Looking North from the Spillway gates

Appendix 5

Plaquemines Basin

Background

The Plaquemines (PL) Basin is made up of 11 sub-basins as shown in Figure 1. It is generally composed of the Plaquemines Parish along the east and west banks of the Mississippi River south of Mile 82. Both the west and east bank protection includes the Mississippi River levees as a part of each sub-basin. There are 134 miles of MRL and floodwall, 53 miles of hurricane protection, 12 miles of floodwall, 19 pump stations, a 110-foot small boat lock, and a marine floodgate. The damage consisted of 20 miles of MRL and HPS levee, 9.4 miles of floodwall, and five pump stations.

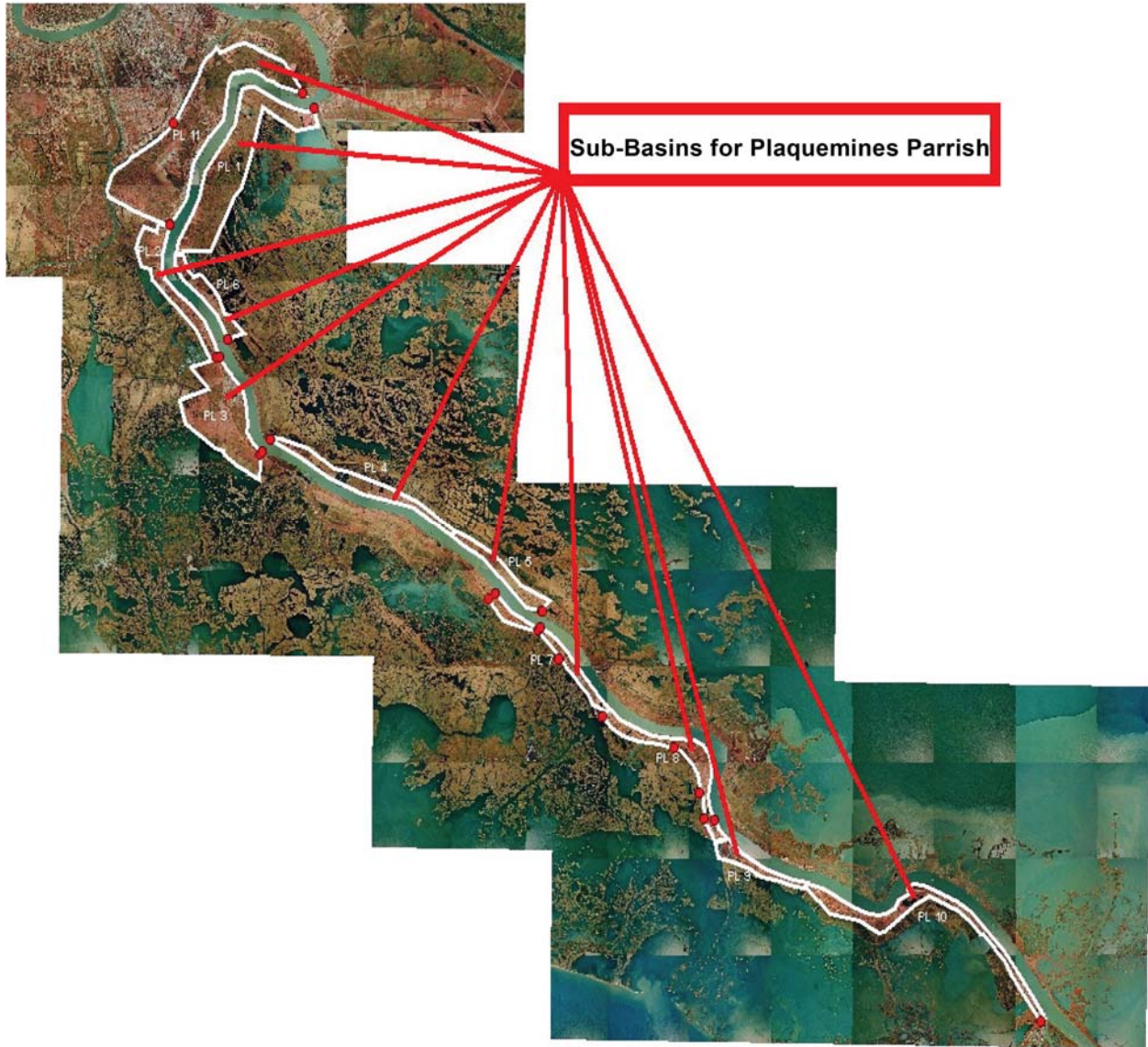


Figure 1. Plaquemines Parrish with levee protection footprint and sub-basins (PL1 – PL11)

PL 11

PL 11 begins along the west back of the MRL, shown in Figure 2, is generally bounded on the east by the Mississippi River, the Intercoastal Waterway on the west, the Plaquemines-Orleans Parrish boundary on the north, and the Hero Canal on the south.

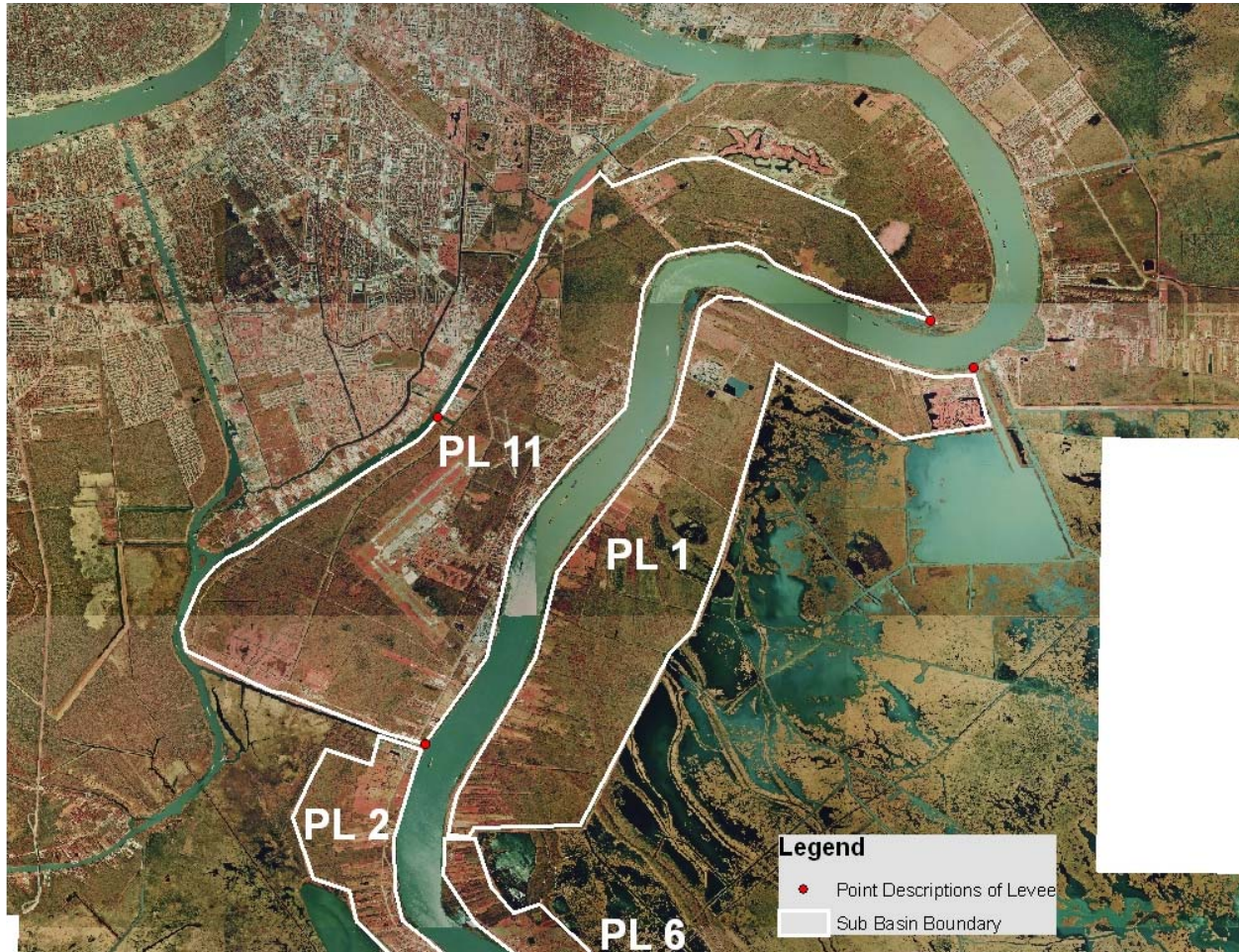


Figure 2. PL 11 and PL 1 Sub-Basins with Reach Beginning and Ending Points (Red Dots)

The federal levee begins at the MRL inside the U.S. Coast Guard station.







Back levee continues inside
U.S. Coast Guard Station

Back levee crossed by roadway
inside U.S. Coast Guard Station.
Roadway is 2 feet lower than
levee. No closure structure



Back levee continues outside U.S. Coast Guard toward GIWW Station



Drainage structure under Back Levee outside U.S. Coast Guard station. Screw gate closure on culvert



Back Levee intersects Hwy 406 looking toward the GIWW and General De Gaulle Bride overpass.
No closure at Hwy



Back Levee passed under General De Gaulle onramp from Hwy 406. Buckling of concrete slab on levee under ramp.

The interior Orleans-Plaquemines Parrish levee ends at the GIWW. The Federal Back levee along the GIWW the proceeds south and passes under the General De Gaulle Highway bridge overpass.



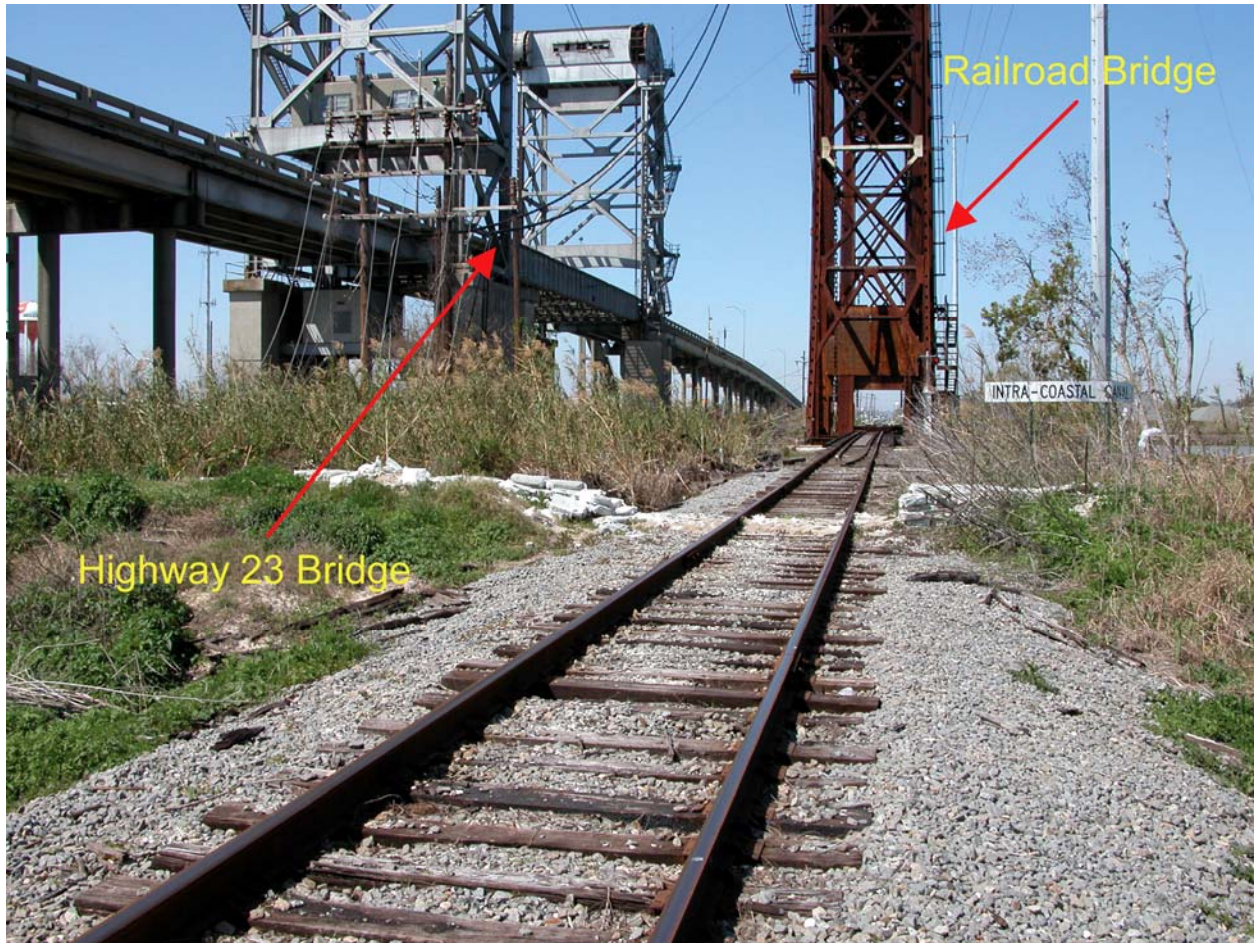


Going south along the GIWW to the Belle Chase Pump Station.

Sub-basin continues south along the GIWW to the Highway 23 and Railroad Bridge Crossing and Tunnel under GIWW.



Highway 23 Bridge over GIWW and Levee





Highway 23 Tunnel under the GIWW



Pipe crossing over the GIWW levee



A point of levee erosion along the GIWW, however most is in good condition



Typical levee section. Numerous gates across levee to contain cattle



Typical levee section along the GIWW



Plaquemines Pump Stations 1 and 2



Plaquemines Pump Stations 1 and 2



PL 11 Back levee intersects Hwy 23 north of Jesuit Bend

The MRL then forms the remaining section of PL 11 as it goes north along the river to the point where it intersects the Plaquemines Parish interior levee inside the U.S. Coast Guard station.



The crown of the levee is generally 10 feet wide, with most paved and some stretches gravel. Numerous pipes cross over the MRL in this area



A number of off-load facilities are located along this portion of the MRL, similar to this grain loading facility



There were a few cases of erosion along the MRL



More typical condition along this section of the MRL, with concrete paved or stone crown and concrete armored floodside

PL 2

PL 2 begins at this point and continues south toward the Alliance Refinery as a non-federal levee. Figure 3 shows the sub-basins PL2, PL3 and PL 6.

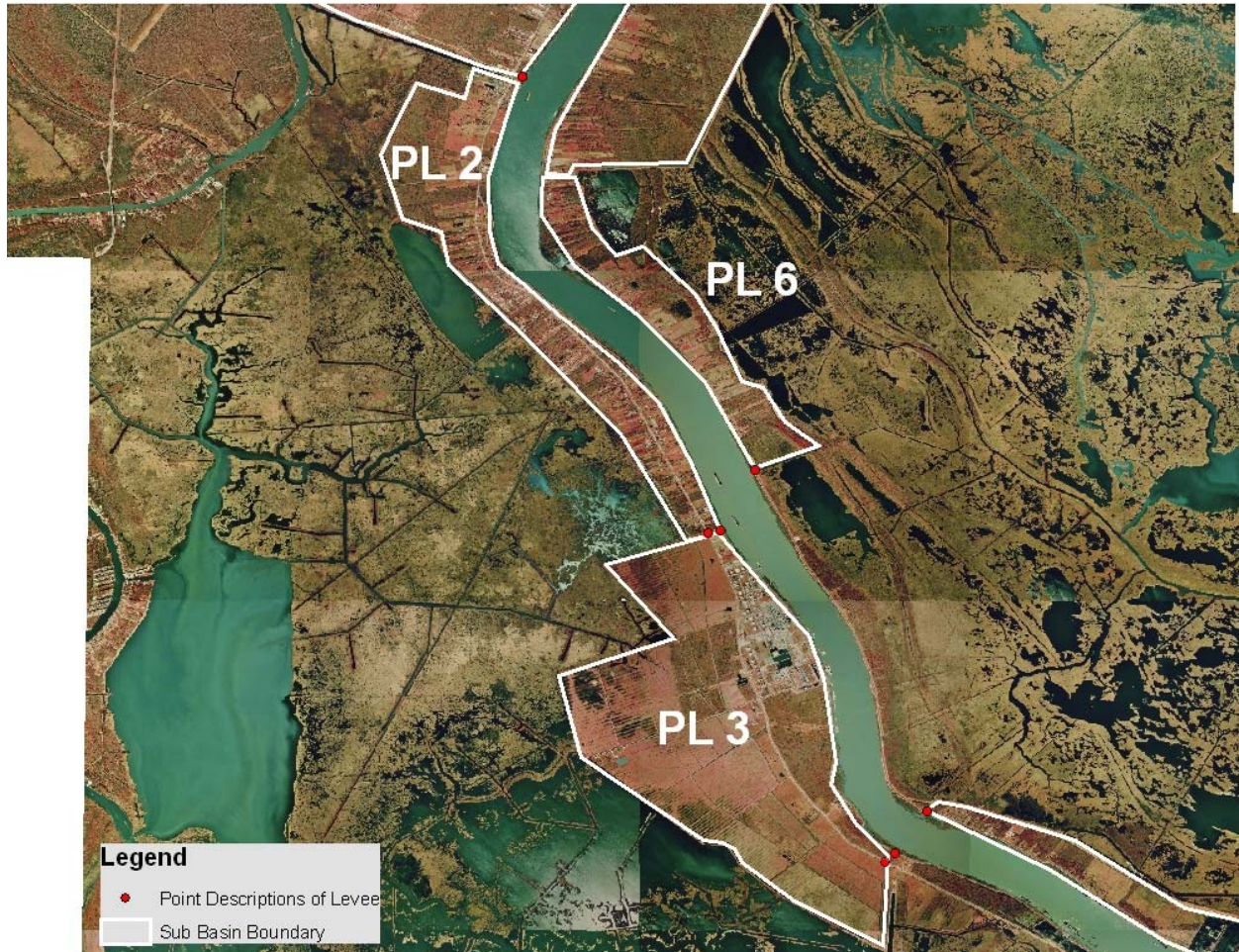


Figure 3. Location of sub-basins PL 2, PL 3, and PL 6



Ollie Pump Station



Ollie Pump Station

The condition of the non-federal levee varies. The crown is generally in better condition if cows are present on the levee.





The PL 2 back levee comes to an end back at Hwy 23 just north of the Alliance Refinery. It then is completed by the MRL as it goes north along the river.

PL 3

PL 3 then begins at this point, just north of the Alliance Refinery, as a non-federal levee and proceeds southward to Myrtle Grove, where it intersects Hwy 23. Levee conditions are generally poorer than the PL 2 back levee, with large overgrowth being common. Many places are impassable by 4 WD vehicles.

The condition of the non-federal levee also varies. The crown is generally poor condition, with much impassable by motorized vehicle.





Continuing southward along the MRL, the sub-basin enclosed by the Citrus Lands Back Levee will not be included. There was an extensive breach in this levee and repairs were difficult. Below is the initial repair.



Citrus Lands Back Levee repairs to breach



Citrus Lands Back Levee repairs to breach

The Back Levee crosses Hwy 23 and connects to the MRL. The sub-basin enclosure then goes north as the MRL.



The Back Levee intersects the MRL after it crosses Hwy 23

As the MRL proceeds north, numerous locations of erosion occurred due to overtopping. Some were repaired and some were not extensive enough to require repair. Debris is located on the levee top and slopes.







Also the MRL has numerous locations where the concrete armor was eroded and was replaced with stone. More cases of erosion.







PL 4, 5, 7, 8, 9, and 10

These sub-basins are on the west bank, south of St. Jude. These sub-basins are in a project named New Orleans to Venice (NOV) Hurricane Protection Project.

NOV

The Mississippi River Levees also serve as the hurricane protection system south of St. Jude and is part of the NOV Hurricane Protection Project. On the East Bank, the project extends 16 miles from Phoenix down to Bohemia. On the West Bank it extends 37 miles from St. Jude to Venice.

Figures 4a and 4b give a comparison the NOV project definitions, and the sub-basin PL 4, 5, 7, 8, 9, and 10 locations.



Figure 4a. New Orleans to Venice, LA, Hurricane Protection Project



Figure 4b. Sub-basins PL 4, 5, 7, 8, 9, and 10

West Bank Back Levees

St. Jude to City Price

The St. Jude to City Price reach includes 3 miles of enlarged back levees from St. Jude to City Price (between approximate river miles 47.1 and 43.9 Above Head of Passes (AHP)). This levee was constructed to elevation 7.0 feet NGVD as a non-federal levee. The non-federal levee was later incorporated into the federal project at 12.5 ft (NGVD). The NOV project area includes approximately 15,600 acres of land including 4,300 acres in Reach A; 3,800 acres in Reach B-1; 2,300 acres in Reach B-2; 4,500 acres in Reach C and 700 acres in the St. Jude to City Price area.

Reach A includes 13 miles of enlarged back levees from City Price to Tropical Bend and two 54-in. flap-gated culverts (between approximate river miles 43.9 and 30.7 AHP). It consists of approximately 12.8 miles of levee system with a net elevation of 12.5-14.5 feet and includes floodwalls at the Hayes Canal and Gainard Woods Pump Stations. The levee enlargement consisted of a marsh side embankment with a wave berm. The base of the levee incorporated geotextile fabric with a sand blanket and a clay cap at least 2 feet thick. The embankment was constructed of uncompacted clay, though a sand core may have been substituted in places. The main levee cross section is 1V on 3H.

Reach B-1 includes 12 miles of enlarged back levees with a net elevation of 15 ft from Tropical Bend to Fort Jackson (between approximate river miles 30.7 and 20.5 AHP) and a marine floodgate at Empire. The main levee cross section is 1V on 4H. The Flood Side (FS) and Protected Side (PS) berms generally vary from 1V on 15-20H and from 1V on 12-20H, respectively. The reach also includes a flood gate at Empire and floodwalls at the Bayou Grand Laird (I- and T-wall) and Sunrise Pump Stations. The Empire Floodgate is in the Empire to Gulf Waterway and consists of a reinforced concrete U-shaped gated bay with a steel gate hinged at the bottom, guide walls and fenders, inverted T-wall reinforce concrete floodwalls extending about 150 feet on each side of the structure, access road and breakwater.

Reach B-2 includes 9 miles of enlarged back levees with a net elevation of 15 ft from Fort Jackson to Venice between approximate river miles 20.5 and 10.4 AHP and includes floodwalls at the Venice Pump Station. The levee consists of a sand core with hydraulic clay fill. The levee construction occurred in three stages or lifts. The main levee cross section is 1V on 4H with the Flood Side (FS) and Protected Side (PS) berms generally varying from 1V on 15-74H FS and from 1V on 29-71H PS.

West Bank River Levee

The West Bank River Levee (WBRL) includes 34 miles of West Bank Mississippi River levees built to a net design elevation of 16 to 17 ft, from City Price to Venice (between Mississippi river miles 44 to 10 AHP) (Note: the lock at Empire is a State of Louisiana facility.)

PL 7

Sub-basin PL 7 begins near City Price at Diamond Pump Station and continues past Hayes Pump Station and on southward near Homeplace as shown in Figure 4b.

PL 8

Sub-basin PL 8 begins at this location and proceeds on to near Empire Lock.

PL 9

Sub-basin PL 9 begins near Empire Lock and proceeds on to near Sunrise Pump Stations.

PL 10

Sub-basin PL 10 begins at Sunrise Pump Stations and proceeds on to near Venice.

East Bank

PL 4 and PL 5

The back levee begins at Phoenix and proceeds southward to Bohemia. The separation between PL 4 and PL 5 occurs near Pointe a La Hache. Reach C of the NOV and the East Bank of the MRL enclose these sub-basins. Reach C consists of approximately 16 miles of enlarged back levees with a net elevation of 17 feet. The back levee has a sand core with clay blanket. It was enlarged with hauled fill and raised from approximately 14-foot elevation to the 17-foot design level. It includes floodwalls (I-type sheet piling) at the pump stations near Bellevue and Pointe a La Hache. Construction of the levee to date has included three of the designed four lifts. It lays between approximate river miles 59.3 and 44.3 AHP and 10 flap-gated culverts.

The NOV was damaged by Hurricane Katrina when it made landfall near Buras-Triumph, which is on Reach B-1. The storm produced storm surge levels that exceed the level of the constructed protection. Numerous breaches occurred along the back levees on both the east and west bank sides of the NOV project. Levees were overtopped and breached, resulting in extensive erosion and scour, along both the back levees and the Mississippi River levees (as enlarged for hurricane protection). In addition there was damage to the floodgate at Empire and to the floodwalls along the MRL and back levees.

PL 1 and PL 6

The final two sub-basins (PL 1 and PL 6) are on the east bank of the river across from PL 11 (Figures 2 and 3). The non-federal back levee begins near the Plaquemines-St. Benard Parrish boundary and continues south, ending south of Belair. The protection level is at elevation 6 feet. These sub-basins are closed by the MRL as it proceeds north along the river to the parrish boundary.

Risk Model Idealization

The Plaquemines Parrish Basin was discretized into 11 sub-basins (PL1 – PL11) as shown in Figure 5. The sub-basins were defined to correspond to the known interior drainage areas. This reach idealization follows from the basin description information presented previously, which was collected from project documents and field inspections. Figures 6, 7 and 8 show the elevations for the Plaquemines Parrish HPS: **Pre-Katrina**-at the time of Katrina, **Current**-as of 1 Jun 2007, and the **Authorized**-at the time Katrina occurred.

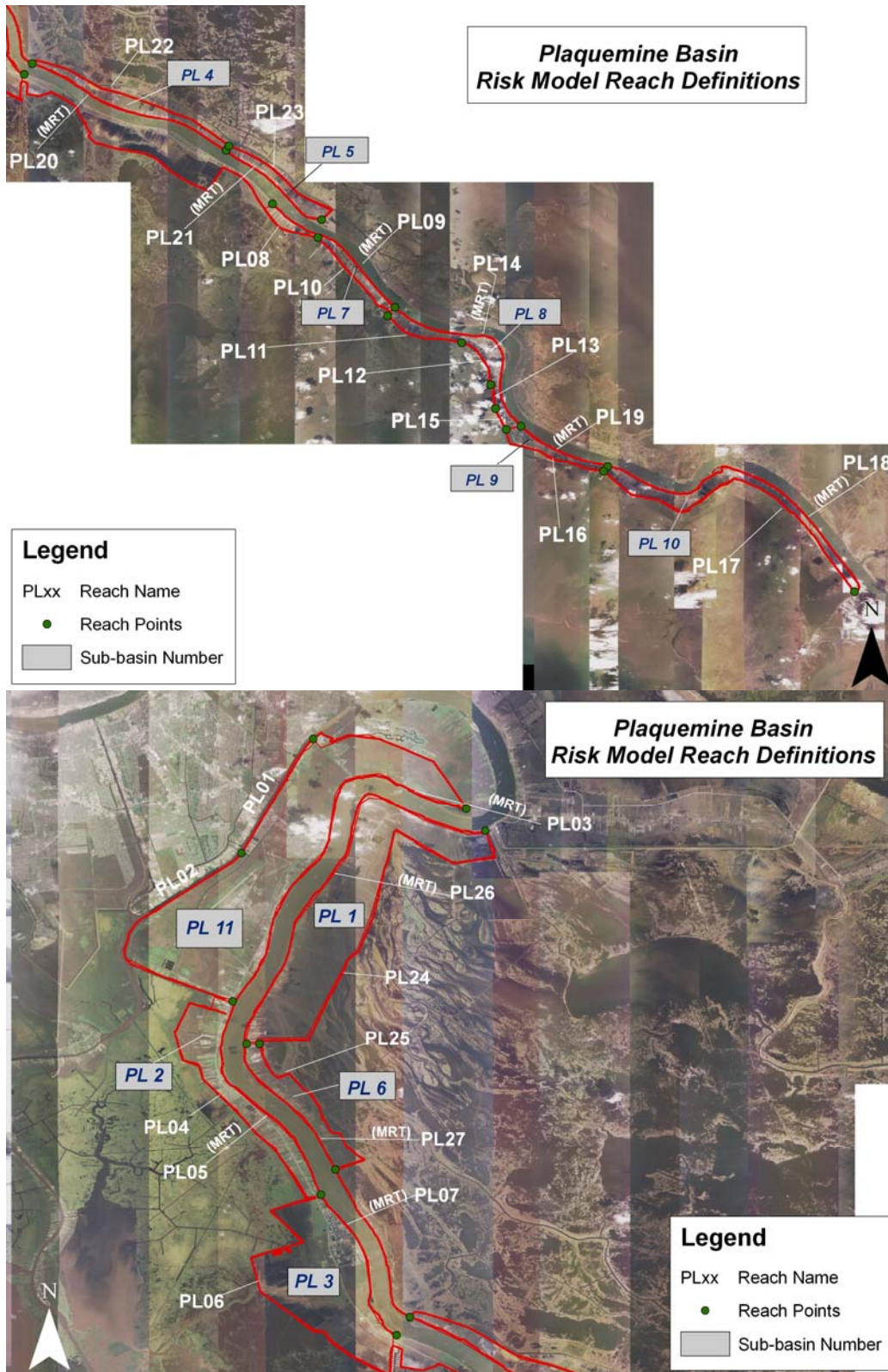


Figure 5. Plaquemines Parrish Basin reaches (PL01-PL28) and sub-basins (PL 1 - PL 11) definition for use in the risk model

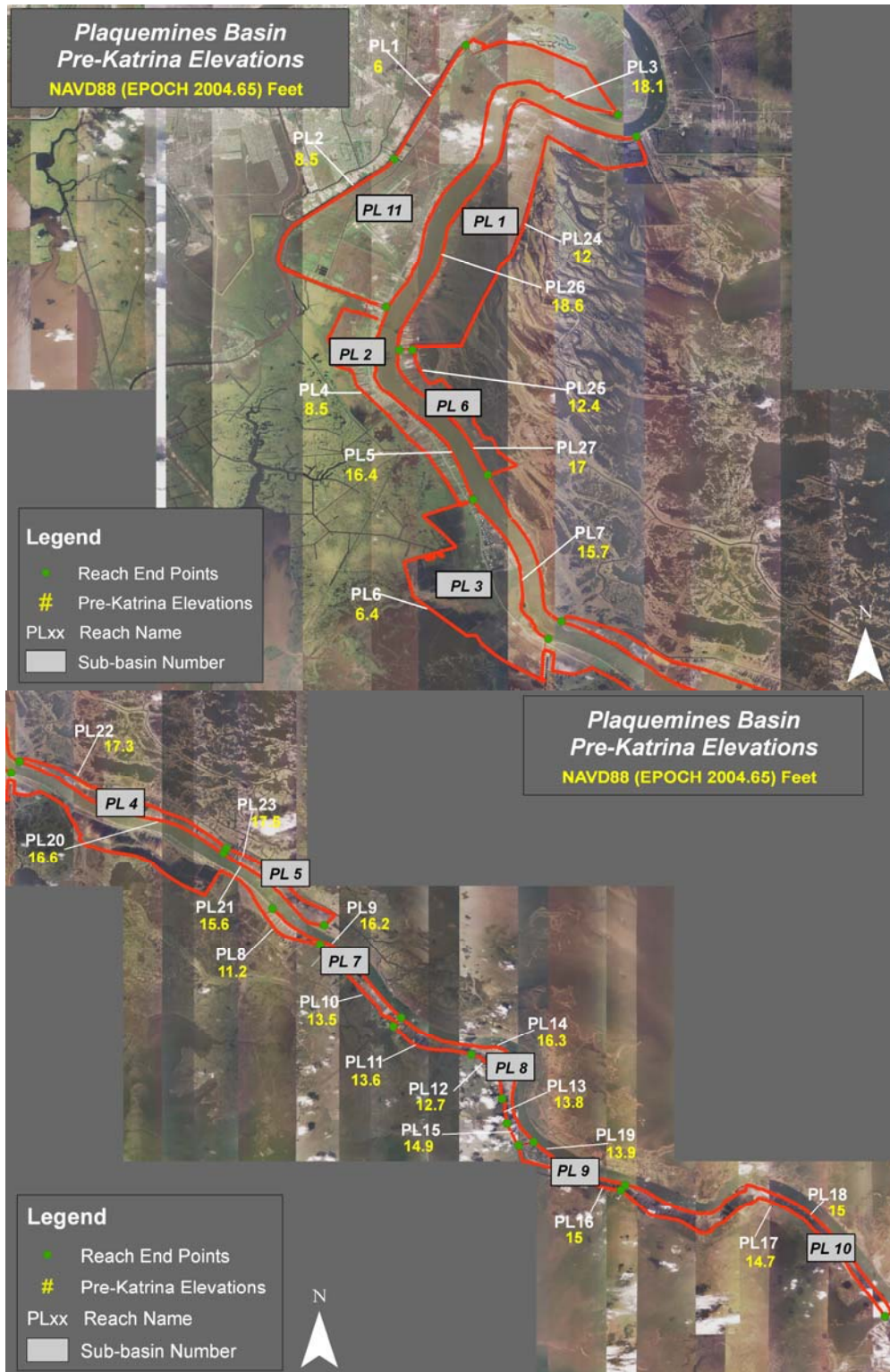


Figure 6. Elevations for the Plaquemines Parrish Basin for the Pre-Katrina HPS (in place when Katrina occurred)

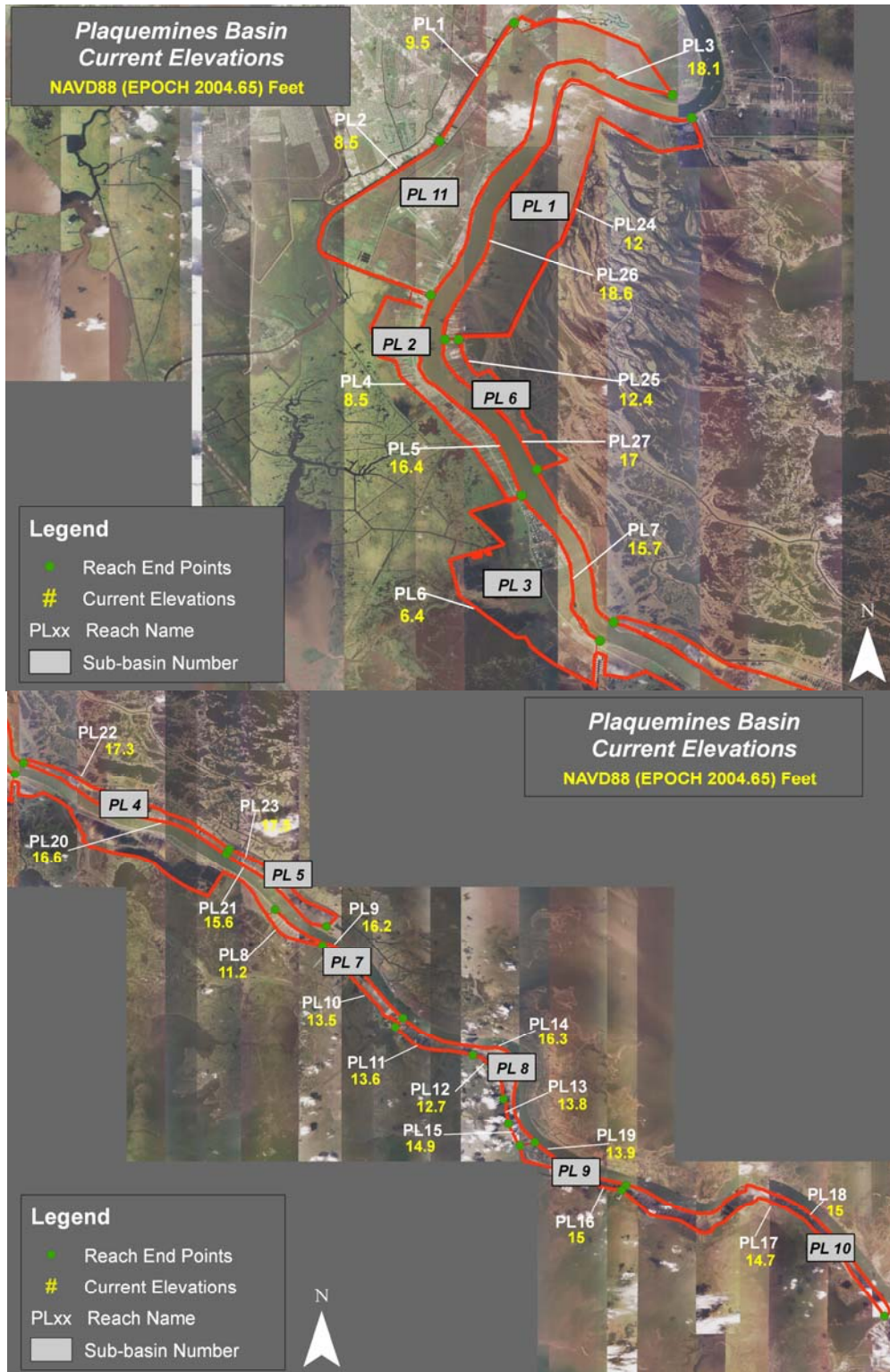


Figure 7. Elevations for the Plaquemines Parrish Basin for the Current HPS (as of 1 June 2007)

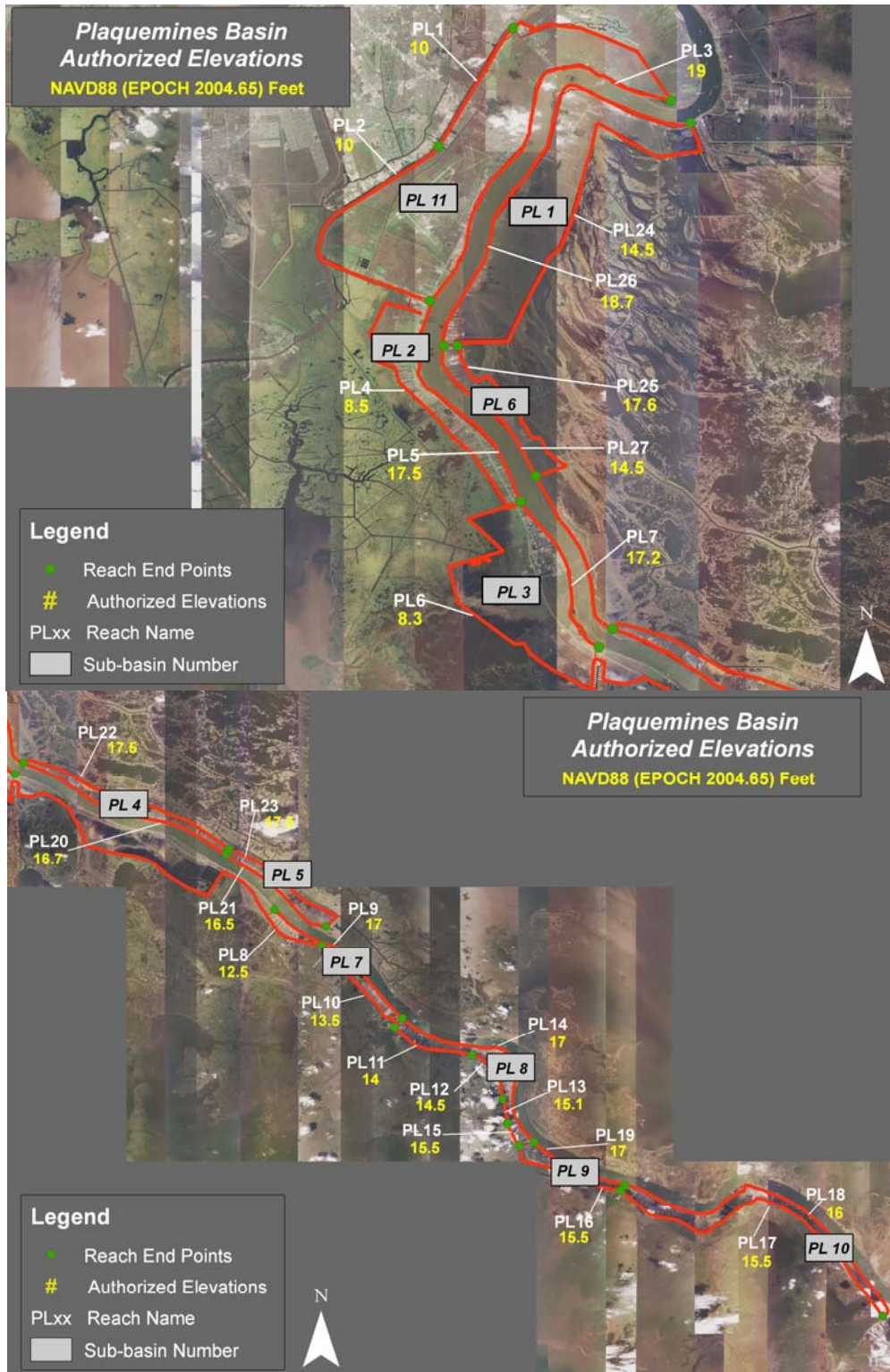


Figure 8. Elevations for the Plaquemines Parrish Basin for the Authorized HPS (authorized at the time of Katrina)

Plaquemines Transitions						
Feature Number	Transition Type	Reach	Width (ft)	Elevation (ft) (NAVD88 2004.65)	Sub-Basin	Description of Feature
132	P	PL1	400.0	8	PL12	Pump Station - Belle Chase #2
133	P	PL1	175.0	10	PL12	Pump Station - Belle Chase #1
134	P	PL4	280.0	10	PL2	Pump Station - Upper Ollie
135	P	PL6	100.0	8	PL3	Pump Station - Wilkerson Canal
136	P	PL8	120.0	18	PL8	Pointe A Lache West Pump Station
137	P	PL8	170.0	10	PL7	Diamond Pump Station
138	P	PL10	342.0	16	PL11	Hayes Pumping Station
139	P	PL11	550.0	17	PL8	Gainard Woods Pump Station
140	P	PL16	1010.0	20	PL9	Sunrise Pumping Station
141	G	PL16	635.0	19.5	PL9	Empire Flood Gate
142	P	PL17	627.0	19	PL10	Venice Pumping Station
143	P	PL17	975.0	19	PL10	Grand Liard (Buras) PS
144	P	PL22	100	18	PL4	Bellevue Pumping Station
145	P	PL27	175	20	PL5	Pointe A La Hache East Pumping Station
146	P	PL25	100	10.5	PL6	Belair Pump Station
147	P	PL25	200	14	PL1	Scarsdale Pump Station
148	P	PL24	80	9	PL1	Braitwaithe Pump Station
149	U	PL2	2200	8	PL2	Unprotected area between PL11 and PL2
150	U	PL1	1650	5	PL1	Unprotected area between PLAQ and STB
151	U	PL1	1730	18	PL1	MRT between PLAQ and STB

Plaquemines Reaches					
Reach No.	Length (ft)	Pre-Katrina Elevation (NAVD88 2004.65)	Reach Type (1)	Foundation Material Type (H, C, P) (2)	Subbasin Reference (3)
81	22,000	6.00	L	H	PL11
82	41,525	8.50	L	H	PL11
83	57,470	18.10	L	C	PL11
84	50,610	8.50	L	H	PL2
85	36,605	16.40	L	C	PL2
86	60,615	6.40	L	H	PL3
87	25,865	15.70	L	C	PL3
88	17,170	11.20	L	H	PL7
89	39,195	16.20	L	C	PL7
90	27,100	13.50	L	H	PL7
91	19,120	13.60	L	H	PL8
92	13,774	12.70	L	H	PL8
93	6,635	13.80	L	H	PL8
94	49,470	16.30	L	C	PL8
95	6,160	14.90	L	H	PL8
96	26,710	15.00	L	H	PL9
97	78,500	14.70	L	H	PL10
98	79,100	15.00	L	C	PL10
99	22,740	13.90	L	C	PL9
100	51,200	16.60	L	C	PL4
101	32,235	15.60	L	C	PL5
102	50,475	17.30	L	H	PL4
103	29,050	17.50	L	H	PL5
104	62,810	12.00	L	H	PL1
105	30,940	12.40	L	H	PL6
106	61,710	18.60	L	C	PL1
107	25,225	17.00	L	C	PL6

Appendix 6

St. Bernard Basin

The St. Bernard (STB) basin is defined by the protection system along the GIWW to the north, MRGO to the east, Caernarvon Canal to the south, and the Mississippi River and Inner Harbor Navigation Canal (IHNC) to the west. Like New Orleans East, it is essentially separated into two distinct areas, a residential/commercial area on the south side of the basin and a marshlands area on the north side. These two sections are separated by a non-federal, interior local levee that runs across the basin from the northwest to the southeast. This area, along with other pertinent information relative to the IPET assessment, is depicted in Figure STB-1.

The levee and floodwall system surrounding the STB basin consists of approximately 157,800 linear feet of varying levels of protection. This provides protection for an area of approximately 81 square miles for the entire basin. The residential area makes up approximately 27 square miles of the basin. In addition, there are two water control sector gate structures along the MRGO at Bayou Bienvenue and Bayou Dupre. There are a total of nine pump stations within the basin, primarily along the interior local levee; one of these is located along the Caernarvon Canal. These major structures are also depicted in Figure STB-1.

Like the other basins, the STB was constructed during different times and modified at various places since the last Design Memorandums. For the purposes of IPET and coupled with varying versions of the most recently completed Design Memorandums (DM), the STB basin is separated into three major stretches. These are as follows:

- **North Side of IHNC Lock thru Caernarvon Canal.** This stretch of the STB basin represents the exterior hurricane protection system and begins at the tie-in to the north side of the IHNC Lock, continues northeast along the GIWW, turns and follows the MRGO to the southeast, then goes west back towards the tie-in to the Mississippi River levee.
- **Mississippi River Levee (MRL).** This section is the flood protection system along the Mississippi River system that contains a combination of floodwalls and levees. For numbering purposes, the MRL reaches begin at the tie-in with the Caernarvon Canal and runs northwest along the Mississippi River until it ties back in with the south side of the IHNC Lock.

- Interior Local Levee (ILL).** This section of levee and floodwall separates the residential and marshland areas of the STB basin. The ILL is actually owned by the State of Louisiana and maintained by the LADOTDD and Lake Borgne Basin Levee District. USACE was provided a one-time waiver from policy and was tasked with repairing the damage to this levee following Katrina. The ILL basically splits the basin in two and begins along the IHNC and heads generally in a southeast direction along the middle of the basin. The ILL “wraps” around the Violet Canal and goes generally east before turning south and tying back into the exterior levee protection system along the Caernarvon Canal.



Figure STB 1. St. Bernard basin

STB Basin – Layout of Reaches for Risk Model by Physical Feature (Pre-Katrina)

Within these major stretches of the STB basin there are shorter reaches, which are defined by physical changes in the protection system, i.e. switching from floodwall to levee, etc., or by significant changes in geotechnical parameters. Within each reach, there are specific “key points” whose reliability needs to be determined in order to calculate the effect on the overall reach being evaluated. An example of a “key point” would be a closure gate at a road or rail line

crossing along a floodwall. Task 10 engineers reviewed existing plans, damage survey reports, and conducted field verification inspections to ensure each basin was accurately defined within the system. As a part of the field verification inspections, GPS coordinates were obtained and stationing from DM's and "as-built" plans was verified. For each basin, this information was transformed into a spread sheet and then a system map for each basin, as shown in Figure STB 2A. Finally, digital photographs with incorporated notes were developed to compliment the spread sheets and system map for further clarification. This collection of information was then categorized to get a clear picture of how the basin should be defined for risk assessment purposes. A summary of the reach and point definitions for STB is shown in Figure 2A with a brief supporting narrative on each reach. The layout shown in Figure STB 2 and the narrative that goes along with this figure relates to the pre-Katrina condition. Task Force Guardian (TFG) made several improvements to the levee/floodwall system which changes the risk for various reaches. These changes by reach are detailed in the next section.

Task 10 basin reach definitions for STB start at the tie-in to the north side of the IHNC Lock. The numbering system for reach definitions continues along the exterior protection system along the GIWW, MRGO, Caernarvon Canal, and then up through the Mississippi River levee system to where it ties back into the south side of the IHNC Lock. Finally, the interior local levee reaches numbers begin at the IHNC and extend until it ends at the Caernarvon Canal. Please refer to Figure STB1, STB2A, and STB2B for further clarification. The STB basin is summarized by the reaches as follows:

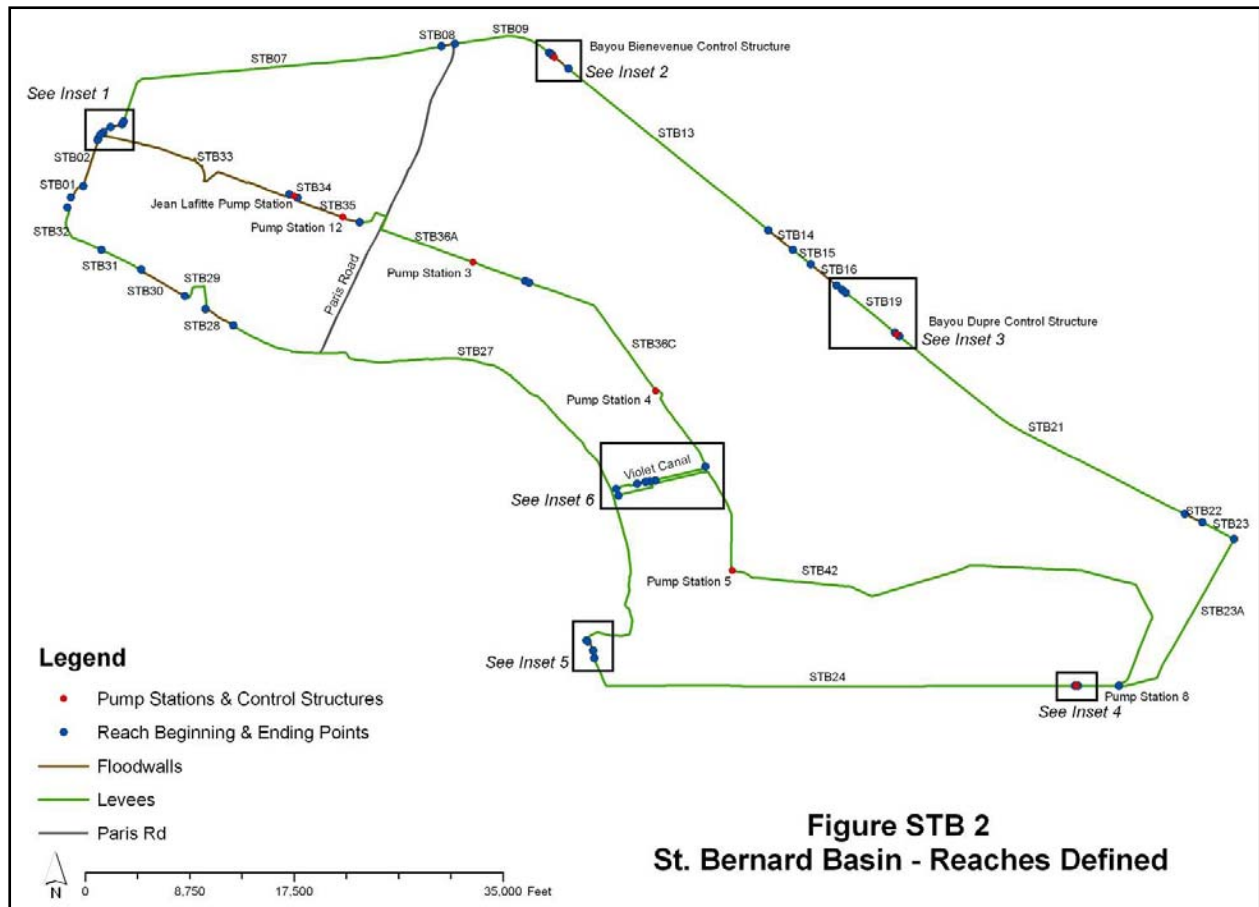


Figure STB 2A. St. Bernard Basin – Reaches Defined

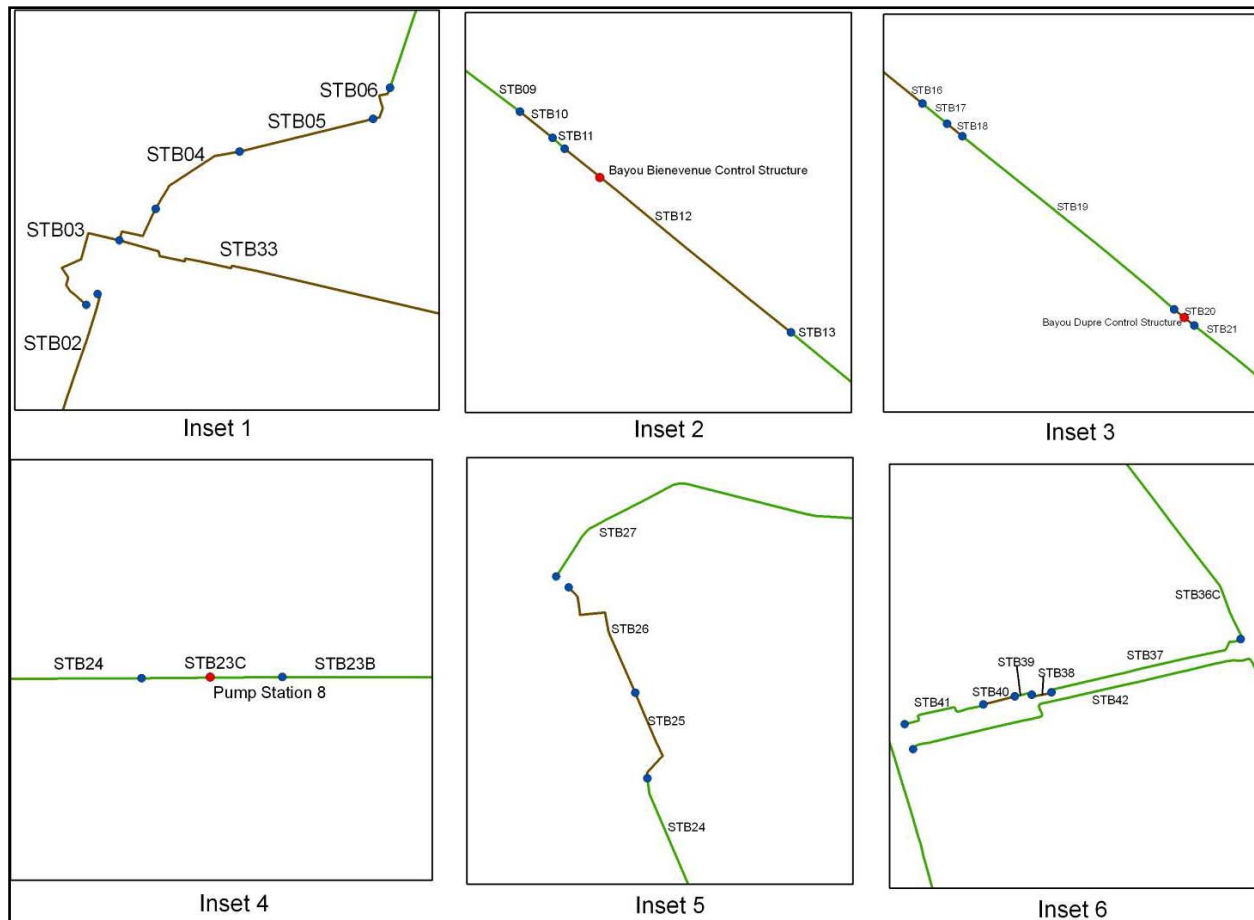


Figure STB 2B. St. Bernard Basin Reaches – Insets 1-6

Reach STB1 (INHC to Caernarvon)

This reach is defined by 1,427 linear feet of concrete capped I-wall that ties into the northeast side of the INHC Lock and generally follows the IHNC north, see Figure STB 3, which shows the beginning of the reach where it ties into the northeast lock wall of the IHNC. There is one key point (stb1a) at the beginning of this reach where the natural ground line transitions between the lock wall and I-wall, as shown in Figure STB 4. The reach ends at the south end of the I-wall failure that occurred in the Lower 9th Ward. Other sections of this reach were overtopped during Katrina, but did not fail, in particular near the Claiborne Bridge, as shown in Figure STB 4. The approximate weighted average top of wall elevation for this reach was 13.0 (NAVD88) prior to Katrina.



Figure STB 3. I-wall section tying into IHNC lock wall (standing on top of lock wall and looking away from IHNC)



Figure STB 4. Section of Reach STB1 overtopped during Katrina (location is just north of Claiborne Avenue Bridge)

Reach STB2 (IHNC to Caernarvon)

This reach *was* defined by a 4,038-ft stretch of I-wall between the Claiborne Avenue Bridge and the railroad bridge near Florida Avenue. There were two separate breaches of this I-wall during Katrina. The southern section of I-wall that failed in the Lower 9th Ward area of St. Bernard during Hurricane Katrina is shown in Figure STB 5. Figure STB 6 shows the authorized design section for this wall, but note the actual elevations for the top of wall were closer to 13.0 when referencing NAVD88 (2004.65) datum. The northern section of I-wall that failed was near the blue railroad bridge close to Florida Avenue. This breach is depicted in Figure STB 7. There were no “key points” within this entire reach. Refer to changes made by Task Force Guardian (TFG) in the post-Katrina narrative.



Figure STB 5. Failed I-wall section of Lower 9th Ward (Reach STB2) (looking south along IHNC)

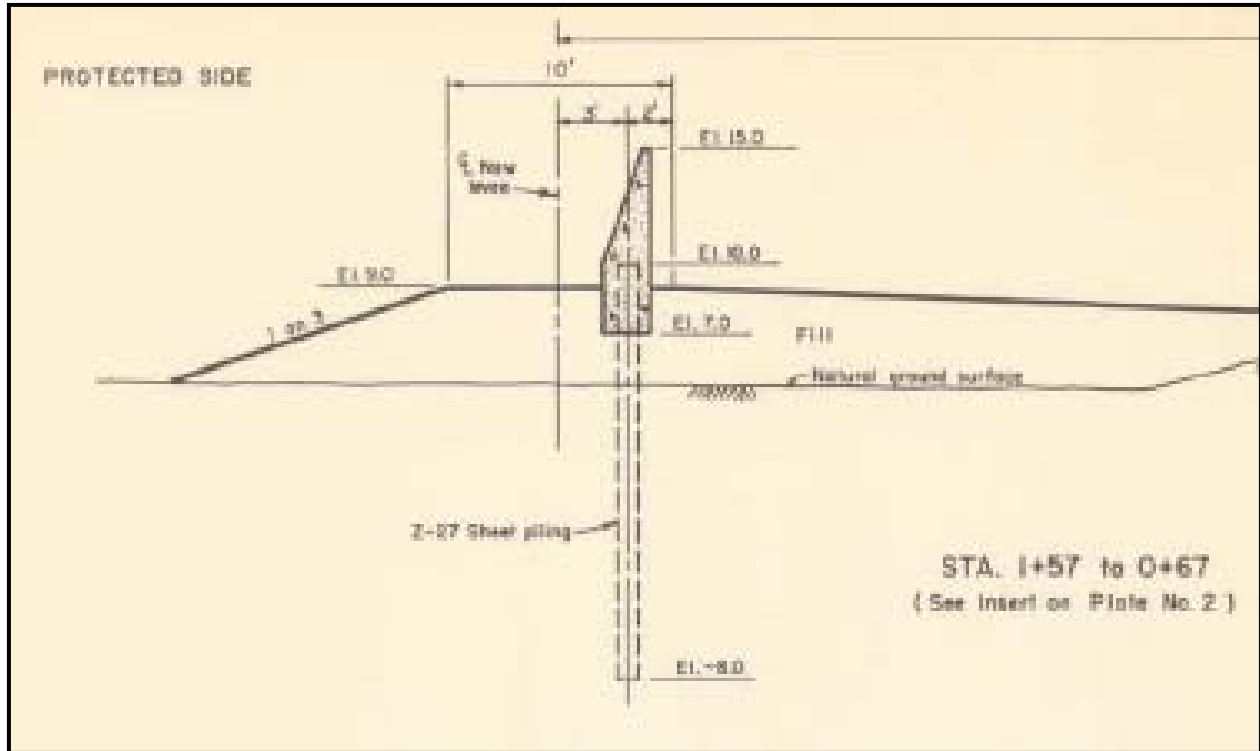


Figure STB 6. Pre-Katrina I-wall design section for Reach STB2 (depicts authorized elevations, not actual elevations)



Figure STB 7. North I-wall failure within Lower 9th Ward (Reach STB2) (Note: pipes on right side of photo are associated with Pump Station #5)

Reach STB3 (INHC to Caernarvon)

This reach is defined by an existing T-wall that is located adjacent to the Surekote Road ramp over the floodwall. The reach is approximately 807 feet in length. There are multiple key points within this reach including the closure gate E-1, as shown in Figure STB 8. Closure gate S-1 at Harbor Road and Florida Avenue and railroad closure gate E-2 are also key points within this reach. The approximate weighted average height of this wall prior to Katrina was elevation 12.5 (NAVD88).



Figure STB 8. Existing T-wall near Florida Ave. Bridge (Reach STB3) (looking from protected side towards IHNC)

Reach STB4 (INHC to Caernarvon)

This reach is defined by 726 linear feet of I-wall that ties into the levee along the GIWW. There are no key points in this reach. This reach ends where the I-wall ties into the levee. This section of I-wall was overtopped during Katrina, but suffered no major damage. It had an approximate weighted average top of wall elevation of 13.3 (NAVD88) prior to Katrina.

Reach STB5 (IHNC to Caernarvon)

This reach is defined by 890 linear of levee between the end of the IHNC I-wall and the floodwalls surrounding closure gates S-2 and S-3 near the Southern Scrap Building. There are no key points within this reach. This levee is depicted in Figure STB 9. There was no significant damage to this section from Katrina. It had an approximate weighted average elevation of 13.1 (NAVD88) prior to Katrina.



Figure STB 9. Beginning of Reach STB5 at end of I-wall (Note TFG improvements to Reach STB4 in foreground)

Reach STB6 (IHNC to Caernarvon)

This reach is defined by a combination of I-walls and T-walls surrounding closure gates S-2 and S-3. The total length of the reach is 340 feet with T-walls located around the gate closures. These walls were overtopped during Katrina but did not fail. The approximate weighted average top elevation of this reach was 13.0 (NAVD88) prior to Katrina. Reference improvements to the scour protection made by TFG in the post-Katrina reach description. The gates themselves serve as the two “key points” within this reach, stb6a and stb6b, respectively.

Reach STB7 (IHNC to Caernarvon)

This reach is defined by 25,722 feet of levee. There is one pipe crossing located within this reach but it does not represent a significant departure from the levee section and can be ignored for the purposes of this assessment. There was no significant damage to this section of levee from Katrina. The approximate top of levee varied along this reach between 13.5 to 16.5 (NAVD88), but had a weighted average elevation of 15.1 (NAVD88) prior to Katrina.

Reach STB8 (IHNC to Caernarvon)

This reach is defined by a 1,016-ft stretch of concrete capped I-walls and T-walls just west of the Paris Road overpass along the GIWW. It is often referred to as the Paris Road floodwall. There is one key point (stb8a), a gate closure, within this floodwall reach. This structure was overtopped during Katrina, but only suffered scour damage. See Figure STB 10 for a photograph depicting this wall during repairs following Katrina. The approximate weighted average top of wall elevation for this reach was 12.4 (NAVD88) prior to Katrina.



Figure STB 10. Paris Road Floodwall (Reach STB8) (looking east from the west end of the floodwall)

STB9 (IHNC to Caernarvon)

This reach is defined by 7,260 linear feet of levee. It goes between the Paris Road floodwall and the floodwalls just prior to reaching the Bayou Bienvenue control structure. There are no key points within this reach. There was some overtopping in this reach during Katrina, but no major damage to the levee. The approximate weighted average for this reach was elevation 17.9 (NAVD88) prior to Katrina.

STB10 (IHNC to Caernarvon)

This section is defined by a relatively short 229-ft stretch of floodwall located just northwest of the Bayou Bienvenue Control Structure. It consists of a 61-ft section of I-wall at elevation 17.0 (NAVD88), a 107-ft stretch of T-wall at elevation 15.5 (NAVD88), and another 61 feet of I-wall at elevation 17.0 (NAVD88). The weighted average top of wall across the entire reach is 16.3 (NAVD88). During original construction, this short section of wall was to serve as an

access point for an industry that was to be located near the Bayou Bienvenue Control Structure. However, the industry went out of business, and it has never been utilized, and the flood gate remains permanently closed. This section of wall was overtopped during Katrina as evidenced in Figures STB 11 and STB 12. Since the gate remains permanently closed, there are no “key points” within this reach.

STB11 (IHNC to Caernarvon)

This reach is defined by a short section of levee between the floodwall described in reach STB10 and the beginning of the floodwall leading to Bayou Bienvenue Control Structure. The levee section is only 96 feet long and received some damage during Katrina at the transitions to adjoining I-wall sections, as shown in Figure STB 12. The levee had an average weighted elevation of 16.0 (NAVD88) prior to Katrina. There are no “key points” within this short reach.



Figure STB 11. Floodwall Northwest of the Bienvenue Structure (Reach STB10) (looking southeast toward Bayou Bienvenue just after Katrina)

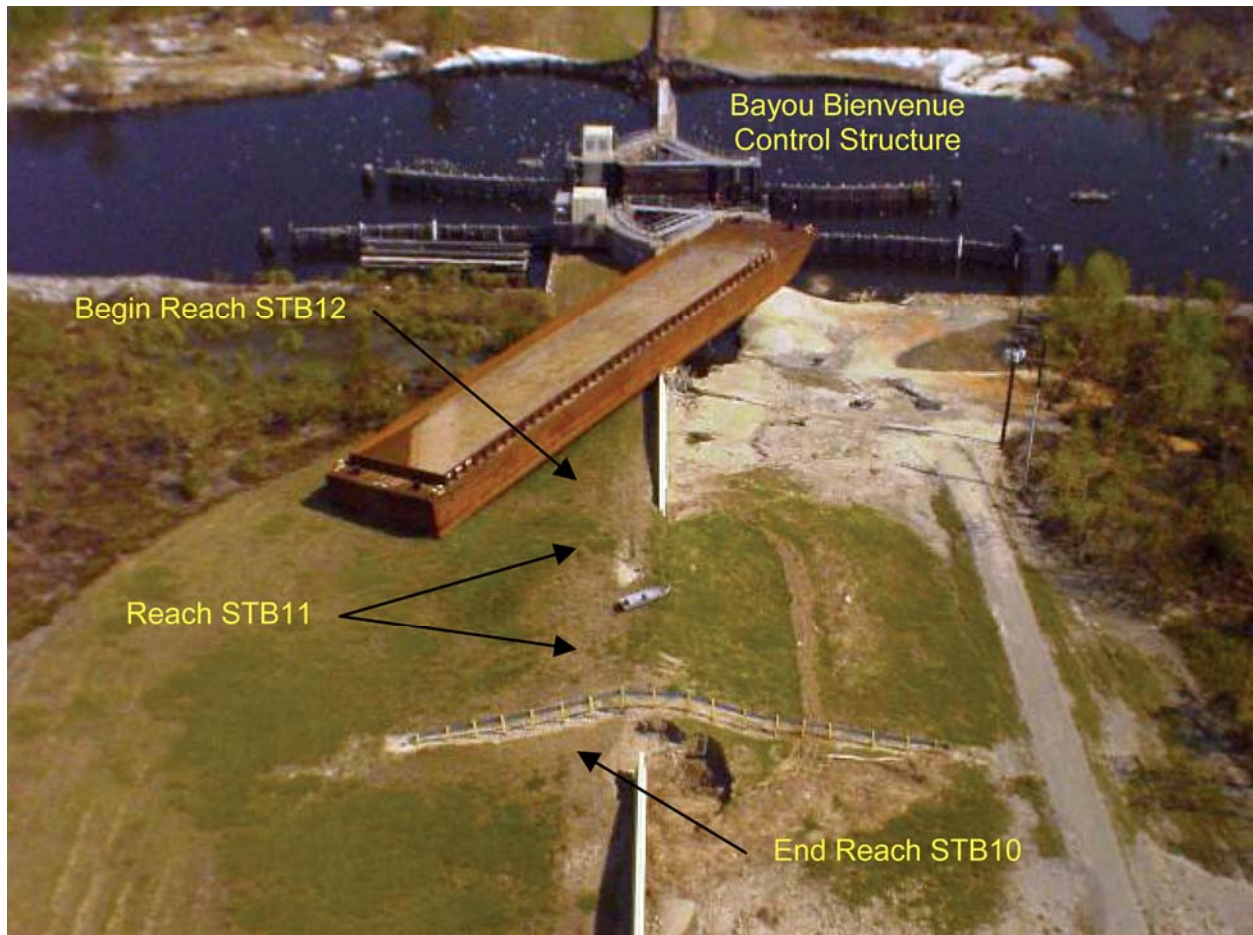


Figure STB 12. Short levee section between floodwalls (Reach STB11)

Reach STB12 (IHNC to Caernarvon)

This reach is defined by the Bayou Bienvenue Control Structure and surrounding floodwalls on either side of it. Prior to Katrina, this reach was made up of 77 feet of concrete capped I-wall at elevation 17.0 (NAVD88), 187 feet of T-wall surrounding the control structure itself at elevation 15.0 (NAVD88), and 1,208 feet of uncapped, sheetpile I-wall at elevation 18.5 (NGVD). As shown in Figures STB12, 13, and 14, the surrounding floodwalls received heavy damage and the uncapped I-wall section breached during Katrina. The sector gate closure itself serves as the only “key point” (stb12a) within this reach.



Figure STB 13. Uncapped I-wall Section on Southeast side of Bayou Bienvenue Control Structure (looking southeast along the MRGO)



Figure STB 14. Picture of breached Bienvenue I-wall from Protected Side

Reach STB13 (IHNC to Caernarvon)

This reach is defined by a 19,858 linear feet stretch of levee. Prior to Katrina, it began at the end of the uncapped sheetpile I-wall on the southeast side of the Bayou Bienvenue Control Structure and continued up to the beginning of an embedded, uncapped I-wall section along the MRGO. This section of levee was overtopped during Katrina and was heavily damaged. It had an approximate weighted average top elevation of 17.5 (NGVD) based upon a 1998 survey. There was one section of embedded uncapped, sheetpile I-wall in about the middle of this reach, but the top of the wall essentially was at the top of the levee. Due to this fact, this section of I-wall will not be included separately in the analysis and is included as part of the overall reach characteristics.

Reach STB14 (IHNC to Caernarvon)

This reach was defined by a 2,427-ft section of uncapped I-wall embedded within the levee. The sheetpile I-wall was installed in 1992 as part of USACE repairs along the MRGO. This section of wall was heavily damaged during Katrina, as evidenced in Figure STB 15. The weighted average top elevation of the uncapped I-wall was 18.5 (NGVD) prior to Katrina, and it had a free standing height of approximately 3.5 feet. As shown in the photo, there are pipe crossings along this reach, but they extend over the levee and do not represent a major change in design or performance parameters; therefore, they are ignored in the risk assessment for this purpose.



Figure STB 15. Breached I-wall along MRGO

Reach STB15 (IHNC to Caernarvon)

This reach consists of a 1,745-linear-ft stretch of levee between uncapped, sheetpile I-wall reaches. This section was overtopped and heavily damaged during Katrina. The weighted average height of this levee section was approximately 16.4 (NGVD) prior to Katrina based upon a detailed 1998 survey. There are no “key points” within this reach.

Reach STB16 (IHNC to Caernarvon)

This reach consisted of a 2,560-ft stretch of uncapped, sheetpile I-wall that was installed in 1992 as part of USACE repairs along the MRGO. This section also was overtopped and heavily damaged during Katrina. The weighted average top of uncapped I-wall along this reach was elevation 18.5 (NGVD) prior to Katrina. It had an approximate free standing height of 3.5 feet. There are no “key points” within this reach.

Reach STB17 (IHNC to Caernarvon)

This reach consists of 566 feet on levee between uncapped, sheetpile I-wall reaches. The approximate weighted average top of levee elevation was 16.5 (NGVD) prior to Katrina based upon a detailed 1998 survey. This section of levee was overtopped during Katrina and heavily damaged. There are no “key points” within this reach.

Reach STB18 (IHNC to Caernarvon)

This reach consists of 359 feet of uncapped, sheetpile I-wall installed in 1992 as part of USACE repairs along the MRGO. The wall had an approximate top elevation of 18.5 (NGVD) with a free standing height of roughly 3.5 feet. It was overtopped and heavily damaged during Katrina. There are no “key points” within this reach.

Reach STB19 (IHNC to Caernarvon)

This stretch of levee runs from the end of the uncapped I-wall in Reach STB18 to the northwest transition wall leading to the Bayou Dupre Control Structure. It is approximately 4,994 linear feet and there are no “key points” within this length. It had an approximate weighted average top elevation of 18.7 (NGVD) prior to Katrina. This reach was heavily damaged during Katrina.

Reach STB20 (IHNC to Caernarvon)

This reach includes the Bayou Dupree Control Structure and the adjoining transition flood walls. Prior to Katrina, the reach started with 92 linear feet of precast concrete sheetpile wall on the northwest side of the gate structure, 69 feet of T-wall on the northwest side of the gate closure, 134 feet across the closure structure, 69 feet of T-wall on the southeast side of the closure structure, and 92 feet of precast concrete sheetpile wall on the southeast side of the closure structure. While the concrete sheetpile walls were designed at a higher elevation, settlement across this area left all walls roughly at elevation 15.2 (NAVD88) prior to Katrina. As shown in Figure STB 16, the northwest precast concrete sheetpile I-wall failed during Katrina. The only “key point” in this reach is the closure structure itself.

Reach STB21 (IHNC to Caernarvon)

This reach starts with the levee tie-in to the southeast side of the Bayou Dupre Control Structure adjoining floodwall. The approximate length of this reach is 25,562 linear feet, and it has no “key points” within the reach. Prior to Katrina, it had a weighted average top elevation of 19.1 (NGVD). The reach was heavily damaged during Katrina from overtopping.



Figure STB 16. Damage at Bayou Dupre Control Structure (note breached section of precast concrete pile wall)

Reach STB22 (IHNC to Caernarvon)

This reach was defined by a 1,401-ft section of uncapped, sheetpile I-wall that was installed during 1992 USACE repairs along the MRGO. The wall had a top elevation of 19.0 (NGVD) prior to Katrina and a free standing height of approximately 4.0 feet. There were no “key points” within this reach. There was scour damage in this area as a result of Katrina.

Reach STB23a (IHNC to Caernarvon)

This reach is defined by the remaining levee along the MRGO between the end of Reach STB22 and where it turns away from along the Caernarvon Canal. The weighted average top of levee elevation for this reach was approximately 19.5 (NGVD) prior to Katrina. There are no “key points” within this reach. Sections of this reach did receive damage during Katrina.

Reach STB23b (IHNC to Caernarvon)

This reach consists of 5,709 feet of levee that begins at the MRGO and continues to the intersection point with the interior local levee. Although the levee along the Caernarvon Canal

continues, a new reach had to be defined because of the potential for varying consequences due to the presence of the interior local levee. This area of levee received minor damage during Katrina. There are two basic areas along this reach where repairs are different. The weighted average top elevation of this reach was approximately 17.0 (NAVD88) prior to Katrina. There is one “key point” within this reach (stb23bd), which is the Bayou Road closure gate.

Reach STB23c (IHNC to Caernarvon)

This section of levee is 2,692 feet long and goes from the interior local levee to the beginning of the east side floodwall surrounding Pump Station #8. There was minimal scour damage along this stretch during Katrina. It had an approximate weighted average top elevation of 16.0 (NAVD88) prior to Katrina. There are no “key points” within this reach.

Reach STB23d (IHNC to Caernarvon)

This reach consists of 231 feet of flood wall around the discharge pipes for Pump Station #8. There are roughly 45 feet of I-walls on both sides of the middle T-wall for the discharge pipes. The T-wall length is approximately 141 feet long. The top of the I-walls are elevation 17.0 (NAVD88) and the T-wall is at 16.5 (NAVD88). The weighted average top of wall elevation is 16.7 (NAVD88). This wall was not damaged or overtopped during Katrina. There are no “key points” within this reach. For a view of this reach, please refer to Figure STB 17.



Figure STB 17. Floodwalls surrounding Pump Station #8 pipes (viewed Looking West Along Caernarvon Canal)

Reach STB24 (IHNC to Caernarvon)

This reach is defined by 36,610 linear feet of levee along the Caernarvon Canal. It starts on the east side at the where it ties into the west end of the Pump Station #8 floodwall and continues until it ties into a sheetpile wall near the Caernarvon Freshwater Diversion Structure. This section received little or no damage during Katrina. There are several utility crossings along this reach, but none significant enough to warrant as a “key point.” The approximate weighted average top elevation of the levee is 15.4 (NAVD88) across this reach.

Reach STB25 (IHNC to Caernarvon)

This reach consists of 693 linear feet of uncapped, sheetpile I-wall near the Caernarvon Freshwater Diversion Structure. There are no “key points” within this reach. It received little or no damage from Katrina. The reach has a weighted average top elevation of 12.8 (NAVD88) taken from a physical survey following Katrina. See Figure STB 18 for a photograph of this reach.



Figure STB 18. Uncapped Sheetpile I-wall near Caernarvon Canal (building on left side is on flood side)

Reach STB26 (IHNC to Caernarvon)

This reach consists of concrete capped I-walls that extend from the end of the sheetpile wall in Reach STB25 to the where the Caernarvon section ties into the Mississippi River levee. This section of wall is 1,104 feet long with a weighted average elevation of 13.0 (NAVD88). It was not damaged during Katrina. There are two “key” points within this reach, and both are closure

gates; one for a rail line and the other for Highway 39. The location where the floodwall ties into the higher Mississippi River levee is shown in Figure STB 19.

Reach STB27 (Mississippi River Levee)

This reach is the most southern section of levee within the STB basin, as reflected as the higher ground area of Figure STB 19. Refer to Figure STB 2 for reference to the reach location relative to the entire basin. The reach consists of 49,877 linear feet of levee, and it ends at the southern end of the concrete capped I-wall near the Battlefield site along the Mississippi River. It has a weighted average top elevation of 20.1 (NAVD88).

Reach STB28 (Mississippi River Levee)

This reach consists of 2,724 feet of concrete capped I-wall near the Battlefield site. There is one key point with this reach, and it is a small access closure gate. A typical stretch of this wall along with the access closure gate is shown in Figure STB 20. The weighted average elevation of the top of the wall for this reach is 17.6 (NAVD88). This reach was not damaged during Katrina.



Figure STB 19. Caernarvon Canal Floodwall tie-in to higher MRL (gate is for Highway 39 closure)



Figure STB 20. Concrete capped I-wall along Miss. River near Battlefield (access closure gate is key point within this reach)

Reach STB29 (Mississippi River Levee)

This reach consists of 3,729 feet of levee along the Mississippi River in and around the Rodriguez Canal. There are four key points within this reach, all gated closures near the Rodriguez Canal. The reach ends where the levee ties into a floodwall near the Domino Sugar Plant. The weighted average top elevation of the levee along this reach is 20.9 (NAVD88). This reach was not damaged during Katrina.

Reach STB30 (Mississippi River Levee)

This reach is defined by 5,180 linear feet of concrete capped I-wall that begins near the Domino Sugar Plant. There are three key points within this reach, all of them closure gates. One is located at the Domino Plant, one at the Port Ship Service Dock, and the last one at Mehle Avenue. The weighted average elevation of the top of the wall along this reach is 18.0 (NAVD88). This reach was not damaged during Katrina. One of the closure areas and typical I-wall along this stretch is shown in Figure STB 21.



Figure STB 21. Concrete capped I-wall near Domino Sugar Plant (closure represents key point within this reach)

Reach STB31 (Mississippi River Levee)

This reach consists of 2,345 feet of levee that is primarily covered with paved slopes and roads. It begins near the Jackson Barracks and ends at the warehouse and dock area near Flood Street. The weighted average elevation along this stretch of levee is 19.0 (NAVD88). There are no key points within this reach, although there are some pipe crossings noted but not considered significant enough to effect the overall reliability of the reach. This reach was not damaged during Katrina. The end of this reach (viewed from the Reach STB30 side) is shown in Figure STB 22.

Reach STB32 (Mississippi River Levee)

This reach consists of 4,870 linear feet of levee along the Mississippi River and southeast side of the Inner Harbor Navigation Canal. It begins at the warehouse/dock facilities on the levee near Flood Street and ends at the southeast side of the Inner Harbor Navigation Canal Lock. The weighted average elevation of the top of this levee is 20.9 (NAVD88). There are no key points within this reach. This reach was not damaged during Katrina.



Figure STB 22. End Reach STB31 where levee ties into Dock Facility (Viewed from Reach STB30 side)

Reach STB33 (Interior Local Levee)

This reach consists of approximately 15,455 linear feet of uncapped sheetpile I-wall. The reach starts at the north side of the interior local levee near Pump Station #5, as shown in Figure STB 23. There are two key points within this reach. The first is a railroad closure near the East Bank Wastewater Treatment Plant, and the second is a timber closure across a road. An aerial view of the location where the interior local levee sheetpile wall ties into the concrete capped I-wall along the IHNC is shown in Figure STB 23. A close-up view of the start of the interior local levee is shown in Figure STB 24. This location is referenced in Figure STB 23. This reach had a weighted average top of wall elevation of 13.5 (NAVD88) prior to Katrina. Most of this reach was not damaged during Katrina. There was a 4,500 feet stretch of uncapped I-wall and levee near the parish line along this reach that was damaged and in need of repair. The general area where the parish line crosses the interior local levee is shown in Figure STB 1.

Reach STB34 (Interior Local Levee)

This reach consists of 685 feet of concrete floodwall surrounding the Jean LaFitte Pump Station. The weighted average top elevation of this reach is 14.0 (NAVD88) taken from a 1999 LADOTDD physical survey of the interior local levee. There was no significant damage during Katrina. There are no key points within this reach.



Figure STB 23. Area showing beginning of interior local levee at the IHNC



Figure STB 24. Close-up of beginning of interior local levee

Reach STB35 (Interior Local Levee)

This reach consists of 5,055 linear feet of uncapped sheetpile I-wall within the levee. The weighted average top elevation of this reach is 13.3 (NAVD88) taken from a 1999 LADOTD physical survey of the interior local levee. There are a couple of pipe crossings along this reach, but no key points for the risk assessment. There was overtopping along this reach during Katrina, but no major damage. The end of the reach where the I-wall ties into an adjoining levee (beginning of Reach STB36) is shown in Figure STB 25.

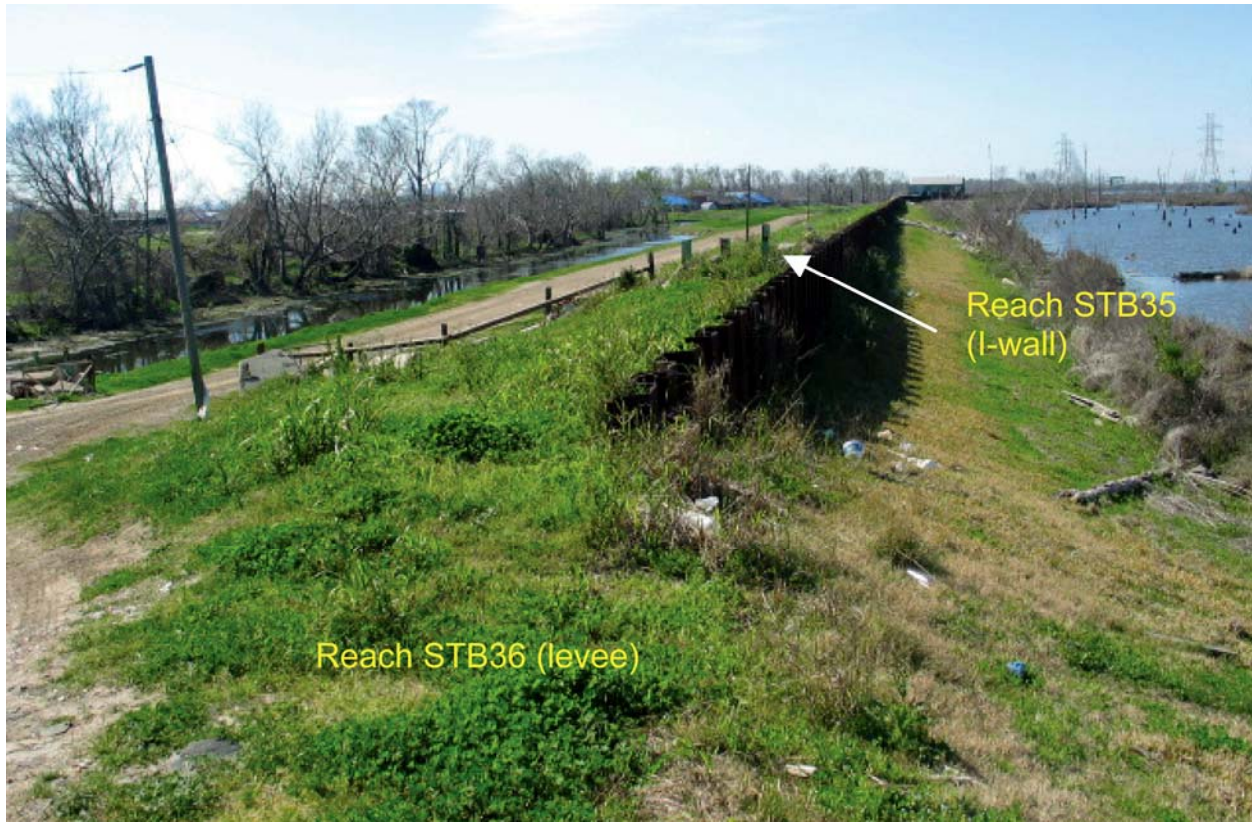


Figure STB 25. End of Reach STB35 at the beginning of Reach STB36 (interior local levee near Paris Road)

Reach STB36a (Interior Local Levee)

This reach is defined by 15,105 linear feet of levee between floodwalls. The reach begins approximately 2,400 feet west of Paris Road (see Figure STB25) and ends where the levee ties into the west end of the sheetpile I-wall leading to Pump Station #7 (Bayou Ducros Pump Station). There are two basic sections within this reach, the first is the short section west of Paris Road that had a weighted average elevation of 11.6 (NAVD88) prior to Katrina. From Paris Road east, the weighted average elevation of this reach was 8.4 (NAVD88) prior to Katrina. The main reason this reach is sub-divided was because of the work carried out by TFG was only done east of Paris Road with respect to raising the levee. The weighted average top of levee for this reach was 8.9 (NAVD88) prior to Katrina. There was significant overtopping damage to the section of levee east of Paris Road during Katrina. There are no key points within this reach.

Reach STB36b (Interior Local Levee)

This reach consists of 350 linear feet of floodwall surrounding Pump Station #7, also referred to as the Bayou Ducros Pump Station. The reach has 140 feet of uncapped sheetpile I-wall west of the discharge pipes, 70 feet of concrete T-wall around the discharge pipes, and 140 feet of uncapped sheetpile I-wall east of the discharge pipes. The weighted average elevation for the top of the 280 feet of uncapped sheetpile I-wall is 9.0 (NAVD88). The weighted average top elevation of the concrete T-wall is 12.5 (NAVD88). The overall weighted average top of wall

elevation for the entire reach is 9.7 (NAVD88). A photograph of the 3.5 feet difference in wall height where the sheetpile ties into the adjoining concrete T-wall at the discharge pipes is shown in Figure STB 26.



Figure STB 26. T-wall and I-wall offset at Pump Station #7 along interior local levee (Note: wall offset is approximately 3.5 feet)

Reach STB36c (Interior Local Levee)

This reach consists of 20,870 linear feet of levee that begins at the east end of Pump Station #7 I-wall and then ends where the levee adjoins the Violet Canal. This reach of levee had a weighted average top elevation of 9.1 (NAVD88). There are no key points within this reach. This reach of levee was overtopped and damaged during Katrina.

Reach STB37 (Interior Local Levee)

This reach is defined by 3,888 linear feet of levee along the north side of the Violet Canal. The weighted average top of levee elevation along this reach was 8.1 (NAVD88) prior to Katrina. There are no key points within this reach. This reach was overtopped and damaged during Katrina.

Reach STB38 (Interior Local Levee)

The floodwall for the Soap Factory along the Violet Canal defines this reach. It is 432 linear feet. The weighted average elevation of the top of the wall was 7.0 (NAVD88) prior to Katrina. This section of wall was overtopped during Katrina, but the wall was not heavily damaged. There are no key points within this reach. See Figure STB 27 for a view of this reach along the Violet Canal.



Figure STB 27. Floodwall Along the North Side of Violet Canal (This is Reach STB38 for the Risk Model, Violet Canal is to the left)

Reach STB39 (Interior Local Levee)

This stretch of levee runs between the end of the concrete floodwall for the Soap Factory and ties into the series of buildings on top of the levee along the north side of the Violet Canal. This section can be seen in the background of Figure STB 27. This levee is approximately 510 feet long and had a weighted average top elevation of 8.5 (NAVD88) prior to Katrina. The reach was overtopped and damaged during Katrina.

Reach STB40 (Interior Local Levee)

Prior to Katrina, this reach was defined by a short concrete floodwall surrounding a shrimp factory along the Violet Canal. This floodwall was 155 linear feet and had a weighted average top elevation of 7.5 (NAVD88). There are no key points within this reach. The reach was damaged during Katrina.

Reach STB41 (Interior Local Levee)

This reach is defined by 2,201 linear feet of levee along the Violet Canal, and it ends where it ties into Highway 46. The weighted average top elevation of this reach was 8.7 (NAVD88). There are no key points within this reach. This reach was overtopped and damaged during Katrina.

Reach STB42 (Interior Local Levee)

This reach starts on the south side of the Violet Canal at Highway 46 and continues to the tie-in to the exterior levee along the Caernarvon Canal. While there are a few ramp and pipe crossings within this 55,227-ft reach; none are considered key points. The weighted average elevation of the top of the levee along this reach was 7.7 (NAVD88). This reach was overtopped and damaged during Katrina.

STB Basin – Layout of Reaches for Risk Model by Physical Feature (Post-Katrina Changes by Task Force Guardian)

Reach STB1 (INHC to Caernarvon)

Although this section of wall did not fail during Katrina, improvements were made to this reach to improve its performance for stability and overtopping. A physical survey of this section of wall taken in November 2005 shows an average elevation of 13.0 (NAVD88) across this reach. The wall was designed with a free standing height of 6 feet (see Figure STB 6 with a top of wall elevation of 15.0 and top of levee elevation of at 9.0). TFG restored the top of levee to 9.0 feet, thus reducing the free standing height to approximately 4.0 feet. In addition, a scour protection slab was placed on the protected side. This is generally 6 to 8 feet wide from the base of the wall at the top of the levee on the protected side.

Reach STB2 (INHC to Caernarvon)

This section of I-wall failed during Katrina (see Figure STB 5 for reference). The top of the I-wall was approximately at elevation 13.0 (NAVD88 2004.65) prior to Katrina. This wall was replaced by a T-wall to the authorized elevation of 15.0. In addition, scour protection was provided on the protected side in the form of an 8-in. concrete slab that is 8-ft wide. See Figure STB 28 for a photograph showing the new T-wall under construction and Figure STB 29 for the design section that was installed.



Figure STB 28. New T-wall being constructed along IHNC (Reach STB2) (looking north along the IHNC)

the 5.5 feet range with a top of levee elevation at 9.0. TFG will provide a stability berm to elevation 9.0 on the protected side. Therefore, the free standing height will be reduced to approximately 4.3 feet with the increased stability berm. In addition, a scour protection pad, as shown in Figure STB 30, was installed on the top of the protected side levee.

Reach STB5 (IHNC to Caernarvon)

There were no improvements made to this reach under TFG.

Reach STB6 (IHNC to Caernarvon)

Scour protection was provided on the protected side of all these walls and around the tie-in to the levee by TFG. Figure STB 31 depicts the completed scour protection pad construction.

Reach STB7 (IHNC to Caernarvon)

There were no improvements made to this reach under TFG.



Figure STB 30. New scour protection pad (typical) (photo taken at end of Reach STB4 looking back toward IHNC)



Figure STB 31. New scour protection around Reach STB6

Reach STB8 (IHNC to Caernarvon)

The floodwall around Paris Road has a couple of modifications made to it by TFG. First, the free-standing height of the wall was returned to the as designed condition. Any location where the free-standing height of wall was greater than designed was reduced back to a height of 6 feet. Secondly, scour protection was added around this wall similar to other sections. The pad extends 10 feet away from the vertical face of the protected side. The repairs that were made are shown in Figure STB 32.



Figure STB 32. TFG repairs to Paris Road floodwall

Reach STB9 (IHNC to Caernarvon)

There were no improvements made to this reach under TFG.

Reach STB10 (IHNC to Caernarvon)

A scour protection pad was added around the transition areas with the adjoining levee sections as well as the protected side of this wall by TFG as shown in Figure STB 33. There were no other changes to this reach.



Figure STB 33. New scour protection around Reach STB10. (viewed from Bienvenue Control Structure side looking northwest)

Reach STB11 (IHNC to Caernarvon)

This short section of levee was topped with heavy riprap between the two floodwall sections as part of repairs made by TFG following Katrina. This will be a significant improvement in scour protection for this section since there is no exposed earthen levee and the transition areas have been topped by a combination of concrete scour pads and heavy riprap.

Reach STB12 (IHNC to Caernarvon)

As shown in Figures STB11-13, this area suffered significant damage during Katrina. Two major repair efforts were undertaken for this set of walls as part of TFG. The first is heavy riprap has been placed around the northwest I-wall/T-wall sections leading to the control gated structure. A photograph of this repair is shown in Figure STB 34 and is also typical of the riprap that was placed on top of Reach STB 11 as part of the repair effort. The second major repair is a sheetpile diaphragm wall that has been installed to replace the failed uncapped I-wall section. This diaphragm wall was constructed to an elevation of 18.5 (NGVD). The basic design section for this sheetpile diaphragm wall is shown in Figure STB 35. Note that this sheetpile diaphragm repair is the same one used for the northwest walls leading to the Bayou Dupree Control Structure (Reach STB 20), and the section shown is actually from the Bayou Dupree drawing set.



Figure STB 34. Riprap placement around Northwest Floodwall adjoining Bayou Bienvenue Control Structure (looking southeast along MRGO)

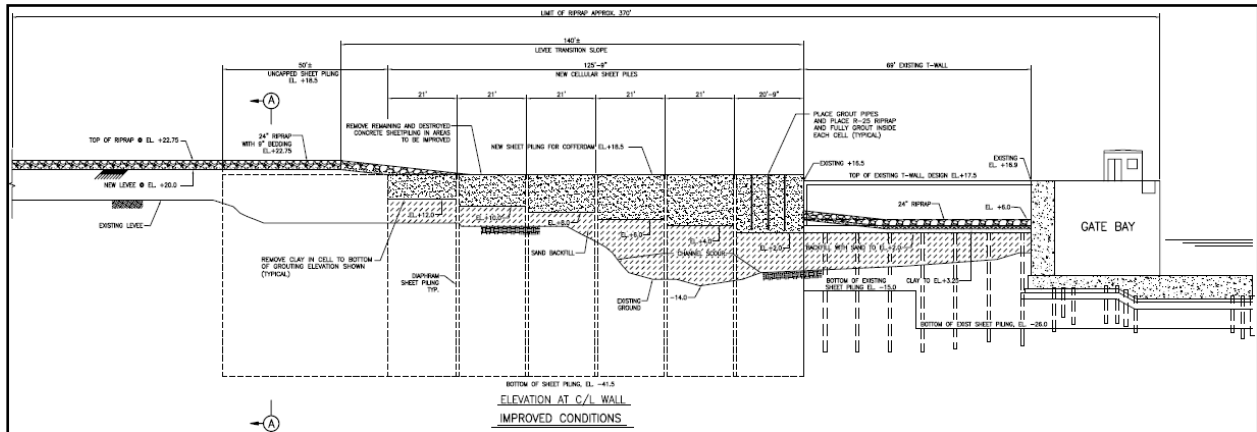


Figure STB 35. New sheetpile diaphragm wall replacing failed uncapped I-wall at Bayou Bienvenue Control Structure. (Note: This is same repair being done for northwest wall at Bayou Dupree)

Reach STB13 (IHNC to Caernarvon)

This reach was rebuilt to a constructed elevation of 20.0 (NGVD) with a final design grade of 17.5 (NGVD). This will allow for 2.5 feet of long-term settlement. There are three locations, each 300 feet long, within this reach where the levee was only rebuilt to elevation 17.5 (NGVD). These are all at utility pipe crossings. As was noted in the pre-Katrina section, this reach failed and had an approximate weighted average top elevation of 17.5 (NGVD). Therefore, the reach will be 2.5 feet higher initially until it begins to settle over time.

Reach STB14 (IHNC to Caernarvon)

The uncapped I-wall that defined this section pre-Katrina was removed by TFG, and the entire stretch was replaced with a rebuilt levee to a constructed elevation of 20.0 (NGVD) with a final design grade of 17.5 (NGVD), thus, allowing for 2.5 feet of long-term settlement. There are two exceptions to this description within this reach. There are two separate 300-ft stretches where the levee was only rebuilt to elevation 17.5 (NGVD) because of utility pipe crossings. See Figure STB 36 for reference of these areas along this stretch.

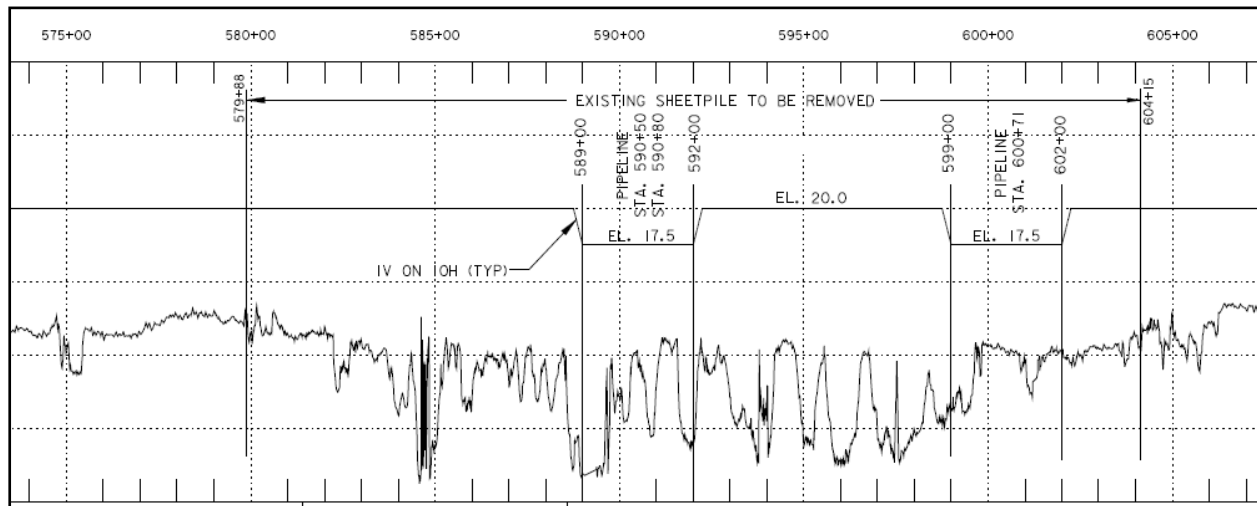


Figure STB 36. Profile of rebuilt levee along MRGO (Reach STB14). (Note: Jagged line represents elevation of levee following Katrina)

Reach STB15 (IHNC to Caernarvon)

This section of levee, which had an approximate weighted average top elevation of 16.4 ft (NGVD) prior to Katrina, was replaced with a new levee between the two control structures constructed to elevation 20.0 (NGVD) to allow for 2.5 feet of long-term settlement. Final design grade is elevation 17.5 (NGVD). Thus, the new levee section will be 3.6 feet higher than the pre-Katrina elevation for this levee initially and then 0.9 feet higher assuming a final design grade after settlement occurs.

Reach STB16 (IHNC to Caernarvon)

The uncapped I-wall that defined this section pre-Katrina was removed by TFG, and the entire stretch replaced with a rebuilt levee to a constructed elevation of 20.0 (NGVD) with a final design grade of 17.5 (NGVD), thus, allowing for 2.5 feet of long-term settlement.

Reach STB17 (IHNC to Caernarvon)

This reach of levee was replaced with a new levee to a constructed elevation of 20.0 ft (NGVD) with a final grade elevation of 17.5 (NGVD). This will allow for 2.5 feet of long-term settlement. This means the new levee will be 3.5 feet higher than pre-Katrina at the time of construction, and its final design elevation should be approximately 1.0 foot higher.

Reach STB18 (IHNC to Caernarvon)

The uncapped I-wall that defined this section pre-Katrina was removed by TFG, and the entire stretch was replaced with a rebuilt levee to a constructed elevation of 20.0 (NGVD) with a final design grade of 17.5 (NGVD), thus, allowing for 2.5 feet of long-term settlement.

Reach STB19 (IHNC to Caernarvon)

This reach of levee was replaced with a new levee to a constructed elevation of 20.0 (NADV88) with a final grade elevation of 17.5 (NAVD88). This will allow for 2.5 feet of long-term settlement. This means the new levee will be 1.3 feet higher than pre-Katrina at the time of construction, and its final design elevation will actually be lower than the pre-Katrina weighted average elevation.

Reach STB20 (IHNC to Caernarvon)

There are several changes to this structure that were made by TFG. First the northwest precast concrete sheetpile wall that failed during Katrina was replaced with a diaphragm sheetpile cell wall (similar to the one shown in Figure 35 for Bayou Bienvenue). This diaphragm cell wall was built to elevation 18.5 (NAVD88). In addition, the adjoining T-walls on both sides remained, but the surrounding earthen sections were covered with heavy riprap for scour protection. Finally, the southeast precast concrete sheetpile wall remained, but now has an earthen berm placed on both the sides of the wall and covered with heavy riprap, as shown in Figure 37.



Figure STB 37. Repairs to Southeast adjoining walls at Bayou Dupre (viewed from southeast side looking northwest along the MRGO)

Reach STB21 (IHNC to Caernarvon)

This reach of levee was replaced with a new levee to a constructed elevation of 20.0 (NGVD) with a final grade elevation of 17.5 (NGVD). This allows for 2.5 feet of long-term settlement. This means the new levee will be 0.9 feet higher than pre-Katrina at the time of construction, and its final design elevation will actually be lower than the pre-Katrina weighted average elevation across this reach if it settles to the design elevation.

Reach STB22 (IHNC to Caernarvon)

The uncapped I-wall that defined this section pre-Katrina was removed by TFG, and the entire stretch was replaced with a rebuilt levee to a constructed elevation of 20.0 (NGVD) with a final design grade of 17.5 (NGVD), thus, allowing for 2.5 feet of long-term settlement. Therefore, the levee will be 1.0 feet higher when constructed, but will be lower if settlement occurs to the design grade.

Reach STB23a (IHNC to Caernarvon)

This section of levee was rebuilt by TFG to a constructed elevation of 20.0 (NGVD) with a final design grade of 17.5 (NGVD). Therefore, the “new” levee will be slightly higher (0.5 feet) than pre-Katrina when constructed, but lower if it settles to design grade.

Reach STB23b (IHNC to Caernarvon)

There were small changes made to this reach under TFG. The first 1,400 feet or so of this levee was topped to an elevation of 19.0 (NAVD88). The remainder only had minimal scour

repairs where necessary, thus, overall the reach will not vary greatly from pre-Katrina conditions.

Reach STB23c (IHNC to Caernarvon)

There were no major changes planned for this section of levee under TFG. There were some minor scour repairs to areas that were damaged during Katrina.

Reach STB23d (IHNC to Caernarvon)

There were no improvements planned for this reach under TFG.

Reach STB24 (IHNC to Caernarvon)

There were no improvements planned for this reach under TFG.

Reach STB25 (IHNC to Caernarvon)

Scour protection was provided along this reach under TFG even though it was not overtopped or damaged during Katrina. A photograph of this protection (same general location as pre-Katrina condition shown in Figure STB18) is shown in Figure STB 38.



Figure STB 38. Scour repairs to Caernarvon sheetpile I-wall area (Note: compare to pre-Katrina condition shown in Figure STB 18)

Reach STB26 (IHNC to Caernarvon)

The only significant repair to this reach undertaken by TFG was to provide a scour protection pad similar to the one shown for Reach STB25 (see Figure STB 38). In addition, any spots that had an I-wall “stick-up” height that was greater than designed were modified to reduce free standing height to design levels.

Reaches STB27 through STB33 (Mississippi River Levee)

There were no improvements to any of these reaches planned under TFG.

Reach STB33 (Interior Local Levee)

Most of this 15,455-ft stretch of levee did not require any modifications by TFG. However, a 4,500-ft section of uncapped sheetpile I-wall embedded within the levee was repaired because of Katrina damage. This repair essentially consisted of replacing the damaged wall and levee that was washed away to its pre-Katrina condition. Therefore, for the purposes of the IPET assessment it was assumed that no improvements to this reach were made compared to the

pre-Katrina condition. A photograph of the construction being carried out to repair the damaged section along this reach is shown in Figure STB 39.



Figure STB 39. Repairs to interior local levee along Reach STB33 near parish border (Note: This section is being returned to pre-Katrina conditions)

Reach STB34 (Interior Local Levee)

There were no improvements to this reach planned under TFG.

Reach STB35 (Interior Local Levee)

There were no improvements to this reach planned under TFG.

Reach STB36a (Interior Local Levee)

TFG repaired Katrina damages and raised the levee east of Paris Road within this reach. Prior to Katrina, the weighted average top elevation east of Paris Road was 8.4 (NAVD88) based upon a 1999 LADOTD physical survey. TFG was granted approval on a one-time basis to raise this portion of the levee to elevation 10 (NAVD88 2004.65).

Reach STB36b (Interior Local Levee)

There were no major improvements to this reach being planned by TFG.

Reach STB36c (Interior Local Levee)

This reach of levee was rebuilt and raised to elevation 10 (NAVD88 2004.65) under TFG. The pre-Katrina weighted average top of levee elevation across this reach was 9.1 (NAVD88).

Reach STB37 (Interior Local Levee)

This reach was rebuilt and raised to elevation 10 (NAVD88 2004.65) under TFG. The pre-Katrina weighted average top of levee elevation across this reach was 8.1 (NAVD88).

Reach STB38 (Interior Local Levee)

There were no improvements planned to this section of wall under TFG.

Reach STB39 (Interior Local Levee)

This 510-ft reach of levee was rebuilt by TFG and raised to elevation 10 (NAVD88 2004.65). Prior to Katrina, the weighted average top elevation of this reach was 8.5 (NAVD88) based upon a 1999 LADOTD physical survey. Figure STB 40 shows the levee being rebuilt by TFG.



Figure STB 40. Repairs and levee raising to Reach STB39 along Violet Canal (viewed looking west from end of Reach STB38)

Reach STB40 (Interior Local Levee)

This reach along the Violet Canal was repaired by TFG. The section was reinforced with gabion baskets in front of the building facilities, as shown in Figure STB 41. The new top elevation of this reach is 10 (NAVD88 2004.65) compared to elevation 7.5 (NAVD88) prior to Katrina.



Figure STB 41. Gabion basket repairs to Reach STB40 (viewed from west side of reach)

Reach STB41 (Interior Local Levee)

This reach of levee was rebuilt and raised to elevation 10 (NAVD88 2004.65) by TFG. Prior to Katrina, the weighted average elevation was 8.7 (NAVD88).

Reach STB42 (Interior Local Levee)

This reach of levee was also rebuilt and raised to elevation 10 (NAVD88 2004.65) by TFG. Prior to Katrina, the weighted average elevation was 7.7 (NAVD88).

TABLE STB 1 - Summary of I-wall Changes from Pre-Katrina to Post Katrina

		Pre-Katrina Information				Post-Katrina Task Force Guardian Improvements				
Reach	Location Description	Primary Type of Protection	Weighted Elevation	Datum Source	Free Standing Height (ft)	Primary Type of Protection	Weighted Elevation	Datum Source	Free Standing Height (ft)	Added Scour Protection
STB1	IHNC to Claiborne Bridge	Concrete I-wall	13.0	NAVD88	6.0				4.0	Yes
STB2	Failed Wall Along IHNC	Concrete I-wall	13.0	NAVD88	6.0	Concrete T-wall	15.0			Yes
STB3	Near Florida Ave Bridge	Concrete T-wall	12.5	NAVD88	6.0					Yes
STB4	Floodwall Ties into GIWW Levee	Concrete I-wall	13.3	NAVD88	5.5				4.3	Yes
STB6	Floodwall Around S-2 and S-3	Concrete I-wall	13.0	NAVD88	6.0					Yes
STB8	Paris Road Floodwall	Concrete I-wall	12.4	NAVD88	6.7				6.0	Yes
STB10	Unused Gate Near B. Bienvenue	Concrete I-wall	16.3	NAVD88	4.9					Yes
STB12	West i-wall of B. Bienvenue	Concrete I-wall	17.0	NAVD88	4.0					Yes
STB12	East i-wall of B. Bienvenue	Sheetpile I-wall	18.5	NAVD88	???	Diaphragm Wall	18.5		n/a	Yes
Numerous	MR-GO Sheet Pile Modifications Between Control Structures	Sheetpile I-wall	18.5	NGVD	3.5	Rebuilt Levee	17.5	NAVD88	n/a	n/a
STB20	West Concrete Sheetpile Wall @ Bayou Dupre	Conc Sheetpile	15.2	NAVD88	12.0	Diaphragm Wall	18.5		n/a	Yes
STB20	East i-wall of B. Bienvenue	Conc Sheetpile	15.2	NAVD88	7.5		15.2		1.0	Yes
STB22	MR-GO Sheet Pile Mods Between Bayou Dupre and Caernarvon	Sheetpile I-wall	19.0	NGVD	3.5	Rebuilt Levee	20.0	NAVD88	n/a	n/a
STB23d	Floodwalls Around Pump Station #8	Concrete I-wall	16.7	NAVD88	6.0					
STB25	Caernarvon Sheet Pile Wall	Sheetpile I-wall	12.8	NAVD88	5.5					Yes
STB26	Caernarvon Sheet Pile Wall	Concrete I-wall	13.0	NAVD88	6.0					Yes
STB33	Interior Local Levee from IHNC to Pump Station #6	Sheetpile I-wall	13.5	NAVD88	???					
STB34	Floodwalls Around Jean Lafitte Pump Station	Sheetpile I-wall	14.0	NAVD88	???					
STB35	Floodwall Between Jean Lafitte PS to Paris Road	Sheetpile I-wall	13.3	NAVD88	???					
STB36b	Floodwall Around Pump Station #7 (Bayou Ducros)	Sheetpile I-wall	9.7	NAVD88	3.5					
STB38	Floodwall for Soap Factory Along Violet Canal	Conc I-wall	7.0	NAVD88	???					
STB40	Floodwall for Shrimp Factory Along Violet Canal	Conc I-wall	7.5	NAVD88	???					

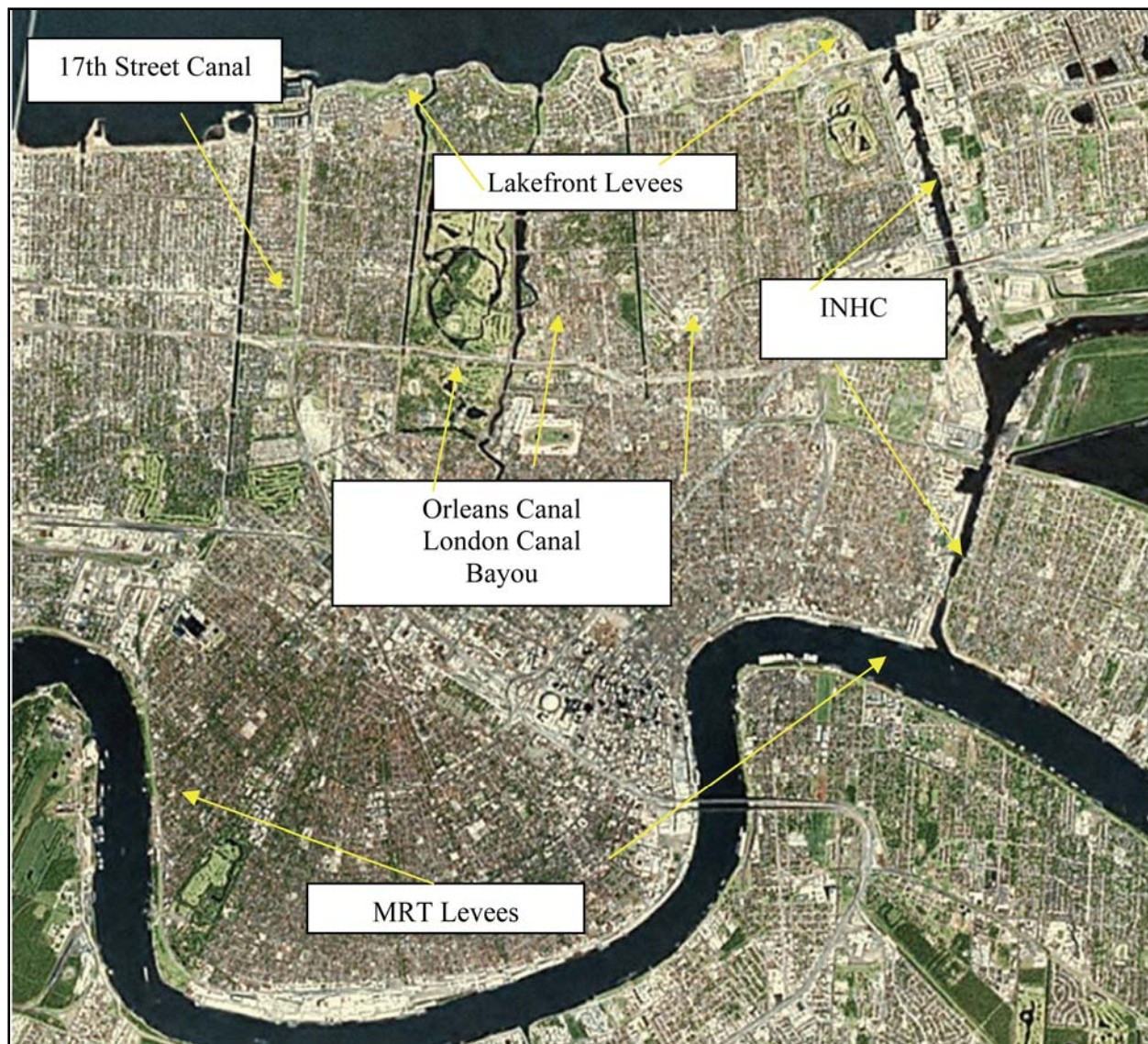
Appendix 7

Orleans Basin

Field Reconnaissance and Definition of Reaches in Orleans East Bank Basin

The basin for Orleans East Bank has been broken down into seven distinct sections to develop both reaches and features definitions for the risk model. These sections are based on General Design Memorandum (GDMs) published by the New Orleans District, USACE and updated by field reconnaissance by IPET Team 10. The Orleans East Bank Basin has been defined by the following sections shown in the figure below:

1. 17th Street Canal
2. Orleans Canal
3. London Canal
4. Bayou St. John Canal
5. Lakefront Levees
6. INHC
7. Mississippi River Levees



Overview of Orleans East Bank Basin

Elevations

All vertical elevations in this report are defined in **NAVD88 2004.65** datum unless otherwise noted within the text. All horizontal datums are defined in State Plane Coordinates NAD83 – 1702 Louisiana South, UTM NAD83 Zone 15, and GCS NAD83. Elevations for transition features are top elevation of feature and elevation for the gates are inverts.

Section 1: 17th Street Canal (East Side)

Narrative

The 17th Street Canal Floodwall cross section is typical from station 125+87.45 W/L to 0+00.00 W/L (also Sta. 340+40.00 B/L Lakefront) with a I-wall section at elevation of 14.0 feet

NGVD. The elevation changes from station 80+10.00 W/L to 80+40.00 W/L, where the I-Wall crosses under Veterans Highway and the elevation is 14.5 feet NGVD. The elevation changes again from station 100+86.00 W/L to 102+06.00, where the I-Wall elevation is 15.0 feet NGVD.

There was a major failure of the I-wall floodwall protection on the east side of the 17th Street Outfall Canal. This failure resulted in a breach located approximately N30°01.02 and W90°07.28. The length of the breach is 455 feet long. Floodwall monoliths, founding levee and foundation materials were scoured away resulting in scour hole with an approximate bottom elevation -21 feet NGVD. A temporary levee was constructed up to elevation +10 NGVD to provide temporary flood protection. Figure 3 shows the breach along the 17th Street Canal. Figure 4 shows the sheetpile repair along the 17th Street Canal.



Figure 3. Breach in the 17th Street Canal



Figure 4. Sheetpile repair along the 17th Street Canal

Elevation Stationing (used East Bank for OEB)										
Section	Start	End	Structure	EL	Section/Point	Length	Avg Height		Weighted Average	
1	0+00	7+45.59	I-Wall	14	S	745.59	14			
2	7+45.59	7+52.09	T-Wall	14	P	6.5	14			
3	7+52.09	8+14.09	Gate No. 3	14	P	62	14			
4	8+14.09	8+20.59	T-Wall	14	P	6.5	14			
5	8+20.59	80+10.00	I-Wall	14	S	7189.41	14	↓	Reach 1	14.0
6	80+10.00	80+40.00	I-Wall Transition	14.0 - El 14.5	S	30	14.25			
7	80+40.00	80+51.70	I-Wall	14.5	P	11.7	14.5			
8	80+51.70	81+63.70	Veterans Hwy	14.5	S	112	14.5			
9	81+63.70	100+86.00	I-Wall	14.5	S	1922.3	14.5	↓	Reach 2	14.5
10	100+86.00	102+06.00	I-Wall Transition	14.5 - El 15.0	S	120	14.75			
11	102+06.00	125+87.45	I-Wall	15	S	2381.45	15	↓	Reach 3	15.0

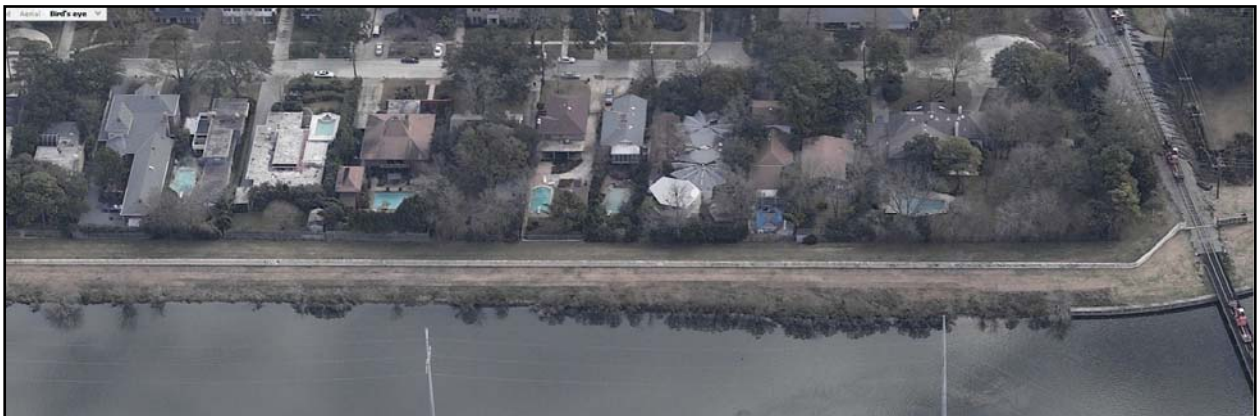
End at Hammond Highway

Features

<u>Elevation</u>	<u>Feature</u>
15	Pump Station #6 - End of 17th Street Canal
15	Pump Station OP#10
10.6	Gate E9 - Southern RR
7	Gate at OP#10 Pump Station
7	Gate north of I-10
7.3	Gate E4 - Veterans Blvd.
7.3	Gate E5 - Veterans Blvd

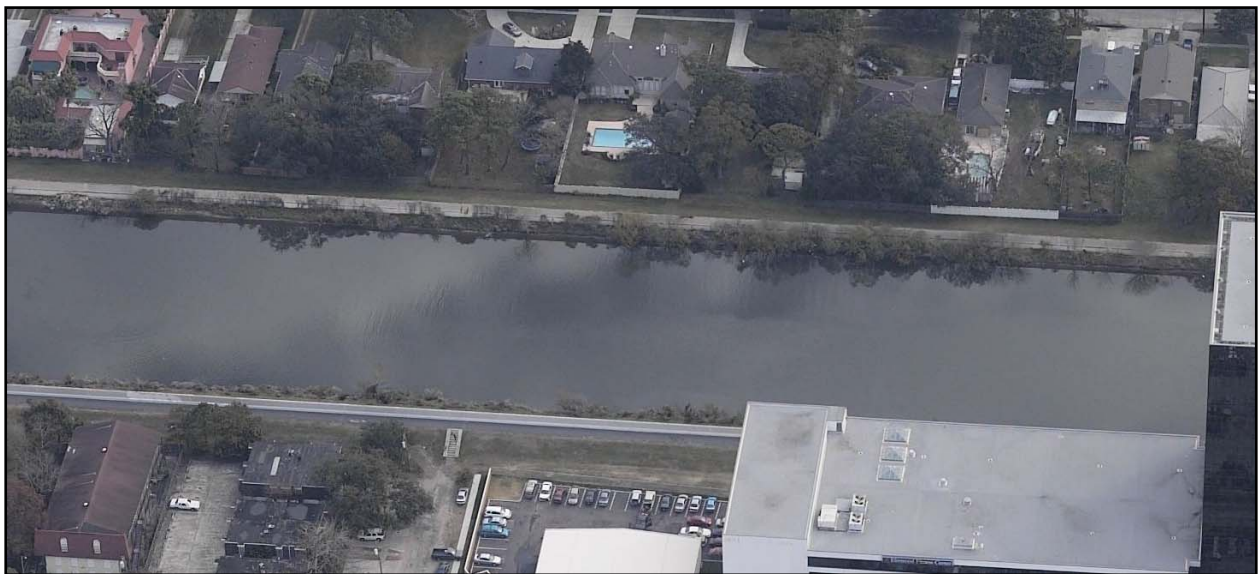
Definition of Reaches

Reach 1-3 (now 45) – This reach consists of I-wall on the east side of the 17th Street Canal at average elevation 15.5 feet with a length of approximately 12,740 feet. There are two transitions (Pump Stations 6 and 10) and five gates in this reach.

















Section 2: Orleans Avenue Canal

Narrative

The protection on the east side of the Orleans Outfall Canal starts at the intersection of Lakeshore Drive and Marconi Drive. After short lengths of floodwall and cantilever sheeting, the protection consists of a levee that extends to Robert E. Lee Boulevard. South of this intersection, the protection consists of floodwall that extends to the pumping station near Interstate Highway 610. This line of protection is in satisfactory condition and does not appear to have been damaged during Hurricane Katrina.

Definition of Reaches

Reach 4-10 (now 46-49) – These reaches consists primarily of I-walls with levees at the lakefront entrance on both on the east side of the Orleans Avenue Canal at average elevation 14.0 feet with a length of approximately 9,280 feet, 3,155 feet, 9,110 feet, and 3,610 feet respectively. There are one transitions (Pump Stations 7) and four gates in this reach.

Section	Structure	Length	Elevation		Section	Structure	Length	Elevation	
1	I-Wall	3404	13.6		1	I-Wall	3430	13.6	
2	I-Wall	2712	13.6		2	I-Wall	2545	13.6	
3	I-Wall	2627	13.4		3	I-Wall	2643	13.4	
4	I-wall	180	13	↓	4	I-wall	160	13	↓
5	Levee	2210	13	Reach 4	5	Levee	2948	13	Reach 8
6	I-wall	500	12	Reach 5	6	Levee	226	12	↓
7	Levee	665	13	Reach 6	7	I-wall	482	13	Reach 9
				Reach 7					Reach 10

Features

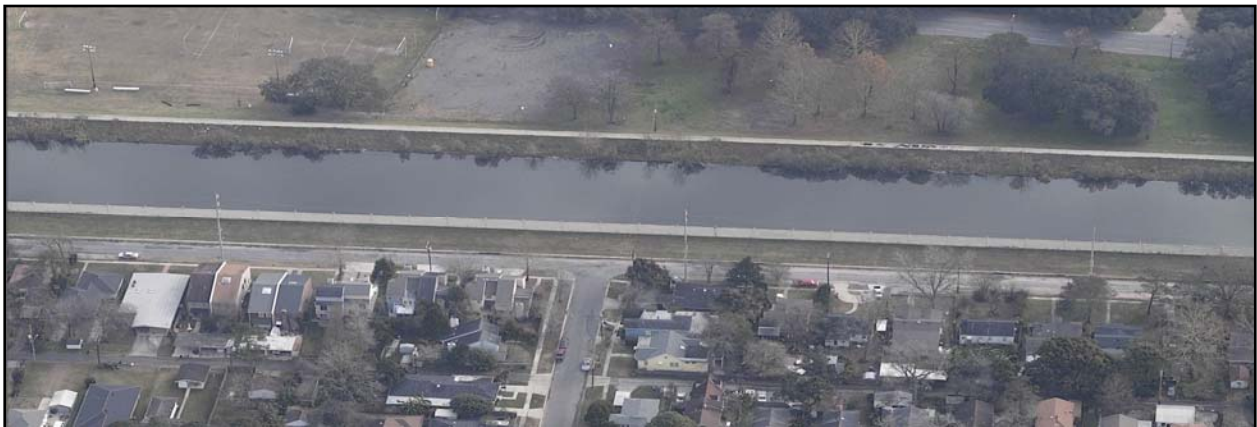
<u>Elevation</u>	<u>Feature</u>
15	Pump Station OP#7 FW - End of Orleans Canal
7	Gate at Harrison Ave
7	Gate at Harrison Ave
7	Gate at Filmore Ave
7	Gate at Filmore Ave

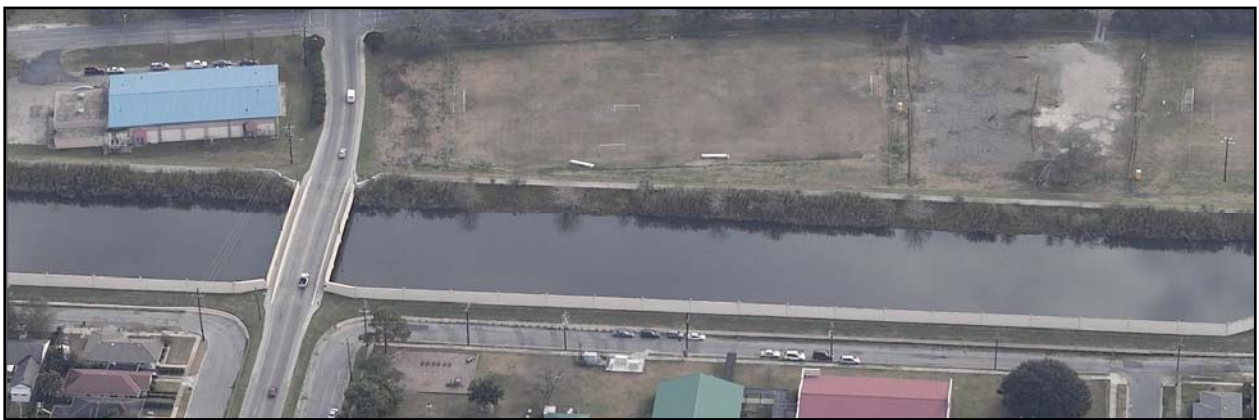


Pump Station #6



I-610 Overpass





Harrison Ave.







Filmore Ave.







Robert E. Lee Blvd









Lakeshore Drive and Marconi

Section 3: London Avenue Canal

Narrative

There was a major failure of the I-wall floodwall protection on the east side of the London Avenue Outfall Canal immediately north of Mirabeau Avenue Bridge. This failure resulted in a breach located approximately $N30^{\circ} 00.52'$ and $W90^{\circ} 04.167'$. The length of the breach was 425 feet long. Floodwall monoliths, founding levee and foundation materials were scoured away resulting in scour hole with an approximate bottom elevation -28 feet NGVD. A provisional levee was constructed up to elevation +10 NGVD to provide temporary flood protection. Figure 5 shows the sheetpile repair along the London Avenue Outfall Canal.

There was a second major failure of the I-wall floodwall protection on the west side of the London Ave Outfall Canal immediately south of Robert E. Lee Boulevard Bridge. This failure resulted in a breach located approximately $N30^{\circ}01.218'$ and $W90^{\circ}04.26'$. The length of the breach was 720 feet long. Floodwall monoliths, founding levee and foundation materials were scoured away resulting in scour hole with an approximate bottom elevation -20 feet NGVD. A provisional levee was constructed up to elevation +10 NGVD to provide temporary flood protection. Figure 6 shows the sheet pile repair and also a failed I-wall floodwall section.



Figure 5. Sheetpile repair along the London Ave Canal – East Side Failure



Figure 6. Sheetpile repair along the London Ave Canal – West Side Failure

Definition of Reaches

Reach 11-18 (now 50-53) – These reaches consists primarily of I-walls with levees at the lakefront entrance on both on the east side of the London Avenue Canal at average elevation 14.0 feet with a length of approximately 12,130 feet, 3,880 feet, 12,765 feet and 3,030 feet respectively. There are two transitions (Pump Stations 3 and 4) and three gates in this reach.

Elevation Stationing - WEST (START AT PUMP STATION #3)				Elevation Stationing - EAST (START AT PUMP STATION #3)						
Section	Structure	Length	Elevation			Section	Structure	Length	Elevation	
1	I-Wall	9712	13	Reach 11		1	I-Wall	9827	13.2	Reach 16
2	T-Wall	300	15	Transition	PS #4	2	T-wall	240	18	Transition
3	I-Wall	1984	13.4	Reach 12		3	I-Wall	1974	13.2	
4	Levee	537	12	Reach 13	Between Robert Lee and Simon	4	I-wall	672	13.1	↓
5	I-wall	190	12.5	↓	Between Robert Lee and Simon	5	I-wall	130	13	Reach 17
6	I-wall	92	13	Reach 14		6	Levee	3647	12.5	Reach 18
7	Levee	3276	12.5	Reach 15						

Features

<u>Elevation</u>	<u>Feature</u>
9.0	Unprotected area adjacent Pump Station #3
14.6	Pump Station #4 West FW - Middle of London Canal
13.6	Pump Station #3 FW - End of London Canal
10	West CSX RR gate near Pump Station #3
7	Gate at Filmore Ave
7	Gate at Filmore Ave



Pump Station #3



Pump Station #3



I-610 overpass

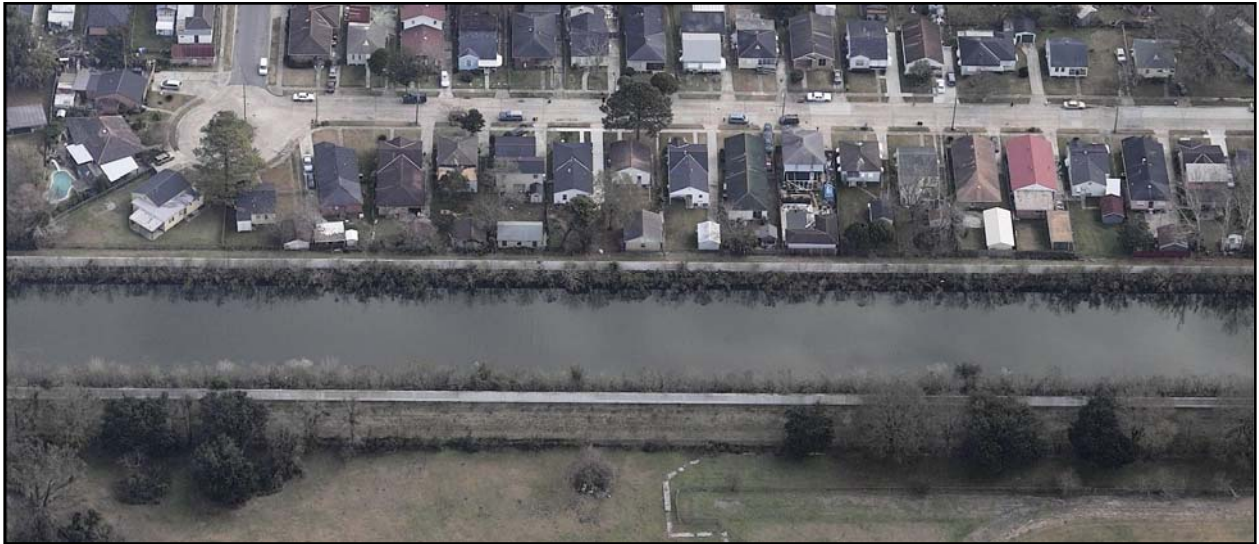


Gentilly Blvd











Mirabeau Ave.



Mirabeau Ave.





Filmore Ave





Pump Station 4





Robert E. Lee Blvd



Leon C Simon Blvd







Lakeshore Blvd

Section 4: Bayou St. John Canal

Narrative

The protection on the east and west banks of the Bayou St. John Canal meets the Lakefront protection. This protection extends approximately 800 feet to the south where there is a closure structure across Bayou St. John. The closure structure has both a sector gate and slice gates. South of the closure structure, the protection along the banks is approximately ten feet lower. There are no reaches considered for this canal. The gate structure is included as both a transition (tie-in on both sides) and a gate structure.



Inlet to Bayou St. John



Protection Gate Structure at Bayou St. John

Section 5: Lakefront Levees

Narrative

Orleans East Bank Lakefront Levee Reaches 9 and 8, as designated in Design Memorandum No.13, extend from the 17th Street Canal at station 340+40 to the Orleans Avenue Canal at station 250+72. Starting at the east bank of the 17th Street Canal, the protection begins with a slide gate across Marina Boulevard. At this junction, construction work was ongoing under contract number W912P8-06-C-0008, titled "17th Street Canal Interim Closure Structure." Contract completion date is scheduled for 1 June 2006. The flood protection along Marina Boulevard consists of an I-wall with a series of street gates that provide access through the line of protection. The I-wall transitions into the levee just beyond the intersection at Lake Shore drive at longitude-latitude coordinates 30°1'19" North by 90°06'47" West.

The typical cross section for the Lakefront Levee has a ten-foot top width with vegetated side slopes. The crest has an undulant profile, and there appears to be a low spot in the protection where Canal Boulevard intersects the levee. Design Memorandum No. 13 indicates the net grade for the levee crest to be elevation 18 feet NGVD. At the Orleans Outfall Canal, the Lakefront Levee drops approximately four feet and transitions into the west levee for the Orleans Outfall Canal. At this junction, construction work was ongoing under Contract Number W912P8-06-C – 0097, titled “Interim Closure Structure, Orleans Avenue.” A review of the contract documents indicates the at the west levee will be raised from Lake Shore Drive to the new Closure Structure and the southern limit of the work will extend to West Robert E. Lee Boulevard. Contract completion date is scheduled for 1 June 2006. South of Robert E. Lee Boulevard, the protection on the west side of the Orleans Outfall Canal consists of floodwall up to the pumping station at 29°59’40” North by 90°06’02” West. South of the pumping station, the canal is contained in an underground conduit.

Orleans East Bank Lakefront Levee Reach 7 extends from the Orleans Avenue Canal at station 246+37 to the Bayou St. John Canal at station 199+42. On the east side of the Orleans Outfall Canal, there is a street gate marked “L8” across Marconi Drive and then an approximate 20-foot length of sheeting that transitions into the typical levee cross-section that Design Memorandum No. 13 indicates to have a net crest elevation of 17.5 feet NGVD. The Lakeshore Levee then continues along the south side of Lake Shore Drive until coordinate point 30°1’39” North by 90°05’17” West where the alignment shifts to the north side of Lake Shore Drive where a flood wall serves as the protection. The point where the protection intersects Lake Shore Drive appears to be a low point. The floodwall transitions back to the typical levee cross section at coordinate point 30°1’39” North by 90°05’-15” West where minor erosion was observed on the lakeside slope. The typical levee cross section then continues toward Bayou St. John where it transitions back to a floodwall that ties into the bridge abutments where Lake Shore Drive passes over Bayou St. John.

Orleans East Bank Lakefront Levee Reach 6 extends from the Bayou St. John Canal at station 196+50 to the London Ave Canal at station 163+98. Starting at the east bridge abutment, the protection consists of floodwall up to Lake Terrace Drive where it then transitions back to the typical levee cross-section that Design Memorandum No. 13 indicates was to be constructed to a net elevation of 18 feet NGVD. The transition area appears to be a low point in the protection. The levee section runs along the north side of Lake Shore Drive until it approaches the London Avenue Outfall Canal where it then crosses to the south side of Lake Shore Drive where it ties into the London Avenue west levee. Corps survey markers were found in this area with spot elevations of 14.47 feet NGVD on the crest of Lakeshore Levee and elevation 12.84 feet NGVD on the crest of the west levee along the canal. The point where the protection crosses Lake Shore Drive appears to be a low point.

Orleans East Bank Lakefront Levee Reach 4 extends from the London Ave Canal at station 161+00.18 B/L to the Inner Harbor Navigational Canal at station 0+00.00. This reach is typically levee. The section from station 136+13.19 B/L to station 102+23.16 B/L has been removed and a new floodwall has been constructed on the back side of the University of New Orleans. The original DM showed the floodwall on the front side of what is not the University of New Orleans. This area includes floodwall and levee. Figure 7 shows the new floodwall and levee.

The majority of the damage in this reach is lake side erosion, scour at the base of the floodwalls, and damaged floodwalls. There are also trees and bushes growing adjacent to and on the levee. Figure 8 shows the bushes on the levee.



Figure 7. Floodwall and Levee behind the University of New Orleans

Reach 23-32 (now 54-60) – These reaches consist primarily of levees on the lakefront with walls at certain protection areas. Elevations range from 12 to 18 feet depending upon the section. The lengths of the reaches are shown with their respective elevations. There are eleven transitions and eighteen gates in this reach.

Reach	Length	Elevations
54	2,925	12.00
55	6,310	18.00
56	9,940	17.00
57	2,380	16.50
58	3,220	16.50
59	7,605	16.50
60	1,155	14.40

Elevation Stationing

Section	Start	End	Structure	EL	Section/Point	Length	Avg Height	Weighted Average
1	0+00	1+13.57	I-Wall	EI 14.5	S	113.57	14.5	
2	1+13.57	1+21.07	I-Wall	EI 14.0	P	7.5	14	
3	1+21.07	1+51.07	Ramp formerly Gate No 1	EI 10.0	P	30	14	
4	1+51.07	1+58.57	I-Wall	EI 14.0	P	7.5	14	
5	1+58.57	2+54.51	I-Wall	EI 14.5	S	95.94	14.5	
6	2+54.51	5+60.00	Levee	EI 14.0	S	305.49	14	Reach 32
7	5+60.00	5+74.37	Levee Transition	EI 14.0 - EI 15.0	S	14.37	14.5	
8	5+74.37	7+04.00	Levee	EI 15.0	S	129.63	15	Reach 31
9	7+04.00	7+62.87	I-Wall	EI 15.5	S	58.87	15.5	
10	7+62.87	7+69.37	I-Wall	EI 15.0	S	6.5	15	
11	7+69.37	8+02.37	Gate No. 2	EI 8.0	S	33	15	
12	8+02.37	8+08.87	I-Wall	EI 15.0	S	6.5	15	
13	8+08.87	8+59.15	I-Wall	EI 15.5	S	50.28	15.5	
14	8+59.15	8+63.15	I-Wall	EI 15.0	S	4	15	
15	8+63.15	8+91.15	Gate No. 3	EI 10.75	S	28	15	
16	8+91.15	8+95.15	I-Wall	EI 15.0	S	4	15	
17	8+95.15	9+88.10	Seabrook Bridge	EI 19.19	S	92.95	19.19	
18	9+88.10	14+31.42	I-Wall	EI 15.5	S	443.32	15.5	
19	14+31.42	14+40.23	Levee	EI 15.0	S	8.88	15	Reach 30
20	14+40.23	15+30.23	Levee Transition	EI 15.0 - EI 18.0	S	90	16.5	
21	15+30.23	15+85.23	Levee	EI 18.0	S	55	18	
22	15+85.23	15+90.23	I-Wall	EI 18.5	S	5	18.5	
23	15+90.23	16+08.23	I-Wall Transition	EI 18.5 - EI 18.0	S	18	18.25	
24	16+08.23	16+27.23	I-Wall	EI 18.0	S	19	18	
25	16+27.23	16+36.23	I-Wall	EI 18.5	S	9	18.5	
26	16+36.23	16+70.23	Gate No. 4	EI 12.25	S	34	17.5	
27	16+70.23	16+79.18	I-Wall	EI 18.5	S	8.95	18.5	
28	16+79.18	16+95.46	I-Wall	EI 18.0	S	16.28	18	
29	16+95.46	17+13.46	I-Wall Transition	EI 18.0 - EI 18.5	S	18	18.25	
30	17+13.46	17+18.46	I-Wall	EI 18.5	S	5	18.5	
31	17+18.46	20+00.00	Levee	EI 18.0	S	281.4	18	
32	20+00.00	20+05.00	I-Wall	EI 18.5	S	5	18.5	
33	20+05.00	20+22.25	I-Wall Transition	EI 18.5 - EI 18.0	S	17.25	18.25	
34	20+22.25	20+33.43	I-Wall	EI 18.0	S	11.18	18	
35	20+33.43	20+40.43	I-Wall	EI 17.5	S	7	17.5	
36	20+40.43	20+62.43	Gate No. 5	EI 12.5	S	22	17.5	
37	20+62.43	20+69.43	I-Wall	EI 17.5	S	7	17.5	
38	20+69.43	20+76.30	I-Wall	EI 18.0	S	6.87	18	
39	20+76.30	20+93.55	I-Wall Transition	EI 18.0 - EI 18.5	S	17.25	18.25	
40	20+93.55	20+98.55	I-Wall	EI 18.5	S	5	18.5	
41	20+98.55	42+10.0	Levee	EI 18.0	S	2111.45	18	
42	42+10.0	42+16.00	Ramp No 1 - Levee Transition	EI 18.0 - EI 14.5	P	6	16.25	
43	42+16.00	42+26.00	Ramp No 1 - Levee	EI 14.5	P	10	14.5	
44	42+26.00	42+62.00	Ramp No 1 - Roadway	EI 14.5	P	46	14.5	
45	42+62.00	42+68.00	Ramp No 1 - Levee	EI 14.5	P	6	14.5	
46	42+68.00	42+80.00	Ramp No 1 - Levee Transition	EI 14.5 - EI 18	P	12	16.25	
47	42+80.00	78+55.24	Levee	EI 18.0	S	3575.24	18	Reach 29
48	78+55.24	78+65.24	Ramp No 2 - Levee Transition	EI 18.0 - EI 14.5	P	10	16.25	
49	78+65.24	78+70.24	Ramp No 2 - Levee	EI 14.5	P	5	14.5	
50	78+70.24	78+98.24	Ramp No 2 - Roadway	EI 14.5	P	28	14.5	
51	78+98.24	79+36.24	Ramp No 2 - Shoulder	EI 15.0	P	38	15	
52	79+36.24	79+64.24	Ramp No 2 - Roadway	EI 14.5	P	928	14.5	
53	79+64.24	79+75.24	Ramp No 2 - Levee	EI 14.5	P	11	14.5	
54	79+75.24	79+81.24	Ramp No 2 - Concrete Capping	EI 18.0	P	6	18	
55	79+81.24	91+50.00	Levee (Now Floodwall)	EI 19.5	S	1168.76	19.5	Reach 28
56	91+50.00	94+60.00	Levee Transition	EI 19.5 - EI 17.0	S	310	18.25	
57	94+60.00	102+23.16	Levee (Ramp 3 included)	EI 17.0	S	763.16	17	Reach 27
58	102+23.16	136+13.19	FLOODWALL AT UNO - 1984			3390.07	20	Reach 26
59	136+13.19	159+70.00	Levee	EI 17.5	S	2356.81	17.5	Reach 25
60	159+70.00	163+98.15	London Ave. Outfall Canal		P	-	-	-
61	163+98.15	166+38.00	Levee	EI 18.0	S	239.85	18	
62	166+38.00	167+02.00	Ramp No. 5 (SEE PLATE 24 FOR DETAILS)		P	64	15.5	
63	167+02.00	196+50.00	Levee	EI 18.0	S	2948	18	Reach 24
64	196+50.00	199+41.52	Bayou St. John		P	-	-	-
65	199+41.52	203+18.00	Levee	EI 17.5	S	376.48	17.5	
66	203+18.00	204+28.30	Gate No 8 (SEE PLATE 17 FOR DETAIL)		P	110.3	17.5	
67	204+28.30	218+14.5	Levee (with 300 ft concrete capped wall at Ramp 6)	EI 17.5	S	1386.2	17.5	
68	218+14.5	218+77.5	Ramp No. 6 (SEE PLATE 24 FOR DETAILS)		P	63	14.5	
69	218+77.5	244+59.81	Levee	EI 17.5	S	2582.31	17.5	
70	244+59.81	246+10.04	Gate No 9 Marconi (SEE PLATE 18 FOR DETAIL)		P	150.23	17.5	
71	246+10.04	246+37.18	Levee (now concrete capped floodwall)	EI 17.5	S	27.14	17.5	Reach 23

Features

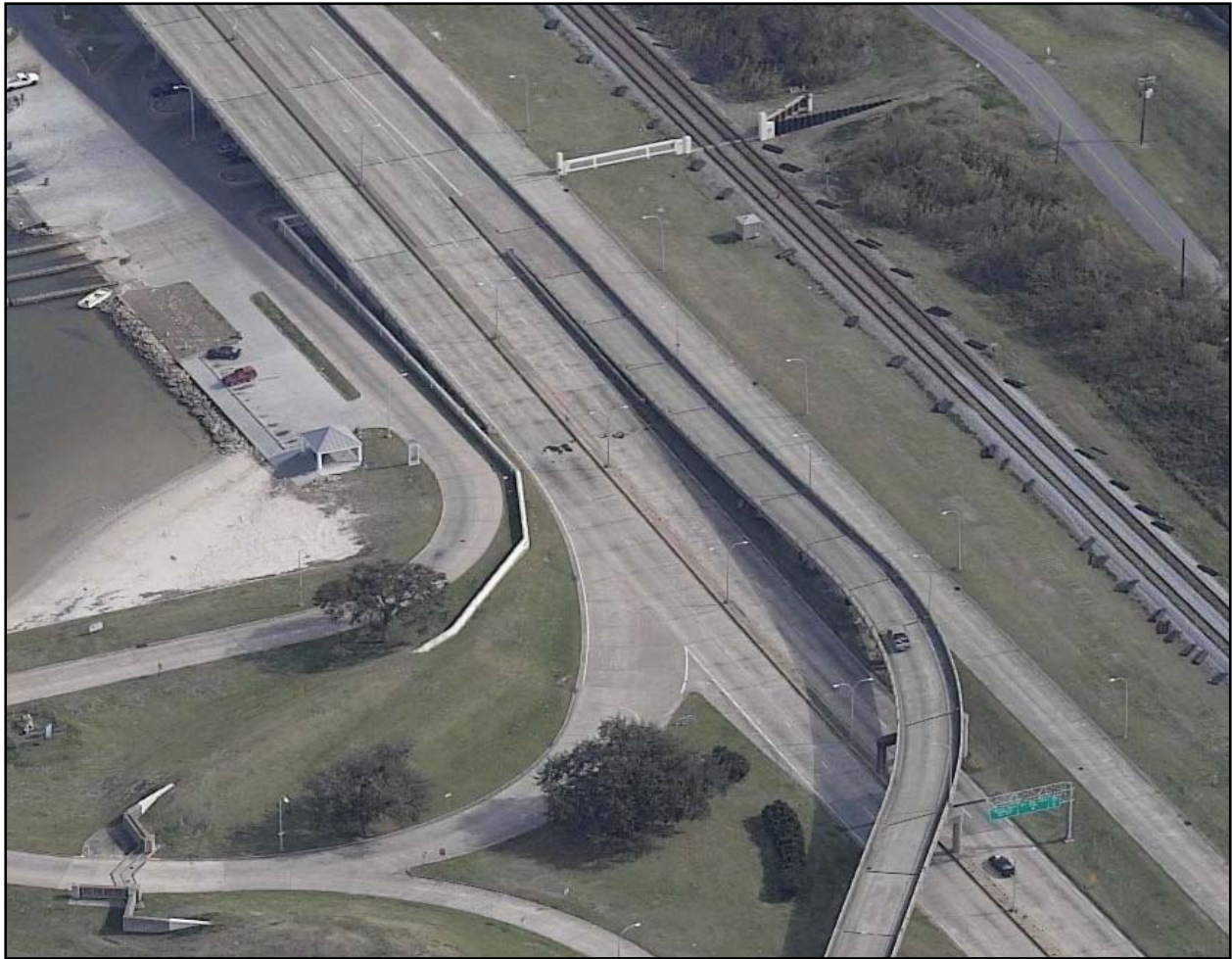
Elevation	Feature
13.8	Gate at W. Roadway Street
14	WLT - OM 10/11
7.55	Gate 10 - Topaz Dr
13.8	NB Ramp at Canal Blvd
13.8	SB Ramp at Canal Blvd
12.05	Gate 9 - Marconi Dr.
16	Ramp 6 - Lakeshore Dr.
16	Ramp Lake Terrace Dr.
16	Ramp 5 - Lakeshore Dr.
16.8	Ramp 4 - Lakeshore Dr.
16.8	Ramp 3 - Lakeshore Dr.
16.3	Ramp 2 - Franklin Ave - double wide ramp
14.5	Ramp 1 - Leroy Johnson Drive
11.8	Gate 5 - Navy Reserve
11.55	Gate 4 - Navy Reserve
14	WLT O 16/15
10.05	Road Gate 3
7.3	RR - Gate 2
7	Gate at Filmore Ave
7	Gate at Filmore Ave
7	Gate at Leon C Simon Blvd
8.8	W. Roadway St
8.8	Gate 15 - Into Marina Parking
8.8	Gate 14 - Into Marina Parking
8.8	Gate 13 - Into Marina Parking
8.8	Gate 12 - Entrance to Marina
6.05	Gate 11 - Lakeshore Dr.
7.55	Gate 10 - Topaz Dr
12.05	Gate 9 - Marconi Dr.
-5	Bayou St John Floodgate
10	Gate 3 UNO
10	Gate 2 UNO
10	Gate 1 UNO
11.8	Gate 5 - Navy Reserve
11.55	Gate 4 - Navy Reserve
10.05	Road Gate 3
7.3	RR - Gate 2



Reach 32



Reach 31



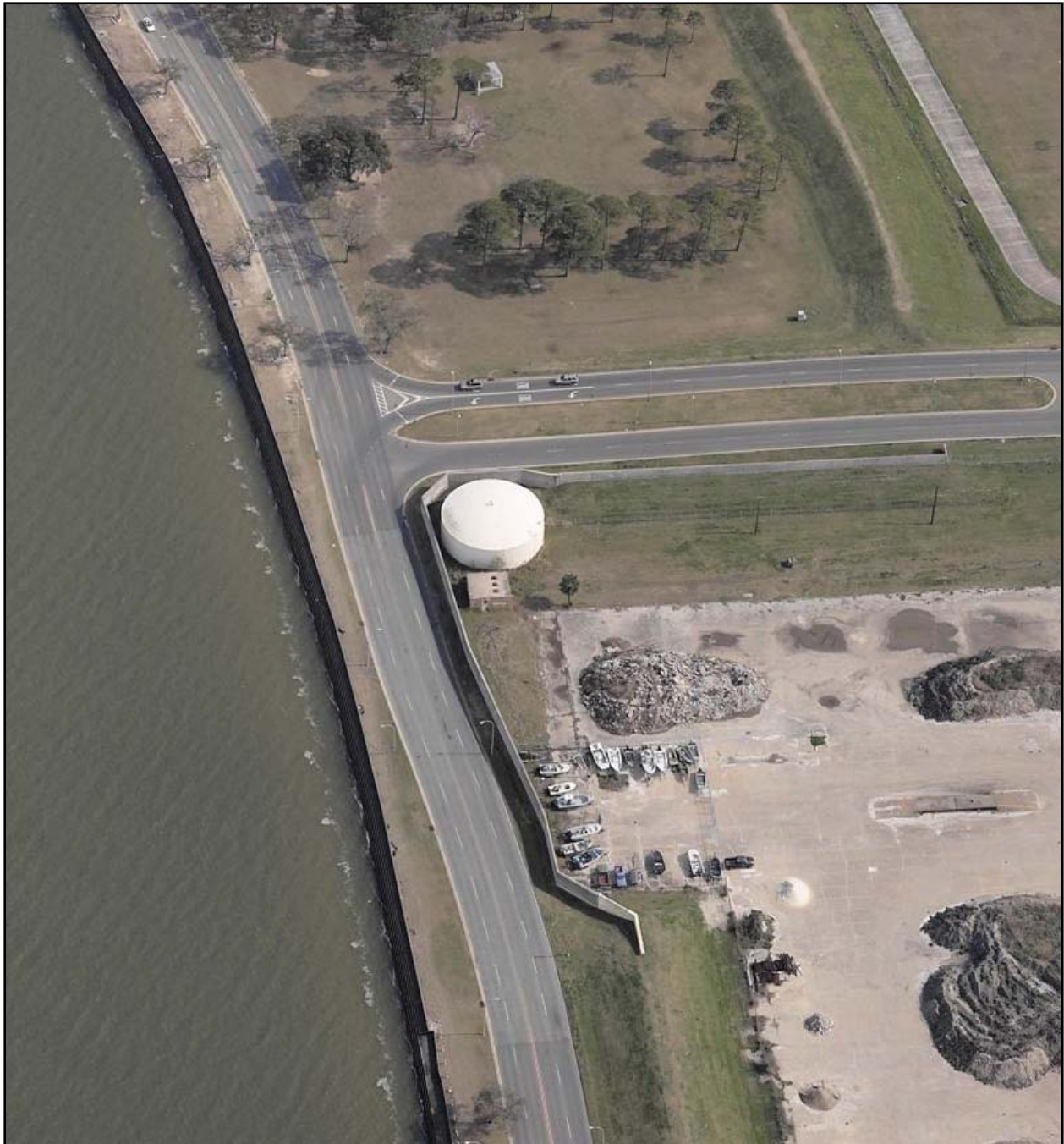
Reach 30



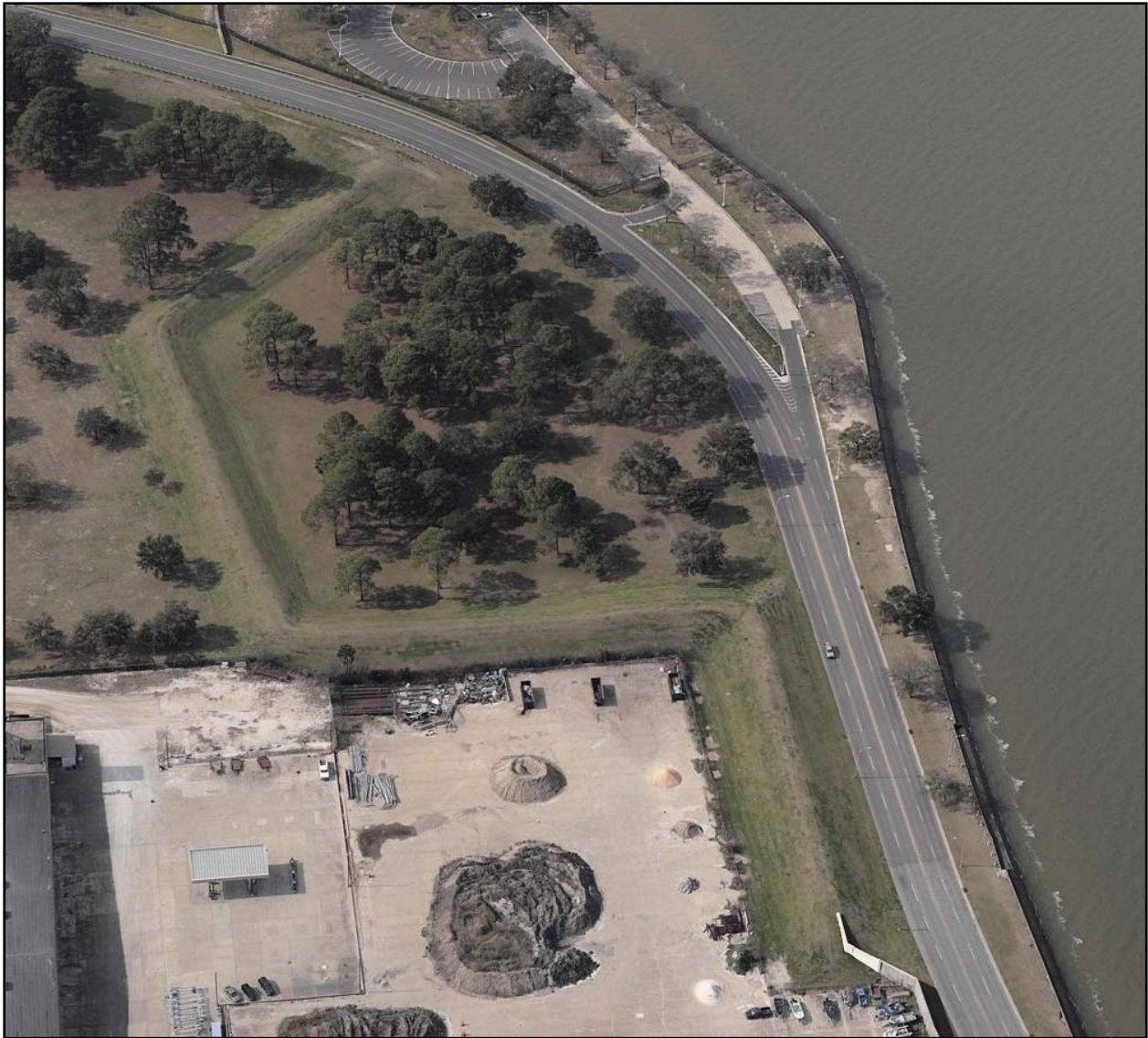
Reach 29



Reach 28



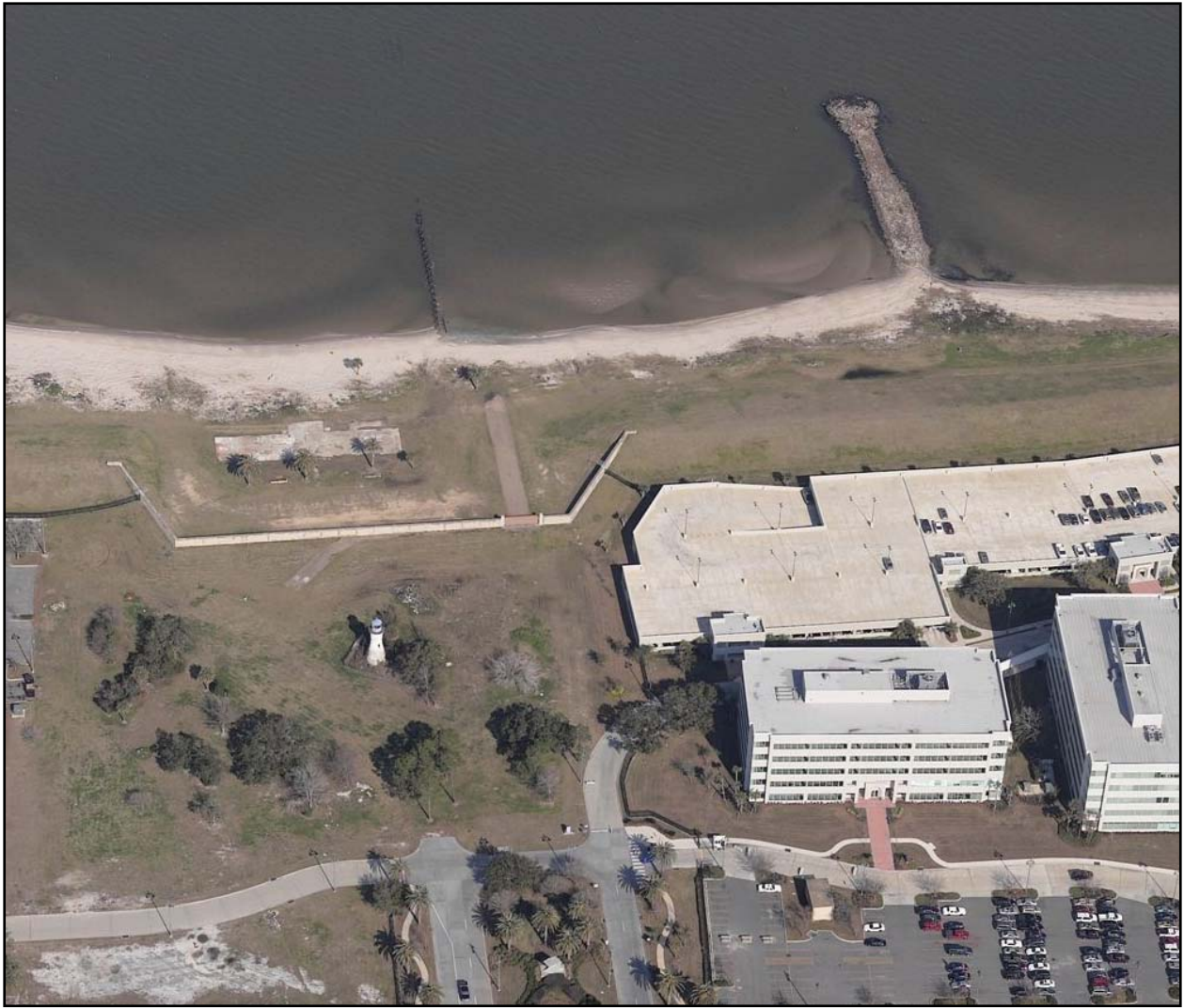
Reach 27



Reach 26



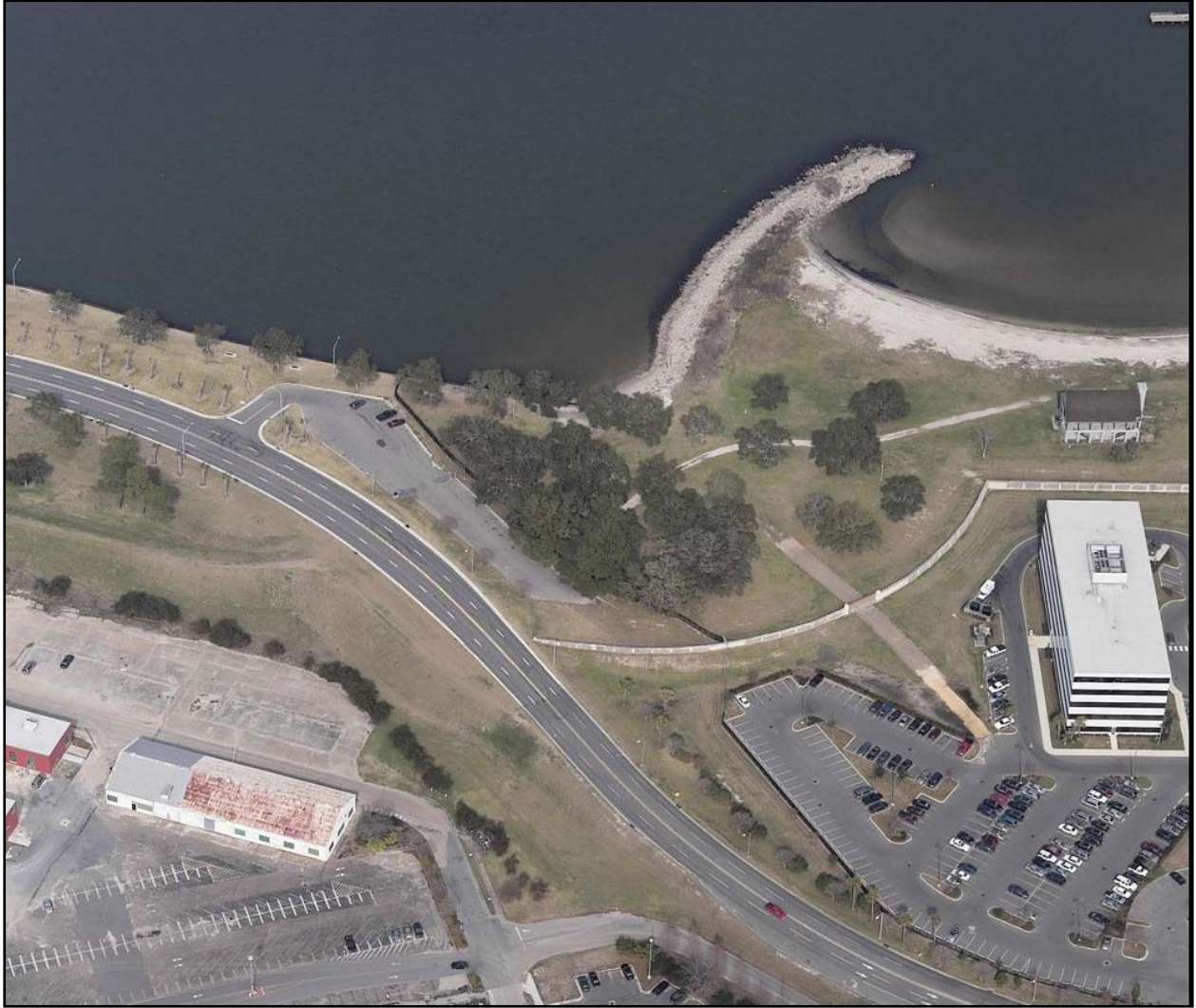
Reach 25



Reach 25



Reach 25



Reach 25



Reach 26



Reach 27



Reach 27



Reach 28



Reach 29



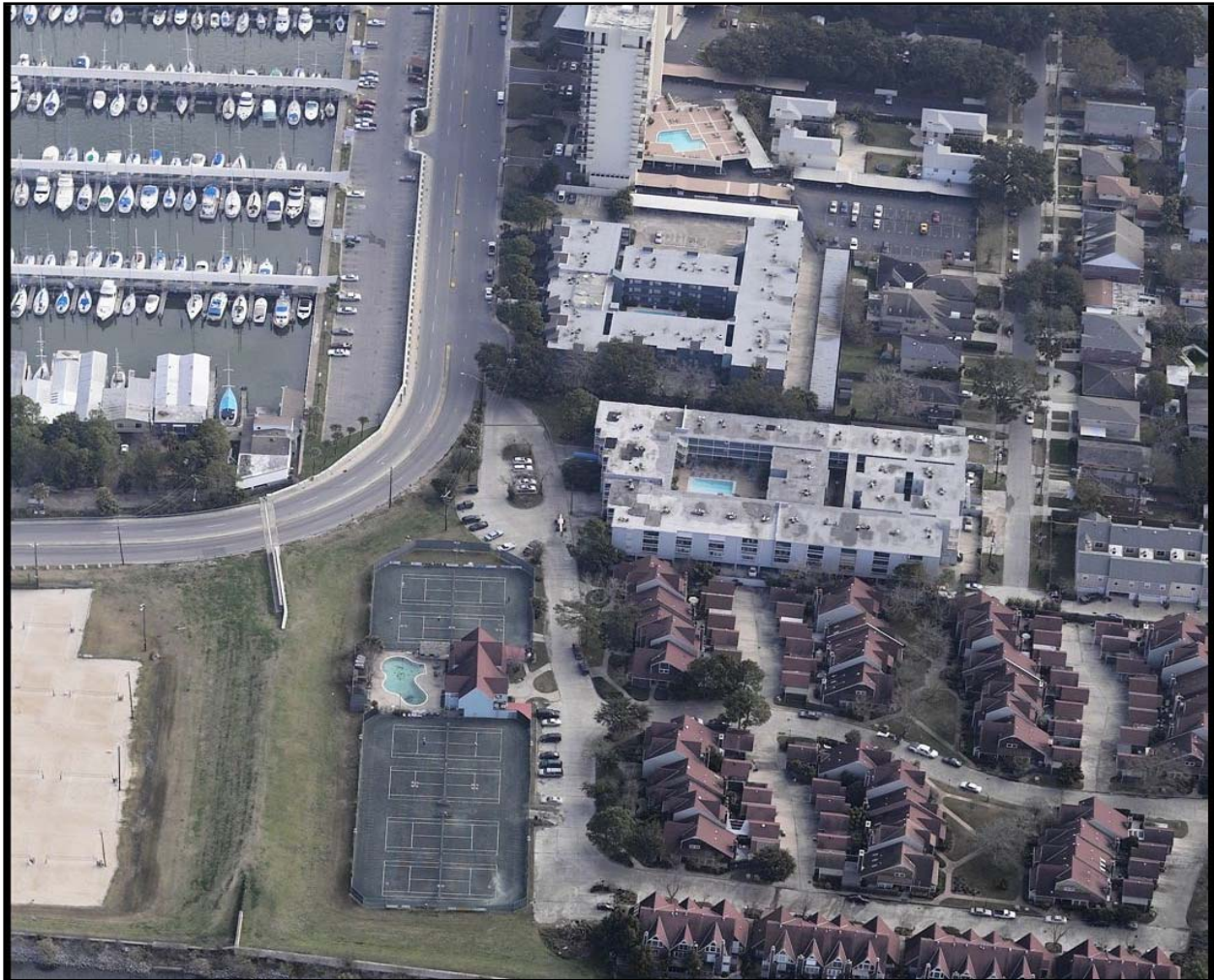
Reach 29



Reach 30 and 31



Reach 31



Reach 31 and 32

Section 6: Inner Harbor Navigation Canal (IHNC)

Narrative

The Inner Harbor Navigational Canal (IHNC) reach extends along the west side of the IHNC from the lock at St. Claude Avenue northward to Lake Pontchartrain. Flood protection along this reach consists of levee and floodwall. From Station 0+00.00 to Highway 90 (Station 118+85.00) the floodwall sustained minor damage in the form of scour along its base. Figure 8 shows the repair to the floodwall scour. The Levee and floodwall between Hwy 90 (Station 118+85.00) and Florida Ave (Station XX+XX.XX) sustained scour damage. In this area, the floodwall breached at N29 59.315 and W90 01.612. Figure 9 shows the repairs in the breached area. The floodwall between Florida Avenue and the Lock sustained damage along the base of the floodwall in the form of scour.



Repair to Scour Along Floodwall.



Repairs Along the IHNC Where The Floodwall Breached Levee Section.

Definition of Reaches

Reach 33-41 (now 61-65)– These reaches consists primarily of I-walls along the canal with a levee section at the Port of New Orleans facility. The elevations of the I-walls and lengths of reaches are shown below. There are fourteen transitions (Pump Stations 3 and 4) and thirty five gates in this reach.

<u>Reaches</u>	<u>Length</u>	<u>Elevations</u>
61	9,095	13.50
62	9,170	13.80
63	1,490	13.80
64	8,390	13.80
65	875	20.10

Elevation Stationing									
Section	Start	End	Structure	EL	Section/Point	Length	Avg Height		Weighted Average
1	31+05	46+00	I-Wall	14	S	1495	14	Reach 33	14.00
2	46+00	46+30	I-Wall Transition	14.0 - 14.25		30	14.125	↓	
3	46+30	61+00	I-Wall	14.25		1470	14	Reach 34	14.00
4	61+00	61+30	I-Wall Transition	14.25 - 14.5		30	14.375	↓	
5	61+30	76+00	I-Wall	14.5		1470	14.5	Reach 35	14.50
6	76+00	76+30	I-Wall Transition	14.5 - 14.75		30	14.625	↓	
7	76+30	90+70	I-Wall	14.75		1440	14.75	Reach 36	14.75
8	90+70	91+00	I-Wall Transition	14.75 - 15.0		30	14.875		
9	91+00	106+25	I-Wall	15		1525	15		
10	106+25	106+57	France Road Ramp	14.5		32	14.5		
11	106+57	106+84.5	I-Wall	15		27.5	15		
12	106+84.5	109+81.5	I-Wall	14.5		297	14.5		
13	109+81.5	110+37.5	Gate 1W / T-Wall	14		56	14		
14	110+37.5	112+15	I-Wall	14.5		177.5	14.5		
15	112+15	112+56	Gate 2W / T-Wall	14		41	14		
16	112+56	116+53	I-Wall	14.5		397	14.5		
17	116+53	118+85	I-Wall	15		232	15		
18	118+85	119+59	Hwy 90	17		74	17		
19	119+59	121+78.5	I-Wall	14.5		219.5	14.5		
20	121+78.5	122+07.5	Gate 3W	14		29	14		
21	122+07.5	124+88.5	I-Wall	14.5		281	14.5		
22	124+88.5	125+17.5	Gate 4W	14		29	14		
23	125+17.5	128+41.5	I-Wall	14.5		324	14.5		
24	128+41.5	128+70.5	Gate 5W	14		29	14		
25	128+70.5	130+53.5	I-Wall	14.5		183	14.5		
26	130+53.5	130+82.5	Gate 6W	14		29	14		
27	130+82.5	132+00	I-Wall	14.5		117.5	14.5		
28	132+00	135+31	I-Wall	15		331	15		
29	135+31	136+10	Gate 7W	14		79	14		
30	136+10	136+27	T-Wall	14		17	14		
31	136+27	136+94.5	Gate 8W	14		67.5	14		
32	136+94.5	137+42	I-Wall	15		46.5	15		
33	137+42	137+72	I-Wall	14.5		30	14.5		
34	137+72	141+20	Levee	15		348	15		
35	141+20	143+94	I-Wall	15		274	15		
36	143+94	144+01	T-Wall	14		7	14		
37	144+01	144+48	Gate 9W	14		47	14		
38	144+48	145+39	I-Wall	15		91	15		
39	145+39	145+76	I-Wall	14.5		37	14.5		
40	145+76	148+28	Levee	15		252	15		
41	148+28	210+10	I-Wall	15		6182	15		
			Double Hung Gates (France Rd Parkw	80					
42	210+10	210+89	T-Wall	14		79	14		
43	210+89	211+03	Gate 10W	14		14	14		
44	211+03	211+17	T-Wall	14		14	14		
45	211+17	211+46	I-Wall	15		29	15		
46	211+46	211+81	I-Wall	14.5		35	14.5	Reach 37	14.88
			France Road Ramp	14.5					
47	211+81	226+44	Levee	15		1463	15	Reach 38	15.00
48	226+44	226+60	I-Wall	15		16	15	↓	
49	226+60	235+77	T-wall	14		917	14	Reach 39	14.02
Start at Pump Station #14									
50		390	I-wall/Twall	15	Transition		Pumping Station #14		
51		2293	I-wall	13	Reach 40				
53		875	Levee	20	Reach 41		IHNC Lock		

Features

Elevation	Feature
13.25	Ramp east of France Road near Hickey Bridge
14.75	France Road Ramp near Chef Mentuer Hwy
6.25	Road Gate 7W
7.4	RR Gate 8W
9	Ramp to Bridge
4.75	RR Gate 9W
14.75	France Rd Ramp
4.25	Gate 10W - RR open

14.75	France Road Ramp
2.25	Gate in Levee at Port of NO
2.25	Gate in Levee at Port of NO
6	Pump Station near Florida Ave Bridge
14	LWT OM 22/23
5	Gate in France Road
7.25	Gate 1W road closed
7.55	Gate 2W RR open
9.5	Gate 3W access open
11.25	Gate 4W access open
11.25	Gate 5W access open
11.25	Gate 6W access open
6.25	Gate 7W road closed – damaged
7.4	Gate 8W RR open – Failed during Katrina
4.75	Gate 9W RR open – damaged
4.25	Double Gates - France Rd Parkway – damaged
4.25	Gate 10W - RR open – damaged
4.25	Gate in levee at Port of NO – Failed during Katrina
4.25	Gate in levee at Port of NO – Failed during Katrina
2.5	Gate in pier access – no damage
2.5	Gate in pier access – no damage
6	Gate next to pump station
2.25	Road closed – Florida Avenue Bridge Gate W20
2	RR closed
2.25	RR open – Gate W21
2.75	Road open – Florida Ave Bridge
7.45	Road open – Florida Avenue Wharf
4.45	RR open – Florida Avenue Wharf
7.25	Road open – Florida Avenue Wharf
8	Road open
8.25	Road open
7.5	Road open
1.75	Road open – Gate W6
2.35	RR closed – Gate W5
5.35	Road open – Gate W4
5.35	RR Access closed – Gate W3
3.5	Road open – Gate W2
2.25	Road open – Gate W1



Reach 33



Reach 33



Reach 33



Reach 33



Reach 33



Reach 33



Reach 33



Reach 34



Reach 34



Reach 35



Reach 35



Reach 35 and 36



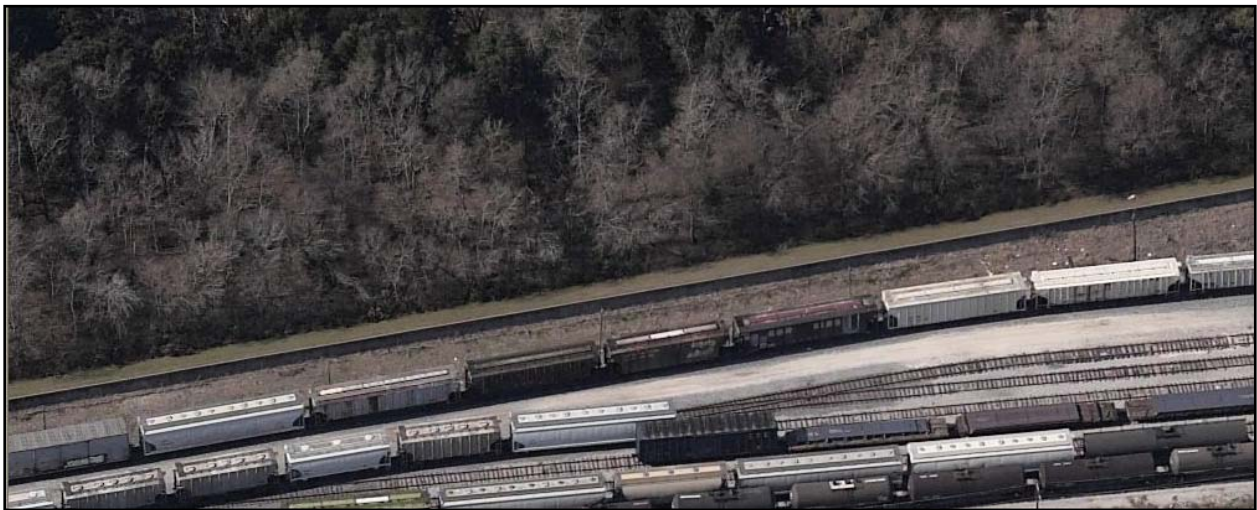
Reach 36



Reach 36



Reach 36



Reach 36



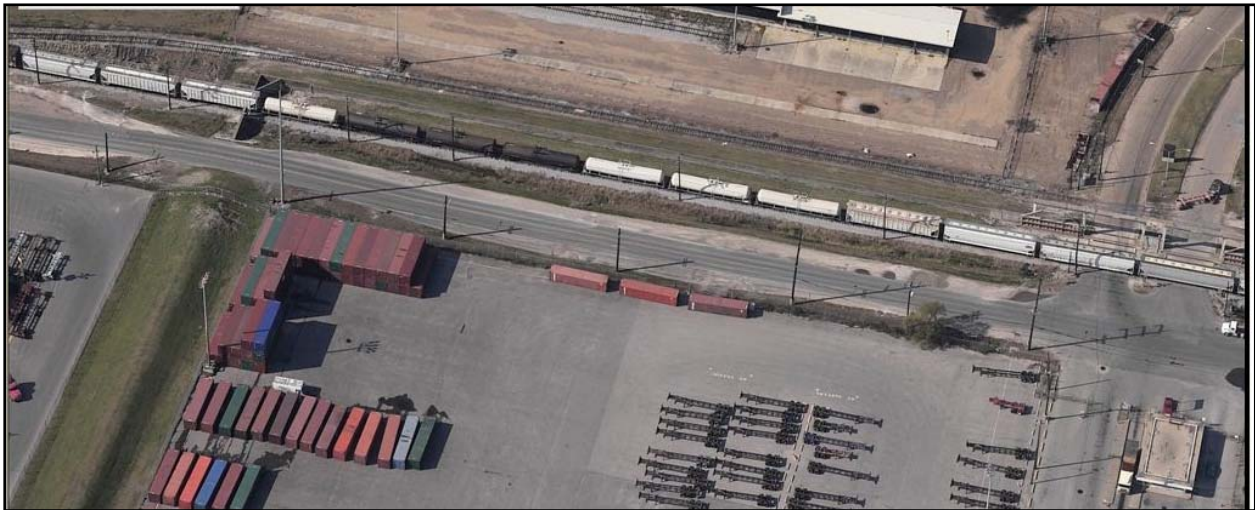
Reach 36



Reach 36



Reach 36



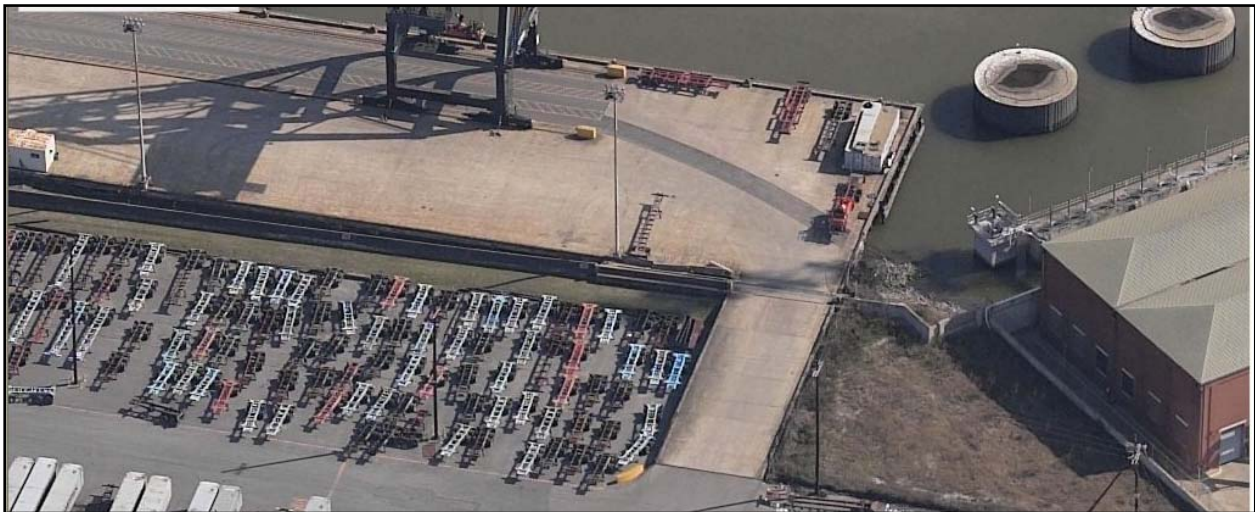
Reach 36 and 37



Reach 37



Reach 37



Reach 38



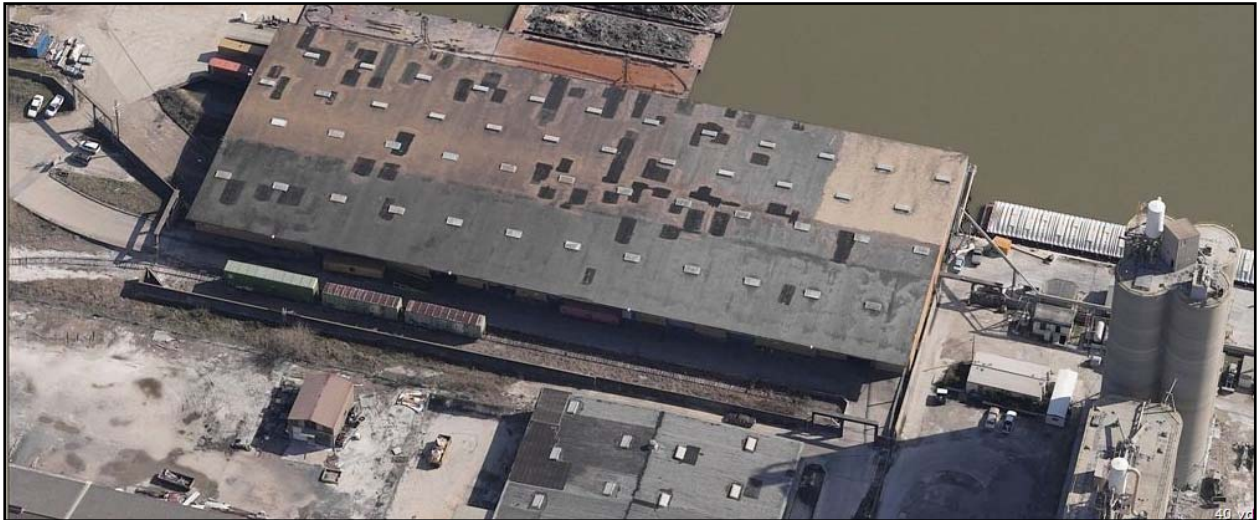
Reach 39



Reach 39



Reach 39



Reach 39



Reach 40



Reach 40



Reach 40



Reach 40



Reach 40



Reach 40



Reach 40



Reach 41

Section 7: Mississippi River and Levees (MRT)

References

General design information was not available for the MRT walls and levees within Orleans Parish at the time of the report. Information was gathered from discussion with the Orleans Parish Levee Board and from the field recon.

Narrative

The MRT connects to the IHNC at the navigation lock facility. The MRT structures consist of levees into the INHC lock, a series of flood walls (as shown below) that surround the City of

New Orleans up to the Port of New Orleans and a MRT levees from the Port of New Orleans to the Jefferson/Orleans Parish border.



Typical Area on the Mississippi River East Levee and Floodwall.

Definition of Reaches

Reach 42-50 (now 66-71) – These reaches consists primarily of I-walls with levees at the lakefront entrance on both on the east side of the London Avenue Canal at average elevation 14.0 feet with a length of approximately 12,130 feet, 3,880 feet, 12,765 feet and 3,030 feet respectively. There are two transitions (Pump Stations 3 and 4) and three gates in this reach.

Reaches	Length	Elevations
66	1,980	21.50
67	8,915	22.50
68	25,450	23.60
69	10,780	24.30
70	14,180	24.80
71	3,350	25.80

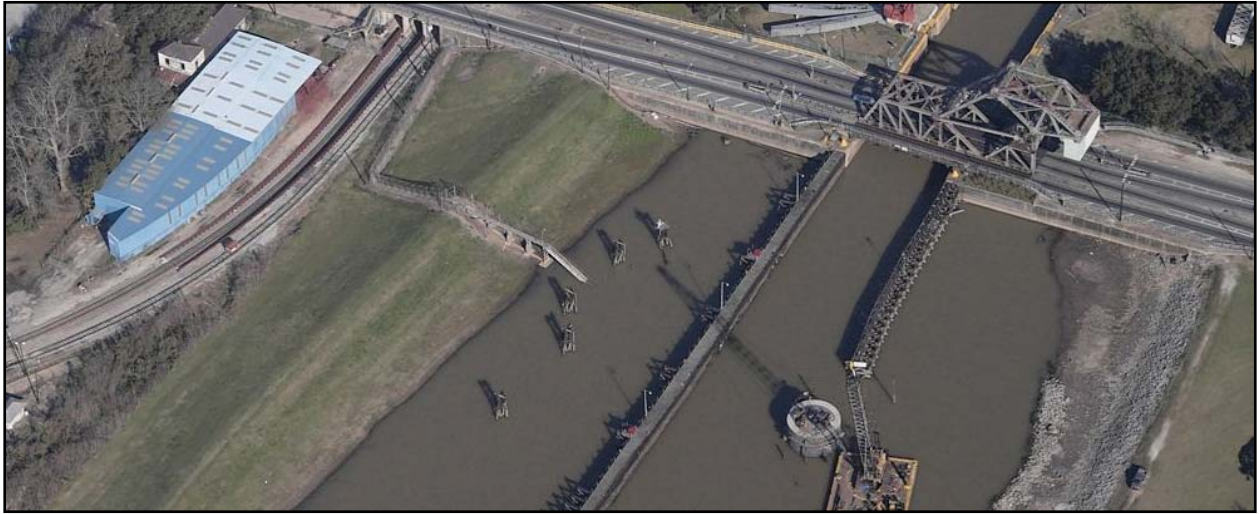
Section	Structure	EL	Length	Section/Point		Weighted Elevations
1	Levee	21	1774	S		21
2	I-Wall	17	19661	S	Reach 42	17
3	I-Wall	20	2951	S	Reach 43	20
4	I-wall	17	1469	S	Reach 44	
5	I-Wall	14	8371	S	↓	
6	I-Wall	17	3437	S	Reach 45	15.1
7	I-Wall	20	1843	S	↓	
8	I-Wall	18	5920	S	Reach 46	18.8
9	I-Wall	20	1902	S	Reach 47	
10	I-Wall	24	2961	S	Reach 48	
11	Levee	24	5917	S	Reach 49	24
12	Levee	20	2732	S	Reach 50	20
13	Levee	24	4526	S		24

Features

Elevation	Feature
7.5	Road Access — Off Poland Ave - Navy Complex
7.5	Road Access — Off Poland Ave - Navy Complex
7.5	RR Gate — Pauline St Wharf
7.5	Road Access — Pauline St Wharf
7.5	RR Gate — Pauline St Wharf
7.5	RR Gate — Off Charles St. – photo
7.5	Road Access — Off Charles St.
7.5	Road Access — Off Charles St.
7.5	RR Gate — Press St. Wharf
7.5	Road Access — Esplande St and Wharf
7.5	Road Access — To riverfront parking off N Peters
7.5	Road Access — To riverfront parking - St Peters
7.5	Road Access — To riverfront parking – Toulouse
7.5	Road Access — To riverfront parking - St. Louis
7.5	Road Access — To riverfront parking - Conti St
7.5	Road Access — To riverfront parking – Bienville
7.5	Pedestrian Crossing — North end of Riverwalk
7.5	Road Access — Convention Center openings
5	Road Access — Henderson Street
5	Road Access — Race Street
5	Road Access — Orange Street
5	Road Access — Celeste St – photo
5	Road Access — Port of NO - near Felicity St
5	Road Access — Port of NO - 3rd St
5	Road Access — Port of NO - Washington St
5	RR Gate — Port of NO - across from 9th ST
5	Road Access — Port of NO
5	RR Gate — Port of NO
7.5	Road Access — Port of NO - Louisiana Ave
7.5	Road Access — Port of NO
7.5	RR Gate — Port of NO - Napoleon Ave
7.5	Road Access — Port of NO - Warehouse Rd
7.5	Road Access — Port of NO
7.5	Road Access — Port of NO - Coffee Dr

7.5
7.5

Road Access — Port of NO - Leake Ave
Road Access — Port of NO - Henry Clay Dr



Reach 42



Reach 42



Reach 43



Reach 43



Reach 43



Reach 43



Reach 43



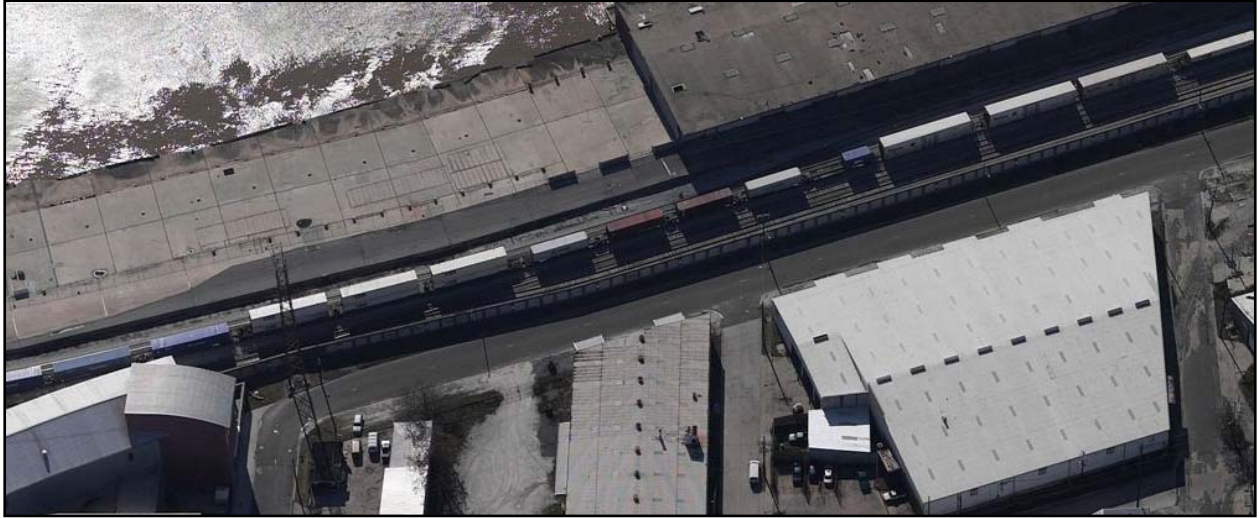
Reach 43



Reach 43



Reach 43



Reach 43



Reach 43



Reach 44



Reach 44



Reach 44



Reach 44



Reach 45



Reach 45



Reach 45



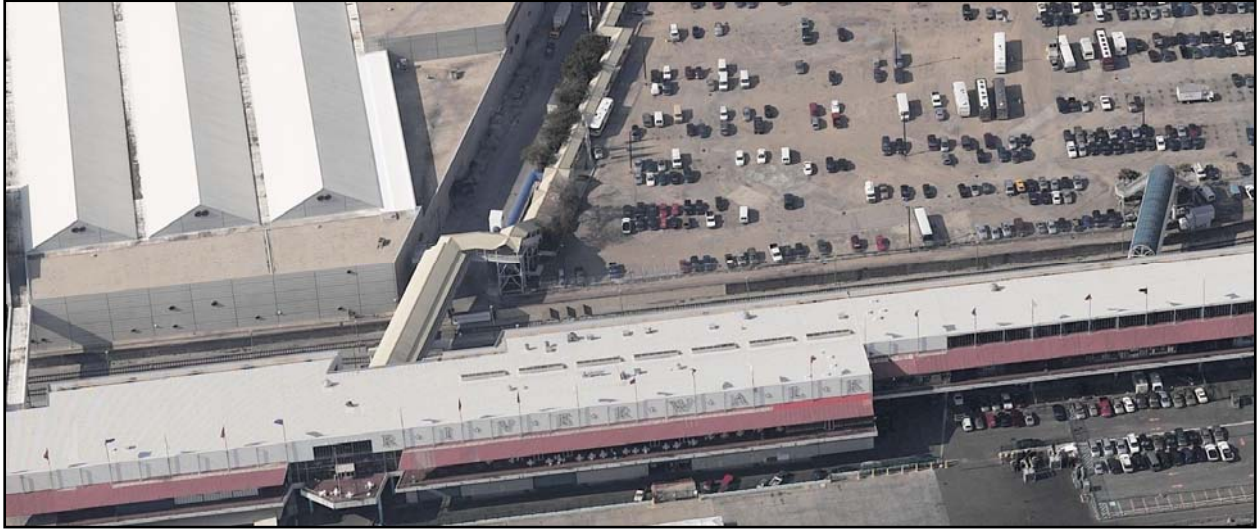
Reach 45



Reach 45



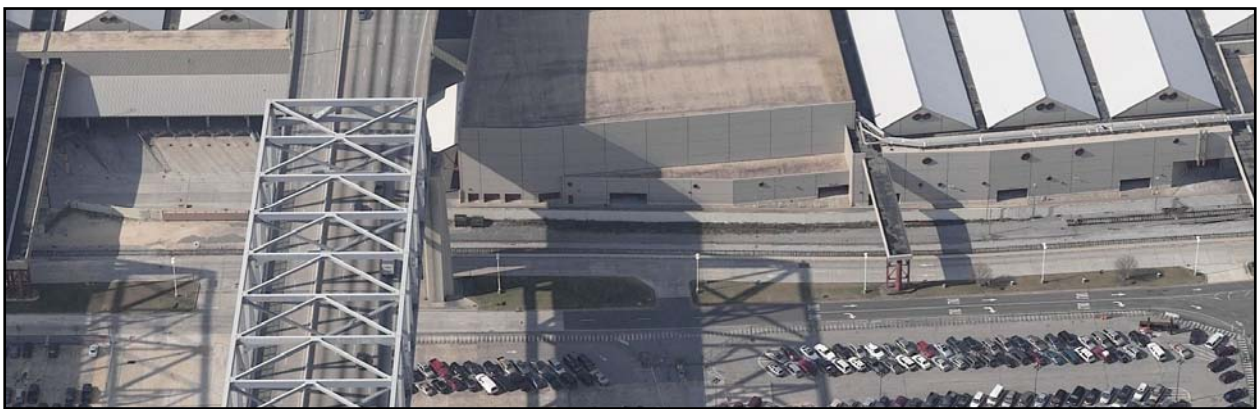
Reach 45



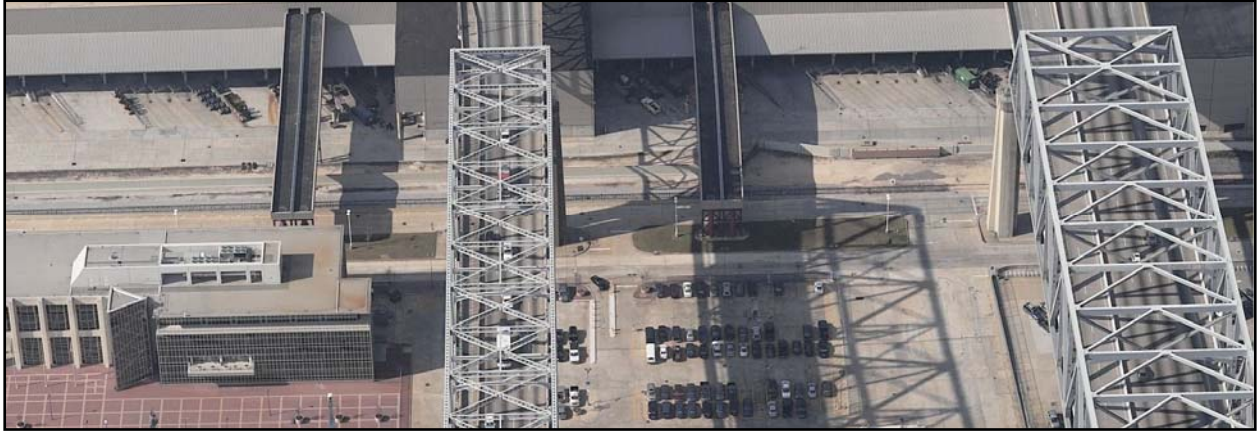
Reach 45



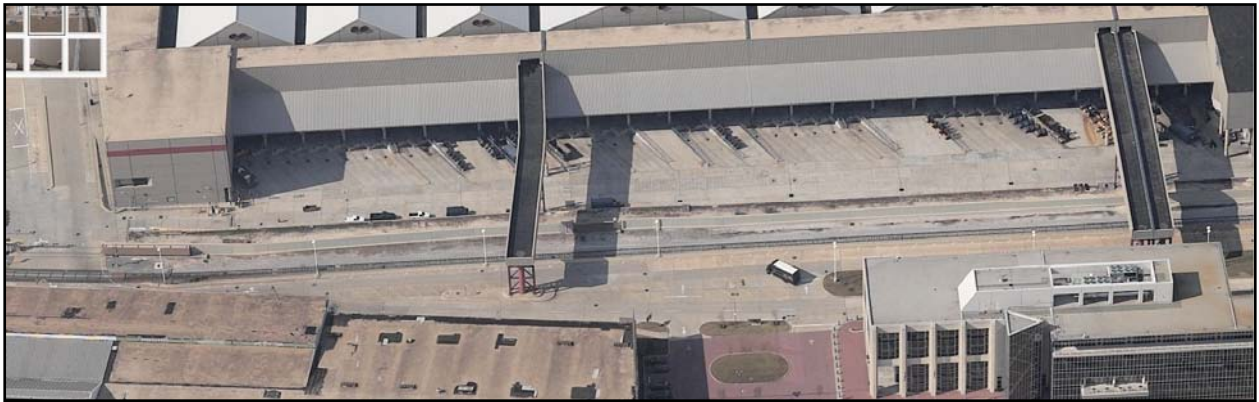
Reach 45



Reach 45



Reach 45



Reach 45



Reach 46 and 47



Reach 47



Reach 47



Reach 47



Reach 47



Reach 47 and 48



Reach 48



Reach 48



Reach 48



Reach 48



Reach 48



Reach 48



Reach 48



Reach 48



Reach 48



Reach 49



Reach 50

Orleans West Bank

The Orleans Parish West Bank Basin is composed of two sub-basins (Figure 1). These are located on either side of the upper end of the Algiers. OW1, on the west side of Algiers Canal, was designed as part of the Algiers Canal to Hero Canal Project. OW2, on the east side of the Algiers Canal, was designed as part of the Harvey Canal to Algiers Project.



Figure 1. Orleans Parish West Bank Basin with sub-basins (OW1 and OW2)

OW1

Orleans West Bank – OW1 (Algiers Canal to Hero Canal Project)

Sub-basin OW1, as shown above, is located on the west bank of the Mississippi River in Orleans Parish and is generally bounded by a portion of the Algiers Canal, the Mississippi River and the Orleans-Plaquemines Parish line. Topography is flat with ground elevations ranging from +5 feet NGVD on the alluvial ridges along the Mississippi River to -7 feet NGVD in the interior of the area. Approximately 40 percent of the area is below sea level. The surface area is 4.7 square miles. The sub-basin area is protected by 15.0 miles of levees and floodwalls. There

are no floodgates, drainage structures or control structures in the protection system. There is one pumping station that drains the protected area (NOS&WB Pumping Station #11 at location 29.90962 -89.978).

Segment 1 is a low, all earth (clay) non-federal levee separating Orleans Parish from Jefferson Parish. It extends from the main line Mississippi River levee (MRL) inside the US Coast Guard Station to the Algiers Canal levee with an elevation of 3–4 ft NVGD.







**Back levee continues inside
US Coast Guard Station**

**Back levee crossed by roadway inside
US Coast Guard Station. Roadway is 2 feet
lower than levee. No closure structure**



Back levee continues outside US Coast Guard toward GIWW Station. Crown is rutted



Drainage structure under Back Levee outside US Coast Guard station. Screw gate closure on culvert



**Back Levee intersects Hwy 406 looking toward the
GIWW and General De Gaulle Bride overpass.**

**Back Levee intersects Hwy 406.
No closure at Hwy**



Segment 2 is the East bank of the Algiers Canal levee that extends between the local interior levee (Segment 1) and the Algiers Lock. This 9.5 ft NVGD clay levee is interrupted by a floodwall segment that crosses in front of NOS&WB Pumping Station #11.



Abandoned pipe crossing through the Algiers Canal



Typical Algiers Canal levee; no armor



South end of Algiers Lock

Segment 3 is the Orleans West Levee District Mississippi River levee. This levee segment closes the North and East side of the sub-basin. It extends from the GIWW and Mississippi River intersection to where it intersects the interior levee (Segment 1) inside the US Coast Guard Station. The MRL is an all clay levee with crushed stone surfacing on the 10-ft wide crown at elevation 22 ft NVGD.





Pipe crossing along MRL just east of GIWW and MRL intersection



Barge sitting on foot of MRL



OW2

Orleans West Bank – OW2 (Harvey Canal to Algiers Canal)

Sub-basin OW2, as shown in figure above, is located on the west bank of the Mississippi River in Orleans Parish. It is generally bounded by the Mississippi River, the Algiers Canal, and the Orleans-Jefferson-Plaquemines Parish boundary. The topography is flat with ground elevations ranging from +10 feet NGVD on the alluvial ridges along the Mississippi River to -5 feet NGVD in the interior of the area. Approximately 25 percent of the area is below sea level. The surface area is 6.3 square miles and the population is approximately 57,000. The sub-basin is protected by 12.6 miles of levees and floodwalls.

Segment 1 is a clay, non-federal levee that begins at the Greater New Orleans Bridge (US 90) crossing of the Mississippi River Levee and runs along the Orleans-Jefferson Parish line to the Algiers Canal levee, near the NOS&WB Pump Station #13. This interior levee is approximately 4 miles long and is at elevation 3–4 ft NGCD.

Segment 2 is the West bank of the Algiers Canal levee (GIWW) that extends between the local interior levee and the Algiers Lock. This clay levee is interrupted by a floodwall segment that crosses in front of NOS & WB Pumping Station #13. It is 1.8 miles long at elevation 9.5 ft NGVD.

Segment 3 is the Orleans West Levee District Mississippi River Levee extending from the Algiers Canal Lock west to the Orleans Parish Line (beneath the Greater New Orleans Bridge, US 90), completing the sub-basin. This MRL is a predominately all clay levee with small reaches of short concrete I-Walls atop the clay levee base. It is 6.8 miles long at elevation 22-23.5 ft NGVD. There are no floodgates, drainage culverts or control structures in the protection system. There is one pumping station that drains the protected area (NOS & WB Pumping Station #13 at location 29.8959, -89.9978).

Risk Model Idealization

The West BankHPS was discretized into two sub-basins (OW 1 and OW 2) as shown in Figure 2. The sub-basins were defined to correspond to the known interior drainage areas. This reach idealization follows from the basin description information presented above, which was collected from project documents and field inspections. Figure 3 shows the elevations for the Orleans Parish West Bank HPS: **Pre-Katrina**—at the time of Katrina, **Current**—as of 1 June 2007, and the **Authorized** system (authorized at the time of Katrina).



Figure 2. Orleans Parrish West bank Basin reaches (HA1,HA 5-HA9) and sub-basins (OW 1 and OW 2) definition for use in the risk model.

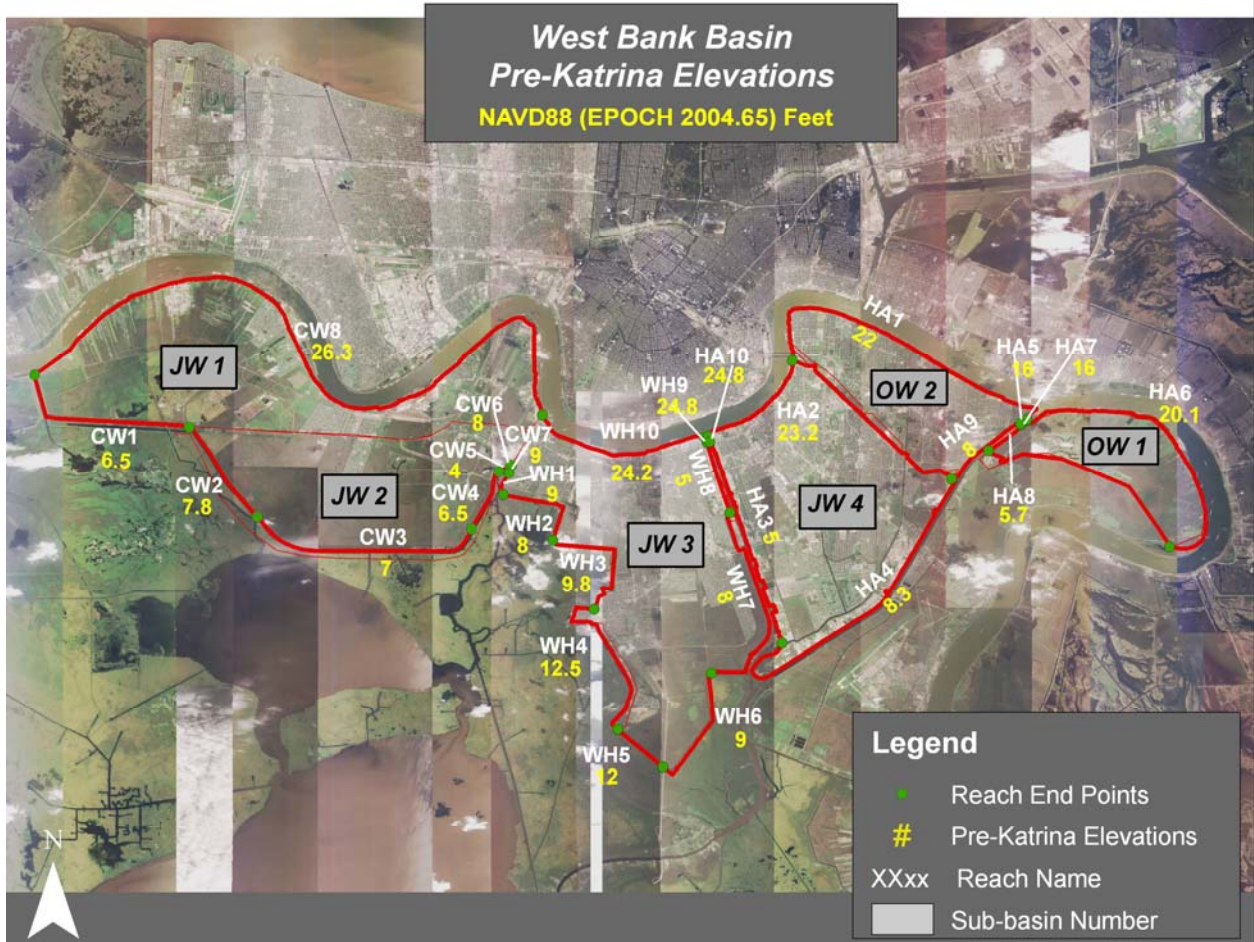


Figure 3. Elevations for the Orleans Parrish West Bank (OW1 and OW2) for the Pre-Katrina HPS (in place when Katrina occurred), the Current HPS (as of 1 June 2007), and the Authorized HPS (authorized at the time Katrina occurred) (continued)

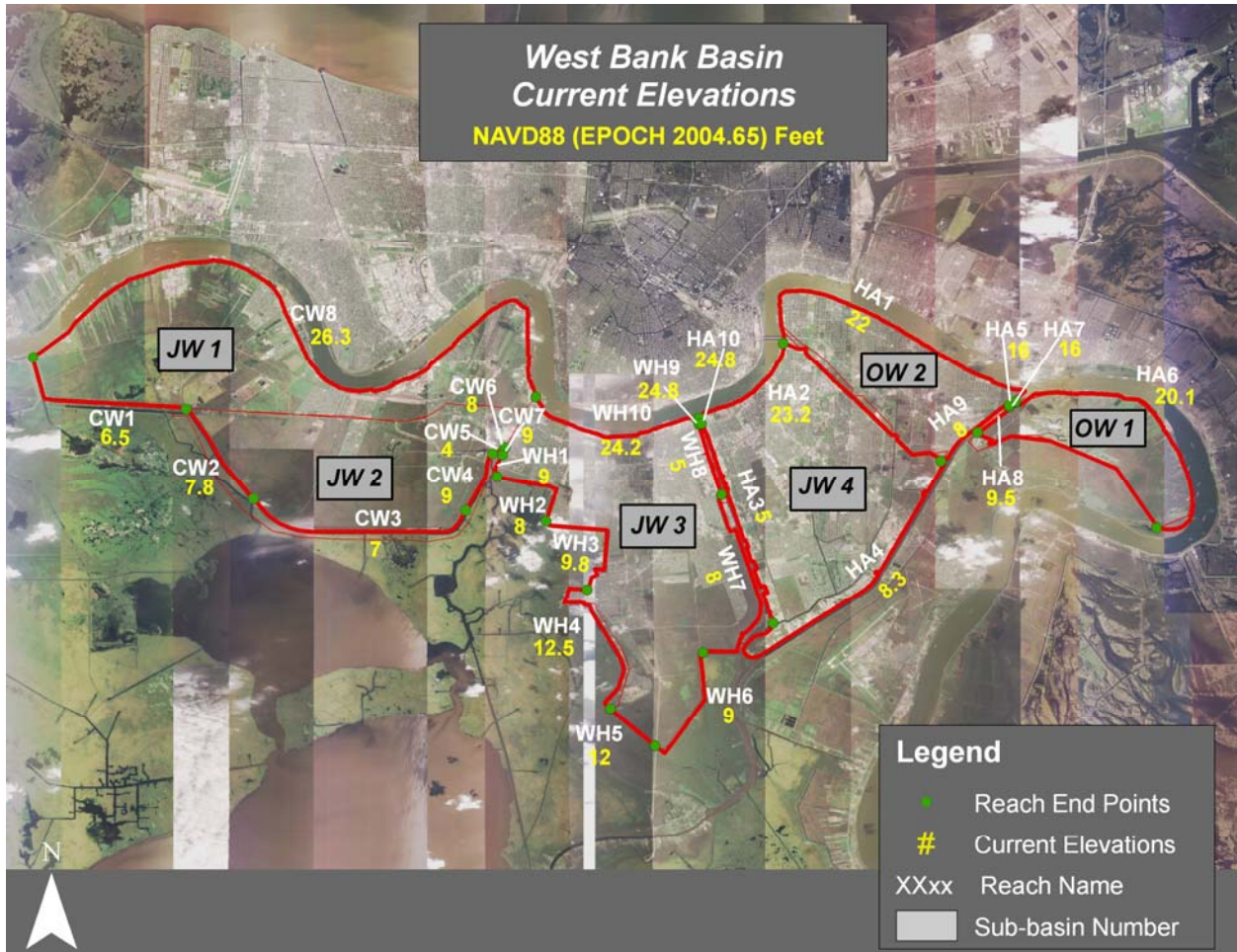


Figure 3. Continued

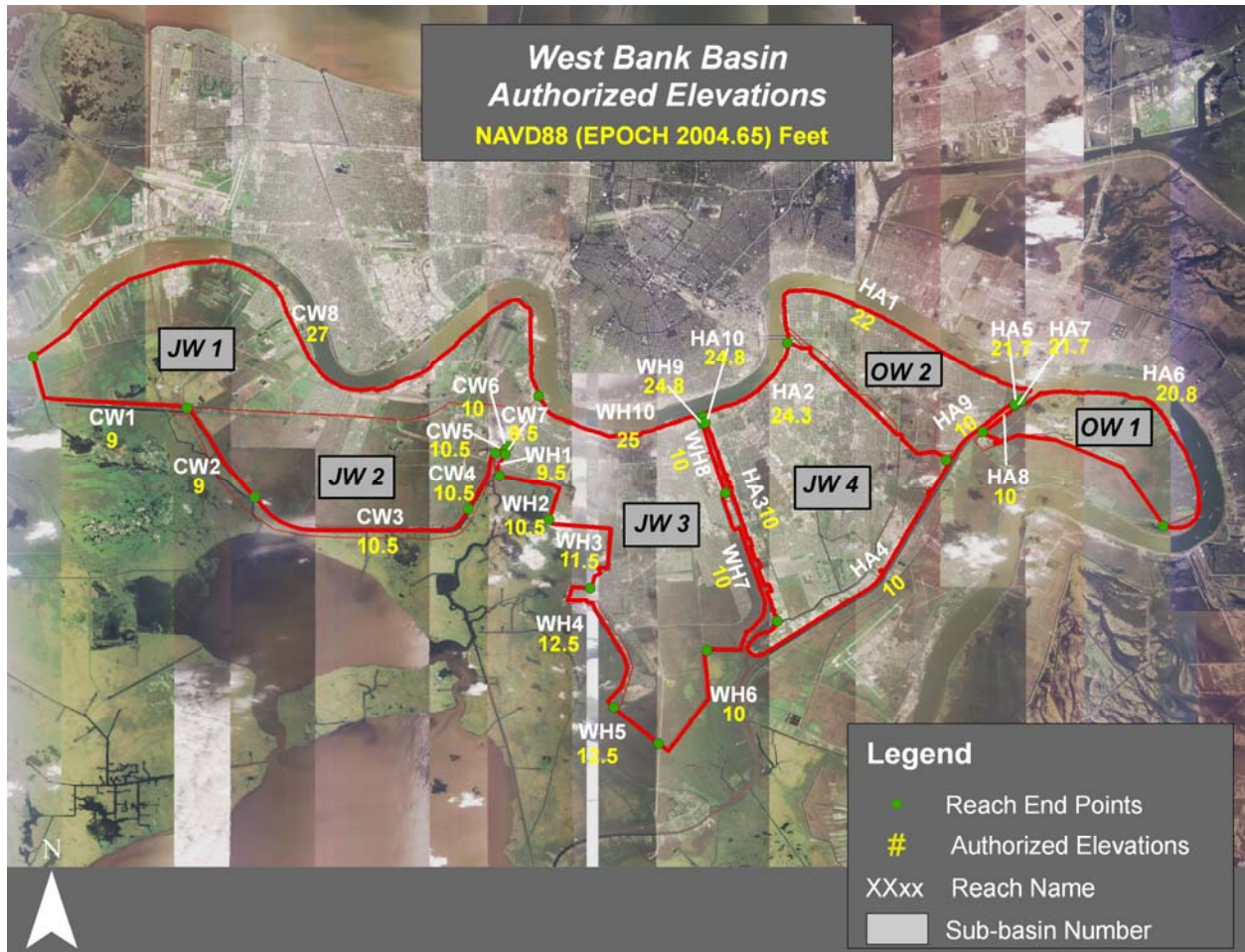


Figure 3. Concluded

Appendix 8

Hazard Analysis

Introduction

This appendix includes several components. First is an overall discussion of the Hazard Analysis modeling effort, describing the surge (ADCIRC) and wave (WAM, STWAVE) modeling. That first section is followed by a subsidiary section labeled Appendix 8-1 that defines the many acronyms used in the modeling discussion. This is followed by a major section labeled Appendix 8-2 consisting of the Whitepaper of Donald T. Resio, ERDC-CHL, which forms the basis of the storm statistics and JPM methods discussed in the main body of the report. Owing to its prominence in the discussion, it has, for convenience, been referred to as R2007. Note that R2007, itself, includes several appendices; these are identified as Appendices A-G within Appendix 8-2. Finally, a discussion of the rainfall model is included here as Appendix 8-3.

Hazard Analysis

The hazard analysis required for the risk assessment was based upon the hurricane modeling conducted by a team of Corps of Engineers, FEMA, NOAA, private sector and academic researchers working toward the definition of a new system for estimating hurricane surges and waves. Following is a discussion of the processes used by this team and the steps taken by the risk team to incorporate the results into the risk analysis.

The hurricane hazard definition required as input to the risk analysis involved several steps:

1. Selection of the methodology to be used for estimating surges and waves
2. Determination of hurricane probabilities
3. Production of the ADCIRC grid models for the different HPS configurations.
4. Production of the computer system for development of the large number of hydrographs required by the risk model.
5. Formatting of the ADCIRC/STWAVE hydrographs for input to the risk computer model
6. Determination of the rainfall volumes expected for each hurricane

The hurricane modeling resulted in a total of 152 storms that were used in the risk analysis. Of these storms, frequencies were developed by the storm team for only 77 storms. The storm parameters and their frequency of occurrence are shown in Table 8-1.

Methodology for Hurricane Modeling

At least five methods have been applied in past studies of environmental extremes due to hurricanes in the United States:

1. Formulation of design storm events
2. Estimates based only on historical storms
3. The empirical simulation technique (EST)
4. The joint probability method (JPM) and
5. The Empirical Track Model

All of the methods referenced above have different strengths and weaknesses for various applications. Appendix 2 (R2007) includes a complete discussion of each of these methods. It considers includes the following topics:

1. Potential extensions of probabilistic methods to future hurricane surges,
2. The JPM with Optimal Sampling (JPM-OS); and
3. A computational methodology for effective simulation of storm surges for hurricane inundation studies.

In each method, it is important to understand that two different statistical measures are required to characterize the expected extremes over an interval of time. The first of these is the measure of the expected values of the distribution and the second is a measure of expected dispersion around these central values.

Hydrograph Production System

Overview

On-going projects for storm-surge and inundation mapping along the US Gulf of Mexico coast require the computation of many simulations using state-of-the-art numerical models and high-performance computational facilities. In this context, the storm-surge model ADCIRC and spectral wave model STWAVE are used in a “coupled” scenario to improve upon the storm surge solutions provided by ADCIRC. Coupling of the models is done through input/output file exchange between the numerical models. The water level and wind field from ADCIRC are provided in the appropriate form for the spectral wave model STWAVE. STWAVE computes the high-frequency wave field, including the wave radiation stress associated with the storm (wind) and simulated water level. This wave radiation stress is then passed to the next ADCIRC simulation as an additional forcing term, in conjunction with the storm wind and pressure field. This model communication through file I/O achieves a first-order coupling of the non-linear interaction between the wind-induced storm-surge and the wind-driven higher frequency wave fields.

The primary difficulty with the large number of compute-resource-intensive simulations required by these projects is ensuring that each simulation uses the correct files and that the compute-jobs run to completion with as little intervention as possible. Avoiding human interaction is critical to prevent errors in file input, compute-job staging, and post-processing. To address this problem, a software system has been developed to prepare each required simulation and submit each simulation to the compute-resource job manager. Basic graphics/visualizations and archiving are included to aid in QA/QC procedures and permanent storage of the computed results.

This document describes the software production system developed for coupled ADCIRC/STWAVE simulations. The software manages the gathering and preparation of input files for the ADCIRC/STWAVE models, and writes the job control script that the user submits to the host machine job manager (e.g., LSF, PBS, LoadLeveler). The production management software is written in the scripting languages *perl* and *bash*. Technical details of the script procedures and operations are reported in a separate technical report.

The primary requirements for the production system are independently verified and validated numerical models; tested and verified model grids; and runtime inputs to the models (forcing functions). Input files that provide initial conditions and forcing functions to the ADCIRC/STWAVE system are required to be pre-computed. This includes the storm realization (wind and pressure fields computed by the Ocean Weather PBL model) and the wave energy spectra for each storm (computed by the WAM model and interpolated onto the STWAVE model boundaries).

Computer system

The components of the production system are independent of the UNIX HPC computer system used, and can be set up on any system with accessible processing elements, large disk and storage capacity, and a job controller (Load Sharing Facility, Portable Batch System, LoadLeveler, etc). The scripting language *perl* and shell language *bash* must exist on the computer system (which is generally the case on Linux-based systems). Additional software packages (GNUplot, GMT) are used to facilitate post-simulation graphical analysis of the solutions.

The production system has been developed on the ERDC Cray XT3 (Sapphire) and the University of Texas Dell cluster LoneStar. However, the system is easily portable to other high-performance computing facilities with minor changes to the scripts and job controller/manager configurations. This has been tested several times on the following system/job scheduler combinations: NAVO IBM P5 (*Babbage*)/LSF, LONI IBM P5 (*Neptune*)/LoadLeveler, Cray Research Cray XT3 (*Salmon*)/PBS.

For the 2005, 2007, and 2010 (LACPR) simulations, the ERDC Cray XT3 *Sapphire* and University of Texas Dell cluster *LoneStar* were used for the computations. The only required changes to the scripts and setup are the specification of different job control parameters and a different home directory for the system. The basic computer system characteristics for *Sapphire* and *LoneStar* are shown in Table A.

Table A: Basic configurations of the High-Performance Computer systems used for the LACPR storm-surge simulations. On 9 April, 2007, the ERDC Cray XT3 Sapphire returned to service after a major hardware upgrade and several related software changes. Its current configuration is indicated in parentheses in the table.

System	ERDC Cray XT3 <i>Sapphire</i>	University of Texas Dell <i>LoneStar</i>
Operating System	SUSE Linux & UNICOS/lc	CentOS Linux
Compute-Nodes	AMD Opteron 2.6GHz single-core, single-processor (dual core, single-processor)	Intel Xeon 5100 series 2.66GHz dual-core, dual-processor
Number of Nodes/Processors	4176/4176 (4096/8192)	1300/5200
Parallel Filesystem (/work)	Lustre	Lustre
Compute-Job Controller	LSF (PBS)	LSF
Website	www.erdchpc.mil	www.tacc.utexas.edu

Numerical Models in the Production System

The “coupled” approach to the required storm-surge solutions uses the shallow-water finite element surge model ADCIRC (Luettich and Westerink, 2004) in conjunction with the steady-state spectral wave model STWAVE (Smith et al, 2001). Software versions are 46_48 and greater, and ep_110306 and greater, for ADCIRC and STWAVE respectively. Figure A shows the extents of the three models’ grids. The ADCIRC grids (boundary drawn in black) cover the western North Atlantic Ocean, with the only open boundary at 60 deg west. All ADCIRC grids in this project use the same footprint and general coverage. Only the details in the Louisiana and surrounding regions differ. The Ocean Weather PBL model boundary is shown in red, covering the Gulf of Mexico and 0.05 degrees resolution. ADCIRC interpolates the PBL grid to the ADCIRC grid and pads the far-field extent with background values. The STWAVE grid boundaries (blue) are shown along the Louisiana, Alabama, and Mississippi coasts. The Lake Pontchartrain domain is barely visible at this scale.

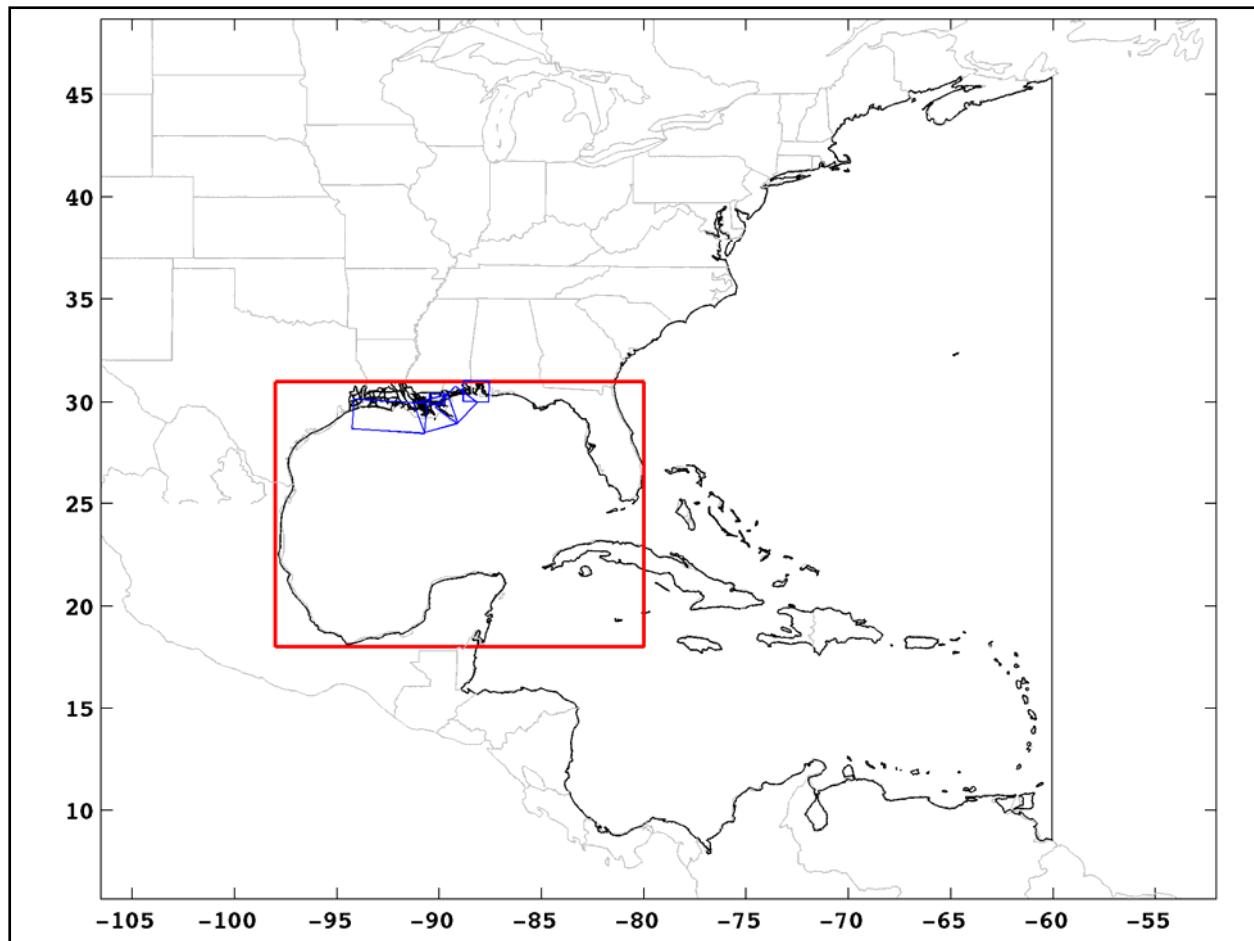


Figure A. Footprints of the various model domains for the coupled ADCIRC/STWAVE system. ADCIRC, OWI/PBL, and STWAVE grid boundaries are shown in black, red, and blue respectively.

Surge Model – ADCIRC

The storm surge model ADCIRC is a state-of-the-art model that solves the generalized wave-continuity equation on linear triangular elements. The depth-integrated (2D) implementation is used, where the water level and depth-averaged velocity are solved for at each triangle vertex (node), after complete specification of the initial conditions and time history of the boundary conditions (forcing). The finite element grids used in this project are the SL15 grid sequence for the 2005, 2007, and 2010 levee configurations. There are approximately 2.1 million horizontal nodes and 4.2 million elements in this sequence of grids. Ninety percent of the computational grid nodes are within the region shown in Figure B1. The computational domain is decomposed into 256 sub-domains, and each sub-domain problem is allocated to a separate computing processor. Inter-domain communication of boundary data is handled through MPI. Each solution is computed with a timestep of 1 second. A detail of the finite element grid is shown in Figure B2 for the New Orleans East area.

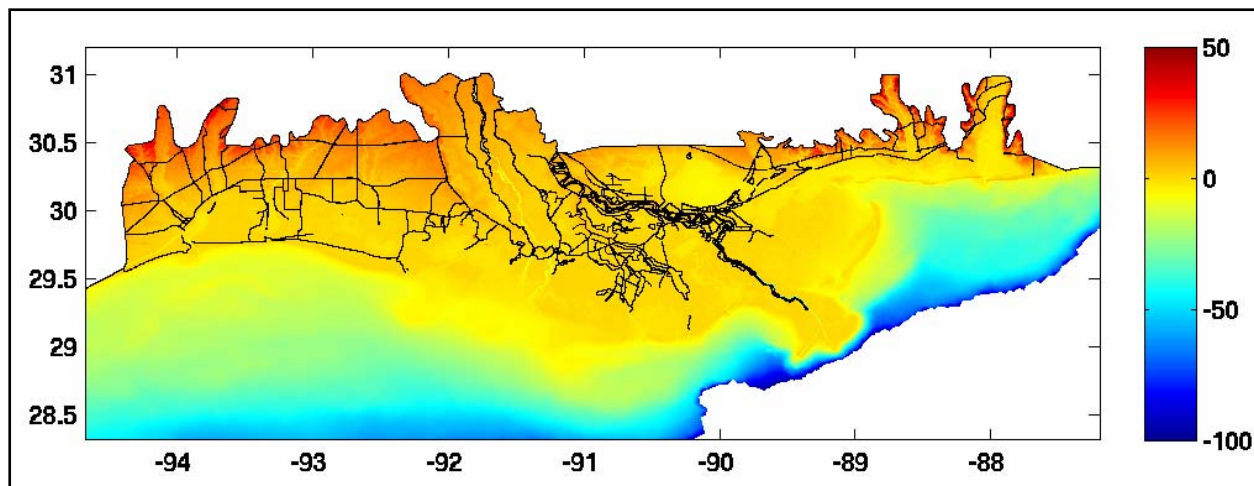


Figure B1. ADCIRC bathymetry (in meters) for the SL15 grids along the northern Gulf of Mexico coast. In this image, the bathymetry is clipped at -100 meters for display purposes. Each of the SL15 grids, for the 2005, 2007, and 2010 simulation sets has details that are not discernable at this scale shown.

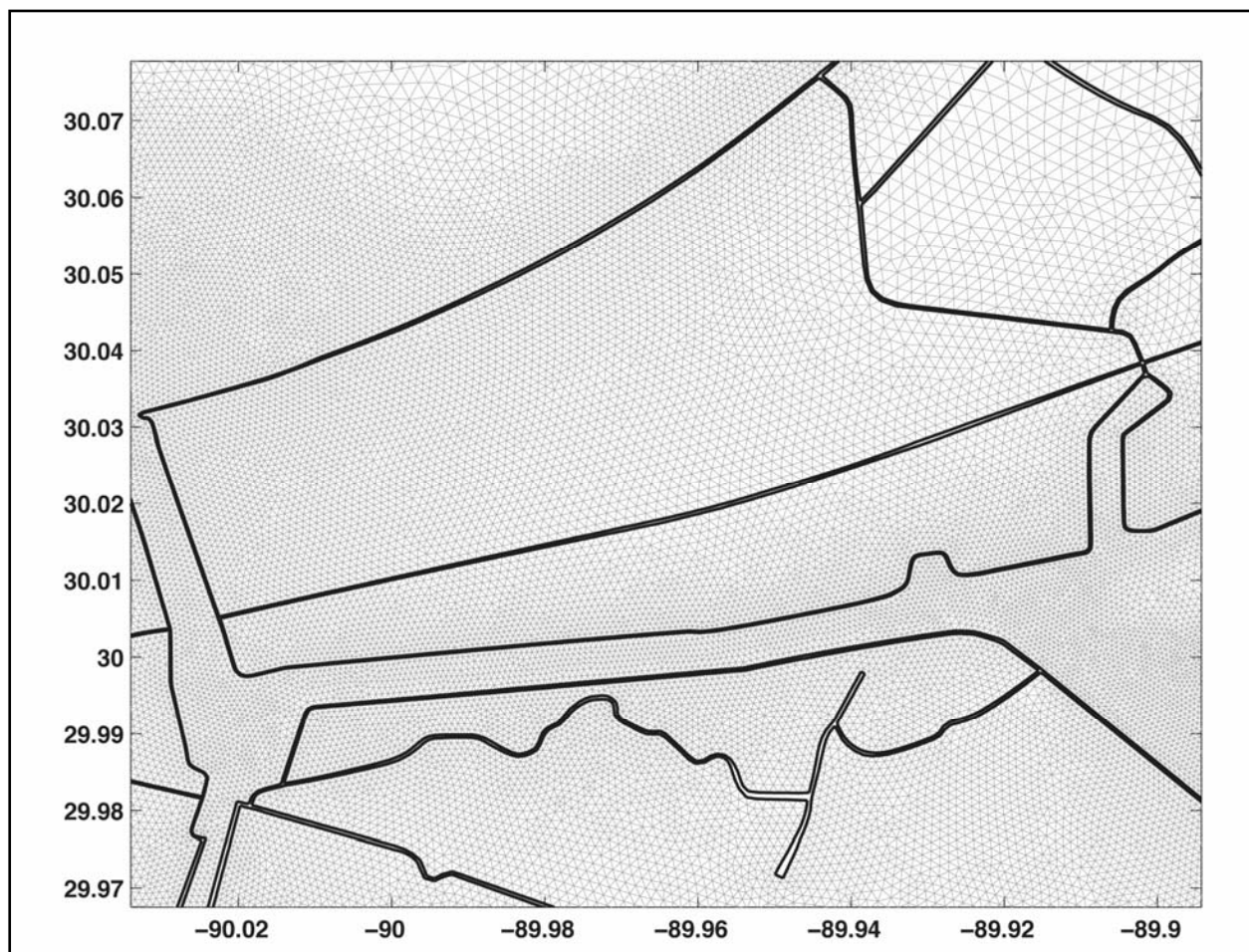


Figure B2. ADCIRC grid detail in the New Orleans East area. The solution is computed at the vertex of each triangle, and the thick black line is the model boundary. Weir boundary conditions are applied at the boundaries shown in this image.

Wave model – STWAVE

Five STWAVE grids are used in the current production system implementation covering the Louisiana, Mississippi and Alabama coastal region. (The “west” W grid is not used for the LA EAST simulations.) The boundaries of the domains are shown in Figure C. The spatial resolution of each STWAVE grid is 200 meters, and the temporal resolution is set to 30 minutes. The parallel STWAVE implementation is used in this system. In this version, each wave field snapshot is solved for on a separate processing element (cpu). The half-plane STWAVE is used for the South (S), Mississippi-Alabama (MS-AL), Southeast (SE) and West (W) grids. The full-plane STWAVE model is used for the Lake Pontchartrain domain.

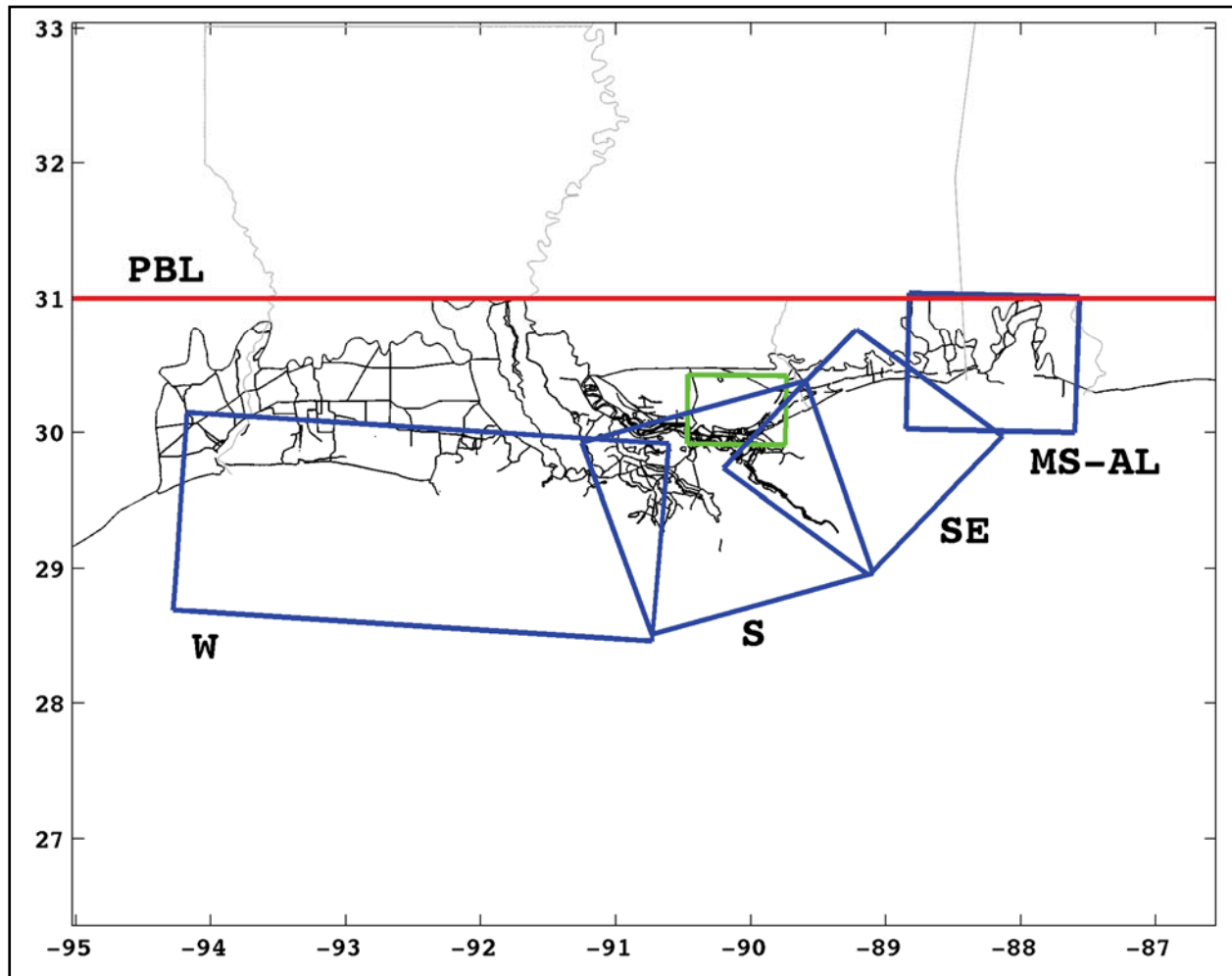


Figure C. Boundaries of the five STWAVE model domains and the PBL wind model northern extent (red) used in the current implementation of the production simulation system. The ADCIRC grid boundary is also shown (black) for one of the production grids. The Lake Pontchartrain (in green and not labeled) simulations use the full-plane STWAVE version; the other domains use the half-plane STWAVE. The “W” west grid is used in the LAWEST simulations, but not in the LAEAST simulations. The actual STWAVE grids to use for a specific simulation are a configurable part of the system.

Initial Condition to Storm Simulations (River Spinup)

The initial condition for the storm-surge simulations is an ADCIRC solution that provides a background river discharge on the Mississippi and Atchafalaya Rivers. River inflow to the Mississippi River at Baton Rouge and to the Atchafalaya River at Simmesport is specified as a flux per unit width as defined by a wave radiation boundary. The radiation condition is based on the relationship between the normal flow and elevation at the boundary. The river condition is spun up for 2.0 simulation days, with forcing of normal flow specified at the head of the rivers. A two-day spin up period with a half-day hyperbolic ramping function is applied to the river boundary forcing prior to any additional model forcing. While the solution has not quite reached a steady state after this period, the subsequent wind-driven solutions continue this river spinup, and the river stages reach steady state over the next simulation day. The water elevations at the default sampling locations within the two rivers are shown in Figure D. This initial condition is a pre-computed requirement to each storm-driven simulation.

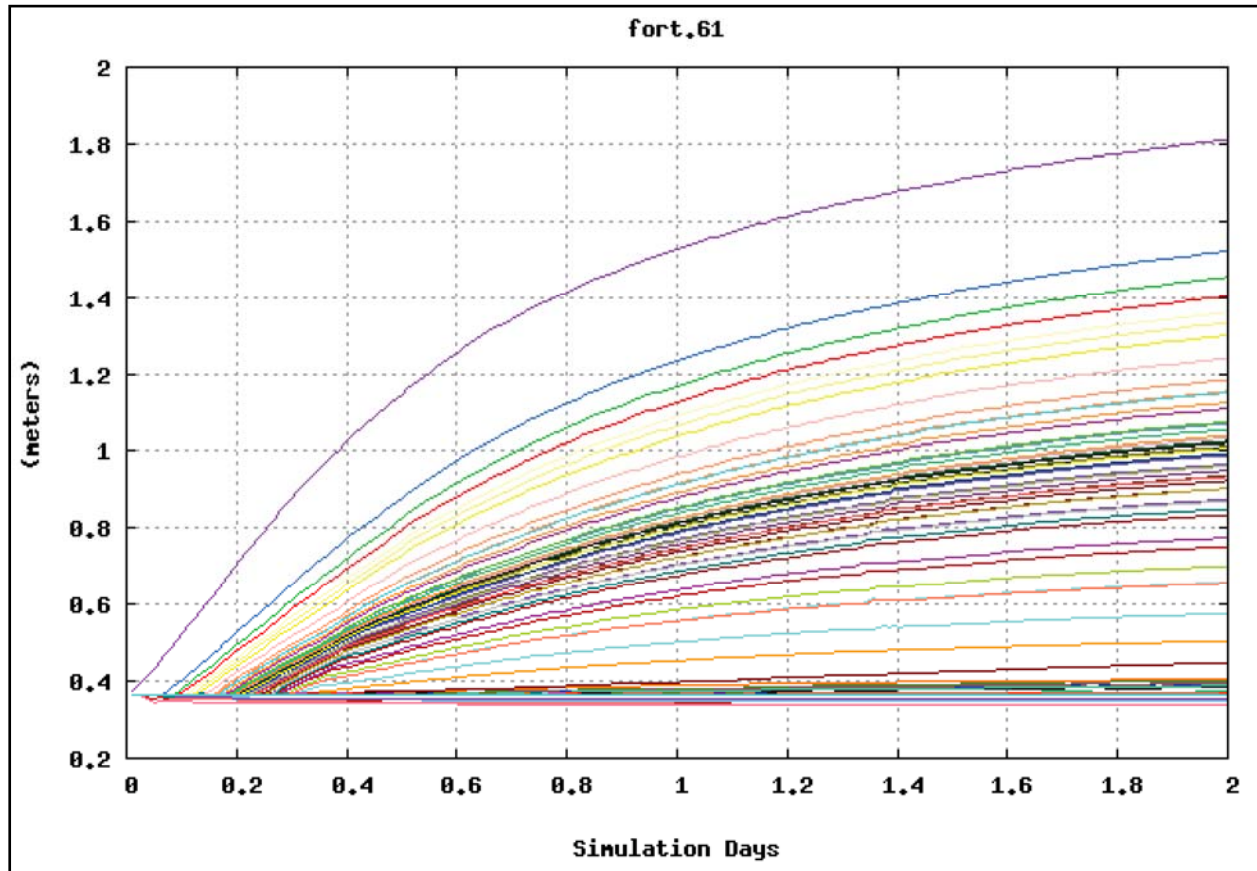


Figure D. Water elevations along the Mississippi and Atchafalaya Rivers showing the spinup of the initial condition. This solution is driven by volume fluxes across the open boundary on the two rivers. The discharge is ramped up over the first 0.5 days. The maximum elevation reached at the top of the Mississippi River is 1.84 meters.

Wind Fields for Storms

The primary inputs to the production system are the wind and pressure fields generated by application of the Ocean Weather Planetary Boundary Layer (PBL) model. The boundary of this domain is shown in Figure A1. Each storm/simulation must be represented by wind and pressure field files (WND/pre) in PBL format, ready to read by ADCIRC and as specified by the parameter $NWS=+/-12,212$ in the fort.15 file. For the LACPR storms, the WND/pre fields were pre-computed, external to the production system and assumed to exist as input to the system. An example of the WND/pre fields is shown in Figure E for LACPR storm number 042 (TPOC: Jay Ratcliff, USACE/MVN).

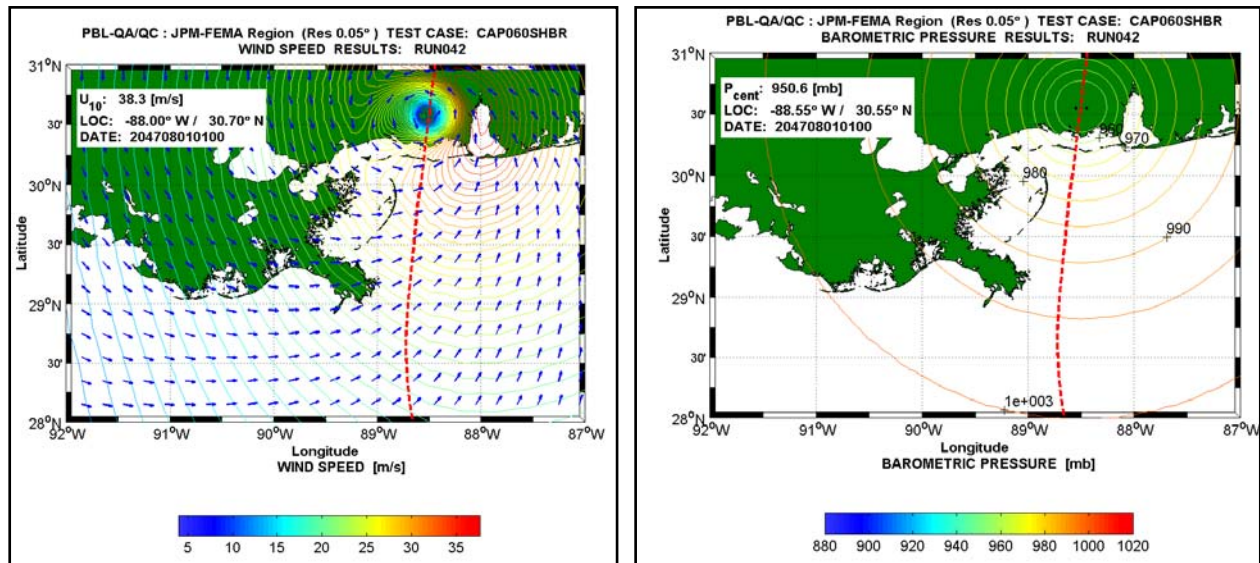


Figure E. Wind (left) and pressure (right) fields for LACPR storm 042 at landfall. The storm track is shown with the dashed, red line. The fields are computed with the Ocean Weather Planetary Boundary Layer (PBL) model, and are used to drive the far-field wave model WAM and ADCIRC. The wind field information is passed to STWAVE through the ADCIRC global output wind file fort.74.

The WND/pre files must be placed in the \$PSHOME/winds directory to be detected by the production system. In the USACE/LACPR specification of the production system, the landfall date is YYYYMMDDHHMN, where the year is arbitrary and MMDDHHMN is 08010200 (2AM on 01 August). This landfall date is conveyed to the production system scripts by specifying it in system control file (ProdSysDef.pm). It is also assumed that the storm center continues past landfall time for 24 hours. The pre-landfall time length is arbitrary. A graphic timeline is shown at the top of Figure F.

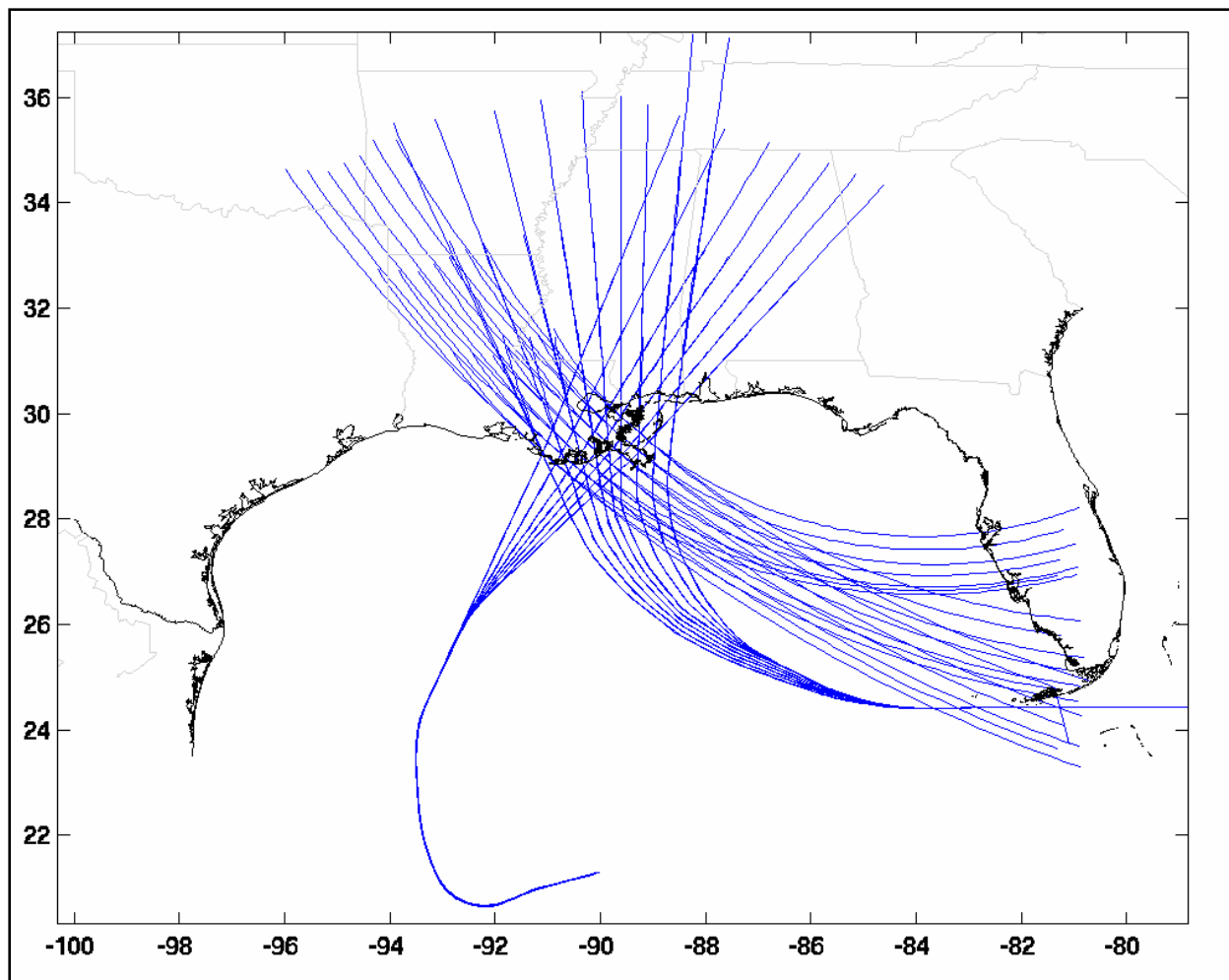


Figure F. Tracks used to define the 152 LACPR storms. Hurricane parameters vary along the tracks, and provide the input to the Ocean Weather PBL wind/pressure field model. This provides the storm forcing required for each production system simulation.

There are 152 storms defined, each of which has a corresponding PBL WND/pre field. The storms are specified by variations of the hurricane parameters along the tracks shown in Figure F. The details of the storm parameter specification are described elsewhere in the technical documentation for this project.

Wave Field Boundary Conditions for STWAVE

All of the half-plane STWAVE grids (the full-plane STWAVE version is used for Lake Pontchartrain) require specification of the wave spectral characteristics on the open boundary. These boundary condition sets are pre-computed by running the WAM ocean wave model for each storm and extracting the wave energy spectra from the WAM solutions at the STWAVE open boundary node locations. The WAM-to-STWAVE procedure is applied for each of the storm wind/pressure fields, and the results are made available to the production system (WAM TPOC: Robert Jensen, USACE/ERDC-CHL).

Solution Sampling Locations

Each ADCIRC storm-surge simulation produces water level timeseries, both for the global model domain and for pre-defined station locations. In the current system implementation, the pre-defined sampling locations are shown in Figure G. There are three sets of points; for LACPR (blue), MSCIP (magenta), and IPET (red). The IPET locations correspond to reach locations as defined in the IPET risk model system definition files. The station output from each solution can be visualized using the post-processing code `plotfort61.pl`. This *perl* script generates a timeseries plot using *GNUplot* to be used for quick inspection of the `fort.61` results. The timeseries plot for the ADCIRC3 (step 4) part of the process is shown in Figure G for storm 042.

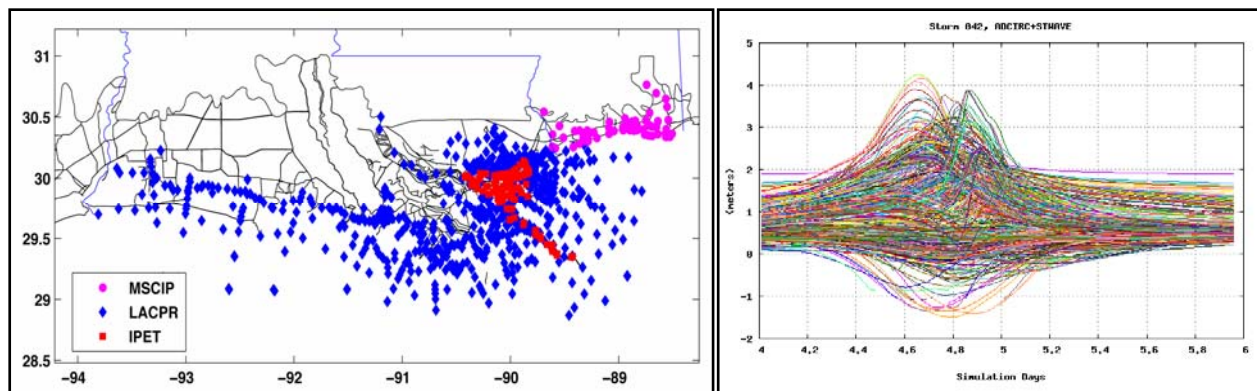


Figure G. Left) ADCIRC solution sampling points that define the station output in the `fort.61` file. The global model solution is interpolated to these locations and output for visualization and analysis. Right) Hydrograph plot generated by `plotfort61.pl`, for the ADCIRC3 step of the production system, for LACPR storm 042.

Solution Procedure (Process Management)

Each simulation is performed in four computational parts, as shown in the “Production Steps” part of Figure H. The initial conditions (River Spinup), PBL wind and pressure fields, and the wave energy spectra boundary conditions (as computed by WAM) are all required inputs to the system.

1. **ADCIRC1:** Each simulation is started from the River Spinup (ADCIRC0). ADCIRC is run from the start of the PBL wind field to 24 hours prior to landfall of the storm (ADCIRC1, River+Winds). The model state is output to disk to provide initial conditions for continuation of the simulation (step 2), and for the subsequent rerun of step 2 that includes wave radiation stresses from STWAVE (step 3).
2. **ADCIRC2:** The ADCIRC1 solution (River+Winds) is then continued to the termination of the PBL wind/pressure fields. The ADCIRC2 global water level (`fort.63`) and wind field (`fort.74`) are output for QA/QC as well as to provide to STWAVE as input.
3. **STWAVE:** The ADCIRC2 solution in step 2 is interpolated to the STWAVE domains, and each STWAVE domain is executed to generate wave radiation stress gradients for input back to ADCIRC in step 4.

4. **ADCIRC3:** ADCIRC2 is re-run over the same time period as in step 2, but including the wave radiation stress gradient computed by STWAVE and interpolated onto the ADCIRC grid. This is the River+Winds+RadStress solution and is also referred to as the ADCIRC+STWAVE step.

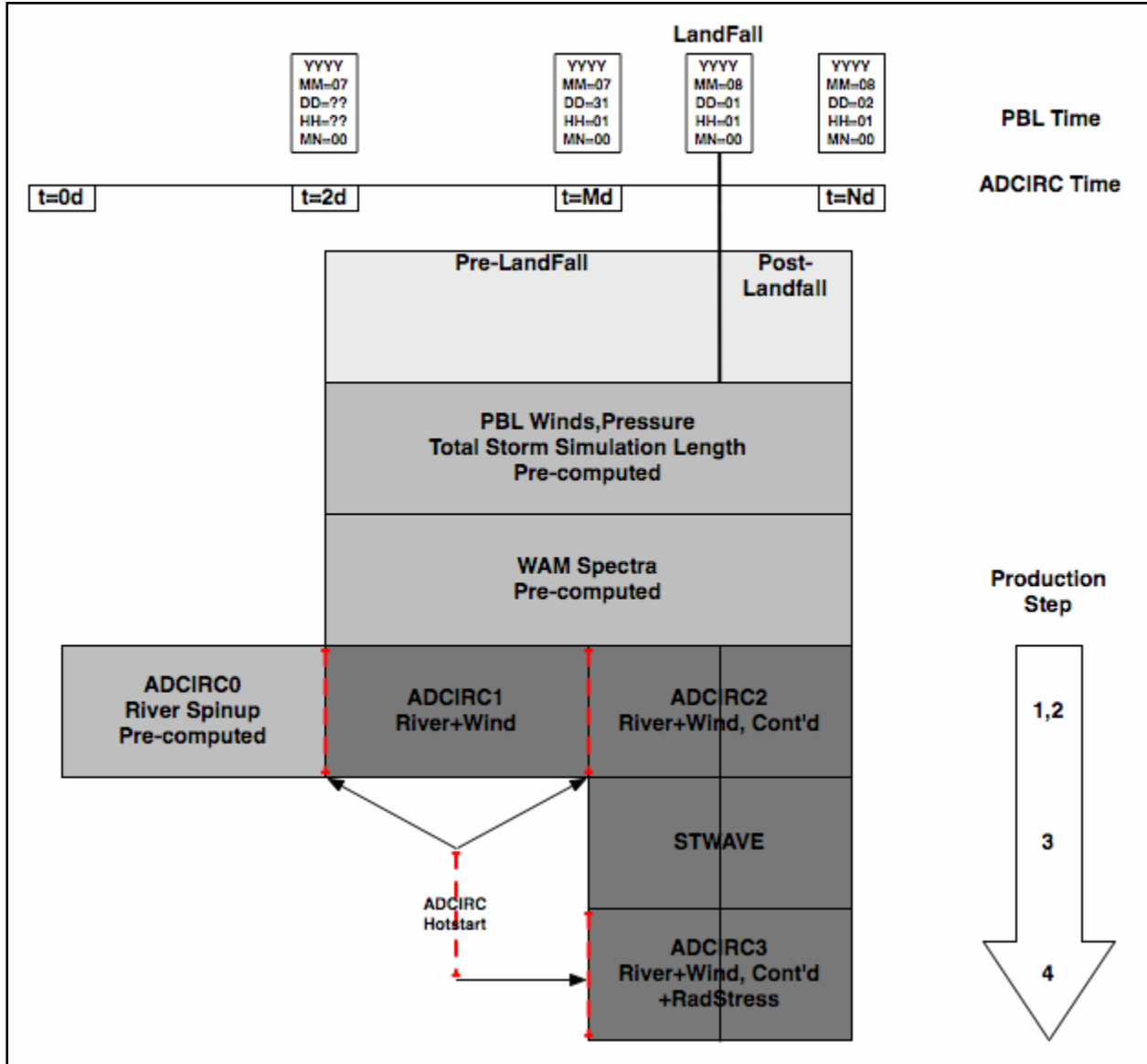


Figure H. Timeline for Production System simulations. The timeline for the wind forcing (PBL) is shown at the top. PBL winds and pressures are used to drive both the WAM wave model and the ADCIRC/STWAVE simulations. Specification of the PBL and WAM fields is a required input to the Production System.

These four steps are coordinated by a *perl* script (`prep_prod_sim.pl`) that organizes the directory structure for each run, gathers the needed input files (grids, initial conditions), edits the files for the specifics of the current simulation, and writes a job control file for the high-performance computer system job controller (PBS on the ERDC Cray Sapphire and LSF on the Uni. of Texas Lonestar Dell cluster). The data file flow controlled by this script is shown in

Figure I. To stage a specific simulation, this script is executed with the storm number specified on the command line.

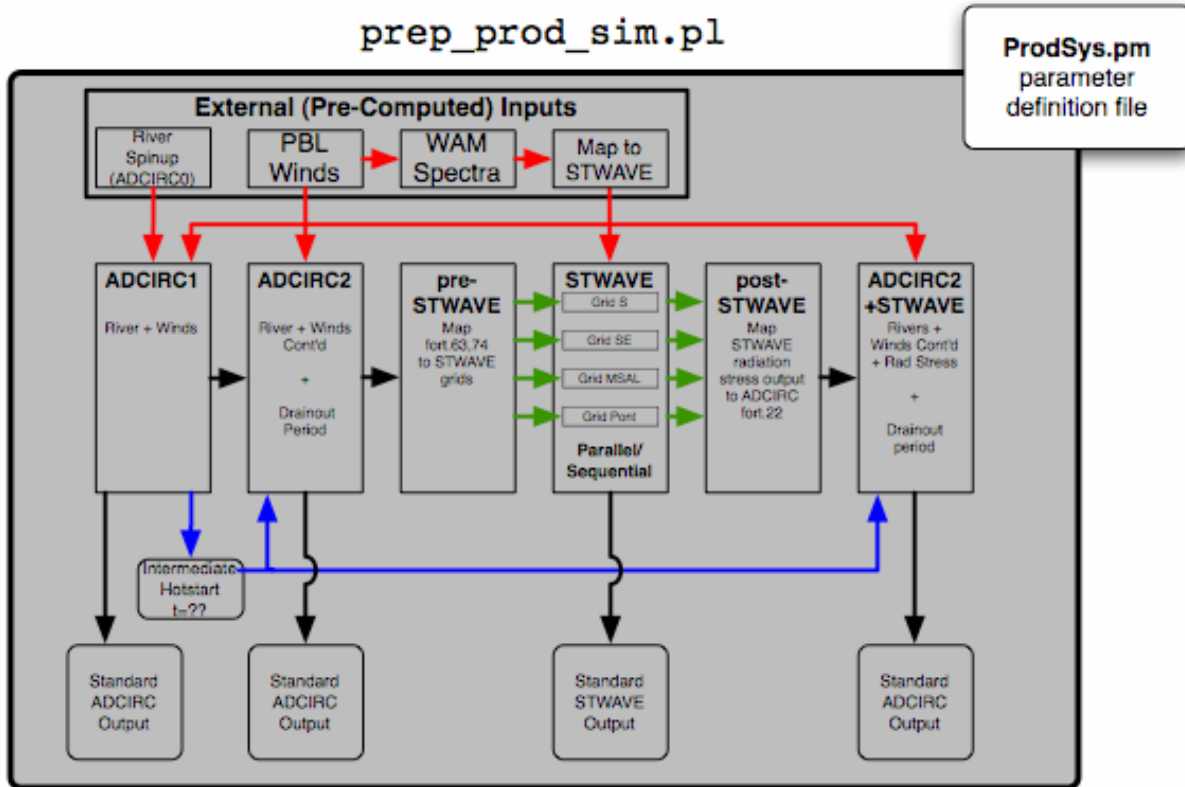


Figure I. Data flow controlled by the production system script `prep_prod_sim.pl`. Pre-computed inputs are shown at the top with red arrows. The middle row of boxes corresponds to the four steps, where the STWAVE step includes interpolation from ADCIRC to the STWAVE grids, the STWAVE simulations, and the interpolation back to ADCIRC. ADCIRC2+STWAVE is the “ADCIRC3” step. Blue lines indicate the ADCIRC hotstart file process. Parameters that are the same for all simulations are defined in the `ProdSysDef.pm` file and read by `prep_prod_sim.pl` at runtime.

Katrina Simulation with PBL Wind Field

A comparison of the observed high-water marks (HWMs) to ADCIRC+STWAVE solutions is shown in Figure J, for the surge that accompanied hurricane Katrina. Two ADCIRC solutions are shown.

The verification solution, forced by the Ocean Weather 95% best-estimate winds, is compared to the observed HWMs (in blue). The overall agreement is very good, with the best-estimate winds solution explaining 94% of the observed HWM variance ($r^2=.94$, $S_e=1.5$). The ADCIRC3 solution forced by the Ocean Weather PBL wind and pressure field is shown in red. The agreement is also very good ($r^2=.88$, $S_e=2.1$).

For each solution, the best-fit line is shown, colored the same as the data points, as well as the 95% confidence region about the data.

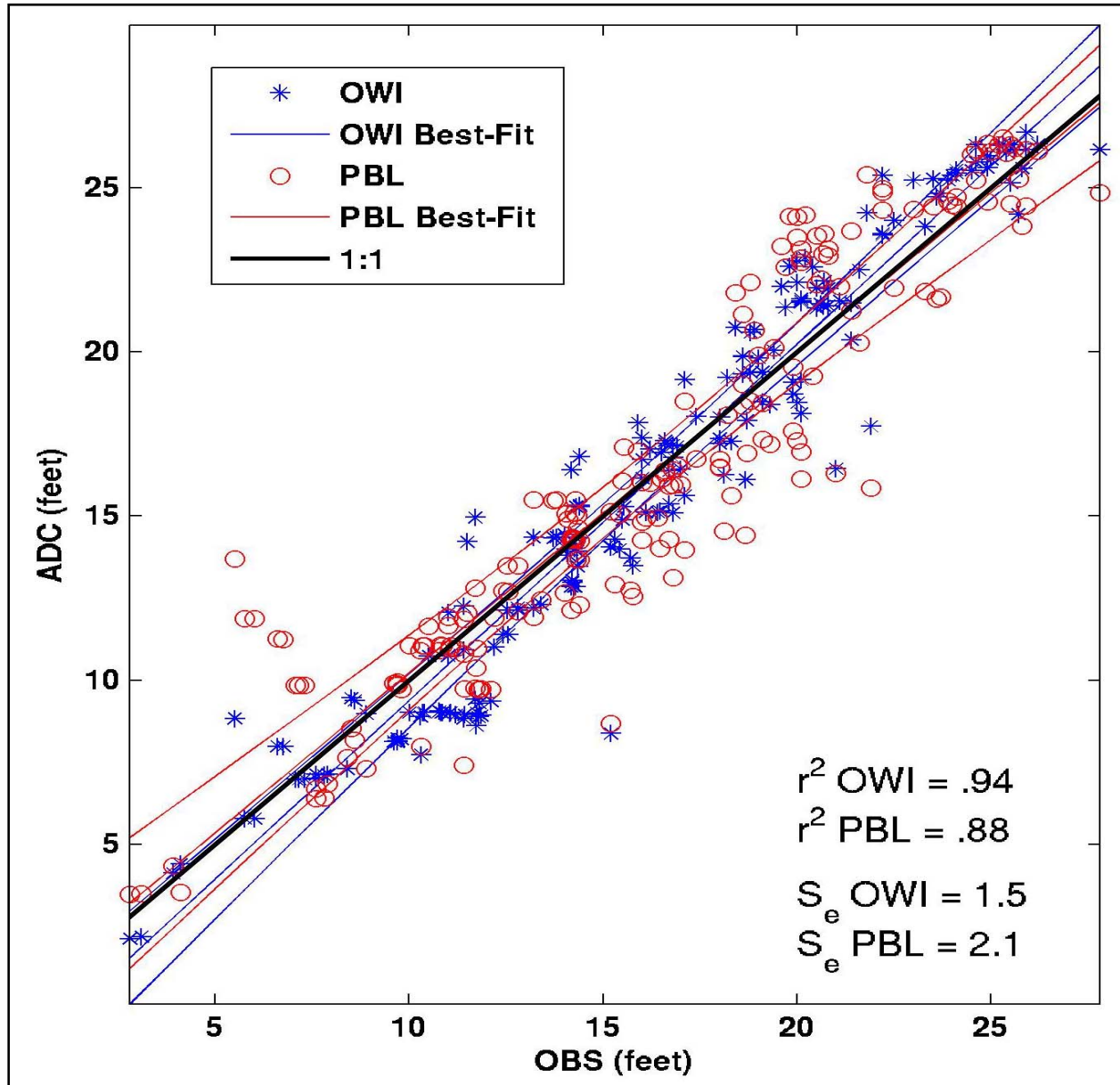


Figure J. Comparison of observed High Water Marks (HWM) for hurricane Katrina, and the Production System Katrina simulation using the PBL wind and pressure fields (red). Also shown is the comparison between the observed HWMs and the verification solution forced by the Ocean Weather 95% wind and pressure field (blue). Observations are on the abscissa, and the ADCIRC3 values are on the ordinate.

References

Luettich, R., and J. Westerink. *Formulation and Numerical Implementation of the 2D/3D ADCIRC, Finite Element Model Version 44.XX*, 2004. http://adcirc.org/adcirc_theory_2004_12_08.pdf

Smith, J., A. Sherlock, and D. Resio. *STWAVE: Steady-State Spectral Wave Model User's Manual for STWAVE Version 3.0*, Tech Report ERDC/CHL SR-01-1, 2001.
<http://chl.erd.c.usace.army.mil/Media/2/4/4/erdc-chl-sr-01-11.pdf>

Appendix 8-1

Acronyms

ADCIRC	ADvanced CIRCulation model for shallow seas
CHL	Coastal Hydraulics Laboratory
ERDC	Engineer Research and Development Center
GMT	Generic Mapping Tools; open-source plotting package used for post-processing graphics generation
HWM	High-water mark
HPC	High-performance computing
I/O	Computer input and output
IPET	Interagency Performance Evaluation Task force
LACPR	Louisiana Coastal Protection and Restoration project
LONI	Louisiana Optical Network Initiative
LSF	Platform Computing's Load Sharing Facility (LSF) job scheduler
MPI	Message-passing interface; parallel programming model used by ADCIRC and STWAVE
NAVO	NAVal Oceanographic computing facility
PBL	Planetary boundary layer model of Ocean Weather Inc.
PBS	Portable Batch System job scheduler
QA/QC	Quality assurance/quality control
STWAVE	STeady-state spectral WAVE model
WAM	NOAA large-scale wave model

Appendix 8-2 (R2007) (May 27, 2007) White Paper on Estimating Hurricane Inundation Probabilities

Written by: Donald T. Resio, Senior Scientist, U.S. Army Corps of Engineers, ERDC-CHL
Incorporating contributions, discussions, data, and comments by: (in alphabetic order)
Stanley J. Boc (ERDC-CHL), Leon Borgman (private consultant), Vincent J. Cardone,
(Oceanweather, Inc), Andrew Cox (Oceanweather, Inc.), William R. Dally (Surfbreak
Engineering), Robert G. Dean (U. of Florida), David Divoky (Watershed Concepts), Emily
Hirsh (FEMA), Jennifer L. Irish (Texas A&M University), David Levinson (NOAA's National
Climatic Data Center), Alan Niedoroda (URS Corporation), Mark D. Powell (NOAA's
Hurricane Research Division, AOML), Jay J. Ratcliff (USACE-MVN), Vann Stutts (USACE-
MVN), Joseph Suhada (URS Corporation), Gabriel R. Toro (Risk Engineering), Peter J.
Vickery (Applied Research Associates), and Joannes Westerink (U. of Notre Dame)

Introduction

Over the last several months, a team of Corps of Engineers, FEMA, NOAA, private sector and academic researchers have been working toward the definition of a new system for estimating hurricane inundation probabilities. This White Paper is an attempt to capture the findings and recommendations of this group into a single document.

At least five methods have been applied in past studies of environmental extremes due to hurricanes in the United States:

1. Formulation of design storm events
2. Estimates based only on historical storms
3. The empirical simulation technique (EST)
4. The joint probability method (JPM) and
5. The Empirical Track Model

In each method, it is important to understand that two different statistical measures are required to characterize the expected extremes over an interval of time. The first of these is the measure of the expected values of the distribution and the second is a measure of expected dispersion around these central values.

All of the methods referenced above have different strengths and weaknesses for various applications. To help understand these, a brief discussion of conventional applications of these methods in the past will be given before moving on to a discussion of the approach recommended for future hurricane surge applications. This will be followed by sections that treat the following:

1. Potential extensions of probabilistic methods to future hurricane surges,
2. The JPM with Optimal Sampling (JPM-OS); and
3. A computational methodology for effective simulation of storm surges for hurricane inundation studies.

Formulation of Design Storm Events

An example of this approach applied to coastal inundation is the Standard Project Hurricane. This approach was adopted by the Corp of Engineers in the 1960's to estimate potential surge hazards along many U.S. coastlines. Due to the paucity of data, it would have been very difficult, if indeed possible, to investigate detailed characteristics of landfalling hurricanes prior to 1960; consequently, the Corps requested that NOAA prepare an estimate of a storm with characteristics that were expected relatively infrequently within some stretch of coastline. Unfortunately, the period prior to 1960 (the input to the statistical analyses performed by NOAA) was a period of relatively low hurricane activity in the Gulf of Mexico; consequently, the SPH, as specified in those earlier studies, is not representative of the characteristics of extreme storms that have occurred in the Gulf since 1960.

In the past, the design storm approach has typically utilized a single storm to characterize environmental factors for design at a given location. This effectively reduces the number of degrees of freedom in storm behavior to one parameter, typically the intensity of the storm. All other storm parameters (for example: storm size, forward storm speed, and track location) are deterministically related to storm intensity. The major problem with this is that, if a second factor (such as angle of storm approach to the coast, storm duration or river stage) significantly affects design conditions and/or considerations, the design storm approach cannot accurately capture all aspects of the storm that affect the design. An extrapolation of the single design storm concept is to define a small set of storms with some range of additional parameters considered. This defines a set of storms that can be used to examine various design alternatives in an efficient manner, while retaining some additional degrees of freedom within the analysis. Because of their use in this context, these storms are often termed "screening storms" rather than design storms.

Estimates Based only on Historical Storms

If at least one sample from a population of interest occurs within each year, it might be possible to apply statistical methods that utilize annual maxima to formulate the stage-frequency curves at a site. However, it is clear that such a situation cannot be well characterized by conventional asymptotic methods which assume many samples in a population occur annually. Since hurricanes are both relatively infrequent and relatively small in terms of the amount of coastline affected by these storms each year, the frequency of storms affecting a site is typically significantly less than 1 storm per year. As an example of this, Figure 1 provides an estimate for the frequency of severe hurricanes (greater than Category 2 intensity) per 1-degree by 1-degree (area) per year for the Gulf of Mexico.

Another sampling problem related to the use of historical storms for specifying extremes is the tendency for intense storms to behave differently than weaker storms. To compensate for this sampling inhomogeneity, many oil-industry groups have adopted the “Peaks Over Threshold,” or POT method for estimating extremes. In this approach, only storms above some threshold value are considered within a statistical analysis of extremes. By screening small storms from the analyzed sample, the effect of small storms on the parameters of fitted distributions (e.g. the parameters of the Gumbel, Frechet, Weibull, Lognormal, Log Pearson or other distributions of choice) is minimized. This approach is inherently parametric due to the need to assume/specify a distribution (or class of distributions such as the Generalized Extreme Value method).

Another potentially more serious problem with the reliance only on historical storms for estimating coastal inundation is related to the small sample of storms at any site. As can be seen from Figure 1, even in the vicinity of New Orleans, the frequency of major storms passing within a given 60 nautical mile region (1-degree) is only about once every 20-25 years. Since we have limited records beyond the middle of the 20th century and since the frequency of storms in the latter half of the century may be markedly different than the frequency of storms in the early part of the century, the historical record for a direct hit (taken here for simplicity as ± 30 nm of a site) would include on the average only about 2-3 storms. Given this small potential sample size, sampling variability can lead to very unrealistic variations in storm frequency and intensities along the coast. For this reason, methods for estimating coastal inundation based solely on historical analyses should not be used for coastal hazard assessment. This point is also pertinent to arguments that the use of historical records for extremal estimation is also difficult to justify in many other, non-coastal applications.

The Empirical Simulation Technique (EST)

Statistics of Expected Extremes

Conventionally, the EST was used as an approach for estimating the expected extremal distribution for surges based on a variation of the “historical record” approach (Borgman *et al.*, 1992; Scheffner *et al.* 1993). In this approach a set of storms above some threshold affecting a particular area are hindcast, similar to the approach used within the POT method. The primary difference is that typically the largest 1 or 2 storms is re-run over a number of track variations in order to distribute the effects of the storm over a wider area. Unfortunately, the rules for this re-distribution of tracks were developed only after some preliminary applications of this approach and tend to be somewhat arbitrary. Results from computer simulations at each point of interest are then ranked and assigned a cumulative distribution value via a formula that links the rank to the cumulative distribution function, $F(x)$, which is abbreviated as CDF in subsequent discussions,

$$F(x) = \frac{m}{N + 1} \tag{1}$$

where m is the rank of the storm (with $m=1$ as the smallest) and N is the total sample number. This is converted to a measure of recurrence via the use of a Poisson frequency parameter, λ

$$T(x) = \frac{1}{\lambda[1 - F(x)]} \quad (2)$$

where $T(x)$ is the expected return period for x . For example, if we hindcast 50 storms from an interval of 100 years, the value of λ would be 0.5; and the estimates of $T(x)$ would span the range from slightly over 100 years to slightly over 2 years.

In the interior of the ranked points, the EST assumes that the best estimate of the expected distribution is the sample itself and does not fit any parametric distribution to the central distribution in order to obtain a “smoothed” distribution. Thus, within this interior range, the distribution is nonparametric. If one is interested in return intervals outside of the range covered by the ranked sample points, it is necessary to invoke some sort of empirical (parametric) function for extrapolation. This is a severe limitation of the conventionally applied EST, since it restricts the non-parametric estimates to approximately the number of years covered by the hindcasts, just as in any other method that relies only on historical storms. In fact, the conventional EST, as used in most past studies, is very similar to the so-called peaks over threshold (POT) method based on historical hindcasts, with three notable exceptions discussed below.

First, the POT method typically uses a parametric fit in the interior region of the distribution, rather than just in the region beyond the largest storms. It can be shown via Monte Carlo simulations that, if the entire sample is drawn from a single parent distribution, the POT method would provide a more stable estimate of the actual distribution in the interior than would the EST. However, in many situations in nature, the interior distribution can consist of samples from several different parent populations. An example of multiple populations would be the case of storm surges due to “direct hits” of hurricanes vs. storm surges due to bypassing storms. Surges from these two sources could have relatively different probability characteristics at a fixed coastal location, as shown in Figure 2. Consequently, the use of nonparametric estimates within the central portion of the distribution seems more appropriate for most coastal flooding applications.

Second, the POT method uses a “fit” to the entire sample to extrapolate into longer return periods. In this case, the problem of mixed populations could potentially introduce serious problems into extrapolations, if the more that one population persists into the region above the “cut-off” threshold. However, many POT methods carefully choose the threshold value to try to restrict the sample to a single population. In some situations this is possible and in others this may not be possible due to lack of sample size (i.e. there may only be 1 or two direct “hits” by hurricanes). On the other hand, the EST uses an empirical “spline” fit to some small number of points near the high end of the distribution combined with a set of secondary restrictions that tend to limit excessive curvature in the extremes. Extrapolations in such situations tends to be subject to considerable judgment, since there is no underlying distribution used as the basis for estimating values larger than those included within the sample.

Third, in hurricane surge studies with the EST, it was observed that a single intense storm could introduce an anomalously large value into a small spatial region, while other areas had much lower maximum surge values. Since there is no reason to believe that all future hurricanes

would strike only points included in the historical data set, some applications of the EST introduced a set of hypothetical storms intended to distribute the effects of large storms throughout the region being studied. In this approach, the largest storm was usually assigned a number of offset tracks and the probability of that storm was distributed over that set of tracks. However, each of these “cloned” storms had exactly the same characteristics as the original storm. In this approach, the extent of the offsets was rather arbitrary, in spite of the fact that the degree of smoothing (distance over which the storm track is replicated) can significantly affect estimated local extremes. Also, only characteristics of storms that fell within the area being analyzed were included in an analysis. Thus, a storm such as Katrina (a large, very intense storm) is difficult to reliably predict from a local sample that does not contain this type of storm within its sample.

Both the POT method and the EST use various statistical methods to incorporate tidal effects into their estimates of water levels at the coast. In a sense, these could be considered as hypothetical storms, since they represent storms that struck the coast at a different tidal phase.

From this discussion, it can be seen that a major problem with the conventional EST is the same as encountered in any approach to hurricane flooding based on local data only: lack of sample. The relatively small spatial extent of hurricanes combined with the small number of storms affecting a given section of coast during the period of reliable records and the apparent existence of long term cycles and trends makes the sampling variability in historical records very large along U.S. coastlines. This same variability affects all estimates of coastal flooding since they all rely on historical data; however, this variability can be greatly exacerbated when only local data is considered. It is perhaps fair to say that the application of the EST requires more experience and judgment than an application of the JPM.

Measures of Variability in Expected Extremes

Since the EST does not contain an underlying theoretical distribution, no theoretical estimates of variability (confidence limits) are possible. Instead, the EST uses a “re-sampling” method to obtain estimates of expected variations in extremes over an interval of time. This method, rather than its methodology for estimating expected extremes, is the strength of the EST. The combination of the re-sampling with the nonparametric distribution provides a sound basis for estimating the variability of the estimated extremes.

The Joint Probability Method (JPM)

Statistics of Expected Extremes

The JPM was developed in the 1970’s (Myers, 1975; Ho and Meyers, 1975) and subsequently extended by a number of investigators (Schwerdt *et al.*, 1979; Ho *et al.*, 1987) in an attempt to circumvent problems related to limited historical records. In this approach, information characterizing a small set of storm parameters was analyzed from a relatively broad geographic area. In applications of this method in the 1970’s and 1980’s, the JPM assumed that storm characteristics were constant along the entire section of coast from which the sample was

drawn. Recent analyses suggest that this assumption is inconsistent with the actual distribution of hurricanes within the Gulf of Mexico.

The JPM used a set of parameters, including 1) central pressure, 2) radius of maximum wind speed, 3) storm forward speed, 4) storm landfall location, and 5) the angle of the storm track relative to the coast, to generate parametric wind fields. Furthermore, initial applications of the JPM assumed that the values of these five parameters varied only slowly in storms approaching the coast; therefore, the values of these parameters at landfall could be used to estimate the surge at the coast. Recent data shows that this is not a good assumption (Figure 3). Kimball (2006) has shown that such decay is consistent with the intrusion of dry air into a hurricane during its approach to land. Other mechanisms for decay might include lack of energy production from parts of the hurricane already over land and increased drag in these areas. In any event, the evidence appears rather convincing that major hurricanes begin to decay before they make landfall, rather than only after landfall as previously assumed.

The conventional JPM used computer simulations of straight-line tracks with constant parametric wind fields to define the maximum surge value for selected combinations of the basic five storm parameters. Each of these maximum values was associated with a probability

$$p(c_p, R_{\max}, v_f, \theta_l, x)$$

where

c_p is the central pressure,

R_{\max} is the radius of maximum wind speed

v_f is the forward velocity of the storm

θ_l is the angle of the track relative to the coast at landfall

x is the distance between the point of interest and the landfall location

These probabilities were treated as discrete increments and the CDF was defined as

$$F(x) = \sum p_{ijklm} | x_{ijklm} < x \tag{3}$$

where the subscripts denote the indices of the 5 parameters used to characterize the hurricanes. Similar to the EST, this method is nonparametric; however, the conventional JPM included a range of parameter combinations that typically made extrapolation beyond the range of simulations unnecessary. This is an advantage over the conventional EST, since it removes the need to assume a particular parametric form for the CDF in critical ranges of values.

Another potential advantage of the JPM over methods which depend heavily on historical storms was that the JPM considered storms that might happen; whereas, the EST considered only storms that did happen. Assuming that, for the purpose of surge generation, storm characteristics can be represented adequately by the set of parameters used, it is possible to construct a Katrina-like storm (high intensity combined with large size) even if one has not happened previously.

Likewise, it is possible to interpolate between re-curved storms such as Opal and Wilma to understand possible hurricane impacts in the Tampa area, even though neither of these storms produced significant surges in the Tampa area.

Perhaps the biggest controversy in JPM applications during the 1970's and 1980's centered on the definition of this 5-dimension joint-probability function. The lack of data on historical storms prior to 1950 made it very difficult to derive representative distributions, even for extended sections of coast. For example, information on storm size (radius of maximum wind speed was lacking for most historical storms; consequently, a statistical estimate of r_{\max} (as a function of latitude and central pressure) was frequently substituted for actual values in the probability distribution. One wind field factor not considered in early JPM applications was the variable peakedness of hurricane wind fields. This term is represented in terms of the Holland B parameter in recent hurricane wind models and will be discussed in a subsequent section of this white paper.

One point of interest that should not be lost here is the importance of capturing the mean statistical behavior of any time-varying properties used in JPM applications. For example, surges derived from previous JPM applications, under the assumption of that storm characteristics near the coast were constant, may have been biased low, since they were based on statistics at landfall. Since storms are consistently more intense off the coast (as shown in Figure 3), the modeled offshore storms are less intense than the actual offshore storms, under this assumption. Of course, some calibration was performed in these studies, so this might have been somewhat accounted for via calibration procedures; however, calibration tends to be somewhat storm specific, so such calibration could still leave considerable residual bias in the final results.

JPM Measures of Variability in Expected Extremes

Most applications of the JPM only considered the definition of the mean CDF from the simulations, and little attention was paid to quantifying the dispersion (uncertainty) of what could happen within a particular time sample. This is potentially a major shortfall in the JPM as it was originally applied.

The Empirical Track Model

Vickery *et al.* (2000) presents a method for modeling hurricane risk in the United States. This method has been adopted for the development of design wind speed maps within the U.S. (American National Standards Institute (ANSI), ASCE 1990, 1996). This method uses a Monte Carlo approach to sample from empirically derived probability and joint probability distributions. The central pressure is modeled stochastically as a function of sea surface temperature along with storm heading, storm size, storm speed, and the Holland B parameter. This method has been validated for several regions along U.S. coastlines and provides a rational means for examining hurricane risks associated with geographically distributed systems such as transmission lines and insurance portfolios.

A key requirement for the application of the Empirical Track Model within its Monte Carlo framework is the ability to efficiently execute storms over many, many years (20,000 years in the Vickery *et al.* (2000) application). Whereas this is not too demanding for an efficiently written PBL wind model, it is well beyond the range of possibility in large, high-resolution ocean and coastal response models (wave models and surge models). For this reason, the Empirical Track Model was not considered for application to coastal inundation; however, it provides an excellent source for validating the statistical characteristics of the winds used for inundation modeling.

Potential Extensions of Probabilistic Methods to Future Hurricane Surges

As noted in the earlier section on the design storm approach, the design storm approach suppresses much of the real variability in storm characteristics and should be used only for screening alternatives and not for final design of critical coastal structures. However, it is sometimes informative to examine the relative return period of specific historical storms. Appendix A provides an estimation method along these lines which estimates the return periods for both Hurricanes Katrina and Rita (found to be 397 and 89 years, respectively).

It should be clear from the previous section that both the EST and the JPM in older applications suffered from a paucity of historical data. Also, older applications did not include many of the modeling advances that are now regarded as necessary for accurate simulations, for example: inclusion of numerically simulated wave set-up, use of detailed grids to capture high-resolution bathymetric effects, and the application of improved near-coast meteorological models for hurricane evolution and wind-field behavior. Many of these effects were recognized and improved methods for treating them were developed during the forensic study of Hurricane Katrina by the Interagency Performance Evaluation Task Force (IPET).

Recognition that waves can play a substantial role in coastal surge levels introduces a key difference between older JPM applications and the applications being considered today. In the older methods, the assumption of constant parameters was intended to span an interval of about 12 – 24 hours, essentially the primary period for direct wind forcing of coastal surges in historical hurricanes. Waves contribute to coastal surges primarily in nearshore areas; however they are generated over a span of days during the approach of the storm to land. Thus, consideration of wave contributions to surges requires some knowledge of the storm behavior 1-4 days prior to landfall. Treatment of hurricanes in terms of straight tracks with constant size and intensity over such a period is a bad assumption, since such tracks would not retain the wave-generation characteristics produced by the curved tracks within the historical record.

This brings us to a crucial point in considering what statistical approach should be used in future applications, i.e. whether to use an approach based strictly on re-sampling historical storms (essentially a modification/extension of the EST) or an approach based on parameterized wind fields over longer tracks (essentially a modification/extension of the JPM). On one hand, it is clear that each historical storm has many, many factors which vary throughout its history which influence hurricane wind fields. For example, eye-wall replacement cycles, interactions

with large-scale wind systems, asymmetries within the eye-wall, and complicated track curvatures can all create significant perturbations within the structure of hurricane wind fields. It is not clear however that such modifications to the winds affect the total wave generation process so much, since the nature of this process integrates the wind input over several 10's of hours. In fact, numerical experimentation with hurricane Katrina showed that all of the versions of the wind field (PBL alone, HWIND, and the most recent Oceanweather version) created minimal variations in the wave field (in the range of 5-7% differences in wave height) in the area off of Mississippi.

In a sense, the critical factor that must be considered here is the number of primary dimensions required for representing wind fields with sufficient accuracy that they provide reasonable, relatively unbiased skill when used to drive coastal wave and surge models. For the case of extratropical storms, there is no known simple set of parameters that meets this criterion and some extension of the EST or POT method may be the suitable choice for such applications. For the case of hurricanes, dynamic models of hurricane wind fields (Thompson and Cardone, 1996; Vickery et al., 2000) can be shown to capture a substantial portion of the wind field structure, when driven with the parameters listed above plus the so-called "Holland B" (Holland, 1980) parameter.

Each hurricane will tend to exhibit some degree of deviation from the theoretical PBL-model estimates. At any fixed time, such deviations could be produced by strong storm asymmetries, variations in R_{\max} around the storm, enhanced spiral bands, etc. Hence, a "best-estimate" wind field crafted by experts to assimilate all the observations in a given hurricane will typically represent the details of that particular storm much more faithfully than possible via a parameterized theoretical model. Such wind fields today are produced primarily by Mark Powell and others at the Hurricane Research Division of the National Hurricane Center of NOAA or by analysts at Oceanweather, Inc. These wind fields are absolutely essential for advancing our understanding of hurricane winds relative to wave and surge forcing in offshore and coastal areas.

It is obvious that "best-estimate" wind fields contain an extremely large number of degrees of freedom in their formulation. Given the relatively small number of historical hurricanes, it is unlikely that we can understand/quantify the probabilistic nature of all the interrelated detailed factors creating these deviations. If these details were absolutely critical to coastal wave and surge estimation, we would be able to represent a past hurricane very accurately but would know little about the probability of future hurricanes unless we retained the same number of the degrees of freedom, including their expected variability in estimates of future storm surge and wave estimates. To demonstrate this point, in the definition of surge probabilities via numerical models, we are considering a relationship of the form

$$p(\eta) = \int \dots \int p(x_1, x_2, \dots, x_n) \delta[\Psi(x_1, x_2, \dots, x_n) - \eta] dx_1 dx_2 \dots dx_n \quad (4)$$

where η ($= \eta_{\max}$ for each individual storm at a fixed spatial location) is the storm surge level, $\delta[.]$ is the Dirac delta function and $\Psi(x_1, x_2, \dots, x_n)$ is a numerical model or system of models

that operate on the set of parameters (x_1, x_2, \dots, x_n) to provide an estimate of the surge level at a fix location. This can be directly integrated to yield the CDF for surge levels

$$F(\eta) = \int \dots \int p(x_1, x_2, \dots, x_n) H[\eta - \Psi(x_1, x_2, \dots, x_n)] dx_1 dx_2 \dots dx_n \quad (5)$$

where $H[.]$ is the Heaviside function. If we retained a sufficient number of degrees of freedom to resolve the wind fields exactly, if our numerical codes were also “exact,” and if our specification of the joint probability function $p(x_1, x_2, \dots, x_n)$ were known exactly, we could treat this equation as an exact integral for the CDF, with no uncertainty in its expected value. The sampling variability could then be estimated by re-sampling methods along the lines of the EST.

The CDF integral (equation 5) shows that the number of dimensions required for an exact representation of the surge CDF must equal the number of degrees of freedom contained within the system (for practical purposes determined by the number of degrees of freedom contained in the wind fields). Since we recognize that all wind fields, wave models, and surge models remain inexact and that our estimates of joint probabilities are greatly hampered by lack of sample size, it is clear that the actual representation of this integral should be written as

$$F(\eta) = \int \dots \int p(x_1, x_2, \dots, x_n, \varepsilon) H[\eta - \Psi(x_1, x_2, \dots, x_n) + \varepsilon] dx_1 dx_2 \dots dx_n d\varepsilon \quad (6)$$

where ε is an “error” term due to wind field deficiencies, model deficiencies, unresolved scales, etc. In this form, we see that there is a trade-off between modeling accuracy and the magnitude of the error term, ε . There is also a similar trade-off between errors/uncertainties in the probability estimates and the overall accuracy in estimates of the surge CDF. These errors will increase substantially if we attempt to split a small sample (for example the historical hurricane record in the Gulf of Mexico) into information for too many dimensions. Following this reasoning, it seems advisable to limit the number of parameters considered in the JPM probability integral and to include an approximation for all of the neglected terms within the error term, ε . As noted previously, PBL models provide a relatively accurate representation of the broad-scale structure within hurricanes. Furthermore, wind fields from PBL models have a very long history of providing accurate wave estimates in Gulf of Mexico hurricanes (Cardone *et al.*, 1976). Consequently, the logical choice appears to be to limit the number of dimensions in the JPM integral to the number of parameters contained within such PBL models

$$F(\eta) = \int \dots \int p(c_p, R_p, v_f, \theta_l, x, B) p(\varepsilon) H[\eta - \Psi(x_1, x_2, \dots, x_n) + \varepsilon] dx_1 dx_2 \dots dx_n d\varepsilon \quad (7)$$

where the error term has been separated from the rest of the probability distribution. In this form, the “error” term allows us to include additional effects on water levels, such as tides (albeit in an uncoupled, linear fashion). Also, in this equation, we have replace R_{\max} with R_p , since the latter term is used in the PBL model selected for application here (see Appendix B) for details.

During the last several months considerable effort has gone into re-analyzing hurricane characteristics and hurricane wind fields. One of the significant findings of this effort is that the Holland B parameter in mature storms within the Gulf of Mexico tended to fall within the range of 0.9 – 1.6. Furthermore, numerical sensitivity tests of both wind fields and coastal surges suggest that the adoption of a constant value of 1.27 for storms centered more than 90 nm from the coast provided a reasonable first approximation to both the wind fields and the surges. Thus, if we add the effects of B-variations into the “error” term, we can reduce the CDF equation to

$$F(\eta) = \int \dots \int p(c_p, R_p, v_f, \theta_l, x) p(\varepsilon | \eta) H[\eta - \Psi(x_1, x_2, \dots, x_n) + \varepsilon] dx_1 dx_2 \dots dx_n d\varepsilon \quad (8)$$

In this form, ε is considered to include, at a minimum, the following terms:

1. tides,
2. random variations in B,
3. track variations not captured in storm set,
4. model errors (including errors in bathymetry, errors in model physics, etc.), and
5. errors in wind fields due to neglect of variations not included in the PBL winds.

It is evident that we can only approximate the overall distribution of ε from ancillary information on errors in comparisons to High Water Marks and comparisons of results from runs with the “best-estimate” wind fields and PBL wind fields. Tides can be factored into this analysis assuming linear superposition, with some degree of error introduced. Based on the best available approximations to all of these terms, assuming that all the “error” contributions are independent, and a loose application of the Central Limit Theorem, we will assume that the “error” term can be represented as a Gaussian distribution with a mean of zero (assuming that the model suite is calibrated to this condition) and a standard deviation equal to some percentage of the modeled surge.

If we were to try to extend the EST to include shifting actual historical storms from one landfall site to another, we would implicitly be holding all the “details” constant by assuming exactly the same storm will occur in the future at different locations. This constrains all future hurricanes to have the same detailed characteristics as the single historical storm upon which it is based. It seems more logical to approach this in two stages as described above, an initial stage to capture the broad-scale wind characteristics and a second stage to understand/quantify the impact of deviations around these broad-scale winds on coastal surges. In this way, the probability analysis can be kept within a sufficiently small number of dimensions to allow reasonable approximation from historical records.

In our own work investigating modifying the EST, we began by making the same assumption as the older JPM application, i.e. that we could take some section of coast and treat it as though it were homogeneous with respect to expected storm parameters. With this assumption, we felt that it would be appropriate to move a storm some distance along the coast without affecting its characteristics. Unfortunately, when we tested this approach, we saw that historical tracks did not translate well spatially. We found that all of the large storms affecting U.S. Gulf of Mexico coastlines entered the Gulf through either the gap between Cuba and the Yucatan Peninsula or through the southern Florida to Cuba area. A simple geometric displacement of a particular

storm track made that track intersect with land in areas that are not suitable for their origin. For example, such a displacement to allow a storm such as Hurricane Opal to strike the western portion of Louisiana would intersect with land at a point slightly south of the border between the United States and Mexico. It is essentially impossible for such a track to generate a storm of Opal's strength. Another example would be the simple translation of Katrina's track to a point farther east. It is highly unlikely that such a track would be able to support a storm of Katrina's size and intensity. Thus, any concept that involves a simple geometric translation of a historical storm track to a position very far from where it actually occurred was found to be very naïve, at least in a meteorological/climatological sense. Still another example of problems associated with the use of a detailed track would be the simplistic shifting of a track with a loop in it, such as Hurricane Elena along the panhandle of Florida. The implication of using this exact track and associated wind field is that all future storms of this type will exhibit exactly this same loop and associated intensity, size, asymmetry, and other detailed characteristics during its approach to land. The probability of this actually occurring is very near zero.

An additional problem in our initial attempt to modify the EST for storm surge application relates to the definition of storm probability. We found that, due to the geographic constraints of entry points for intense storms into the Gulf, it was a very bad assumption to treat any extended section of coast as though it were a homogeneous area in terms of expected hurricane characteristics. Instead, several independent analyses have shown that the statistical properties of hurricanes vary continuously and substantially throughout the Gulf of Mexico. This means that it is not advisable to shift a storm track from one section of coast to another and treat it as an equivalent sample to a storm that actually occurred in that section of coast. A related problem in attempting to modify the EST for hurricane surge applications is assigning the probability of exceedance of some characteristic in a particular storm. For example, most critical reviews conducted recently have advocated limiting the period of record to be used in climatological estimates of hurricane characteristics to a period from no earlier than the mid-1940's to the present. Thus, if we adopt the conventional plotting position, Katrina will represent somewhere in the neighborhood of a 60 year event. We can probably increase this a little by spreading Katrina over some section of coast; but as noted above, this is not a simple exercise. The degree of spreading, the reasonableness of the tracks, and the spatial variation of statistical properties all make this a procedure that should not be trivialized.

The final point worth noting is that prior to 2005, there was no Katrina in the historical record. Straightforward estimates of surges using the EST method prior to Katrina suggest that such a surge only occurs once every 1200 years, or so. Most analyses suggest that this is a substantial overestimation of the return period for such a surge. The problem here is that, prior to Katrina, no historical storm combined both intensity and size in a fashion equivalent to Katrina. Thus, Katrina was outside the sample range of the EST. Although this particular deficiency in the sample has been remedied for at least some of the Gulf coast (since Katrina has now occurred there), one must ask what other gaps in the sample of historical storms might exist. Given this point along with all the other discussion points in this section, it was decided that it would be more straightforward to modify the JPM for hurricane surge applications than to modify the EST. As noted previously, both of the methods are nonparametric in the interiors of their cumulative distribution functions.

The Modified JPM Method (JPM-OS)

In this section, a method for estimating storm surges via a modified JPM will be developed, including estimation of some key climatological characteristics of hurricane tracks, intensities, and sizes. The term JPM-OS will be used here to denote this new methodology, since the underlying concept of this methodology is to provide a good estimate of the surges in as small a number of dimensions as possible, while retaining the effects of additional dimensions by including the ε term within the estimated CDF for surges. This approach will also attempt to minimize the number of runs required by improving methods used for interpolating between combinations of variables in different simulations.

Estimation of Spatially Varying Probabilities

In our new approach, the recommended treatment of geographic variation is to use the Chouinard et al. (1997) method for determining optimal spatial size for estimating hurricane statistics. In this method, the optimal size for spatial sampling is estimated in a manner that balances the opposing effects of spatial variability and uncertainties related to sample size. Although the final, definitive statistics are still being developed, a brief description of the method is included here, along with the preliminary results.

We begin by estimating the omni-directional statistical properties for storm frequency and intensity. Work performed by Gabriel Toro of Risk Engineering showed that the optimal spatial sample (kernel) size was in the range of 160 km for frequency analyses, but found that the optimal spatial size for intensities reached a plateau above about 200 km and did not drop off substantially at higher spatial kernel sizes. For our purposes, we took the basic data set of 22 hurricanes, which had central pressures less than 955 mb, shown in Figures A3 through A5 and defined their locations and intensities along the line shown in Figure A2. Although this line includes the west coast of the Florida peninsula for completeness within the analysis, results will only be presented for the section of coast west of this peninsula. Our hurricane sample covers the interval 1941 through 2005. Appendix C provides a synopsis of some work supporting the selection of this period of record.

For our frequency analysis, we selected a “line-crossing” methodology, rather than an “area-crossing” (such as used in the Toro analysis presented in Figure 1) since the frequency of landfalling storms is inherently better posed in this context. The location of this line is shown in Figure A2 and distance in this system will be referenced in this white paper via an “increment number.” This “increment number” is based on integer values of the distance in degrees (longitude at 29.5 degrees latitude) as explained in the figure caption in Figure A2.

After a number of sensitivity studies we were able to show that the results for spatial samples for spatial kernels above 250 km or so did not vary markedly and settled on a sample size of ± 3 degrees (333 km) along this line. Results from this analysis are converted into an estimate of the frequency of hurricanes (which attain a minimum central pressure of 955 mb or less) making landfall within contiguous 1-degree increments along the reference line. Figure 4 gives the results of this analysis. As can be seen here, the “line-crossing” frequency estimate is fairly consistent with the spatial-area frequency estimates obtained by Toro in Figure 1. It should be

noted that the Toro analysis was based on 52 storms (all storms above Category 2 intensity within the Gulf of Mexico) rather than the 22-storm subset used here.

For each 1-degree increment along the coast, pressure differentials at the time of landfall for all storms making landfall within the ± 3 -degree distance along the reference line were used to define a best-fit (conditional) Gumbel distribution, i.e. the distribution of hurricane intensity given that a hurricane (with central pressure less than 955 mb) does occur. The Gumbel coefficients for the pressure differentials are shown in Figure 5. Combining the storm frequency estimates with these values we can estimate the omni-directional probability of intensity along the Gulf coast at the time of landfall.

Figure 6 shows the (smoothed) distribution of the 50-year, 100-year, and 500-year central pressures based on the Oceanweather information. Also shown in this Figure is the estimates using the same derivation methodology, but based on the official NOAA values for landfalling central pressures. As can be seen here, the two methods yield very similar results, except for some divergence as the Louisiana-Texas border is approached. This curious aspect of the otherwise excellent agreement was found to be related to a single spurious value in the Oceanweather files for Hurricane Audrey. Once this was fixed, the region of good agreement extended across the entire region.

Interpretation of these values to “off-coast” values should refer to Figure 3, which suggests that the off-coast central pressures should be on the average around 10-15 mb lower than these values. For comparison, return periods based on independent analyses performed by David Levinson (National Climate Center) suggest that the 100-year central pressure offshore was in the range of 894-908 for a broad portion of the central Gulf of Mexico, which is reasonably in agreement with the values derived here, based on 1-degree increments of coast. However, in performing this comparison, it is essential to bear in mind that the estimates are appropriate for the recurrence within a 1-degree section of coastline. To compare the estimates in Figure 6 with values for the entire Gulf of Mexico, Peter Vickery performed an independent analysis of extremes based on 1) a statistical combination of all of the coastal segments and 2) an extremal analysis of the NOAA’s landfalling pressures. As can be seen in Figure 7a, the estimates of landfalling central pressures shown in Figure 6 can be used to provide a very consistent estimate for landfalling central pressures along the U.S. coast from Texas to the northwest Florida coast. And, as can be seen in Figure 7b, a similar analysis for a single 1-degree increment shows, as expected, a little more randomness for this (smaller) set of points but a similar good general agreement in the tail of the distribution. Figure 7c shows a comparison of another independent check on the probability distribution based on a comparison to the results of Toro’s analysis performed for FEMA Region 4, along the Mississippi coast. These tests confirm the general estimation methodology used here is quite robust for hurricanes along the U.S. Gulf of Mexico coasts.

Several independent analyses over the last several months have shown that storm size is not independent of storm intensity; and recently, Shen (2006) has shown that the potential intensity achievable by a hurricane is very sensitive to the size of a hurricane eye. Figures 8a and 8b show the relationships between R_p and central pressure from Oceanweather analyses of all storms exceeding Category 2 within the Gulf of Mexico at their time of maximum strength (52 storms –

shown in Figure 8a) and the 22-storm sample of landfalling storms (Figure 8b). Equation A3 in Appendix A gives an estimate of the conditional probability of storm size as a function of central pressure. Figure 8 gives the mean angle of storm heading as a function of distance along the reference line shown in Figure A2, along with the standard deviation of the heading angles around this mean value. The direction convention used here is that a heading of due north represents an angle of zero degrees. Storms heading more westerly than due north will have positive angles, while storms heading more easterly will have negative angles. These estimates were derived by the same spatial averaging procedure used in deriving the central pressures and frequencies. A circular normal distribution is used here to represent the storm heading probability distribution as a function of location along the reference line.

Figure 10 presents the estimated forward storm speed as a function of central pressure. This figure suggests that storm intensity and the forward speed of the storm are approximately independently distributed. However, if we plot forward storm speed as a function of storm heading at landfall for the 14 storm subset that intersect with the 29.5-degree latitude portion of the reference line in Figure A2 and for the entire 22-storm sample of landfalling storms (shown in Figures 11a and 11b), we see that there is a tendency for higher forward speeds to be associated with lower storm heading angle (a correlation of 0.52 which is significant at the 0.05 level of significance with 21 degrees of freedom in a “Student’s *t*” test). This is consistent with the expected behavior of re-curving storms that become swept up in stronger westerly circulations. The primary exception to the overall relationship is Hurricane Betsy, represented by the point in the upper right-hand corner of this Figure. This storm moved very fast into the New Orleans area after crossing the lower portion of the Florida peninsula.

Putting all of the pieces of information together, for any point in our five-dimensional parameter space (retaining appropriate interrelationships among parameters), we see that the final estimates of joint probability densities can be written as

$$p(c_p, R_p, v_f, \theta_l, x) = \Lambda_1 \cdot \Lambda_2 \cdot \Lambda_3 \cdot \Lambda_4 \cdot \Lambda_5$$

$$\Lambda_1 = p(c_p | x) = \frac{\partial F[a_0(x), a_1(x)]}{\partial c_p} = \frac{\partial}{\partial x} \left\{ \exp \left\{ -\exp \left[-\frac{c_p - a_0(x)}{a_1(x)} \right] \right\} \right\} \quad (\text{Gumbel Distribution})$$

$$\Lambda_2 = p(R_p | c_p) = \frac{1}{\sigma(\Delta P)\sqrt{2\pi}} e^{-\frac{(\bar{R}_p(\Delta P) - R_p)^2}{2\sigma^2(\Delta P)}}$$

$$\Lambda_3 = p(v_f | \theta_l) = \frac{1}{\sigma\sqrt{2\pi}} e^{-\frac{(\bar{v}_f(\theta_l) - v_f)^2}{2\sigma^2}}$$

$$\Lambda_4 = p(\theta_l | x) = \frac{1}{\sigma(x)\sqrt{2\pi}} e^{-\frac{(\bar{\theta}_l(x) - \theta_l)^2}{2\sigma^2(x)}}$$

$$\Lambda_5 = \Phi(x)$$

where the overbars denote average values of the dependent variable for a specified value of an independent variable in a regression equation, $a_0(x)$ and $a_1(x)$ are the Gumbel coefficients for

the assumed Gumbel form of the central pressures, and $\Phi(x)$ is the frequency of storms per year per specified distance along the coast (taken as one degree in examples presented here).

Figures 12-14 show three sets of synthesized tracks that are being used in the ongoing New Orleans area study. These central tracks (Figure 12) essentially mimic the behavior of intense landfalling historical storms in the record, while preserving the geographic constraints related to land-sea boundaries. These storms preserve the historical pattern of the tracks better than simply shifting the same storm tracks east or west along the coast, since they capture the observed variations in mean storm angles along the coast.

Estimation of the ε Term

Although there may be some degree of nonlinearity in the superposition of tides and storm surges, numerical experiments have shown that for the most part linear superposition provides a reasonable estimate of the (linearly) combined effects of tides and surges. Thus, the tidal component of the ε term, represents the percentage of time occupied by a given tidal stage and can be directly derived from available tidal information along the coast.

Careful analyses appropriate for formulating Holland B parameters for ocean response modeling have shown that this parameter falls primarily in the range of 1.1 - 1.6 offshore and 0.9 - 1.2 at the coast (Appendix E). For Gulf of Mexico hurricanes, a mean value of 1.27 in offshore areas is assumed with a standard deviation of 0.15, while at the coast the corresponding mean and standard deviation is 1.0 and 0.10, respectively. Via numerical experiments, the maximum storm surge generated by a hurricane has been found to vary approximately linearly with variations in the Holland B parameter, at least for changes of the Holland B parameter in the range of 10-20%.

Off-coast track variations affect surges at the coast primarily through the effects of these track variations on wave fields, rather than by their effects on direct wind-driven surges. As noted previously, wave fields tend to integrate wind field inputs over 10's of hours; consequently, off-coast track variations tend to shift the wave fields somewhat while maintaining the general form and magnitude of the wave height contours. Near-coast radiation stresses are approximately proportional to gradients in wave energy fluxes, which, in turn, can be related to the square of the wave height gradient. In shallow water, where contributions of radiation stresses to surges are most important, wave heights tend to be depth limited. It is only in the incremental region, where larger waves make additional contributions due to increased energy losses offshore, that larger wave conditions affect the total wave set-up at the coast. Numerical sensitivity studies suggest that once incident waves become much larger than about 10 meters, most of the additional energy loss is in depths that do not contribute very much to wave set up. For this reason plus the fact that in general the wave set-up term tends to be only about 15-30% of the total surge, we expect the effect of storm track variations on wave set-up at the coast to be fairly small (due to the fact that surge response is on a much faster scale than wave generation, where we noted that the "straight-track" approximation was not very good). We will assume that the deviations around the mean surge will be approximately Gaussian. A standard deviation of 20% of the calculated wave-set up contributions to the total surge (determined by subtracting the

direct wind-only surge from the total surge due to winds and waves combined) will be used within this distribution.

Model errors combined in calibration/verification runs of ADCIRC have shown that this combination of model and forcing in the Louisiana-Mississippi coastal area provides relatively unbiased results with a standard deviation in the range of 1.75-2.50 feet. Relative errors associated with the use of PBL winds increase the value of the standard deviation to 2.00 to 3.50 feet. This is not to surprising, since the accuracy of HWM's (the primary measurements to which the model results are compare) are quite variable in and of itself.

Combining all of these terms, under the assumption that they are each independently distributed, gives

$$p(\varepsilon) = \iiint \delta(\varepsilon_1 + \varepsilon_2 + \varepsilon_3 + \varepsilon_4 - \varepsilon) p(\varepsilon_1) p(\varepsilon_2) p(\varepsilon_3) p(\varepsilon_4) d\varepsilon_1 d\varepsilon_2 d\varepsilon_3 d\varepsilon_4$$

where

- ε_1 is the deviation between a storm at a random tide phase and a zero tide level;
- ε_2 is the deviation created by variation of the Holland B parameter;
- ε_3 is the deviation created by variations in tracks approaching the coast; and
- ε_4 is the deviation created primarily by errors in models and grids.

Three of the terms ε_1 , ε_3 , and ε_4 are treated here as though they are approximately independent of the magnitude of the surge, while the remaining term, ε_2 has been found to depend essentially linearly with the magnitude of the surge. For a monochromatic tide, the tidal elevation distribution, ε_1 , is known to be bimodal distributed around its zero value; however, in nature, the effect of combining several tidal components with varying phases is to force the distribution toward a unimodal distribution. The probabilities of terms ε_3 and ε_4 are assumed to be normally distributed; thus, the probability distribution of the sum of these two terms will also be a normal distribution with the variance given by the sums of the individual variances of the two terms.

Figure 15 gives a numerical example of the combination of all four terms assuming a storm surge of 15 feet, as might be associated with a particular deterministic model execution based on a set of track and PBL parameters. As can be seen in this figure, the overall magnitude of these effects can add or subtract substantially to the total water depth. In this case, the distribution appears similar to a Gaussian distribution, since it is dominated by the term with the largest variance (deviations due to the omission of the Holland B parameter); however, the other terms have been included within the integral for $p(\varepsilon)$. Table 1 shows an example of the effect of adding this term on expected surge levels for selected return periods. In this example, a Poisson frequency of 1/16 was used in combination with a Gumbel distribution, with parameters $a_0 = 9.855$ and $a_1 = 3.63$. For this example, the effect of adding the ε -term is less than 1/2 foot for return periods up to 175 years and only exceeds 1 foot at return periods greater than

400 years. However, for risk-based calculations which often include very large return periods (1,000-10,000 years), this term can become as large as 2-3 feet, even for the case where the effects of all neglected factors are assumed to be distributed around a mean deviation of zero. The effect could of course be larger if the deviations were biased.

From Table 1 and the above discussion, we see that the effect of the ε -term becomes much more pronounced at large return periods. Thus, older applications of the JPM that neglected this term were probably reasonably accurate at the 100-year return period, but were likely to have been progressively biased low at higher return periods. The important points to stress here are twofold. First, any neglect or suppression of natural variability in a procedure to estimate extremes will lead to some degree of underestimation of the estimated extremes, whether using a JPM or an EST approach; therefore, it is important to recognize and attempt to quantify all significant factors affecting surge heights at the coast. Second, to avoid making the number of dimensions in the JPM unmanageable, the estimated effects of the neglected factors contributing to extreme surges should be addressed statistically, such as we have done here via the addition of the ε -term to the JPM integral.

Treatment of Subsidence and Sea-Level Rise

Rather than treat subsidence and sea-level rise within the ε -term, it is simpler to include this in a separate analysis. For purposes of design, as a first approximation to the non-overtopping situations, estimates of subsidence and sea-level rise can be added linearly to the expected surge levels. Thus, (as a purely hypothetical scenario) if two feet of local subsidence is anticipated along with one-foot of sea-level rise over a design lifetime (say 100 years as an example), a levee design set for 20 feet would need to “evolve” to 23 feet in order to provide the same level of protection at the end of the design lifetime. Other options might be to overbuild the design at the outset to account for anticipated subsidence and sea-level rise. In either case, it will be critical to constantly monitor the changing water levels to ensure that the design level of protection is maintained.

Sampling of Storm Parameters for the JPM-OS

In the conventional JPM each simulation was typically treated as representative of its entire discrete probability range (i.e. all of the probability for each multi-dimensional box centered on its mean position). In these applications, the computational burden was considerably less than what is considered appropriate for surge simulations today (see subsequent section on the computational effort recommended for today’s applications). Even in the original JPM, however, a scaling relationship between the pressure differential of a storm and computed surge levels was used to reduce the number of computer runs. This relationship, based on theoretical considerations and confirmed numerically in several studies, shows that surges are linearly proportional to the pressure differential of a storm at all areas close to the area of maximum storm impact. This information can be used effectively to interpolate between two different numerical results within the JPM integral. Such an interpolation provides added resolution along the pressure differential axis in this integral, which is very important due to the highly nonlinear characteristics of the probability of pressure differentials [$p(\Delta P)$].

In addition to the scaling relationship between surge levels and pressure differentials, the JPM-OS attempts to sample the parameter space in a fashion that can be used to estimate surges (develop the response surface) in an optimal manner. This method has been developed via hundreds of simulations on relatively straight coasts, as well as on coasts with other simple geometries, and is in the process of being extended to more complex coasts. It attempts to alleviate the need for very closely spaced parameter values in numerical simulations (essentially track spacing and number of storm sizes, forward speeds, and track angles considered); thereby potentially greatly reducing the total number of computer runs required for JPM execution. The initial set of runs for the New Orleans area consists of 152 hurricanes traveling along tracks shown in Figures 12-14. To put this number of runs in perspective, since a major storm only affects each one-degree section of coast once per 16 years and the section of coast being studied is only about 2.5 degrees, this number of hurricanes would only be expected in the simulated area every 853 years. Consequently, unless we have selected these storms in a very unrepresentative fashion, we expect this number of storms (combined with an accurate methodology for surge simulation) to provide a fairly accurate description of the general characteristics of hurricane surges at least up to the 500-year return period. A description of the parameters of these storms is given in Appendix D, along with a discussion of some scaling relationships between storm parameters and surges that have been found in our numerical studies.

Specification of Variations in Pre-landfalling Hurricanes

Whereas the original JPM considered storm size, intensity, and wind field distribution to be constant in storms approaching the coast, the new JPM uses information from recent storms to estimate the rate of change of these parameters for pre-landfall conditions. In general these trends show that storms tend to fill by about 10-15 millibars (Figure 3), become slightly (15-30%) larger (Figure 16) and have less peaked wind speed distributions (Holland B parameter decreasing from about 1.27 to around 1.0) over the last 90 nautical miles of coastal water before landfall. Since all of our probabilities have been developed based on landfalling characteristics, the offshore characteristics must be estimated from a generalized transform

$$p(\Delta P, R_p, v_f, \theta_l, x)_{\text{offshore}} = p(\Delta P, R_p, v_f, \theta_l, x)_{\text{landfall}} J^{-1}$$

where J is the Jacobian for the transform from nearshore to offshore conditions. However, since 1) storm heading during approach to the coast is relatively constant, 2) the forward speeds are assumed to be constant during approach to land and 3) the points of intersection (x) are identical for each offshore and landfall case, the transform can be viewed in only two dimensions, ΔP and R_p . Details will be given in Appendix D.

A Computational Methodology for Effective Simulation of Storm Surges for Hurricane Inundation Studies

For completeness, we include here a brief description of the computational methodology that has been adopted for calculating inundation levels/probabilities. The first step in this procedure is to develop appropriate surge and wave model grids and verify them. The second step is to use both “best available” winds and best PBL winds to verify the modeling system performance within the area of interest. The “best available” winds, which include all appropriate data assimilation and expert analyses, are used to verify the model and grid and to provide calibration guidance, if required. The second set of runs with winds from the PBL model are used to establish any additional tuning required and to determine the actual modeling error term to be used in the ε -term in the JPM integration. Following this procedure, the complete production system is exercised for all of the selected combinations of storm tracks and wind parameters required for the JPM-OS application. A schematic diagram of this system is shown in Figure 17.

Step 1

As seen here, for each defined storm (a track and its time-varying wind field parameters) the Oceanweather PBL model (Thompson and Cardone, 1996) is used to construct 15-minute snapshots of wind and pressure fields for driving surge and wave models.

Step 2

Using “warm-start” condition with all major rivers already “spun up,” initiate ADCIRC (version 46.50 or higher as they come online) for simulation of direct wind-driven surge component (assuming zero tide). In parallel with the initial ADCIRC runs, execute a large-domain, discrete, time-dependent spectral wave model (WAM or WAVEWATCH) to calculate directional wave spectra that serve as boundary conditions for local-domain, near-coast wave model runs in Step 3.

Step 3

Using initial water levels from ADCIRC, winds that include the effects of sheltering due to land boundaries, and spectral boundary conditions from the large-domain wave model, execute either STWAVE or SWAN model runs (again using the PBL winds) to produce a wave fields and estimated radiation stress fields.

Step 4

Using the radiation stress fields from Step 3 added to the PBL-estimated wind stresses, rerun the ADCIRC model for the time period during which the radiation stresses potentially make a significant contribution to the water levels. In this step, care must be taken to “match” the grids in the wave model and ADCIRC model.

Step 5

Using the water levels from Step 4, in locations adjacent to structures, a method based on Boussinesq modeling (either direct application or interpolations from generic runs) is used to provide estimates of the following key information along man-made structures and steep-sided natural flood barriers: incremental contribution to the water level at the structure (which should be considered as the final water level for inundation efforts at these locations); estimated total overtopping at structure; and estimated velocities on the front face, crest, and rear face of the structures. The boundary conditions for driving the Boussinesq-based runs are taken from the closest points in the nearshore grids used in Step 3.

Summary

Some of the key issues addressed in this paper, along with relevant conclusions, are as follows:

1. The Joint Probability Method (JPM) provides a sound method for estimating inundation probabilities. However, given the number of degrees of freedom in hurricanes characteristics affecting coastal surges and the computational burdens associated with coastal surge simulations, it is critical to reduce the number of factors considered to a minimum, while maintaining sufficient detail to properly model hurricane wind fields for surge prediction.
2. After a discussion of various alternatives, it is recommended that the same five parameters used in older JPM studies (storm intensity, storm size, forward speed of the storm, angle of the storm track with the coast, and track location) be used to characterize storms for simulating coastal surges. With this number of dimensions within the JPM integral, it is essential 1) to allow these characteristics to exhibit observed variations during their approach to land and 2) to retain and quantify a statistical “error” term that adds the suppressed variability back into the estimated extremes. Previous applications of the JPM did not consider this term.
3. Similar to the Empirical Simulation Technique (EST), it is recommended that uncertainty in the stage-frequency relationships be estimated via re-sampling methods.
4. As discussed in Appendix C and as has been noted in many journal publications, it appears that a 40-year cycle is a dominant feature within the recent hurricane record. We have experienced one full “high-activity” portion of a cycle and about 2/3 of a second “high-activity” portion of a cycle. It is recommended that a comparable proportion of “low-activity” years be included within the record being used for estimating inundation probabilities. Following this logic, we will use the full “low-activity” interval (approximately 30 years) between the two recent “high-activity” intervals plus a period equivalent to 2/3 of the recent “low-activity” interval within our sample period. This yields 1941 through 2005 as our period of record for coastal inundation analyses.

5. The topic of future climatic variability has been dealt with in a recent manuscript by Resio and Orelup. In this manuscript, it is shown that the hurricane record within the Gulf of Mexico does not exhibit a strong secular trend, in contrast to the record in the Atlantic Basin. The Resio and Orelup manuscript showed that the “high-activity” intervals dominated the extreme surge population for return periods greater than 50 years or so. As a sensitivity study, they investigated the consequences of a doubling of “high-activity” years, even though there is no evidence that such a doubling is imminent. Results of this study showed that such a climate scenario would produce about a 12% increase in surge levels at the 100-year level, with decreasing effects at longer return periods.
6. Historically, the storms which appear to have had the most impact on coastal areas within the Gulf of Mexico have all moved along the central paths shown in Figure 12. These storms include Rita, Ivan, Camille, Katrina, and Andrew in the historical record from 1941 through 2005; thus the set of tracks in this figure have been nicknamed the RICK-fan.
7. The JPM-OS represents an attempt to combine statistical information over an interval of the coastline in order to gain more confidence in information relevant to the definition of extreme surges at a point. This approach also allowed us to incorporate information on the general behavior of storms in coastal areas (such as storm decay and variations in storm size and the peakedness of the wind distribution along a transect) into our simulations of extreme events.

References, Tables, and Figures for R2007

- ASCE, 1990: Minimum design loads for buildings and other structures, ASCE 7-88, New York.
- ASCE 1996: Minimum design loads for buildings and other structures, ASCE 7-95, New York.
- Borgman, L.E, Miller, M., Butler, L. and R. Reinhard, 1992: Empirical simulation of future hurricane storm histories as a tool in engineering and economic analysis, Proc. Fifth Intn'l, Conf. on Civil Engr. In the Ocean, ASCE, November, College Station, Texas.
- Cardone, V.J., Pierson. W.J., and E.G. Ward, 1976: Hindcasting the directional spectra of hurricane generated waves, J. Petrol. Technol., 28, 385-394.
- Collins, J.I., and M.J.Viehmann, 1971: A simplified model for hurricane wind fields, Paper 1346, Offshore Technology Conference, Houston, TX.
- Chouinard, L.E., Liu, C. and C.K. Cooper, 1997: A model for the severity of hurricanes in the Gulf of Mexico, J. Waterways, Harbor and Coastal Engr., ASCE, 123, 113-119.
- Chow, S., 1971: A study of the wind field in the planetary boundary layer of a moving tropical cyclone, M.S. Thesis, New York University.
- Ho, F.P and V.A. Myers, 1975: Joint Probability Method of Tide Frequency Analysis applied to Apalachicola Bay and St. George Sound, Florida, NOAA Tech. Rep. NWS 18, 43p.

- Ho, F.P., Su, J.C., Hanevich, K.L., Smith, R.J. and F.P. Richards, 1987: Hurricane Climatology for the Atlantic and Gulf Coasts of the United States, NOAA Tech. Rep. NWS 38, completed under agreement EMW-84-E-1589 for FEMA, 194 p.
- Holland, G.J., 1980: An analytic model of the wind and pressure profiles in hurricanes, *Mon. Wea. Rev.* 108, 1212-1218.
- Irish, Resio, & Ratcliff, 2006: The influence of hurricane size on coastal storm surges, submitted to *J. Phys. Oceanogr.*
- Kimball, S.K., 2006: A modeling study of hurricane landfalls in a dry environment, *Mon. Wea. Rev.*, 134, 1901-1918.
- Myers, V.A., 1954: Characteristics of United States hurricanes pertinent to levee design for Lake Okeechobee, Florida, Hydromet. Rep. No. 32, U.S. Weather Bureau, Washington, D.C.
- Myers, V.A., 1975: Storm Tide Frequencies on the South Carolina Coast, NOAA Tech. Rep. NWS-16, 79 p.
- Resio, D.T. and E.A. Orelup, 2006: Potential effects of climatic variability in hurricane characteristics on extreme waves and surges in the Gulf of Mexico, submitted to *J. Climate*.
- Scheffner, N., Borgman, L. and D. Mark, 1993: Empirical simulation technique applications to a tropical storm surge frequency analysis fo the coast of Delaware, Proc. Third Intn'l Conf. on Estuarine and Coastal Modeling.
- Schwerdt, R.W., Ho, F.P., and R.R. Watkins , 1979: Meteorological criteria for Standard Project Hurricane and Probable Maximum Hurricane Windfields, Gulf and East Coasts of the United States, Tech. Rep. NOAA-TR-NWS-23, National Oceanic and Atmospheric Administration.
- Shen, W., 2006: Does the size of hurricane eye matter with its intensity?, *Geophys. Res. Let.*, 33, L18813.
- Thompson, E.F. and V.J. Cardone, 1996: Practical modeling of hurricane surface wind fields, *ASCE J. Waterway, Port, Coastal, and Ocean Engineering*, 122, No. 4, 195-205.
- Vickery, P.J., Skerjil, P.F., and L.A. Twisdale, 2000: Simulation of hurricane risk in the U.S. using empirical track model, *J.Struct. Engr.*, 1222-1237.

**Table 1.
Example of Expected Surge Values as a Function of Return Period With and Without ϵ -Term Included**

Return Period (years)	Without ϵ-Term (feet)	With ϵ-Term (feet)
50	11.98	12.06
75	13.64	13.90
100	14.82	15.21
125	15.74	16.22
150	16.49	17.04
175	17.12	17.74
200	17.67	18.35
225	18.15	18.88
250	18.59	19.36
275	18.98	19.79
300	19.33	20.18
325	19.66	20.55
350	19.97	20.88
375	20.25	21.20
400	20.52	21.49
425	20.76	21.76
450	21.00	22.02
475	21.22	22.27
500	21.43	22.50

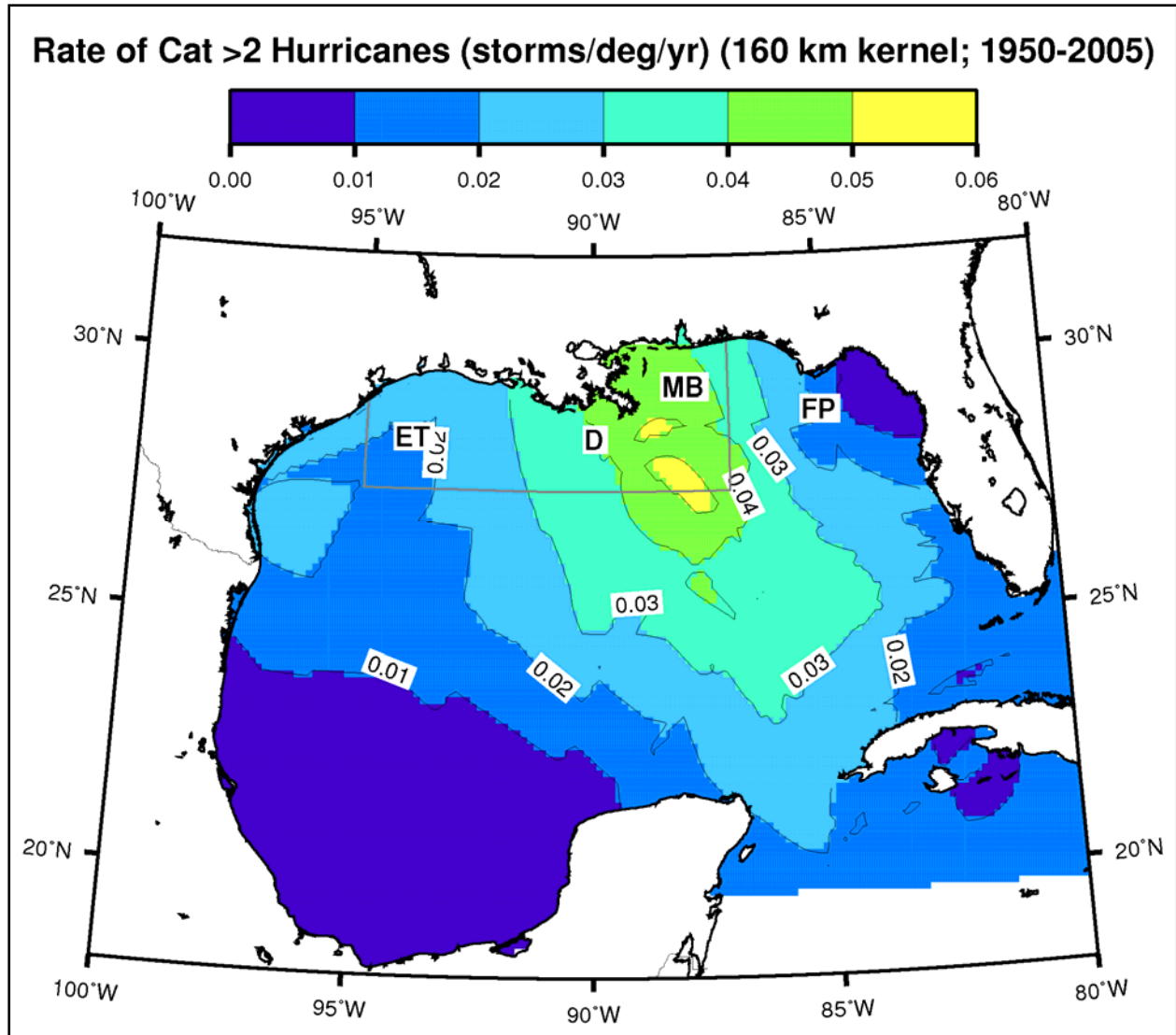


Figure 1. Analysis of hurricane frequency from Toro (Risk Engineering) from an analysis using an optimized spatial kernel.

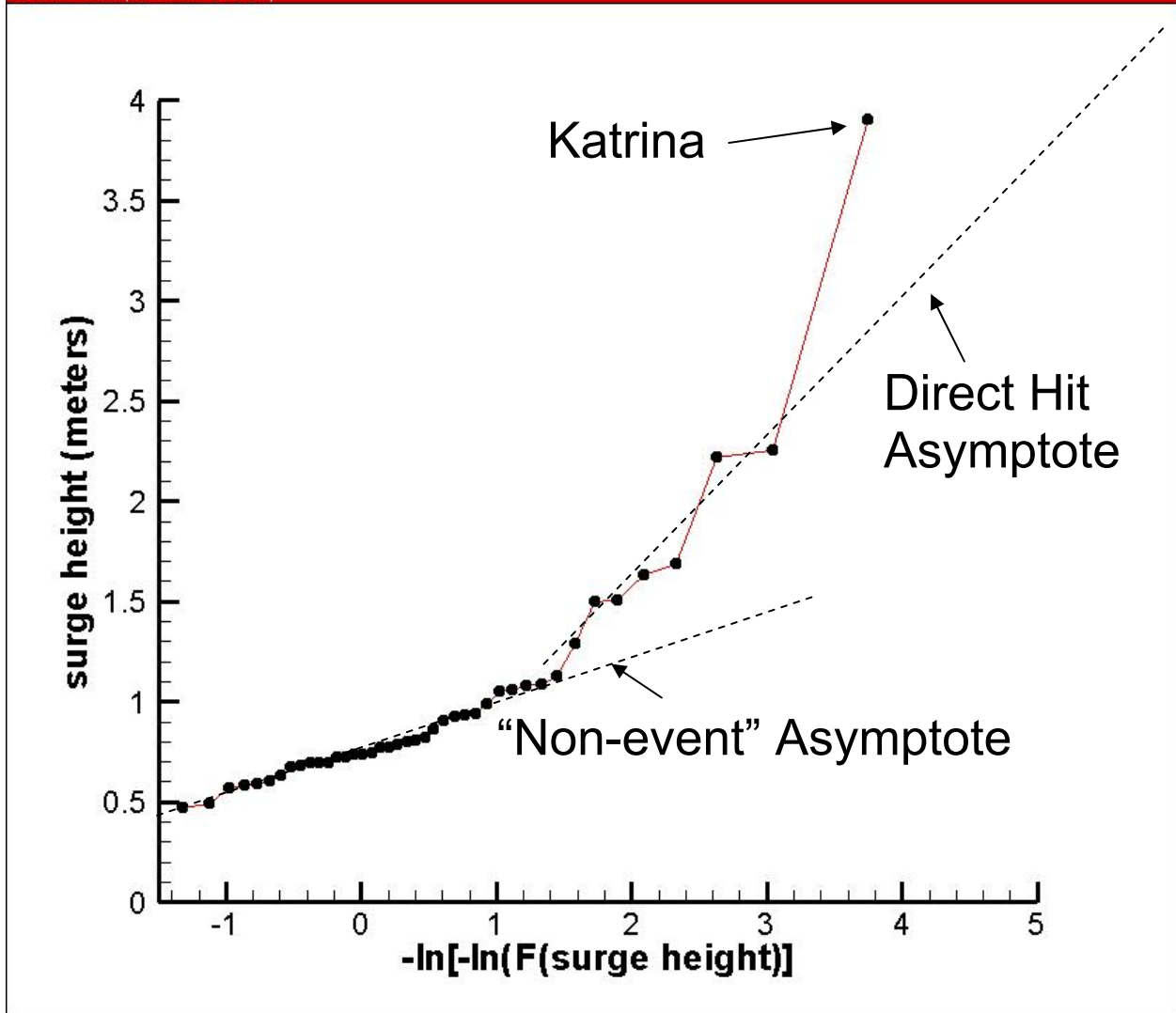


Figure 2. Distribution of the maximum surge heights from ADCIRC simulations for a site in Lake Pontchartrain. Storms within the “non-event” asymptote consist of storms which do not make landfall close to the site of interest; whereas, storms within the “direct-hit” asymptote represent storms that pass very close to the site of interest. The different slopes of these line segments suggests that it may not be justifiable to combine these points into an analysis that treats all of the points as though they are drawn from a single analysis.

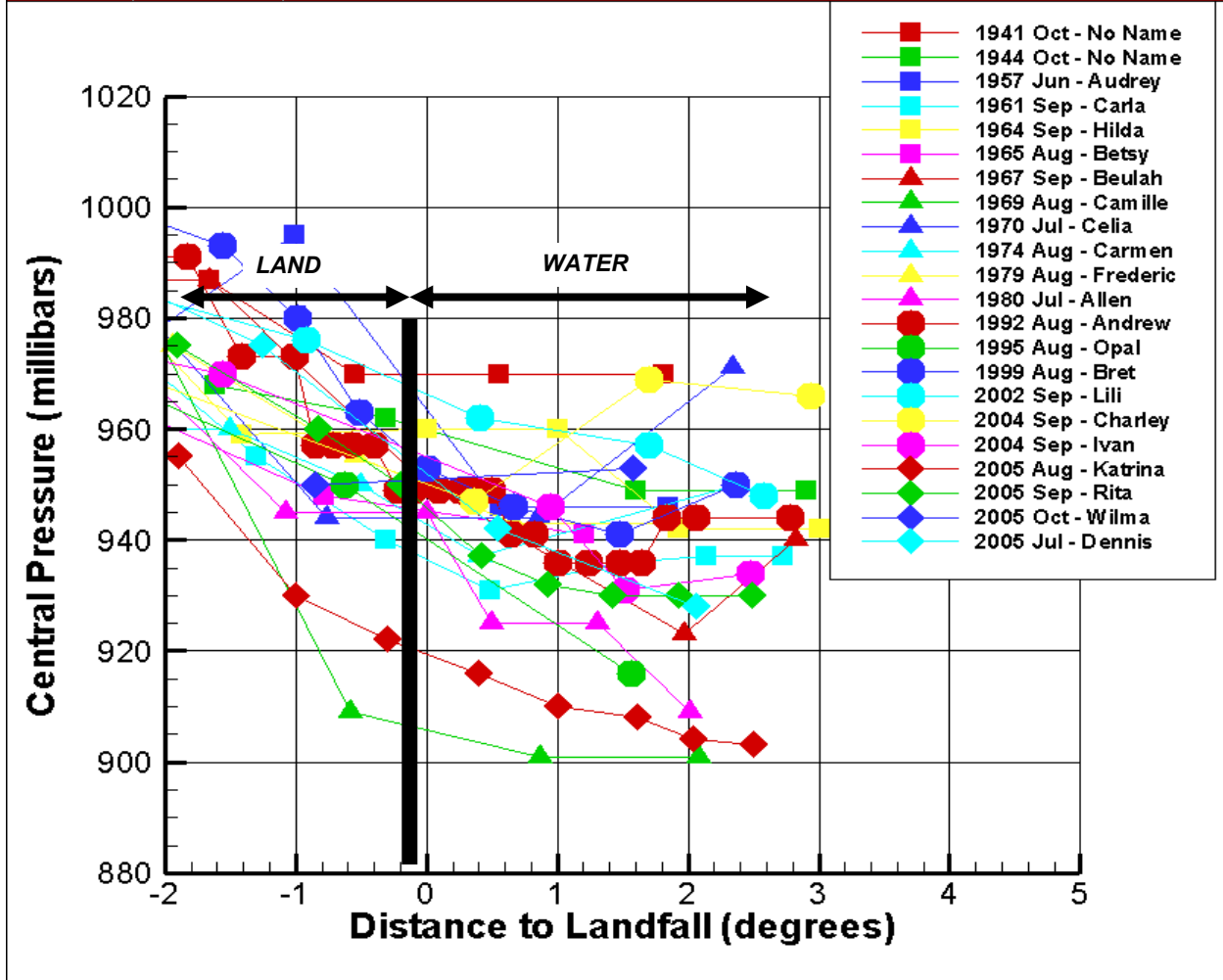


Figure 3. Central pressure in landfalling storms plotted against distance from the coast. Previously it was believed that storm decay began only after landfall. These data from Oceanweather, Inc. show clearly that decay begins offshore.

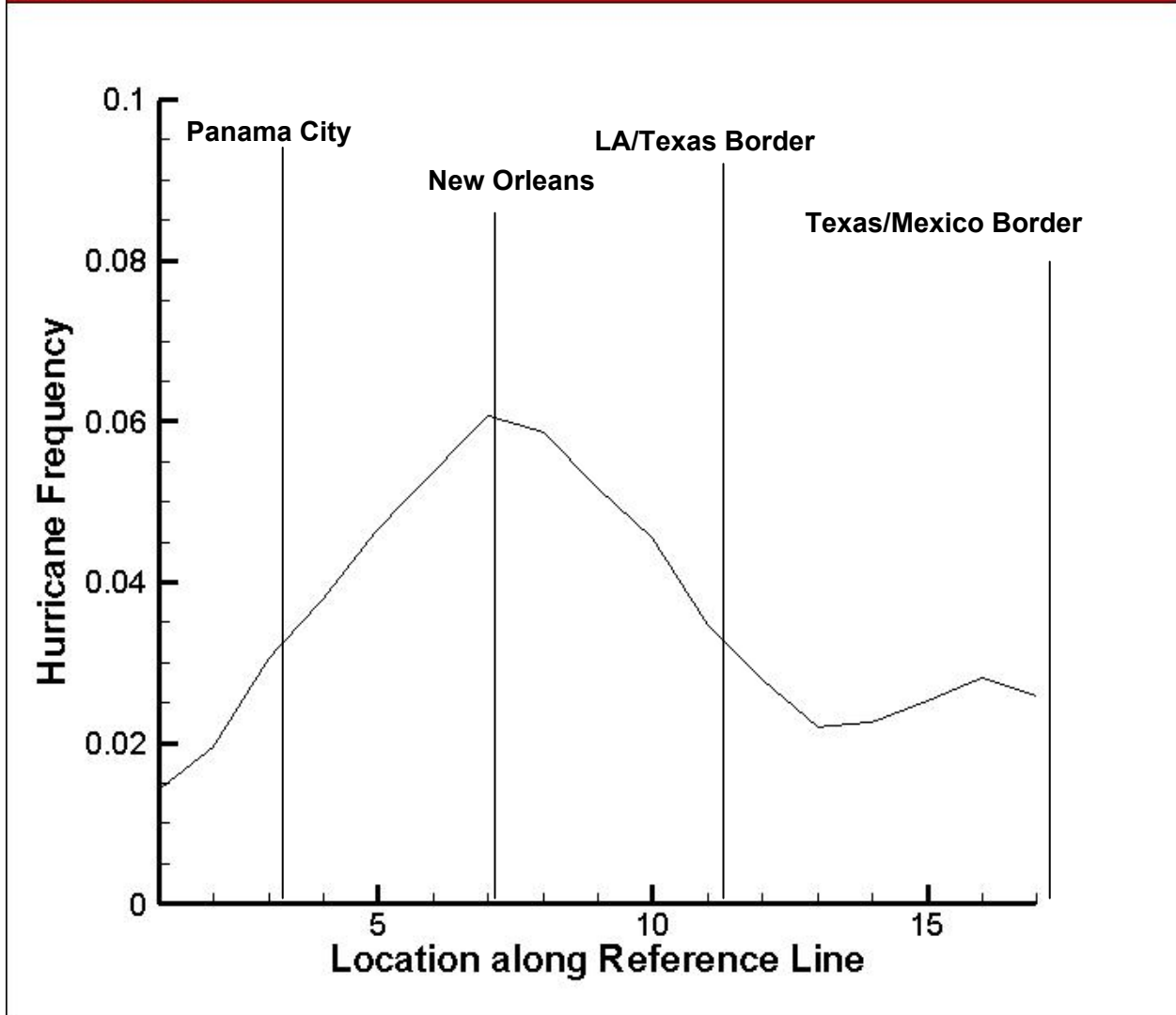


Figure 4. Frequency of hurricanes along reference line with annotated geographic locators, based on 22-storm sample. Location along this line can be taken as equivalent to 1-degree increments along the coast, with the New Orleans area falling within increment 7.

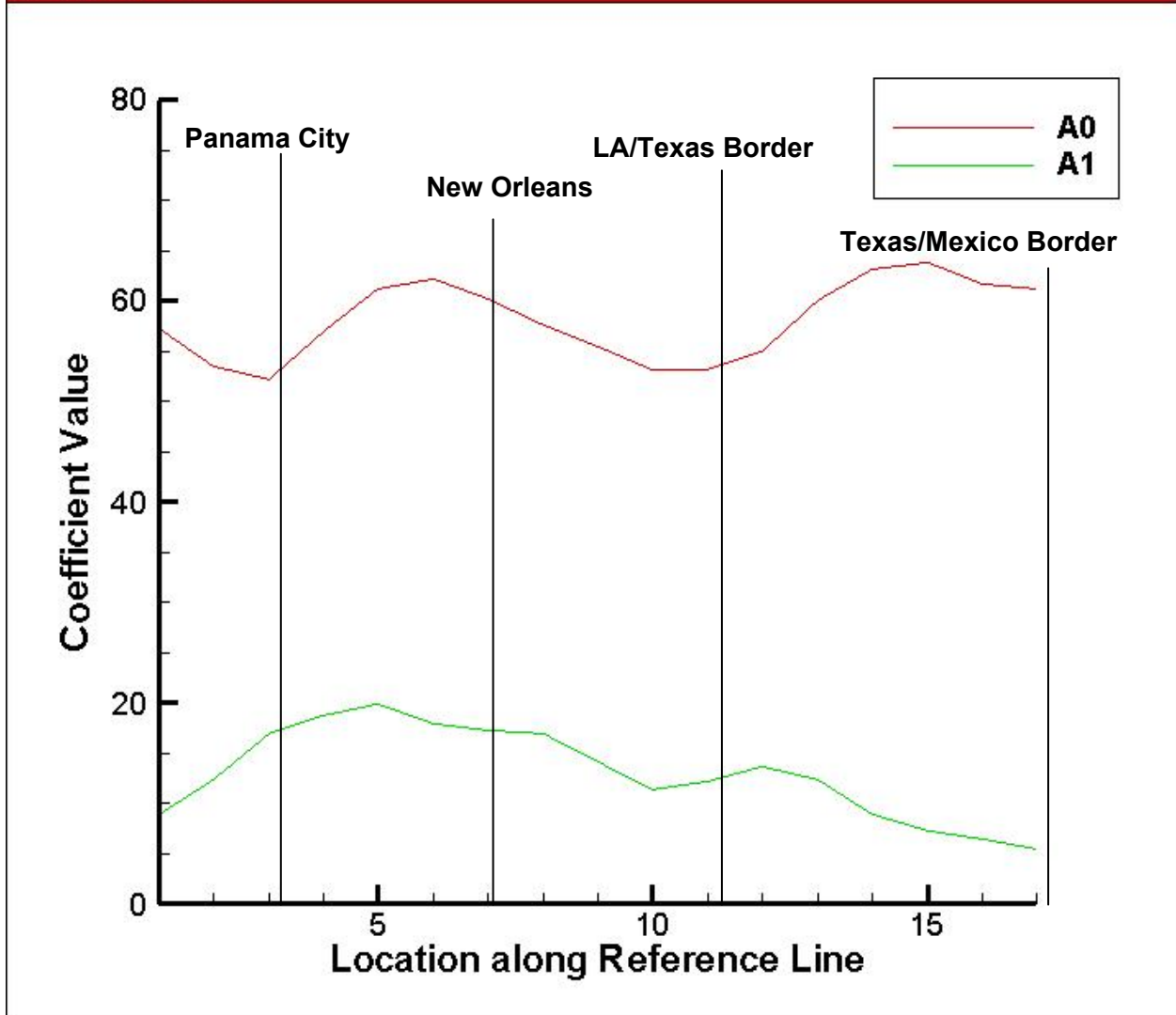


Figure 5. Gumbel coefficients for locations along reference line, based on 22-storm sample. For reference, the Gumbel equation is reproduced here in terms of its explicit dependence on x,

$$F(\Delta P | x) = \exp\left\{-\exp\left[-\frac{\Delta P - a_0(x)}{a_1(x)}\right]\right\},$$

where ΔP is the pressure differential (peripheral pressure minus central pressure). It should be recognized that the frequency is assumed to be equal to 1 in this equation. Location along this line can be taken as equivalent to 1-degree increments along the coast, with the New Orleans area falling within increment 7.

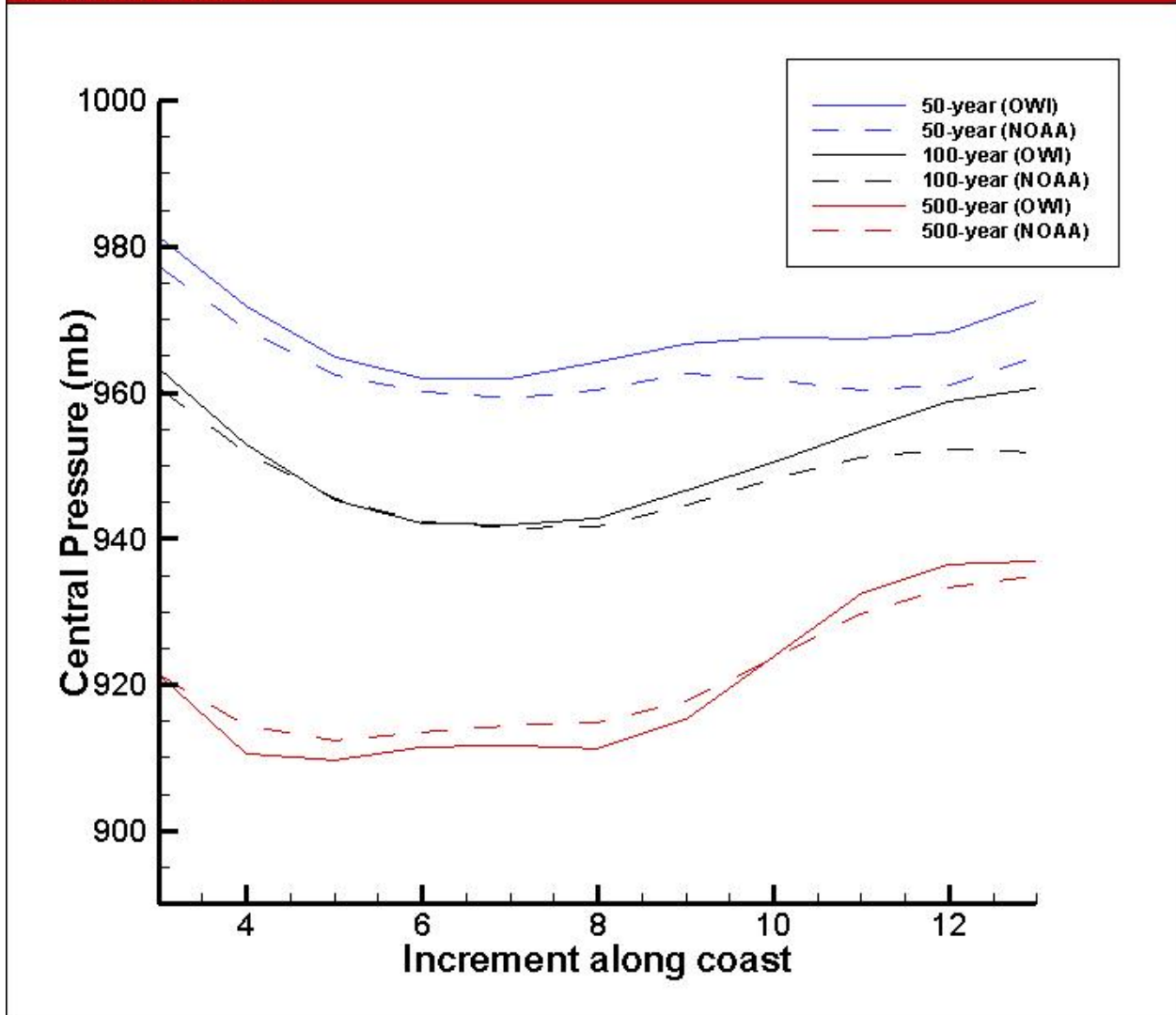


Figure 6. Distribution of 50-year, 100-year, and 500-year central pressures along the reference line shown in Figure A2, using both Oceanweather, Inc. (OWI) data and official NOAA values. Location along this line can be taken as equivalent to 1-degree increments along the coast, with the New Orleans area falling within increment 7.

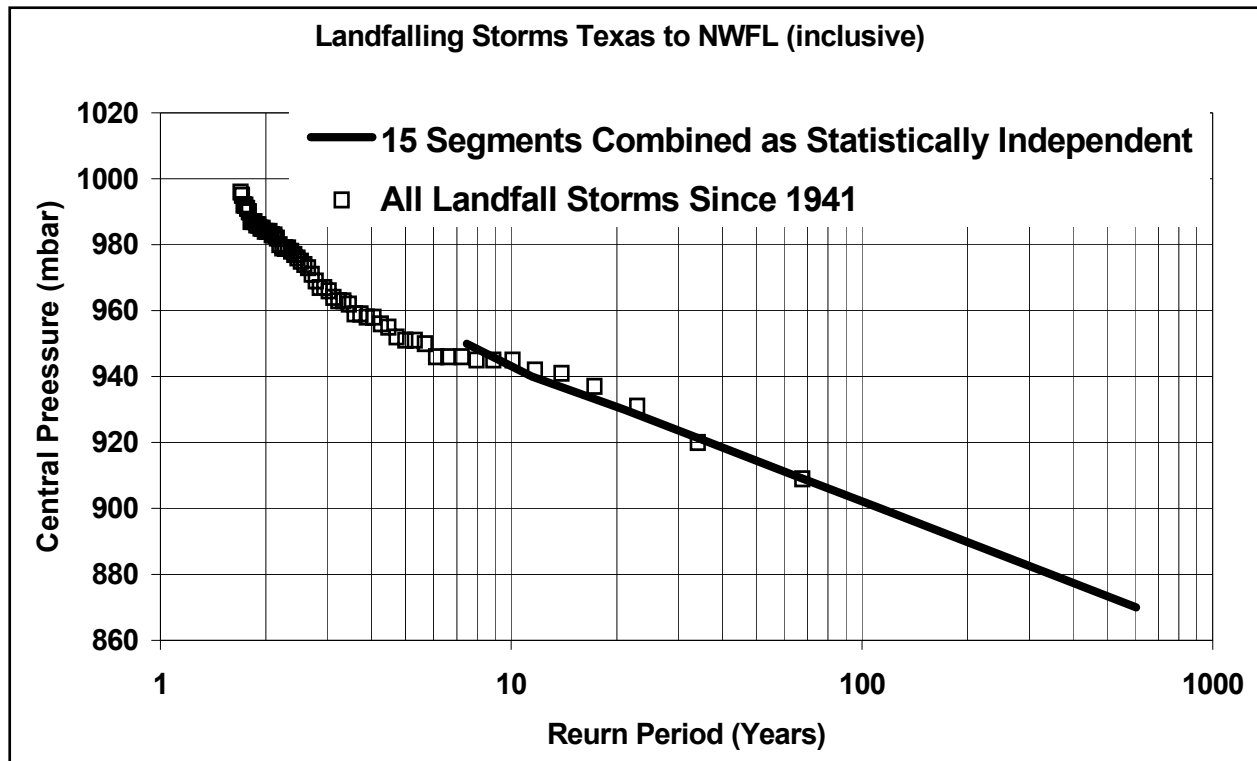


Figure 7a. Comparison of Vickery's analysis of the combination of distributions for landfalling central pressures from all coastal segments (taken from the NOAA results shown in Figure 6) compared to the distribution of all (NOAA) landfalling central pressures within the Gulf of Mexico.

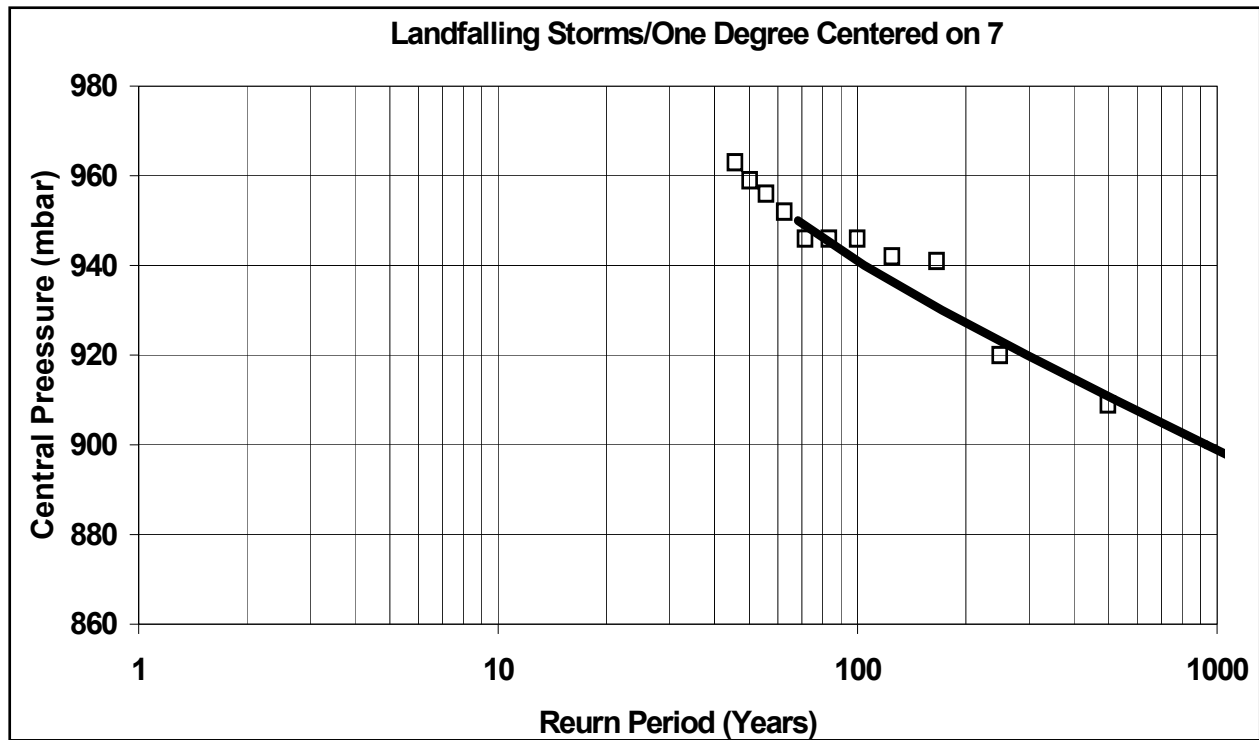


Figure 7b. Same as Figure 7a except specific to the 1-degree increment centered on 7.

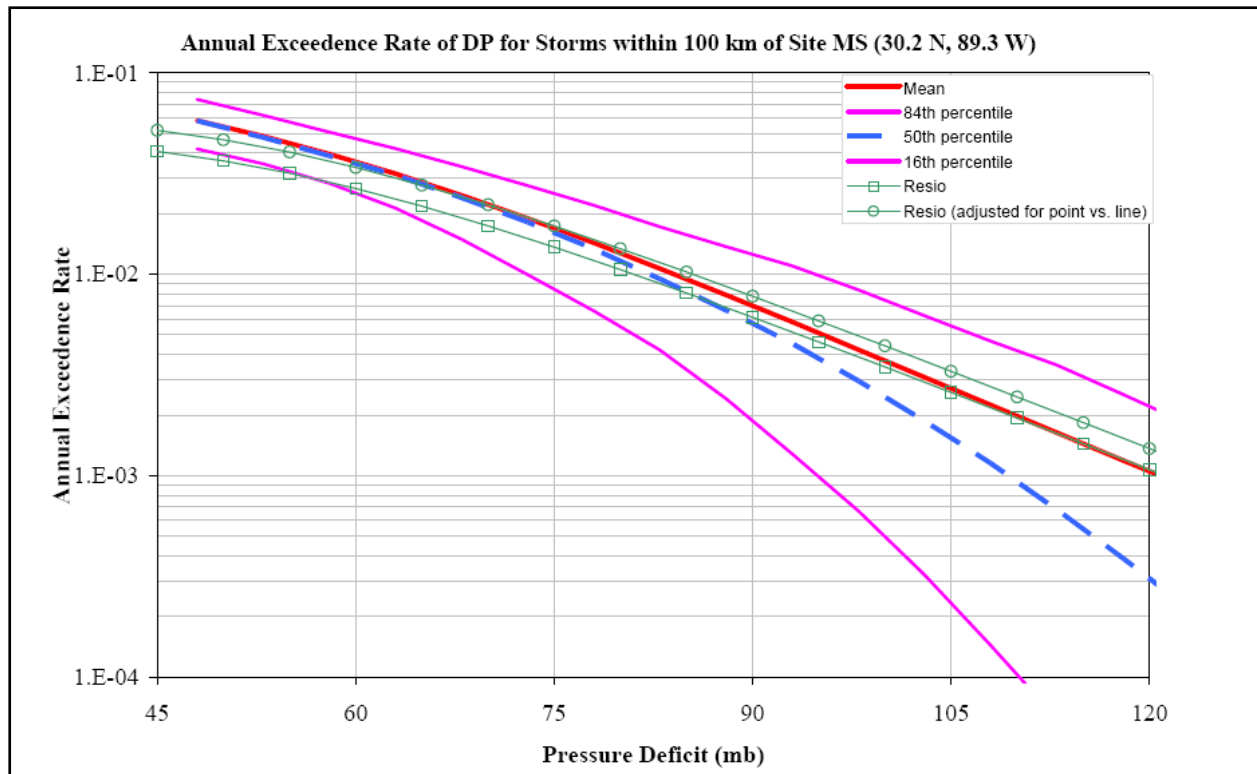


Figure 7c. Independent estimate of storm probabilities in the Mississippi coastal area by Gabriel Toro (for FEMA Region 4) compared to estimate based on Gumbel segments developed in this White Paper. As can be seen here the mean curve is in very good agreement with Toro's results.

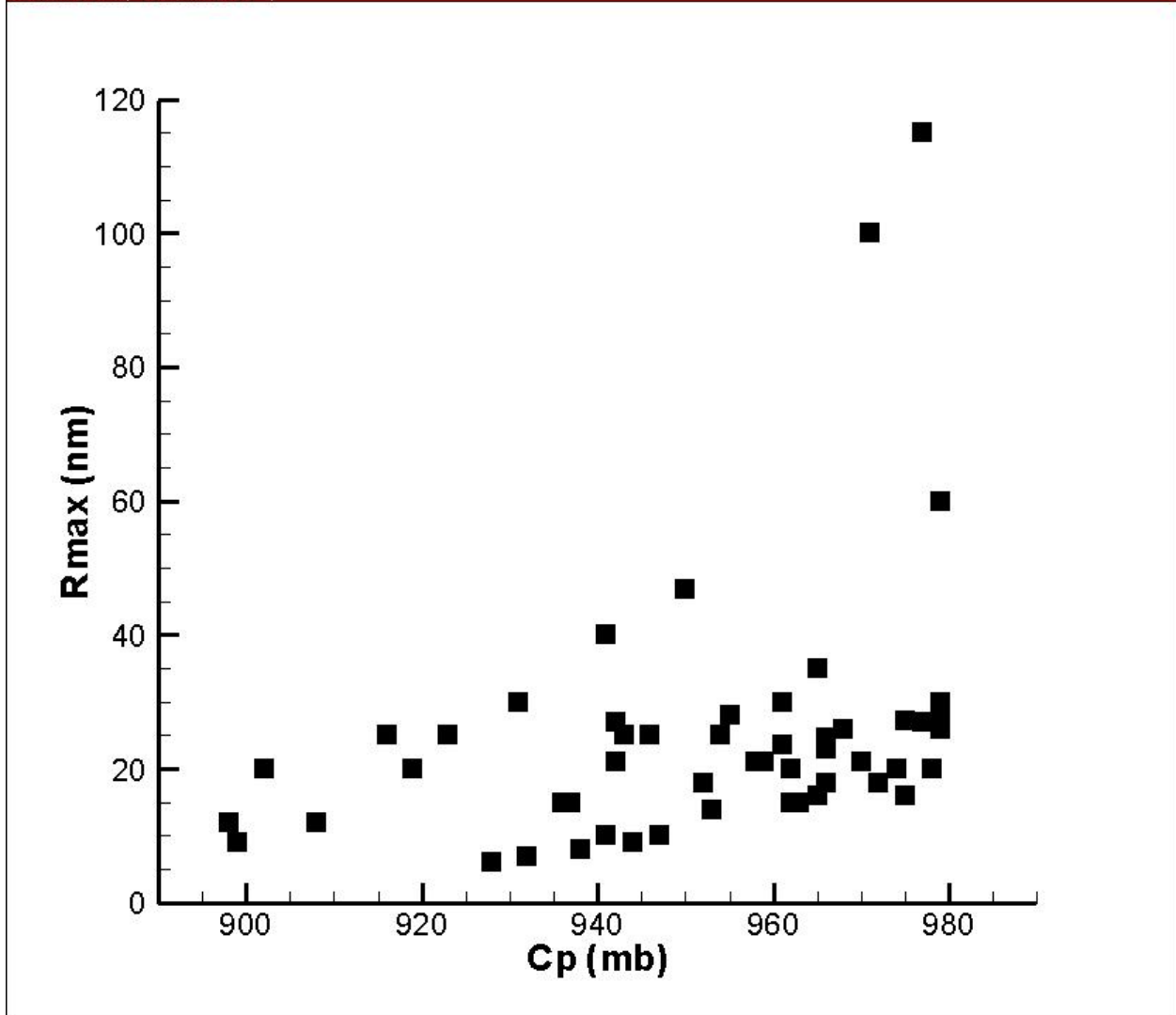


Figure 8a. Relationship between size scaling parameter (R_p) versus Central Pressure for 52 storm set in Gulf of Mexico (offcoast; all storms > Cat 2).

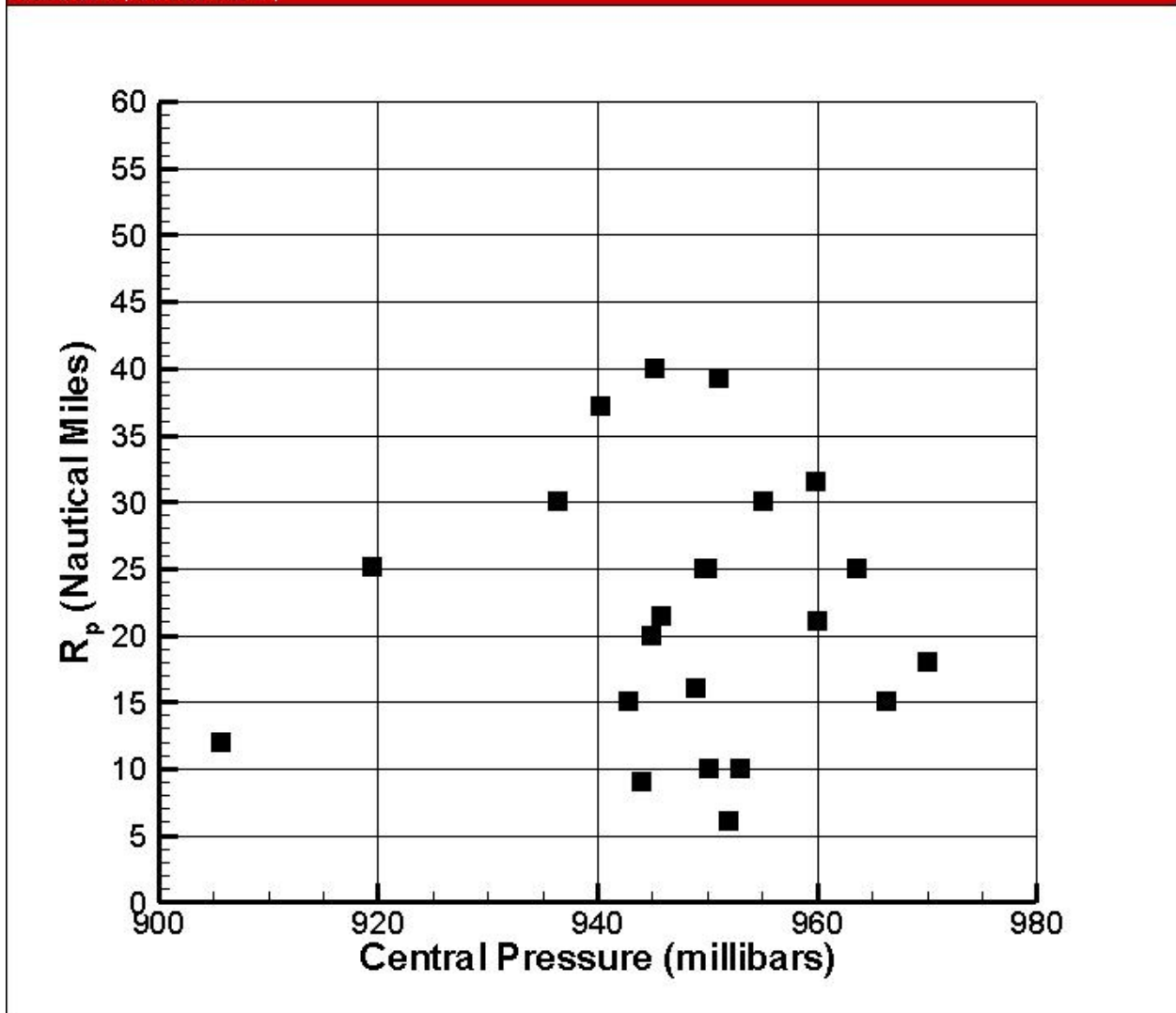


Figure 8b. Relationship between size scaling parameter (R_p) at landfall versus Central Pressure for 22 storm set in Gulf of Mexico (offcoast; all storms with central pressure < 955 at time of minimum pressure in the Gulf of Mexico).

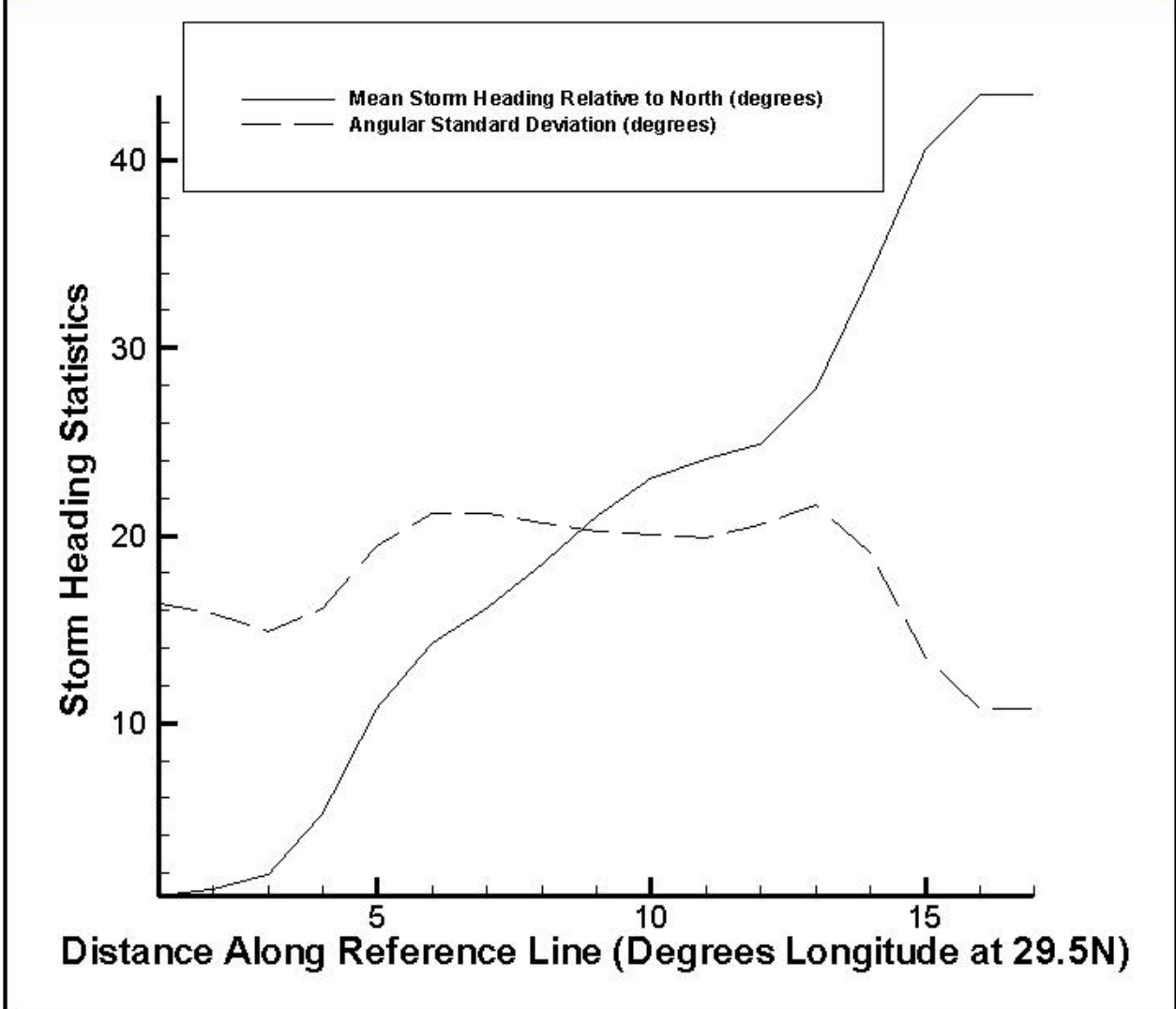


Figure 9. Plot of mean storm heading angle and standard deviation around this angle as a function of location along reference line. Distance along the x-axis can be taken as equivalent to 1-degree increments along the coast, with the New Orleans area falling within increment 7.

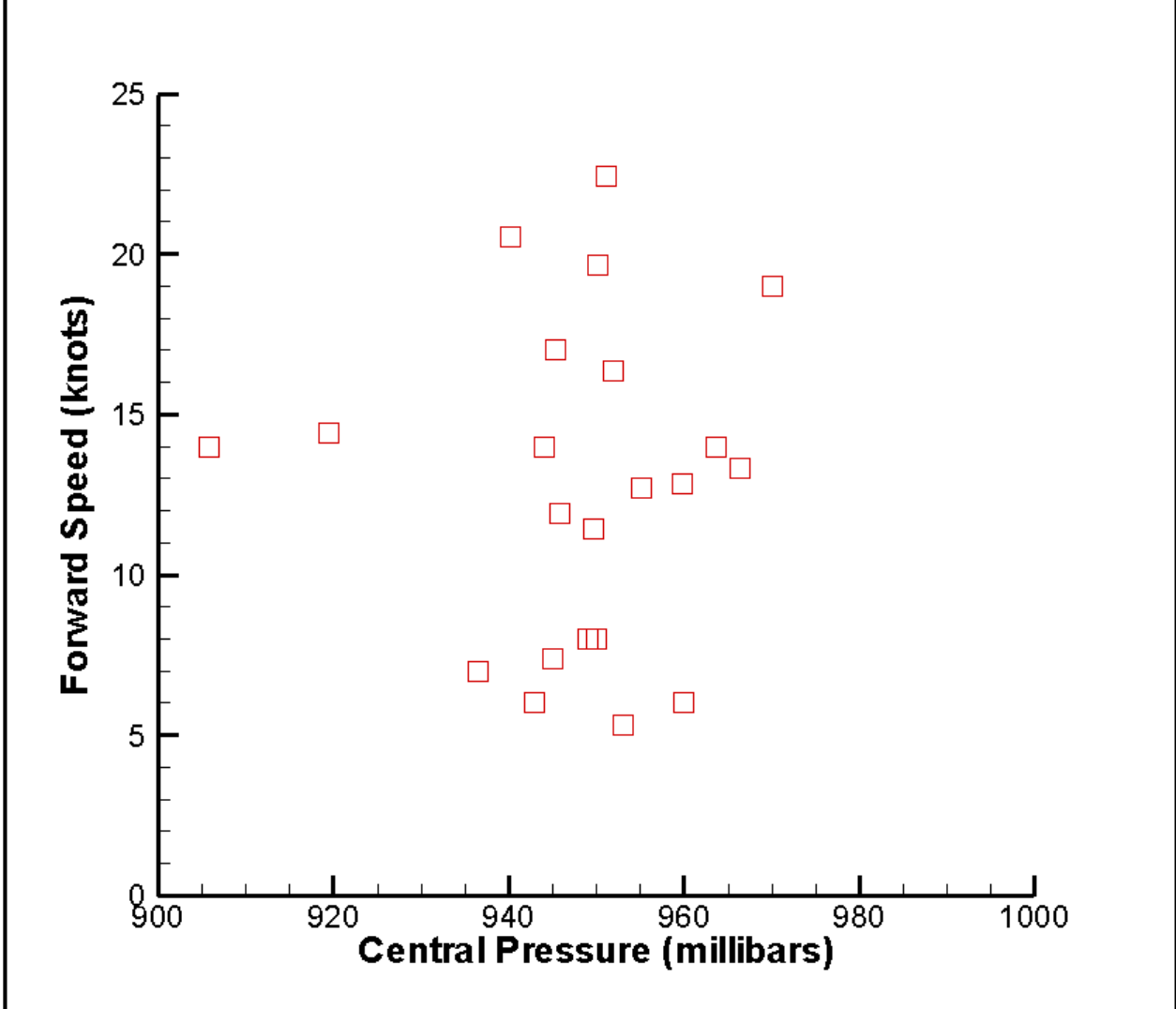


Figure 10. Plot of forward speed of storm at landfall versus central pressure at landfall.

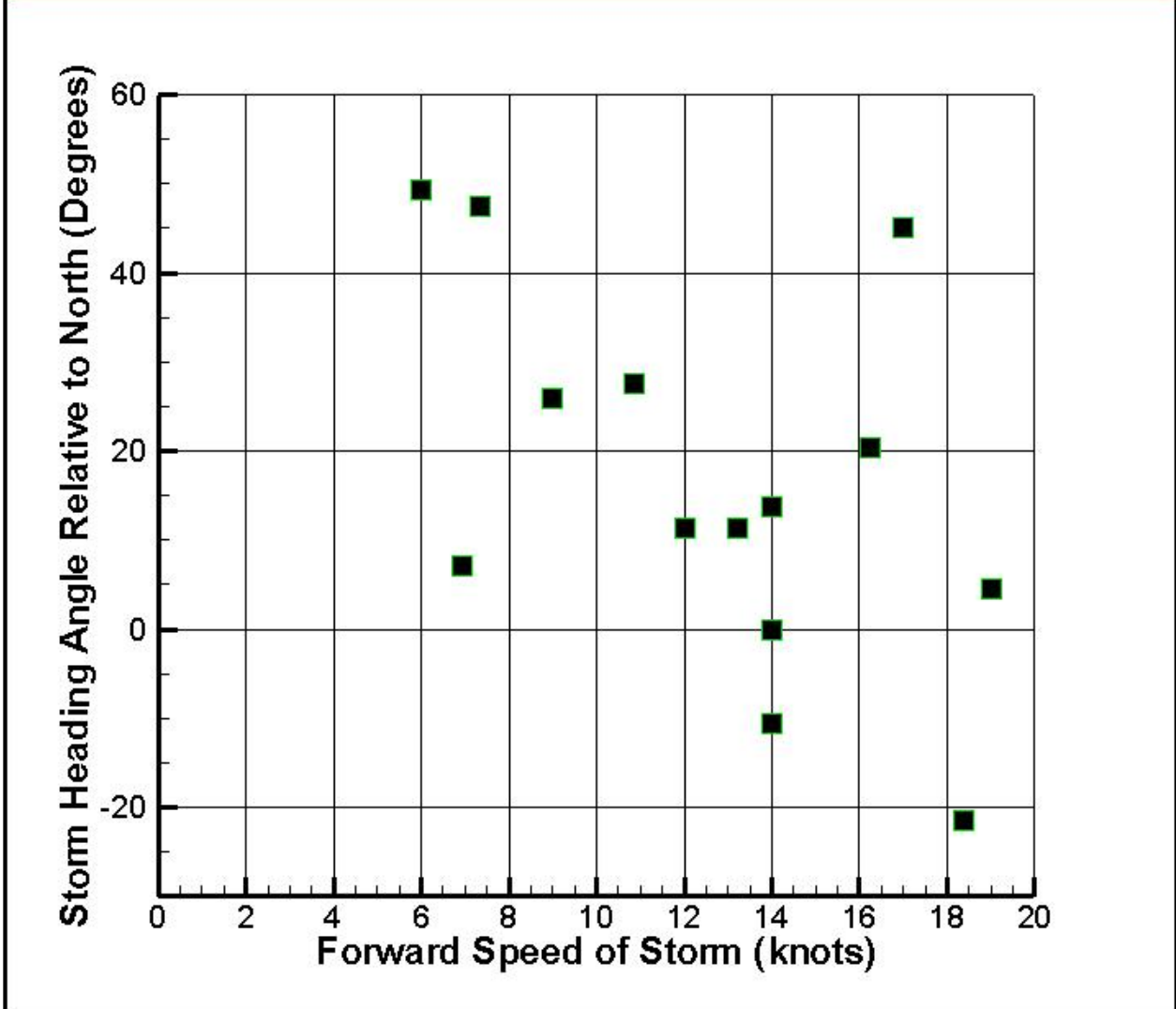


Figure 11a. Plot of storm heading and forward speed at time of landfall for only central Gulf landfalling storms.

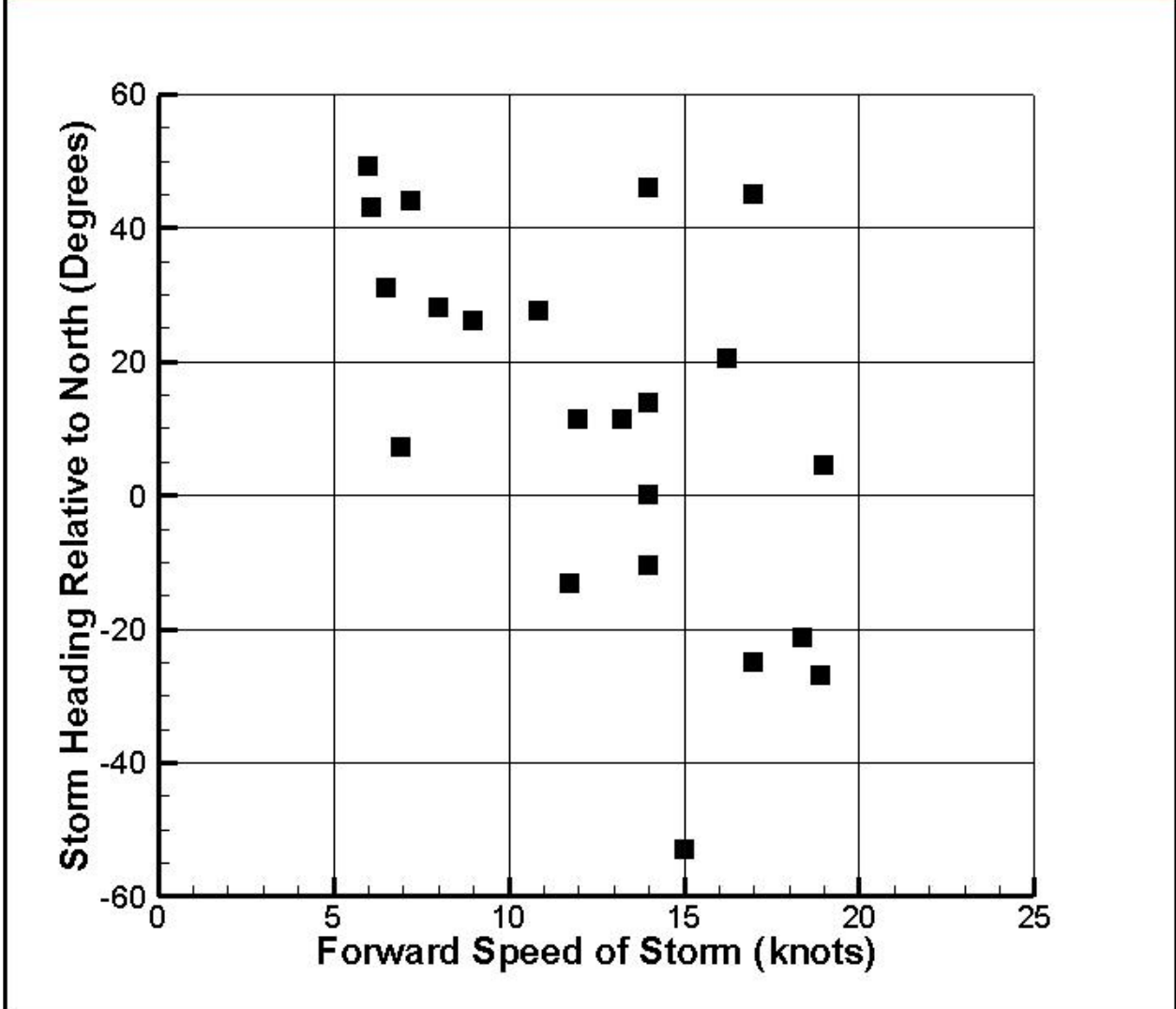


Figure 11b. Plot of storm heading and forward speed at time of landfall for the entire 22-storm sample.

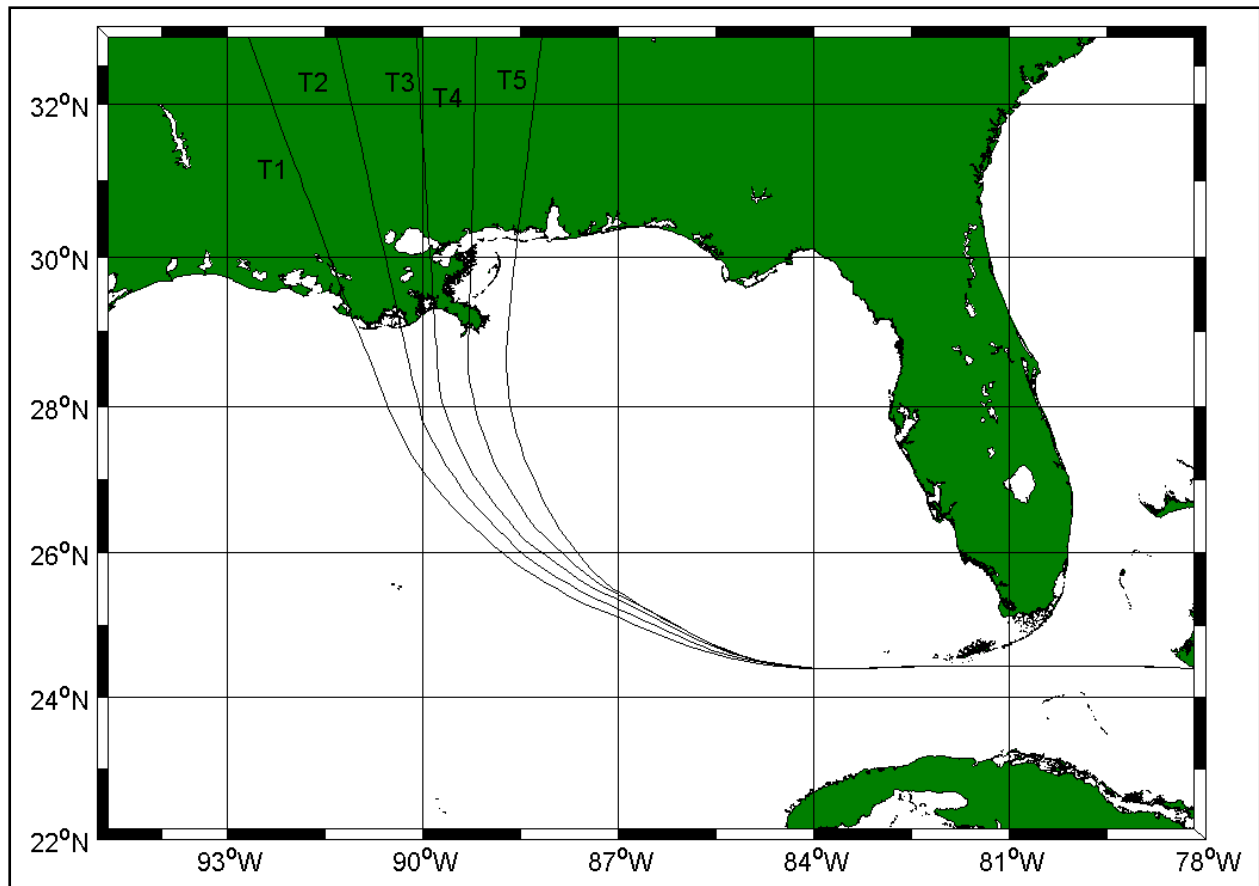


Figure 12. Central angle tracks (RICK-fan set).

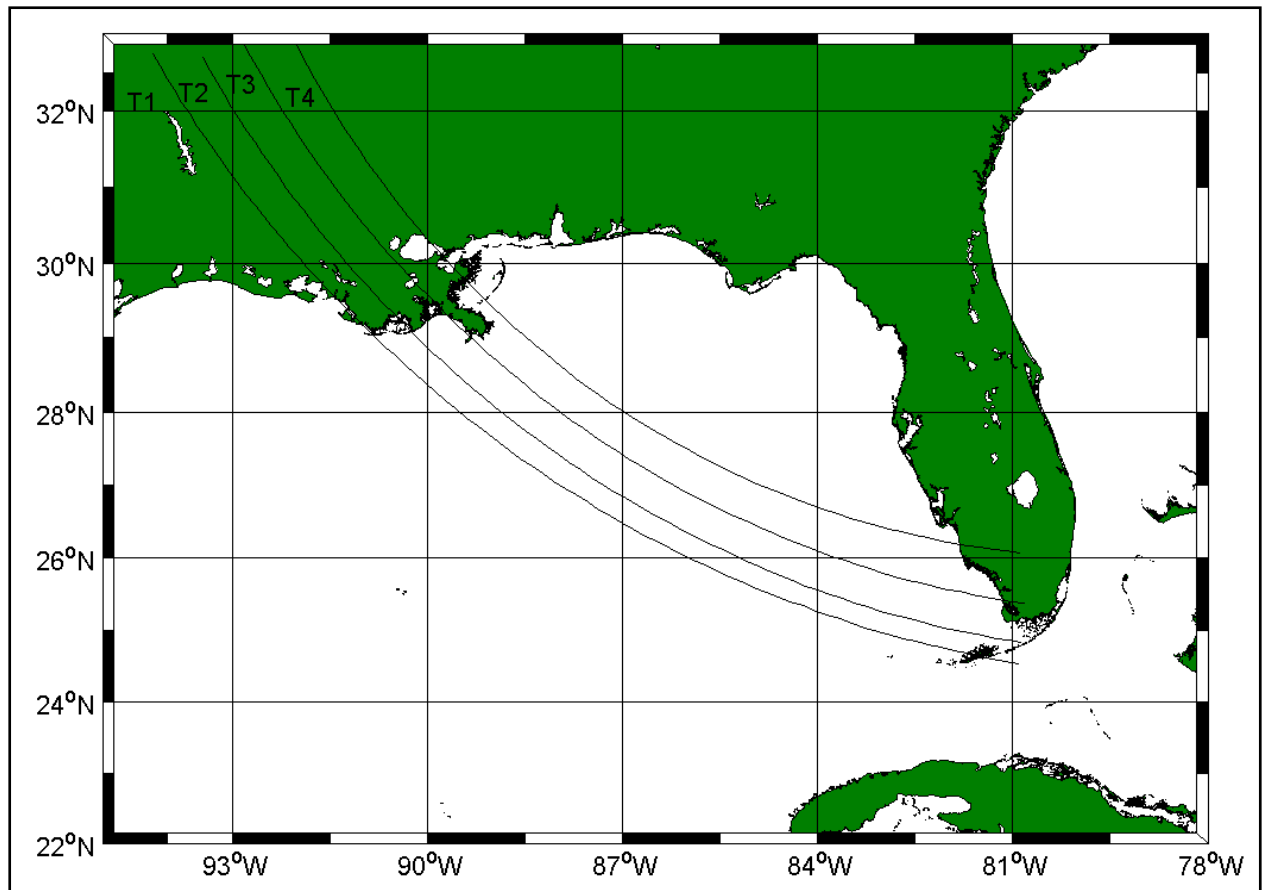


Figure 13. Tracks from southeast at 45-degree angle to RICK-fan set.

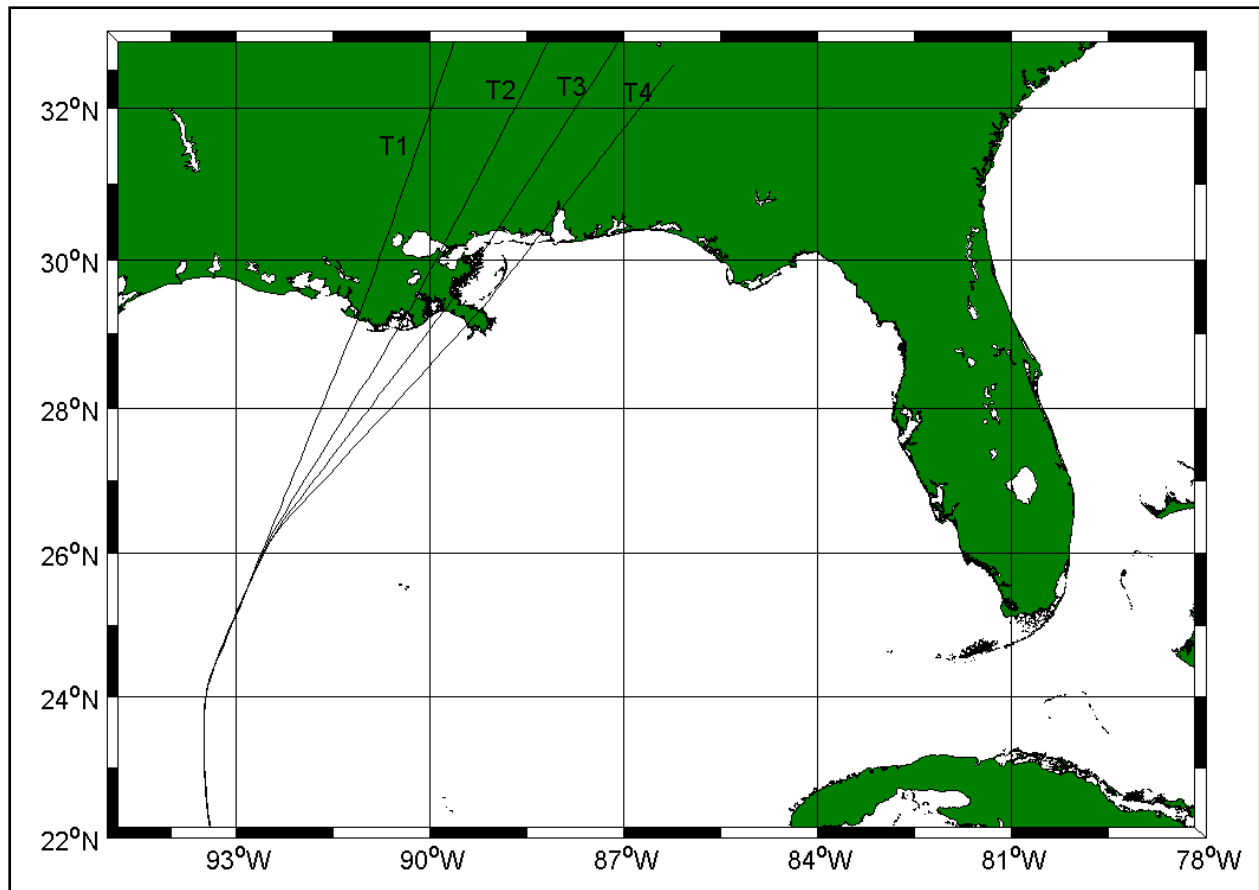


Figure 14. Tracks from southwest at 45-degree angle to RICK-fan set.

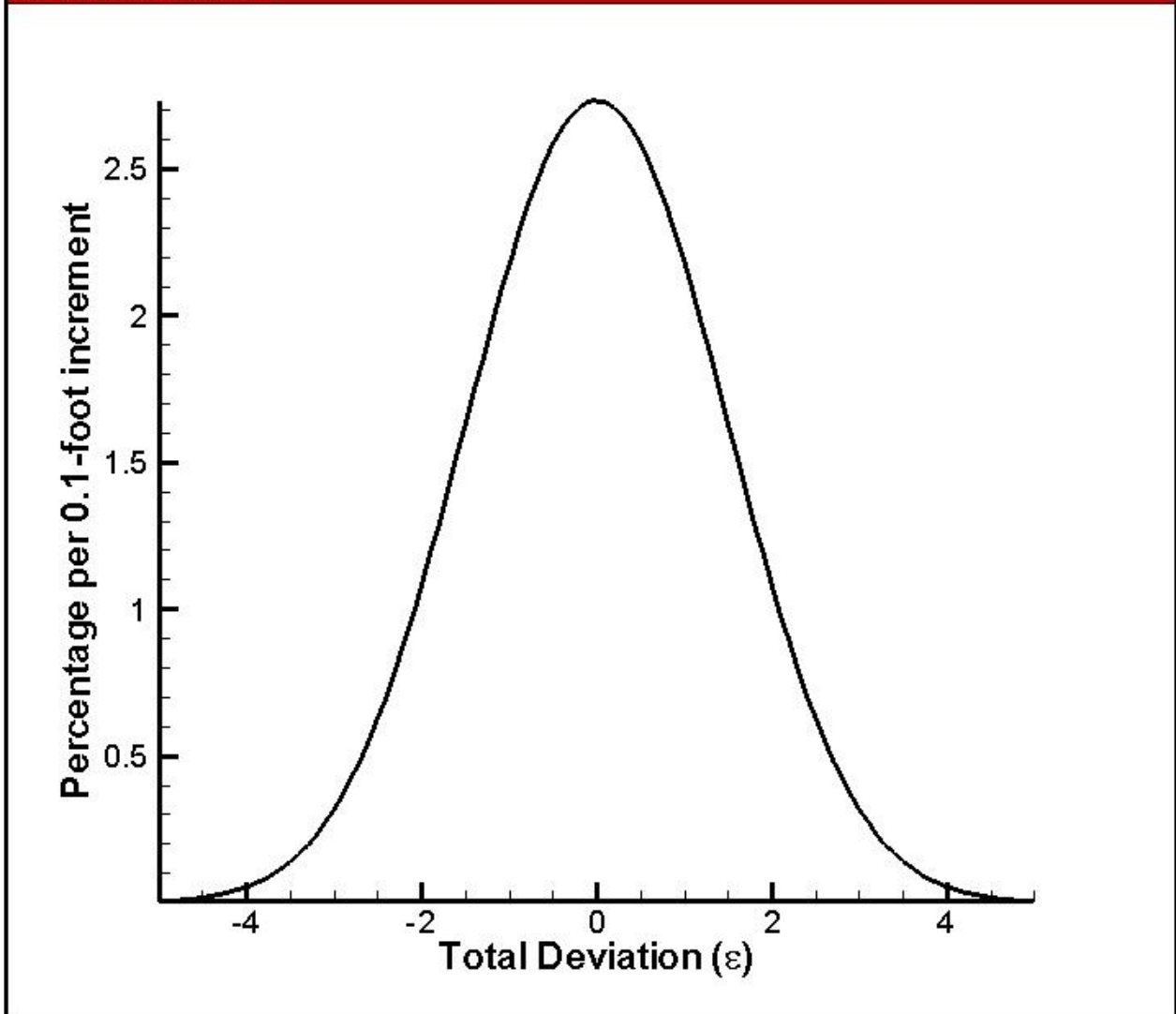


Figure 15. Percentage of deviations per 0.1-foot class as a function of deviation in feet.

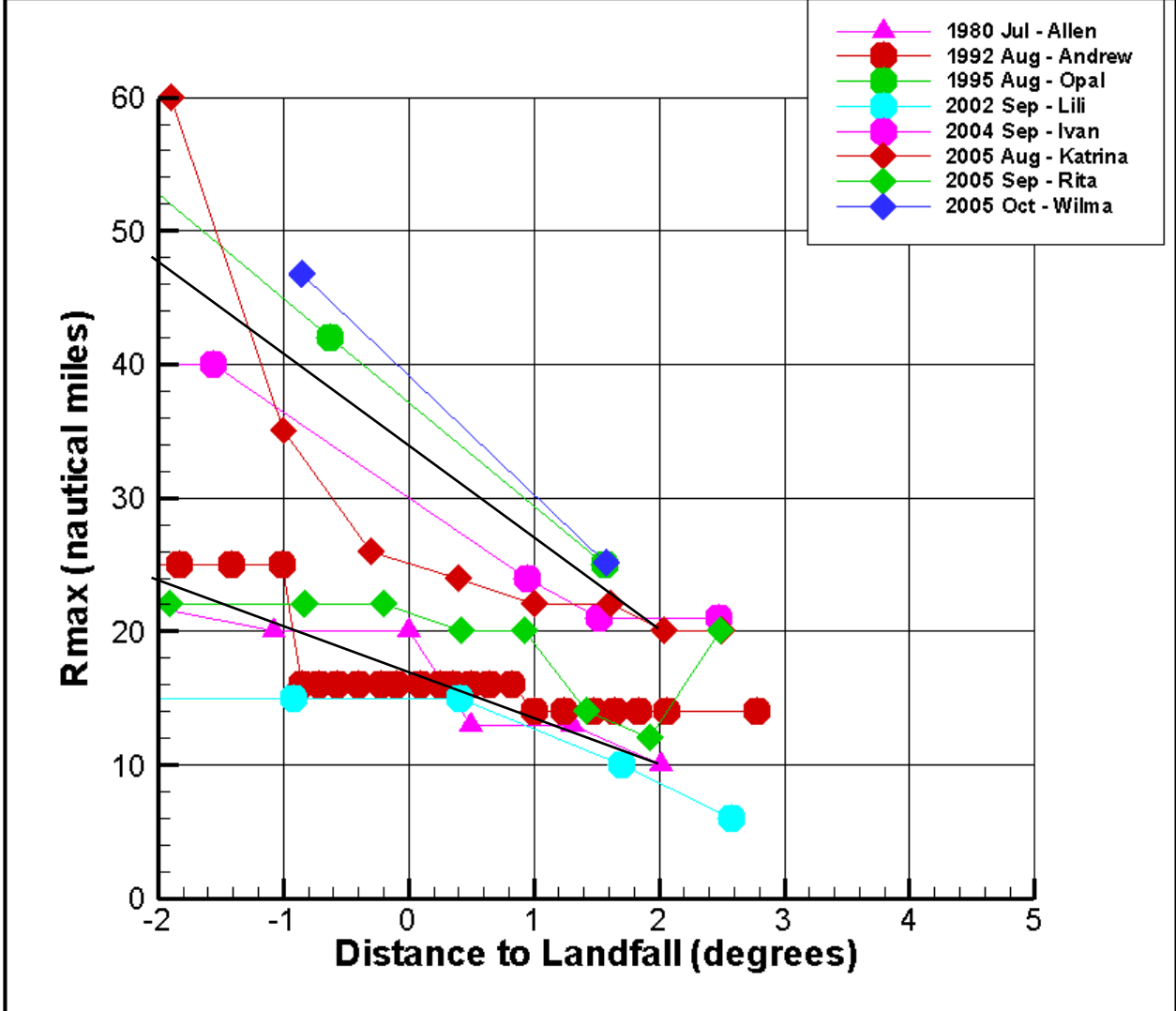


Figure 16. Increase in hurricane size during approach to coast, as seen in recent, well-documented storms.

**Probability Characteristics for Set of PBL Parameters and Tracks
(including potential climate variability)**

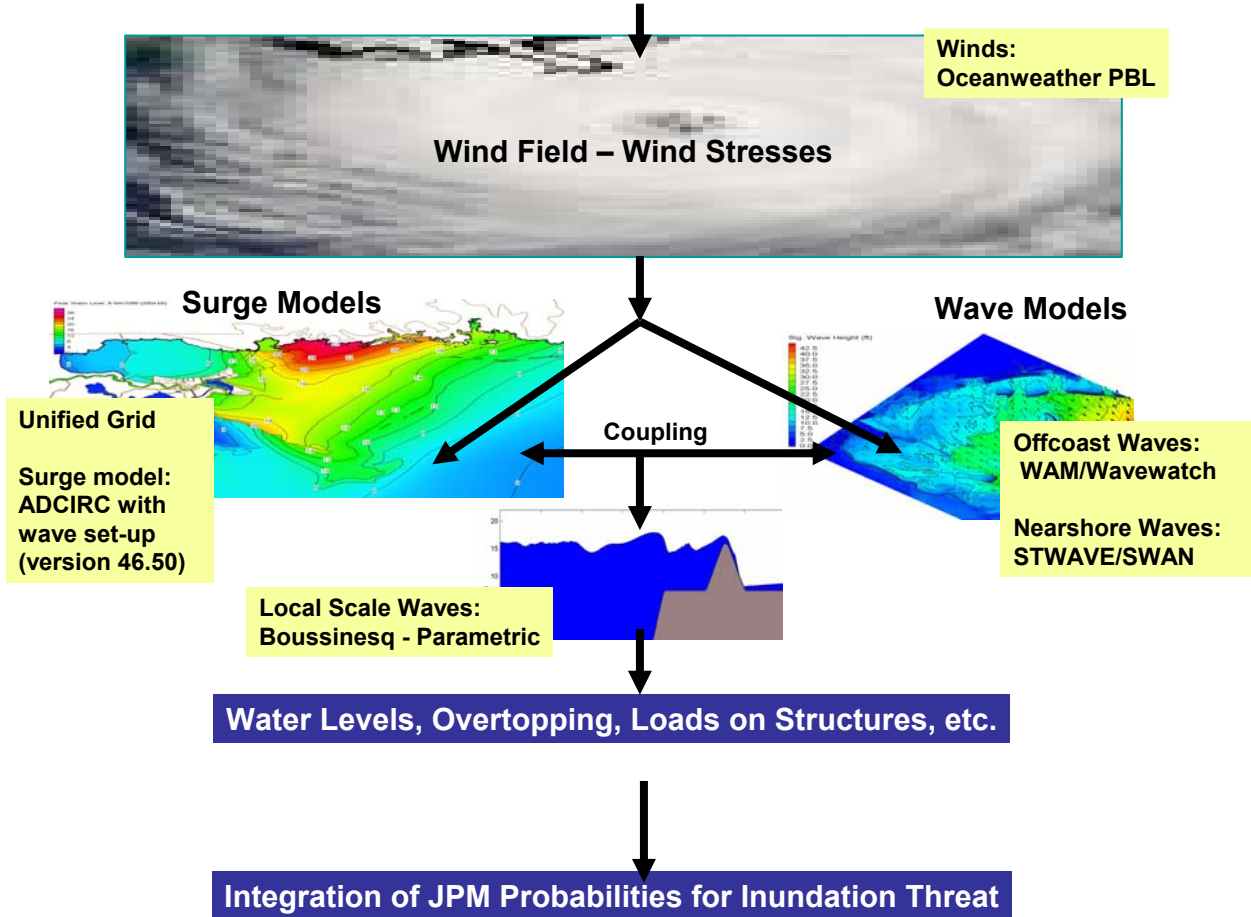


Figure 17. Schematic diagram of “production” modeling system for coastal inundation applications.

APPENDIX A of R2007

Expedient Estimation of Return Periods for Specific Historical Storms

On one hand, the most accurate characterization of the return period for a specific storm water level is to wait until the stage-frequency relationships have been developed and see where the water levels from that storm fall on this curve. Inspection of such an approach would show that water levels from a specific storm would fall at different return periods at different locations. A different, albeit more approximate approach which does not have to wait until the final results of simulations are complete, is to treat the storm water level potential in terms of the primary parameters affecting peak surge levels, typically storm intensity, storm size, angle of approach to the coast, forward storm speed, the geometry of the coast, and the offshore bathymetric slope.

Application to Hurricane Katrina

Figure A1, taken from Irish et al. (submitted for journal publication), shows the dependence of peak surge on storm intensity (peripheral pressure minus central pressure) and size (scaling radius for the pressure field). These values were generated from ADCIRC simulations using the Oceanweather Planetary Boundary Layer (PBL) model for wind fields. In these runs, storms were held at constant intensity and size during the approach to the coast. This figure is appropriate for a very shallow offshore slope (1:10000), found to be approximately representative of the continental shelf east of the Mississippi River in this area. Sensitivity studies of the effects of storm speed and storm approach angle showed that these factors were of secondary influence on surges at the coast, at least within the ranges of expected values for large, intense storms. Sensitivity studies also showed that although the coastal geometry in the New Orleans area (the presence of the Mississippi River Delta and river levees) tends to modify local storm surge levels, this factor did not change the relative ranking of the different storms.

Assuming that we can neglect the secondary factors, the relative ranking, and thus the return period for a specific event, can be deduced from a combination of Figure A1 and a specification of the joint probability structure of storm intensity and storm size. The estimation of the latter is a key part of the same methodology being used in the JPM-OS application in this area.

The frequency of storms along a coast has units of number of storms per year per length of coastline. For our application, we will assume that a storm within 1/2 degree longitude is the relevant parameter for our purpose here. This is equivalent to assuming that the surge within $\pm 1/2$ degree remains sufficiently close to the peak value that it can be considered approximately equal to the peak (within 10%). Although a continuous method can be used for this estimation method, the results were quite similar and the discretized method is easier to explain. Figure A2 shows a line along the Gulf of Mexico coastline that will be taken as the “sample line” for landfalling conditions in our analysis. A centered, running average of landfalling conditions over a distance of 6 degrees along this line was used to estimate the frequency of storms and to accumulate samples for extremal analysis within contiguous 1-degree (longitude – at 29.5 degrees) increments along the coast. The New Orleans area is located in Increment 7 along the coast in this scheme.

The storm sample used in this analysis is the 22-storm sample shown in Figures A3-A5 (essentially all storms with central pressures less than 955 mb during their transit through the Gulf of Mexico since 1941). Eleven of these storms fell within ± 3 degrees of the center of the New Orleans section of coast. Since this is not a very large number, we restrict our analysis to a 2-parameter (Gumbel) distribution here. The conditional Gumbel distribution of hurricane pressure differential was found to be given by

$$A1. F(\Delta p | hurricane) = e^{-e^{-z}}$$

where F is the condition cumulative distribution function (i.e. the expected CDF given a hurricane) and z is given by the best 2-parameter fit

$$z = \frac{\Delta p - a_0}{a_1}$$

where a_0 and a_1 are the distribution parameters and Δp is the pressure differential. For Increment 7 along the coast, the value of a_0 and a_1 are 56.557 and 16.463, respectively. The frequency of occurrence of hurricanes for this coastal segment is 0.0486 per year per degree (or once per every 20.6 years, or so).

Since, the contours in Figure A1 denote lines of equal surge, The probability of a storm capable of generating a storm surge equal to or greater than that produced by Hurricane Katrina can be estimated by the sum of the probabilities in regions A, B, and C, delineated by different R_p limits in Figure A6 or

$$F(\eta) = \int A + \int B + \int C$$

It can be shown that all three of these integrals can be written in a common form

$$A2. \int (A, B, C) = \int_{R_1}^{R_2} \int_{\Delta p(R)}^{\infty} \frac{\partial F(\Delta p)}{\partial \Delta p} P(R_p | \Delta p) d\Delta p dR_p$$

where the limits of the first integral are made to match the region shown in Figure A6. The conditional probability for size is given by a Gaussian distribution of the form

$$P(R_p | \Delta p) = \frac{1}{\sigma(\Delta p)\sqrt{2\pi}} e^{-\frac{x^2}{2}}$$

A3. *where*

$$x = \left(\frac{R_p - \bar{R}_p(\Delta p)}{\sigma(\Delta p)} \right)$$

In this equation a linear regression ($\bar{R}_p = 14. + 0.3*(110. - \Delta p)$ – with units for R_p and \bar{R}_p in nautical miles and units for Δp in millibars implied) was used to represent the conditional mean for storm size and the standard deviation was taken as $\sigma(\Delta p) = 0.44\bar{R}_p(\Delta p)$. The sum of all three integrals is 0.0518, which can be interpreted as slightly more than 1 hurricane in 20 can produce a surge of Katrina’s level in the New Orleans area. When 1 is divided by the product of the two frequency parameters, it yields an estimate of 397.6 years for the return period of a storm capable of producing a surge of comparable magnitude to Katrina. For practical purposes, Katrina would seem to fall in the range of a 400-year storm, in terms of storm surge generation. It should be noted that the methodology described here pertains to the area of maximum surges within a storm; consequently, the surges at some distance from area of maximum surge will certainly not be 400-year surges for those points.

Application to Hurricane Rita

The same procedure outlined above, modified to consider the different offshore slope, was applied to Hurricane Rita, with a landfall in Increment 10 of our analysis. A slope of 1:1000, which is characteristic of the shelf region in the area west of the Mississippi River, was adopted here in the idealized surge modeling referenced here. The return period for this storm from this analysis is 89.7 years. Again, for practical purposes, this can be taken to imply that Rita was somewhere in the neighborhood of a 90-year storm, in terms of storm surge.

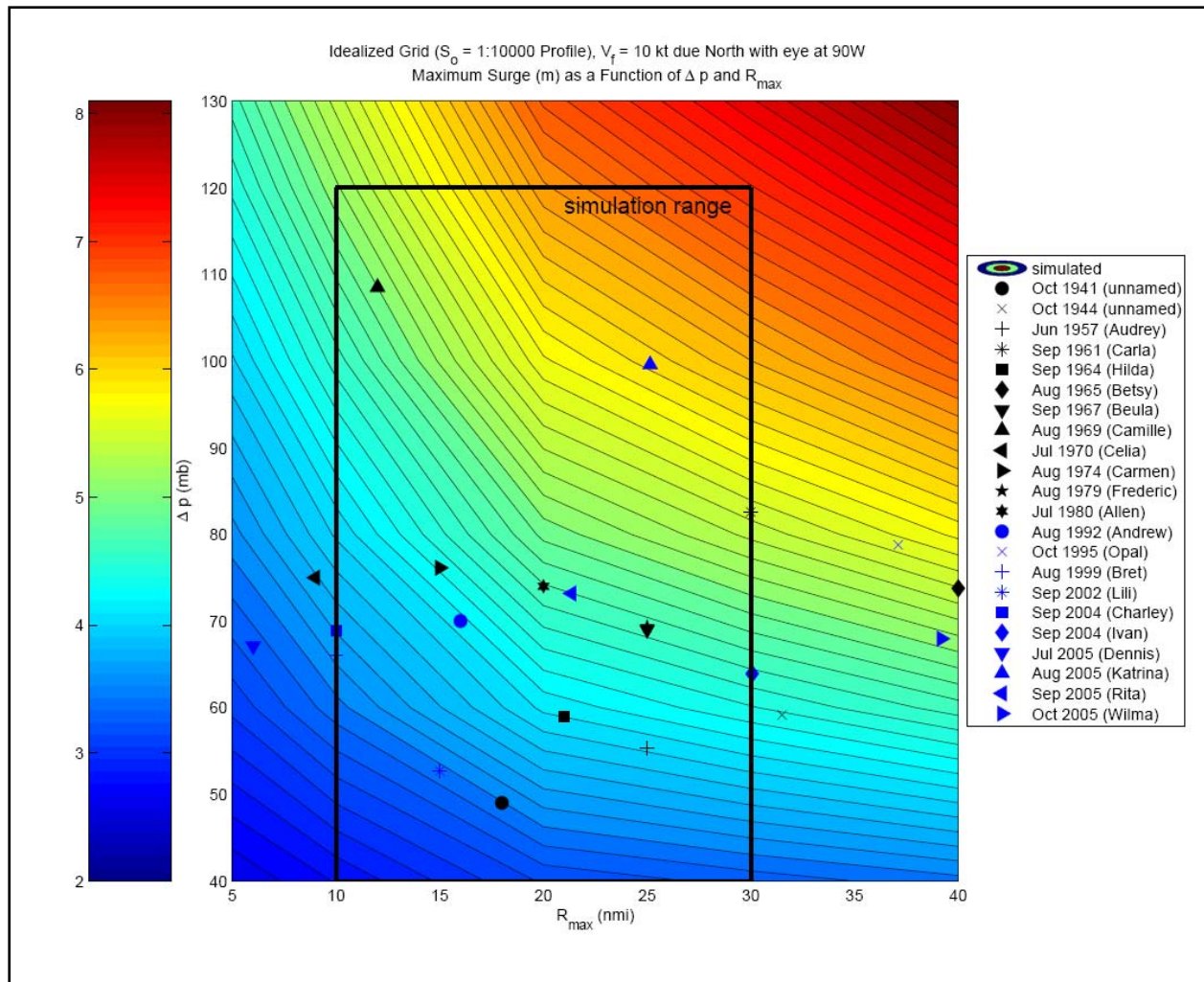


Figure A1. Contour plot of peak surge levels along a straight coast with a constant offshore slope as a function of storm size ($R_{max} = R_p$ in our terminology) and storm intensity (peripheral pressure minus central pressure). The storm values used in this plot are the offshore conditions, rather than the conditions at the coast.

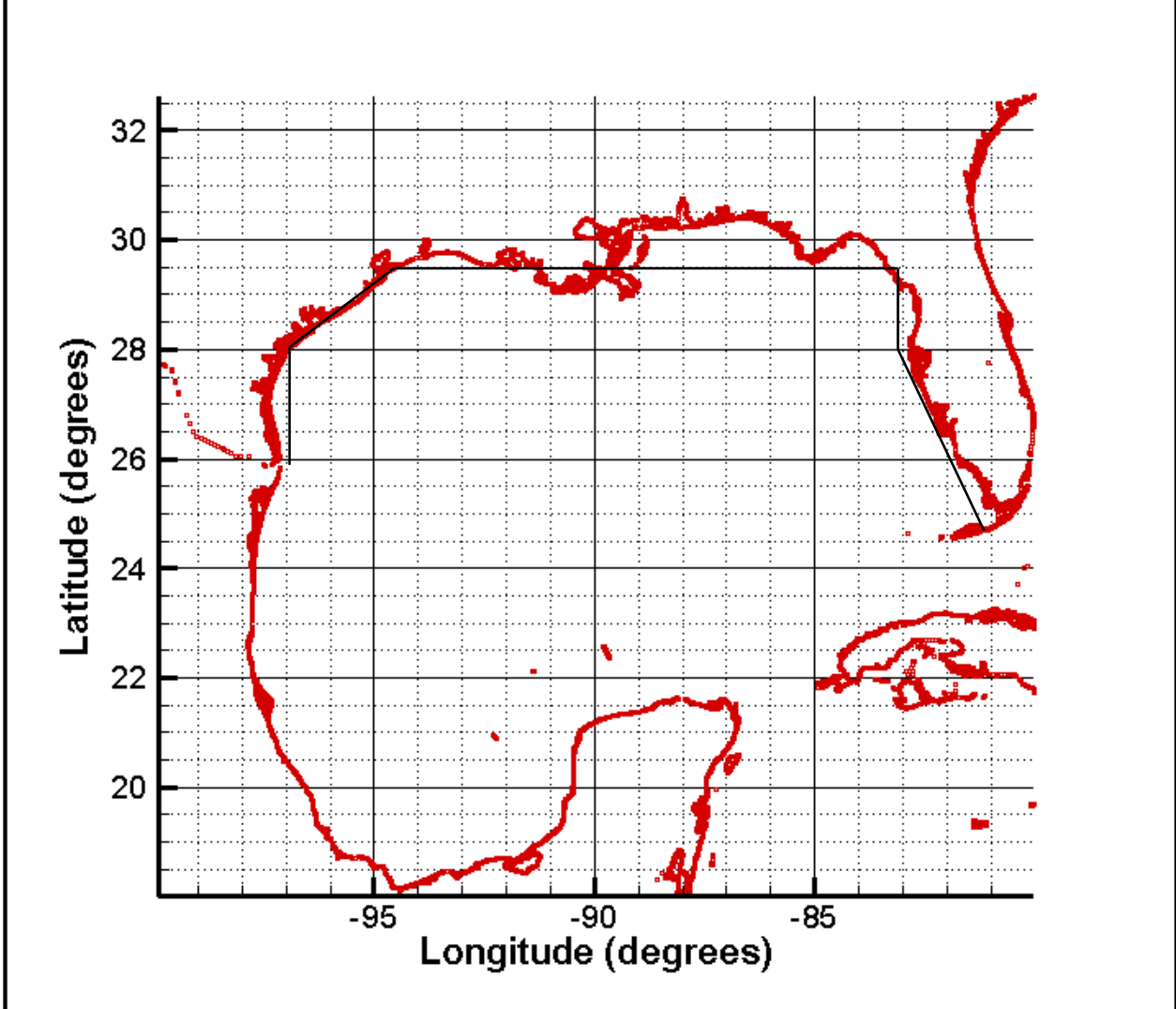


Figure A2. Location of line for analysis of hurricane landfalling characteristics. Throughout this white paper, one-degree increments of distance along this line from east to west, with the “zero-value” taken at -83 degrees longitude, will be used as a locator for discretized sections of coast. In this convention, the increment number for any section being analyzed is given by $N_{increment} = Integer(-83-longitude)$. For example, any point with a longitude less or equal to -83 and greater than -84 would fall in increment 0, any point with a longitude less than or equal to -85 and greater than -85 would fall in increment 1, etc.

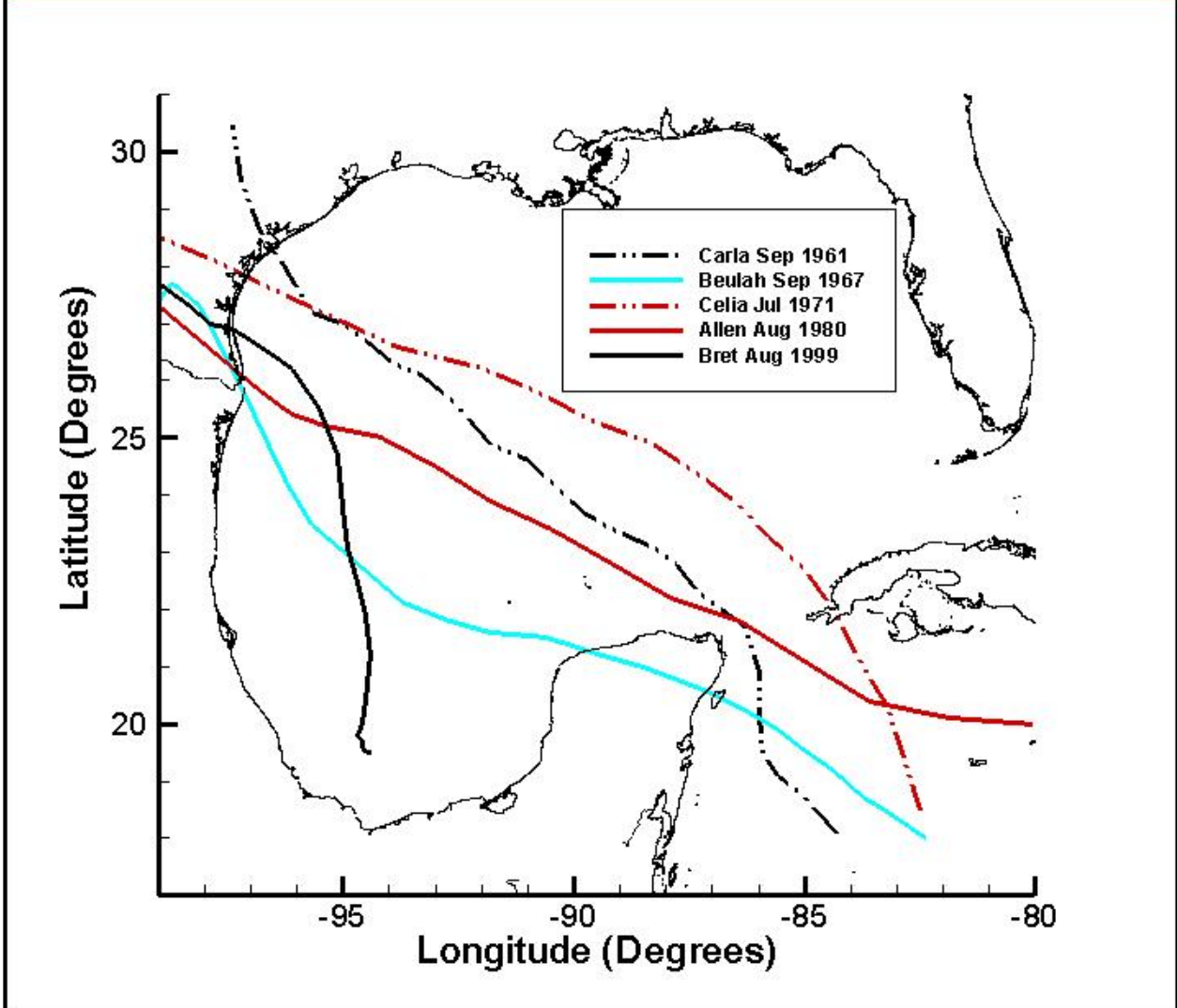


Figure A3. Tracks of all hurricanes (1941-2005) making landfall in the Western Gulf of Mexico for storms that attained a central pressure of 955 millibars or lower during its transit through the Gulf of Mexico.

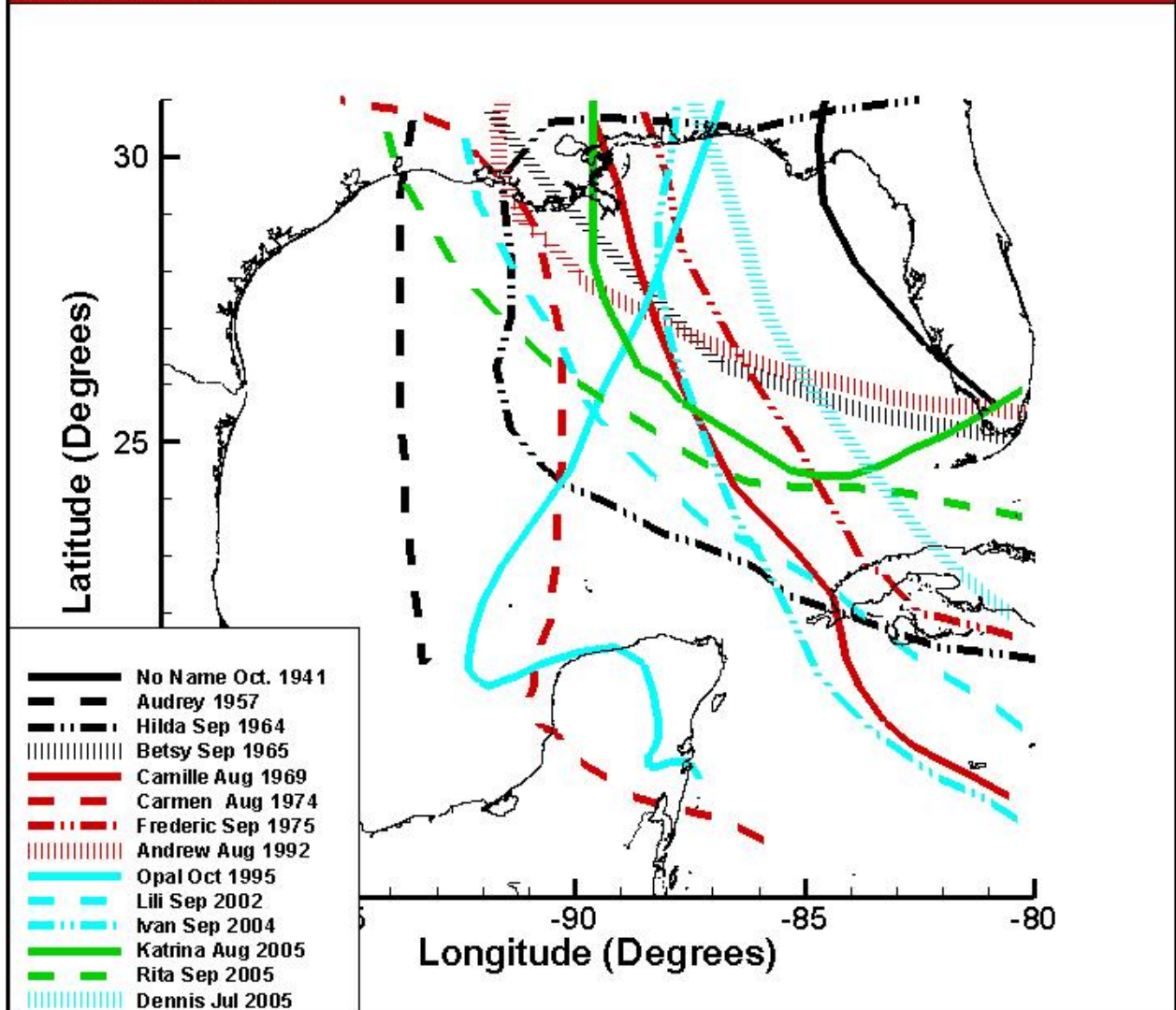


Figure A4. Tracks of all hurricanes (1941-2005) making landfall in the Central Gulf of Mexico for storms that attained a central pressure of 955 millibars or lower during its transit through the Gulf of Mexico.

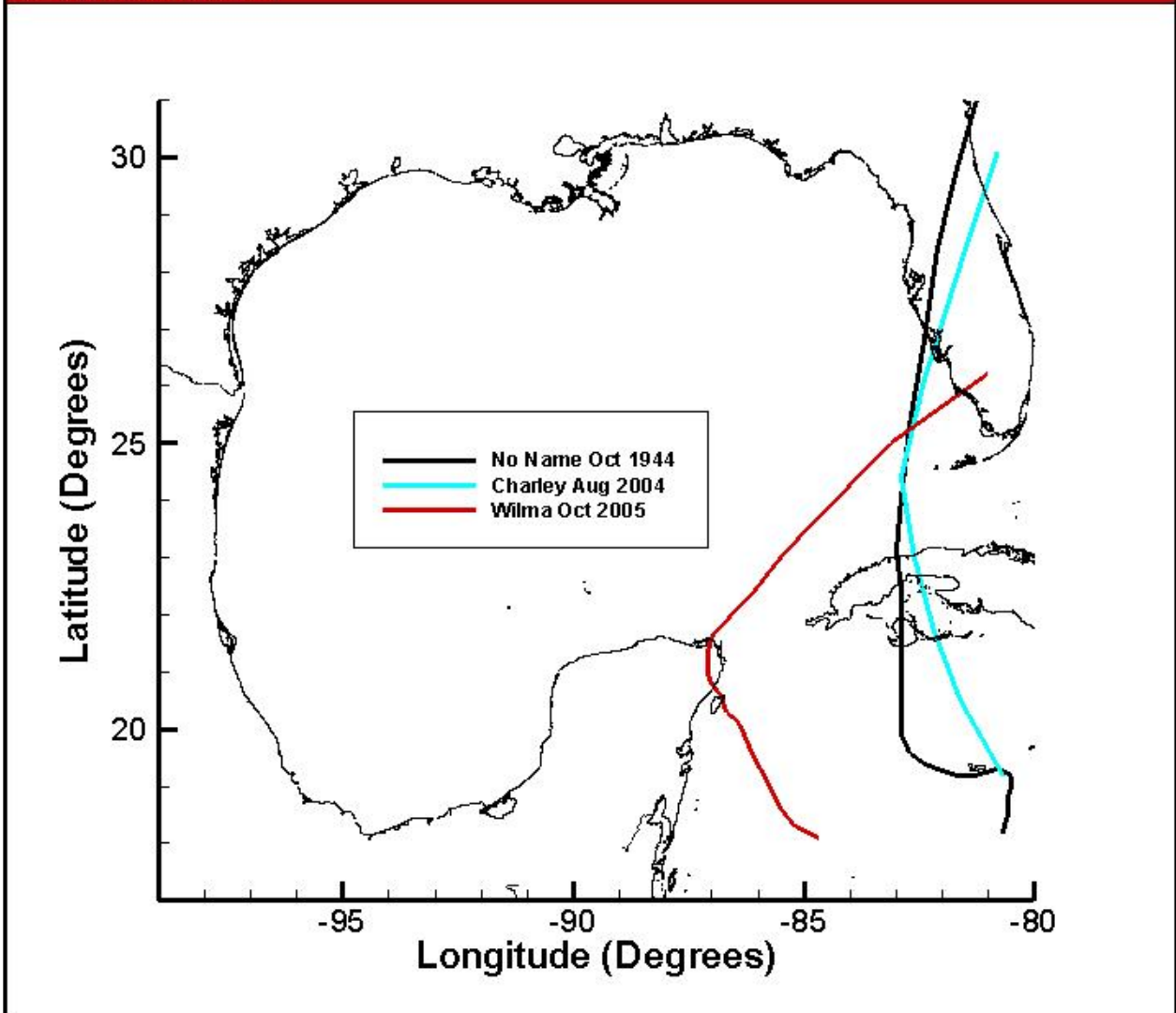


Figure A5. Tracks of all hurricanes (1941-2005) making landfall in the Eastern Gulf of Mexico for storms that attained a central pressure of 955 millibars or lower during its transit through the Gulf of Mexico.

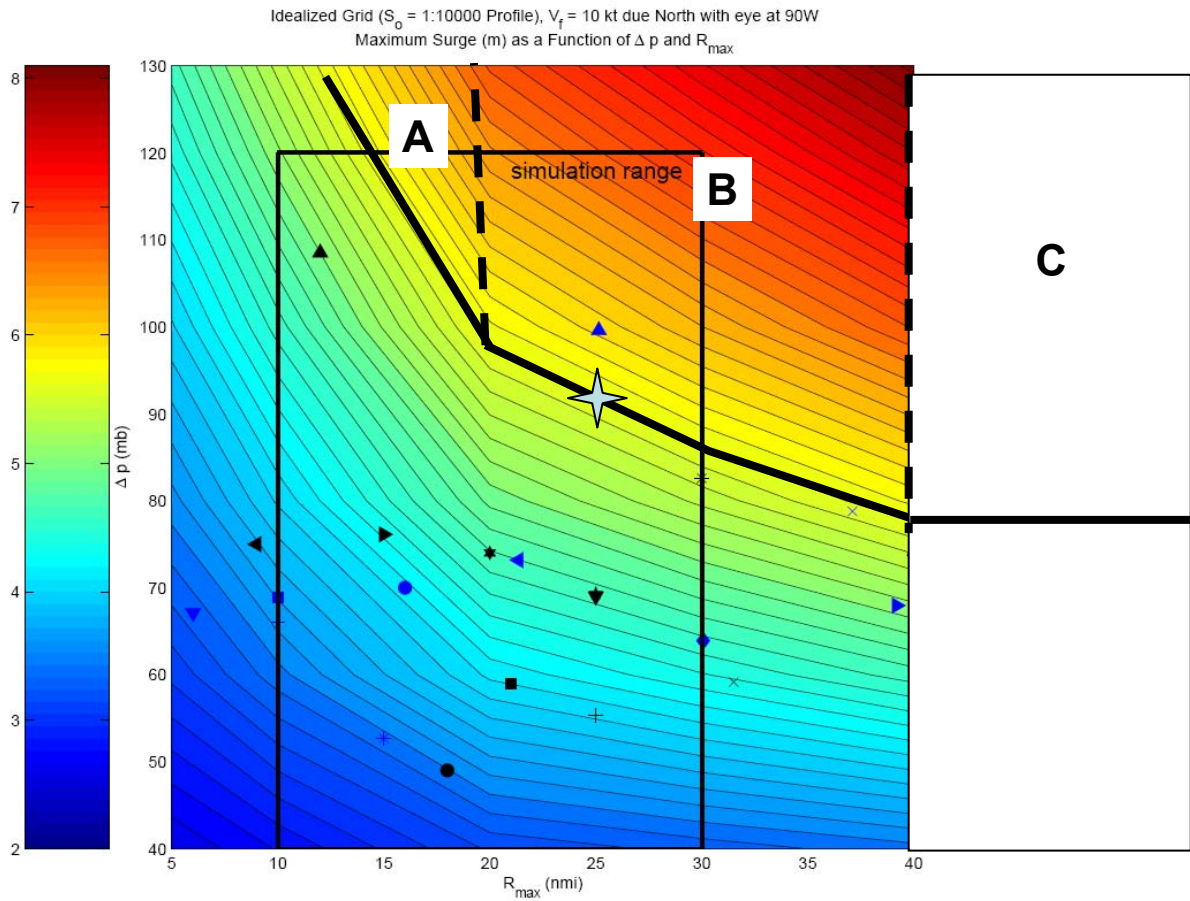


Figure A6. Regions of size-intensity domain expected to contribute to surges greater than or equal to that of Hurricane Katrina. The Blue “star” represents Katrina’s characteristics at time of landfall, with a somewhat lower intensity than shown in Figure A1.

APPENDIX B of R2007

Selection of Wind Model for Coastal Surge Estimation

Ocean response models for waves and surges require winds at a constant reference level with some suitable averaging interval (typically around 20-30 minutes) and a specified drag law to convert these winds into estimates of momentum fluxes from the atmosphere to the ocean. Two different models (Thompson and Cardone, 1996; Vickery *et al.*, 2000) were investigated for application to coastal surge modeling as part of a general investigation of modeling for coastal inundation.

The dynamic (Planetary Boundary Layer – PBL) model of Thompson and Cardone (1996) has been selected for use in estimating hurricane wind fields. In older storms, the “best-estimate” wind fields will be virtually identical to the initial guess wind fields due to the lack of information available for assimilation into the PBL wind fields. Comparisons of Oceanweather and Vickery PBL winds from Hurricane Katrina, along east-west and north-south transects through the center of the storm, to Oceanweather’s “best-estimate” winds are shown in Figures B1 and B2, respectively. Figure B3 shows a similar set of comparisons for both the east-west and north-south transects for Hurricane Betsy. As can be seen in these figures, Oceanweather’s PBL winds capture most of the broad-scale structure of the wind fields.

The Vickery PBL model does not perform as well as the Oceanweather PBL model in comparisons with the Oceanweather “best-estimate” winds. This is not too surprising, since the Oceanweather analysis “best-estimate” analysis is likely to have been considered in deriving the PBL parameters. The abrupt drop-off of wind speeds in the Vickery wind is an artifact of the version of the Vickery code that was available for testing during the time of this comparison. This problem is being remedied and is not a property of the general solution capabilities inherent to the Vickery model.

Since the relaxation time for coastal surge is on the order of hours rather than 10’s of hours, as for the generation of waves, offshore complexities of storm tracks tend to affect wave fields much more than they affect coastal surges. Since tracks of major storms tend to lack the complexity exhibited by minimal hurricanes and tropical storms and since wave generation tends to produce a wave field that represents the integrated effects of winds over many hours, the effect of track variation on wave fields should be rather minimal. It should also be recognized that PBL winds have long been shown to be capable of providing accurate wind field estimates for purposes of hindcasting waves in hurricanes (Cardone *et al.*, 1976).

The use of PBL winds is also consistent with the approach of Vickery *et al.* (2000) or estimating wind hazards in U.S. coastal areas, which were found to provide very reasonable wind estimates when compared to both onland and offshore wind observations. Given all of the problems associated with using historical wind fields with indefinite degrees of freedom in their formulation, it would seem that a very careful study of the differences between PBL-driven surges and “best-estimate”-driven surges should be undertaken for a small set of hurricanes before any clear advantage to using “best-estimate” wind fields for surge prediction can be claimed.

A very important improvement pertinent to PBL wind field estimation is the availability of carefully estimated size parameters for all historical storms (from Oceanweather). These parameters were compiled specifically for driving ocean response models (e.g. wave and surge models) and allow improved estimation of the joint probability of intensity-size relationships in Gulf of Mexico hurricanes.

As a final element of this Appendix, the Holland B parameter will be briefly described. This description is excerpted from the section on Meteorology in the *Coastal Engineering Manual* (Resio, Thompson, and Bratos), which can be found online for reference.

Myers (1954), Collins and Viehmann (1971), Schwerdt *et al.* (1979), and Holland (1980) all present descriptions and justifications of various parametric approaches to wind-field specification in tropical storms. Cardone *et al.* (1992) use a modified form of Chow's (1971) moving vortex model to specify winds with a gridded numerical model. However, since this numerical solution is driven only by a small set of parameters and assumes steady-state conditions, it produces results which are of similar form to those of parametric models. The Holland model differs from previous parametric models in that it contains a parameter (the Holland B parameter) which allowed the peakedness of winds in a hurricane to vary. This model will be described here to demonstrate the role of the Holland B parameter in this model.

In the Holland model, hurricane pressure profiles are normalized via the relationship

$$B1. \quad \beta = \frac{p - p_c}{p_n - p_c}$$

where

- p is the surface pressure at an arbitrary radius (r);
- p_c is the (surface) central pressure in the storm; and
- p_n is the ambient surface pressure at the periphery of the storm.

Holland showed that the family of β-curves for a number of storms resembled a family of rectangular hyperbolas and could be represented as

$$r_p^B \ln(\beta^{-1}) = A$$

or

$$B2. \quad \beta^{-1} = \exp\left(\frac{A}{r_p^B}\right)$$

or

$$\beta = \exp\left(\frac{-A}{r_p^B}\right)$$

where

A is a scaling parameter with units of length; and

B is a dimensionless parameter which controls the peakedness of the wind speed distribution.

This leads to a representation for the pressure profile as

$$\text{B3. } p = p_c + (p_n - p_c) \exp\left(\frac{-A}{r_p^B}\right)$$

which then leads to a gradient wind approximation of the form

$$\text{B4. } U_{gr} = \left[\frac{AB(p_n - p_c) \exp\left(\frac{-A}{r_p^B}\right)}{\rho_a r^B} + \frac{r^2 f^2}{4} \right]^{1/2} - \frac{rf}{2}$$

where

U_{gr} represents the gradient approximation to the wind speed.

In the intense portion of the storm, this equation reduces to a cyclostrophic approximation (a flow in which the pressure gradient force is balanced only by centrifugal acceleration) given by

$$\text{B5. } U_c = \left[\frac{AB(p_n - p_c) \exp\left(\frac{-A}{r_p^B}\right)}{\rho_a r^B} \right]^{1/2}$$

where

U_c represents the cyclostrophic approximation to the wind speed; which yields explicit forms for the radius to maximum winds as

$$\text{B6. } R_{\max} = A^{\frac{1}{B}}$$

where R_{\max} is the distance from the center of the storm circulation to the location of maximum wind speed, compared to r_p which is the pressure-scaling radius.

The maximum wind speed can then be approximated as

$$B7. U_{\max} = \left(\frac{B}{\rho_d e} \right)^{1/2} (p_n - p_c)^{1/2}$$

where

U_{\max} is the maximum velocity in the storm; and
 e is the base of natural logarithms, 2.718.

If B is equal to 1 in this model, the pressure profile and wind characteristics become similar to results of Myers (1954), Collins and Viehmann (1971), Schwerdt et al. (1979), and Cardone et al. (1976). In the case of the Cardone et al. model this similarity would exist only for the case of a storm with no significant background pressure gradient. Although the Cardone et al. PBL model initially did not consider the effects of the Holland B parameter, it now does include this term in its formulation (Thompson and Cardone, 1996). The Vickery et al. (2000) model also includes the Holland B term in its formulation.

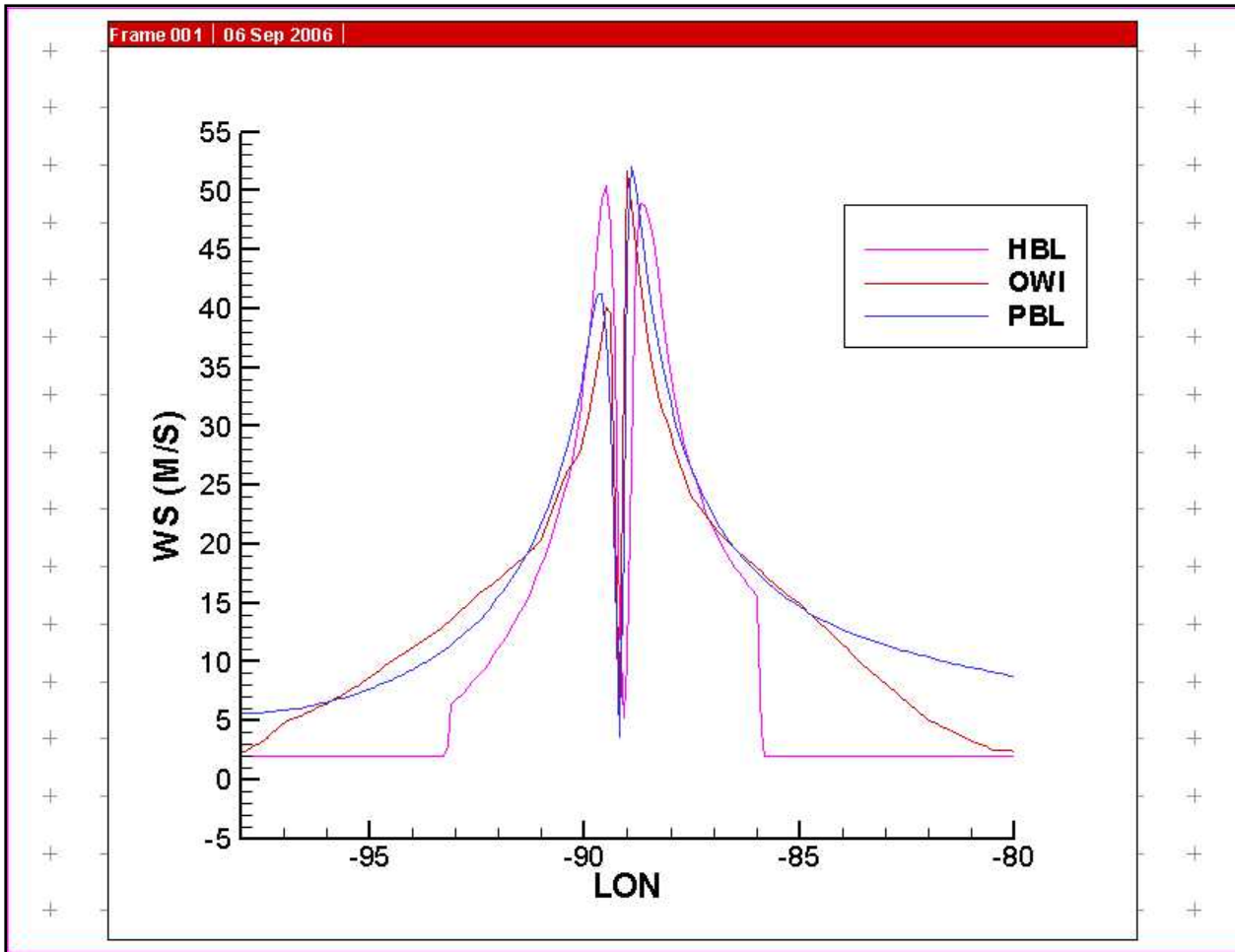


Figure B1. Plot of wind speeds (in meters per second) along east-west transects through Hurricane Katrina. HBL denotes wind speeds from the Vickery et al. (2000) hurricane boundary layer model. PBL denotes wind speeds from the Thompson and Cardone (1996) planetary boundary layer (PBL) model; and OWI denotes wind speeds from the “best-available” wind speeds from analysts at Oceanweather, Inc., which include the HWIND inputs from Mark Powell in NOAA’s Hurricane Research Division.

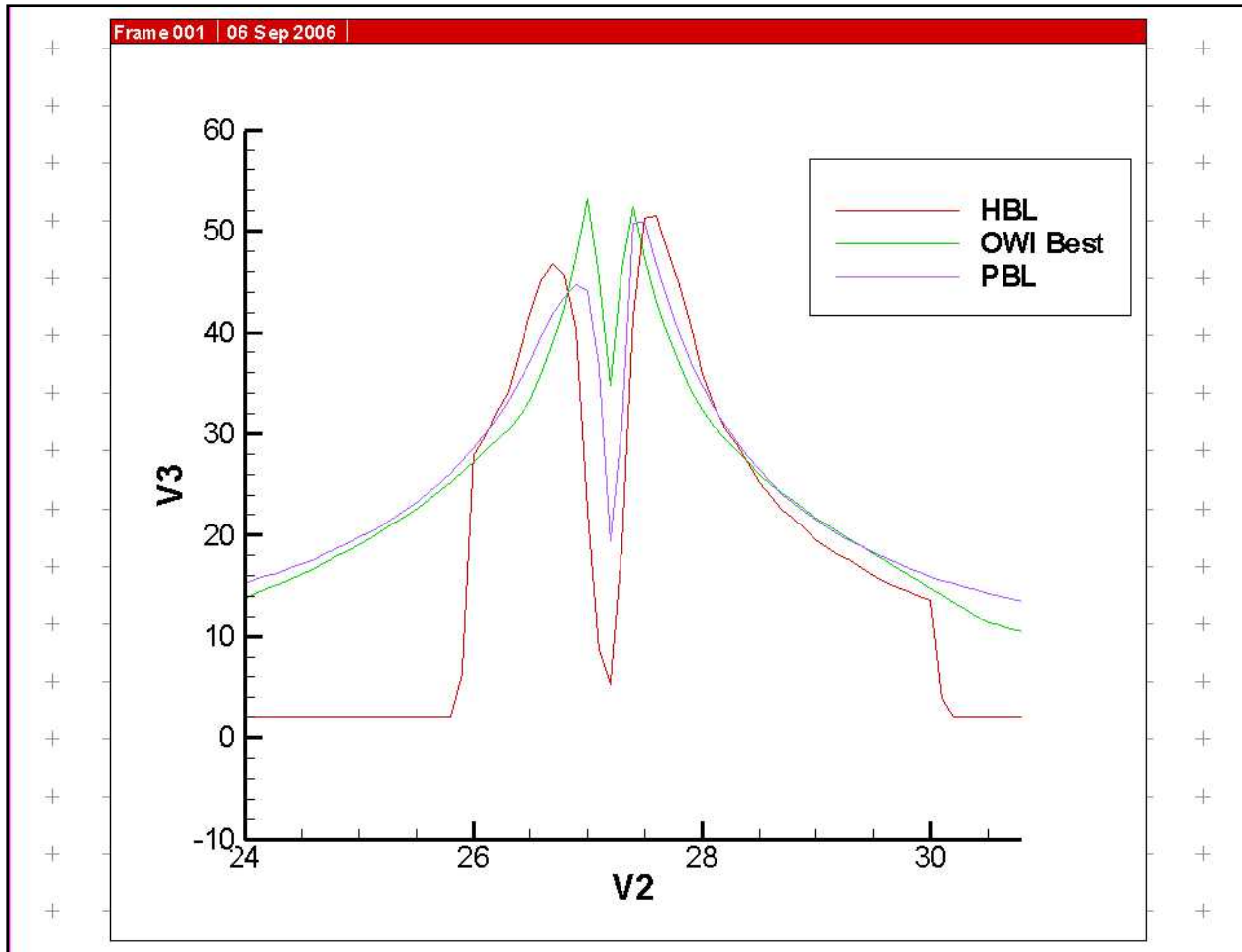


Figure B2. Plot of wind speeds (in meters per second) along north-south transects through Hurricane Katrina. HBL denotes wind speeds from the Vickery et al. (2000) hurricane boundary layer model. PBL denotes wind speeds from the Thompson and Cardone (1996) planetary boundary layer (PBL) model; and OWI denotes wind speeds from the “best-available” wind speeds from analysts at Oceanweather, Inc., which include the HWIND inputs from Mark Powell in NOAA’s Hurricane Research Division.

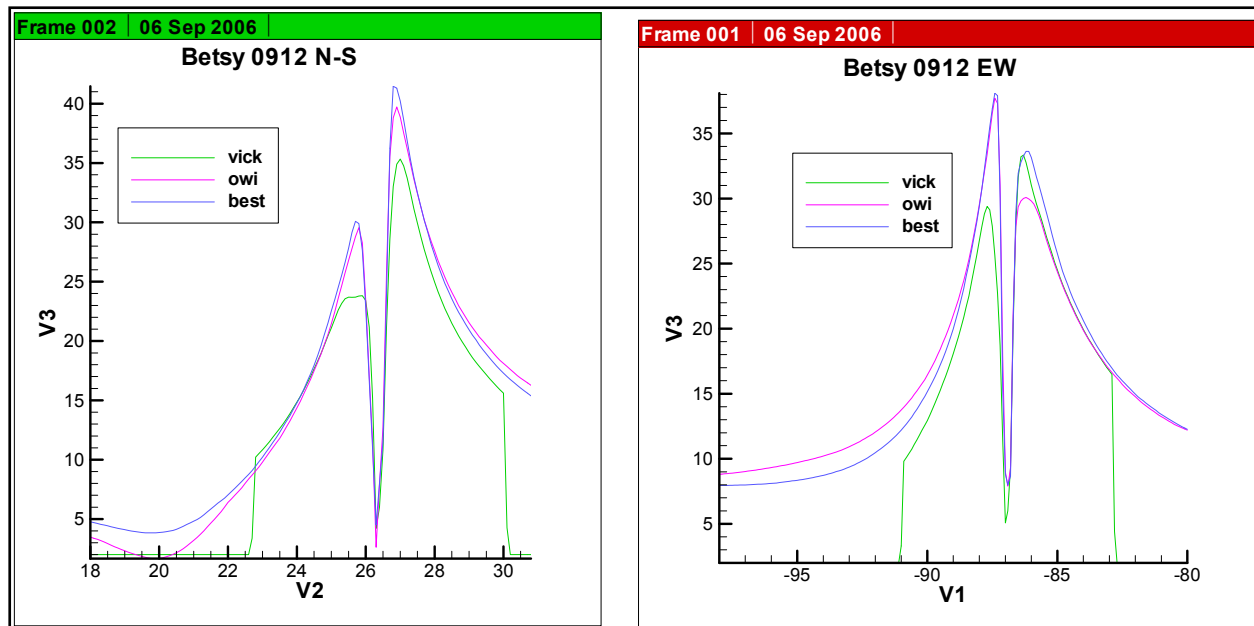


Figure B3. Plot of wind speeds (in meters per second) along north-south (N-S) and east-west (E-W) transects through Hurricane Betsy. Vick denotes wind speeds from the Vickery et al. (2000) hurricane boundary layer model. OWI denotes wind speeds from the Thompson and Cardone (1996) planetary boundary layer (PBL) model; and “best-available” denotes wind speeds from the “best-available” wind speeds from analysts at Oceanweather, Inc.

APPENDIX C of R2007

Selection of Period of Record for Surge Estimation and Consideration of the Effects of Climatic Variability on Surge Extremes

An analysis of climatic variability was undertaken by Resio and Orelup (submitted for publication to J. Climate). Enclosed here are some of the findings relevant to the selection of the period of record and the estimated effects of climatic variability on expected surge extremes. Three fundamental data sets are used in this study: 1) sea-level pressures (SLP's) from the NOATL-tropic data set (a sub-domain of the total NCEP SLP data set that covers from 0° to 40° N latitude and from 5° to 110° W longitude); 2) sea surface temperature (SST) data downloaded from Extended Reconstructed Sea Surface Temperature (ERSST); and 3) information on hurricane characteristics taken from Oceanweather, Inc files, now available in the public domain. Details on these data sets are available on appropriate web sites.

Empirical Orthogonal Functions (EOF's) have long been recognized as a powerful tool for encapsulating natural patterns within the atmosphere. In this study we used data from the 1950-2005 period (56 years) and defined five-day mean sea level pressure (SLP) fields on a 2.5° by 2.5° grid. This resulted in 73 five-day intervals for every year without a leap year. Leap year was handled by adding that day into the time interval starting on February 25th, which created one element encompassing six days once in every four years. Given that we were not interested in the seasonality of hurricane but rather in inter-annual and longer variability, we defined mean pressure fields for each five-day interval throughout the year, with the average taken over the 56 years included in this analysis. Calculated mean pressure fields for each five-day interval were subtracted from individual mean five-day pressure fields to produce a set of 73 x 56 pressure fields that were input into an EOF analysis.

The SST data used here represent a subset of the total ERSST data set and covers from 18° to 30° N latitude and from 58° to 98° W longitude on a 2° by 2° grid, with a land mask that restricts the data to only water points. Although SST patterns within the Gulf exhibit considerable spatial variability, it is not clear that the variations in the spatial characteristics of these patterns play a major role in the inter-annual variability of hurricane genesis and/or development. Consequently such variations are not considered here. Instead, mean monthly data for the entire Gulf of Mexico region for July through October were averaged together to provide a single measure of sea surface temperature for each hurricane season from 1950 through 2005.

The data set for hurricane characteristics includes estimates of six-hourly storm position, along with several parameters that relate to hurricane shape, size and intensity. Unlike previous data sets which have focused on short-duration (typically 1-minute maximum) wind speeds from flight level, this new data set also contains estimates of the highest sustained (30-minute average) surface-level (10-meter) wind speeds along the path of the storms. Since these are the appropriate winds for driving ocean response models, they provide a much more direct measure of hurricane surge and wave production. In the earlier storms in this data set (prior to 1990) these wind estimates were derived primarily from simulated wind fields based on a "slab model" of the lowest region of the atmosphere combined with a planetary boundary layer model (Thompson

and Cardone, 1996). For most of the later storms these wind fields have been extensively reworked by analysts to assimilate available measurements.

Most past studies of climatic variability have used storm frequency (sometimes stratified by Saffir-Simpson scale) to categorize storm activity in each year. However, for our purposes we will define a single parameter that incorporates both intensity and frequency into one measure of hurricane activity. This measure of annual hurricane activity is obtained by calculating the estimated kinetic energy for each storm passing through the Gulf of Mexico at the time of its maximum intensity and then adding all maxima within a given year. At a fixed time, the total kinetic energy in a hurricane can be related to storm size and storm intensity as

$$E_k \sim \iint V^2(x, y) dx dy = \iint V^2(r, \theta) r dr d\theta$$

C1. given that $V(r, \theta) = V_{\max} \phi_1\left(\frac{r}{R_{\max}}\right) \phi_2(\theta - \theta_0)$ then

$$E_k \sim V_{\max}^2 R_{\max}^2$$

where V_{\max} is the maximum (30-minute average, 10-m) wind speed within the storm and R_{\max} is the radius to maximum winds at the same time. The value of the parameter E_k at the time of maximum wind speed during a storm's passage through the Gulf of Mexico provides a good integrated measure of the storm intensity and size at the time of the storm's maximum intensity. Summing all values of E_k for a season yields a surrogate for combined number, size, and intensity of storms in a year.

Figure C1 shows the cumulative hurricane kinetic energy per season as defined previously in this paper, smoothed over a running five-year period. Since we are trying to extend the data as long as possible, the "smoothed" data at either end of this record is defined only in terms of the existing data within the five-year window. For example, the 2005 data considers only data from 2003, 2004, and 2005 in its average. Thus as the ends are approached, a slight bias is created in terms of the mean position of the years contributing to this mean, culminating in a one-year displacement at the beginning and end of the analysis along with a reduced averaging window. This Figure shows two very notable peaks, one that commenced in the late-1950's and persisted until about 1970 and a second that began around 2000 and has persisted through 2005, with a broad trough in Gulf hurricane activity between these two peaks. There does not appear any strong secular signal within this record. The first of these periods coincides with the very active hurricane seasons that included Hurricanes Carla, Hilda, Betsy, Beulah and Camille that devastated much of the Gulf coast during the 1960's; while the second contains the recent set of intense hurricanes, including Lili, Charley, Ivan, Dennis, Katrina, and Rita.

Figure C1 shows that there are two intervals of high hurricane activity separated by an interval of relatively low hurricane activity in the years from 1950 to 2005. If this cycle is real, it seems advisable to use a sampling scheme that preserves the expected long-term ratio of high-activity and low-activity years. Since we obviously want to retain both the early (1960-1970) interval of high activity latest (partial?) interval (2000-2005) of high activity in our sample, we should include about 2/3 of the 30-year low-activity interval preceding 1960 in order to achieve

this balance. This suggests that including approximately 20 years of the 30-year low-activity interval (1941-1960) is appropriate. Thus, the total record sample length recommended for surge estimation in the Gulf of Mexico is 1941-2005.

Figure C2 shows estimated return periods for central pressures for the total sample within the Gulf of Mexico for different estimation methods. The estimation methods examined are 1) analysis of only quiescent years (Group 1); 2) analysis of only active years (Group 2); 3) analysis of both quiescent-year and active-year samples, treated as though they are drawn from separate populations (Equation 4 from the Resio and Orlup manuscript, reproduced below); and 4) analysis of both quiescent-year and active-year samples as though they are a single population.

Eq. 4 from Resio and Orlup:

$$T(x) = \frac{1}{1 - \sum \lambda_n \beta_n F_n(x)}$$

where

$T(x)$ is the return period for x ;

C2. λ_n is the frequency of storms in Group n ;

$F_n(x)$ is the cumulative distribution function (CDF)

for storms in Group n ; and

β_n is the proportion of years in Group n .

These results combined with integrations of the full probability integral for surges along a straight coast from the Irish *et al.* computer runs yields the results shown in Table C1 for the expected variations in wave and surge extremes within the Gulf of Mexico, given a doubling of the high-activity years (from $\frac{1}{4}$ of the total time to $\frac{1}{2}$ of the total time). There is nothing in the Gulf of Mexico record that suggests such a scenario is imminent, so this prediction should probably be taken as an upper limit of what could happen rather than what will happen.

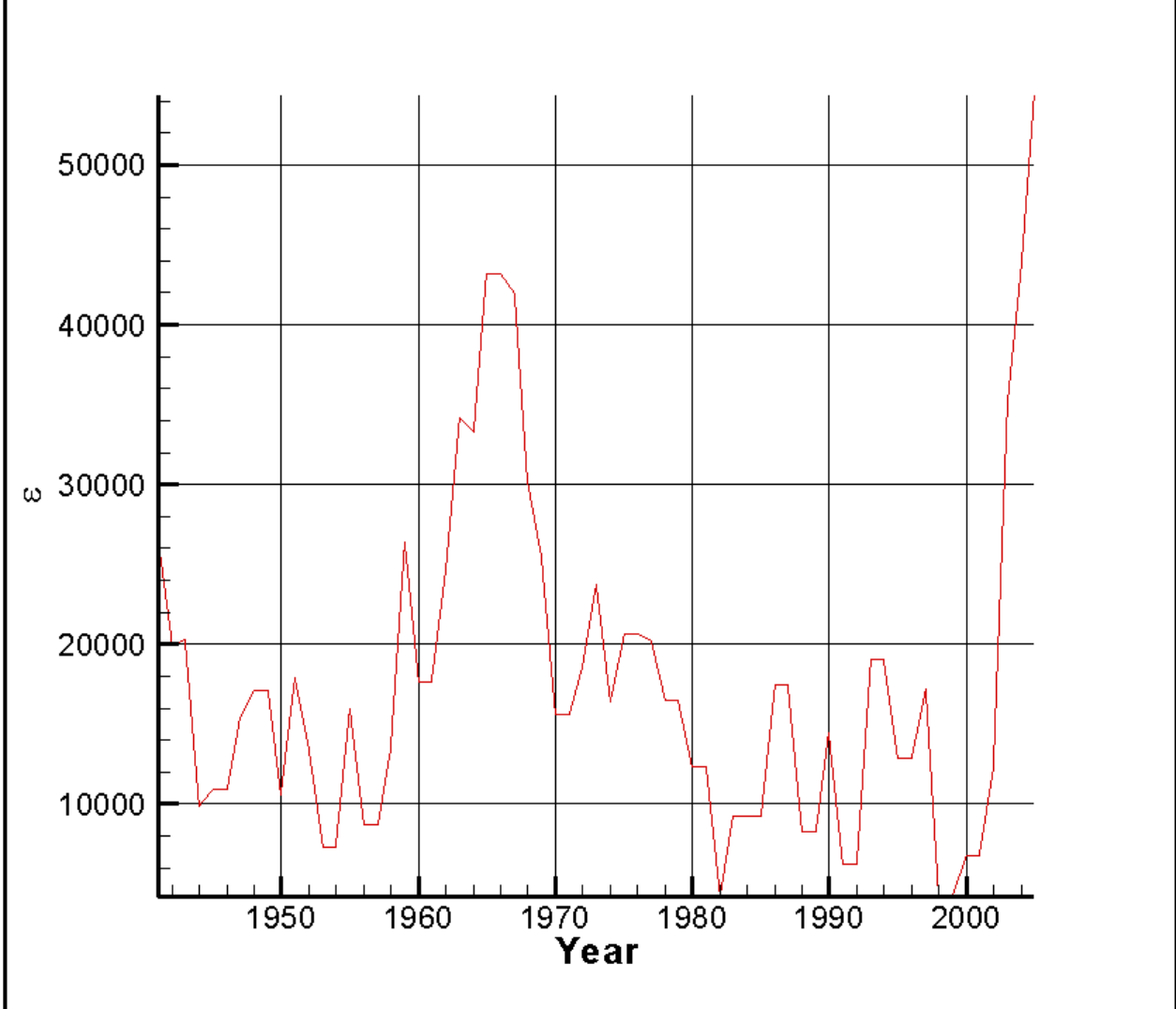


Figure C1. Plot of estimated cumulative kinetic energy for all storms at time of maximum surface winds within each year: 1941-2005. The units of ϵ are l^4/t^2 , since we have factored out the mass term (consistent with equation C1). Note: ϵ is termed E_k in Appendix C.

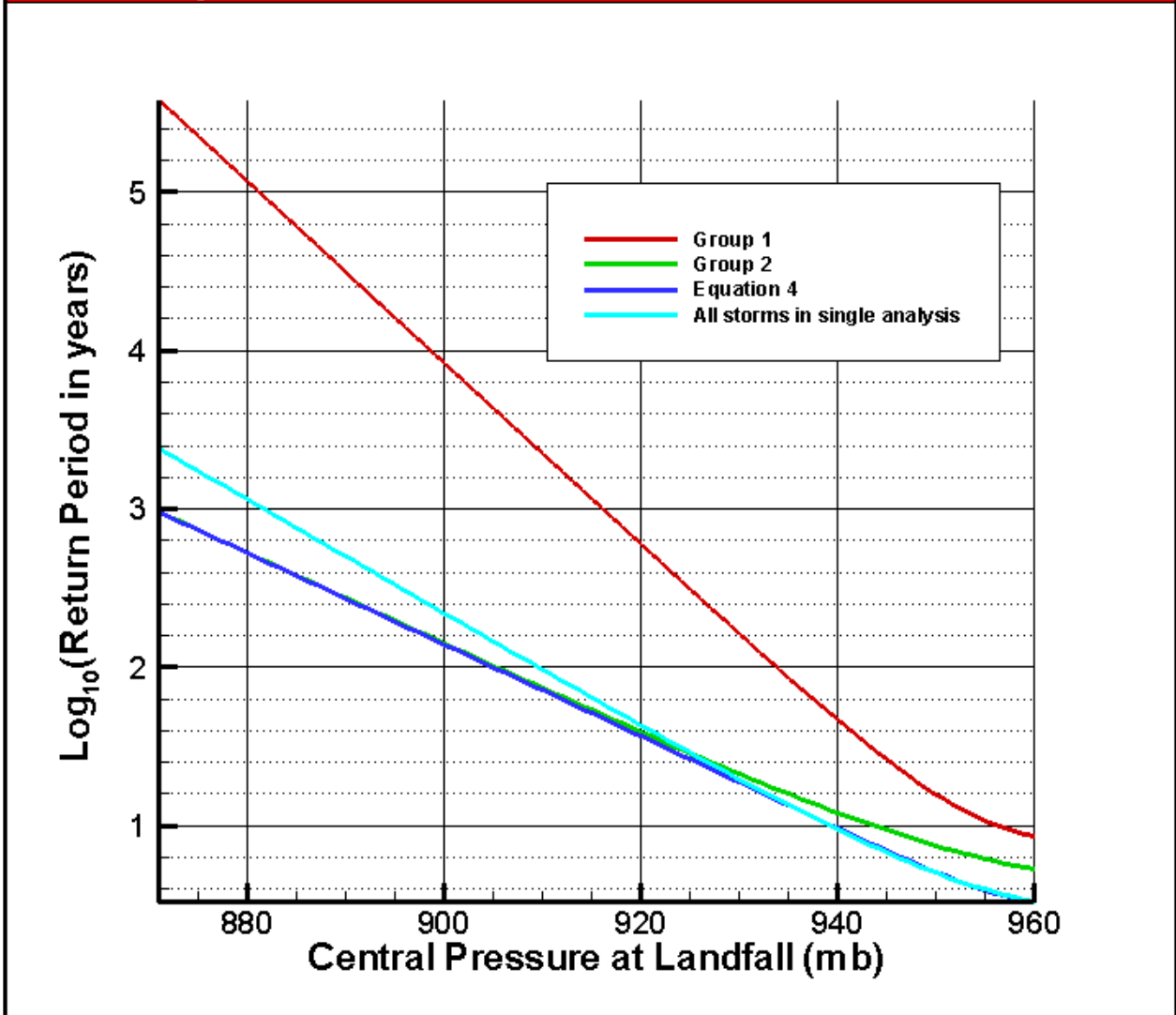


Figure C2. Estimated return periods for 4 separate analyses: Low-Activity years only (Group 1 – red line); High-Activity Years only (Group 2 – green line); All years into a single analysis (light blue line); and estimate based on combined analysis of two populations (equation 4 from Resio and Orelup - dark blue line).

Return Period (years)	Change in Wave Height (percent)	Change in surge (percent)
25	+15	+18
50	+13	+16
100	+12	+15
250	+11	+12
500	+10	+9

APPENDIX D of R2007

Selected Storm Sample for Simulations

In this Appendix, the terms R_{\max} (storm-size scaling radius) and C_p (central pressure) should be taken as equal to R_p and C_p , as defined elsewhere in this white paper. Tracks 1-5 are defined as shown in Figure 12 of the main text. This set of tracks has been nicknamed the “RICK-fan” since it mimics the tracks of Rita, Ivan, Camille, and Katrina. Track 1 is the westernmost and Track 5 is the easternmost track in this set. Tracks 1b-4b fall midway between the five primary tracks. One primed track 4’ is located about 40 nm north of the landfall point for Track 4 to allow for storms entering the N-S aligned portion of the coast in this area.

One of the issues affecting our storm selection is implicit in the spacing of the tracks shown in Figure 12. This spacing is approximately 0.6 degrees longitude at a latitude of 29.5 degrees, equivalent to a distance of about 31 nautical miles in the along-coast direction. Studies of surge response on idealized, open coasts have shown the distribution of surges along the coast scale quite nicely with this parameter for a wide range of storm sizes and offshore slopes (Figures D1-D3). Figure D4 provides a plot with all three of the storm sizes plotted together. A second factor which influences along-coast surge variations is the presence of large geometric features in the coastal configuration, such as the Mississippi River, its deltas, and the river levees south of New Orleans. Figure D5-A shows a general set-up for a numerical study to examine this effect. Figure D5-B shows the distribution of surges along the coast. It is apparent in this figure that the effect of the land protrusion is to add a second scale to the along-coast surge distribution. In the New Orleans area, this scale is likely to be of more significance than the simple open coast scaling. In the New Orleans area, this effect will tend to dominate the second source of along coast variation for storm within about 30 nm or so of the eastern edge of the land protrusion. In this context, the storm track spacing for the New Orleans area should be quite reasonable.

In the more general case of storms along a straight coast, any single storm will produce a patten with a shape similar to those shown in Figures D1-D3. Figure D6 shows a plot of where surges from two storm tracks might fall if they were separated by 31 nautical miles on each of these figures. This represents the worst case in which neither of the simulated storms captures the peak condition that could be generated by these hurricanes. This case is the worst possible since it has the maximum distance from the peak on both sides. Since tracks are assumed to be distributed uniformly along the coast, the expected value would be the mean of all points between the two lines. The bias introduced into the estimated extreme from this set of tracks can be estimated as

$$D1. \frac{E(\eta_1 + \eta_2)}{E(\eta_{1-2})} = \frac{\frac{\eta_1 + \eta_2}{2}}{\frac{1}{(x_2 - x_1)} \int_{x_1}^{x_2} \eta(x) dx}$$

which can be calculated numerically for each of the different radii to maximum winds considered. For the three cases shown, the calculated values are 0.794, 0.907, and 0.959 for the

10 nm, 20 nm, and 30 nm cases, respectively, which translates into low biases of approximately 20%, 9% and 4% in these “worst-case” situations. It should be noted that the sampling pattern itself should not introduce a bias in either direction (high or low); consequently, in other sections of the coast, where the exact peak is attained, the simulated value is actually higher than the denominator in this equation. Historically, this problem of low and high values along the coast has been addressed by some sort of smoothing along the coast. The smoothing interval of approximately $\frac{R_{\max}}{2}$ should work relatively well for this purpose.

Along each of the tracks modeled, the central pressure is allowed to vary during a simulated intensification interval until its intensity reaches a plateau. This plateau is maintained until the storm comes within 90 nautical miles of the coast at that time, the pressures decay according to the (linear interpolation) relationship

$$C_p(s) = \lambda_0 C_p(s_0) - (1 - \lambda_0) \Delta P_{decay}$$

where

- D2. C_p is the central pressure at s
 s is the distance along the storm track, with s_0 located 90 nm from landfall
 λ_0 is an interpolation multiplier (=1 at 90 nm from landfall and =0 at landfall)
 ΔP_{decay} is the total change in central pressure over 90 nm approach to landfall

The pressure decay term is somewhat dependent on storm size, so the following relationship was used to represent this term

- D3. $\Delta P'_{decay} = R_p - 6$ (with R_p given in nautical miles)
 constrained by $\Delta P_{decay} = \text{Max}(\Delta P'_{decay}, 18); \text{Min}(\Delta P'_{decay}, 5)$

Once a storm is one hour past landfall the pressure decay factor due to Vickery is applied

$$C_p = P_\infty - \delta P$$

where

$$\delta P = \delta P_0 e^{-a\Delta t}$$

- D4. where
 δP is the local pressure differential
 δP_0 is the pressure differential one hour after landfall
 a is an empirical constant
 Δt is time after landfall minus 1 hour

As noted in the main section of this white paper, R_{max} and the Holland B parameter are allowed to vary linearly over the same distance as C_p for all storms except the smallest storm class used in this application. For that class ($R_{max} = 6nm$), the storm is assumed to retain its intensity, its size, and its Holland B parameter all the way to landfall. Figure D6 shows a typical variation of storm parameters for a storm in which the characteristics vary during their approach to the coast. This figure shows the characteristic “spin-up” time for the hurricane (based on historical times required to reach peak storm intensities) and the variations during its approach to the coast.

Four different $C_p - R_p$ (central pressure – size scaling radius) combinations are defined as

A. 3 C_p and 3 R_{max} values

$C_p=960$ $R_{max} = (21.0, 35.6, 11.0)$
 $C_p=930$ $R_{max} = (17.7, 25.8, 8.0)$
 $C_p=900$ $R_{max} = (14.9, 21.8, 6.0)$

The loop structure for JPM run sequencing is (from inner loop working outward)

- R_{max}
- C_p
- Track

Thus, the sequence of runs for any track using Combination A is

	C_p	R_{max}
1.	960	15.4
2.	960	21.0
3.	960	35.6
4.	930	11.7
5.	930	17.7
6.	930	25.8
7.	900	6.0
8.	900	14.9
9.	900	21.8

B. 2 C_p and 2 R_{max} values

$C_p=960$ $R_{max}=(18.2,24.4)$
 $C_p=900$ $R_{max}=(12.5,18.4)$

The sequence of runs for any track using Combination B will be

	C_p	R_{max}
1.	960	18.2
2.	960	24.4
3.	900	12.5
4.	900	18.4

C. 2 Cp and 1 Rmax values

Cp=960 Rmax=17.7
Cp=900 Rmax=17.7

The sequence of runs for any track using Combination C will be

	Cp	Rmax
1.	960	17.7
2.	900	17.7

D. 1 Cp and 1 Rmax value

Cp=930 Rmax=17.7

Defining three angles as the central angles in the RICK-fan +/- 45 degrees should cover most of the important range for estimating the response surface of the surges. With the secondary variables (tidal phases, Holland B variations, wind field variations around the PBL central estimate, etc.) added to the integral, this should provide a very reasonable estimate of the surge CDF. Figures 13 and 14 in the main text provide the geographic information on these tracks. The tracks approaching the New Orleans area from the southeast are extremely similar to the tracks of the 1947 Hurricane, Betsy, and Andrew in this area. During the 1941-2005 interval, no tracks approached New Orleans from the southwest; however, other storms such as the 1893 storm did approach New Orleans from this direction. In fact, the 1893 track is fairly similar to one of the hypothetical tracks out of the southwest. A track from this direction represents the fact that these storms have to become caught up in the more westerly flow (winds blowing toward the east). For a storm to maintain its strength it cannot move too far west or too close to land; consequently, the track of a major storm is constrained somewhat to come from the region from which all the hypothetical (+45 degree) tracks emerge in order for these storms to strike the New Orleans area.

The effect of storm heading angle on surges at the coast appears to be twofold. First, the overall along-coast pattern is broadened; since the storm moves along the coast at the same time that it moves toward landfall. Second, there is a relatively slow variation in the maximum surges produced by a storm as a function of the angle of the storm track with the coast; however, as seen in Figure D8, maximum surge is relatively weakly dependent on the angle of storm intersection with the coast. In general, the hurricane approaching slightly (15-30 degrees) from west of straight onto a straight east-west coast produce a somewhat higher surge (5% or so) than hurricanes moving perpendicularly to the coast. On the other hand, hurricanes approaching the straight east-west coast from a more easterly direction will tend to produce lower surges than produced by hurricanes moving perpendicular to such a coast. This appears to be a fairly broad pattern that can be represented via interpolation.

The effect of forward storm speed is addressed by considering three different forward velocities $V_f=(11,6,17)$ knots, where 11 is around the mean and the 6-kt and 17-kt speeds span almost the entire range of V_f values at landfall for storms with C_p 's less than 950. Note that a few of the track-angle combinations are dropped due to either their very oblique angle with respect to the shore or they were exiting storms from the New Orleans area moving toward the

northeast. Increased forward storm speed contributes to higher wind speeds in the hurricane PBL model. Consequently, one effect of increasing forward storm velocity is to increase the surge at the coast by a factor which similar to increasing the wind speeds within the hurricane, i.e.

$$\eta_1 = \eta_2 \left(\frac{v_{\max} + 0.5v_{f_1}}{v_{\max} + 0.5v_{f_2}} \right)^2$$

where

- D5. η_1 is the surge at the coast in storm 1, with forward speed = v_1
- η_2 is the surge at the coast in storm 2, with forward speed = v_2
- v_{\max} is the maximum wind speed of a stationary storm
- v_{f_i} is the forward storm velocity of the i^{th} storm

A second effect of storm speed is to change the duration that a flood wave has to propagate inland. Thus, a slowly moving storm may produce more extensive inland flooding than a faster moving storm. By covering essentially the entire range of forward storm speeds observed in major storms within the Gulf (see Figures 11a and 11b), we should be able to quantify the range of the effects of storm speed on surges in the New Orleans area.

The information below provides information on the variation parameter combinations used in the New Orleans 152-storm study.

Primary Tracks

	Track						
(Vf=11)	1	2	3	4	4'	5	
Mean angle	9	9	9	9		9	(use Cp-Rmax combination set A) – storms 1-45
-45	4	4	4		4		(use Cp-Rmax combination set B) – storms 46-61
+45	4	4	4	4			(use Cp-Rmax combination set B) – storms 66-81
TOTAL = WAS 81 — NOW 77							

	Track						
(Vf= 6)	1	2	3	4	4'	5	
Mean angle	2	2	2	2		2	(use Cp-Rmax combination set C) – storms 82-91
-45	1	1	1		1		(use Cp-Rmax combination set D) – storms 92-95
+45	1	1	1	1			(use Cp-Rmax combination set D) – storms 97-100
TOTAL = 19							

(Vf=17)	Track						
	1	2	3	4	4'		5
Mean angle	1	1	1	1		1	(use Cp-Rmax combination set D) – storms 101-105
-45	1	1	1		1		(use Cp-Rmax combination set D) – storms 106-109
+45	1	1	1	1			(use Cp-Rmax combination set D) – storms 111-114
TOTAL = WAS 14 – NOW 13							

Secondary Tracks

(Vf = 11)	Track						
	1b	2b	3b	4b			
Mean angle	2	2	2	2		(use Cp-Rmax combination set C) – storms 115-122	
-45	2	2	2			(use Cp-Rmax combination set C) – storms 123-128	
+45	2	2	2			(use Cp-Rmax combination set C) – storms 131-136	
TOTAL = 20							

(Vf = 6)	Track						
	1b	2b	3b	4b			
Mean angle	2	2	2	2		(use Cp-Rmax combination set C) – storms 137-144	
-45	1	1	1			(use Cp-Rmax combination set D) – storms 145-147	
+45	1	1	1			(use Cp-Rmax combination set D) – storms 149-151	
TOTAL = 14							

(Vf = 17)	Track						
	1b	2b	3b	4b			
Mean angle	1	1	1	1		(use Cp-Rmax combination set D) – storms 152-155	
-45	1	1	1			(use Cp-Rmax combination set D) – storms 156-158	
+45	1	1	1			(use Cp-Rmax combination set D) – storms 160-162	
TOTAL = 10							

GRAND TOTAL = 152

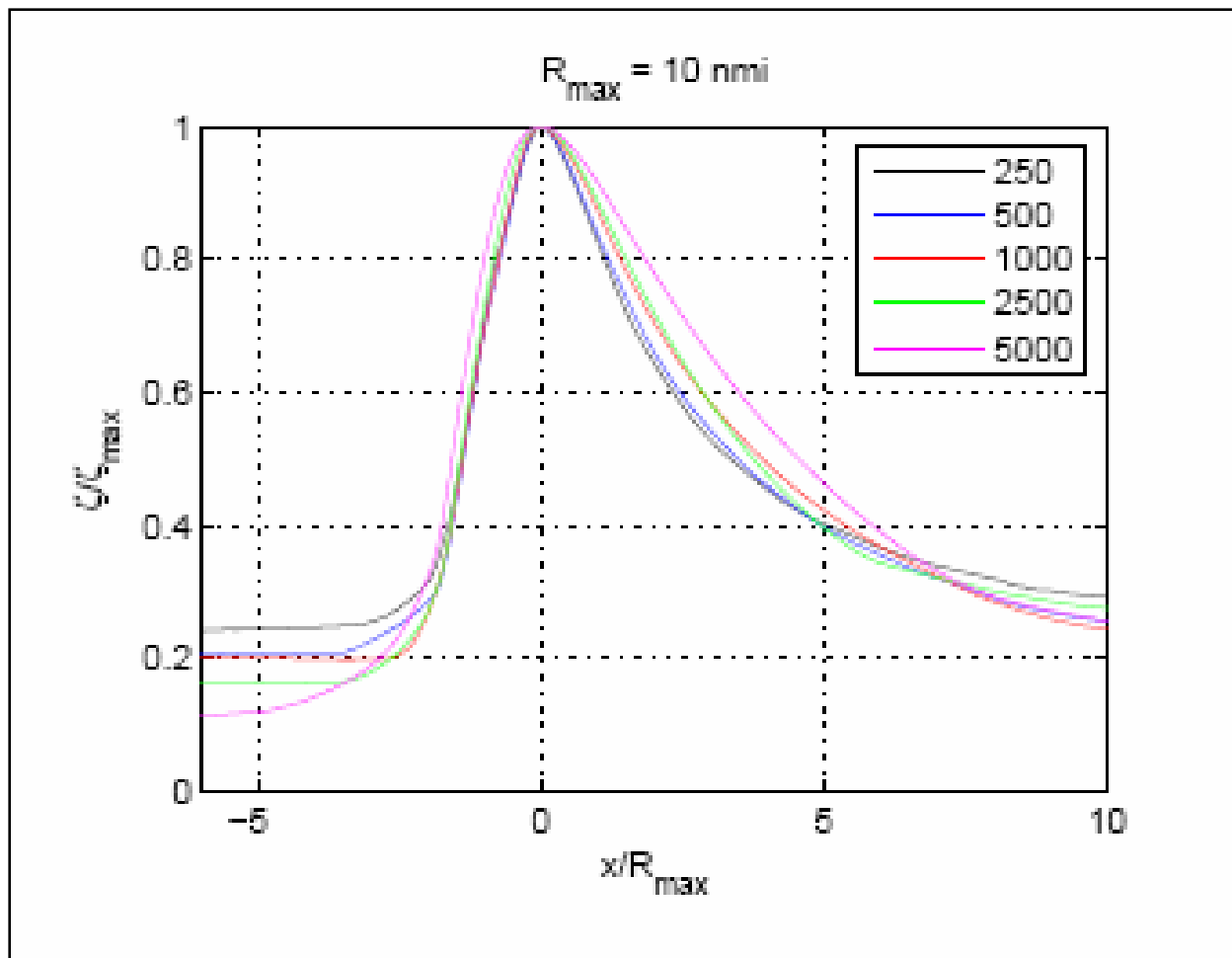


Figure D1. Distribution of normalized maximum surges along the coast (local surge maximum (ζ) divided by the maximum surge within the entire storm (ζ_{\max}) versus normalized distance along the coast (distance from storm peak divided by radius scaling parameter, R_{\max} , for offshore slopes in the range of 1:250 to 1:5000. Results are from numerical simulations on an idealized, straight coast for hurricanes for relatively small storm: R_{\max} ($= R_p$ scaling radius in Cardone PBL model) = 10 nm.

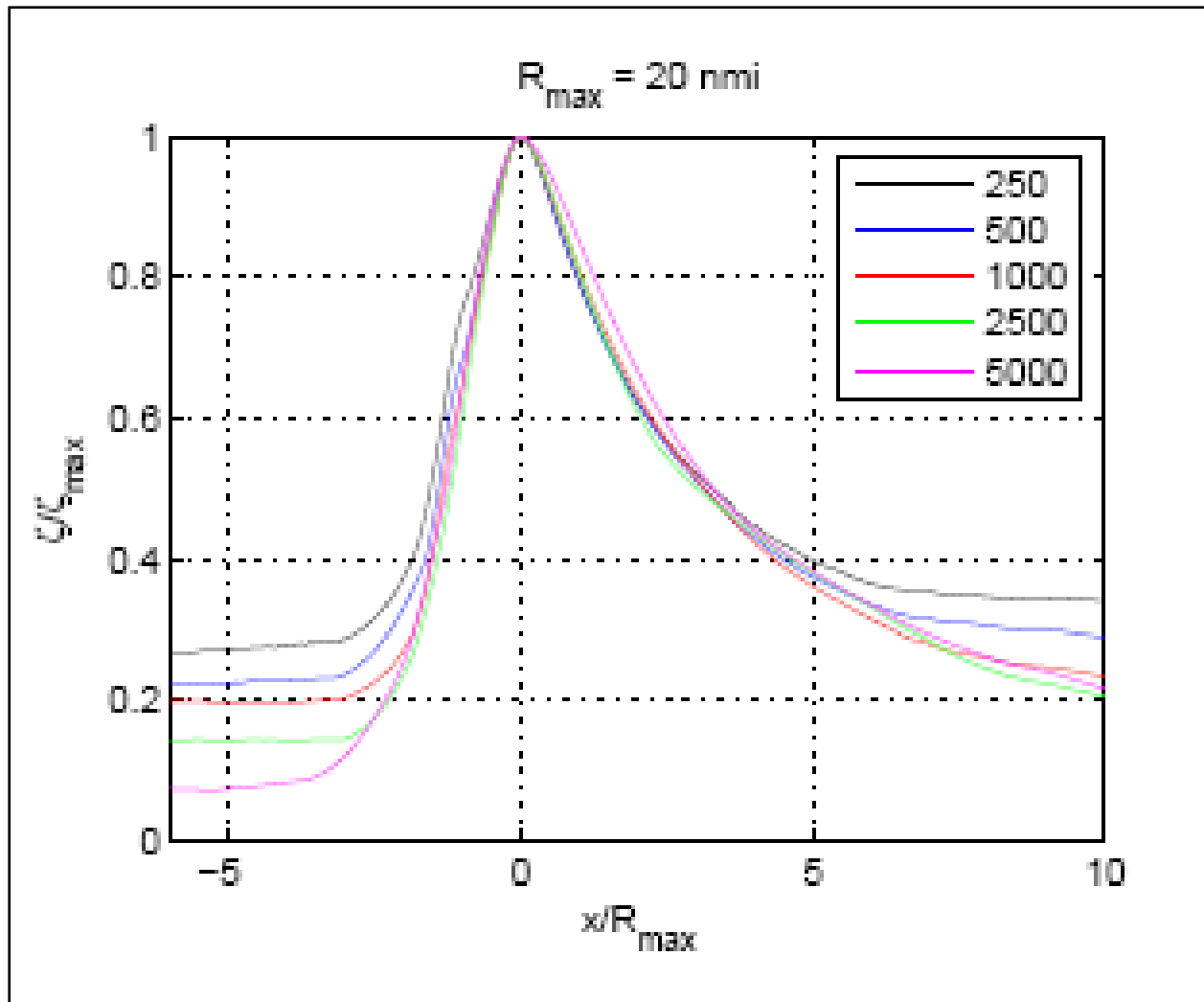


Figure D2. Distribution of normalized maximum surges along the coast (local surge maximum (ζ) divided by the maximum surge within the entire storm (ζ_{\max}) versus normalized distance along the coast (distance from storm peak divided by radius scaling parameter, R_{\max} , for offshore slopes in the range of 1:250 to 1:5000. Results are from numerical simulations on an idealized, straight coast for hurricanes for relatively small storm: R_{\max} ($= R_p$ scaling radius in Cardone PBL model) = 20 nm.

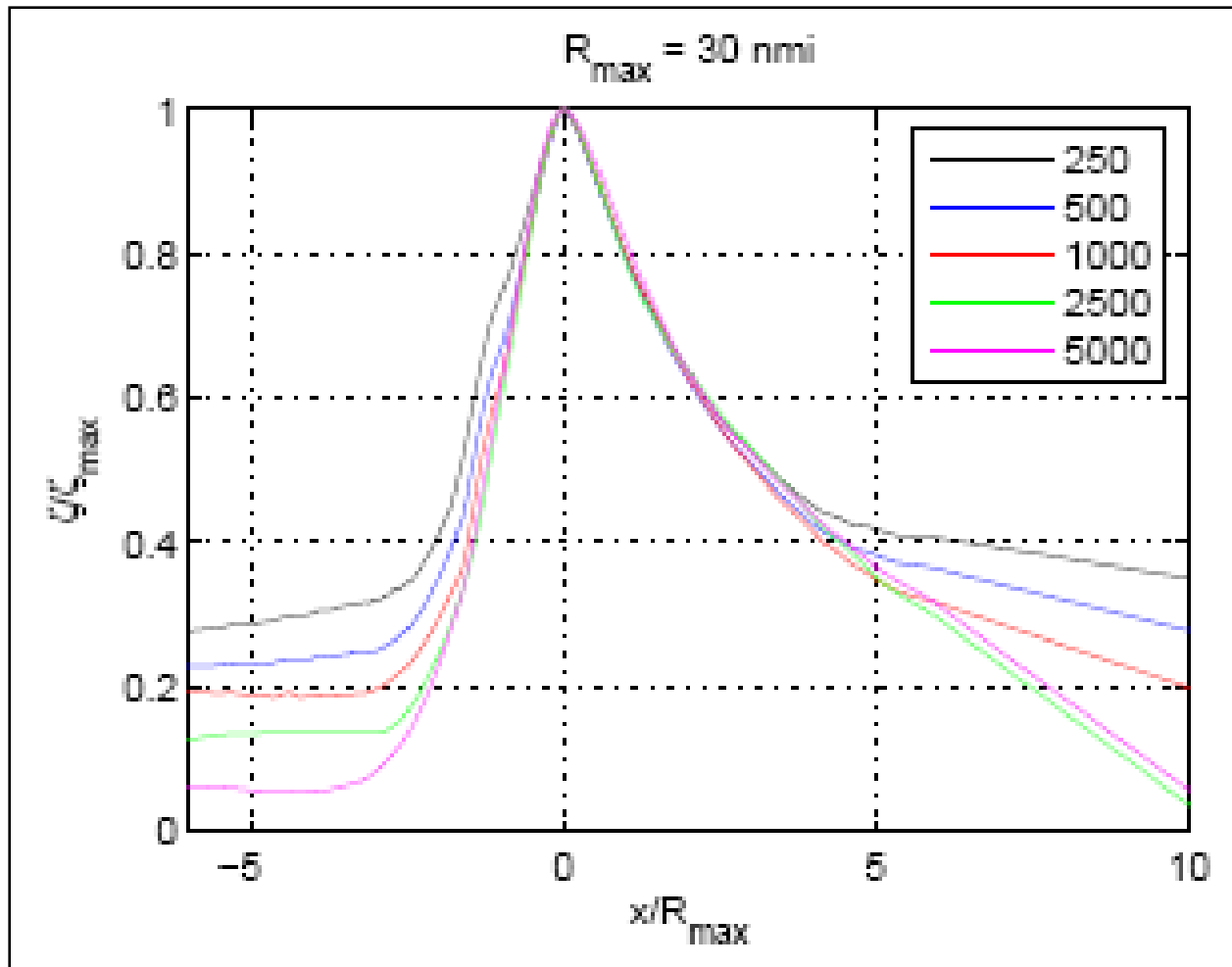


Figure D3. Distribution of normalized maximum surges along the coast (local surge maximum (ζ) divided by the maximum surge within the entire storm (ζ_{\max}) versus normalized distance along the coast (distance from storm peak divided by radius scaling parameter, R_{\max} , for offshore slopes in the range of 1:250 to 1:5000. Results are from numerical simulations on an idealized, straight coast for hurricanes for relatively small storm: R_{\max} ($= R_p$ scaling radius in Cardone PBL model) = 30 nm.

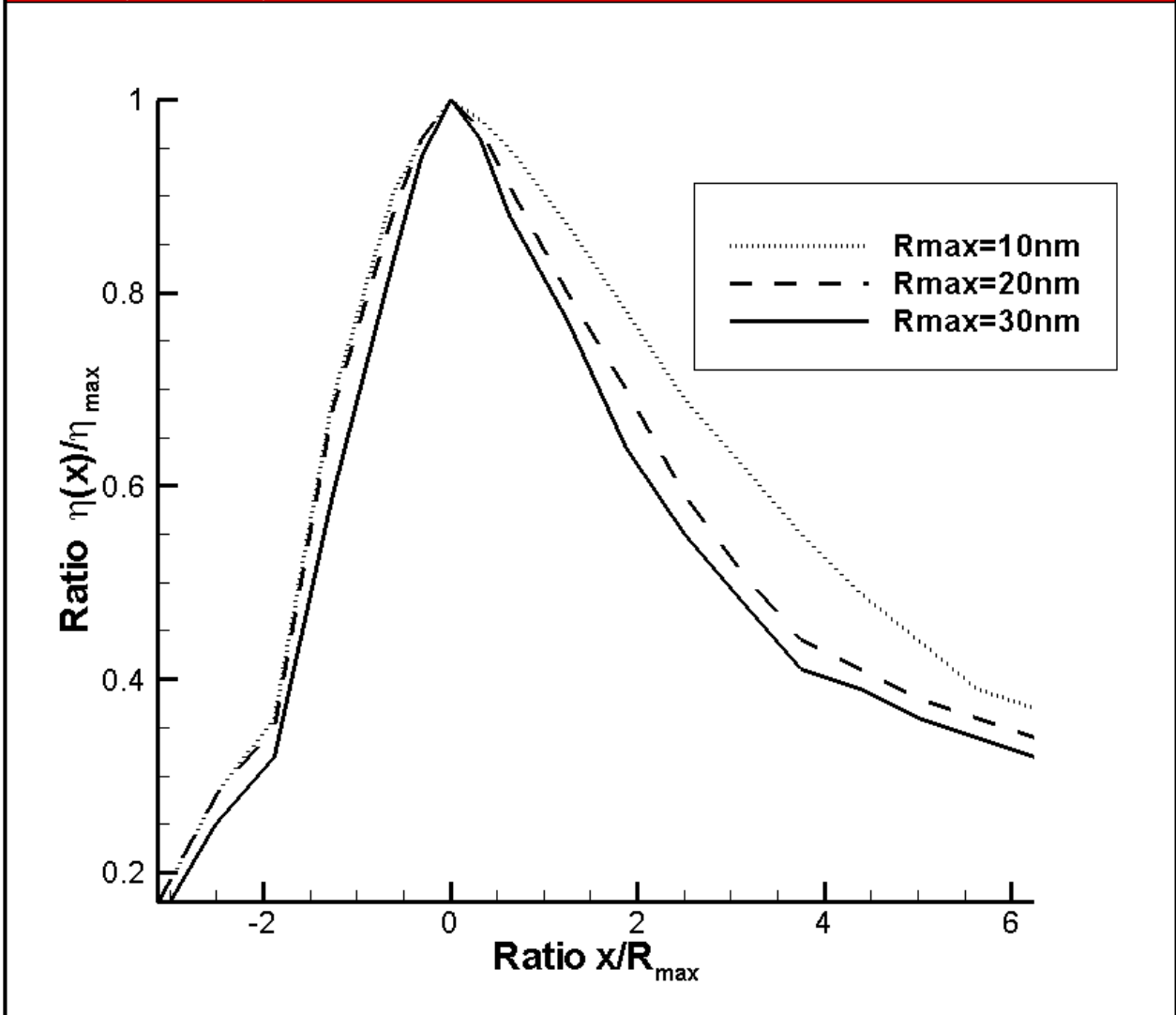
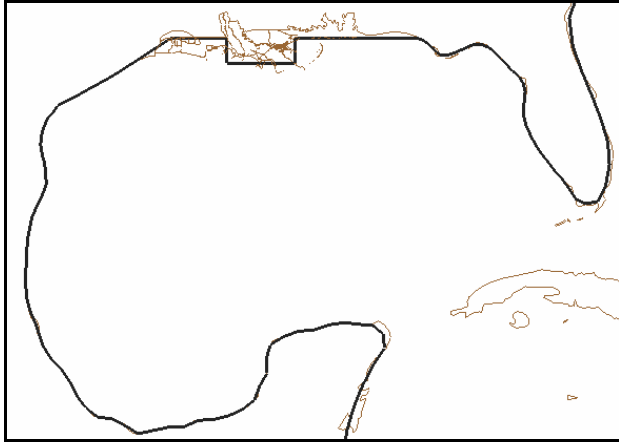
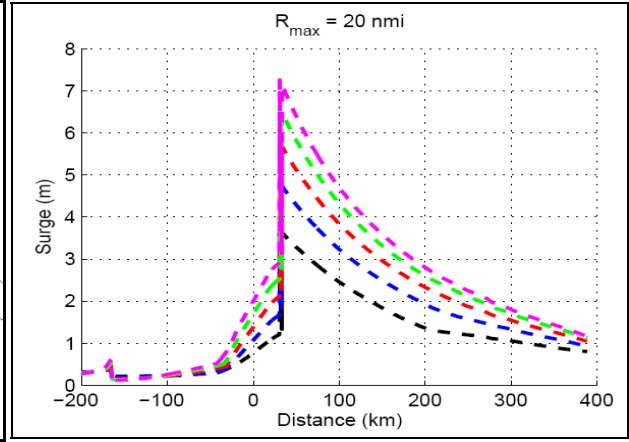


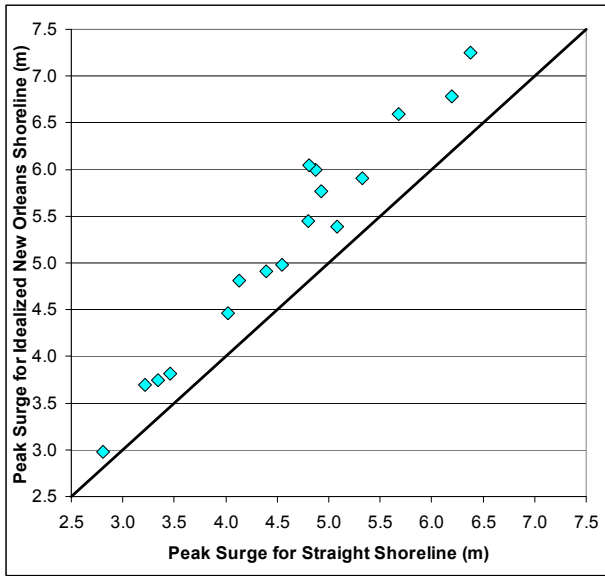
Figure D4. Distribution of normalized storm surge (local maximum ($[\eta(x)]$) divided by maximum over entire storm (η_{max}) as a function of normalized distance along the coast.



A. 1:10000



B.



C.

Figure D5(A-C). Figure D5-A shows an idealized representation of the New Orleans coastal area, with a section of land protruding from a generalized straight-line coast. Figure D5-B shows that the resulting surge distributions along the coast. Figure D5-C shows that surge values for this coastal configuration tend to be about 10-20% higher than the corresponding surges on a straight-line coast.

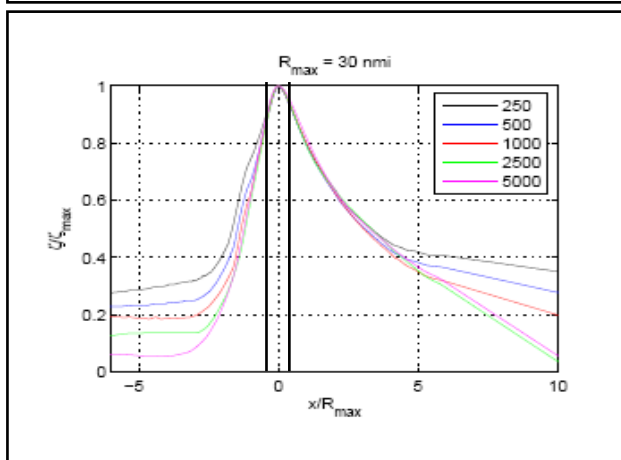
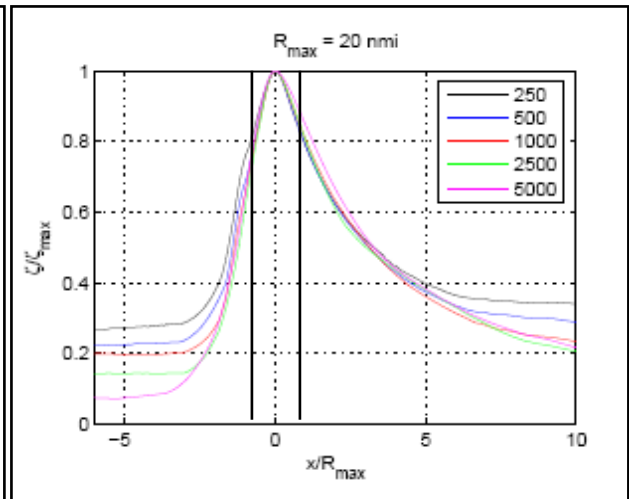
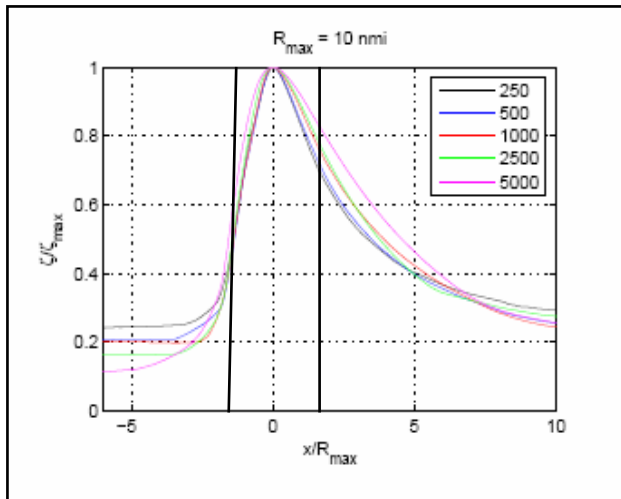


Figure D6. Figures D1-D3 re-plotted with lines approximately 31 nm drawn for the case in which the peak falls midway between the two tracks.

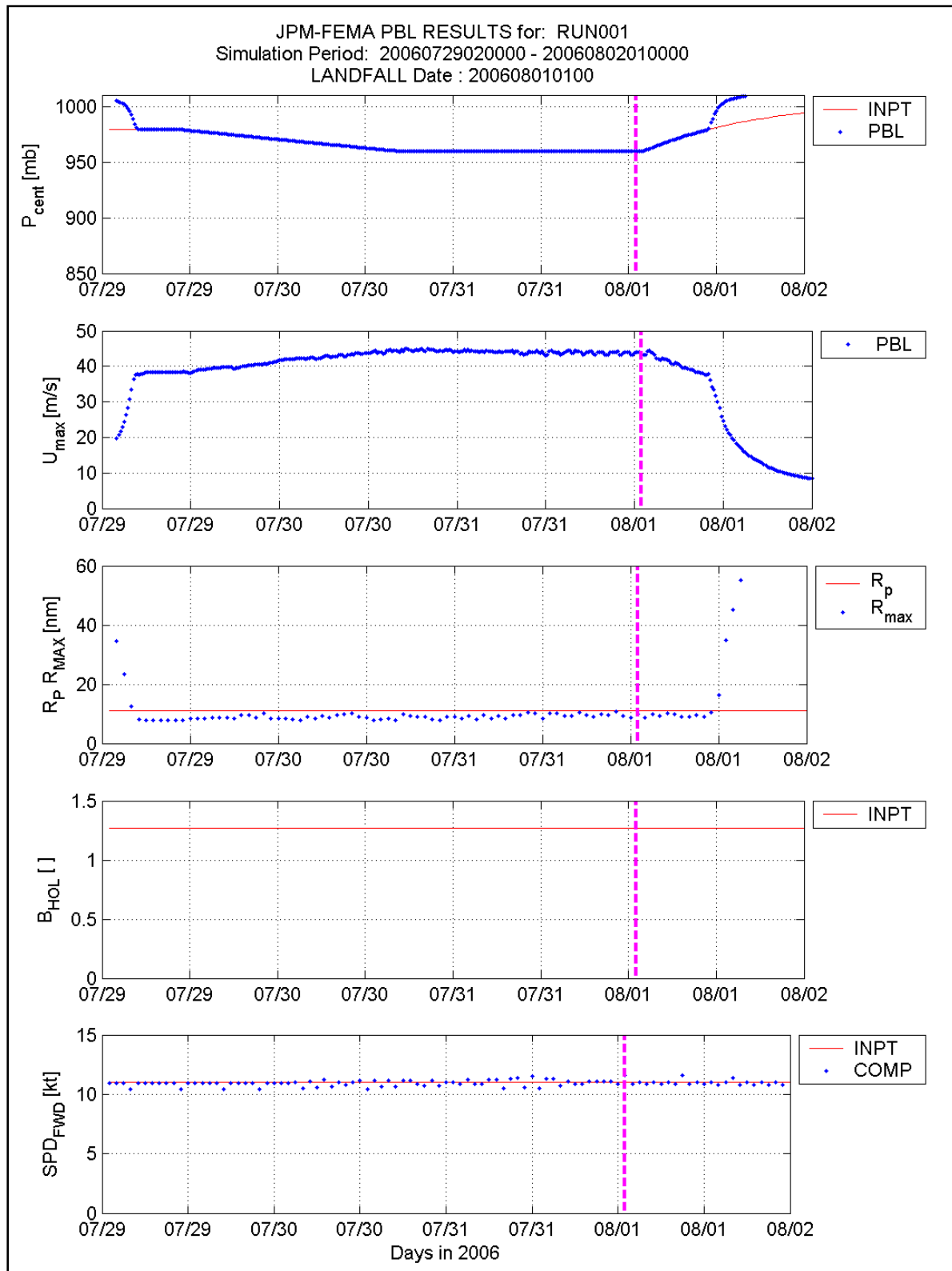


Figure D7. Sample time plot of the variation in central pressure, maximum wind speed, R_p , and forward storm speed used in quality control check of storm parameter behavior for first storm in JPM sequence.

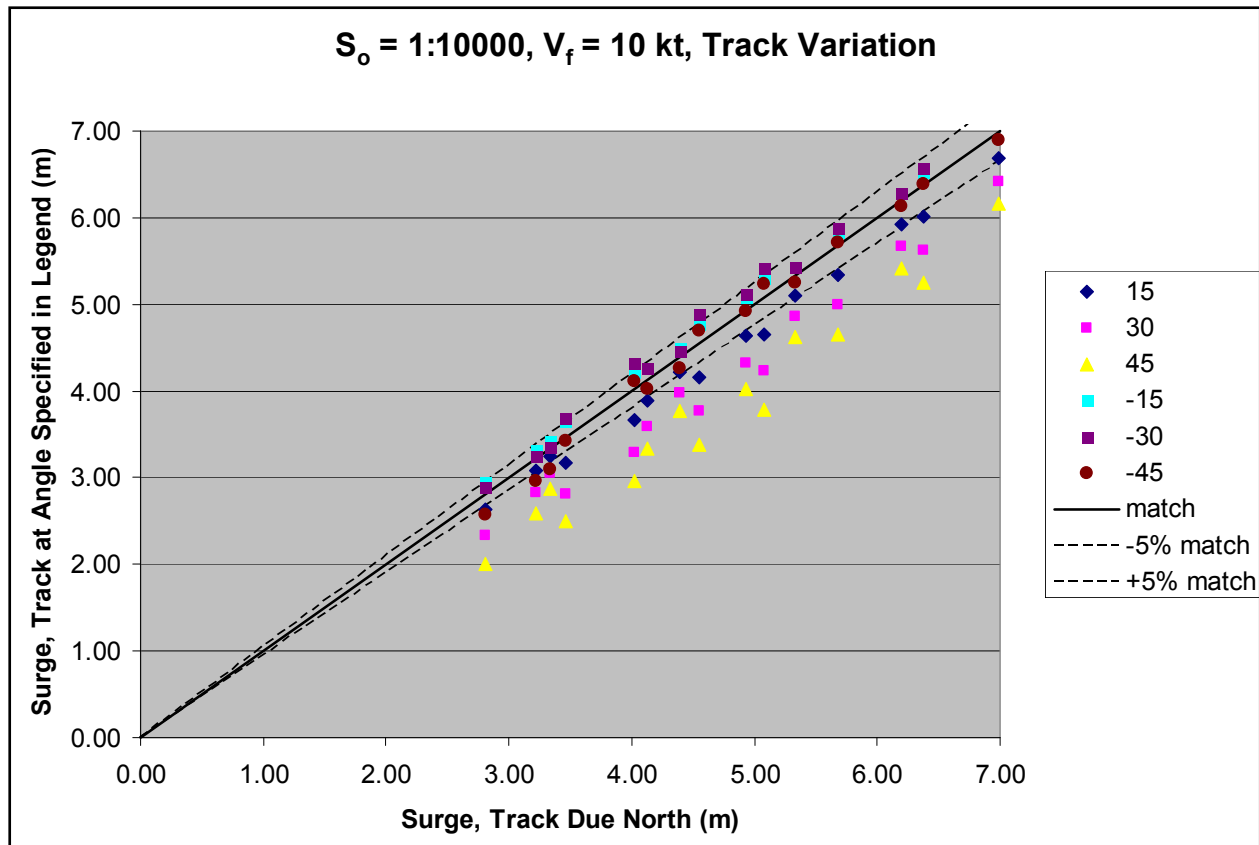


Figure D8. Variation in maximum storm surge produced by hurricanes approaching a straight, shallow-sloping (1:10,000) coast relative to the maximum surge produced by a storm moving perpendicularly to the coast.

APPENDIX E of R2007

The Characteristics of the Holland Pressure Profile Parameter and the Radius to Maximum Winds for Gulf of Mexico and Atlantic Hurricanes as Determined from an Analysis of Flight Level Pressure Data and H*Wind Surface Wind Speed Data

Introduction

Using pressure data collection during hurricane reconnaissance flights, coupled with additional information derived from the Hurricane Research Division's H*Wind snapshots of hurricane wind fields, an analysis of the radius to maximum winds and the Holland B parameter was performed. The reconnaissance data incorporates flights encompassing the time period 1977 through to 2001, but the analysis was limited to include only those data collected at the 700 mbar or higher level.

The Holland B parameter was found to be inversely correlated with both the size of a hurricane and the latitude of a hurricane. A weak positive correlation of B with central pressure deficit and sea surface temperature was also observed. A statistical relationship between the Holland B parameter and a non-dimensional parameter incorporating central pressure, radius to maximum winds, sea surface temperature and latitude was developed.

A qualitative examination of the variation of B , central pressure and radius to maximum winds as a function of time suggests that along the Gulf of Mexico coastline (excluding Southwest Florida), during the final 6 hrs to 24 hrs before landfall the hurricanes weaken as characterized by both an increase in central pressure and the radius to maximum winds, and a decrease in the Holland B parameter. This weakening characteristic of landfalling storms was not as evident for hurricanes making landfall elsewhere along the United States coastline.

Flight Level Data Analysis Methodology

Upper level aircraft data available at NOAA site were used to estimate Holland's pressure profile parameter (B). The upper level aircraft dataset used here contains a total of 4546 radial profiles from 62 Atlantic storms. For every storm, data has been organized based on the different flights that passed through the storm. For each flight, the airplane traversed through the hurricane a number of times in different directions. For every pass the data was collected from the center of the storm to a certain radius (usually 150 km). Available data is then organized according to their radial distance from the center of the storm. For each bin (based on the radius from the center of the storm) flight level pressure, flight altitude, dew point temperature, wind speed and air temperature are available. Each profile from every flight and every storm is treated as an independent observation. Holland, (1980) describes the radial distribution of surface pressure in a hurricane in the form:

$$p(r) = p_0 + \Delta p \cdot \exp\left[-\frac{A}{r^B}\right] \quad (1)$$

where $p(r)$ is the surface pressure at a distance r from the storm center, p_0 is the central pressure, Δp is the central pressure difference, A is the location parameter and B is the Holland's pressure profile parameter. Holland (1980) showed that $RMW = A^{1/B}$ where RMW is the radius to maximum winds, and thus Equation (1) can be expressed as:

$$p(r) = p_0 + \Delta p \cdot \exp\left[-\left(\frac{RMW}{r}\right)^B\right] \quad (2)$$

The surface pressure and radial distance are transformed to the form of Equation (2). The missing quantities in Equation (2) are RMW and B . First estimate of RMW is made from the recorded wind speed profile i.e. RMW is the radius to the measured maximum wind speed. From here on, the radius corresponding to the maximum wind speed in a profile is referred to as RMW . To estimate the optimum values of B and RMW , RMW and B are varied over the range $[0.5RMW, 1.5RMW]$ and $[0.5, 2.5]$ respectively. The algorithm calculates an optimum B value by minimizing the mean of the square differences between the measured and the modeled surface pressure in a range of $0.5RMW$ to $1.5RMW$ for different B and RMW values. Mathematically, the mean square error between the measured and the modeled surface pressure can be written as:

$$\varepsilon^2 = \frac{\sum_{i=0.5RMW}^{1.5RMW} (P_{obs_i} - P_{theo_i})^2}{n} \quad (3)$$

where P_{obs_i} is the measured pressure, P_{theo_i} is the theoretical pressure calculated using equation (2) and n is the number of data points in the range $[0.5RMW, 1.5RMW]$. The values of B and RMW chosen correspond to those yielding the minimum mean square error, ε^2 . The corresponding r^2 value for the fit is given by:

$$r^2 = 1 - \frac{\varepsilon^2}{\sigma^2} \quad (4)$$

where σ is the standard deviation of the measured pressure data in the range of $[0.5RMW, 1.5RMW]$.

Quality control criteria

A quality control criterion was used to filter out profiles. Each of the filtered profiles has at least one of the following characteristics associated with it, (a) Flight level pressure is less than 700 mbar i.e. height greater than 3000 m, (b) Central pressure difference is less than 25 mbar, (c) Radius to maximum winds is greater than two-third of the sampling domain, (d) the distance of aircrafts closest approach to the center is greater than half of the radius to maximum winds, (e) Data is available for less than one third of the sampling range i.e. less than 50 km, (f) visual inspection which involved eliminating profiles with a considerable amount of data missing in the

range of interest $[0.5RMW, 1.5RMW]$. The rationale for using criteria (a) is that higher the measurement height, less representative measurements are of the surface observations. Criteria (b) results in the data associated with Category 1 or higher hurricanes only. The rationale for using criteria (c), (d), (e) and (f) is to ensure that there is a sufficient number of measurements on both sides of the radius to maximum winds to have a clear representation of the shape of the profile.

The use of the quality control criteria eliminated a total of 2291 profiles from a set of 4556 profiles. Table 1 presents the count of the eliminated pressure profiles based on the filtering criteria. It is clear that criteria (a) and (b) are the most common reasons for profile elimination. Storm by storm percentage of the retained profiles is given in Table 2. For some storms, no profiles were retained as all the profiles either had a central pressure difference of less than 25 mbar (e.g. Chantal 1995) or a flight level pressure of less than 700 mbar (e.g. Hugo 1989). Figure 1 presents a few examples of pressure profiles that were eliminated from the analysis. Both the measured pressure data and the corresponding fit to Holland’s equation are shown. It is observed that each of the subplots in Figure 1 is compromised by at least one of the above mentioned quality control criteria.

Figure 2 presents examples of pressure profiles that were retained for analysis. Each row in Figure 2 corresponds to a complete airplane traverse in one direction. The shaded regions in Figure 2 represent the error minimizing range of $0.5RMW$ to $1.5RMW$. The fit parameters i.e. the B value, the central pressure difference and the RMW are also provided in the title of every profile. For a given traverse through a hurricane, differences in the B values for two different profiles is due to the change in the radius to the maximum winds and the central pressure difference. The geographical distribution of the filtered profiles, based on the storm center, is shown in Figure 3. The filtered profiles have a wide geographical distribution and provides with a wide domain of hurricane climatic characteristics. The filtered dataset has an average RMW of 46 km (standard deviation of 22 km), an average central pressure difference of 51 mbar (18 mbar) and an average location of $25.84^{\circ}N$ ($5.74^{\circ}N$) and $74.78^{\circ}W$ ($12.82^{\circ}W$). 71% of the fits yield r^2 values greater than 0.95 and 80% of the fits have a mean square error less than 2.5 mbar. The maximum mean square error was 24.6 mbar which occurred for one of Hurricane Opal’s profiles where Holland’s equation overestimated the pressures at all points.

Table 1.	
Distribution of filtered pressure profiles based on filtering criteria.	
Filter criteria	Number of profiles eliminated
(a)	459
(b)	1180
(c)	121
(d)+(e)+(f)	531
Total number of filtered profiles	2291

Table 2.
Percentage of flight level pressure profiles retained.

Storm	Year	Total	Retained	%Retained	Comments
no-name	1938	5	5	100.00	Data extracted manually from Myers & Jordan (1956)
Anita	1977	20	20	100.00	
David	1979	24	17	70.83	
Frederic	1979	62	38	61.29	
Allen	1980	125	43	34.40	
Gert	1981	78	1	1.28	$\Delta p < 25\text{mb}$ for all the cases, except one.
Alicia	1983	50	39	78.00	
Arthur	1984	22	0	0.00	$\Delta p < 25\text{mb}$ for all the cases.
Diana	1984	128	67	52.34	
Danny	1985	26	0	0.00	$\Delta p < 25\text{mb}$ for all the cases.
Elena	1985	122	99	81.15	
Gloria	1985	42	24	57.14	
Isabel	1985	48	0	0.00	$\Delta p < 25\text{mb}$ for all the cases.
Juan	1985	36	6	16.67	
Charley	1986	28	0	0.00	$\Delta p < 25\text{mb}$ for all the cases.
Emily	1987	56	1	1.79	40 out of 56 profiles have flight level pressure $< 700\text{mb}$.
Floyd	1987	22	0	0.00	$\Delta p < 25\text{mb}$ for all the cases.
Florence	1988	20	11	55.00	
Gilbert	1988	50	39	78.00	
Joan	1988	6	5	83.33	
Dean	1989	12	1	8.33	
Gabrielle	1989	12	10	83.33	
Hugo	1989	40	0	0.00	Flight level pressure $< 700\text{mb}$ for all the cases
Jerry	1989	17	5	29.41	
Gustav	1990	84	82	97.62	
Bob	1991	92	34	36.96	
Claudette	1991	73	71	97.26	
Andrew	1992	141	95	67.38	
Debby	1994	10	0	0.00	$\Delta p < 25\text{mb}$ for all the cases.
Gordon	1994	83	8	9.64	57 out of 83 profiles have $\Delta p < 25\text{mb}$.
Allison	1995	39	3	7.69	35 out of 39 profiles have $\Delta p < 25\text{mb}$.
Chantal	1995	72	0	0.00	$\Delta p < 25\text{mb}$ for all the cases.
Erin	1995	97	66	68.04	
Felix	1995	130	59	45.38	
Gabrielle	1995	16	0	0.00	$\Delta p < 25\text{mb}$ for all the cases.
Iris	1995	132	41	31.06	
Luis	1995	130	77	59.23	
Marilyn	1995	116	96	82.76	
Opal	1995	76	21	27.63	
Roxanne	1995	141	52	36.88	
Bertha	1996	78	56	71.79	
Cesar	1996	34	0	0.00	$\Delta p < 25\text{mb}$ for all the cases.
Edouard	1996	178	135	75.84	
Fran	1996	143	102	71.33	
Hortense	1996	109	59	54.13	
Josephine	1996	23	1	4.35	

Storm	Year	Total	Retained	%Retained	Comments
Kyle	1996	8	0	0.00	$\Delta p < 25\text{mb}$ for all the cases.
Lili	1996	68	28	41.18	
Marco	1996	67	1	1.49	$\Delta p < 25\text{mb}$ for all the cases, except two.
Erika	1997	56	36	64.29	
Bonnie	1998	193	113	58.55	
Danielle	1998	133	48	36.09	
Earl	1998	32	3	9.38	
Georges	1998	202	125	61.88	
Mitch	1998	86	57	66.28	
Bret	1999	102	49	48.04	
Dennis	1999	158	83	52.53	
Floyd	1999	163	103	63.19	
Keith	2000	50	40	80.00	
Leslie	2000	29	0	0.00	$\Delta p < 25\text{mb}$ for all the cases.
Michael	2000	21	11	52.38	
Humberto	2001	46	13	28.26	
Michelle	2001	89	61	68.54	

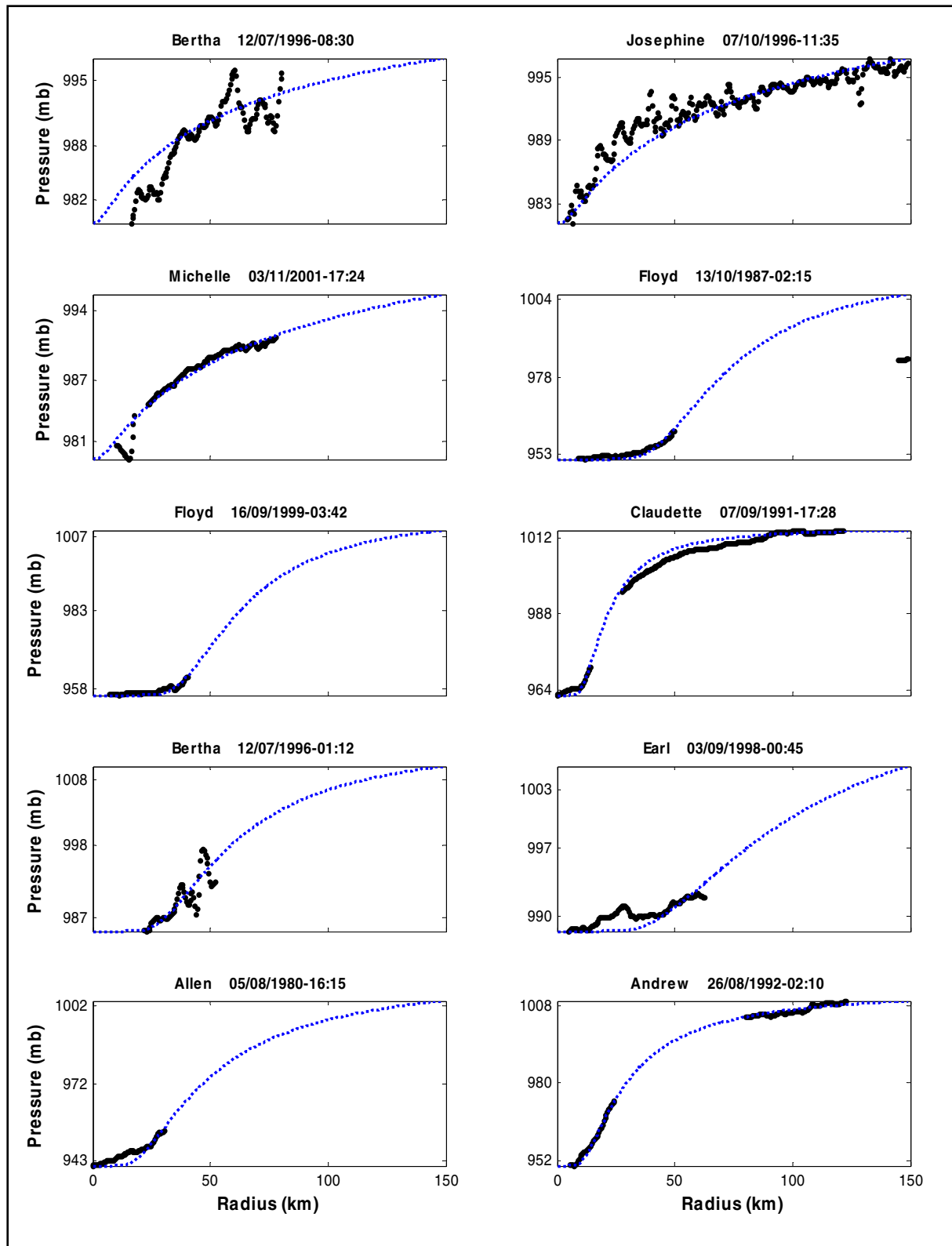


Figure 1. Examples of the eliminated profiles.

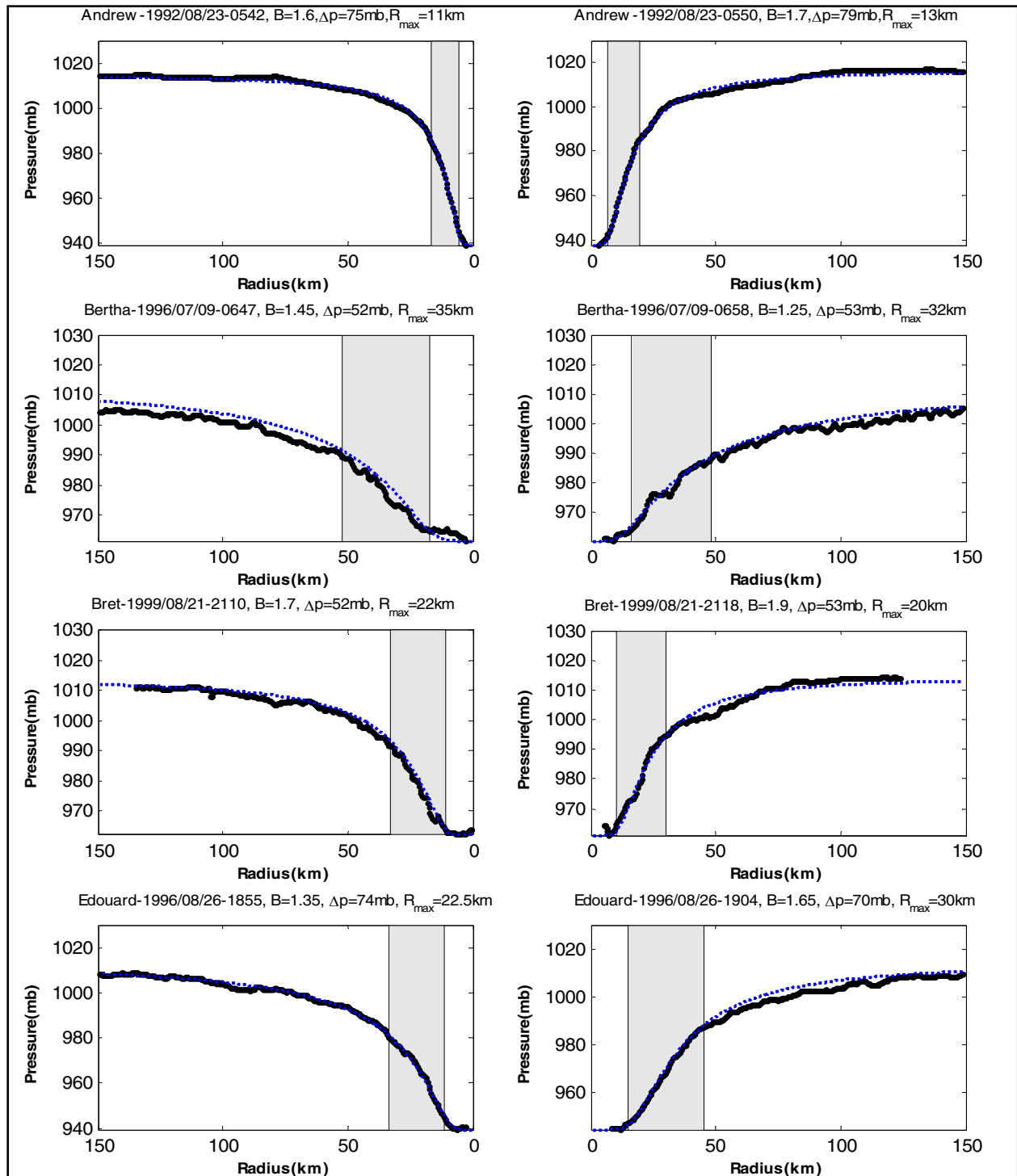


Figure 2. Examples of surface pressure profiles for a traverse across a given hurricane.

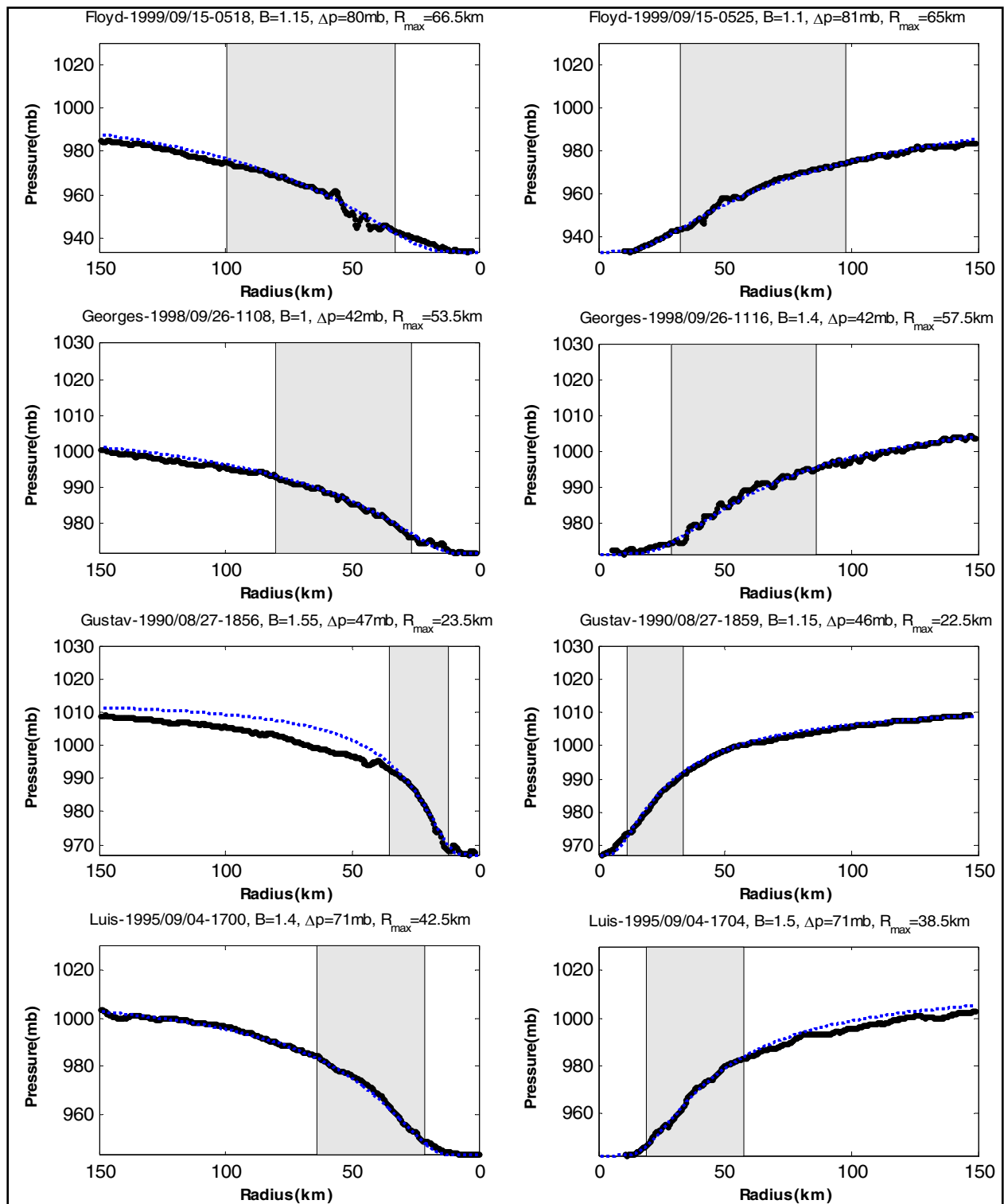


Figure 2. (continued) Examples of surface pressure profiles for a traverse across a given hurricane.

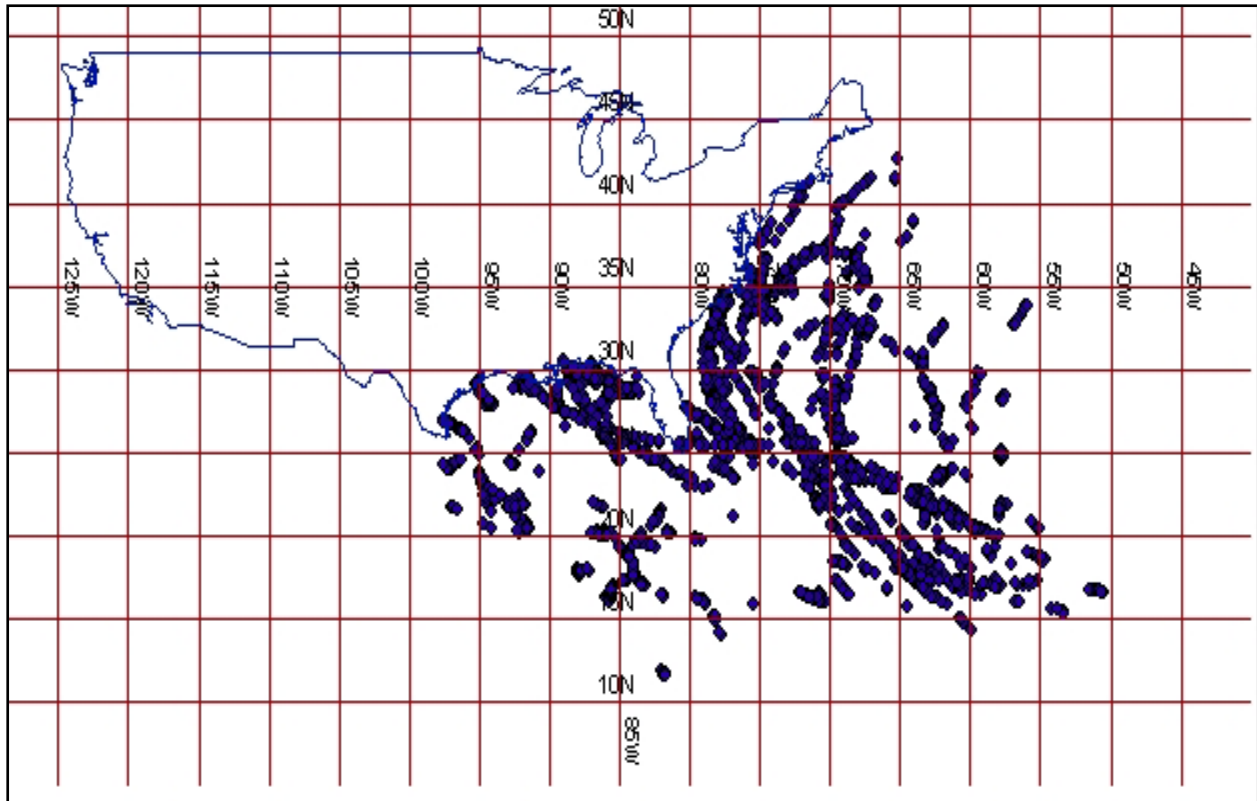


Figure 3. Geographical distribution of all the filtered profiles.

The approach for analyzing the B and RMW data involved the estimation of RMW and B from each single pass of a flight through the storm, and then smoothing the variations in B and RMW as a function of time. Figure 4 presents ten examples of both the single flight (point estimates) and the smoothed estimates of B and RMW plotted vs. time, for landfalling hurricanes. The landfall time is indicated with a vertical line in each plot. Using the smoothed data, values of B and RMW were extracted at intervals of approximately 3 hrs and retained for use in the statistical analyses. The mean values of B and RMW for the smoothed data set are 1.21 and 47 km respectively. The corresponding standard deviations are 0.29 and 21 km respectively. Note that in only one of the 11 landfall's indicated in Figure 4, does the Holland B parameter appear to increase as a hurricane approaches land (Hurricane Floyd near the NC coast). Table 3 summarizes, qualitatively, the tendency in the changes of B over the final few hours before landfall.

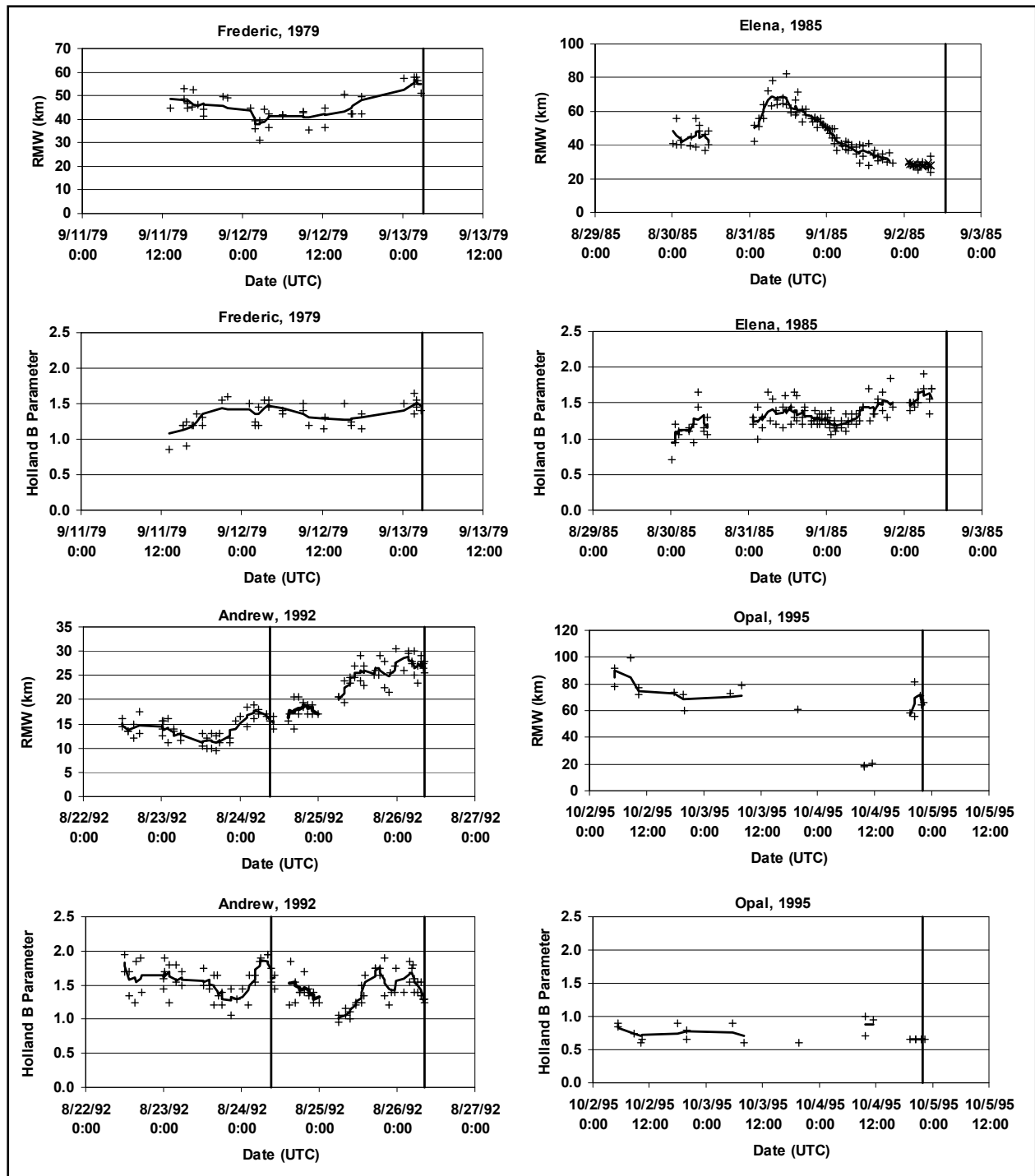


Figure 4. Examples of Smoothed (line) and Point Estimates (symbols) of *RMW* and *B* derived from 700 mbar level pressure data. Vertical line(s) represent time of landfall.

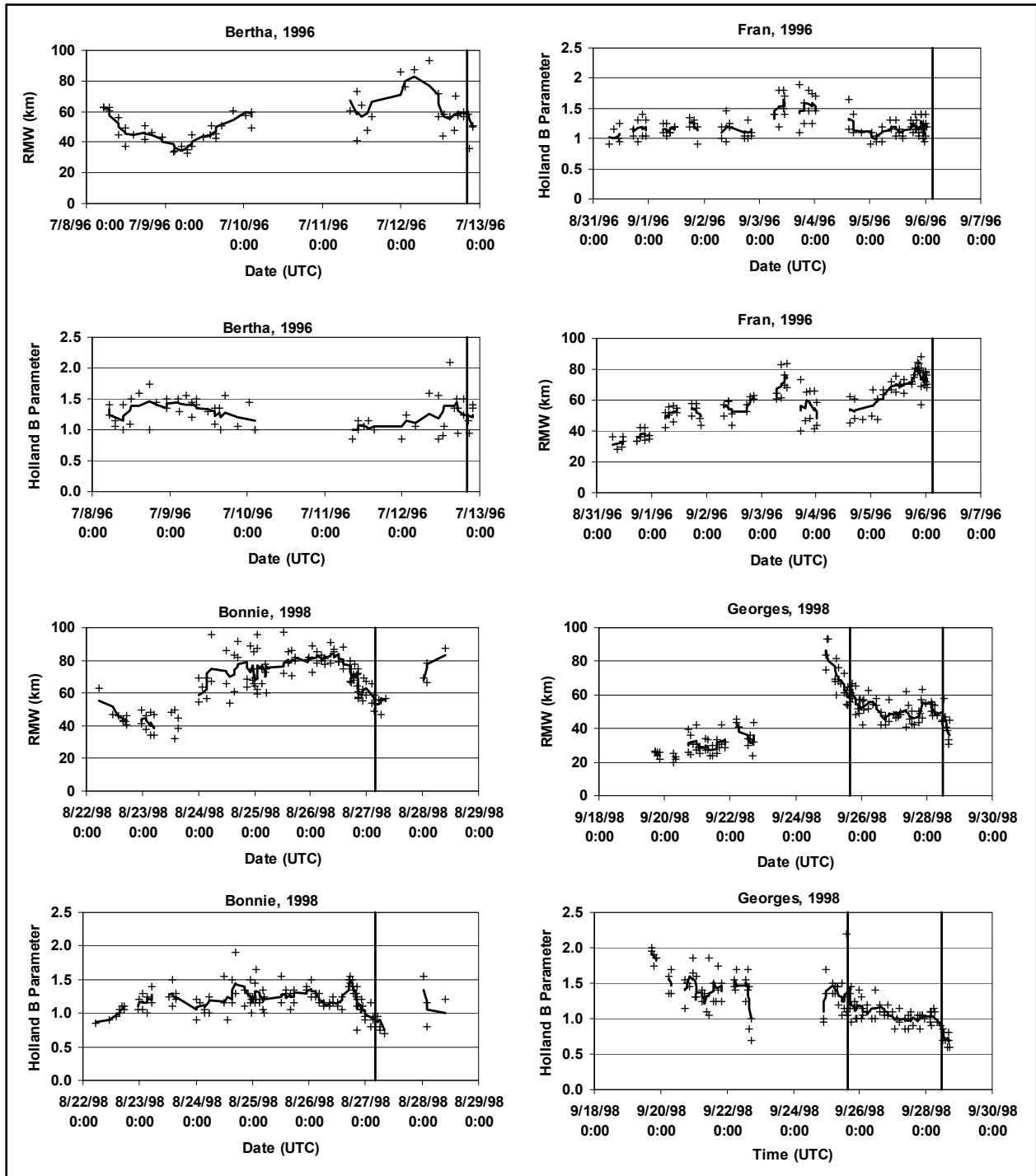


Figure 4. (continued) Examples of Smoothed (line) and Point Estimates (symbols) of RMW and B derived from 700 mbar level pressure data. Vertical line(s) represent time of landfall.

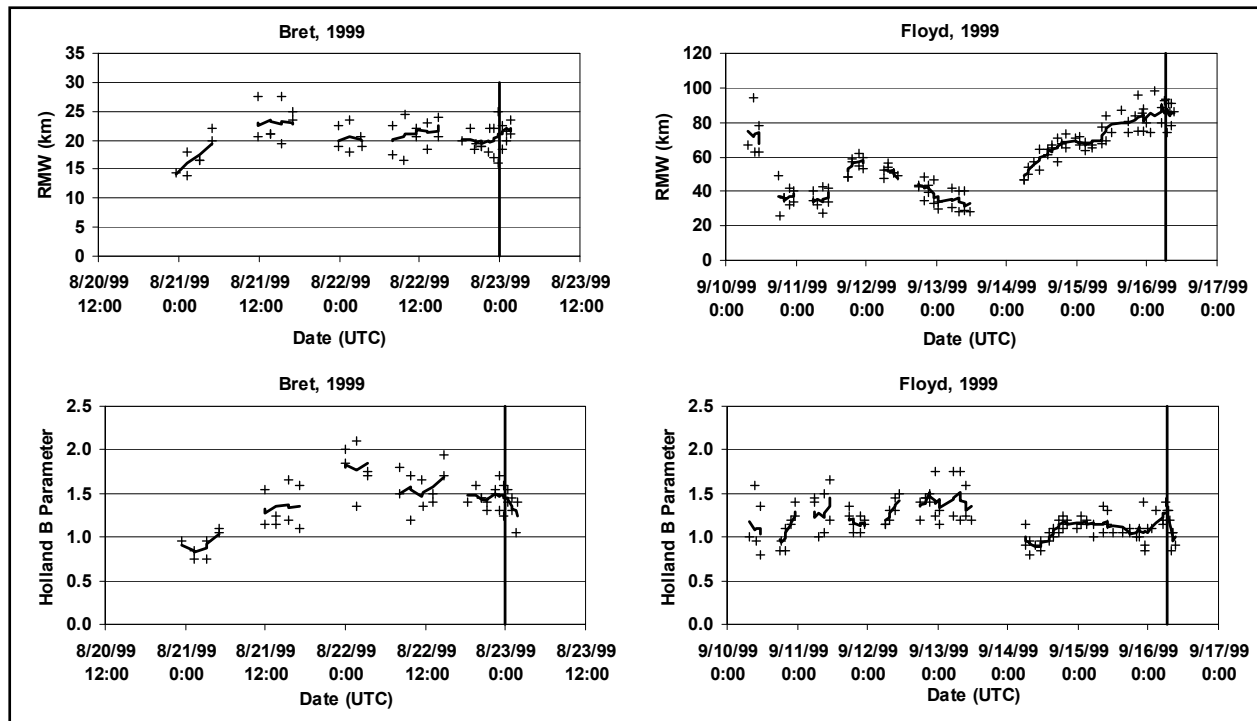


Figure 4. (concluded) Examples of Smoothed (line) and Point Estimates (symbols) of *RMW* and *B* derived from 700 mbar level pressure data. Vertical line(s) represent time of landfall.

Table 3.	
Tendency of Holland B Parameter for Landfalling Storms	
Hurricane and Landfall Location	B Tendency at landfall
Frederic (Alabama)	~ constant
Elena (Mississippi)	~ constant
Andrew South Florida	~constant to ~negative
Andrew Louisiana	negative
Opal (North West Florida)	constant
Bertha (North Carolina)	negative
Fran (North Carolina)	~constant
Bonnie (North Carolina)	negative
Georges (Mississippi)	negative
Bret (Texas)	~constant
Floyd (North Carolina)	positive

Supplemental H*Wind Data

The flight level data encompasses storms through to 2001, and thus to supplement the data set with more recent storms, some additional storms analyzed using the H*Wind methodology were added. The only storms added were the intense storms from the 2004 and 2005 seasons that had been re-analyzed using the most recent SFMR calibrations. The intense storms that have been reanalyzed include Hurricanes Katrina (2005) and Hurricane Ivan (2004). Hurricane Rita was added to the data set even though it had not been re-analyzed, because at its most intense, the storm had a minimum central pressure of less than 900 mbar. Using the wind field model described in Vickery, et al. (2007)., and the values of central pressure, RMW , storm translation speed, and the maximum sustained wind speed, a B value chosen so that the maximum surface level wind speed (one minute sustained value) obtained from the model match the H*Wind estimate of the maximum wind speed. Thus the estimated B values are obtained through an indirect measure, matching the maximum wind speed rather than the shape of the entire wind field.

Figure 5 presents plots of RMW , maximum one minute surface level wind speed, the derived B parameter and central pressure as a function of time for the three aforementioned hurricanes, in addition to the data derived for hurricanes Dennis (2005), Bret (1999) and Lili (1999). These three additional storms are given to examine the change in the characteristics of the storms as they approach land. Each plot also presents the central pressure(s) at land fall as given in the NHC hurricane reports.

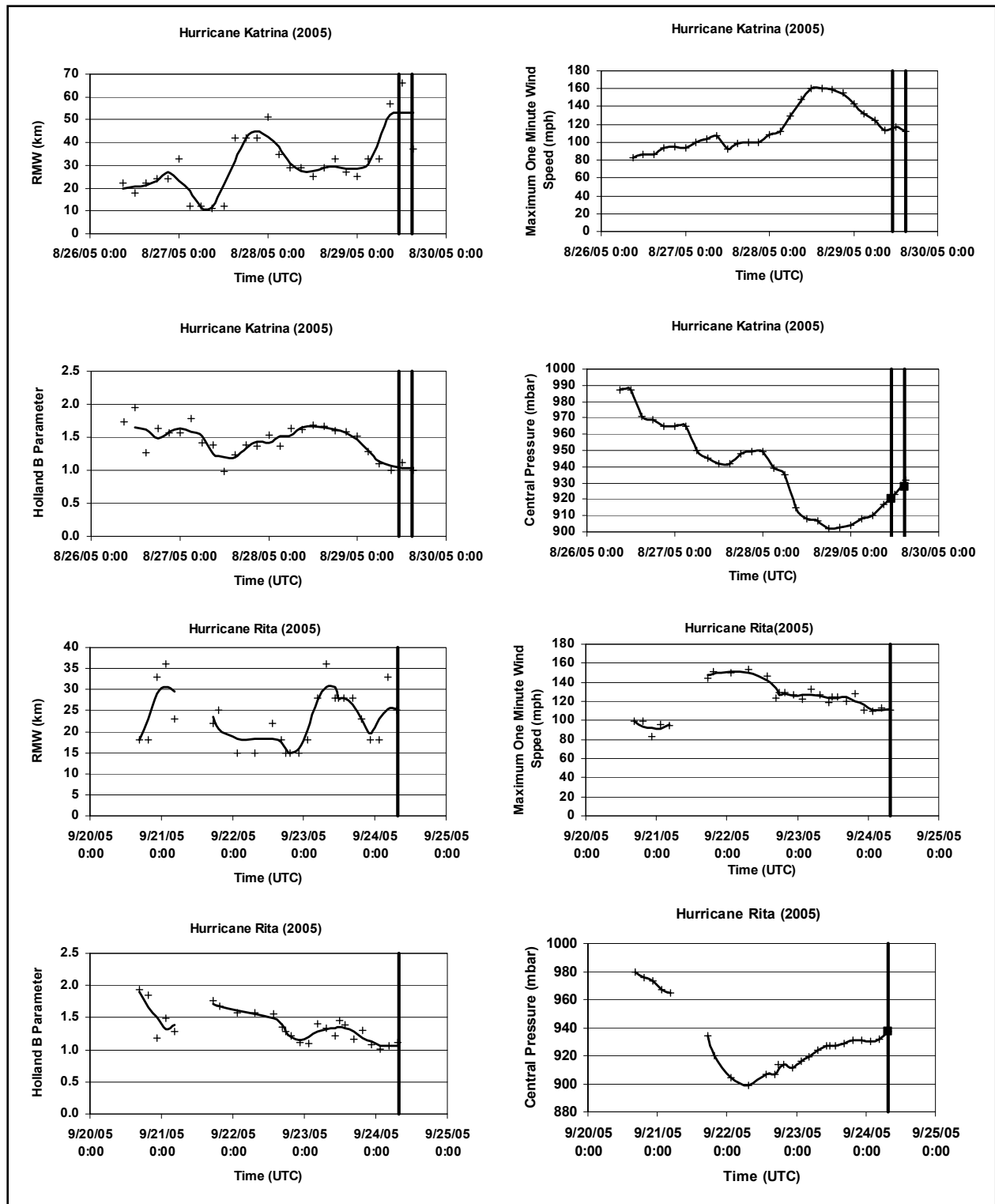


Figure 5. Smoothed (line) and Point Estimates (symbols) of *RMW* and *B* derived from H*Wind data. Vertical line(s) represent time of landfall. Solid square point at time of landfall represents NHC landfall pressure value.

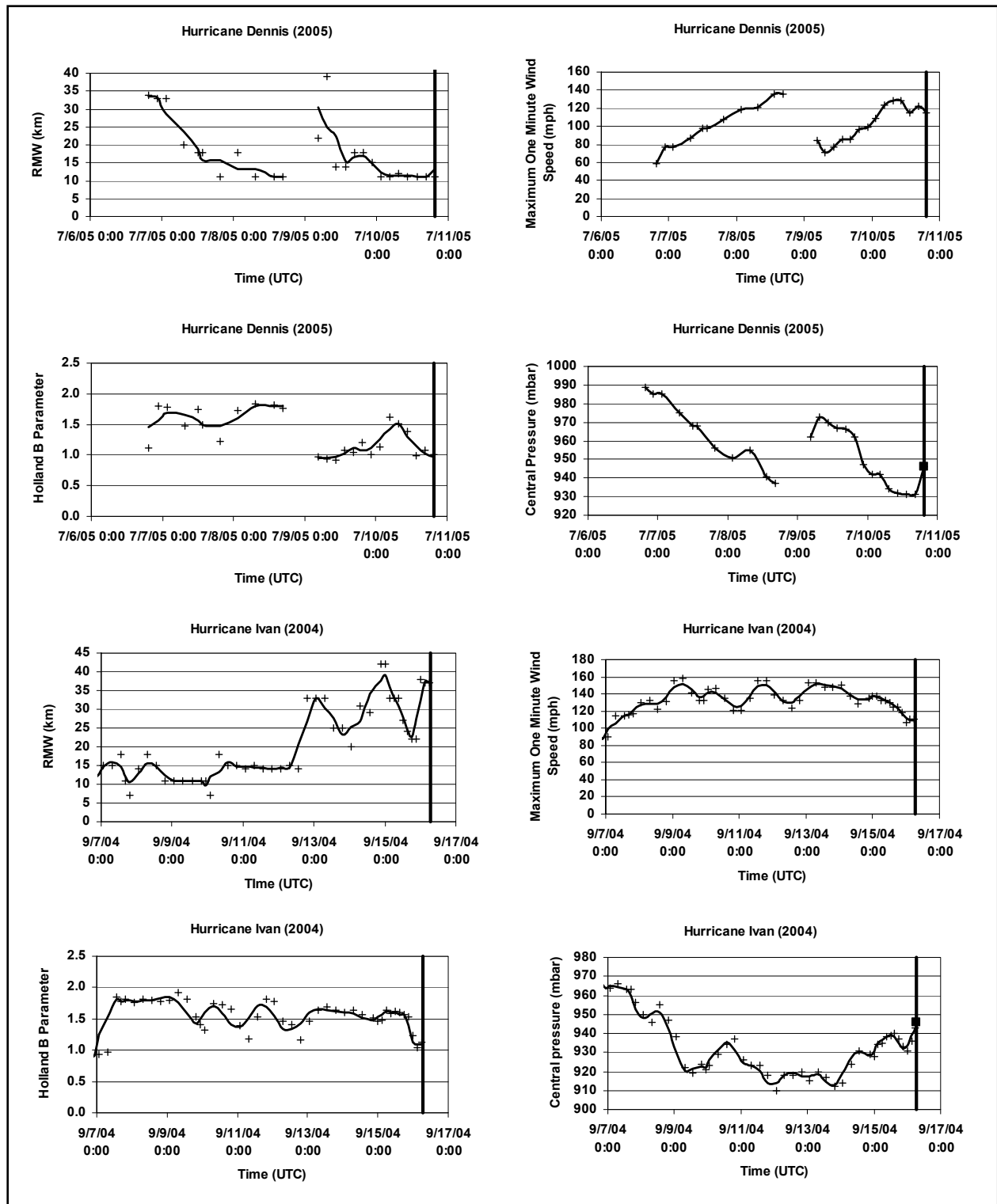


Figure 5. (continued) Smoothed (line) and Point Estimates (symbols) of *RMW* and *B* derived from H*Wind data. Vertical line(s) represent time of landfall. Solid square point at time of landfall represents NHC landfall pressure value.

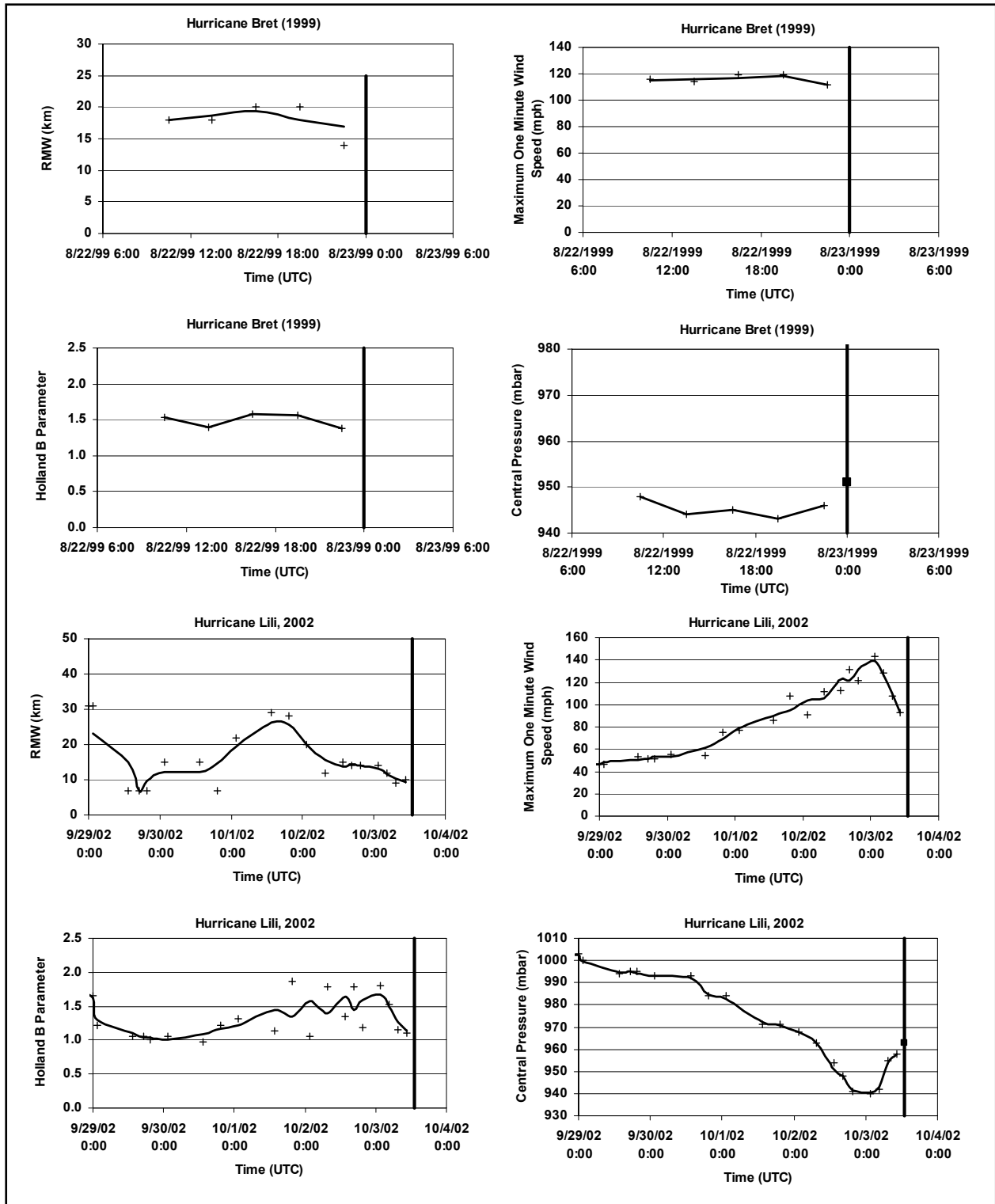


Figure 5. (concluded) Smoothed (line) and Point Estimates (symbols) of *RMW* and *B* derived from H*Wind data. Vertical line(s) represent time of landfall. Solid square point at time of landfall represents NHC landfall pressure value.

These six hurricanes represent all the Gulf of Mexico landfalling hurricanes in the H*Wind database that include information on both wind speeds and central pressure in each of the H*Wind snapshots. Additional storms are given in the H*Wind database that do not have central pressures provided on the H*Wind snapshots. All of the six hurricanes show an increase in central pressure and a decrease in the magnitude of the Holland B parameter as they approach the Gulf Coast. An increase in the radius to maximum winds as the hurricanes approach landfall is also evident in five of the six cases examined.

A similar analysis of hurricane characteristics for hurricanes making landfall in regions other than along the Gulf of Mexico coast did not indicate that there is a strong tendency for the storms to weaken and enlarge before landfall.

Statistical Model for Radius to Maximum Winds

All Hurricanes. The RMW for all points (flight level data plus H*Wind data) in the data set having a central pressure of less than 980 mbar were modeled as a function of central pressure difference and latitude in the form:

$$\ln(RMW) = 3.559 - 7.229 \times 10^{-5} \Delta p^2 + 5.296 \times 10^{-4} \Psi^2; r^2=0.266, \sigma_{\ln RMW}= 0.449 \quad (4)$$

An analysis of the errors (difference between the regression model estimates and the data) indicates that the model error reduced with increasing Δp , as indicated in Figure 6.

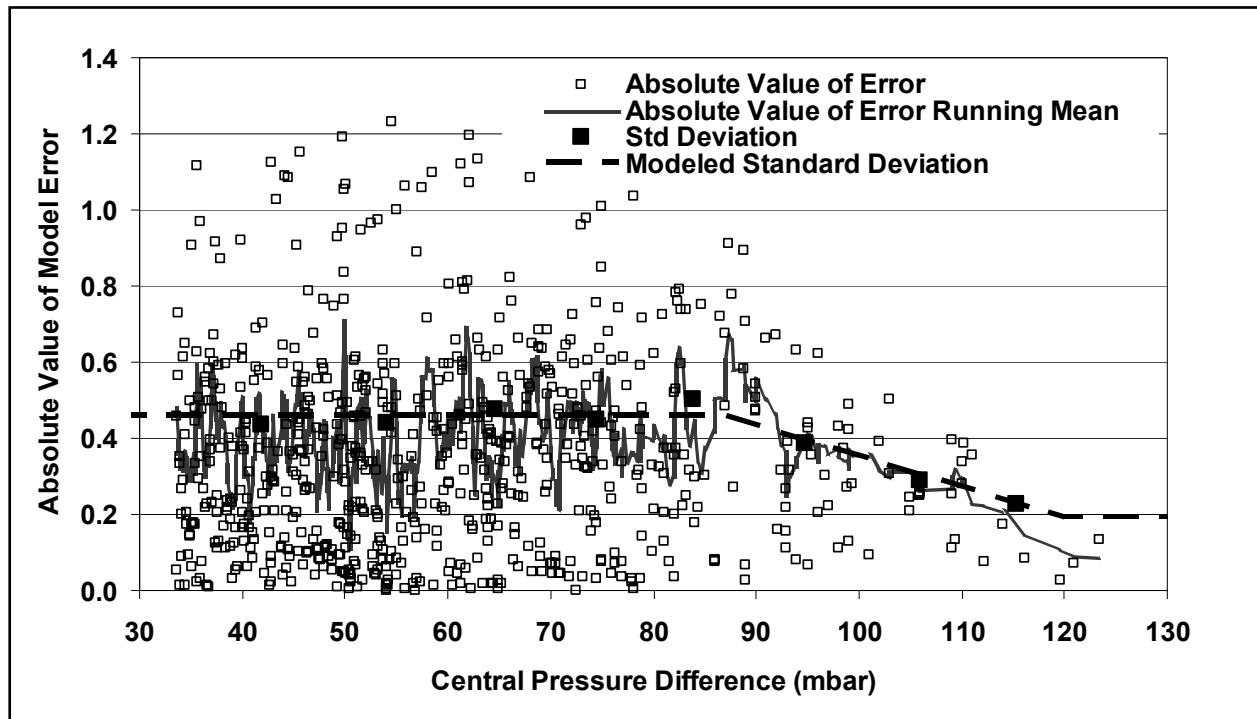


Figure 6. Absolute value of RMW model error vs. Δp

The error, $\sigma_{\ln RMW}$, is modeled in the form:

$$\sigma_{\ln RMW} = 0.460 \quad \Delta p \leq 87 \text{ mbar} \quad (5a)$$

$$\sigma_{\ln RMW} = 1.1703 - 0.00817\Delta p \quad 87 \text{ mbar} \leq \Delta p \leq 120 \text{ mbar} \quad (5b)$$

$$\sigma_{\ln RMW} = 0.190 \quad \Delta p > 120 \text{ mbar} \quad (5c)$$

Figure 7 presents the modeled and observed values of RMW plotted vs. Δp . The modeled data are given as the median estimates and the range defined by $\pm 2\sigma_{\ln RMW}$. The modeled range reflects the reduction in $\sigma_{\ln RMW}$ as a function of Δp .

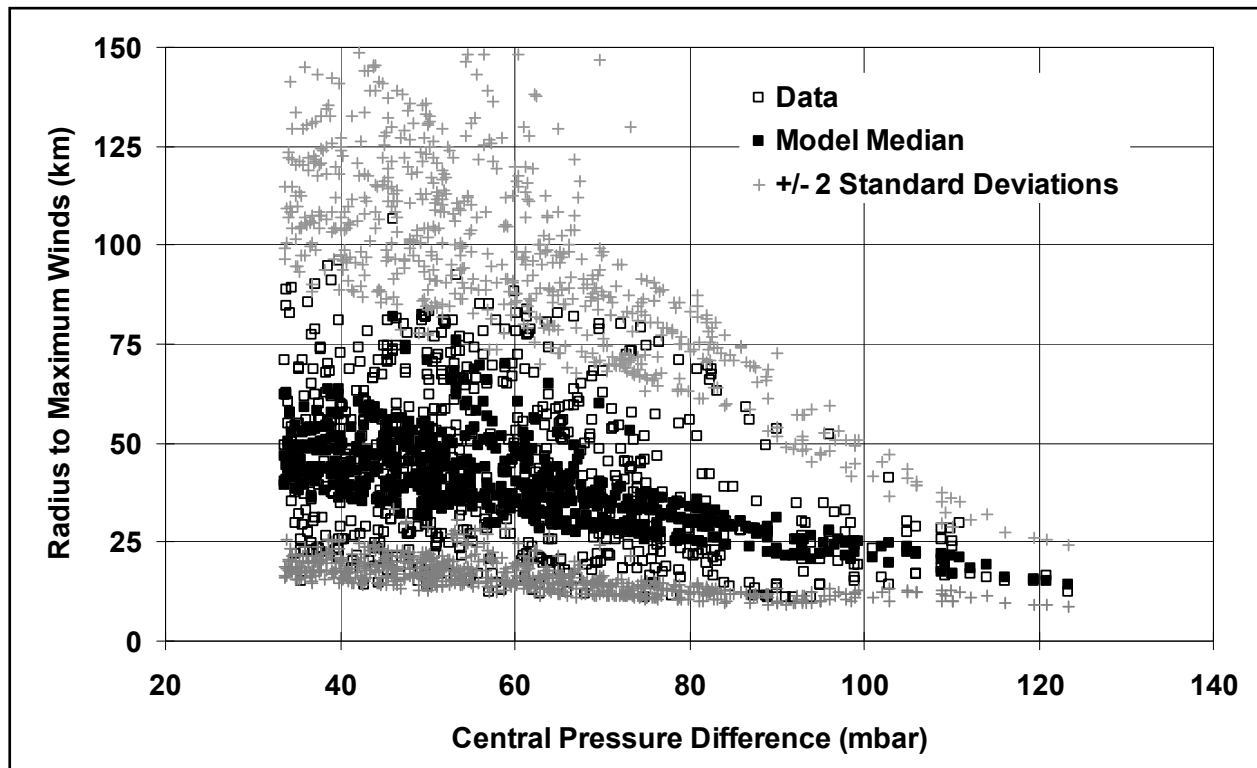


Figure 7. Modeled and observed RMW vs. Δp for all hurricanes

Gulf of Mexico Hurricanes. In order to determine if the characteristics of the RMW associated with the Gulf of Mexico storms differed from that obtained using the all storm data, the $RMW - \Delta p$ and $RMW - \psi$ relationships were re-examined. For this analysis the Gulf of Mexico storms included all hurricanes west of $81^\circ W$ and north of $18^\circ N$. The RMW for all storms (flight level data plus H*Wind data) in the Gulf of Mexico data set with central pressures less than 980 mbar were modeled as a function of central pressure difference in the form:

$$\ln(RMW) = 3.859 - 7.700 \times 10^{-5} \Delta p^2 \quad r^2=0.290, \sigma_{\ln RMW} = 0.390 \quad (6)$$

The *RMW* was found to be independent of latitude. As in the all storm case, the model error reduces with increasing Δp , as indicated in Figure 8.

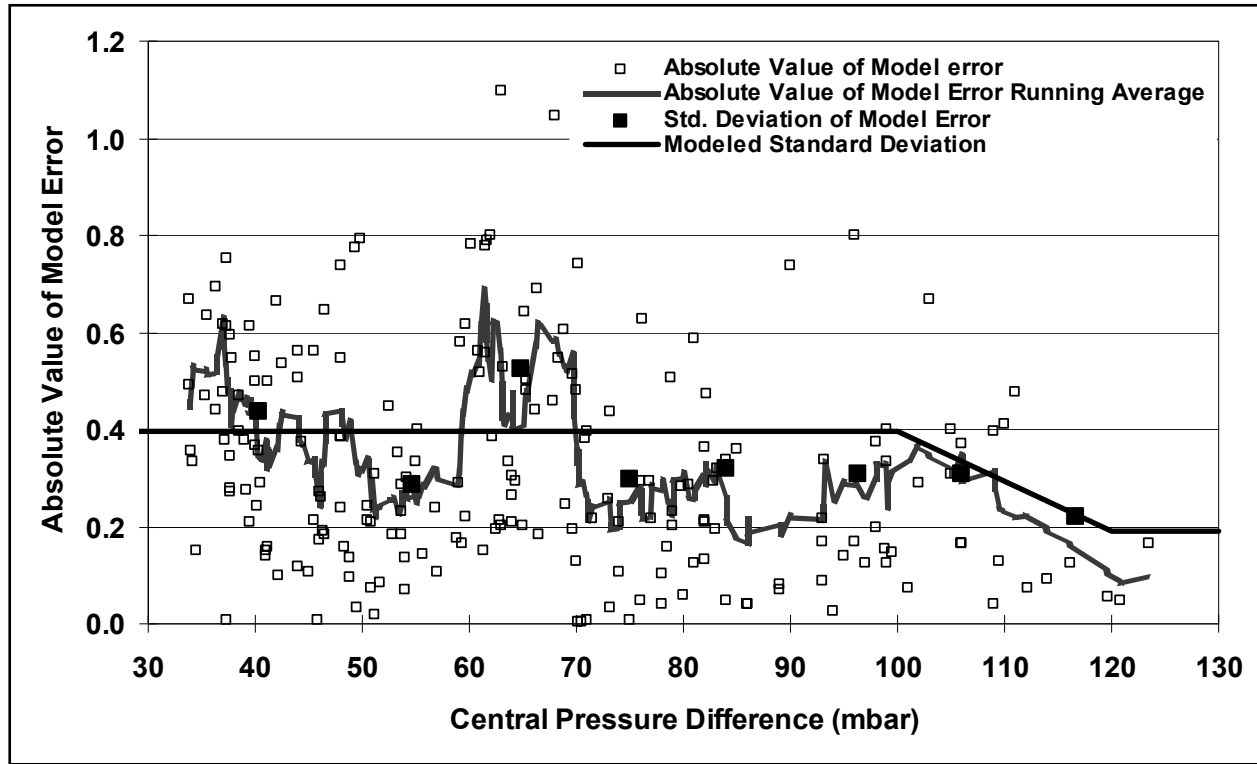


Figure 8. Absolute value of *RMW* model error vs. Δp for Gulf of Mexico hurricanes

The error, $\sigma_{\ln RMW}$, for Gulf of Mexico hurricanes is modeled in the form:

$$\sigma_{\ln RMW} = 0.396 \quad \Delta p \leq 100 \text{ mbar} \quad (7a)$$

$$\sigma_{\ln RMW} = 1.424 - 0.01029\Delta p \quad 100 \text{ mbar} \leq \Delta p \leq 120 \text{ mbar} \quad (7b)$$

$$\sigma_{\ln RMW} = 0.19 \quad \Delta p > 120 \text{ mbar} \quad (7c)$$

Figure 9 presents the modeled and observed values of *RMW* plotted vs. Δp for the Gulf of Mexico hurricanes. The modeled data are given as the median estimates and the range defined by $\pm 2\sigma_{\ln RMW}$. The modeled range reflects the reduction in $\sigma_{\ln RMW}$ as a function of Δp .

Figure 10 presents the median values of the *RMW* computed using Equation 4 (all hurricane *RMW* model) computed for latitudes of 25°N (Southern Gulf of Mexico) and 30°N (Northern Gulf of Mexico), where it is seen that for the Northern Gulf of Mexico storms, the all hurricanes *RMW* model over estimates the size of the Gulf of Mexico hurricanes, indicating that Gulf of Mexico hurricanes, are smaller than Atlantic hurricanes.

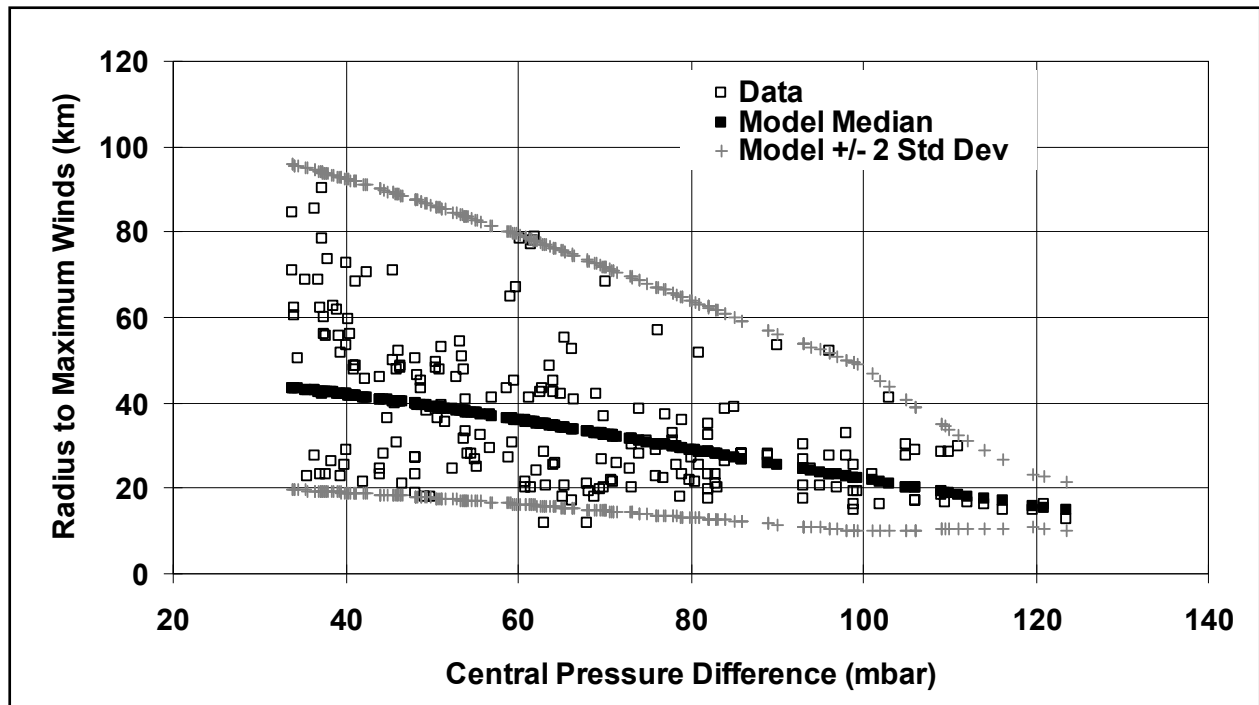


Figure 9. Modeled and observed *RMW* vs. Δp for Gulf of Mexico hurricanes.

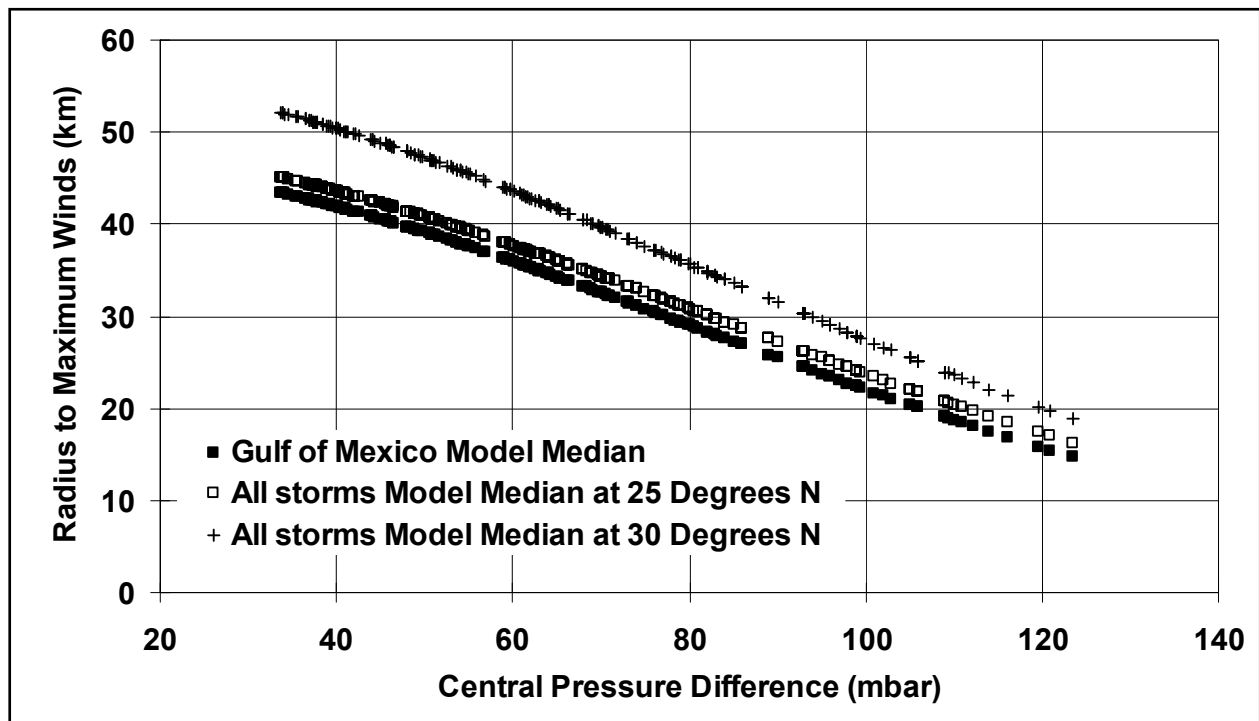


Figure 10. Comparison of all hurricanes model predicted median *RMW* to Gulf of Mexico model median *RMW*.

***RMW* for Landfalling Storms**

Figure 11 presents the values of the *RMW* for storms making landfall along the Gulf and Atlantic coasts of the United States. In the case of Gulf Coast storms, no statistically significant correlation exists between the *RMW* and either latitude or Δp . In the case of hurricanes making landfall along the Atlantic coast, the *RMW* is positively correlated with latitude, and negatively correlated with the Δp^2 . As a group (i.e. both Atlantic and Gulf Coast landfalling hurricanes), the *RMW* is also positively correlated with latitude, and negatively correlated with the Δp^2 . Using only landfall values of *RMW* the following statistical models best define the relationship between *RMW*, Δp and latitude.

1. Gulf of Mexico landfalling hurricanes:

$$\ln(RMW) = 3.558 \quad \sigma_{\ln RMW} = 0.457 \quad (8a)$$

2. Atlantic Coast landfalling hurricanes:

$$\ln(RMW) = 2.556 - 5.963 \times 10^{-5} \Delta p^2 + 0.0458\psi; \quad r^2=0.336, \sigma_{\ln RMW} = 0.456 \quad (8b)$$

3. Gulf and Atlantic Coast landfalling hurricanes:

$$\ln(RMW) = 2.377 - 4.825 \times 10^{-5} \Delta p^2 + 0.0483\psi; \quad r^2=0.203, \sigma_{\ln RMW} = 0.457 \quad (8c)$$

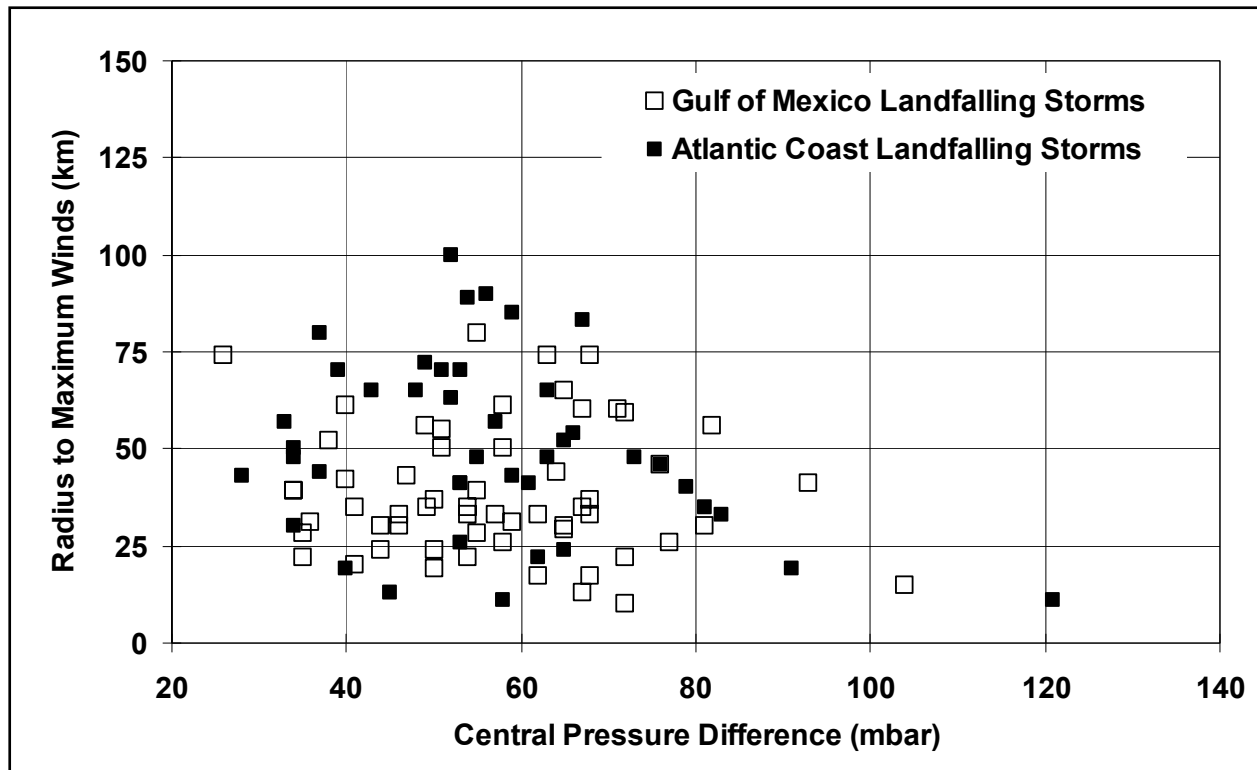


Figure 11. *RMW* for landfalling storms along the Gulf and Atlantic Coasts of the US

The ability of the *RMW* models developed using the flight level and H*Wind data (primarily open ocean data) to model the landfalling hurricane *RMW* was tested by computing the mean errors (in log space) and the resulting standard deviations and r^2 values using the landfall *RMW* data and the flight level/H*Wind derived *RMW* models. The error, $\mu_{\ln RMW}$, is defined as model *RMW* minus observed *RMW*, thus a mean positive error indicates the model overestimates the size of the landfalling hurricanes. The comparisons yield the following findings:

1. Gulf of Mexico landfalling hurricanes with GoM *RMW* model:

$$\mu_{\ln RMW} = 0.032 ; \quad r^2 = -0.008 \quad \sigma_{\ln RMW} = 0.459$$

2. Atlantic Coast landfalling hurricanes with the all hurricane *RMW* model:

$$\mu_{\ln RMW} = 0.058 ; \quad r^2 = 0.356 \quad \sigma_{\ln RMW} = 0.450$$

3. Gulf and Atlantic Coast landfalling hurricanes with the all hurricane *RMW* model for the Atlantic Coast and GoM *RMW* model for the Gulf Coast:

$$\mu_{\ln RMW} = 0.043 ; \quad r^2 = 0.219 \quad \sigma_{\ln RMW} = 0.453$$

A comparison of the model errors noted above to those resulting from the statistical analyses of the landfalling storms alone indicates that the models derived from the flight level and H^* Wind data can be used to define the characteristics of landfalling hurricanes. In the case of landfalling Gulf of Mexico hurricanes, the use of the GoM RMW model which contains the negative correlation between RMW and Δp^2 , is not statistically significantly different from the uncorrelated RMW - Δp relationship derived from the landfalling hurricanes alone. This observation suggests that there are an insufficient number of landfalling intense storms in the historical data to discern such a relationship.

Statistical Model for Holland's Parameter (B)

The B values computed as discussed above were found to be correlated to the radius to maximum winds, central pressure difference, latitude and sea surface temperature. Only points associated with central pressures of less than 980 mbar are included in the analysis. Figure 12 presents the variation of B as separate linear functions of the RMW , Δp , latitude (ψ) and the mean sea surface temperature T_s . It is clear from the data presented in Figure 12 that B decreases with increasing RMW and increasing latitude. A weak positive correlation of B with Δp is seen as is a weak positive correlation with sea surface temperature.

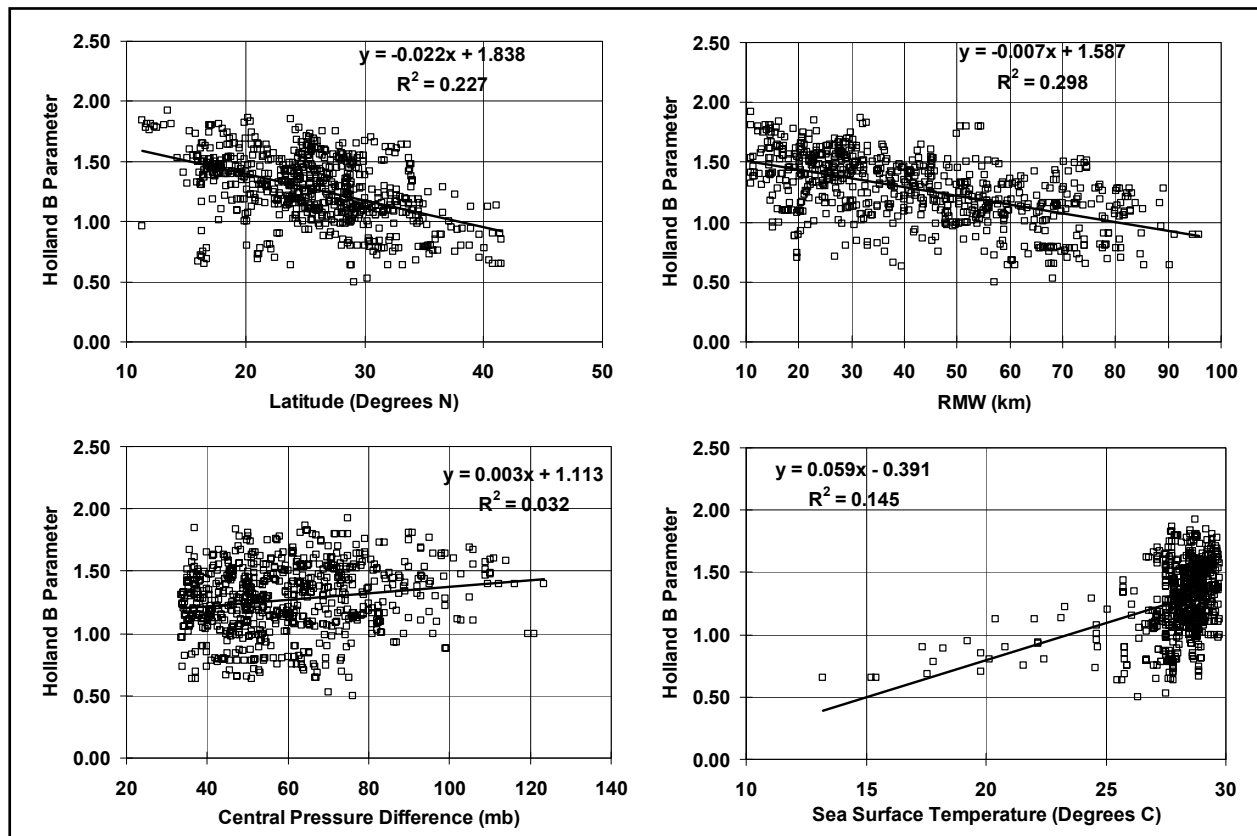


Figure 12. Relationships between the Holland B parameter, latitude, RMW , Δp , and T_s

In order to incorporate the effects of RMW , Δp , latitude (ψ) and T_s into a single model, new non-dimensional variable, A , was developed defined as:

$$A = \frac{RMW \cdot f_c}{\sqrt{2R_d T_s \cdot \ln\left(1 + \frac{\Delta p}{P_c \cdot e}\right)}} \quad (9)$$

The numerator of A is the product of the RMW (in meters) and the Coriolis force, defined as $2\Omega \sin\phi$ and represents the contribution to angular velocity associated with the coriolis force. The denominator of A is an estimate of the maximum potential intensity of a hurricane. From Emanuel (1988), the maximum wind speed in a tropical cyclone is:

$$V_{\max} = \sqrt{2R_d T_s \ln\left[\frac{p_{\max}}{p_c}\right]} \quad (10)$$

where V_{\max} is the maximum wind speed, R_d is the gas constant for dry air, p_{\max} is the pressure at $r=RMW$, T_s is the sea surface temperature in degrees K and p_c is the pressure at the storm center.

Using Holland's Equation it can be shown that

$$\frac{p_{\max}}{p_c} = 1 + \frac{\Delta p}{p_c e} \quad (11)$$

Hence, both the numerator and denominator of A have the units of velocity, and thus A , is non-dimensional. Modeling B as a function of the square root of A yields a linear model (Figure 13) with B negatively correlated with \sqrt{A} and has an r^2 of 0.34, with a the standard deviation of the error equal to 0.225. The relationship between B and \sqrt{A} is expressed as:

$$B = 1.732 - 2.237\sqrt{A}; \quad r^2=0.336, \sigma_B = 0.225 \quad (12)$$

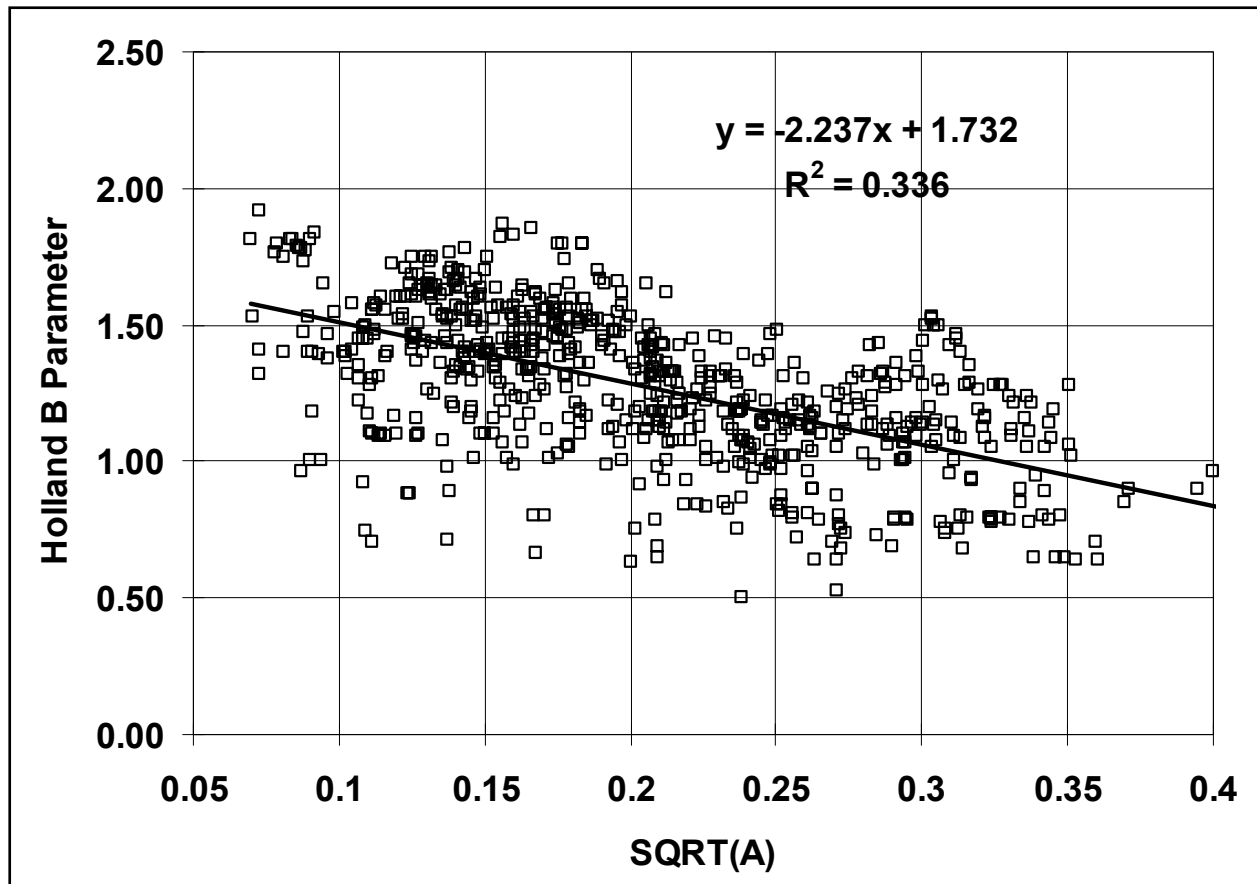


Figure 13. Relationship between the Holland B parameter dimensionless parameter, A .

In order to determine if the relationship between B and A is valid for intense storms, the point values of B and the model values of B were plotted as a function of RMW for strong hurricanes (i.e. storms with a central pressure of < 930 mbar) as shown in Figure 14. The data presented in Figure 14 indicates that in the case of strong storms with large RMW ($RMW > 40$ km) the relationship between B and A described earlier breaks down, with the true values of B being less than those predicted by the model. Although only two storms with large RMW and low central pressures exist in the data analyzed (Hurricane Katrina in the Gulf of Mexico and Hurricane Floyd in the Atlantic), the data indicate that the likelihood of a storm with a central pressure less than 930 mbar, a RMW greater than 40 km, combined with a B value greater than about 1.1 is remote. The mean value of B for these large, strong hurricanes is 1.01, and the estimated standard deviation is 0.082. In cases where these strong storms are simulated, B should be constrained to lie within the range of 0.85 to 1.18 (i.e. mean $\pm 2\sigma$).

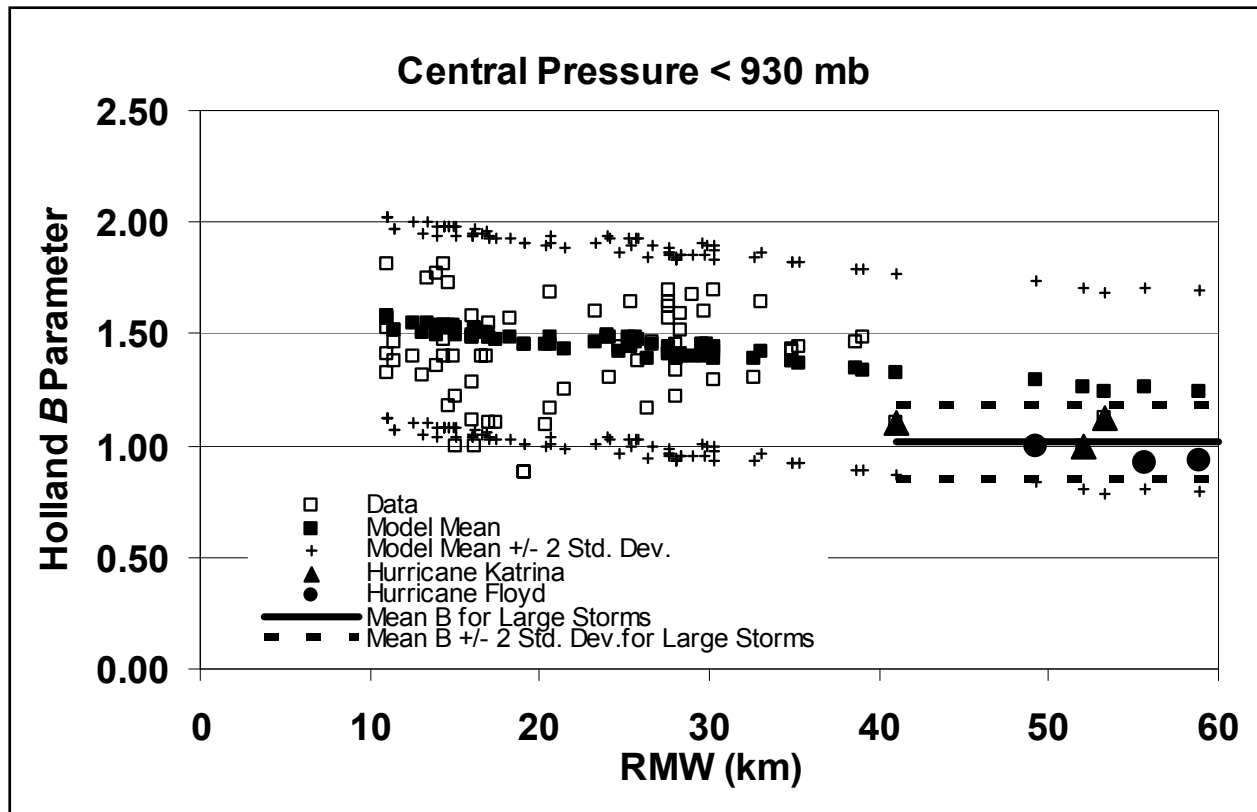


Figure 14. Holland B parameter vs. RMW for storms with central pressure < 930 mbar

As in the case of the analysis of Gulf of Mexico (GoM) hurricanes with respect to the behavior of RMW with Δp and latitude, B values for all hurricanes within the Gulf of Mexico were extracted and analyzed alone. Unlike the results seen for the RMW where the GoM hurricanes were found to be smaller than the other hurricanes, the variation of B with A for the GoM hurricanes is essentially identical to that seen in the all hurricane case. Figure 15 presents the individual B values for the GoM and Atlantic hurricanes along with the model predicted mean values of B where it is clearly evident that there is, for practical purposes, no difference in the variation of B with A between the two regions.

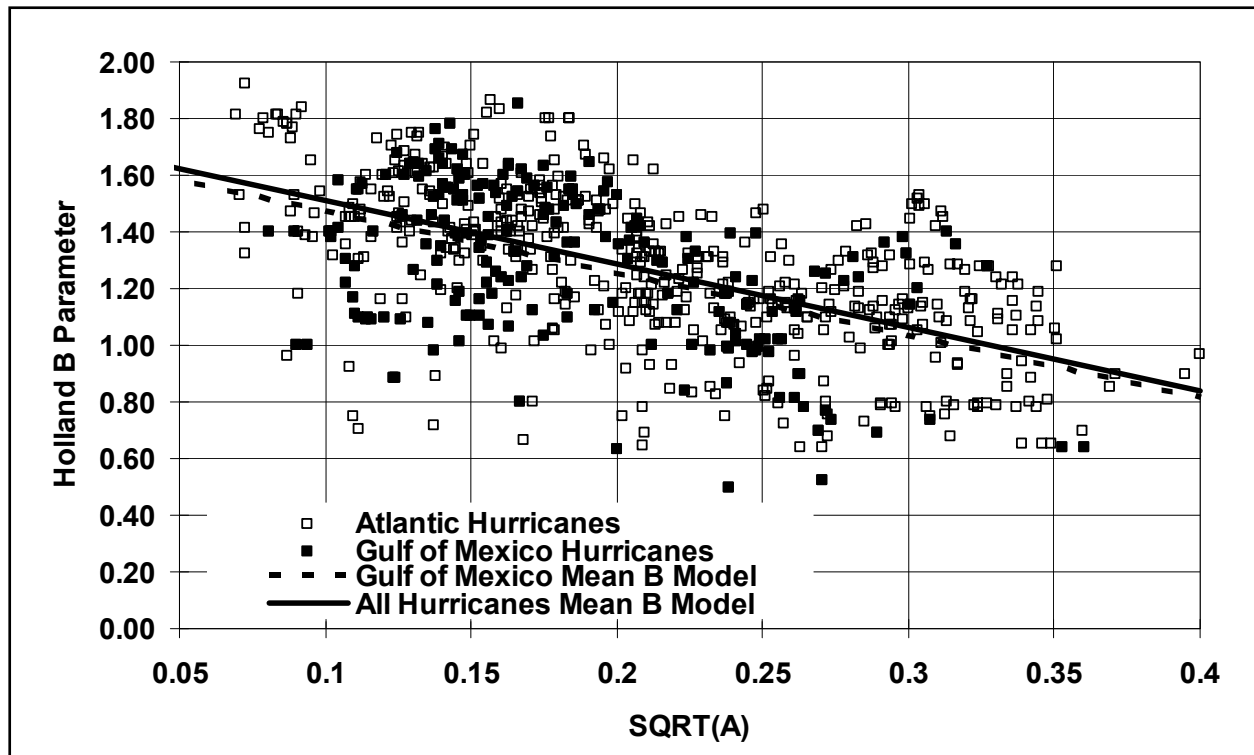


Figure 15. Relationship between the Holland B parameter and the dimensionless parameter, A , comparing the all hurricane data with the GoM hurricane data.

Note that two simpler, but less elegant models, relating B with RMW and latitude were examined modeling B as a function of $f_c RMW$ and B as a function of \sqrt{C} , where C is defined as:

$$C = \frac{RMW \cdot \sin \psi}{\sqrt{T_s \cdot \ln \left(1 + \frac{\Delta p}{P_c \cdot e} \right)}} \quad (13)$$

Where in Equation (13) T_s is expressed in degrees C rather than degrees K.

The regression model relating B to \sqrt{C} is given in the form:

$$B = 1.756 - 0.194\sqrt{C}; \quad r^2=0.368, \sigma_B = 0.220 \quad (14)$$

The regression model relating B to $f_c RMW$ is given in the form:

$$B = 1.793 - 0.326\sqrt{f_c RMW}; \quad r^2=0.357, \sigma_B = 0.221 \quad (15)$$

Both of these models yield marginally improved r^2 values than does the model relating B to the non-dimensional relative intensity parameter, but have the small disadvantage in that the independent variable is not non-dimensional. The limitations of these models when applied to large intense storms are the same as those evident in the case of the non-dimensional model. The reduction the r^2 value seen when changing the independent variable in the non-dimensional parameter given in Equation (9) to the dimensional parameter given in Equation (13) is due solely to the conversion of the sea surface temperature from degrees C (Equation 13) to degrees K (Equation 9). For practical purpose, any of the three linear regression models given in Equations 12, 14 or 15 can be used to model the Holland B parameter, with Equation 15 requiring the least computational effort.

Comparisons of Flight Level B Values with Landfall Analysis B Values

Figure 16 presents a comparison of the Holland B parameters derived from the flight level data to those used in the wind field model described in Vickery, et al. (2007) used for estimating the wind speeds associated with land falling storms. Overall, the comparisons indicate that the two values of B are similar, with the B values used within the windfield model in post storm analyses being slightly lower than those derived from the flight level data. The largest difference between the two estimates of the Holland B parameter occurs in the case of Hurricane Erin for the landfall along the Florida Panhandle.

Figure 17 presents the same information as Figure 16, but is limited to hurricanes with central pressures of 964 mbar or less. The comparisons indicate that the B values used within the hurricane wind field model to match the surface observations of wind speeds and pressures is about 7% less than those derived from the flight level data. This difference could be due to either changes in the characteristics of the pressure field between the 700 mbar level and the surface, or biases in the windfield model. Note that a 7% reduction in B corresponds to approximately a 3.5% reduction in the maximum modeled wind speed. However, comparisons of modeled and observed peak gust wind speeds and time series of the surface level pressures suggests that there is no such bias in the wind model.

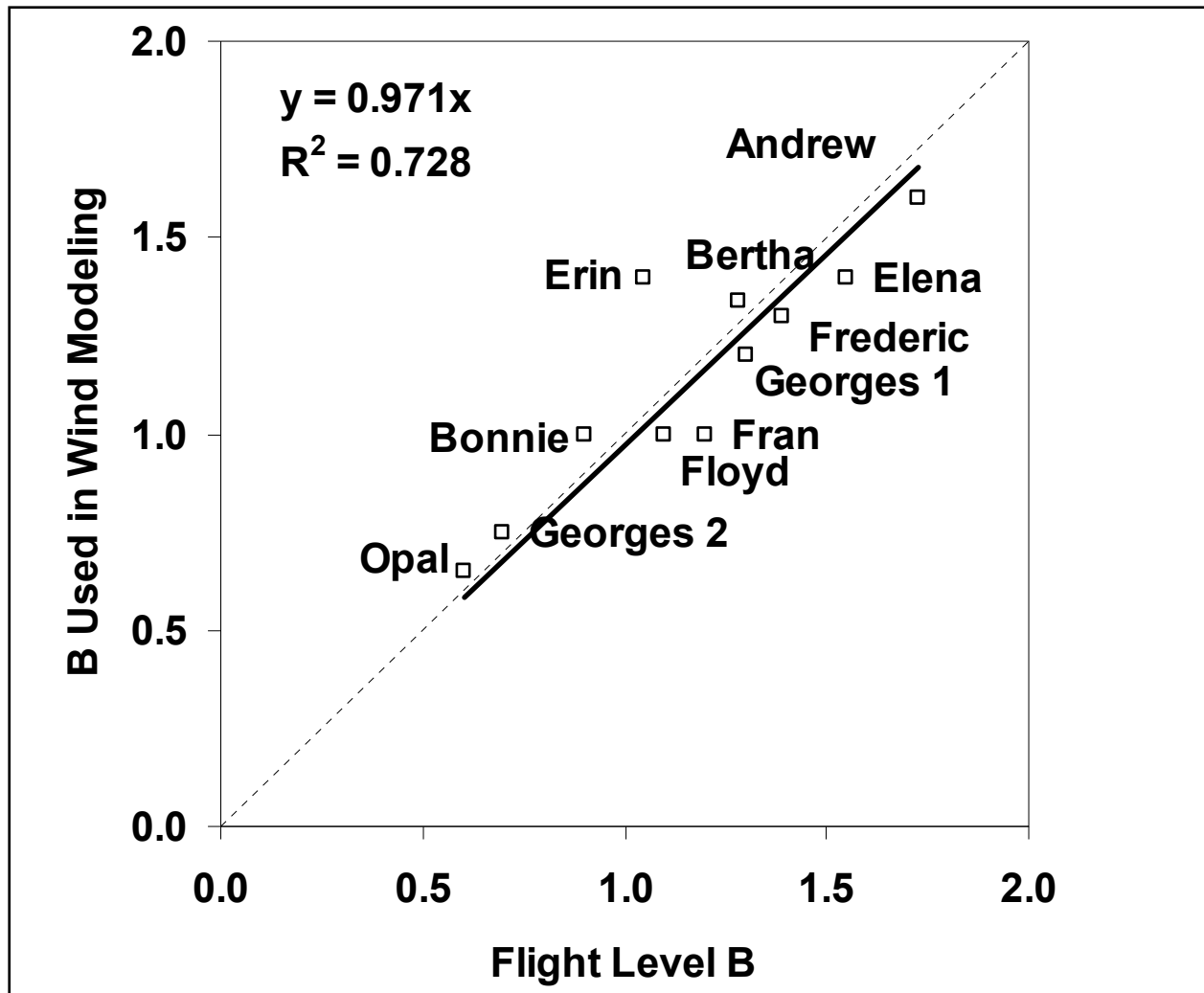


Figure 16. Comparison of Holland B parameters derived from flight level data to those derived using a post landfall windfield analysis.

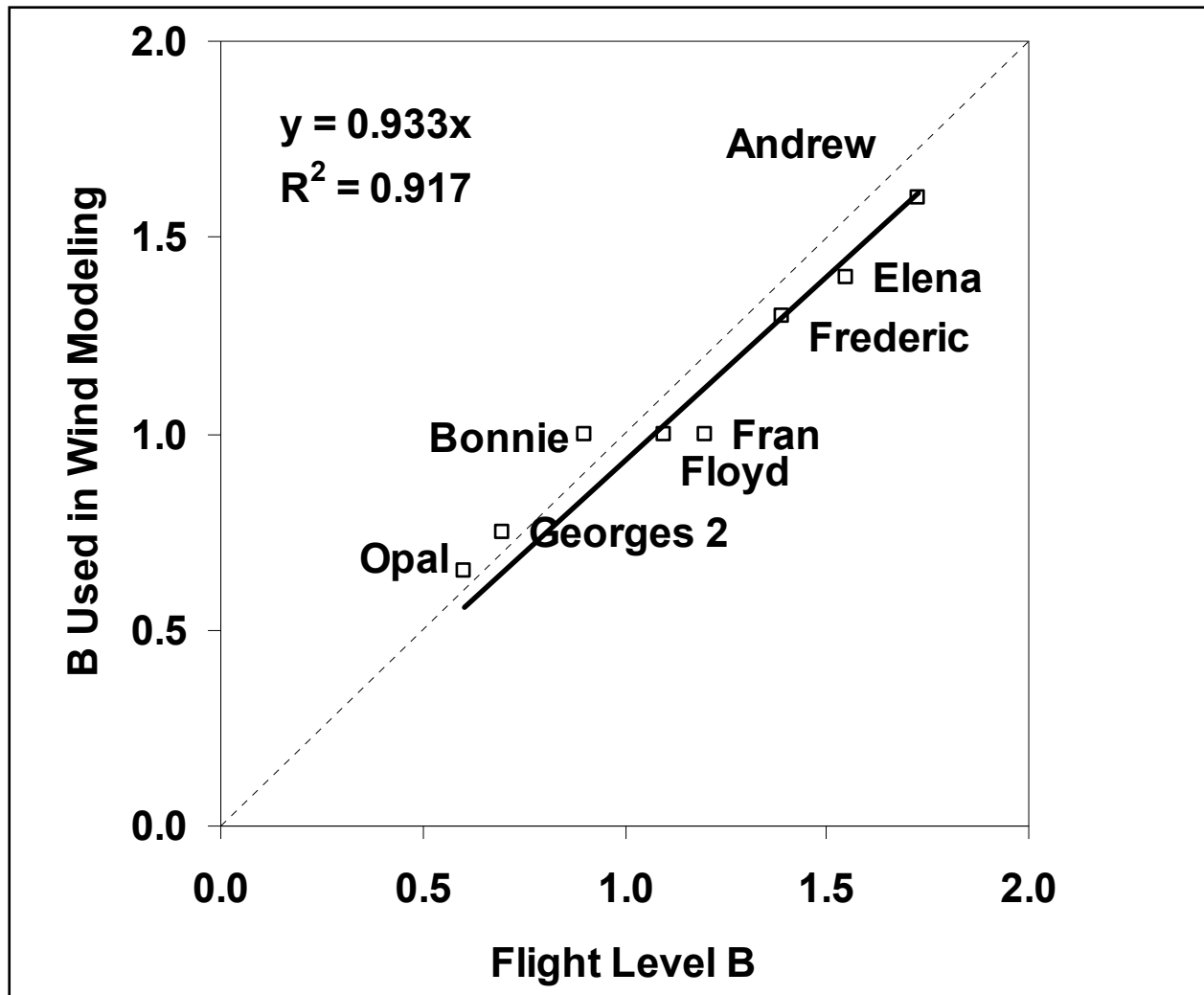


Figure 17. Comparison of Holland B parameters derived from flight level data to those derived using a post landfall windfield analysis for hurricanes with central pressures ≤ 964 mbar.

Summary

The Holland pressure profile parameter, B , was found to decrease with increasing latitude and increase with decreasing RMW . A weak positive correlation between B and both Δp and sea surface temperature was also observed. The effect of all four of these parameters was accounted for by defining a new non-dimensional parameter, A , defined by Equation 12, however; a two parameter model (with dimensions) relating B to the RMW and the coriolis parameter is an equally good predictor of B .

The limited data for large (as defined by RMW) hurricanes, having low central pressures ($p_c < 930$ mbar) indicates that B has an upper limit of ~ 1.2 . The relationship between B and A was found to be the same in the Atlantic Basin and in the Gulf of Mexico.

A qualitative examination of the characteristics of intense hurricanes making landfall along the coast of the Gulf of Mexico (excluding Southwest Florida) suggests that these hurricanes

weaken in the last 6 – 24 hours, with this weakening characterized by an increase in the central pressure, and increase in the radius to maximum winds and a decrease in the Holland B parameter. The reason for this weakening is beyond the scope of this investigation.

The few cases where flight level data were available up to the time a hurricane makes landfall indicates that in most cases, B , tends to decrease as the hurricane approaches land. Recognizing that the data set is limited, this observation suggests that using the statistical model for B derived using open ocean (or open Gulf) data may result in an overestimate of B for landfalling storms. This potential overestimate of the magnitude of the Holland B parameter along the Gulf Coast associated with the use of a statistical model developed using open water hurricane data may be further exaggerated because of the decrease in the Holland B parameter just before landfall observed in the limited number of landfalling cases examined.

Appendix F of R2007 Integration Method

There are several ways that one could approach the integration of the storm probabilities within the JPM. Each of these can be justified under a particular set of assumptions. Three of these will be discussed here; but before we proceed to examine these, a brief overview of the integration procedure is in order.

The integration is performed by summing discretized probabilities to approximate equation 6 in the main text of this white paper (with ε now included within the same probability function as the other five parameters), i.e.

$$F(\eta) = \sum \sum \dots \sum p(c_p, R_{\max}, v_f, \theta_l, x, \varepsilon) H[\Psi(c_p, R_{\max}, v_f, \theta_l, x) - \eta + \varepsilon] \Delta(c_p, R_{\max}, v_f, \theta_l, x, \varepsilon)$$

where

$F(\eta)$ is the CDF for surge levels (η)

$p(c_p, R_{\max}, v_f, \theta_l, x, \varepsilon)$ is the probability density function for the multivariate set of parameters;

$H[z]$ is the Heaviside function (=1 if $z \geq 0$, = 0, otherwise);

$\Psi(c_p, R_{\max}, v_f, \theta_l, x)$ is the result of the numerical simulation for a particular parameter combination;

$\Delta(c_p, R_{\max}, v_f, \theta_l, x, \varepsilon)$ is the increment of parameter space encapsulated within a discretization.

F1.

There are three primary aspects of this equation that contribute to the accuracy of approximations to $F(\eta)$:

1. The accuracy in the specification of $p(c_p, R_{\max}, v_f, \theta_l, x, \varepsilon)$;
2. The accuracy in the numerical simulations, $\Psi(c_p, R_{\max}, v_f, \theta_l, x)$; and
3. The influence of the discretization size on the approximation.

The first two of these are fairly intuitive, but the third is often more difficult to explain and quantify, since the size of the discrete increments required for a given accuracy is dependent on the behavior of the probability function itself. We shall now proceed to examine three approaches to the integration.

1. The Case of Simple Models Combined with Many Simulations

One approach to estimating coastal hazards would be to utilize simple models with many, many simulations. In this context, one could discretize the each parameter in the hurricane parameterization considered here ($c_p, R_{\max}, v_f, \theta_l, x$) and even add some additional probabilistic attributes to the storms (for example: variations in the Holland B parameter, variable storm decay during approach to the coast, suite of variations in offshore storm tracks associated with

each landfalling storm, etc.). Given n parameters with m categories used to represent each parameter, n^m simulations would be required in this approach. For example, for the five-dimensional representation, with 5 categories in each parameter, 3125 simulations would be required to populate the JPM integral.

This approach would produce a very accurate discretization of the probability function; however, inaccuracies in the simulations do not vanish by simply increasing the number of simulations. For example, if simplified models predict values that are 30% too high or too low at a given point along the coast for the portion of the parameter space that contains the primary contribution to surges at the $1 - F(\eta) = 0.01$ level (the range of the nominal “100-year” surge event), no increase in the number of simulations will converge to the correct answer for this range, nor will the addition of uncertainty make the error vanish.

For the case of wind fields, Vickery *et al.* (2002) have shown that a parametric wind field approach, which includes physical effects captured within an accurate planetary boundary layer model, can provide reasonable representations of wind speeds in coastal areas. This method also allows many simulations to be run and, therefore, represents a good application of this type of approach. Coastal surge generation requires that wave fields, direct wind-driven surges, and the interaction between these two driving mechanisms be modeled correctly. Parametric wave models for hurricanes have been known to be quite inaccurate for a number of years and are not used by any major wave modeling group in the world today, even in offshore areas. In nearshore areas, refraction, wave breaking, sheltering and other physical mechanisms cannot be captured by parametric models. Also, surge models such as ADCIRC include much improved capabilities for depicting critical shallow-water physics and for representing small-scale coastal features. Because of this, the methodology described in the main text, which relies on state of the art models to ensure unbiased estimates of coastal surges is recommended; however, it is practical limitations related to computer run time (even on the largest supercomputers available today) presently preclude the execution of multiple thousands of runs using this complete prediction system.

2. The Case of Optimized Category Definition

Given that *a priori* information is available for the variation and co-variation of the variables used in the probability function, as well as for the sensitivity of coastal surges to variations in each of the variables, it is possible to construct an optimized set of discrete samples to simulate surges from the overall multivariate distribution. This approach is presently under development by Toro for applications within FEMA Region 4. As shown in Figure 7c in the main text, Toro’s independent check on the pressure distribution used here showed very good agreement. Similarly, preliminary comparisons between the two statistical methods appear to show good agreement for JPM applications.

3. The Case of Structured Interpolation on a Response Surface

Numerical studies using ADCIRC have shown that coastal surge response is very dependent on pressure differential (peripheral pressure minus central pressure), storm size (R_{\max}), and storm

location relative to a site, as discussed in Appendix D. Storm surge is less sensitive to forward storm speed and angle of the storm relative to the coast. Figure F1 shows the characteristic variation of surge elevations at coastal stations as a function of variations in pressure differential ($p_0 - c_p$), based on SLOSH tests along the coast of Mississippi. As noted in Appendix B, the maximum wind speed in a slowly varying, stationary hurricane can be approximated as

$$U_{\max} = \left(\frac{B}{\rho_a e} \right)^{1/2} (\Delta P)^{1/2}$$

where

B is the Holland B parameter;

ρ_a is the density of air;

e is natural logarithm base (= 2.718...); and

ΔP is the pressure differential between the storm periphery and its center.

Since surges tend to be proportional to the wind stress, which for a capped coefficient of drag is proportional to the wind speed squared, it follows that the linear relationship between ΔP and surge is consistent with our theoretical expectation for this relationship.

Since a major portion of the surge response to hurricanes is captured by the variation of ΔP and R_p , the integration method selected for application here is based on the estimation of $\Delta P - R_p$ planes within the 5 dimensional parameter space used in the JPM. Thus, for a fixed value of storm landfall location (x), storm track angle relative to the coast (θ_l), and storm speed (v_f), we can define a response function,

$$\eta_{\max}(x, y) = \phi_{kmn}(\Delta P, R_p, x, y) \tag{F2}$$

where ϕ_{kmn} is the surge response function and the subscripts “k, m and n” denote a specific track angle, storm speed, and landfall location, respectively. This notation reflects the fact that this response function must be defined for each spatial (x, y) point in the computations. Figure F2 shows an example of such a response function. As expected, the surge values increase essentially linearly with increasing pressure differential and also increase with increasing values of R_p .

Figures F3 and F4 show the characteristic variations of coastal surges as a function of storm angle relative to the coast (θ_l) and forward storm speed (v_f), respectively. As can be seen here, the variations tend to be quite smooth with either linear or slightly curved slopes in these figures. The JPM integration method employed here makes use of the “smoothness” of these functions to interpolate between discretized storm parameters.

An advantage of the approach used here is that the surge response is characterized with some level of detail in the important $\Delta P - R_p$ plane. To drive the relevance of this point home, let us examine the effects of discretization on a probability integral along the “pressure-differential”

axis. Given the linear variation of surge elevation with pressure differential, surge elevation can be written as

$$\eta = \lambda \Delta p \tag{F3}$$

where λ is a site-specific constant, and hence

$$F(\eta) = F(\lambda \Delta p) \tag{F4}$$

If we assume that the pressure differential probability follows a Gumbel distribution, we can calculate this probability directly. Figure F5 shows a comparison of the CDF's for three different approximations to the return period as a function of surge level, given the value of $\lambda = 0.2$ in equation F4 (just for an example here). As can be seen in this figure, for a fixed return period deviations between the 3-category approximation (categories with a width of 30-millibars) and the continuous function can be as large as ± 3.0 feet. For the 3-millibar categories, the deviations are, as expected, only about ± 0.3 feet. Although this pattern will be smoothed and obscured by the addition of many categories of storms, it is clear that the smaller categories provide an improved representation for the probabilities. Also, due to the physical basis for the pressure differential scaling used here, we can extrapolate to larger storms than those actually utilized in the storms. This will provide a somewhat conservative estimate if there is substantial levee overtopping; but since the level of extrapolation used here is only about 18% ($\Delta P = 113$ mb to $\Delta P = 133$ mb), this should not present a serious problem.

In this approach, we do not treat the set of 9 storms simulated for a given track, forward storm speed, and track angle as a discrete set of storms each with its own associated probability increment, since this would give only a relatively crude representation of the actual probability structure. Instead, we interpolate between simulated values and extrapolate over relatively short distances in Δp and (R_{\max}). For the integration used in the New Orleans area, the 3 Δp and 3 R_{\max} values were interpolated to increments of 1-mile in R_{\max} and 3 millibars in Δp , over the range of 960 mb to 882 mb for offshore pressures (i.e. before they begin to decay) and 5 nm to 40 nm for R_{\max} values. This provides a very smooth response surface for the primary storm tracks in this area (the so-called RICK-fan tracks). For the ± 45 -degree tracks, the 2 values of Δp and R_{\max} are likewise used to develop a finely discretized (1 nm by 3 mb) set of values over the Δp - R_{\max} plane. At this point, we have finely discretized categorizations within the Δp - R_{\max} plane for the five primary (RICK-fan) tracks and the eight additional ± 45 -degree tracks. Thus, we have a set of response functions $[\varphi_{kmn}(\Delta P, R_p, x, y)]$ that are quite well defined for the central storm speed (11 knots) for these tracks.

Since the effect of variations in storm speed is fairly small and tends to have fairly linear slopes that are roughly independent of (R_{\max}) and Δp , only a small number of storms can be used to modify the functional form of $[\varphi_{kmn}(\Delta P, R_p, x, y)]$ as a function of forward storm speed. This retains the overall structure of the response function for the alternative speeds, rather than assigning only a single surge value to all the responses for that storm speed. For the New Orleans area, two storms (with different combinations of Δp and R_{\max}) were used to estimate the impact of a slower storm speed on the surge response function $[\varphi_{kmn}(\Delta P, R_p, x, y)]$ compared to the

primary (central) speed category (11 knots) for the RICK-fan set of tracks. Single storms were also used to estimate the impact of varying the forward speed from 11 knots to 6 knots, along the ± 45 -degree tracks and to estimate the effects of varying the forward speed from 11 knots to 17 knots for all storms. In the approach used here, the value of $[\phi_{kmn}(\Delta P, R_p, x, y)]$ for different speeds is obtained from the relationship

$$\phi_{kmn}(\Delta P, R_p, x, y) = \phi_{k_0 m_0 n}(\Delta P, R_p, x, y) \Psi_{kmn}(\Delta P, R_p, x, y)$$

where

The subscript "0" refers to the central speed and angle categories for a specific landfall location; and

$$\Psi_{kmn}(\Delta P, R_p, x, y) = \frac{\partial \phi_{kmn}(\Delta P, R_p, x, y)}{\partial v_f} \delta v_f$$

For the cases in which a single storm is used to infer the variation with forward speed $\Psi_{kmn}(\Delta P, R_p, x, y)$ reduces to a constant.

This now provides a suitable set of interpolated, finely-discretized values of surge heights as a function of Δp and R_{\max} for all forward storm speeds, storm angles and storm tracks and the summation in Equation F1 can be rewritten as

$$F(\eta) = \sum \sum \dots \sum p(\Delta p_i, R_{\max_j}, v_{f_k}, \theta_l, x_m, \varepsilon_n) H[\Lambda(\Delta p_i, R_{\max_j}, v_{f_k}, \theta_l, x_m) - \eta + \varepsilon] \Delta(\Delta p_i, R_{\max_j}, v_{f_k}, \theta_l, x_m, \varepsilon_n)$$

where

$F(\eta)$ is the CDF for surge levels (η)

$p(\Delta p_i, R_{\max_j}, v_{f_k}, \theta_l, x_m, \varepsilon_n)$ is the probability density function for the multivariate set of parameters;

$H[z]$ is the Heaviside function ($=1$ if $z \geq 0$, $=0$, otherwise);

$\Lambda(\Delta p_i, R_{\max_j}, v_{f_k}, \theta_l, x_m)$ is the interpolated value between simulations with a particular parameter combination;

$\Delta(\Delta p_i, R_{\max_j}, v_{f_k}, \theta_l, x_m, \varepsilon_n)$ is the increment of parameter space encapsulated within a discretized category.

One concern addressed briefly in Appendix D is the sensitivity of the probability estimates to track spacing. The sufficiency of the spacing used here can be investigated by comparing results from the runs on the set of tracks that fell between the 5 major RICK-fan tracks to results of interpolations based on only the 5 initial tracks. Figures F6-F9 show the results of these comparisons. In general little or no bias is introduced into the probability integration, even if only the information from the primary tracks is used. Only at Track 4a, where the sites are switching from the "right-hand" (onshore winds) side of the storm to the "left-hand" (offshore winds) side of the storm in the area east of the Mississippi River does the variability exceed 10% of the surge values for surges greater than 10 feet.

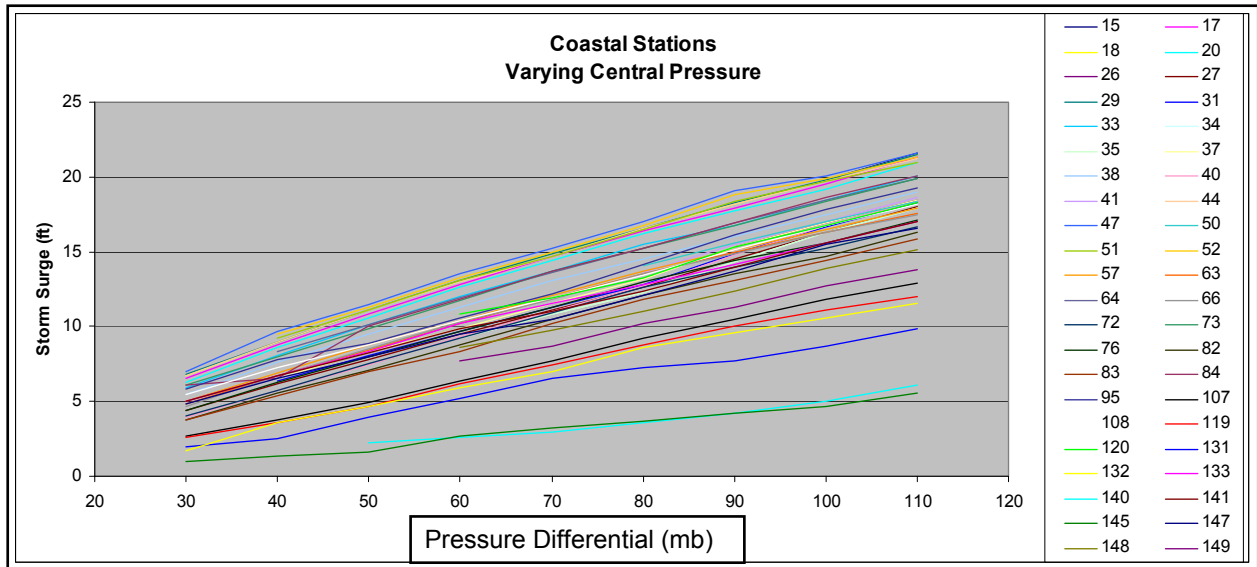


Figure F1. Surge levels (feet) at coastal stations (Station Numbers denoted on right hand side of chart) along Mississippi coast as a function of pressure differential (mb).

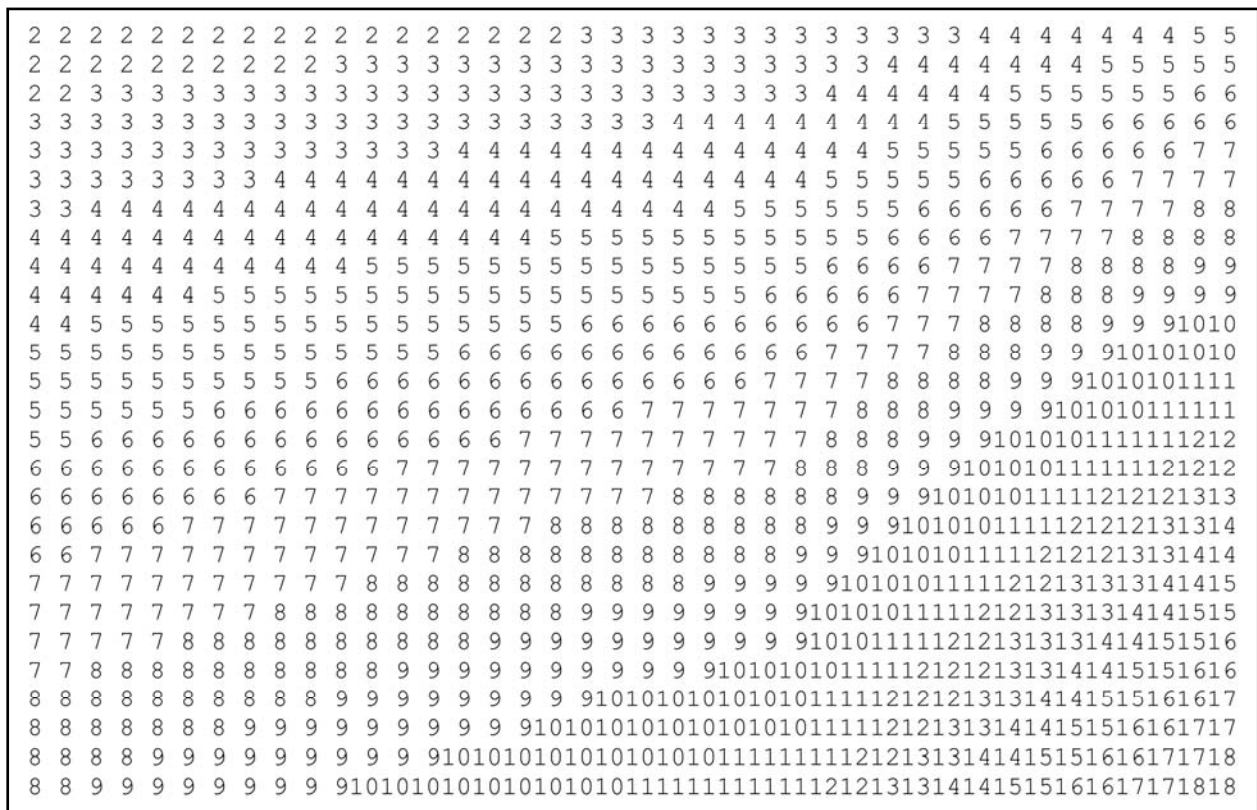


Figure F2. Response surface showing integerized surge values in feet as a function of row from top to bottom (ΔP from 53 to 133 mb in increments of 3 mb) and column from left to right (R_p from 1 nm to 40 nm in increments of 1 nm).

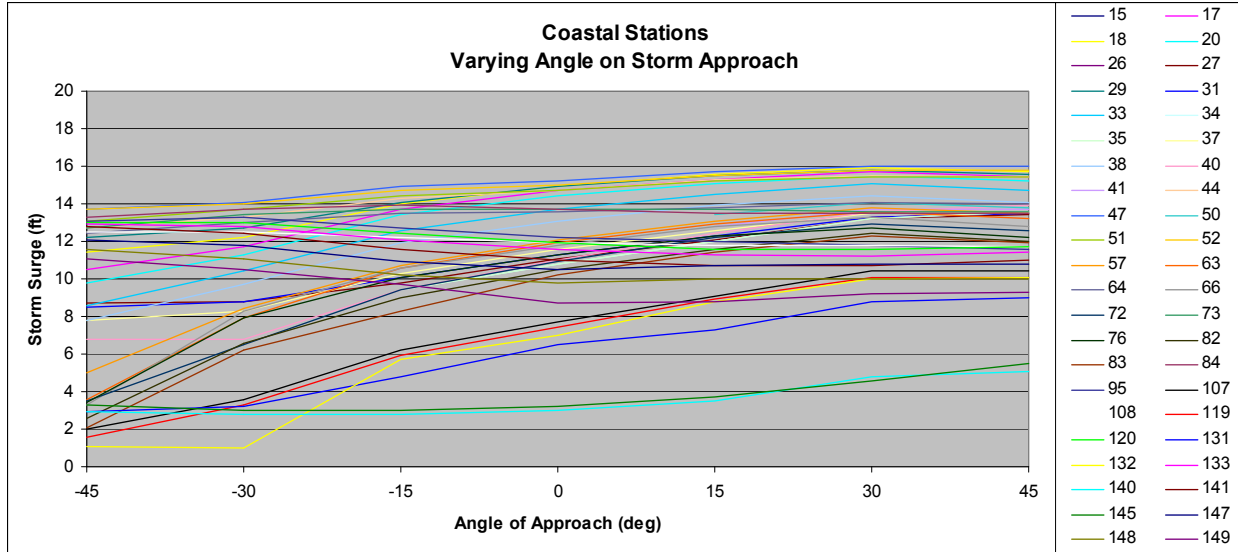


Figure F3. Surge levels (feet) at coastal stations (Station Numbers denoted on right hand side of chart) along Mississippi coast as a function of angle of storm approach to land.

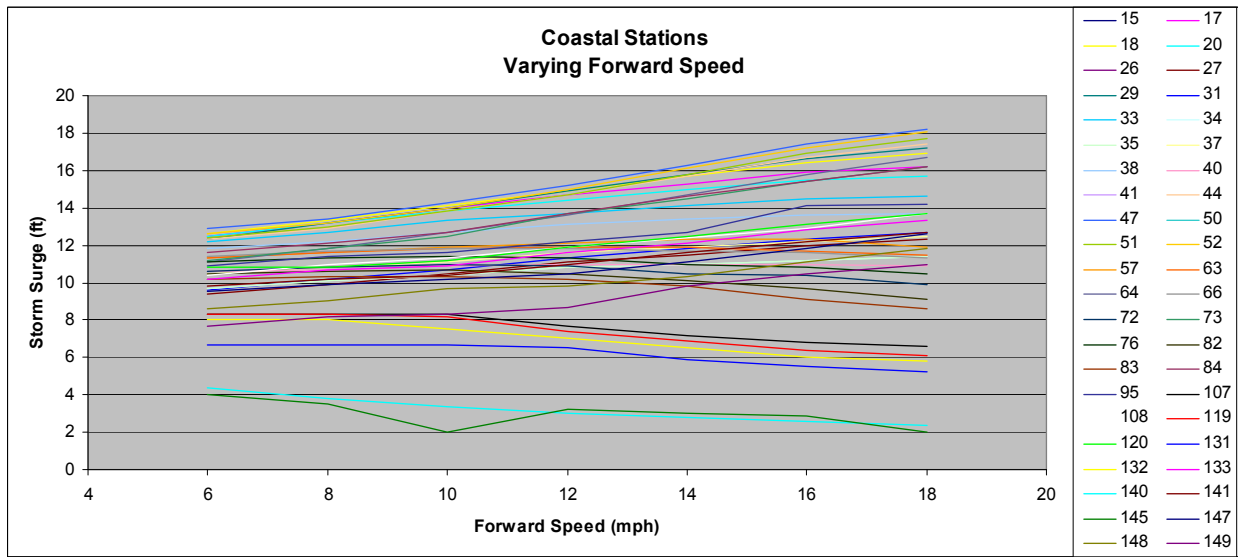


Figure F4. Surge levels (feet) at coastal stations (Station Numbers denoted on right hand side of chart) along Mississippi coast as a function of forward speed of storm (mph).

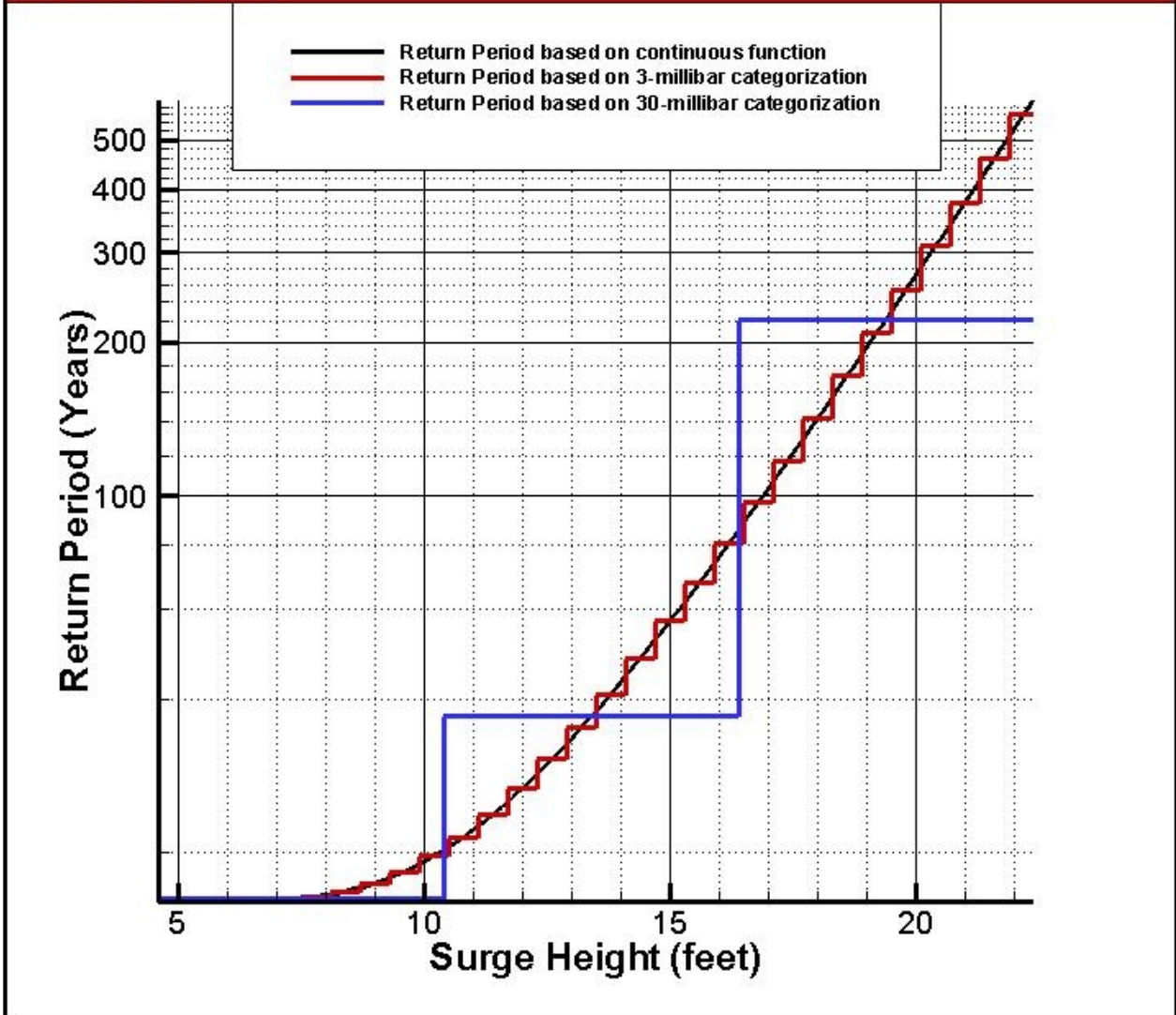


Figure F5. Comparison of Return Periods for surges estimated from 3-millibar and 30-millibar categories compared to a continuous function.

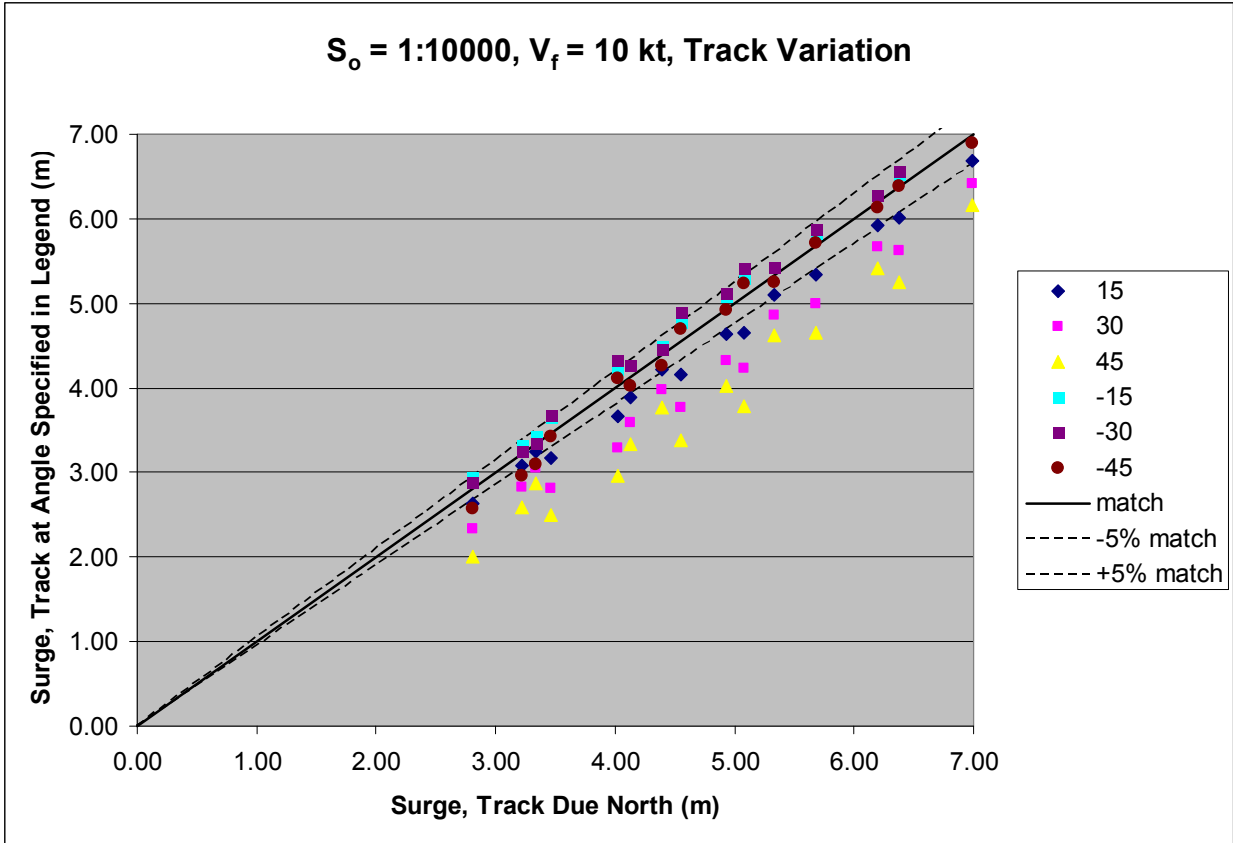


Figure F6. Maximum surges produced along a straight east-west coast by storms approaching the coast at variable angles compared to storms approaching perpendicular to the coast (tracking due north).

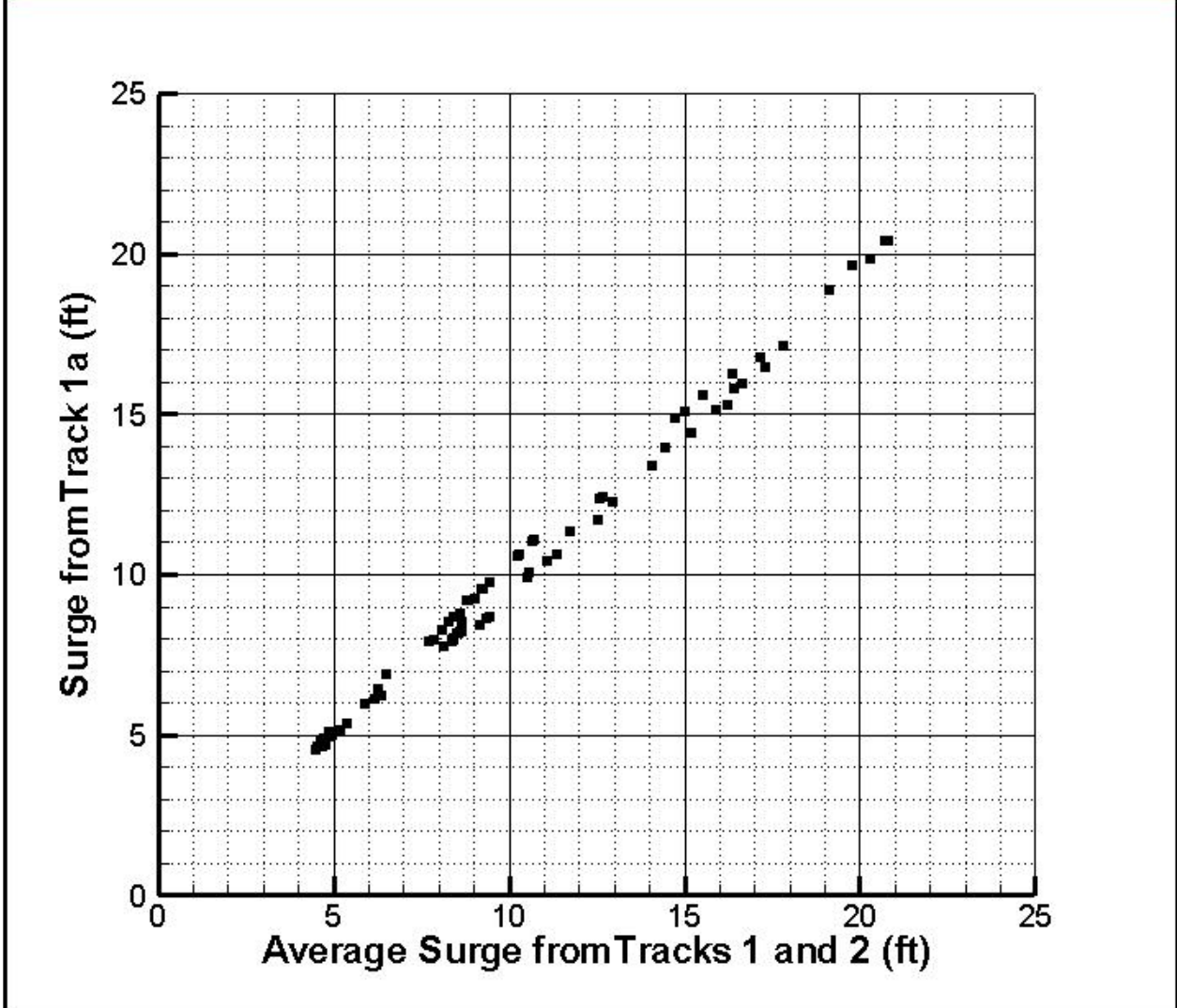


Figure F7. Comparison of results from Track 1a (midway between Tracks 1 and 2) to interpolated values using information from Tracks 1 and 2 for a set of points spread throughout the entire New Orleans region.

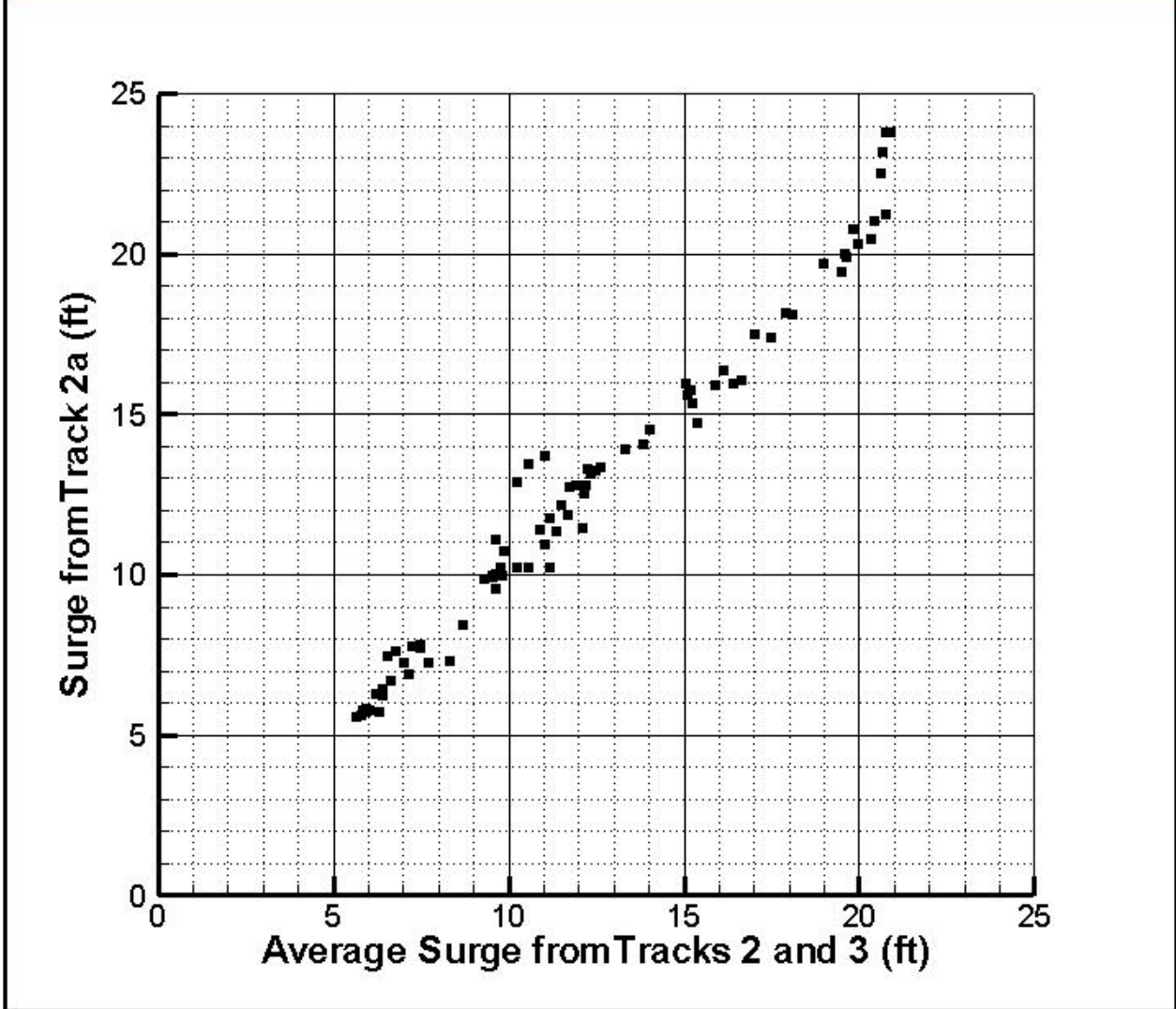


Figure F8. Comparison of results from Track 2a (midway between Tracks 2 and 3) to interpolated values using information from Tracks 2 and 3 for a set of points spread throughout the entire New Orleans region.

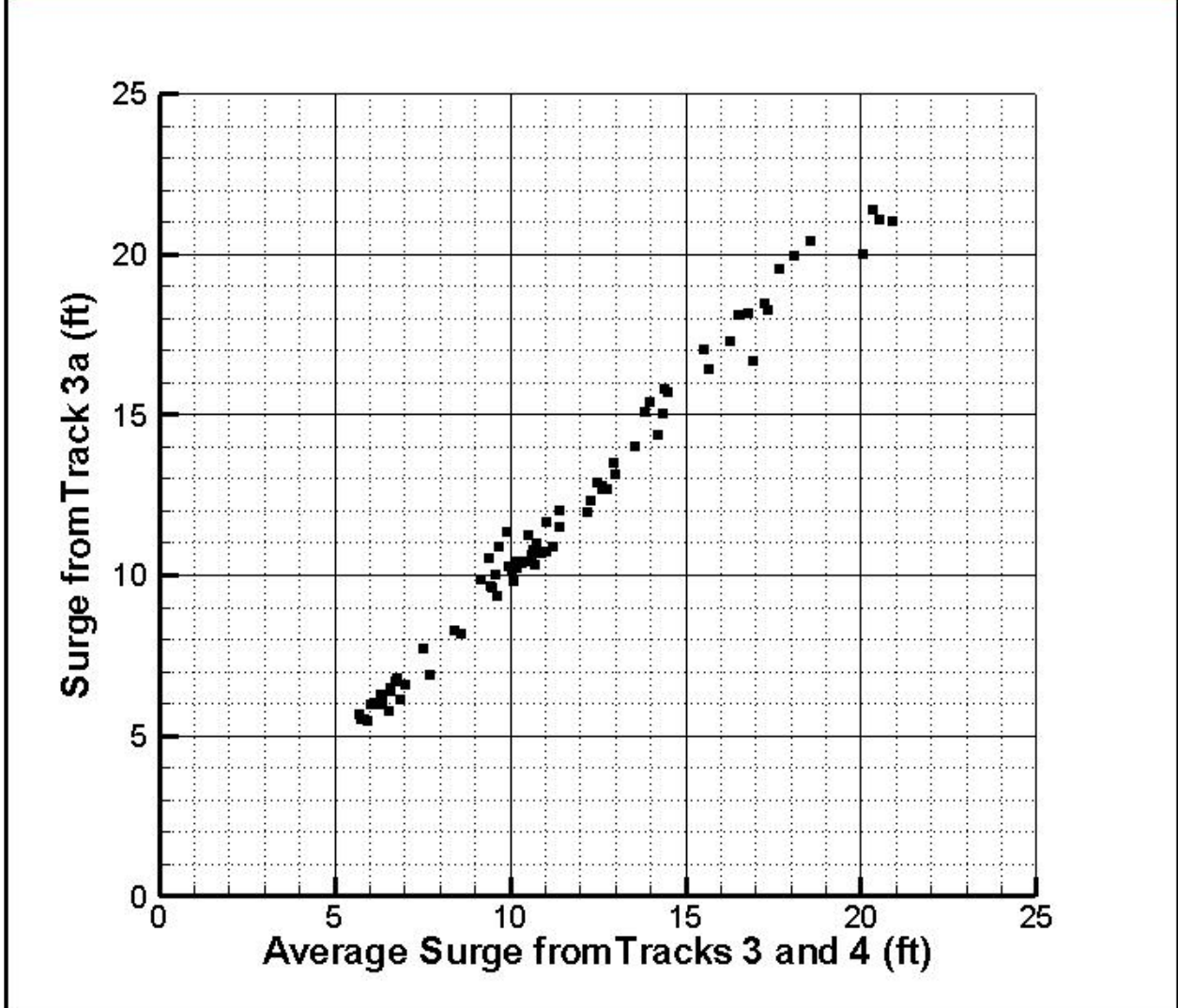


Figure F9. Comparison of results from Track 3a (midway between Tracks 3 and 4) to interpolated values using information from Tracks 3 and 4 for a set of points spread throughout the entire New Orleans region.

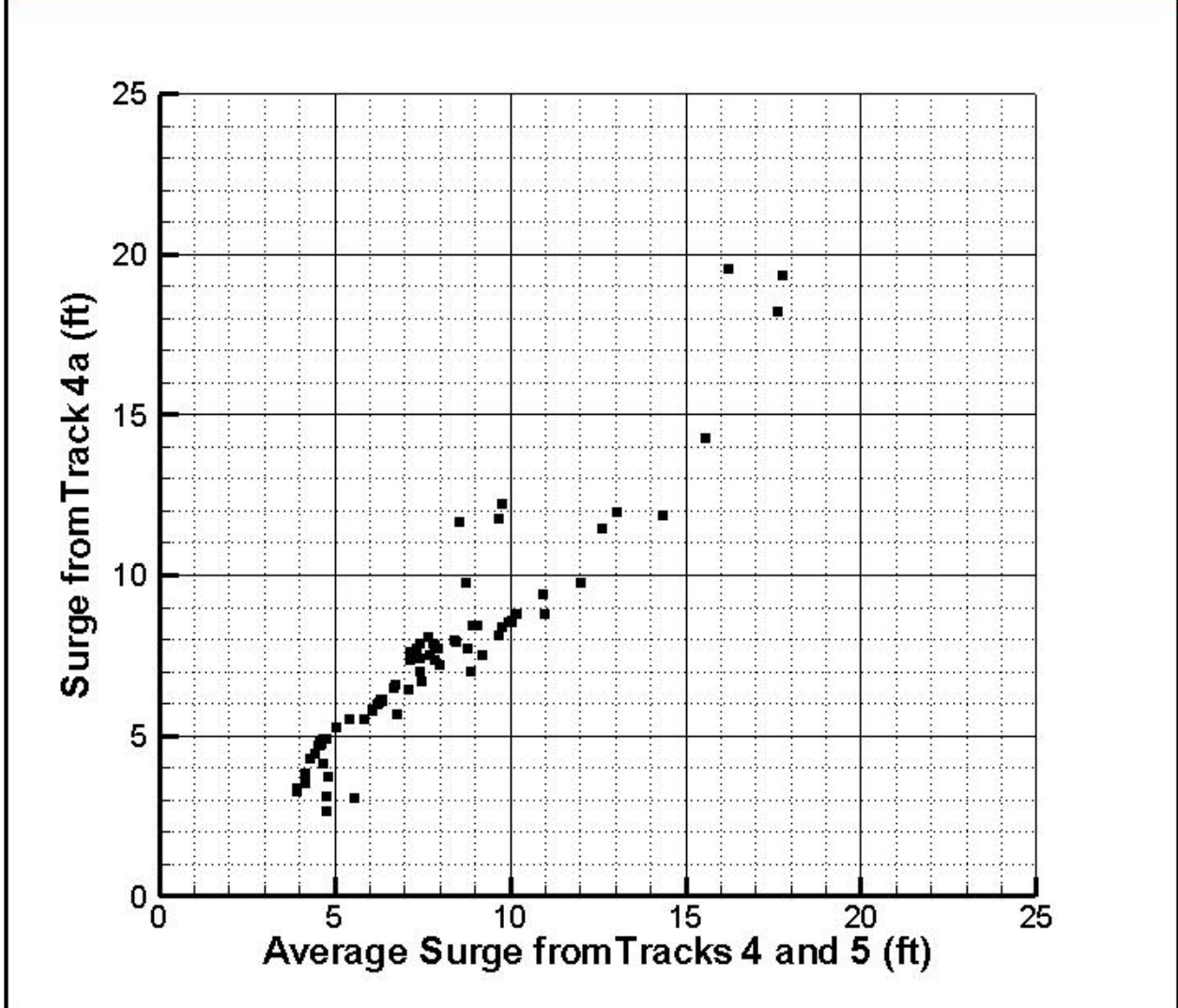


Figure F9. Comparison of results from Track 4a (midway between Tracks 4 and 5) to interpolated values using information from Tracks 4 and 5 for a set of points spread throughout the entire New Orleans region.

Appendix G of R2007

Estimation of Confidence Bands for Surge Estimates

Three main types of uncertainty with respect to the estimation of extremes are relevant to understanding hurricane hazards along coasts. First, there is uncertainty that the actual sample of storms is representative of the “true” climatology today. Second, there is uncertainty in the events within future intervals of time, even if the “true” climatology is known exactly. And, third, there is uncertainty that some non-stationary process (sea level rise, subsidence, climate change, new development patterns, man-made alterations to the coasts, marsh degradation, etc.) will affect future hazards. The first of these has traditionally been addressed via sampling theory. The second can be addressed via re-sampling or “bootstrap” methods. And, the third must be estimated from ancillary information, often not contained within the initial hazard estimates themselves.

The first type of uncertainty listed above pertains to what used to be termed confidence bands (or control curves) for estimates of extremes. It cannot be estimated using re-sampling techniques, since these techniques use the initial sample as the basis for their re-sampling and implicitly assume that the initial sample represents the actual population characteristics. Thus, some parametric method must be used to obtain this information. There are many classes of distributions which can be used to fit the data. Since we are only using the parametric fits to estimate uncertainty and not to replace the non-parametric estimates obtained from the JPM, we are somewhat free to use any distribution for which the sampling uncertainty is known. Gringorten (1962, 1963) has shown that the expected root-mean-square (rms) error of an estimated return period in a two-parameter Fisher-Tippett Type I (Gumbel, 1959) distribution is given by

G1.

$$\sigma_T = \sigma \sqrt{\frac{1.1000y^2 + 1.1396y + 1}{N}}$$

where

σ is the distribution standard deviation;

σ_T is the rms error at return period, T;

N is the number of samples used to estimate the distribution parameters; and

y is the reduced Gumbel variate given by

$$y = (\eta - a_0) / a_1;$$

η is the variate of interest (surge level in this case); and

a_0 and a_1 are the parameters of the Gumbel distribution.

The reduced variate and return period are related by

$$y = -\ln \left[\ln \left(\frac{T}{T-1} \right) \right] \quad \text{G2.}$$

which for $T > 7$ approaches an exponential form given by

$$\left(T - \frac{1}{2} \right) \rightarrow e^y \quad \text{G3.}$$

Equation G1 shows that the rms error at a fixed return period is related to the distribution standard deviation and the square root of a nondimensional factor involving the ratio of different powers of y (y^2 , y^1 , and y^0) to the number of samples used to define the parameters. By the method of moments, the Gumbel parameters can be shown to be given by

$$a_0 = \gamma a_1 - \mu \quad a_1 = \frac{\sqrt{6}}{\pi} \sigma \quad \text{G4.}$$

where γ is Euler's constant ($= 0.57721\dots$) and μ is the distribution mean.

Thus, the distribution standard deviation is related to the slope of the line represented by equation G3.

Although equation G1 was initially derived for applications to annual maxima, it can be adapted to any time interval for data sampling in a straightforward manner. For the case of hurricanes, the average interval between storms (the inverse of the Poisson frequency used in the compound Gumbel-Poisson distribution) can be used to transform equation G1 into the form

$$\sigma'_T = \sigma \sqrt{\frac{1.1000y'^2 + 1.1396y' + 1}{N'}}$$

where

σ is the distribution standard deviation;

G5.

σ'_T is the rms error at return period, T'

(T/\hat{T} , where \hat{T} is the average years between hurricanes); and

N' is the number of samples used to estimate the distribution parameters (N/\hat{T}).

Since the form of equation G3 is logarithmic, the slope is not affected by a multiplicative factor, and thus, the distribution standard deviation remains the same. N' in equation G5 can be estimated from the equivalent total number of years in the sample divided by \hat{T} . The total number of years for this case is 65 (1941-2005, inclusive) times a factor, Z , which relates the spatial area covered by the sample used to the spatial extent of a hurricane surge. For relatively intense storms capable of producing surges that are exceeded only every 100 years or more, the along-coast extent of very high surges at least 60% of the peak value is about 60 nm for a storm

with a 20-nm radius to maximum winds (see Figure D4 in Appendix D). The parameter estimation used to derive the values shown in Figure 5 of the main text covered ± 3.5 degrees longitude along 29.5 north latitude. The value of Z is given by

$$Z = \frac{\text{Distance along coast}}{\text{Width of a single sample}} \quad \text{G6.}$$

which in this case is 365.5 nm divided by 60 nm, or approximately 6.1. Thus, the effective number of years is 396.

Appendix 8-3

Rainfall Analysis

Rainfall Intensity

Rainfall is an additional mechanism that contributes to the inundation of the sub-basins. While rainfall is not of primary concern for the hurricane protection system, it is a contributor to the frequency of low-level flood losses. Hence it was decided that a relatively coarse model of hurricane-induced rainfall would suffice.

Prior to NASA's Tropical Rainfall Measuring Mission (TRMM) (Simpson et al., 1988), information on hurricane rainfall was scanty. The TRMM mission, which started in November 1997, produced significant rainfall data for tropical storms and hurricanes at a spatial scale of about 5 km in various tropical regions, including the Atlantic basin. These rainfall products have been analyzed statistically by Lonfat et al. (2004) and Chen et al. (2006). The model proposed below is based primarily on those two studies and on discussions with Dr. Shuyi Chen at the University of Miami.

Mean Rainfall Intensity

Hurricane rainfall intensity I (mm/hr) varies with distance r from the hurricane center and azimuth β relative to the direction of motion. Moreover, the mean intensity field $m_I(r, \beta)$ varies with the central pressure deficit ΔP , the radius of maximum winds R_{\max} , the storm velocity V , and the vertical wind shear S (in the above quoted references, S is measured as the difference between the horizontal wind fields at the 200 and 850 hPa levels). Finally, rainfall intensity displays strong fluctuations at different scales around the mean value $m_I(r, \beta)$.

The azimuthal average of $m_I(r, \beta)$, $m_I(r)$, gives the symmetrical component of the mean rainfall field. This component has a maximum at a distance from the hurricane center close to R_{\max} and decays in an approximately exponential way at larger distances. This decay is contributed by the approximately exponential decay of both the fraction of rainy area and the mean rainfall intensity at the rainy locations. The rate of exponential decay $m_I(r)$ is inversely proportional to the size of the hurricane; hence, in good approximation, it is inversely proportional to R_{\max} .

The value of $m_I(r)$ for $r = R_{\max}$ increases with increasing ΔP , approximately doubling from a Cat2 to a Cat4-5 event. Considering the Cat12 and CAT3-5 results in Lonfat et al. (2004) as representative of the Cat1-2 boundary and of Cat4, respectively, assuming linear dependence of the mean rainfall intensity at R_{\max} on Δp , and fitting an exponential decay with distance as mentioned above, one obtains

$$m_I(r) = \begin{cases} 1.14 + 0.12\Delta P, & \text{for } r \leq R_{\max} \\ (1.14 + 0.12\Delta P)e^{-0.3\left(\frac{r-R_{\max}}{R_{\max}}\right)}, & \text{for } r > R_{\max} \end{cases} \quad (10)$$

where m_I is in mm/h and ΔP is in mb.

The asymmetric component of the mean rainfall field, i.e. the way $m_I(r, \beta)$ depends on the azimuth β , is affected mainly by the storm velocity V and the vertical wind shear S . This influence is complex, as the asymmetric pattern and its strength vary with the absolute and relative values of V and S , the relative direction of wind shear and storm motion, the distance r from the center, and the geographic location. For hurricanes in the Atlantic region, there is a general tendency for rainfall to intensify in the front-east quadrant relative to the direction of storm motion and de-intensify in the rear-west quadrant. This tendency is especially evident for fast-moving storms and away from the hurricane center, reaching about 30-40% of $m_I(r)$ for $r \approx 3R_{\max}$. The effect is stronger over land than over water.

Variability of Rainfall Intensity

For each TRMM observation of each hurricane, Lonfat et al. (2004) extracted the average rainfall intensity $\bar{I}^+(r, r+10)$ at rainy locations inside annular regions of 10 km width. Using these values, they found the empirical distribution of $\bar{I}^+(r, r+10)$ for different r and different storm intensity classes. A consistent result is that $\bar{I}^+(r, r+10)$ varies by a factor of about 7 above and below the median value. The standard deviation of $\log(\bar{I}^+(r, r+10))$ corresponds to a factor of about 2-2.5. Hence the variability of this average rainfall intensity is very large.

In addition, there is variability in the fraction of rainy area. The latter variability is not given in Lonfat et al. (2004), but it can be bounded and roughly estimated as follows. The mean fraction of rainy area, m_{F^+} , is given by Lonfat et al. as a function of r and storm intensity range. Given m_{F^+} , an upper bound to the variance of F^+ is obtained by assuming that F^+ is either 0 (no rain in the region) or 1 (it rains everywhere in the region). In this case $\text{Var}[F^+] = m_{F^+}(1 - m_{F^+})$,

with a coefficient of variation $V_{F^+} = \sqrt{\frac{1}{m_{F^+}} - 1}$. A more realistic estimate of the coefficient of variation is perhaps one half of this theoretical upper bound, or

$$V_{F^+} \approx 0.5 \sqrt{\frac{1}{m_{F^+}} - 1} \quad (11)$$

For distances r up to 150 km, which are those that contribute the most to intense rainfall, m_{F^+} is around 0.9 irrespective of hurricane intensity and Eq. 11 gives $V_{F^+} \approx 0.17$. This coefficient of

variation is much smaller than the coefficient of variation of rainfall intensity inside the rainy area, which is on the order of 1.0. Therefore, the variability of the rainy area may be neglected.

Assessment of Rainfall Intensity inside the Sub-basins

Based on the above considerations, the following simplified model of rainfall inside the sub-basins was adopted. First, the mean rainfall contribution from the symmetric component of the mean rain field, $m_I(r)$ is specified; then the asymmetric component is discussed, and finally an assessment of the variability of rainfall around the mean is given.

Denote by $m_{I_k}(r, t)$ the temporal variation of $m_I(r)$ for hurricane k (in this model, temporal variation is due to the variations of ΔP). The contribution of $m_{I_k}(r, t)$ to the mean rainfall intensity in subbasin j is evaluated as $m_{I_k}(r_{jk}(t), t)$, where $r_{jk}(t)$ is the distance to a representative point of subbasin j from the center of hurricane k at time t . The appropriate distance was taken to be the instantaneous distance between the eye of the storm and the centroid of the subbasin.

For hurricanes that pass to the right or near the subbasin, one may conservatively neglect the azimuthal dependence of the rainfall field. For hurricanes that pass to the left of the sub-basin centroid, the asymmetric component has been accounted for by multiplying the above symmetric mean rainfall values by 1.5. This factor includes intensification due to land effects.

Uncertainty may be expressed by a lognormal random variable with mean value 1 and log standard deviation 0.69, which corresponds to an uncertainty factor of 2. This random factor should be applied to the entire mean rainfall time history. In reality, rainfall intensity inside a subbasin would display significant fluctuations in time and space, which locally could far exceed a factor of 2. However, the above random factor should adequately reflect uncertainty on the total precipitation in a sub-basin during the passage of a hurricane.

Appendix 9

Risk Methodology

Introduction

This Appendix describes the risk analysis philosophy and methodology used to evaluate the performance of the New Orleans hurricane protection system. Probabilistic risk analysis as described by Ayyub (2003), Kumamoto and Henley (1996), and Modarres et al. (1999) was used to develop the basic risk analysis methodology of the hurricane protection system. The basic elements of the risk analysis methodology are illustrated in the flow chart presented in Figure 9-1. The analysis was developed as a series of modules which interface to provide a risk model for the New Orleans HPS. An Excel spreadsheet program, Flood Risk Analysis for Tropical Storm Environments (FoRTE), was developed to implement the many water volume calculations and exceedance values required to determine the risk of inundation for the suite of hurricanes investigated. The spreadsheet (FoRTE) is described in Appendix 17. The results of the many FoRTE program runs were post processed and modified to include wave runup, interflow between sub-basins for the aggregated storm water volumes, and pumping, and to adjust the program outputs based on historic experience. The results of the analyses are described in Appendix 13.

In the engineering community, *risk* is generally defined as the potential that a component or system will incur losses from exposure to a hazard or as a result of an uncertain event. Risk is quantified as the rate (measured in events per unit time) that lives, economic, environmental, and social and cultural losses will occur due to the non-performance of an engineered system or component. The non-performance of the system or component can be quantified as the probability that specific loads (or demands) exceed respective strengths (or capacities) causing the system to fail, and losses if that failure occurs. Risk can be viewed to be a multi-dimensional quantity that includes event-occurrence rate (or probability), event-occurrence consequences, consequence significance, and the population at risk; however, it is commonly measured as a pair of the rate (or probability) of occurrence of an event, and the outcomes or consequences associated with the event's occurrence that account for system weakness, i.e., vulnerabilities. Another common representation of risk is in the form of an exceedance rate (or probability) function of consequences. In a simplified form, risk is commonly expressed as:

$$\text{Risk} = \text{Event rate (or probability)} \times \text{Vulnerability} \times \text{Consequences of failure}$$

This equation not only defines risk but also offers strategies to control or manage risk, i.e., by making the system more reliable or by reducing the potential losses resulting from a failure. The vulnerability, or probability of failure, part of the equation can be influenced by engineers by strengthening of existing structures, increasing reliability or by adding additional protection. However, the consequence part is highly dependent upon the actions and decisions made by residents, government and local officials, including first-response and evacuation plans and practices. In densely populated areas, simply increasing system reliability may not reduce risks to acceptable levels and increasing consequences through continued flood plain development can offset any risk reductions or cause an increase in risk.

A reliability analyses is used to model the performance of individual elements and features (such as, floodwalls, levees, pumps, levee closures, etc.) located throughout the hurricane protection system to the overall performance of the integrated HPS. The reliability of the various elements and features considers the varying material properties of the structures and of foundation conditions that exist throughout the HPS. The impact of this performance on public safety and, social and economic welfare is incorporated into the risk analysis.

Implementation of risk analysis to the HPS of New Orleans and S.E. Louisiana was challenging because it is a complex system of levees, floodwalls and pumping stations, constructed over many years by different entities that serve a large geographical region. In addition, existing capability to accurately predict and model hurricanes in regions as complex as the Mississippi delta was limited. Nonetheless, mathematical modeling of hurricanes and risk analysis methodologies have improved greatly in recent years to make them important, viable tools for supporting investment decisions as the HPS is restored and improved. In developing the risk analysis strategy, the following requirements were identified as key guiding principles:

- **Analytic.** The methodology must provide a systematic framework for assessing risk by decomposing risk into its basic elements.
- **Transparent.** All assumptions and analytical steps are clearly defined.
- **Defensible.** Values for each parameter are supported by all available data, including knowledge from previous studies and expert opinion.
- **Quantitative.** Risk is expressed in meaningful and consistent units (e.g., dollars and fatalities) so as to provide a basis for performing tradeoffs and benefit-cost analysis.
- **Probabilistic.** The mathematics of probability theory is used for expressing uncertainty in all model parameters and assessing the likelihood of alternative scenarios.
- **Consistent.** It is consistent with established and accepted practices of probabilistic risk assessment (PRA) used in many other fields.

The quantification of risk also required that the analysis consider uncertainty in both the input values and the modeling capabilities. For example, detailed knowledge of the engineering parameters that influence the performance of the HPS and of the hurricane characteristics of storms expected to impact New Orleans is limited. This includes properties of foundation soils underlying the extensive levee and floodwall system, and the frequency with which hurricanes will occur in the future. As other examples, Dixon, et al. (2006) provides an overview of subsidence and flooding in New Orleans; Dokka (2006) describes the tectonic subsidence in coastal Louisiana; and Muir-Wood and Bateman (2005) describe uncertainties and constraints on

breaching and their implications for flood loss estimation. Hurricane models can predict winds, waves and surges only with limited accuracy, and the reliability models used to predict levee performance when subjected to hurricane forces are similarly limited. Hence, the risk profiles of hurricane-induced flooding cannot be established with certainty. Risk analysis, therefore, must include not just a best estimate of risk, but also an estimate of the uncertainty in that best estimate. By identifying the sources of uncertainty in the analysis, measures such as gathering additional data can be taken to reduce the uncertainty and improve the risk estimates.

Several key considerations and limitations of the IPET risk study which should be noted are:

- Defining the physical features of the system required an accurate inventory of all components that provide protection against storm surge and waves. This included cross sections, strength parameters of components, transitions between elements, crest elevations and foundation conditions along reaches. The characterization of the physical features of the protection system was, however, limited by the availability of up-to-date information, the resources to conduct detailed field surveys, and the ability to process the large amount of information that was changing during the course of the study.
- The hurricane modeling and reliability analyses required an accurate depiction of the elevations of the tops of levees and walls that make up the HPS. This was complicated by the different datum used in the area over many years, the lack of up-to-date pre-Katrina survey data and the damage caused by Katrina. The risk team utilized the work by other IPET teams to define the datum to be used. The datum used for all elevations cited in the risk study was NAVD88 2004.65. The risk team used data provided by the New Orleans District, Task Force Guardian and others to establish the pre- and post-Katrina crest elevations.
- The pumping system is an important element of the HPS that controls flooding during and after rain and tropical storms, but was not designed to handle overtopping and breaching during hurricane events. This is also complicated by the human factors that affect the operation of the pumping system. For these reasons, several levels of pumping performance were investigated to provide a range of potential performance levels.
- The consequences associated with pre- and post-Katrina flooding are different due to changes in population and economic activity.
- The effectiveness of the protection system depends on human factors as well as engineered systems (e.g., timely road and railroad closures, gate operations, and functioning of pumping stations). Lessons learned from Katrina and other natural disasters were used in modeling the closures.
- Wave runoff, interflow between sub-basins for aggregated storm water volumes, and pumping was considered outside of the FoRTE program using a simplified analysis. Adjustments to the FoRTE outputs were based on historic data.

Key Factors Influencing Risk

The development of a risk analysis model was facilitated by the preparation of an influence diagram. The process of creating an influence diagram helped establish a basic understanding of the elements of the hurricane protection system and their relationship to the overall system performance during a hurricane event and defined input required for the analysis of consequences and risks.

Figure 9-2 shows the influence diagram for the hurricane protection system and the analysis of consequences. There are four parts to the influence diagram:

- Value nodes (rounded-corner box)
- Chance nodes (circular areas)
- Decision nodes (square-corner boxes)
- Factors and dependencies in the form of arrows.

The influence diagram was used to develop an event (or probability) tree for the hurricane protection system. Figure 9-3 shows an initial probability tree derived from the influence diagram in Figure 9-2. The top events across the tree identify the random events whose state following the occurrence of the hurricane could contribute to flooding in a protected area. The tree begins with the initiating event which is a hurricane that generates a storm surge, winds and rainfall in the region.

Analysis Boundaries

An important initial step in the analysis is to clearly define the bounds of the study and the physical descriptions of the various components of a HPS. These bounds included defining the geographic bounds of the study region, the elements of the hurricane protection system, the resolution of information and analyses to be performed, and analysis constraints or assumptions associated with the risk and reliability analyses.

Study Region and Hurricane Protection System

Figure 9-4 identifies the region of southeast Louisiana considered and the major parishes of the area protected by the hurricane protection system. The HPS study area is limited to the six parishes that make up the metropolitan New Orleans area.

Physical Description of the HPS

The HPS is comprised of a variety of sub-systems, structures, and components, which include earthen levees, floodwalls, pumping stations, drainage canals, road and railway closures, and power supply systems. The system is a combination of low lying tracts surrounded by flood

barriers that form drainage basins, which are independently maintained and operated by local parishes and levee boards. Detailed physical descriptions for each basin based on current conditions are provided by Appendices 2 through 7. Data collected during site inspections by the risk team were used to define characteristics of the basins and their interdependence for use in the risk model. This was a critical and time consuming step in the development of the risk model that has yielded a comprehensive description of the HPS. These descriptions were developed by examining available information gathered by IPET including:

- Design memorandums and supporting documents,
- Pre- and post-Katrina construction documents,
- Inspection reports,
- Katrina damage reports, and
- Detailed field surveys conducted by the Risk Team to verify the location and configurations of the HPS.
- Comprehensive studies conducted by other IPET teams
- Information collected by Task Force Guardian during repair of the HPS.

The information gathered was incorporated into detailed geographic information system (GIS) based maps of each basin that included: locations of all features (walls, levees, pumping stations, and closure gates), geotechnical information (boring logs, geologic profiles), aerial photographs, photos of each feature and elevations of the tops of levees and walls.

Analysis Assumptions and Constraints

As part of the process of developing the risk analysis model, it was necessary to identify key assumptions and analysis constraints. Constraints refer to events or situations that were not modeled or considered explicitly in the analysis. The analysis limitations or constraints of the risk model development are summarized by the following:

- Only modeling procedures that existed prior to Katrina were used.
- Geographic area was limited to elements of the hurricane protection system in the following basins:
 - St. Charles
 - Jefferson (East and West Bank)
 - Orleans (East and West Bank)
 - New Orleans East
 - St. Bernard
 - Plaquemines
- The risk model does not produce temporal profiles, but rather spatial profiles accumulated over the durations of respective storms.
- The risk model includes assumptions based on the information collected to select the parameters used in various major aspects of the hurricane protection system

characterization, hurricane simulation, reliability analysis, inundation analysis, and consequence analysis.

- Hazards, and thus consequences, not considered in the risk analysis are: wind damage to buildings, fire, civil unrest, indirect economic consequences, effect of a release of hazardous materials, and environmental consequences.
- The performance of the evacuation plan New Orleans was not modeled in the risk analysis.

Hurricane Protection System

The hurricane protection system (HPS) for the New Orleans metropolitan area shown in Figure 9- 4 is sub-divided into basins that follow parish boundaries and sub-basins that define the interior drainage characteristics of the basins. Basins and sub-basins are divided into sections, or reaches, that have similar cross-sections, material strength parameters and foundation conditions. Features such as: pumping stations, road and railway closures, drainage structures, etc. within a reach are defined as points within the reach that have the potential for allowing water inflow in the event of their failure. The HPS has been discretized for the reliability and risk analysis tasks as schematically shown in Figure 9- 5 which shows an example of how the HPS was discretized to define the system in the risk model. A complete definition of the system is provided in the appendices. The system consists of basins, sub-basins, reaches, features, and transitions. The definition of these components of the HPS are based on the following considerations:

- Local jurisdiction,
- Floodwall type and cross section,
- Levee type and cross section,
- Engineering parameters defining structural performance,
- Soil strength parameters,
- Foundations parameters,

Reaches of each basin are uniquely identified using sequential numbers as illustrated in the Figure 9-5. The figure also shows the approximate locations of pumping stations for the purpose of illustration.

Definition of Basins, Sub-basins, Reaches and Features

The hurricane protection system is divided into basins, sub-basins, reaches, features and transitions. Table 9-1 illustrates the information structure needed for this definition for selected reaches. The definition includes the following basins with their respective numeric identification:

1. Orleans West Bank (OW)
2. New Orleans East (NOE)
3. Orleans (OM)
4. St. Bernard (SB)
5. Jefferson East (JE)
6. Jefferson West (JW)
7. Plaquemines Area (PL)
8. St. Charles (SC)

Reach Descriptions

The HPS perimeter is discretized into reaches that define sections that have similar physical and engineering characteristics. Initially the reaches were defined using the beginning and ending stations shown in the design memoranda (DM). The stations were then adjusted based on examinations of the subsurface material information to form reaches that were expected to have similar performance (reliability). For each reach, the following information, as shown in Table 9-1, is required:

- Reach numeric identification that can be associated with a unique station in hurricane simulation
- Reach length (ft)
- The reach crest elevation (ft)
- Reach type, either a levee (L) or a floodwall (W)
- Reach weir coefficient needed to compute overtopping water volume of either 2.6 for a levee or 3.0 for a floodwall (in units of ft and sec)
- Basin reference that defines the location of the reach in reference to the overall HPS
- Sub-basin reference that defines where water from overtopping or breaching of the reach will collect.

Table 9-1. Definition of Reaches						
Reach No.	Length (ft)	Elevation (ft)	Design Water Elevation (ft)	Reach Type	Reach Weir Coefficient	Subbasin Reference
1	5,000	14.00	8.00	Levee	2.6	Basin1-1
2	10,000	15.00	9.00	Floodwall	3.0	Basin1-2
3	22,500	16.00	11.00	Levee	2.6	Basin1-3
4	6,000	14.00	10.00	Floodwall	3.0	Basin1-4
5	9,000	18.00	13.00	Levee	2.6	Basin1-5
6	7,000	14.00	8.00	Levee	2.6	Basin2-1
7	11,000	15.00	9.00	Floodwall	3.0	Basin2-2
8	7,500	16.00	11.00	Levee	2.6	Basin2-3
9	500	11.00	8.00	Transition	3.0	Basin1-2
10	400	12.00	8.00	Transition	2.6	Basin2-2

Feature Descriptions

Table 9- 2 illustrates the definitions of features within each reach for selected reaches. For each feature, the following information is required:

- Feature number for unique identification
- Type of features of drainage structure (D), or closures (i.e., gate G), or transition structure (T)
- Reach reference where the feature is located
- A reference value for correlated gates for assigning the same probability of closure
- Width of opening (ft) for water inflow through open gates
- Bottom elevation (ft) of gates
- Probability of gate not closed during a hurricane

Feature No.	Reach No.	Correlated Features	Length (ft)	Bottom Elevation (ft)	Not-closed Probability
1	1	1	500	5.00	0.10
2	1	1	500	5.00	0.15
3	2	3	400	6.00	0.10
4	2	3	400	7.00	0.20
5	2	3	400	5.00	0.10
6	3	3	600	5.00	0.15
7	4	7	600	7.00	0.20
8	4	8	600	6.00	0.10
9	5	9	500	6.00	0.10
10	5	9	500	5.00	0.01

Sources of Information

The Risk Team collected data from design documents, construction drawings and studies conducted by other IPET teams to develop detailed descriptions of the basins. Maps were assembled from aerial photos and information was overlaid in GIS files that included: lat/long data, geotechnical profiles and boring logs, crest elevations, stationing used to define reaches and the locations of critical features such as closure gates and pump stations. The information on these maps was confirmed by field surveys of the entire system by members of the Risk Team who traveled every mile of the system. Photos, GPS coordinates and notes were taken during these surveys to document each feature and reach used in the risk model. In addition to the maps, data was compiled for use in the reliability analyses and the risk model. This process has resulted in a comprehensive description of the HPS. The basin descriptions are provided in Appendices 2 thru 7.

Elevations of Crests

The elevations of the tops of walls and levees, adjusted to the current datum, of the entire New Orleans area HPS were developed for use in the suite of hurricane simulations and the risk assessment model calculations of water volumes from overtopping and breaching. Various sources for elevations of segments of the HPS existed, some adjusted to current datum, but most were not. The 1 ft² and 15 ft² lidar data on the IPET repository have been adjusted to current datum and gave about a 99% coverage of the HPS system. The adjusted lidar data gave good values for portions of the HPS that had levees that were clear of vegetation. In addition, there were numerous field surveys that were available for short portions of the walls, some of which been adjusted to the latest datum.

Using the 1 ft² lidar where it was available, cross section profiles were created for lengths of approximately 200 to 500 ft along the entire HPS. Where the 1 ft lidar was not available, the 15 ft² lidar was used. For the levees, these elevations were compared to the current expected values obtained from various MVN records, Taskforce Guardian, and any available field survey information for verification. The location of walls, drainage structures, closures, and gaps were

known from the field survey of the entire HPS that was documented with photos and notes. Some walls had adjusted survey information available, but for most walls it was necessary to go back to the lidar data and examine the areas by drawing numerous profiles, searching for lidar data patterns of “good hits” on wall tops and determining the elevations of the surrounding soil. Then, using the photos and notes obtained from the site visits, estimates of the wall elevations were made. This same process was used for transition regions. A final comparison to the elevations used in the grid developed by the Storm Team for use in the computer program ADCIRC was made for consistency.

Performance of HPS Structures

The performance of the structures providing hurricane protection against potential water elevations due to surge and waves was quantified using structural and geotechnical reliability models integrated within a larger system description of each drainage basin. The reliability models for the HPS components were developed based on design and construction information, and on the results of the IPET Performance Team and the Pump Stations Team studies. Reliability models were developed and evaluated to determine dominant, or most likely, failure modes for each reach defined in a drainage basin. Failure modes, performance functions, basic random variables, and computational procedures used to model failure probability are provided in Appendix 10, Reliability Methodology.

The reliability models included uncertainties in structural material properties, geotechnical engineering properties, subsurface soil profile conditions, and engineering performance models of levees, floodwalls, and transition points. Uncertainties due to spatial and temporal variation, and due to limited knowledge are tracked separately in the analysis. The reliability models provided a best estimate of the frequency of failure under given loads, along with a measure of the uncertainty in that frequency.

Engineering performance models and calculations were adapted from the Geotechnical Design Manuals (GDM) and engineering parameter and model uncertainties were propagated through those calculations to obtain approximate fragility curves as a function of water height for components of the HPS. These results were calibrated against the analyses of the Performance Team, which applied more sophisticated analysis techniques to similar structural and geotechnical profiles in the vicinity of failures. Failure modes identified by the Performance Team were incorporated into the reliability analyses as those results became available.

Reliability assessments were performed for individual reaches of the HPS for given water elevations. The assessments resulted in fragility curves for each reach by dominant or most likely mode of failure. A fragility curve gives the probability of failure, conditional upon an event (water elevation in this study), at which a limiting failure state is exceeded. A sample fragility curve is shown in Figure 9-6 and the actual curves used in the risk analysis are shown in Appendix 10.

Hurricane Hazard Analysis

The hurricane hazard analysis method parameterizes hurricanes using their characteristics at landfall. The hazard analysis was conducted by an independent team that included representatives from USACE, FEMA, consulting firms and academia. Details of the analysis are presented in Appendix 8. The following parameters were considered:

- Central pressure deficit at landfall,
- Radius to maximum winds at landfall,
- Longitudinal landfall location relative to downtown New Orleans,
- Track of storm motion at landfall,
- Storm translation speed at landfall, and
- Holland's radial pressure profile parameter at landfall (Holland 1980).

Using parameter values based on historic events, the recurrence rate and the joint probability density function of the hurricane parameters were estimated for hurricane events in the New Orleans region of interest. The parameters used by the hurricane team to develop the storms they provided to the risk team are shown in Table 9-3. Note that frequencies of the storms highlighted in yellow in Table 9-3 were not provided; therefore, these hurricanes were not used in the risk analysis.

The selected hurricanes were used as input to the ADCIRC models which used several finite element grids for the various conditions of the HPS. The grids corresponded to the condition of the HPS before Katrina and after repairs and improvements had been completed following Katrina.

Since the possible combinations of winds, surges and waves would be computationally demanding if every combination was run through the ADCIRC models, the number of runs was reduced by using a response surface approach. In this approach a relatively small number of hurricanes were selected and used to calculate the corresponding surge and wave levels at the sites of interest. Then a response surface model was fitted to each response variable (surge or wave level at a specific site). Finally, a refined discretization of the parameter space was used with the response surface to represent the hurricane hazard. The outcomes of these computations were combined surge and effective wave setup elevations at particular locations of interest along the hurricane protection system, e.g., representative values at points along the reaches.

A hydrograph with time-varying surge plus wave setup elevations at each reach was produced, based on the ADCIRC analyses, and provided as input to the risk model. Example hydrographs for a single reach are shown in Figure 9-7. Wave runup elevations were added using a simplified approach.

Risk Quantification

The quantification of risk associated with a hurricane protection system required establishing a performance measure for the HPS. The selected performance measure was the amount of water expected to enter protected areas during a particular hurricane. The water entered protected areas as a result of one or more of the following cases:

1. Non-breach events such as overtopping, water entering through closures (i.e., gates) that are left open, precipitation, and potential backflow from pumping stations
2. Breaching events caused by levee or flood wall failure that lead to water inflow into protected areas
3. Rainfall during hurricane events

The risk quantification framework has, therefore, the objective of estimating water volumes and elevations in basins according to these cases. The event tree presented in Figure 9-8 shows the quantities of interest in the net water levels (W) column resulting from open closures, overtopping, breaching, and operation of pumping stations in non-breach cases. The branches for the rainfall volume are shown separately for clarity, but were added to all the other branches during calculations. Figure 9-8 shows a total of 12 branches that were evaluated for each hurricane. These branches were numbered sequentially as shown in the event tree. The top events of the tree are defined in Table 9-3.

The results for each storm event were evaluated by aggregating the individual results for each basin. This provided an estimate of water inundation volumes in each basin along with the frequencies of occurrence. These were then converted to elevations using the stage-storage curves for each basin thereby yielding elevation – exceedence relationships. The evaluation of consequences relative to basin inundation levels were provided by the Consequence Team based upon the elevations selected for the 50, 100 and 500 year events.

Table 9- 3 Summary of the Event Tree Top Events	
Top Event	Description
Hurricane initiating event	The hurricane initiating event maps the peak flood surge and wave effects with a hurricane rate λ . This event can be denoted, $hi(x,y)$, and has a probability of occurrence, $P(hi(x,y))$ and a rate of occurrence of $\lambda P(hi(x,y))$.
Closure structure and operations (C)	The closure event models whether the hurricane protection system closures, i.e., gates, have been sealed prior to the hurricane. This event depends on a number of factors, as illustrated in the influence diagram. The closure structures were grouped by basins in terms of probability of being closed in preparation for the arrival of a hurricane. This event can be used to account for variations in local practices and effectiveness relating to closures and their operations.
Precipitation inflow (Q)	The precipitation event models the rainfall that occurs during a hurricane event. The precipitation inflow per subbasin is treated as a random variable.
Drainage, pumping and power (P)	The drainage event treats pumping in aggregate with drainage effectiveness and power reliability, including backflow through pumps.
Overtopping (O)	This event models the failure of the HPS due to overtopping.
Breach (B)	The breach event models the failure of the HPS during the hurricane. This event includes all failures other than overtopping. This event is treated using conditional probabilities as provided in Figure 9-8.

Risk associated with the hurricane protection system was quantified through a regional hurricane rate (λ) and the probability $P(C > c)$ where a consequence measure C exceeds different levels c . The loss exceedance probability per event was evaluated as

$$P(C > c) = \sum_i \sum_j P(h_i)P(S_j | h_i)P(C > c | h_i, S_j) \quad (9-1)$$

An annual loss exceedance rate was estimated as follows

$$\lambda(C > c) = \sum_i \sum_j \lambda P(h_i)P(S_j | h_i) \times P(C > c | h_i, S_j) \quad \text{Eq. (9-2)}$$

where $P(h_i)$ is the probability of hurricane events of type i , $P(S_j|h_i)$ is the probability that the system is left in state j from the occurrence of h_i , and $P(C > c | h_i, S_j)$ is the probability that the consequence C exceeds level c under (h_i, S_j) . Summation was over all hurricane types i and all system states j in a suitable discretization. Simulation studies of hurricanes for risk analysis required a set of hurricane cases h_i and their respective rates of occurrence λ_i .

Evaluation of the regional hurricane rate λ and the probability $P(h_i)$, the conditional probabilities $P(S_j | h_i)$, and the conditional probabilities $P(C > c | h_i, S_j)$ was obtained from the hurricane model, the HPS risk assessment model, and the consequence model, respectively.

Water Inflow Volume Models

The hydrographs and HPS system descriptions and fragilities were used to compute whether water entered a basin by levee overtopping or breach, and to determine the resulting water elevation (H_{ps}) within the basin. In the case of levee overtopping, H_{ps} within a basin was based on the water volume computed using the duration of overtopping. If a breach occurred and the invert of the breach was below the final elevation of an adjacent body of water, H_{ps} was set to the elevation of that body of water. If the breach invert was above the final elevation of an adjacent body of water, H_{ps} was based on a water volume computed using the duration that the surge elevation was above the breach invert. The topography, stage-storage curves, and the drainage and pumping models for a basin were used to construct such a relationship. The major basins were subdivided into sub-basins according to the drainage and pumping characteristics within the basin. These subdivisions are show in Figure 9-9.

Water Volumes from Other Features of the Protection System. The hurricane protection system includes features that could allow water volume to enter the protected areas during a hurricane. These features include:

1. Closure structures, i.e., gates, that were left open or failed to close
2. Local changes in elevations at transitions in the HPS, typically between levees and floodwalls

These features are identified within each reach and assigned to a subbasin. The water volume resulting from failure of closure structures for a given hurricane was computed using the closure structure failure probability, width of the closure structure, and the elevation at the bottom of the structure. The water volume associated with localized changes in transitions required the change in elevation and the lengths over which the elevation varied.

Hurricane Run No.	Hurricane Rate (events/ year)	Overtopping Volume (ft ³)					
		For Basin1-1		For Basin1-2		For Basin2-1	
		Mean	Standard Deviation	Mean	Standard Deviation	Mean	Standard Deviation
1	1.00E-01	0.00E+00	0.00E+00	0.00E+00	0.00E+00	8.28E+07	1.66E+07
2	5.00E-02	0.00E+00	0.00E+00	0.00E+00	0.00E+00	1.07E+08	3.31E+07
3	1.00E-02	6.57E+07	1.22E+07	8.28E+07	1.66E+07	8.28E+07	1.66E+07
4	1.00E-02	7.87E+07	2.11E+07	8.28E+07	1.66E+07	8.28E+07	1.66E+07
5	1.00E-02	0.00E+00	0.00E+00	0.00E+00	0.00E+00	9.67E+07	3.30E+07
6	1.50E-01	0.00E+00	0.00E+00	0.00E+00	0.00E+00	7.92E+07	1.89E+07
7	5.00E-03	1.24E+08	2.39E+07	1.90E+08	3.76E+07	1.90E+08	3.76E+07
8	9.00E-02	8.69E+07	2.99E+07	7.99E+07	1.99E+07	6.78E+06	1.79E+07
9	1.00E-02	0.00E+00	0.00E+00	0.00E+00	0.00E+00	1.03E+08	2.43E+07
10	5.00E-02	0.00E+00	0.00E+00	0.00E+00	0.00E+00	1.03E+08	3.21E+07

Pumping, Rainfall and Total Water Volume in a Subbasin. The total volume entering a sub-basin (as a random variable with mean and standard deviation) was calculated for each branch of the event tree by summing volumes of water due to overtopping, breaching, and closure structures, as well as the water volume from rainfall and wave runup minus the effect of pumping.

The pumping system in New Orleans was designed to remove rainfall from tropical storms up to about a 10-year event. The effect of pumping on sub-basin inflow water volumes was approximated by subtracting a portion of the 10-year rainfall (that considered degraded pump reliabilities and efficiencies) as a function of water level accumulated in a sub-basin. The water volume that could be pumped by a given pump station within a particular subbasin was estimated by taking the total individual pump station capacity and multiplying it by the duration of the intense portion of the rainfall for each storm. These volumes were then summed for all the stations within a sub-basin. This volume was considered to be the 100-percent pump station capacity and was subtracted from the rainfall of storm, up to the estimated 10-year rainfall volume. Volumes were also determined for 50-percent pump station capacity and no pump station capacity.

Water Interflow between Basins and Sub-basins. Within a basin, water entering a sub-basin may, under certain conditions, overflow into adjacent sub-basins. Thus, prior to calculating the final volume of water in the sub-basins for each of the 16 branches in the event tree of Figure 9-8, interflow among sub-basins was considered. This was done by modeling the elevations of the interfaces between sub-basins and determining the volume of water that would pass between

sub-basins for the amount of time the interface elevation was exceeded. Table 9-4 shows a tabulated structure for computing volumes associated with sub-basins.

Breaching Models

Three cases of breach failure were examined that corresponded to the breaching branches presented in the event tree of Figure 9- 8. The three cases are:

1. Breach given overtopping
2. Breach given no overtopping
3. Breach due to feature (closure gate, pump house, etc.) or transition failures

The first case of breach given overtopping is primarily driven by erosion, resulting from overtopping water flow. Fragility curves for these cases were developed as described in the Reliability Methodology (Appendix 10). Table 9-5 summarizes the breaching model used in the risk analysis.

Breach Parameters

The breaching scenarios require knowledge of the average breach length and depth and of the hydrograph at the breach location to determine basin inflows. The HPS condition after Katrina was reviewed to identify basic characteristics of the major breaches. The identified characteristics were used to develop general rules for estimating breach dimensions in the risk model. One critical characteristic for determining the volume of water flowing through a breach is the duration of time that the breach is open. During Katrina, the breaches could not be repaired in time to have an effect on the level of water achieved inside the basins. Therefore the time at which the breach occurred was assumed to have no effect on inflow volumes and water elevations.

Breach without Overtopping

IPET studies indicated that the London Ave. and 17th St. Canal breaches occurred during Katrina before the water level in the canals reached the top of the floodwall; the breaches appeared to have been the result of a foundation and/or design failure. Therefore, these breaches were modeled in the risk analysis as having occurred without overtopping. The high water marks (HWM) identified inside the Orleans Basin (where the canal breaches occurred) and the length of time that surge elevations exceeded lake levels in the canals were examined. The HWM during Katrina in the Orleans Basin was within about 1 ft of the peak surge in the canals. For example, it appears that the London Ave. South breach occurred when the canal water level was at about 7 to 8 ft, or about 3 ft below the top of wall. The peak surge in the canal was about 10 to 11 ft, and the HWM in the Orleans Basin was about 10 ft. There was a time lag of several hours between the surge elevation that failed the floodwall and the peak surge elevation. This was a sufficient time period for the water elevation inside the Orleans Basin to reach the peak surge

elevation in the canal. The inverts of the canal breaches were well below the normal lake level, so water flowed back into the lake after the surge passed. Based on these observations, it seemed appropriate to use the peak surge level as the water elevation achieved inside the basin when a catastrophic breach (full levee height) occurred during a non-overtopping event. Therefore, for breaching without overtopping, the following assumptions were used in the breaching model:

- All breaches were considered to be a result of a structural or foundation failure and the breach depth was set to lowest elevation of the levee or floodwall.
- The breach depth was extended below the adjacent lake or river level.
- The maximum basin water elevations caused by the breach were set to the maximum surge elevation experienced adjacent to the breach.

Breach during an Overtopping Event

For levees subject to overtopping and erosion, general rules were developed that determined breach invert elevation based on the depth of overtopping relative to the top of levee and the type of soil in the levee. In the case where the breach invert elevation was higher than adjacent lake or river levels, the depth and length of the breach, the duration of time that the surge level exceeded the breach invert, and the weir coefficient were required to calculate inflow water volumes for the breach. The breach lengths for the levees were assumed to be similar to that experienced during Katrina. Breach lengths at the major canal breaches varied (450 to 1000+ ft), but were all on the order of several hundred feet. At the industrial canal (IHNC) where overtopping did occur, the two Lower Ninth Ward breaches were similar in length to breaches at canals where overtopping did not occur. The depth of the breaches at canals where overtopping did not occur were below the normal canal water levels; water flowed out through these breaches when the surge passed. Based on these observations, it was assumed that using the peak surge level as the maximum water elevation achieved inside the basin was appropriate when a full-depth breach occurred during an overtopping event.

For the case of a less than full-depth breach given overtopping, breach parameters for width and height were not available for determining inflows. The risk model did not consider breaches that were less than full-depth. This refinement should be added once an erosion model for levees subject to overtopping is available. The risk model only computed full-depth breaches. This approach provided a conservative estimate of basin inflows by assuming a full-depth breach.

The following assumptions were made in the breaching events given overtopping:

- Breaches occurred as a result of an erosion failure due to surge and/or waves.
- All breach depths were assumed to be full levee height; however, the depth of overtopping required to cause a breach was dependent upon soil properties. Assumed values are shown in Table 9-5.
- Durations of overtopping were calculated from the hydrographs.

- The maximum basin water elevations caused by the breach were set to the maximum surge elevation experienced adjacent to the breach.

Table 9-5 Breaching Model						
Reaches						
Levee/Floodwall Breach Model Given Overtopping (erosion breach)						
Material	Symbol	0 to 1ft		1ft to 3ft		
		Depth (ft)	Breach Width (w), Reach Length <1000ft	Depth (ft)	Breach Width (w) (ft), Reach Length <1000ft	Depth (ft)
Hydraulic Fill	H	0	0	9	0.50*L to max 400	18
Clay	C	0	0	3	0.50*L to max 135	13
Unknown (Average)	U	0	0	6	0.50*L to max 290	17
Wall	W	0	0	0	0	17
Length Modifiers Reach L>1000 ft						
Overtopping Depth (ft)						
Material	Symbol	0 to 1ft		1ft to 3ft		>3 ft
		Depth (ft)	Breach Width (w), Reach Length <1000ft	Depth (ft)	Breach Width (w) (ft), Reach Length <1000ft	Depth (ft)
Hydraulic Fill	H	0.0	0.0	400 < w < 0.40*L	400 < w < 0.40*L	430 < w < 0.40*L
Clay	C	0.0	0.0	135 < w < 0.10*L	135 < w < 0.10*L	135 < w < 0.10*L
Unknown (Average)	U	0.0	0.0	290 < w < 0.30*L	290 < w < 0.30*L	315 < w < 0.30*L
Wall	W	0.0	0.0	0.0	0.0	315 < w < 0.10*L
Levee/Floodwall Breach Model Given No Overtopping						
Material	Symbol	Depth (ft)	Breach Width (w), (ft)			Notes
			L ≤ 1000 ft	1000 < L ≤ 10,000 ft	L > 10,000 ft	
Hydraulic Fill	H	18	0.50*L to max 500	500 < w ≤ 0.15*L	0.15*L	3 Breaches / 10,000 reach
Clay	C	13	0.50*L to max 500	500 < w ≤ 0.10*L	0.10*L	2 Breaches / 10,000 reach
Unknown (Average)	U	17	0.50*L to max 500	500 < w ≤ 0.125*L	0.125*L	2.5 Breaches / 10,000 reach
Wall	W	17	0.50*L to max 500	500 < w ≤ 0.075*L	0.075*L	1.5 Breaches / 10,000 reach
Transitions						
Transitions Breach Model Given Overtopping						
Transition Type	Symbol	Breach size (ft)				
		width	Depth			
Ramps	R	25	3			
Floodwall-Levee	T	50	3			
Drainage Structures	D	65	5.5			
Pump Stations	P	100	5			
Gates	G	25	5			
Unprotected sections	U	N/A	N/A			
Transitions Breach Model Given No Overtopping						
Transition Type	Symbol	Breach size (ft)				
		width	Depth			
Ramps	R	-	-	Treated as opened or closed (sand bagged)		
Floodwall-Levee	T	-	-	No breaching until OT		
Drainage Structures	D	-	-	No breaching until OT		
Pump Stations	P	-	-	No breaching until OT		
Gates	G	-	-	Treat as opened or closed		
Unprotected sections	U	N/A	N/A			

Overtopping Volume and Rates

The overtopping rate was computed using the rectangular weir formulae (Daugherty et al. 1985). If the water is assumed to be an ideal liquid, it can be shown using the energy conservation law that the flow rate Q is given by the following equation:

$$Q = \frac{2}{3}(2g)^{1/2} LH^{3/2} \quad \text{Eq. (9-3)}$$

where g is the acceleration of gravity, H is the water elevation relative to the top of the levee or floodwall, and L is the reach length. The actual flow rate over the weir is known to be less than ideal (Daugherty et al. 1985) because the effective flow area is considerably smaller than the product LH .

The model can be enhanced further for engineering applications by replacing the term $\frac{2}{3}(2g)^{1/2}$ in Eq. 9-3 by an empirical coefficient, known as the weir coefficient C_w , so that Eq. 9-3 takes on the following form:

$$Q = C_w LH^{3/2} \quad \text{Eq. (9-4)}$$

where

$$C_w = \begin{cases} 3.33 & \text{if } L \text{ and } H \text{ are given in English units} \\ 1.84 & \text{if } L \text{ and } H \text{ are given in SI units} \end{cases}$$

Note that the C_w for the ideal fluid case is $\frac{2}{3}(2g)^{1/2}$ which is equal to 2.95 m/s². This coefficient is assumed to have a coefficient of variation (COV) of 0.2. C_w takes a value of 3.0, 2.6, and 2.0 for floodwalls, levees, and gates, respectively, with a coefficient of variation of 0.2 in English units (L and H in feet).

For the application considered, the mean volume of the overtopping (OT) water μ_V for a given reach can be calculated as

$$\mu_V = C_w L \int [\max(X_s h_s(t) - H_r, 0)]^{3/2} dt \quad \text{Eq. (9-5)}$$

where a hydrograph is represented by $h_s(t)$ as illustrated in Figure 9-7; H_r is the reach height; L is the reach length; C_w is the weir coefficient with a coefficient of variation of 0.2, and a mean $\mu(C_w)$ of 3.0, 2.6, and 2.0 for floodwalls, levees, and gates, respectively; X_s is a random factor

with a lognormal distribution (0.20 log standard deviation and a median of 1.0). The lognormal distribution was applied with the following parameters:

$$\mu = E(\ln(x)) = 0, \text{ and } \sigma(\ln(x)) = 0.2 \quad \text{Eq. (9-6)}$$

The resulting volume is the mean volume due to overtopping. The computations account for X_s by numerically using a step size of Δx_{si} and n steps as follows:

$$\mu_{Vi} = \mu_{C_w} L \int_0^{\infty} (x_{si} h_s(t) - H_r)^{3/2} dt \quad \text{Eq. (9-7)}$$

where the probability $P(\Delta x_{si})$ can be computed based on the density function f_{X_s} as follows:

$$P(\Delta x_{si}) = \int_{\Delta x_{si}} f_{X_s}(x_s) dx_s \quad \text{Eq. (9-8)}$$

such that

$$\sum_{i=1}^n P(\Delta x_{si}) = \sum_{i=1}^n \int_{\Delta x_{si}} f_{X_s}(x_s) dx_s = 1 \quad \text{Eq. (9-9)}$$

For each hurricane, the event tree was evaluated n times, and the branch probabilities for these evaluations were multiplied by the respective $P(\Delta x_{si})$ according to Eq. 9-9. This step resulted in the number of branches produces being multiplied by n .

The variance of the water volume for each case was computed based on the coefficient of variation (δ) of the weir coefficient as follows:

$$\sigma_{Vi}^2 = (\mu_{Vi} \delta_{C_w})^2 \quad \text{Eq. (9-10)}$$

where μ_{Vi} is provided by Eq. 9-7, and the coefficient of variation (δ) of the weir coefficient is taken as 0.2.

Failure and Overtopping Probability

The cumulative distribution function (CDF) of the total water volume contained in a subbasin of n reaches was computed as follows:

$$F_V = \sum_{i=1}^n p_i F_{V_i} \quad \text{Eq. (9-11)}$$

where p_i = a overtopping probability, and F_V = CDF of the total water volume. The overtopping probability was treated as a binary variable. For the case of point estimates of flooding per reach, computations were based on order statistics. Once the total volume was obtained from all overtopping and breach cases, the net volume (as a random variable) was computed by adding (or subtracting) water volumes from rainfall, wave runup and the effect of pumping.

Event Tree Branch Probabilities

The event tree of Figure 9-8 consists of 12 branches per hurricane. This section develops and summarizes the probabilities for these branches.

The event tree includes the following primary independent sub-basin-level events:

- C is the event that all gates within a sub-basin are closed,
- P is the event that all pumps in the sub-basin work, and
- B is the event that at least one reach (or one of its transition features) in a sub-basin is breached.

These events were used to construct Table 9-6 that summarizes the expanded expressions for the probability of each branch in the event tree of Figure 9-8. Table 9-7 summarizes the respective procedures for water volume and elevation computation. It should be noted that the water volume associated with the branches involving *not-all-gates closed* required a procedure to account for all possible combinations of not-all-gates closed. Let i be the index denoting a unique scenario among the set of 2^n scenarios of gate open/closed combinations (n = number of uncorrelated gates). The mean water volume (μ) used in the not-all-gates closed branches was:

$$\mu_{\underline{C}} = \frac{\sum_{i=1}^{2^n} p_i \mu_{\underline{C}_i}}{(1 - p_C)} \quad \text{Eq. (9-12)}$$

where p_C is the probability of all gates closed, $\mu_{\underline{C}_i}$ the mean volume associated with not-closing gates according to the i^{th} scenario, and p_i the multinomial probability of the i^{th} scenario. The volume variance used in the not-all-gates closed branches was:

$$\sigma_{\underline{C}}^2 = \frac{\sum_{i=1}^{2^n} p_i^2 \sigma_{\underline{C}_i}^2}{(1 - p_C)^2} \quad \text{Eq. (9-13)}$$

where $\sigma_{C_i}^2$ is the volume variance associated with not-closing gates according to the i^{th} scenario.

The subbasin interflow analysis as previously described was performed subsequent to Table 9-6 procedures. Water volumes were converted to elevations with a tabulated stage-storage relationship for each subbasin based on linear interpolation. Uncertainty propagation from the volume (V) moments (μ_V and σ_V^2) to elevation (E) moments (μ_E and σ_E^2) also used the tabulated stage-storage relationship. Linear interpolation was used since the stage-storage data was tabulated in increments of 1 ft.

The results produced at this point were summarized by subbasin, for all storms and branches of the event tree, in the form of water elevation (mean and variance) and occurrence rate. These results were used to estimate an elevation-exceedance rate for a subbasin at selected elevation (e) values as follows:

$$\lambda(E > e) = \sum_{\text{All storms \& branches}} \lambda P(h) P(S|h) P(E > e|h, S) \quad \text{Eq. (9-14)}$$

This linear relationship can be expressed as

$$E = a + bV \quad \text{Eq. (9-15)}$$

where coefficients a and b were determined from interpolation. The moments of E were computed as

$$\mu_E = a + b\mu_V \quad \text{Eq. (9-16)}$$

and

$$\sigma_E^2 = b^2 \sigma_V^2 \quad \text{Eq. (9-17)}$$

**Table 9- 6
A Computational Summary for Branches of the Event Tree of Figure 9- 6 for a Hurricane and a Basin**

Branch	Branch Probability (See Figure 9-6)
1. Non-Breach	$P(C)P(P)P(\underline{B} \cap \underline{O}) = P(C)P(P) \left(\prod_i (1 - P_i(B O)) P_i(O) \right)$
2. Non-Breach	$P(C)P(P)P(\underline{B} \cap \underline{O}) = P(C)P(P) \left(\prod_i (1 - P_i(B O)) P_i(O) \right)$
3. Breach	$P(C)P(B \cap \underline{O}) = P(C) \left(1 - \left(\prod_i (1 - P_i(B O)) P_i(O) \right) \right)$
4. Non-Breach	$P(C)P(P)P(\underline{B} \cap \underline{O}) = P(C)P(P)(P(\underline{B}) - P(\underline{B} \cap \underline{O})) =$ $P(C)P(P) \left(\prod_i ((1 - P_i(B O)) P_i(O) + (1 - P_i(B O)) P_i(O)) - \prod_i (1 - P_i(B O)) P_i(O) \right)$
5. Non-Breach	$P(C)P(P)P(\underline{B} \cap \underline{O}) = P(C)P(P)(P(\underline{B}) - P(\underline{B} \cap \underline{O})) =$ $P(C)P(P) \left(\prod_i ((1 - P_i(B O)) P_i(O) + (1 - P_i(B O)) P_i(O)) - \prod_i (1 - P_i(B O)) P_i(O) \right)$
6. Breach	$P(C)P(B \cap \underline{O}) = P(C)(1 - P(\underline{B}) - P(\underline{B} \cap \underline{O})) =$ $P(C) \left(1 - \prod_i ((1 - P_i(B O)) P_i(O) + (1 - P_i(B O)) P_i(O)) - \prod_i (1 - P_i(B O)) P_i(O) \right)$
7. Non-Breach	$(1 - P(C))P(P)P(\underline{B} \cap \underline{O}) = (1 - P(C))P(P) \left(\prod_i (1 - P_i(B O)) P_i(O) \right)$
8. Non-Breach	$(1 - P(C))P(P)P(\underline{B} \cap \underline{O}) = (1 - P(C))P(P) \left(\prod_i (1 - P_i(B O)) P_i(O) \right)$
m9. Breach	$(1 - P(C))P(B \cap \underline{O}) = (1 - P(C)) \left(1 - \left(\prod_i (1 - P_i(B O)) P_i(O) \right) \right)$
10. Non-Breach	$(1 - P(C))P(P)P(\underline{B} \cap \underline{O}) = P(C)P(P)(P(\underline{B}) - P(\underline{B} \cap \underline{O})) =$ $(1 - P(C))P(P) \left(\prod_i ((1 - P_i(B O)) P_i(O) + (1 - P_i(B O)) P_i(O)) - \prod_i (1 - P_i(B O)) P_i(O) \right)$
11. Non-Breach	$(1 - P(C))P(P)P(\underline{B} \cap \underline{O}) = P(C)P(P)(P(\underline{B}) - P(\underline{B} \cap \underline{O})) =$ $(1 - P(C))P(P) \left(\prod_i ((1 - P_i(B O)) P_i(O) + (1 - P_i(B O)) P_i(O)) - \prod_i (1 - P_i(B O)) P_i(O) \right)$
12. Breach	$(1 - P(C))P(B \cap \underline{O}) = P(C)(1 - P(\underline{B}) - P(\underline{B} \cap \underline{O})) =$ $(1 - P(C)) \left(1 - \prod_i ((1 - P_i(B O)) P_i(O) + (1 - P_i(B O)) P_i(O)) - \prod_i (1 - P_i(B O)) P_i(O) \right)$
Combined Branches 3 and 9	$(P(C) + P(\underline{C}))(P(P) + P(\underline{P}))(B \cap \underline{O}) = 1 - \left(\prod_i (1 - P_i(B O)) P_i(O) \right)$
Combined Branches 6 and 12	$(P(C) + P(\underline{C}))(P(P) + P(\underline{P}))(1 - P(\underline{B}) - P(\underline{B} \cap \underline{O})) =$ $1 - \prod_i ((1 - P_i(B O)) P_i(O) + (1 - P_i(B O)) P_i(O)) - \prod_i (1 - P_i(B O)) P_i(O)$

**Table 9- 7
A Computational Summary for the Water Volumes Associated with the Branches of the Event Tree of Figure 9- 6 for a Hurricane and a Basin**

Branch	Branch Water Volume (See Figure 9- 6)
1. Non-Breach	Use precipitation volume, and apply pumping factor
2. Non-Breach	Use precipitation volume without pumping
3. Breach	Use post-surge breach water elevation, no pumping
4. Non-Breach	Use overtopping and precipitation volume, apply pumping factor
5. Non-Breach	Use overtopping and precipitation volume without pumping
6. Breach	Use post-surge breach water elevation, no pumping
7. Non-Breach	Use precipitation and not-all-closed-closure volume apply pumping factor
8. Non-Breach	Use precipitation and not-all-closed-closure volume without pumping
9. Breach	Use post-surge breach water elevation, no pumping
10. Non-Breach	Use overtopping, precipitation and not-all-closed-closure volume apply pumping factor
11. Non-Breach	Use overtopping, precipitation and not-all-closed-closure volume without pumping
12. Breach	Use post-surge breach water elevation, no pumping

Risk Profiles

The construction of risk profiles required that all storms be evaluated for all possible combinations of events (all event tree branches) for all the basins. The number of combination per storm for eight basins and 12 branches of the event tree was 1,073,741,824. Dependency among the basins was not examined in order to reduce the number of possible combinations; however, the risk results obtained by examining the individual basins were considered adequate for evaluating the relative risks and vulnerabilities of the HPS.

By Water Elevation

Forte results were summarized by sub-basin, for all storms and the branches of the event tree in the form of water elevation (mean and variance) and occurrence rate. These results were used to evaluate elevation-exceedance rates for a subbasin at selected elevation e values according to Eq. 9-18 as follows:

$$\lambda(E > e) = \sum_{\text{All storms \& branches}} \lambda P(h) P(S | h) P(E > e | h, S) \quad (9-18)$$

An example of an elevation exceedance curve is shown in Figure 9-11. Given elevation-exceedance probabilities and hurricane occurrence rates for a subbasin, and considering all storms, flood water inundation maps were developed as illustrated in Figure 9-12. The inundation maps show the return periods corresponding to respective elevations.

Forte conducted interflow analyses between subbasins at the basin level for individual storms. The Forte analyses did not include overtopping water volumes due to wave runup,

pumping, or interflow analyses at the basin level when the storms were aggregated. For each basin, these volumes were added to the Forte water volumes using deterministic calculations. Three states of pumping system effectiveness were considered: no pumping, pumping at 50 percent of capacity, and at 100 percent of capacity. The basin analyses modified the final 50, 100 and 500 year sub-basin elevations by adding wave run-up overtopping volumes and by subtracting the averaged value for pumping volume expected over the entire storm set. Pumping volumes were estimated deterministically based on each storm's duration and intensity within each sub-basin, averaged over the set of storms, and subtracted from the 50, 100 and 500-yr elevations using the stage-storage relationship for each sub-basin.

After modifying the basin water volumes due to wave runup and pumping, the Forte results at the 50, 100 and 500 year exceedence rates were examined and balanced at a basin level by looking at the water volumes produced at each exceedence level using the stage-storage relationships for the sub-basins. If the interflow elevations between subbasins were exceeded, water volumes were redistributed and new water surface elevations were determined. Note that the exceedence rates were conditional on the storm set provided to the risk team with frequencies as shown in Appendix 8 which do not consider tropical storms and lower intensity, more frequent hurricanes. The actual inundation maps developed from the final results of the risk analysis are shown in Appendix 13.

By Economic and Life losses

Using the elevation-exceedence curve, economic and life loss profiles were estimated and results were provided as elevation-loss curves per sub-basins. The risk profiles for the HPS are expressed in terms of the life loss consequences (as illustrated in Figure 9-13) and the direct economic (as illustrated by Figure 9-14) based upon the stage-damage curves. The stage-damage curves used to construct these profiles were provided by the IPET Consequence Team. The life and economic risk profiles developed from the final results of the risk analysis are shown in Appendix 13.

Conclusions and Recommendations

In developing the risk analysis methodology for the New Orleans hurricane protection system, the needs of decision and policy makers led to the requirements of producing an analytic, transparent, defensible, quantitative, probabilistic, and consistent methodology. Quantifying risk using a probabilistic framework produced elevation and loss exceedance rates based on a spectrum of hurricanes according the joint probability distribution of the characteristic parameters that define hurricane intensity and the resulting surges, waves and precipitation. The methodology provides a process for evaluating the performance of a hurricane protection systems consisting of levees, floodwalls, transitions, closure gates, drainage systems and pumping stations, and estimates the population and property at risk by considering the best estimate flood levels of each basin for occurrence rates of 0.02, 0.01, and 0.002 (i.e., average return periods of 50 years, 100 years, and 500 years). The quantification of risk will assist decision makers as they consider various alternatives to manage risk through the enhancement of the hurricane protection system, controlling land use, improving evacuation effectiveness, and

improving drainage system operations. It also provides public and private stakeholders with information that can be used to increase hurricane preparedness and the awareness of the risks associated with living in a hurricane prone environment.

References

- ADCIRC, 2006. Finite Element Hydrodynamic Model for Coastal Oceans, Inlets, Rivers and Floodplains, <http://www.nd.edu/~adcirc/index.htm>.
- Ayyub, B. M. 2003. Risk Analysis in Engineering and Economics, Chapman & Hall/CRC Press, FL.
- Ayyub, B. M., and McCuen, R. H. 2003. Probability, Statistics and Reliability for Engineers and Scientists, Chapman & Hall/CRC Press, FL.
- Daugherty, R., Franzini, J., and Finnemore E., 1985, Fluid Mechanics with Engineering Applications, 598 p., McGraw-Hill Book Co., NY.
- Dixon, T. H., Amelung, F., and Ferretti, A.. 2006. "Subsidence and Flooding in New Orleans," Nature 441, 587-588.
- Dokka, R. K., 2006. "Modern-Day Tectonic Subsidence in Coastal Louisiana," Geology 34(4), 281–284.
- Eijgenraam, C. J. J., 2006. Optimal Safety Standards for Dike-Ring Areas. CPB Netherlands Bureau for Economic Policy Analysis: CPB Discussion Paper 62.
- Federal Emergency Management Agency (FEMA), 2006. Mitigation Assessment Team Report: Hurricane Katrina in the Gulf Coast - Building Performance Observations, Recommendations, and Technical Guidance (July 2006). <http://www.fema.gov/library/viewRecord.do?id=1857>
- Grossi, P. and Kunreuther, H., 2005. Catastrophe Modeling: A New Approach to Managing Risk. Springer-Verlag, New York.
- Holland, G. J., 1980. "An Analytic Model of the Wind and Pressure Profiles in Hurricanes." Monthly Weather Review, 108, 1212-1218.
- Kumamoto, H., and Henley, E.J., 1996, Probabilistic Risk Assessment and Management for Engineers and Scientists, Second Edition, IEEE Press, New York.
- McGill, W. L., Ayyub, B. M., Kaminskiy, M., "Risk Analysis for Critical Asset Protection," Risk Analysis, Society for Risk Analysis, (accepted for publication).
- Modarres, M., Kaminskiy, M., Krivstov, V., 1999. Reliability Engineering and Risk Analysis: A Practical Guide, Marcel Decker Inc., New York, NY.
- Muir-Wood, R. and Bateman, W., 2005. "Uncertainties and Constraints on Breaching and Their Implications for Flood Loss Estimation." Philosophical Transactions of the Royal Society A: Mathematical, Physical, and Engineering Sciences, 363(1831), 1423-1430.

National Flood Insurance Program (NFIP), 2006. Flood Insurance Manual: May 2005 (Revised October 2006). <http://www.fema.gov/business/nfip/manual200610.shtm>

US Senate, 2006. Hurricane Katrina: A Nation Still Unprepared, Report to the Committee on Homeland Security and Government Affairs, US Senate, Washington, DC. USACE, 2006. Interagency Performance Evaluation Task Force Draft Report on “Performance Evaluation of the New Orleans and Southeast Louisiana Hurricane Protection System,” Draft Volume VIII – Engineering and Operational Risk and Reliability Analysis, USACE, Washington, DC. (1 June 2006).
<https://IPET.wes.army.mil>

Van Gelder, M., 2000. Statistical Methods for Risk-based Design of Civil Structures, PhD Thesis, Delft University of Technology, Report No. 00-1, The Netherlands.

Van Manen, S. E., Brinkhuis, M. 2005. “Quantitative Flood Risk Assessment for Polders.” Reliability Engineering & System Safety, 90, 229-237.

Voortman, H., 2003. Risk-based Design of Large Scale Flood Defence Systems, PhD Thesis, Delft University of Technology, Report No. 02-3, The Netherlands.

White House, 2006. The Federal Response to Hurricane Katrina: Lessons Learned.
<http://www.whitehouse.gov/reports/katrina-lessons-learned/>

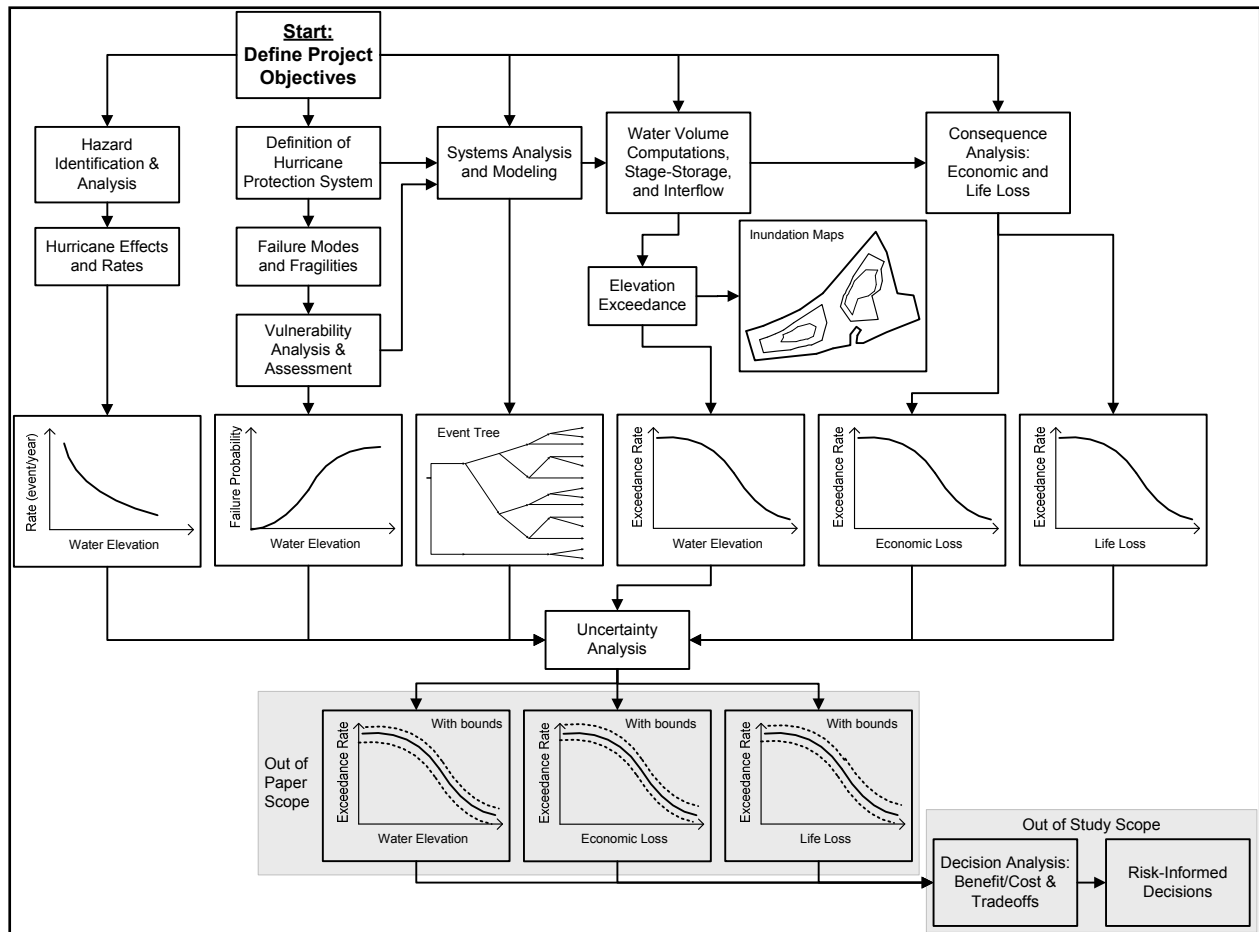


Figure 9-1. Risk Analysis Logic Diagram

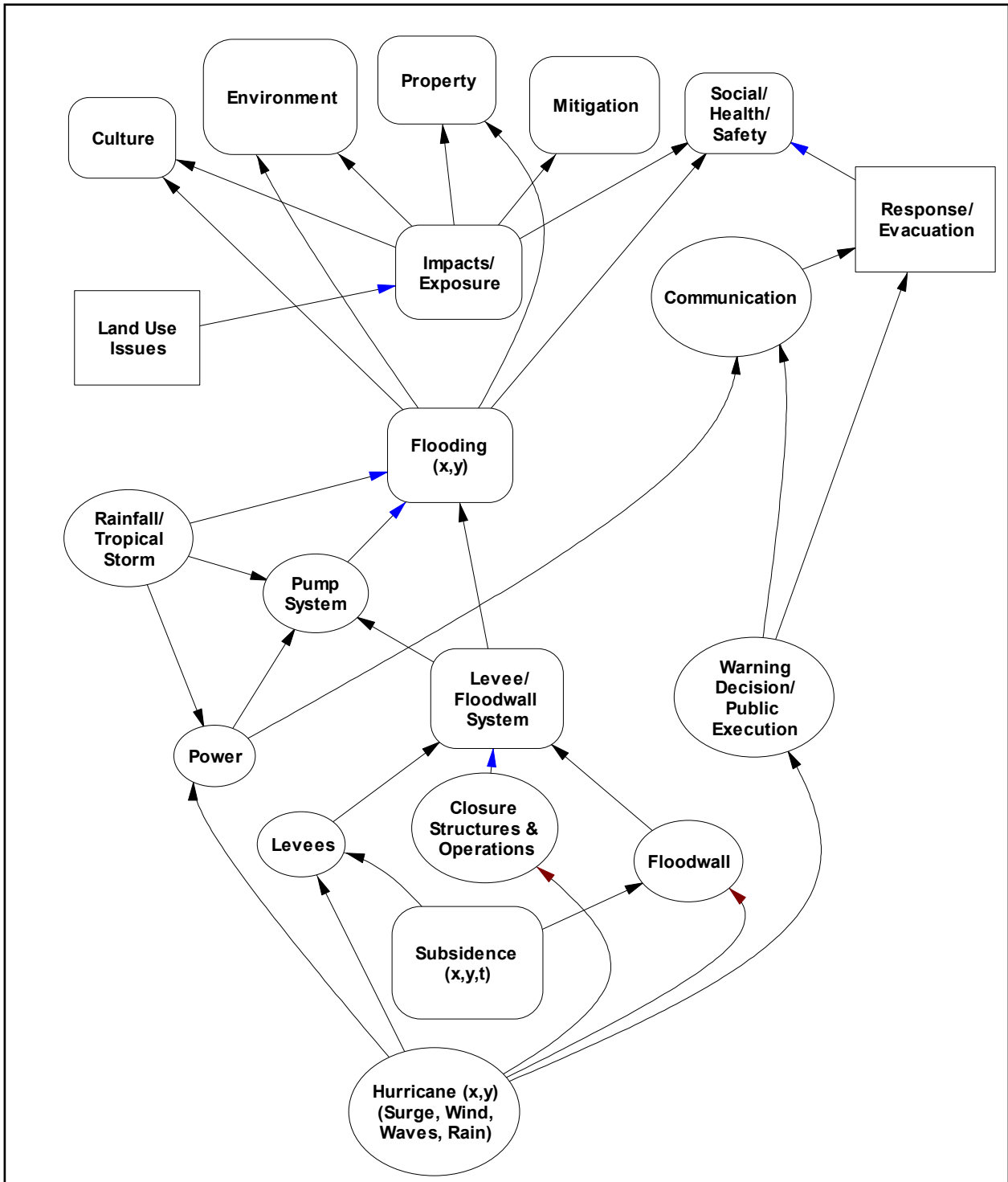


Figure 9-2. Influence Diagrams for Risk Analysis

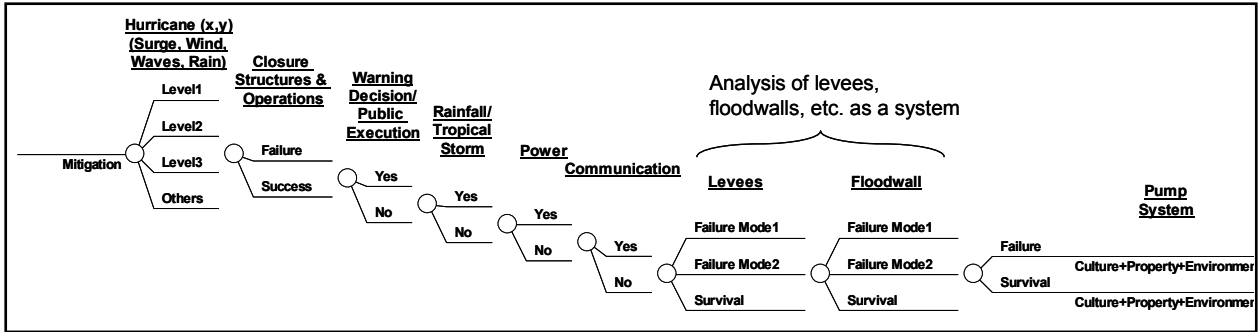


Figure 9- 3. Probability Tree for the Hurricane Protection System

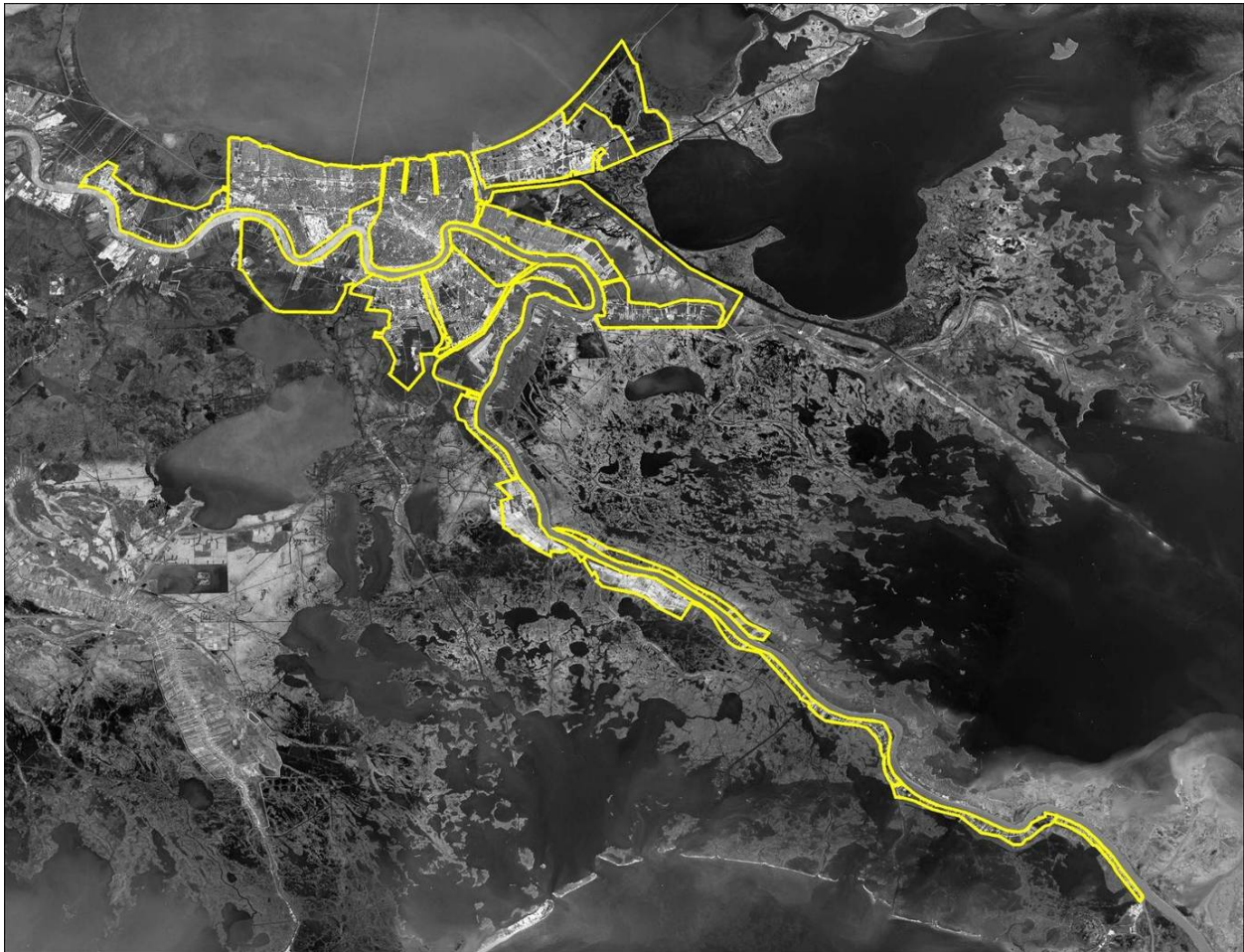


Figure 9-4. Map of New Orleans and the South East Louisiana Area Showing the Geographic Bounds of the Study Region Considered in the Risk Analysis

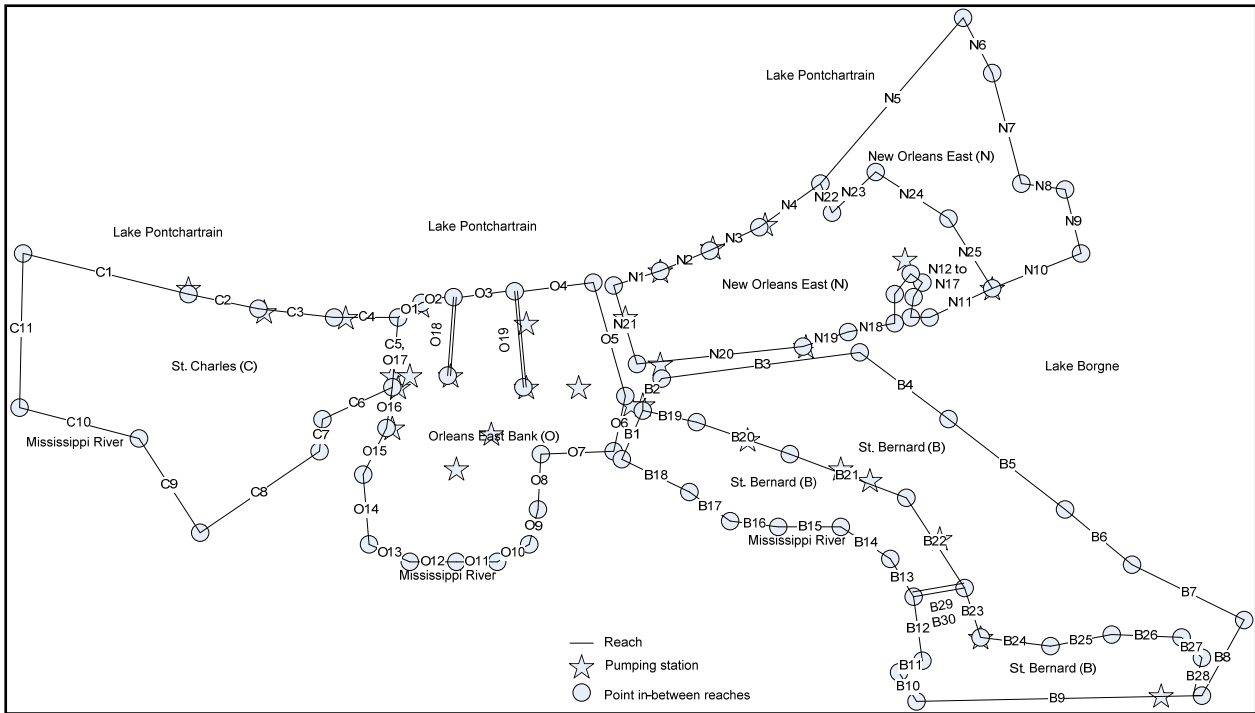


Figure 9- 5. Hurricane Protection System Defined by Basins and Reaches

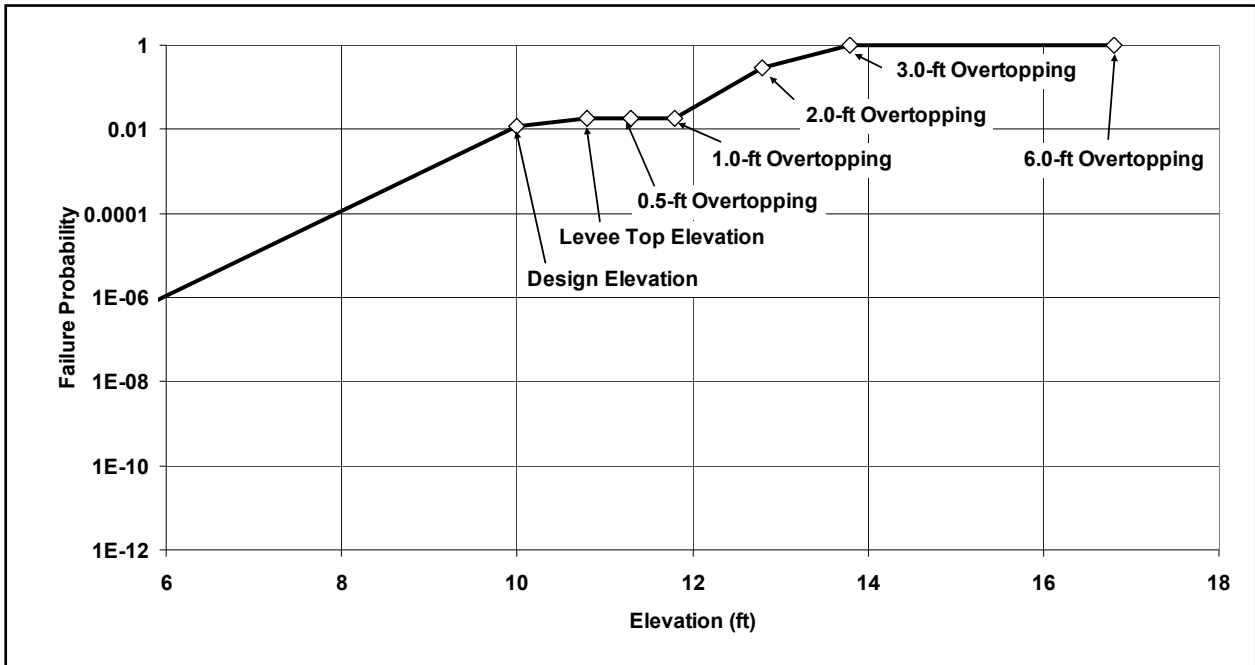


Figure 9-6 Example of a Fragility Curve

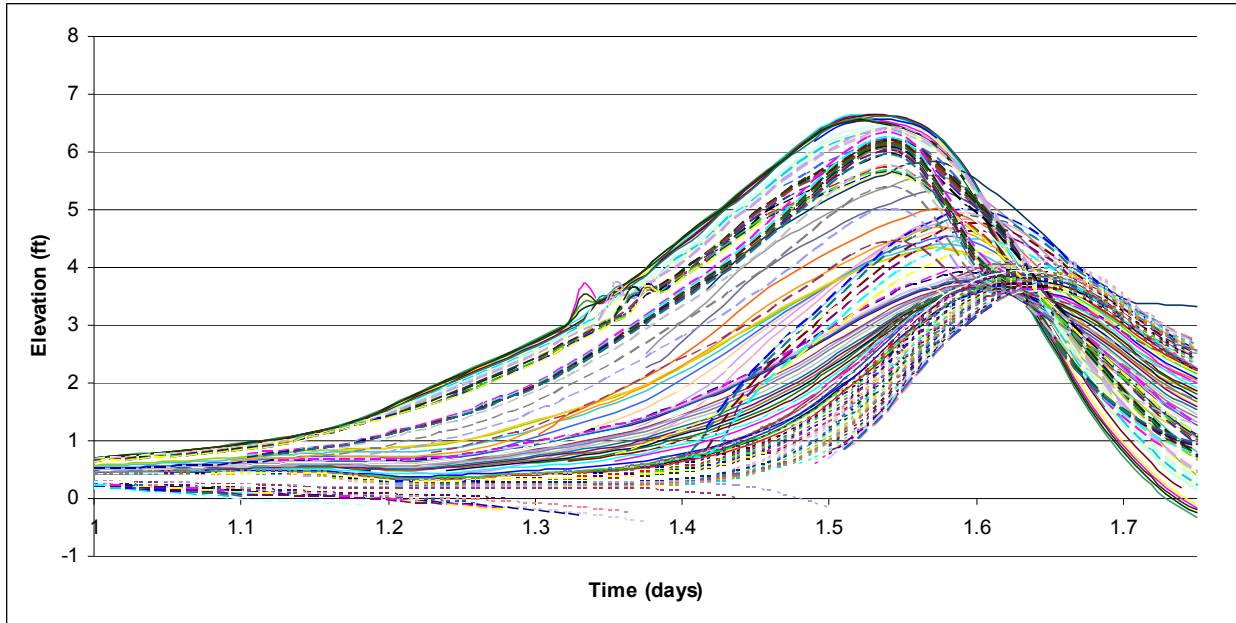


Figure 9-7. Hydrographs of Storm Surge at Defined Stations in the Hurricane Protection System for a Single Storm Event.

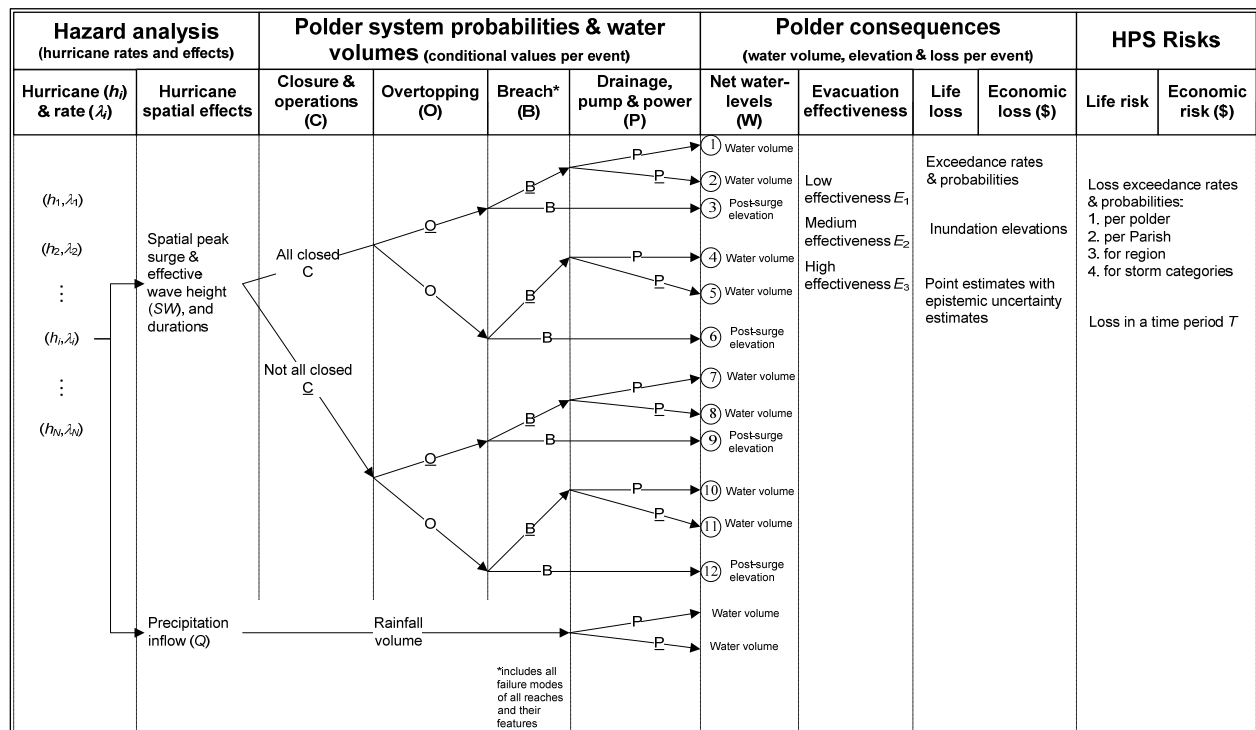


Figure 9-8. Event Tree for Quantifying Risk.

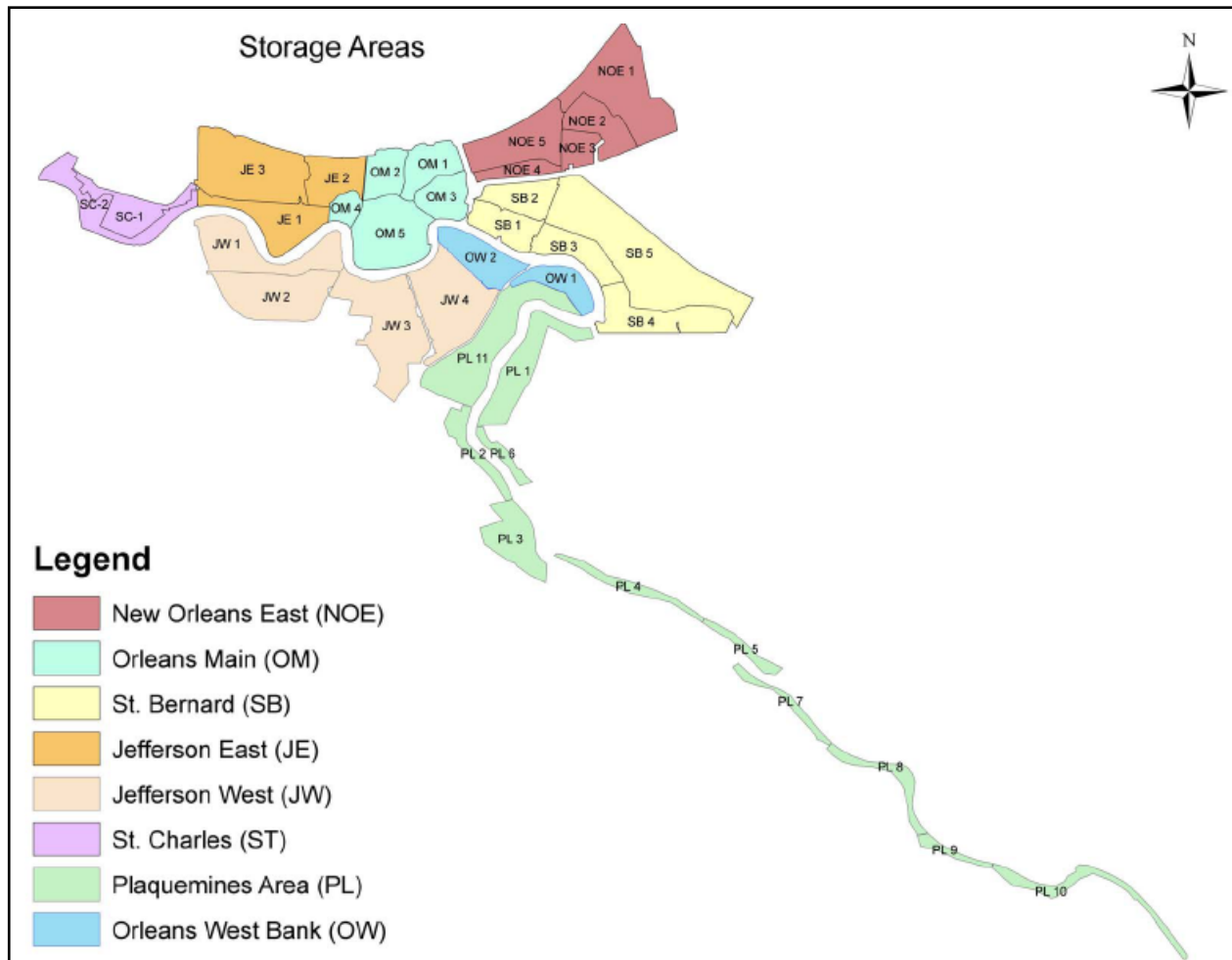


Figure 9-9. Definition of Sub basins for New Orleans HPS.



Figure 9-10. Typical Stage-Storage Curve

**Table 9-3
Storm Frequencies and Parameters**

Sequential number - IPET R&R Storm	Storm Frequency (Events/yr)	Central pressure deficit at landfall (P0)	Radius to maximum winds at landfall (Rp)	Forward speed at landfall (Vf) (Mph)	Holland's parameter (B)	Track angle at landfall wrt vertical (A)	Track Identifier	Lat	Long
1	7.90E-04	960	11	11	1.27	0	1	24.43	-79.1
2	9.19E-04	960	21	11	1.27	0	1	24.43	-79.1
3	4.92E-04	960	35.6	11	1.27	0	1	24.43	-79.1
4	2.50E-03	930	8	11	1.27	0	1	24.43	-79.1
5	2.73E-03	930	17.7	11	1.27	0	1	24.43	-79.1
6	2.30E-03	930	25.8	11	1.27	0	1	24.43	-79.1
7	1.13E-03	900	6	11	1.27	0	1	24.43	-79.1
8	1.39E-03	900	14.9	11	1.27	0	1	24.43	-79.1
9	3.46E-04	900	21.8	11	1.27	0	1	24.43	-79.1
10	7.90E-04	960	11	11	1.27	0	2	24.42	-78.6
11	9.19E-04	960	21	11	1.27	0	2	24.42	-78.6
12	4.92E-04	960	35.6	11	1.27	0	2	24.42	-78.6
13	2.50E-03	930	8	11	1.27	0	2	24.42	-78.6
14	2.73E-03	930	17.7	11	1.27	0	2	24.42	-78.6
15	2.30E-03	930	25.8	11	1.27	0	2	24.42	-78.6
16	1.13E-03	900	6	11	1.27	0	2	24.42	-78.6
17	1.39E-03	900	14.9	11	1.27	0	2	24.42	-78.6
18	3.46E-04	900	21.8	11	1.27	0	2	24.42	-78.6
19	7.90E-04	960	11	11	1.27	0	3	24.42	-78.5
20	9.19E-04	960	21	11	1.27	0	3	24.42	-78.5
21	4.92E-04	960	35.6	11	1.27	0	3	24.42	-78.5
22	2.50E-03	930	8	11	1.27	0	3	24.42	-78.5
23	2.73E-03	930	17.7	11	1.27	0	3	24.42	-78.5
24	2.30E-03	930	25.8	11	1.27	0	3	24.42	-78.5
25	1.13E-03	900	6	11	1.27	0	3	24.42	-78.5
26	1.39E-03	900	14.9	11	1.27	0	3	24.42	-78.5
27	3.46E-04	900	21.8	11	1.27	0	3	24.42	-78.5
28	7.90E-04	960	11	11	1.27	0	4	24.4	-77.9
29	9.19E-04	960	21	11	1.27	0	4	24.4	-77.9
30	4.92E-04	960	35.6	11	1.27	0	4	24.4	-77.9
31	2.50E-03	930	8	11	1.27	0	4	24.4	-77.9
32	2.73E-03	930	17.7	11	1.27	0	4	24.4	-77.9
33	2.30E-03	930	25.8	11	1.27	0	4	24.4	-77.9
34	1.13E-03	900	6	11	1.27	0	4	24.4	-77.9
35	1.39E-03	900	14.9	11	1.27	0	4	24.4	-77.9
36	3.46E-04	900	21.8	11	1.27	0	4	24.4	-77.9
37	7.90E-04	960	11	11	1.27	0	5	24.43	-78.9
38	9.19E-04	960	21	11	1.27	0	5	24.43	-78.9
39	4.92E-04	960	35.6	11	1.27	0	5	24.43	-78.9
40	2.50E-03	930	8	11	1.27	0	5	24.43	-78.9
41	2.73E-03	930	17.7	11	1.27	0	5	24.43	-78.9
42	2.30E-03	930	25.8	11	1.27	0	5	24.43	-78.9

43	1.13E-03	900	6	11	1.27	0	5	24.43	-78.9
44	1.39E-03	900	14.9	11	1.27	0	5	24.43	-78.9
45	3.46E-04	900	21.8	11	1.27	0	5	24.43	-78.9
46	3.50E-04	960	18.2	11	1.27	-45	1	24.54	-80.9
47	3.90E-04	960	24.6	11	1.27	-45	1	24.54	-80.9
48	7.16E-04	900	12.5	11	1.27	-45	1	24.54	-80.9
49	5.48E-04	900	18.4	11	1.27	-45	1	24.54	-80.9
50	3.50E-04	960	18.2	11	1.27	-45	2	24.83	-80.8
51	3.90E-04	960	24.6	11	1.27	-45	2	24.83	-80.8
52	7.16E-04	900	12.5	11	1.27	-45	2	24.83	-80.8
53	5.48E-04	900	18.4	11	1.27	-45	2	24.83	-80.8
54	3.50E-04	960	18.2	11	1.27	-45	3	25.38	-80.8
55	3.90E-04	960	24.6	11	1.27	-45	3	25.38	-80.8
56	7.16E-04	900	12.5	11	1.27	-45	3	25.38	-80.8
57	5.48E-04	900	18.4	11	1.27	-45	3	25.38	-80.8
58	3.50E-04	960	18.2	11	1.27	-45	4.1	26.08	-80.8
59	3.90E-04	960	24.6	11	1.27	-45	4.1	26.08	-80.8
60	7.16E-04	900	12.5	11	1.27	-45	4.1	26.08	-80.8
61	5.48E-04	900	18.4	11	1.27	-45	4.1	26.08	-80.8
63	2.50E-04	960	24.6	11	1.27	45	1	21.28	-90
64	3.02E-04	900	12.5	11	1.27	45	1	21.28	-90
65	2.01E-04	900	18.4	11	1.27	45	1	21.28	-90
66	1.54E-04	960	18.2	11	1.27	45	2	21.3	-90
67	2.50E-04	960	24.6	11	1.27	45	2	21.3	-90
68	3.02E-04	900	12.5	11	1.27	45	2	21.3	-90
69	2.01E-04	900	18.4	11	1.27	45	2	21.3	-90
70	1.54E-04	960	18.2	11	1.27	45	3	21.27	-90.1
71	2.50E-04	960	24.6	11	1.27	45	3	21.27	-90.1
72	3.02E-04	900	12.5	11	1.27	45	3	21.27	-90.1
73	2.01E-04	900	18.4	11	1.27	45	3	21.27	-90.1
74	1.54E-04	960	18.2	11	1.27	45	4	21.28	-90
75	2.50E-04	960	24.6	11	1.27	45	4	21.28	-90
76	3.02E-04	900	12.5	11	1.27	45	4	21.28	-90
77	2.01E-04	900	18.4	11	1.27	45	4	21.28	-90
Total	7.45E-02								
62		960	18.2	11	1.27	45	1	21.28	-90
78		960	17.7	6	1.27	0	1	24.43	-78.9
79		900	17.7	6	1.27	0	1	24.43	-78.9
80		960	17.7	6	1.27	0	2	24.42	-78.4
81		900	17.7	6	1.27	0	2	24.42	-78.4
82		960	17.7	6	1.27	0	3	24.42	-78.3
83		900	17.7	6	1.27	0	3	24.42	-78.3
84		960	17.7	6	1.27	0	4	24.4	-77.7
85		900	17.7	6	1.27	0	4	24.4	-77.7
86		960	17.7	6	1.27	0	5	24.42	-78.7
87		900	17.7	6	1.27	0	5	24.42	-78.7
88		930	17.7	6	1.27	-45	1	26.94	-80.9
89		930	17.7	6	1.27	-45	2	27.09	-80.9
90		930	17.7	6	1.27	-45	3	27.52	-80.9

91		930	17.7	6	1.27	-45	4.1	28.21	-80.9
92		930	17.7	6	1.27	45	1	20.66	-92.3
93		930	17.7	6	1.27	45	2	20.75	-92.6
94		930	17.7	6	1.27	45	3	20.91	-92.8
95		930	17.7	6	1.27	45	4	21.17	-93
96		930	17.7	17	1.27	0	1	24.43	-79.1
97		930	17.7	17	1.27	0	2	24.42	-78.6
98		930	17.7	17	1.27	0	3	24.42	-78.5
99		930	17.7	17	1.27	0	4	24.4	-77.8
100		930	17.7	17	1.27	0	5	24.43	-78.9
101		930	17.7	17	1.27	-45	1	23.29	-80.8
102		930	17.7	17	1.27	-45	2	23.68	-80.9
103		930	17.7	17	1.27	-45	3	24.27	-80.8
104		930	17.7	17	1.27	-45	4.1	24.94	-80.7
105		930	17.7	17	1.27	45	1	21.28	-90
106		930	17.7	17	1.27	45	2	21.27	-90.1
107		930	17.7	17	1.27	45	3	21.27	-90.1
108		930	17.7	17	1.27	45	4	21.26	-90.1
109		960	17.7	11	1.27	0	1.5	24.42	-78.8
110		900	17.7	11	1.27	0	1.5	24.42	-78.8
111		960	17.7	11	1.27	0	2.5	24.42	-78.5
112		900	17.7	11	1.27	0	2.5	24.42	-78.5
113		960	17.7	11	1.27	0	3.5	24.41	-78.3
114		900	17.7	11	1.27	0	3.5	24.41	-78.3
115		960	17.7	11	1.27	0	4.5	24.43	-79.1
116		900	17.7	11	1.27	0	4.5	24.43	-79.1
117		960	17.7	11	1.27	-45	1.5	24.76	-81.2
118		960	17.7	11	1.27	-45	1.5	25.15	-81.1
119		960	17.7	11	1.27	-45	2.5	25.79	-81.2
120		900	17.7	11	1.27	-45	2.5	24.76	-81.2
121		900	17.7	11	1.27	-45	3.5	25.15	-81.1
122		900	17.7	11	1.27	-45	3.5	25.79	-81.2
123		960	17.7	11	1.27	45	1.5	21.29	-90
124		900	17.7	11	1.27	45	1.5	21.29	-90
125		960	17.7	11	1.27	45	2.5	21.29	-90
126		900	17.7	11	1.27	45	2.5	21.29	-90
127		960	17.7	11	1.27	45	3.5	21.28	-90
128		900	17.7	11	1.27	45	3.5	21.28	-90
129		960	17.7	6	1.27	0	1.5	24.42	-78.6
130		900	17.7	6	1.27	0	1.5	24.42	-78.6
131		960	17.7	6	1.27	0	2.5	24.42	-78.3
132		900	17.7	6	1.27	0	2.5	24.42	-78.3
133		960	17.7	6	1.27	0	3.5	24.41	-78.1
134		900	17.7	6	1.27	0	3.5	24.41	-78.1
135		960	17.7	6	1.27	0	4.5	24.43	-78.9
136		900	17.7	6	1.27	0	4.5	24.43	-78.9
137		930	17.7	6	1.27	-45	1.5	26.93	-81.3
138		930	17.7	6	1.27	-45	2.5	27.23	-81.2
139		930	17.7	6	1.27	-45	3.5	27.79	-81.2

140		930	17.7	6	1.27	45	1.5	20.71	-92.5
141		930	17.7	6	1.27	45	2.5	20.83	-92.7
142		930	17.7	6	1.27	45	3.5	21.04	-92.9
143		930	17.7	17	1.27	0	1.5	24.42	-78.8
144		930	17.7	17	1.27	0	2.5	24.42	-78.5
145		930	17.7	17	1.27	0	3.5	24.41	-78.2
146		930	17.7	17	1.27	0	4.5	24.43	-79.1
147		930	17.7	17	1.27	-45	1.5	23.64	-81.3
148		930	17.7	17	1.27	-45	2.5	24.08	-81.1
149		930	17.7	17	1.27	-45	3.5	23.73	-81
150		930	17.7	17	1.27	45	1.5	21.27	-90.1
151		930	17.7	17	1.27	45	2.5	21.27	-90.1
152		930	17.7	17	1.27	45	3.5	21.27	-90.1

**Table 9- 5
A Tabulated Structure for Water Volumes for Sub basins and Basins**

Subpolder Number	Overtopping Volume (V _{OT})		Precipitation		Closures		Breach Volume			
			Rainfall Volume		Water Volume		Elevation		Volume	
	Mean (ft ³)	StD (ft ³)	Mean (ft ³)	StD (ft ³)	Mean (ft ³)	StD (ft ³)	Mean (ft)	StD (ft)	Mean (ft ³)	StD (ft ³)
OW1	0.000E+00	0.000E+00	0.000E+00	0.000E+00	0.000E+00	0.000E+00	1.187E+00	5.937E-02	1.743E+08	4.571E+06
OW2	0.000E+00	0.000E+00	0.000E+00	0.000E+00	0.000E+00	0.000E+00	1.187E+00	5.937E-02	4.858E+08	9.056E+06
NOE1	0.000E+00	0.000E+00	1.655E+04	3.310E+03	4.724E+02	7.162E+01	1.187E+00	5.937E-02	4.461E+08	3.157E+07
NOE2	0.000E+00	0.000E+00	3.775E+06	7.551E+05	4.977E+02	9.954E+01	1.187E+00	5.937E-02	1.109E+09	1.355E+07
NOE3	0.000E+00	0.000E+00	2.703E+06	5.406E+05	0.000E+00	0.000E+00	1.187E+00	5.937E-02	3.059E+08	5.171E+06
NOE4	0.000E+00	0.000E+00	1.550E+01	3.100E+00	5.972E+02	1.194E+02	1.187E+00	5.937E-02	8.688E+07	2.631E+06
NOE5	0.000E+00	0.000E+00	9.367E+07	1.873E+07	0.000E+00	0.000E+00	1.187E+00	5.937E-02	2.463E+09	2.281E+07
OM1	0.000E+00	0.000E+00	0.000E+00	0.000E+00	0.000E+00	0.000E+00	1.187E+00	5.937E-02	7.075E+08	9.807E+06
OM2	0.000E+00	0.000E+00	0.000E+00	0.000E+00	0.000E+00	0.000E+00	1.187E+00	5.937E-02	6.399E+08	8.787E+06
OM3	0.000E+00	0.000E+00	0.000E+00	0.000E+00	0.000E+00	0.000E+00	1.187E+00	5.937E-02	2.480E+08	6.962E+06
OM4	0.000E+00	0.000E+00	0.000E+00	0.000E+00	0.000E+00	0.000E+00	1.187E+00	5.937E-02	7.016E+07	2.248E+06
OM5	0.000E+00	0.000E+00	0.000E+00	0.000E+00	0.000E+00	0.000E+00	1.187E+00	5.937E-02	4.371E+08	1.257E+07
SB1	0.000E+00	0.000E+00	0.000E+00	0.000E+00	0.000E+00	0.000E+00	1.187E+00	5.937E-02	1.753E+08	5.671E+06
SB2	0.000E+00	0.000E+00	0.000E+00	0.000E+00	0.000E+00	0.000E+00	1.187E+00	5.937E-02	1.367E+06	4.737E+04
SB3	0.000E+00	0.000E+00	0.000E+00	0.000E+00	0.000E+00	0.000E+00	1.187E+00	5.937E-02	1.491E+08	4.839E+06
SB4	0.000E+00	0.000E+00	0.000E+00	0.000E+00	0.000E+00	0.000E+00	1.187E+00	5.937E-02	1.581E+07	2.990E+06

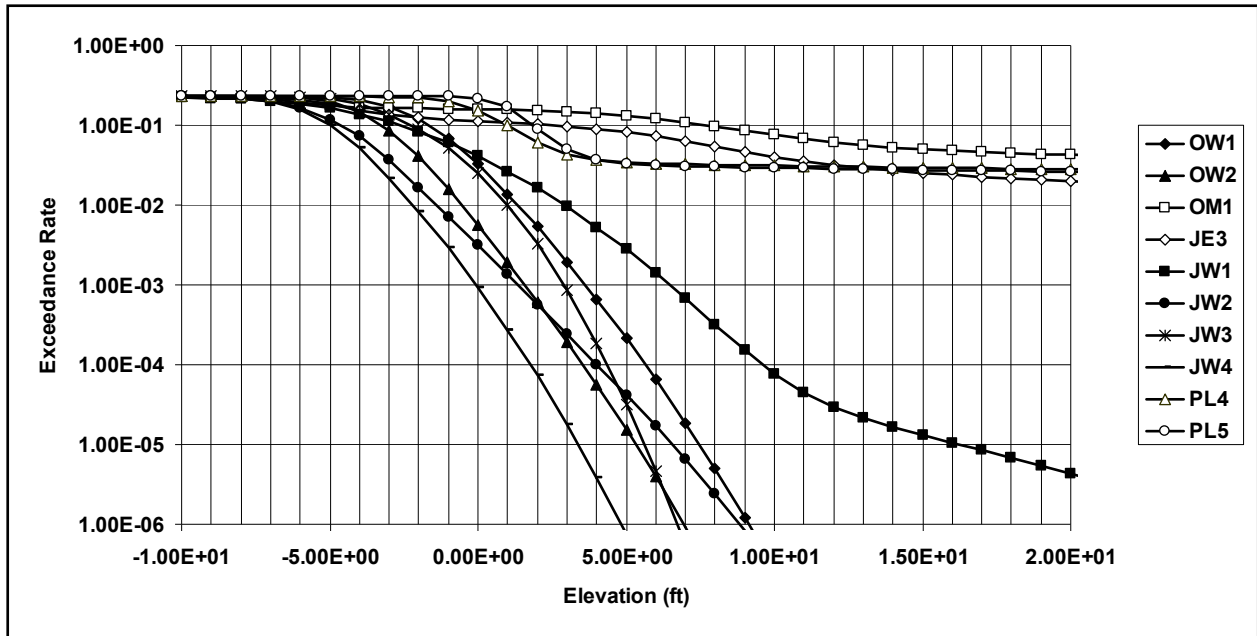


Figure 9-11 Example Elevation-Exceedance Curve

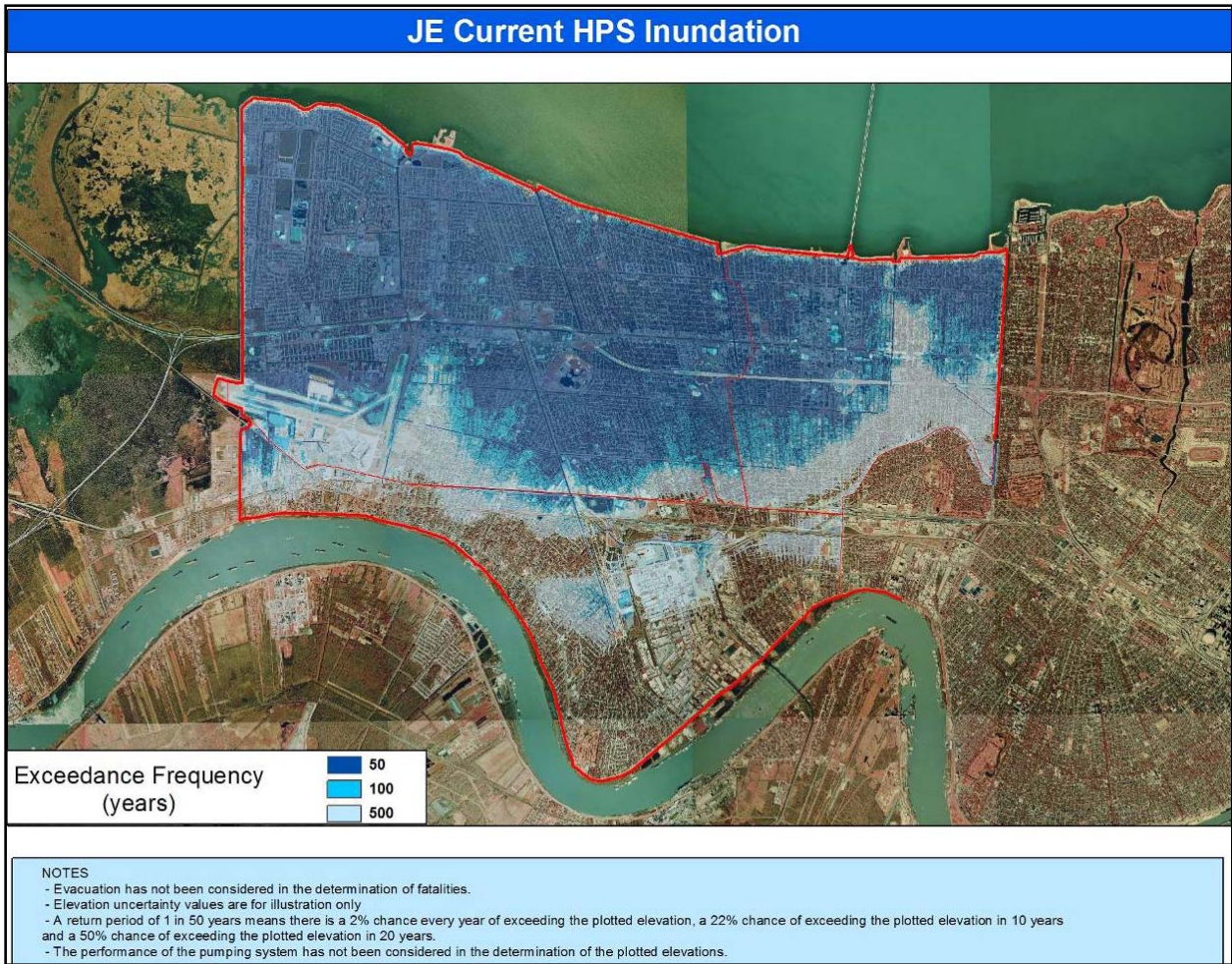


Figure 9-12. Sample Inundation Map

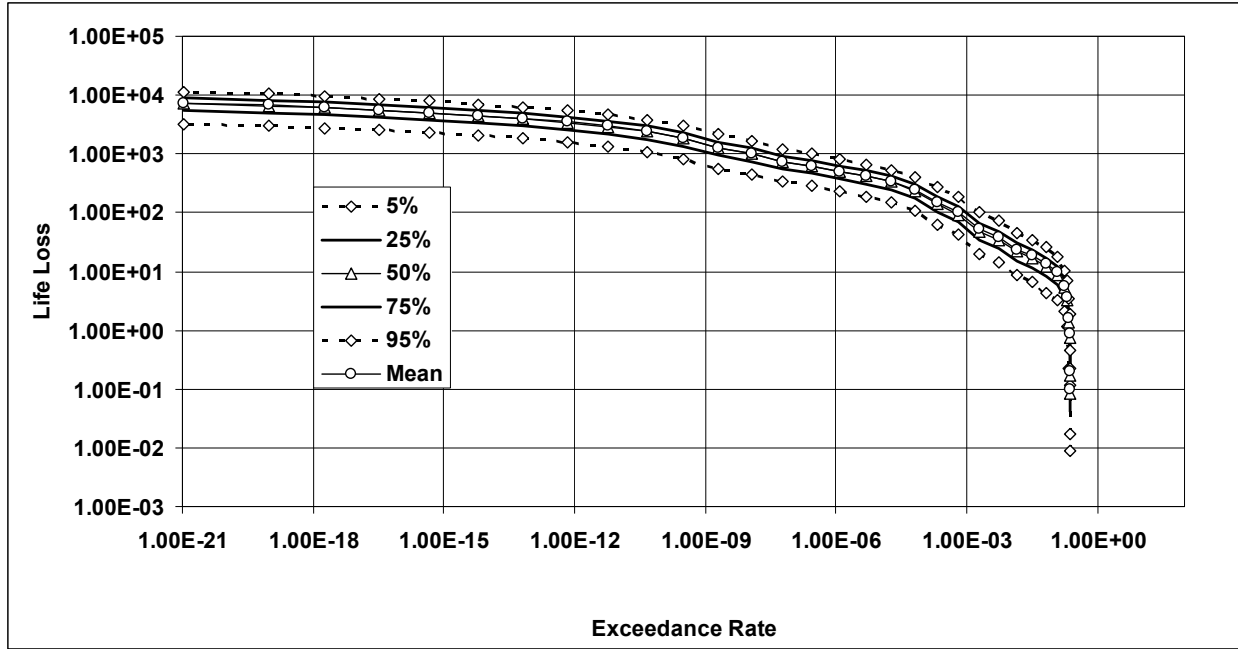


Figure 9-13 Example Life Loss –Exceedance Curve

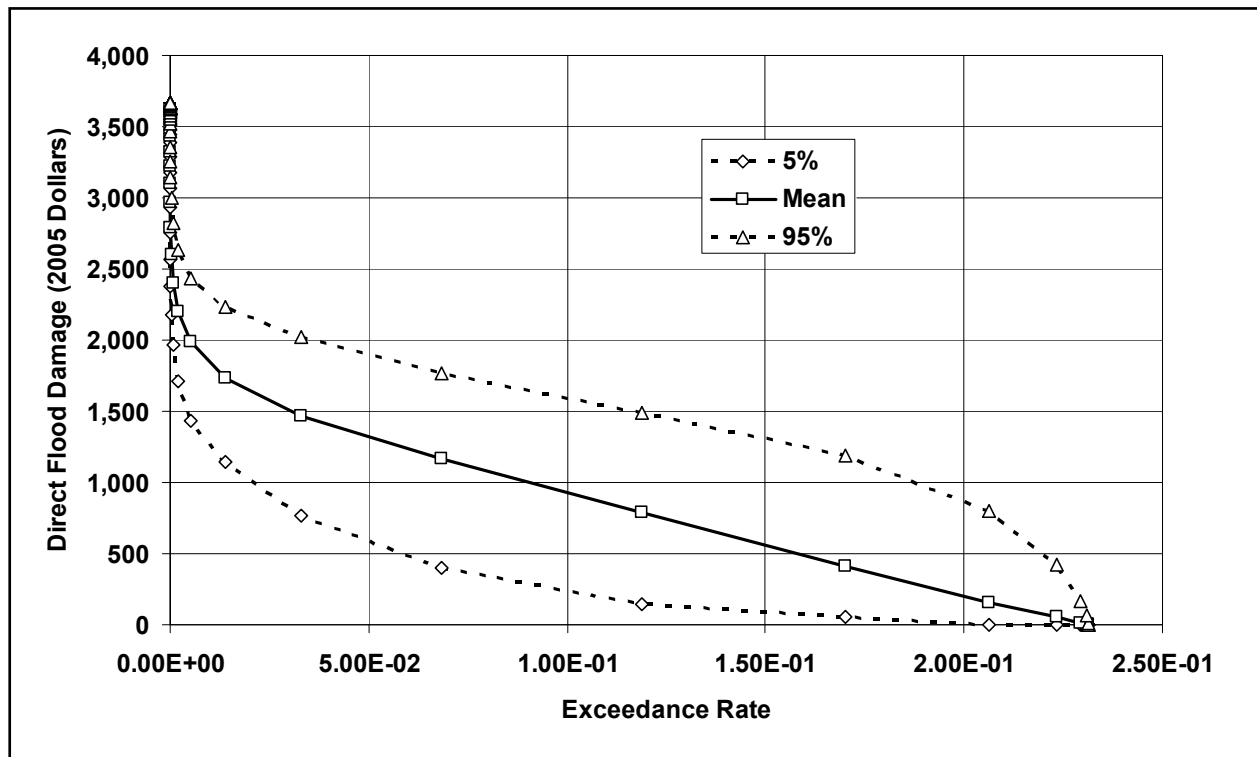


Figure 9-14. Example Damage-Exceedance Curve. Note: Direct Flood Damages (Millions of 2005 Dollars)

Appendix 10

Reliability Modeling

Introduction

Reliability analysis is that part of the risk study that leads to an evaluation of the conditional probability of failure (i.e., reliability) of structures, systems, and components when they are exposed to the loads of a hurricane. The reliability analysis had three steps:

1. Define and characterize the structures, components, and features constituting the hurricane protection system (HPS) for each drainage basin.
2. Define *failure* and identify failure modes and limit states for each structure, system, component, and feature.
3. Assign conditional probabilities to HPS failure states for given water elevations and wave heights caused by hurricane conditions.

Two conditions were analyzed for the reliability of levees, flood walls, and pumping stations: pre-Katrina and post-reconstruction and repair as existing in June 2007.

Earlier appendices contain an inventory of the structures, systems, and components in each drainage basin that were considered in the risk analysis.

Approach

The reliability of the hurricane protection system under potential water elevations due to surge and waves was quantified using structural and geotechnical reliability models integrated within a larger system description of each drainage basin. The reliability models for the HPS components were developed based on design and construction information, and on the results of the Performance Team (IPET v.V 2006) and the Pump Stations Team (IPET v.VI 2006) studies. Reliability models were developed and evaluated to determine dominant, or most likely, failure modes for each reach in each drainage basin.

The reliability models included uncertainties in structural material properties, geotechnical engineering properties, subsurface soil profile conditions, and engineering performance models

of levees, floodwalls, and features. Uncertainties due to spatial and temporal variation, and those due to limited knowledge are tracked separately in the analysis, providing a best estimate of the frequency of failure under given loads, along with a measure of the uncertainty in that frequency.

Physical system definition

The HPS comprises levees, floodwalls, levees with floodwalls on top, and various points of transition or localized features such as pumping stations, drainage works, pipes penetrating the HPS, and gates. Each drainage basin perimeter was divided into segments, referred to as reaches, which were deemed to be homogeneous in three respects: structural cross-section, elevations in the cross-section, and geotechnical cross-section. In total, 135 such reaches were identified across all of the drainage basins, and 197 point features.

Geometric and engineering material properties were identified for each reach and summarized in systems definition tables (Table 10-2). Structural cross-sections were initially identified by review of as-built drawings, aerial photographs, and GIS overlays; and were subsequently confirmed in on-site reconnaissance. Elevations were assessed in the same reconnaissance, supplemented by LIDAR and field surveys provided to the Risk Team. Geotechnical cross-sections and corresponding soil engineering properties were derived from original USACE General Design Memoranda (GDM) for the respective project areas of each drainage basin, supplemented by site characterization data collected post-Katrina at levee and flood wall failure sites (cone penetrometer and laboratory measurements on undisturbed samples). GDM's are available in PDF format at the IPET Project web site (<https://IPET.wes.army.mil>).

1	Levees	a. Embankment section (Reaches were defined on the basis of physical discontinuities - geometric, physical, soils, and construction characteristics) b. Levee Foundation
2	Walls	a. Wall structure (I or T-wall) b. Wall foundation
3	Point Features	a. Gates b. Position – open or closed
4	Transitions	a. Wall-Levee and Levee-Wall b. Gates c. Pump stations d. Drainage Structures e. Ramps f. Unprotected reaches

Engineering performance models and calculations were adapted from the GDM's. Engineering parameter and model uncertainties were propagated through those calculations to obtain approximate fragility curves as a function of water height for components of the HPS. These results were calibrated against the analyses of the Performance Team, which applied more sophisticated analysis techniques to similar structural and geotechnical profiles in the vicinity of failures. Failure modes identified by the Performance Team were incorporated into the reliability analyses as those results became available.

Reliability assessments were performed for individual reaches of the HPS for given water elevations. This resulted in fragility curves for each reach by mode of failure.

Fragility curve. A fragility curve gives the probability of failure, conditional upon an event (water elevation in this study), at which a limiting failure state is exceeded.

Reliability assessments for each reach and component of the drainage basin perimeter were combined in the HPS risk model. The risk model (Appendix 9) used water elevations from the hurricane hazard and the HPS fragilities to calculate probability of volume and duration of flooding within each drainage basin. The system risk model is structured around an event-tree description of the occurrence of hurricane events, corresponding water and wave heights, and the resulting response of the HPS. The risk model separately tracks natural variations and knowledge uncertainties from both the hurricane hazard and the structural and geotechnical response, to give a best estimate of frequency and duration of flooding, along with measures of uncertainty in those frequencies.

Uncertainties and probabilities of failure

The Corps of Engineers Technical Letter ETL 1110-2-556, “Risk-Based Analysis in Geotechnical Engineering for Support of Planning Studies,” (USACE 1999) suggests that the principal sources of uncertainty in predictions of levee performance requiring evaluation are:

1. **Uncertainty in loadings.** Loadings such as floods, earthquakes, and impacts are random events for which magnitude and time of occurrence may be modeled by probabilistic methods. This often involves the use of binomial or Poisson distributions fit to observed event data.
2. **Uncertainty in parameter values.** Geotechnical parameters such as soil strength and permeability have several components of uncertainty. The value of a parameter at any point and the average value over any distance are inherently uncertain because of soil’s natural spatial variability. Secondly, there is uncertainty due to testing errors and uncertainty in estimating the mean and variance of the properties due to the finite number of tests performed. The normal and lognormal distributions are often used to model parameter values, which may be the value at a point or the spatially averaged value calculated over some distance or area.
3. **Uncertainty in analytical models.** Analytical models such as slope stability analysis methods, seepage equations, etc., have an inherent model uncertainty arising from the fact that they are mathematical simplifications of more complex problems, and unsatisfactory performance such as slope instability or piping may occur in the prototype at factors of safety above or below the limit state $FS = 1.0$ corresponding to these conditions in the model. Model uncertainty has not been systematically considered in most Corps studies to date. Where probabilistic methods are used to make economic comparisons of alternatives, probability values calculated using consistent models should provide a consistent basis for comparison even though model uncertainty is not included.

4. **Uncertainty in performance.** As parameter values and analytical models both have inherent uncertainty, the performance of a structure with respect to some quantifiable performance mode (slope stability, seepage, settlement, etc.) is likewise uncertain. The probability of satisfactory or unsatisfactory performance for modes with well-defined models and parameters is often calculated using first-order, second-moment (FOSM) methods, such as the Taylor's series method, which yield a reliability index or probability of unsatisfactory performance $Pr(U)$. This approach quantifies uncertainty in performance as a function of uncertainty in parameter values and the analytical model.
5. **Performance modes without defined limit states.** In some cases, engineering models may not be formulated to include limit states (e.g., $FS = 1$) and hence may not be easily reformulated to provide a reliability index or probability of unsatisfactory performance. Instead, satisfactory performance is expected to be attained by the adoption of experienced-based practices. An example is the design of filter materials, where equations can be used to design filters expected to perform adequately and prevent internal erosion, but there is no measure such as the factor of safety on which to base a mathematical procedure for comparing the relative reliability of filters. These situations are not directly compatible with FOSM methods. To obtain required probability values for these modes, one must either use frequency models based on observed events or judgmental values based on expert elicitation.
6. **Frequency and magnitude of physical changes or failure events.** Physical conditions may change at some uncertain time within the lifetime modeled in a simulation. These may directly lead to unsatisfactory performance or may require changing the values of parameters in an analytical model. Examples include scour of foundations, plugging of well screens by incrustation, failure of well screens by corrosion, development of seepage windows in sheet piling, and dislodging of fill material in rock joints. The occurrence of such events cannot be easily predicted by a model based on physical parameters. The occurrence may be modeled using a frequency-based approach such as those based on the exponential and Weibull distributions where sufficient data exist.
7. **Condition of unseen features.** The condition of unseen features is inherently uncertain. Examples include the effects of unknown cracks, burrows, or other defects in levees, and the adequacy of grout cutoffs under dams. A similar uncertain, but non-calculable, situation would be determining the probability of locating and plugging the source of a piping channel in a foundation before destructive erosion occurs. Such situations may contribute considerable uncertainty regarding performance but often can only be accounted for in a risk assessment or reliability analysis by quantifying the experience and judgment of experts rather than estimating uncertainty in parameters or fitting distributions to historical data.

ETL 1110-2-556 goes on to observe that geotechnical problems have a number of unique aspects that also require consideration in reliability analyses:

1. In geotechnical engineering, coefficients of variation are related to the variability of natural materials, which may need to be assessed on a site-specific basis.

2. Geotechnical parameters may have relatively high coefficients of variation (the value for the coefficient of permeability may exceed 100 percent) and may be correlated.
3. Soil strength parameters can be defined and analyses performed in either a total stress context or an effective stress context. In the former, the uncertainty in strength and pore pressure are lumped; in the latter, they are treated separately.
4. Soils are continuous media where properties vary from point to point, requiring consideration of spatial correlation. For problems such as slope stability, the location of the critical free body must be searched out. Furthermore, its location varies with parameter values, and varying parameter values (in an FOSM or Monte Carlo analysis) results in different free-body locations for each set of parameter values.
5. Although one slip surface may be “critical,” a slope can fail on any of an infinite number of slip surfaces; hence a slope is a system of possible failure surfaces which are correlated to some extent.
6. Some earth structures such as levees may be exceedingly long, such as levees which may be tens of miles long. These can be treated as a number of equivalent independent structures; however, determining the appropriate length and number is problematical, and the reliability of the system may be sensitive to the assumptions made.

The reliability analysis undertaken as part of IPET attempts to incorporate all of these uncertainties and considerations.

Aleatory vs. epistemic uncertainty

In modern practice, engineering risk analysis usually incorporates uncertainties of two distinct types: aleatory and epistemic.

Aleatory uncertainty is attributed to inherent randomness, natural variation, or chance outcomes in the physical world; in principle, this uncertainty is irreducible because it is assumed to be a property of nature. Aleatory uncertainty is sometimes called random or stochastic variability.

Epistemic uncertainty is attributed to lack of knowledge about events and processes; in principle, this uncertainty is reducible because it is a function of information. Epistemic uncertainty is sometimes called, subjective or internal uncertainty, and divides into two major sub-categories: model uncertainty and parameter uncertainty.

An example of the interplay of aleatory and epistemic uncertainties in practice is the flood frequency curve (USACE 1998). The flood frequency curve describes natural variability or aleatory uncertainty of flood flows, while error bands about the curve describe epistemic uncertainty in the parameters of the flood frequency model. The frequency curve reflects the irresolvable variation of nature. The error bands reflect limited knowledge about the statistically

estimated parameters of the frequency curve. Collecting more data would improve our estimates of the parameters, and thus reduce the error bands about the frequency curve, but no amount of data can reduce the underlying probability distribution represented by the exceedance curve.

Separating uncertainty into aleatory and epistemic parts is a modeling decision. Consider drawing a flexible curve through a set of data. A high-order curve may fit the data closely, but the uncertainty in the parameters of the curve will be large because there are many parameters to be estimated. In contrast, a straight line may not fit the data as closely, but the uncertainty in the slope and intercept of the line will be small. The data scatter about the curve is aleatory; the uncertainty in the parameters of the curve is epistemic.

This modeling decision on whether and how to separate aleatory and epistemic uncertainty has important implications in a levee safety analysis. A schematic example is given in Figure 10-1, in which the variability of some engineering property is shown as a function of location. This spatial variability of the property is divided into sections thought to be homogeneous, and averages (means) are estimated for each. When the variability is modeled this way, the variations about the respective means are assumed to be aleatory uncertainties, while that in the estimates of the means are assumed to be epistemic uncertainties. Additional information can reduce the error in the estimates of the means, but it will only better characterize the variance about the means within each zone and not reduce that variance itself. This standard model of spatial variation has many implications, which are discussed in greater detail in Hartford and Baecher (2004).

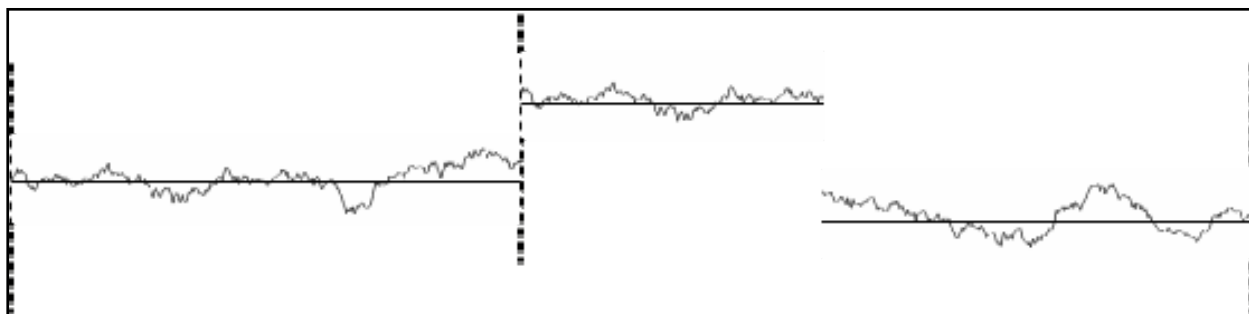


Figure 10-1. Schematic diagram showing the variability of some engineering property in space (e.g., soil strength, surge elevation, etc.). The spatial variability is divided into sections assessed to be homogeneous, and means are estimated for each.

Aleatory and epistemic uncertainty affect the outcomes of a reliability analysis in different ways. Aleatory uncertainty manifests as variations, or frequencies of occurrence, over space or time. Epistemic uncertainties manifest as statistical error and systematic biases in probability estimates, and may introduce correlations among aleatory frequencies.

Reach definitions

The HPS was divided into 135 reaches. A *reach* is defined for the purpose of the reliability analysis as,

Reach. A continuous length of levee or wall exhibiting homogeneity of construction, geotechnical conditions, hydrologic and hydraulic loading conditions, consequences of failure, and possibly other features relevant to performance and risk.

Thus, reaches are homogeneous lengths of levee or wall that differ from neighboring reaches in at least one of the above properties, and which are considered internally homogeneous for the purposes of reliability modeling and risk analysis.

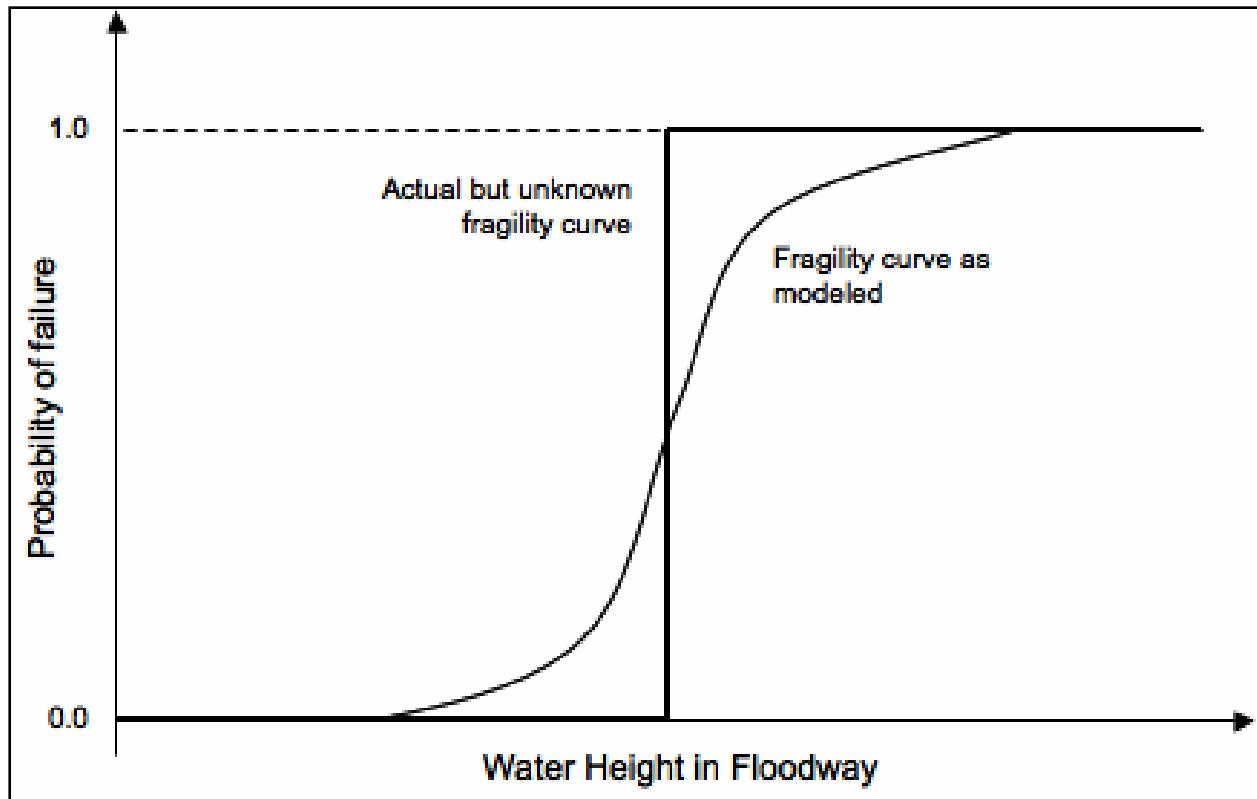


Figure 10-2. The actual but unknown fragility curve for a section is a step function at the loading conditions that causes failure; this is approximated by an “S-shaped” probability curve reflecting what is known about the levee and loads.

All two-dimensional sections within a reach are considered to be the same with respect to those properties relevant to risk and reliability; thus, the fragility of the levee (i.e., probability of failure as a function of load) is modeled as the same everywhere within an individual reach.

In actuality, the fragility at a particular cross section within a reach is a step function at that deterministic loading condition that initiates failure (Figure 10-2). Presumably, there is such a failure loading condition, which if it occurs will cause failure; however, that loading condition varies along the length of the reach and is not precisely known before a failure occurs. The S-shaped fragility curve reflects uncertainty about the unique loading condition that causes failure at a particular location.

Philosophically, the uncertainty represented by the S-shaped fragility curve is epistemic; that is, it reflects lack of knowledge. Gathering more information, for example, by performing a proof loading, can dramatically change the fragility curve. This is suggested in Figure 10-3, taken from McDonald (2002), which shows fragility curves estimated before and after high water—that is, a proof loading—is observed on an embankment, under which the structure performs successfully. Before the loading, the fragility curve is estimated as curve B. Then a higher water load is successfully resisted, and the fragility curve is updated to curve C. Nothing has changed in the structure; only the state of knowledge about the dam has changed. It may be that the water level that actually causes failure is that shown in curve A; but this is unknown with certainty until such a loading is experienced.

The S-shaped fragility curve reflects uncertainty about the unique loading condition that causes failure at a particular location. Part of the uncertainty in the S-shaped fragility curve has to do with systematic uncertainties, such as the average soil strength or average permeability along the reach, or the simplifications introduced in the performance models that apply everywhere; but another part has to do with spatial variability within the reach. Some cross sections may be more fragile than others, but without detailed site characterization one can't know exactly where these sections are, or how much more fragile they are than the stronger sections. This part of the S-shaped fragility curve also reflects epistemic uncertainty, because if more detailed information were available the weak spots could be identified and perhaps treated as separate reaches. But, the detailed information is not available, which is why those potentially weak sections are included in the present reach, and thus the true fragility curve varies from one location to another in an uncertain way. In most risk and reliability analysis, this spatial variability is modeled as if it were aleatory—that is, as if it were random—and stochastic models are used to characterize it.

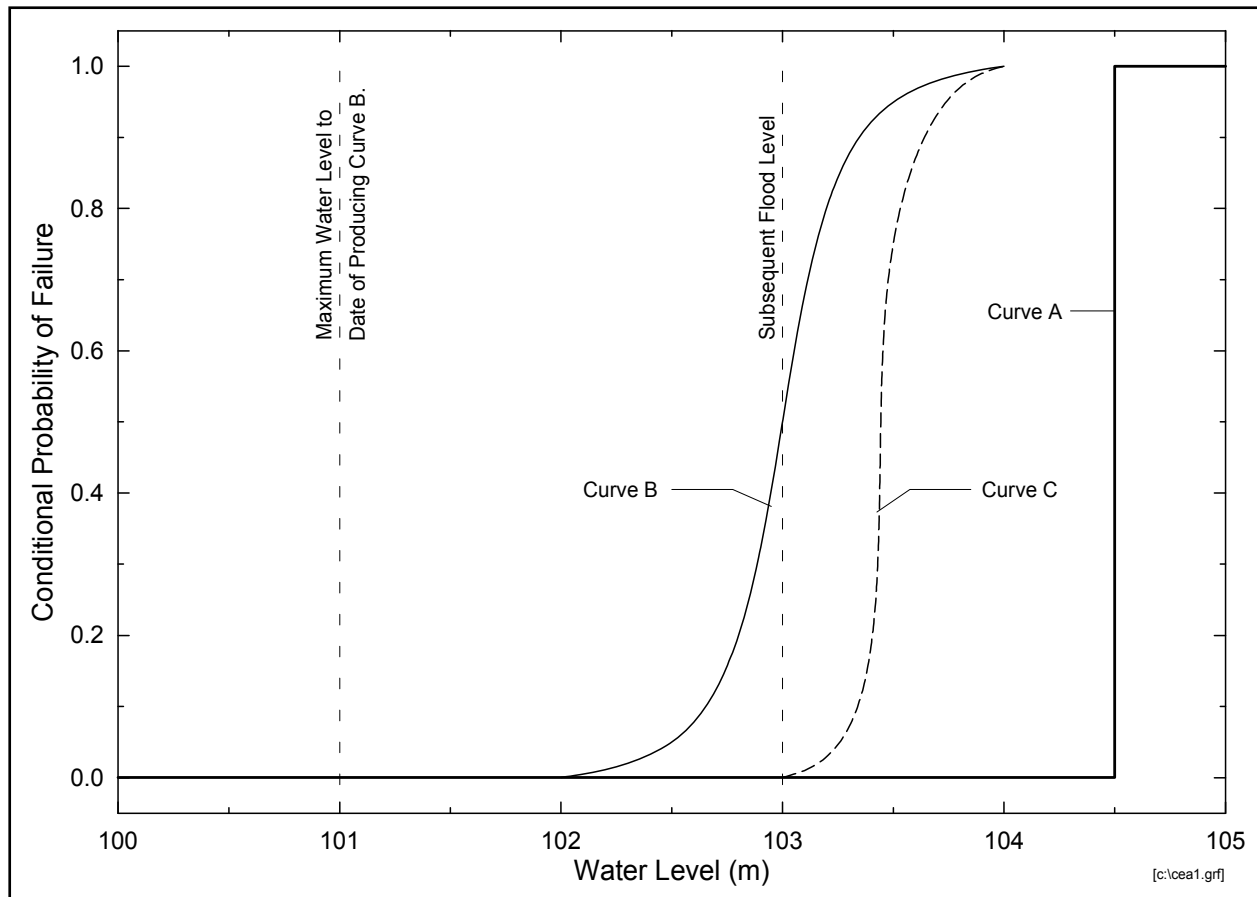


Figure 10-3. Hypothetical fragility curves for an earth dam as a function of pool elevation (McDonald 2002).

This separation of uncertainty in how fragility curves are modeled within a single reach introduced a length effect caused by the way we model uncertainty. Matheron (1989) is famously quoted as having said, “probability is in the model, not in the world.” The systematic uncertainties, which cause a bias in the modeling, affect every section within the reach in the same way: if the mean soil permeability is underestimated at one spot it is similarly underestimated everywhere. The spatial variability, on the other hand, does not affect every section in the same way: some spots are more fragile and some are less fragile. Therefore, the longer the reach, the higher the probability of encountering a particularly weak variation. Note, this length effect is due to incomplete knowledge: collect enough information and it goes away, but there is seldom that much information.

Reach information was summarized in a *systems definition file*, which is a flat-file data base summarizing physical characteristics of each reach along with eight-point fragility curves. An example for the first 33 defined reaches is shown as Table 10-2.

Allowance for sea-level rise and subsidence

In follow on risk and reliability studies, for example those addressing the 2011 (100-year) system, an allowance is made for a potential of two (2) feet of combined sea-level rise and subsidence. In the IPET risk and reliability studies of the pre-Katrina conditions and “current” conditions as of June 2006, no allowance is made for future sea-level rise and subsidence.

Engineering uncertainties in the reliability model

Four categories of engineering uncertainty were included in the reliability analysis:

1. Geological and geotechnical uncertainties, involving the spatial distribution of soils and soil properties within and beneath the HPS.
2. Structural uncertainties, involving the performance of man-made systems such as levees, floodwalls, and point features such as drainage pipes; and the engineering modeling of that performance, including geotechnical performance modeling.
3. Erosion uncertainties, involving the performance of levees and fills around floodwalls during overtopping, and at points of transition between levees and floodwall, in some cases leading to loss of grade or loss of structural support, and consequently to breaching.
4. Mechanical equipment uncertainties, including gates, pumps, and other operating systems, and human operator factors affecting the performance of mechanical equipment.

The reliability analysis takes water elevations and wave characteristics from the hurricane loading conditions as given, and calculates conditional probabilities of failure for specifically stated water elevations. Thus, hurricane effects, wind loads, water heights, and other factors of the loading conditions are not considered to be uncertainties in the reliability modeling. Uncertainties in water elevations from hurricane conditions are convoluted with the results of the reliability analysis in the systems risk model to generate marginal (i.e., unconditional) probabilities.

Definition of Breach

Breaches that lead to breach of the drainage basin perimeters were associated with four principal failure modes: (1) levee or levee foundation failure, (2) floodwall or floodwall foundation failure, (3) levee or floodwall erosion caused by overtopping and wave run-up, and (4) failure modes associated with point features such as transitions, junctions, and closures. The Performance Team found no failures in the HPS which originated in structural (as opposed to geotechnical) failure of the I-wall or T-wall components. All documented failures at I-wall and T-wall locations were geotechnical in nature, with structural damage resulting from the geotechnical failures.

Each reach within the drainage basin perimeter was analyzed and tracked separately, so that the number of breached reaches and their location around the drainage basin perimeter was known for each repetition of the HPS risk model.

The pumping system may have had a mitigating effect on the water elevation of each drainage basin. If the capacity of the pumping system was exceeded by the inflow volume from a single breach then the number and location of the breaches may not matter and the pumping system can be ignored in the risk analysis. If, however, the inflow volume is within the capacity of the pumping system to remove, then the probability that the pumps are operating must also be calculated. The Risk Team relied on other IPET Teams to clarify technical issues. Technical input from other Teams helped the Risk Team determine the level of detail with which failure states need to be represented.

Table 10-2. Reach systems definition table (partial section, schematic only); showing geometric, material, and design properties to the left; and fragility estimates to the right as a function of still-water level with respect to design elevations.

Reach	Length (ft)	Weighted elevation (ft) (1) (NAVD88 2004.65)	Fragility water elevation (ft) (2) (NAVD88 2004.65)	Reach type	Foundation material type (H, C, S)	Polder reference	Subpolder reference (3)	PF fragility curve (breach no overtopping)				PF fragility curve (breach overtopping)			
								Erosion Modifier for W/L	Minimum Elevation for Pf=0	Design Elev. (L) 6ft from TOW (W)	Top of Levee/Top of Wall	1/2 ft Overtopping	1 ft Overtopping	2 ft Overtopping	3 ft Overtopping
1	2,290	11.5	9.52	W	H	2	NOE5	1	0.0000	0.0023	0.0034	0.0000	0.0569	0.7464	0.8787
2	97	13.3	10.27	L	H	2	NOE5	1	0.0000	0.0000	0.0000	0.0002	0.0134	0.0565	0.0658
3	2,325	13.5	11.50	W	H	2	NOE5	1	0.0000	0.0023	0.0035	0.0000	0.0094	0.5269	0.8825
4	2,330	13.3	10.25	L	H	2	NOE5	1	0.0000	0.0002	0.0003	0.0047	0.2760	0.7524	0.8049
5	2,270	13.7	11.72	W	H	2	NOE5	1	0.0000	0.0023	0.0034	0.0000	0.0184	0.6484	0.8764
6	19,112	12.9	9.93	L	H	2	NOE5	1	0.0000	0.0019	0.0029	0.0377	0.9293	1.0000	1.0000
7	1,474	12.1	10.12	W	H	2	NOE5	1	0.0000	0.0015	0.0022	0.0000	0.0370	0.5865	0.7427
8	2,724	12.6	9.64	L	H	2	NOE5	1	0.0000	0.0003	0.0004	0.0055	0.3145	0.8045	0.8520
9	33032	18.6	15.64	L	H	2	NOE5	1	0.0000	0.0033	0.0049	0.0642	0.9897	1.0000	1.0000
10	133	18.6	15.64	L	H	2	NOE1	1	0.0000	0.0000	0.0000	0.0003	0.0183	0.0766	0.0891
11	27,665	15.1	12.13	L	H	2	NOE1	1	0.0000	0.0028	0.0041	0.0541	0.9784	1.0000	1.0000
12	8,942	16.7	13.72	L	H	2	NOE1	1.05	0.0000	0.0009	0.0013	0.0187	0.7359	1.0000	1.0000
13	7,190	17.7	14.65	L	H	2	NOE1	1.1	0.0000	0.0007	0.0011	0.0158	0.6828	1.0000	1.0000
14	22,257	15.5	12.50	L	H	2	NOE1	1.1	0.0000	0.0022	0.0033	0.0480	0.9714	1.0000	1.0000
15	111	17.5	15.50	W	H	2	NOE1	1.05	0.0000	0.0001	0.0002	0.0000	0.0010	0.0624	1.0000
16	382	20.7	18.70	W	H	2	NOE2	1.05	0.0000	0.0004	0.0006	0.0000	0.0033	0.1988	1.0000
17	10,210	16.8	13.80	L	H	2	NOE2	1.1	0.0000	0.0010	0.0015	0.0223	0.8042	1.0000	1.0000
18	10,757	17.9	14.92	L	H	2	NOE2	1.1	0.0000	0.0011	0.0016	0.0000	0.0923	1.0000	1.0000
19	9,318	20.8	18.75	W	H	2	NOE3	1.05	0.0000	0.0093	0.0139	0.0000	0.2220	1.0000	1.0000
20	7,905	17.2	14.19	L	H	2	NOE3	1.1	0.0000	0.0008	0.0012	0.0173	0.7170	1.0000	1.0000
21	539	16.7	14.72	W	H	2	NOE3	1.05	0.0000	0.0005	0.0008	0.0000	0.0144	0.4758	1.0000
22	5616	16.7	14.72	W	H	2	NOE4	1.05	0.0000	0.0056	0.0084	0.0000	0.1404	0.9988	1.0000
23	15,940	14.0	11.02	L	H	2	NOE4	1.1	0.0000	0.0016	0.0024	0.0346	0.9216	1.0000	1.0000
24	1,820	12.1	10.14	W	H	2	NOE4	1.05	0.0000	0.0018	0.0027	0.0000	0.0077	0.4868	1.0000
25	3,453	13.4	10.35	L	H	2	NOE4	1.1	0.0000	0.0003	0.0005	0.0076	0.4239	1.0000	1.0000
26	1,587	14.5	12.50	W	H	2	NOE4	1.05	0.0000	0.0016	0.0024	0.0000	0.0067	0.4410	1.0000
27	2,348	13.8	10.77	L	H	2	NOE4	1.1	0.0000	0.0002	0.0004	0.0052	0.3127	1.0000	1.0000
28	3,803	12.2	9.22	L	H	2	NOE4	1.05	0.0000	0.0004	0.0006	0.0080	0.4323	0.9895	1.0000
29	537	12.4	6.37	W	H	2	NOE4	1.05	0.0000	0.0550	0.1129	0.0000	0.0023	0.1787	1.0000
30	526	12.6	9.60	L	H	2	NOE5	1.05	0.0000	0.0001	0.0001	0.0011	0.0753	0.4676	1.0000

Hurricane Protection System

The HPS for each drainage basin has four components: (1) levees, (2) I-walls (which may be atop levees), (3) T-walls (which may be atop levees), and (4) transitions and closures. The reliability analysis examined the performance of the each of component, separately and in combination.

The following structures in the HPS were not independently evaluated for their failure modes: (1) concrete aprons associated with some I-walls, and (2) sheetpiles with a short (3 to 4 ft) concrete cap. Either could be addressed with failure modes developed for I-walls, but were not included in the present study.

The following failure modes or contributing factors were not considered in the reliability analysis:

1. Internal erosion (piping) of levees due to seepage; note, this is in contrast to high pore pressures in sand strata, which was considered, as in the vicinity of the London Avenue Canal or the northern end of the IHNC. Internal erosion may be reconsidered in later studies.
2. The effects of maintenance on the HPS capacity over time. Improper maintenance or neglect can lead to reduced capacity of the levees; in particular, gates and other moving components also require maintenance. Trees, landscaping, and pools were observed on protected embankments after Hurricane Katrina, indicating a lack of code enforcement and maintenance of the levees. However, there was insufficient information to include maintenance considerations.
3. Impact by a barge, floating debris, or other large object on the floodwalls or levees.
4. Failure of 3-bulb water stops between I-wall sections.

Component Performance

For each component, a performance level was defined such that its occurrence corresponded to a failure to perform an intended function. The critical components within the HPS, as stated above, are the levees, I-walls, T-walls, and transitions and closures. These components can fail in a variety of modes. For each mode of failure a limit state was defined, which, if it were to occur, would result in a failure to keep water out of the drainage basin.

Engineering models of the mechanics of component performance are limited in their ability to explicitly model a failure state. As a result, an analysis is usually carried out for incipient failure by examining the limits of stability. If this state is equaled or exceeded, the structure or component is expected to fail to perform as intended. Incipient failure models were usually similar to design calculations, and in many cases were adapted from the GDM's.

For the purpose of evaluating the performance of the levees and floodwalls, *failure* was defined as complete breaching, which allowed water to enter the drainage basin. This failure

occurred in two ways: (1) loss of levee or wall stability when the strength of the levee or wall and its foundation was insufficient to withstand the forces placed upon the structure for a given water elevation below the top of the wall or levee (no overtopping); or (2) overtopping caused the protected side of the levee or wall to erode substantially and result in a wall or levee breach, which allowed water to flow freely into the drainage basin.

System Failure

Depending on the performance of individual components in the HPS, various outcomes may result. For purpose of evaluating the performance of the HPS, the outcome of most interest is whether a protected area was flooded or not.

The HPS was assumed to “fail” for the purposes of the risk calculations if flooding occurred in a protected area, beyond that expected from rainfall and runoff which can be handled by pumping. Given this definition, a failure of the HPS occurred even if the components making up the system did not fail, for example, if levees or walls were overtopped but not breached. Note, the main IPET report distinguishes between “engineering failures” and “breaching;” but the risk analysis does not.

Flooding can occur as a result of chains of events occurring individually or in combination. Among these are:

1. Levee or floodwall breaching.
2. Inflow into an area due to levee or flood wall overtopping that does not result in breaching, and which exceeds the capacity of the pumping system.
3. Inflow to an area that occurs as a result of rainfall.
4. Inflow to an area that occurs when the capacity of the pump system is exceeded as a result of backflow through pump houses.

Flooding that occurs as a result of rainfall or transient overtopping in most cases will not be as consequential and may be mitigated by the pumping system.

Geological Profile

The stratigraphy of the New Orleans area is Pleistocene and Holocene in age. Observed levee and floodwall failures during Katrina principally involved shallow Holocene aged sediments. Generally, sediments constituting the New Orleans area are less than 7,000 years old (Holocene). Formation of the present day New Orleans began with the rise in global sea level, beginning about 12,000 to 15,000 years before present.

A typical profile for much of the New Orleans HPS shows a layer of fill at the top, underlain by organic clays (‘marsh’), in turn underlain by lacustrine (distributary) plastic clays, in turn

underlain by stiffer Pleistocene clays. Fig. 10-1 shows the profile under the New Orleans East (NOE) Lakefront Levee, which is typical of this profile.

As sea level rise slowed, five short-lived delta complexes evolved across the Louisiana coast by depositing Mississippi River sediments through branching distributary channels. These channels transported and deposited fluvial sediments along the margin of the delta and built into shallow coastal water. Distributary channels from one of these, the St. Bernard delta, are responsible for filling the shallow Gulf waters in the greater New Orleans area (Frazier 1967). On top of these distributary clays grew cypress swamps which would eventually become the marsh formations. On top of these came fills, mostly clayey, on which the present levees and floodwalls were constructed.

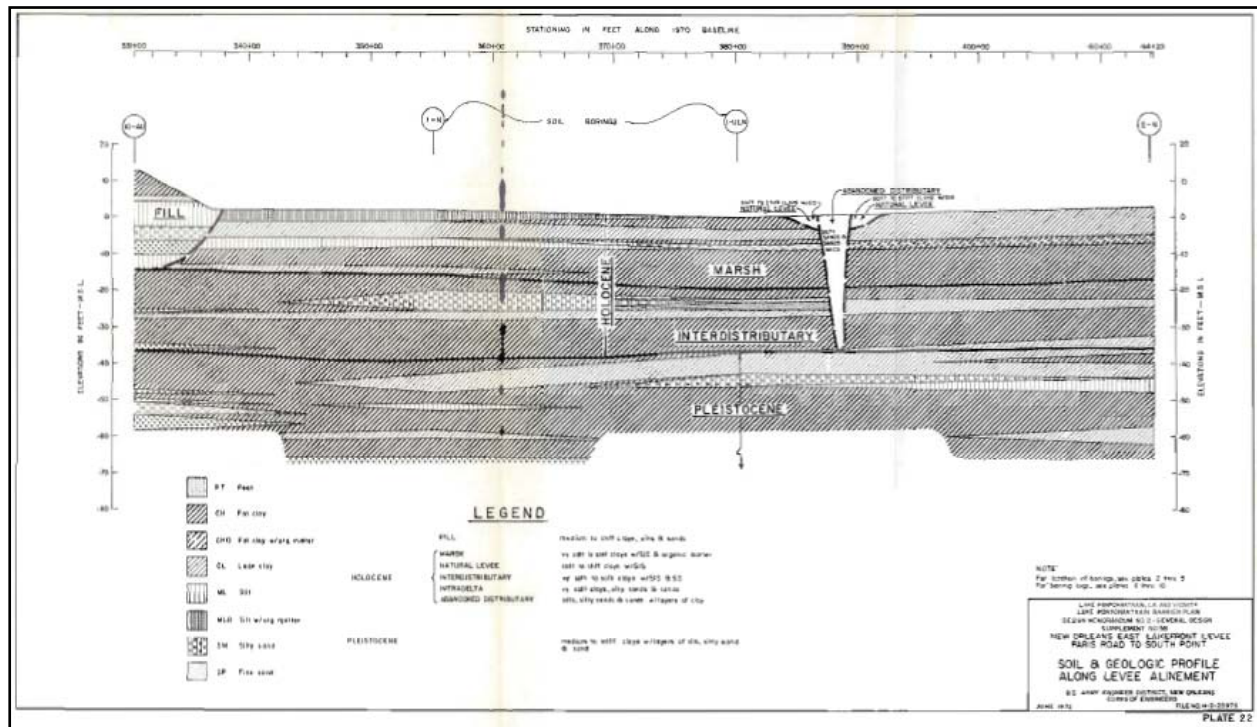


Figure 10-4. Typical geological profile, NOE lakefront section (USACE 1972).

The spatial variability of this typical section has to do with variations in thickness of the various strata, and inter-bedding of sand or silt lenses and other local conditions. In some places, for example, the marsh can be thicker than average, as for example in the vicinity of the 17th Street Canal failure.

Equally important to the performance of levees in Orleans East Bank (OEB) and NOE is the Pine Island Beach deposit, a buried, barrier island or beach dating to ca. 5,000 years before present (see Fig. 10-2). This feature extends northeast along the southern shore of Lake Pontchartrain, adjacent to and north of the Metairie and Gentilly ridges, former natural levees of the Mississippi. Sea level was 10 to 15 ft lower than the current level when the beach ridge formed. Consequently, foundation soils beneath OEB and NOE are affected by this buried sand,

which provides a high permeability channel for pore pressures. Under the London Avenue Canal and the northern end of the IHNC, the sand rises close to the present ground surface.

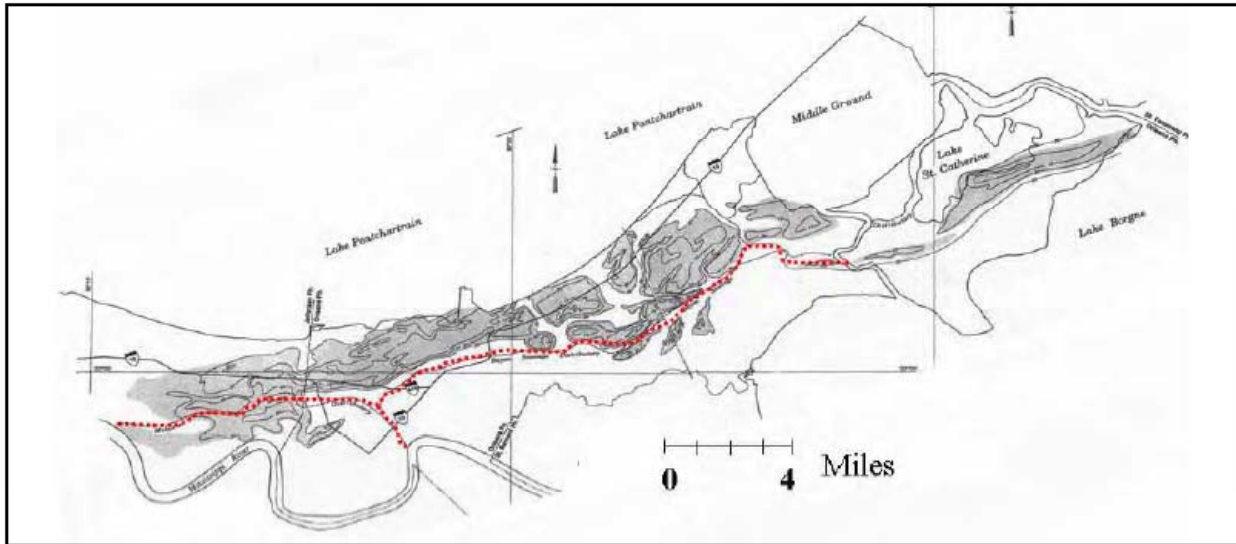


Figure 10-5. Pine Island (buried) beach ridge, and locations of the canal breaches (after Saucier 1994). The 17th Street breach is located behind the axis of the beach ridge while the London Ave. Canal breaches are located on the axis of the ridge. Bayou Metairie is identified in red and forms the Bayou Sauvage distributary course.

Soil Engineering Properties

The principal uncertainty contributing to probability of failure of the levee and I-wall sections in the reliability analysis is soil engineering properties, specifically undrained shear strength, S_u . Uncertainties in soil engineering properties are presumed to have two main components: (1) data scatter caused by actual variation of soil properties in space and by random measurement errors, and (2) systematic errors caused by limited numbers of measurements (i.e., statistical estimation error), and by measurement bias (see Figure 10-6).

Uncertainty model

The variance in soil properties is a composition of these four terms,

$$Var(S_u) = Var(x) + Var(e) + Var(m) + Var(b) \quad (10-1)$$

in which $Var(\cdot)$ is variance, S_u is the soil property as input to the analysis (in this case, undrained strength), x is the soil property *in situ*, e is measurement error (noise), m is the spatial mean of the soil property (which has some error due to the statistical fluctuations of small sample sizes), and b is a model bias or calibration term caused by systematic errors in measuring soil engineering properties.

The NOE drainage basin is used here to describe the reliability analysis approach. Analyses of the other drainage basins are similar. The soil profile underlying NOE consists typically of clayey fill overlying ‘marsh’ (OH, CH), in turn overlying ‘distributary clays’ (CH), as shown in Figure 10-4. Critical sections in the GDMs and failures observed during Katrina occur in these uppermost strata. The engineering properties of deeper, stronger strata of the Pleistocene formations were not statistically characterized.

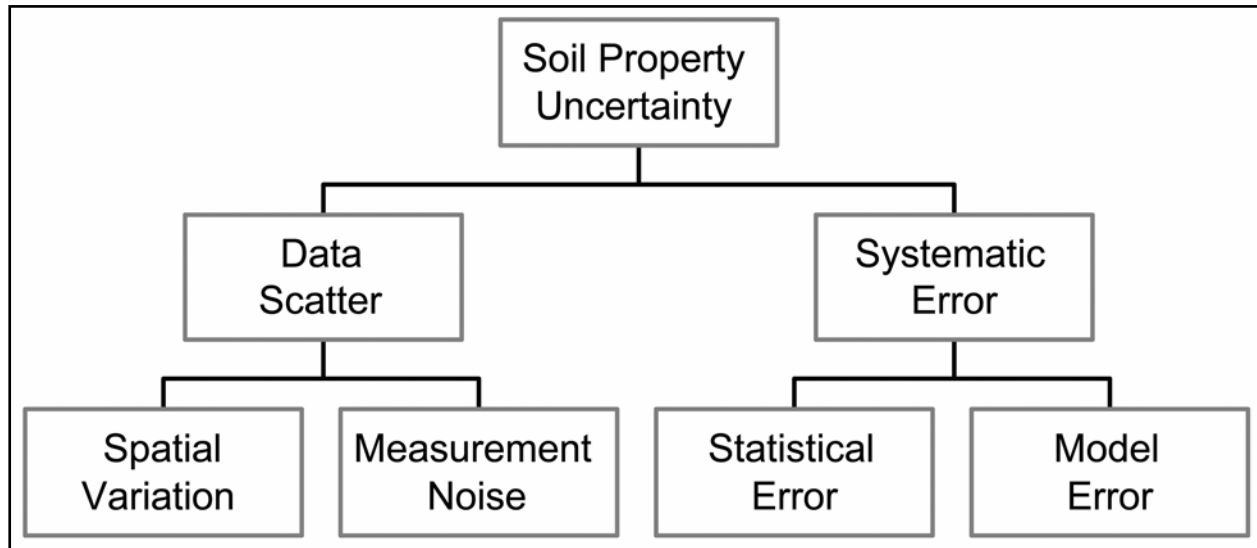


Figure 10-6. Sources of soil property uncertainty in geotechnical reliability model.

Measured Q-test results reported in the GDMs of NOE are shown as histograms in Figure 10-9.

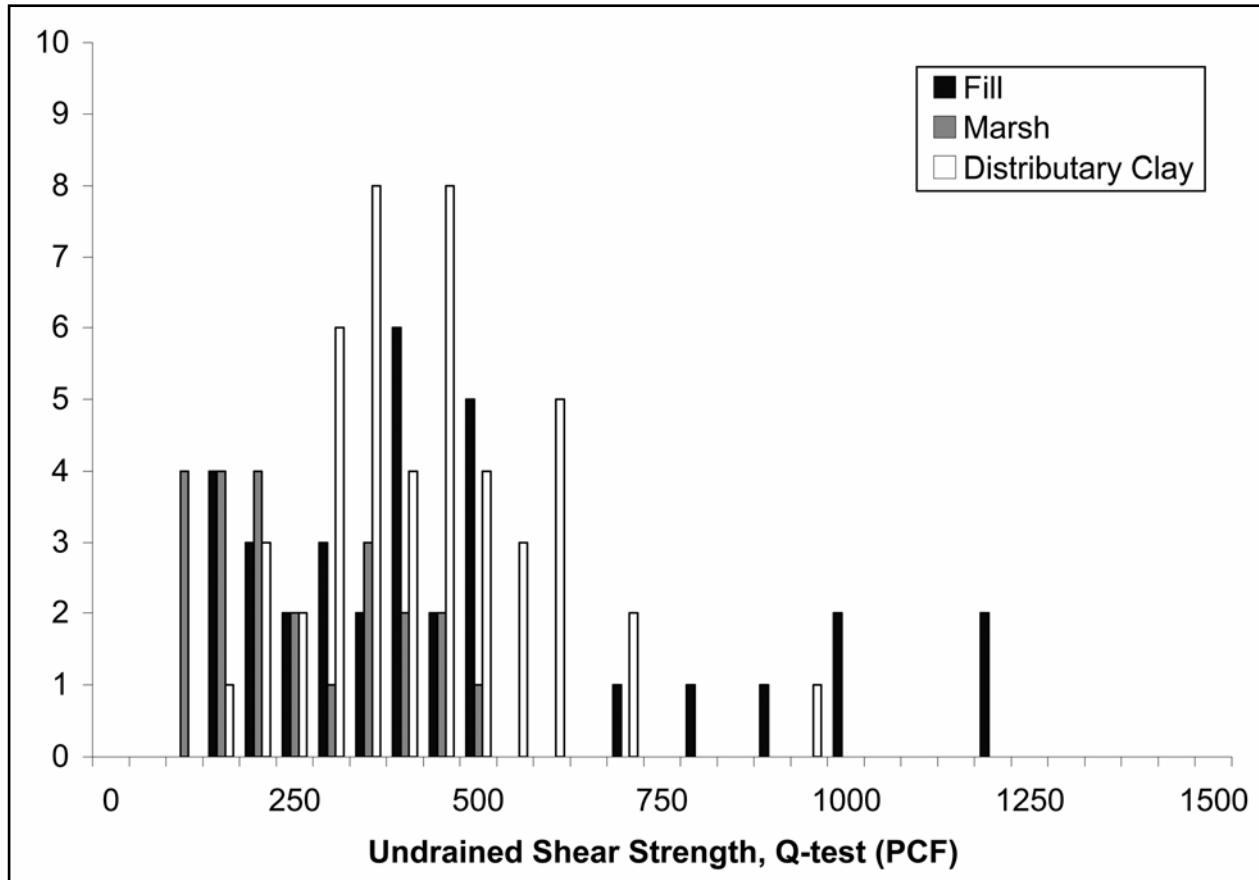


Figure 10-7. Second-moment statistical properties of these data are shown in Table 10-3. Test values larger than 750 PCF were assumed to be local effects and removed from the statistics to the right in the table. These moments were used in subsequent calculations.

Spatial variation

The spatial pattern of soil variability is characterized by auto-covariance functions. These describe the covariance of soil properties as a function of separation distance. Soils whose properties vary erratically from spot to spot display little spatial covariance, while soils whose properties vary with more waviness display more spatial covariance.

The auto-covariance function of a soil property z is defined as $C_z(\delta) = E[z(i), z(i + \delta)]$, in which $E[\cdot]$ is expectation, $z(i)$ is the soil property at some location i , and $z(i + \delta)$ is the property at another location at distance δ from the first. The autocorrelation function is found by normalizing the auto-covariance by the variance, $R_z(\delta) = E[z(i), z(i + \delta)] / Var^{-1}(z)$. The auto-covariance distance is indexed as that separation distance at which $R_z(\delta) = e^{-1}$. This is a representative or characteristic length of the spatial correlation.

The auto-covariance function can only be estimated for distances at least as great as the minimum spacing among observations, that is the minimum boring spacing in the present case. The minimum boring spacings in NOE are on the order of many hundred feet, with some

spacings between adjacent borings as much as several thousand feet. To supplement the information in the GDMs, post-Katrina borings made in the vicinity of the 17th Street and London Avenue Canal breaches were used to estimate auto-covariance functions, and correspondingly the magnitude of measurement noise and the autocorrelation distance.

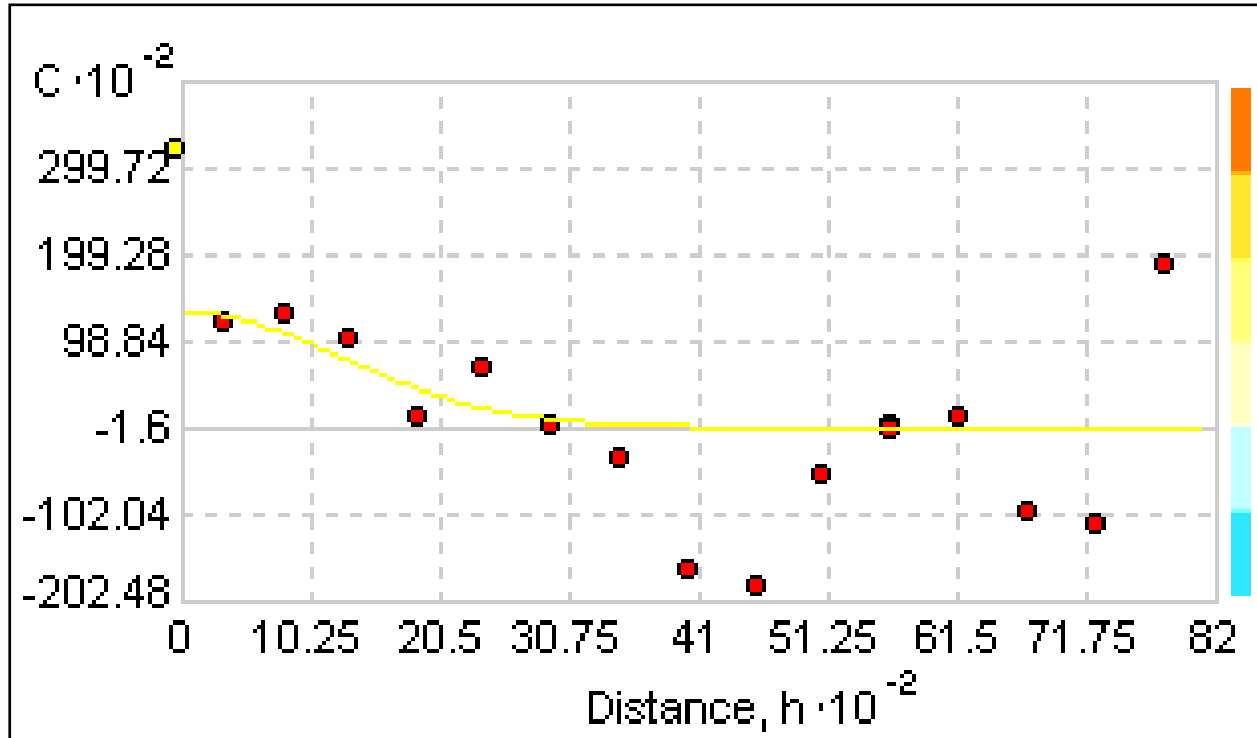


Figure 10-8. Typical auto-covariance function for CH soils in 17th Street Canal area post-Katrina borings, undrained strength (PCF) from Q tests at uniform depth below grade.

Statistical estimates of the auto-covariance were made using the ESRI *Geostatistical Analyst*[®], an application running in *ArcMap*[®]. Results for the undrained strength (Q-tests) of London Avenue the Distributary Clay clays are shown in Figure 10-8. Analyses for Marsh and Fill show similar patterns.

Table 10-3. Statistics of undrained strength data (Q-tests), NOE General Design Memoranda. COV is the coefficient of variation, or standard deviation divided by the mean.						
Parameter	All data			Data less than 750PCF		
	Fill	Marsh	D.Clay	Fill	Marsh	D.Clay
Mean (PCF)	452	405	238	333	392	238
Std Dev (PCF)	297	154	124	142	132	124
COV (data scatter)	0.66	0.38	0.52	0.43	0.34	0.52

Measurement noise

Soil strength is measured destructively, therefore replicate measurements cannot be used to estimate the magnitude of random measurement error. However, the spatial covariance structure provides an indirect way to make the estimate (DeGroot 2006). Assuming that the measurement z of soil property x is corrupted by a zero-mean error e that is independent from one measurement to the another and independent of the value x , the measurement can be expressed as $z=x+e$. The auto-covariance function of z is the summation of the auto-covariance functions of x and of e : $C(z)=C(x)+C(e)$. But, the auto-covariance function of e is a spike at the origin and zero otherwise. Thus, the difference between the intersection of the observed auto-covariance function of z extrapolated back to the origin, and the total variance $\text{Var}(z)$, provides an estimate of the variance of the error, $\text{Var}(e)$.

The conclusions drawn from these auto-covariance analyses were: (1) the measurement noise (or fine-scale variation) in the Q-test data is roughly 1/2 to 3/4 the total variance of the data (suggesting the COVs in the top row of Table 10-4); (2) the representative auto-covariance distance in the horizontal direction is on the order of 1000 feet; (3) the representative auto-covariance distance in the vertical direction is assumed to be on the order of 1/100 of the horizontal distance, or about 10 feet, although there are too few Q-test data in individual borings to statistically estimate this value.

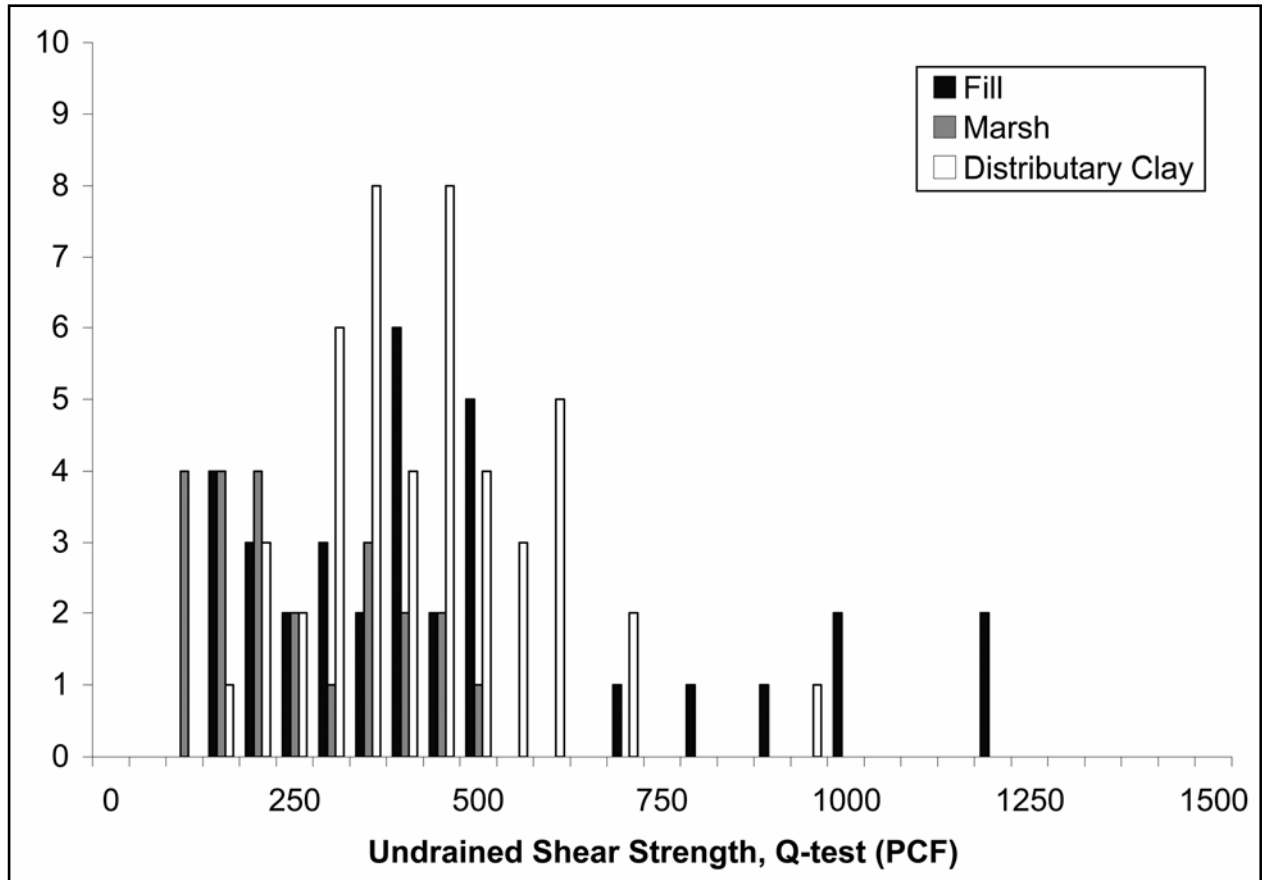


Figure 10-9. Histograms of undrained strength data (Q-tests), by soil type, NOE General Design Memoranda: (black) Fill, (gray) Marsh, (white) Distributary Clay.

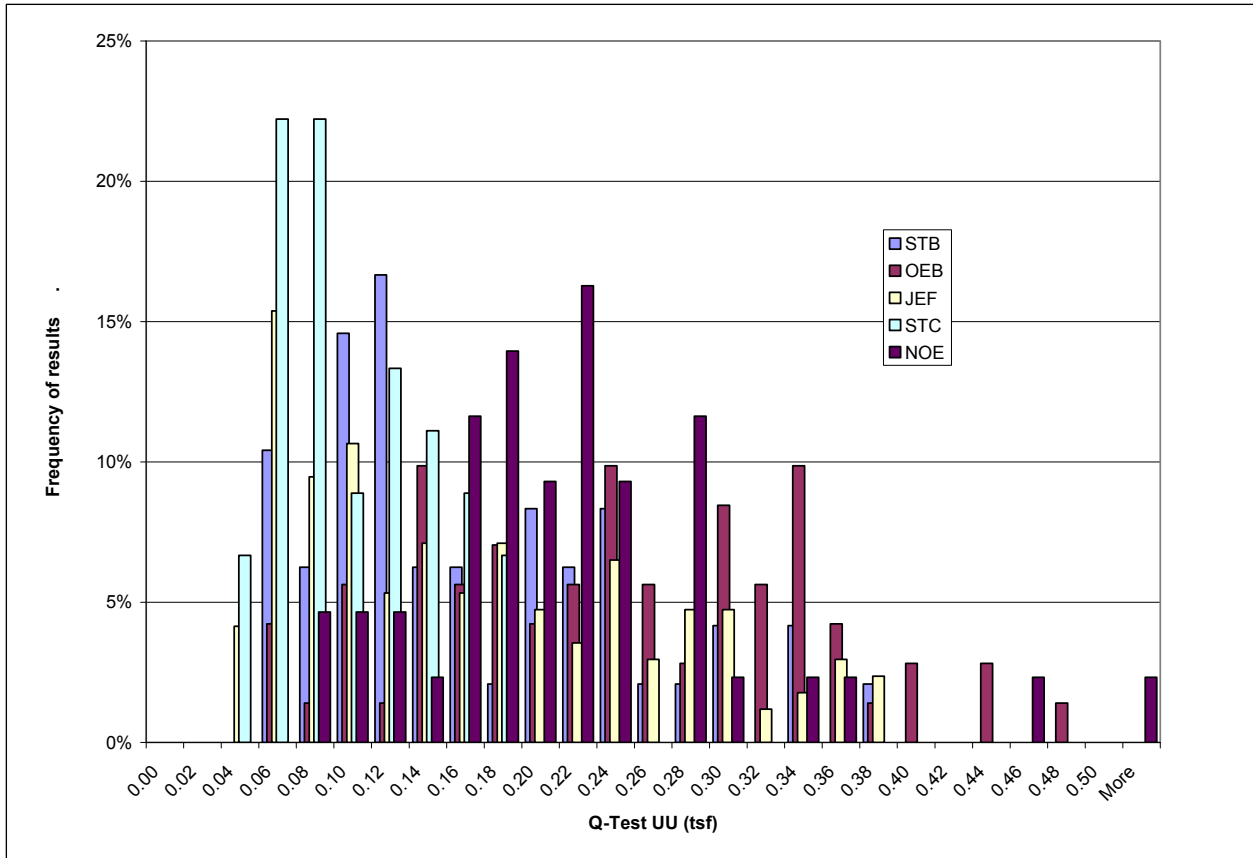


Figure 10-10. Histograms of undrained strength data (Q-tests), by parish, from USACE General Design Memoranda of various projects.

Statistical error

Statistical estimation error in the mean soil property is caused by limited numbers of data within a reach and is approximated from the standard error of sampling. The variance of the error is approximated as $Var(m) \approx Var(x)/n$, in which m is the mean soil property, x is the spatial variation component of data scatter, and n is the number of measurements (Table 10-4).

Table 10-4. Estimates of component uncertainties to soil engineering property model.			
Component	Fill	Marsh	D.Clay
Spatial COV	0.20	0.17	0.25
Number of measurements	48	21	23
Statistical error in mean	0.06	0.07	0.11
Model bias	0.1	0.1	0.1

Geotechnical model error

Model bias was calculated based on a comparison of the detailed modeling results of the Performance Team compared to the more simple general method of planes used in the GDMs. On average, the GDMs calculated factors of safety that were approximately 10% lower than more precise model analysis, varying from about 7% to about 18% (IPET v.V 2006).

Fragility Curves

Fragility curves summarize the probability of components reaching their respective limit states (i.e., failure), conditioned on levels of water elevation from hurricane conditions. For example, the fragility curve of Figure 10-11 schematically represents the probability of failure by deep-sliding instability of a levee section as a function of water height. Design basis water elevation indicates the probability of failure at the design water level (i.e., 3 ft from the top of the levee).

Fragility curves for levees and floodwalls were calculated for two conditions: (1) global stability without overtopping, for which reliability was calculated at two water elevations, design elevation and top of levee, and a smooth curve approximated to lower water elevation at sea level; and (2) overtopping with subsequent erosion, for which reliability was estimated from empirical experience during Katrina at four water elevations of overtopping: ½ foot, 1 foot, 2 feet, and 3 feet above the top of levee or flood wall.

Once the fragility curves for each component failure mode were determined, they were input to the HPS risk model, which is based on event tree analysis. For each sequence in the event tree, a ‘sequence’ fragility curve is determined by evaluating the event tree logic at each successive water elevation level. Once each sequence of events has been evaluated, the composite or total fragility for system failure can be determined for each system performance state of interest (e.g., no flooding has occurred in any area protected by the HPS, or flooding occurred as a result of levee or floodwall failure, or flooding occurred as a result of overtopping) by simply summing the fragility curves for the sequence of events for the same state.

Reliability assessments were performed for individual reaches of approximately homogeneous structural type, elevation, geotechnical conditions, and water elevations. This resulted in fragility curves for each reach by mode of failure. Such fragility curves represented the aleatory (i.e., random) uncertainties from one hurricane to another.

Failure mode	Hazard	Models and parameters	Source of inputs	Principal uncertainty
Static instability	Still-water surge; weak foundation soils	Limiting equilibrium stability	IPET v.IV, V; Soil test data; Design Memoranda; In situ surveys	Soil properties; Still water levels; Existing elevations; Geotechnical model
Under seepage	Still-water surge; high permeability soils	Flownet calculations; Limiting equilibrium stability	IPET v.IV, V; Soil test data; Design Memoranda; In situ surveys	Soil properties; Still water levels; Existing elevations; Geological profile geometry
Still-water overtopping and scour	Still-water surge; erodable fill	Empirical correlations from post Katrina data	IPET v.IV, V;	Still water levels Soil fill properties Existing elevations Scour model
Transition point feature erosion	Still-water surge; erodable fill	Empirical observations during Katrina	IPET v.V;	Still water levels Soil fill properties Existing elevations Scour model
Wave run-up	Wave heights and periods; erodable fill	Empirical (Dutch) correlations and model test results	IPET v.IV	Wave height and period; Still water levels; Existing elevations

Levee fragility, no overtopping

Engineering performance models were adapted from the GDM for the respective reaches of levee. Engineering parameter and model uncertainties were propagated through those calculations using a first-order, second-moment approximation to obtain approximate fragility curves as a function of water height. The geotechnical models used in the GDMs were calibrated against the analysis work of the Performance Team which used more refined calculations.

The reliability analysis was based on limiting equilibrium calculations of factor of safety against instability. For levees, the analysis was based on GDM calculations of factor of safety against wedge instability (Figure 10-12). The calculations were based on undrained ($\phi=0$) failure conditions. Undrained strengths of soils underlying the levees and walls are based on Q-test (unconsolidated -undrained) results.

Best estimate calculations

Best estimate calculations were based on average (mean) soil properties, adjusted from calculations in the GDMs, which used factored average soil properties. That is, the calculation of factor of safety in the GDMs was not based on mean observed undrained strengths, but factored strengths, using a reduction factor of 1.2 to 1.3. These were corrected for the reliability analysis to yield a mean factor of safety.

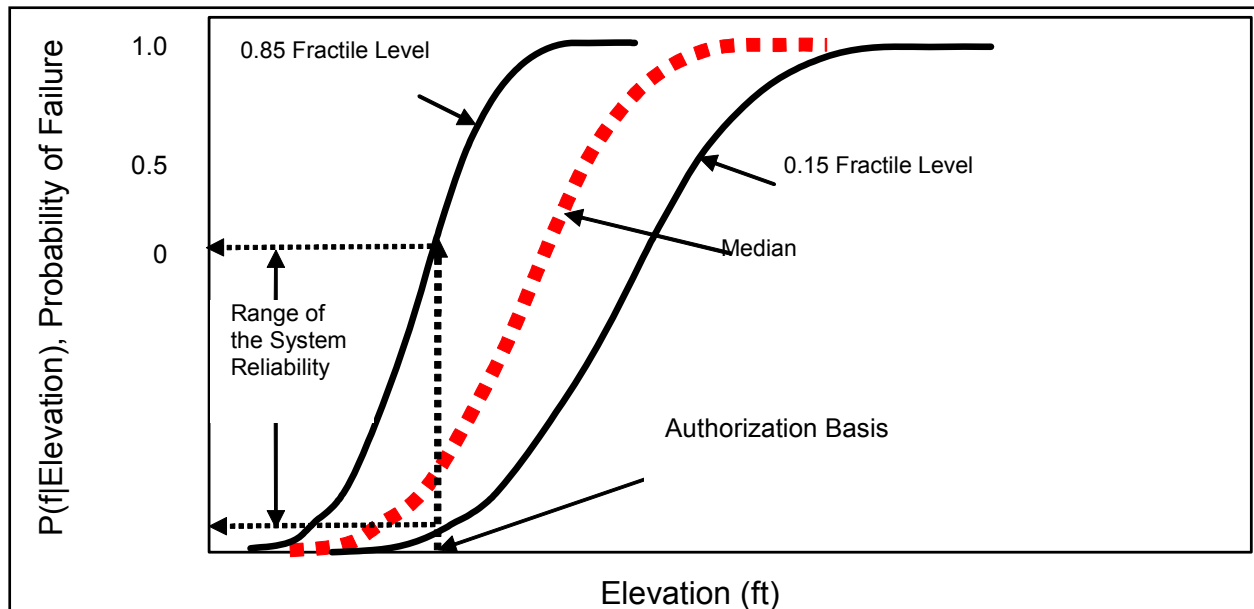


Figure 10-11. Schematic fragility curve

Table 10-6. Soil property uncertainty by parish									
PARISH	MEAN SU (TSF)	POINT COV	POINT COV less noise	SPATIAL reduction	COV Averaged	N	DEPTH of data	BOUND for outliers	STD DEV in mean
OEB	0.24	0.43	0.22	0.70	0.15	71	0 to -40	0.4	0.05
STB	0.16	0.53	0.27	0.70	0.19	64	0 to -40	0.4	0.07
NOE	0.22	0.58	0.29	0.70	0.20	43	0 to -40	0.4	0.09
STC	0.09	0.41	0.21	0.70	0.14	45	0 to -40	0.4	0.06
JEF	0.16	0.62	0.31	0.70	0.22	169	0 to -40	0.4	0.05

Uncertainties in undrained shear strength were propagated through the GDM calculations to estimate a coefficient of variation in the calculated factor of safety. The factor of safety was assumed to be normally distributed, and a fragility curve was approximated through a limited number (typically two) of calculation points.

Soil property uncertainty in the form of coefficients of variation for undrained soil strengths underlying the levees and walls was propagated through the limiting equilibrium wedge stability calculations to obtain coefficients of variation on factors of safety, shown in Table 4. In most cases, the stability analyses were linear functions of undrained soil strength so that the coefficient of variation of the factor of safety was the same as the coefficient of variation of the input soil strengths. The mean factor of safety was taken as that calculated in the GDMs, adjusted for factored strengths.

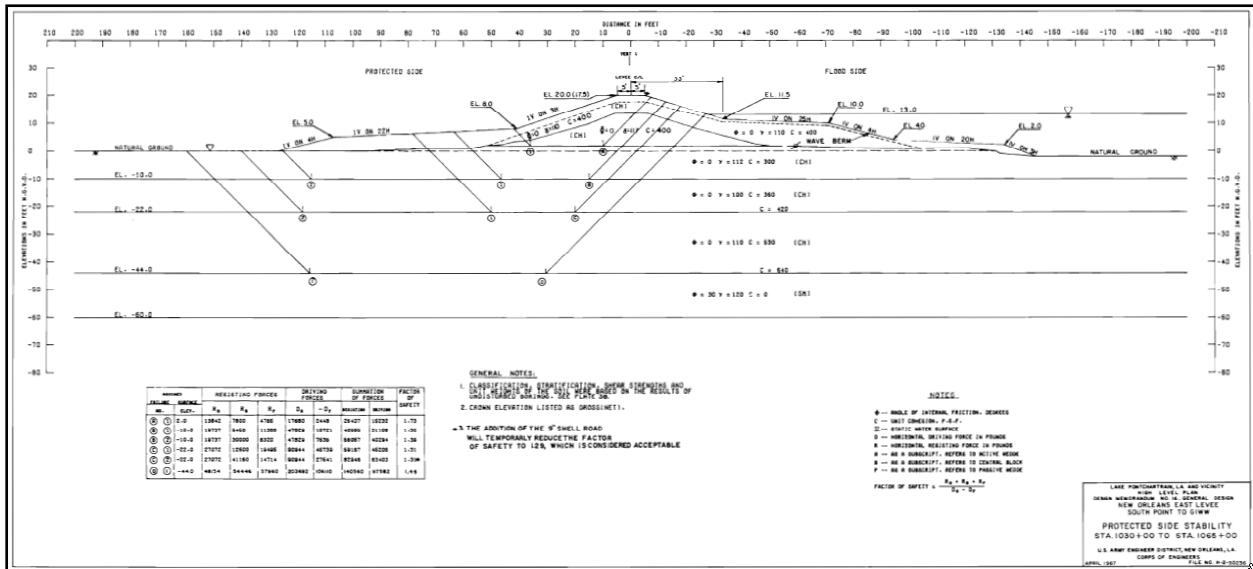


Figure 10-12. Typical wedge stability analysis of levee section from GDM (USACE 1972).

Table 10-7. Uncertainty analysis for example levee reach in NOE.

Water level	Design basis	% design basis	Top of levee
Mean FS	1.3	2	1.2
Spatial COV	0.17	0.17	0.17
Spatial average reduction factor	0.8	0.8	0.8
Systematic COV	0.07	0.07	0.07
Total COV	0.15	0.15	0.15
Reliability Index, b	2.2	6	1.7
Pf for specific 1000 ft reach	0.014	0	0.045
Increase in Pf per 1000 feet reach	2%	0.0	5%

Fragility curves summarize the conditional probability of levee or wall failure as a function of water elevation. Calculations were made for a three specific water elevations: typically design water level, some level lower than design (i.e. sea level), and at the top of the levee or wall.

Uncertainty in realized factor of safety

For a given water elevation, uncertainty in the realized factor of safety against sliding depends principally on the average soil strength, S_u , across the area of the failure surface. This average strength varies from cross-section to cross-section because the soil properties themselves vary from spot to spot (Figure 10-13). The variability in the average soil strength is less than the variability in the point-to-point properties because, to some extent, the highs and lows of the soil strength balance against each other over the failure surface. The larger the failure surface relative to the autocorrelation of the soil properties, the greater the variance reduction from the local averages. VanMarcke (1977a,b) has shown that the variance of the spatial average for a unit-width plain strain cross section decreases approximately in proportion to (L/r_L) , for $L > r_L$, in which L is the cross-sectional length of the failure surface, and r_L is an equivalent auto-

covariance distance of the soil properties across the failure surface weighted for the relative proportion of horizontal and vertical segments of the surface. For the wedge failure modes this is approximately the vertical auto-covariance distance. The variance across the full failure surface of width b along the axis of the levee is further reduced by averaging in the horizontal direction by an additional factor (b/r_H) , for $b > r_H$, in which r_H is the horizontal auto-covariance distance. At the same time that the variance of the average strength on the failure surface is reduced by the averaging process, so, too, the auto-covariance function of this averaged process stretches out from that of the point-to-point variation.

For a failure length of approximately 1000 feet along the levee axis and 30 feet deep, with horizontal and vertical auto-covariance distances of 1000 feet and 10 feet, respectively, the corresponding variance reduction factors are approximately 0.75 for averaging over the cross-sectional length L , and between 0.73 and 0.85 for averaging over the failure length b , assuming either an Exponential or squared-exponential (Gaussian) auto-covariance. The corresponding reduction to the COV of soil strength based on averaging over the failure plane is the root of the product of these two factors, or between 0.74 and 0.8.

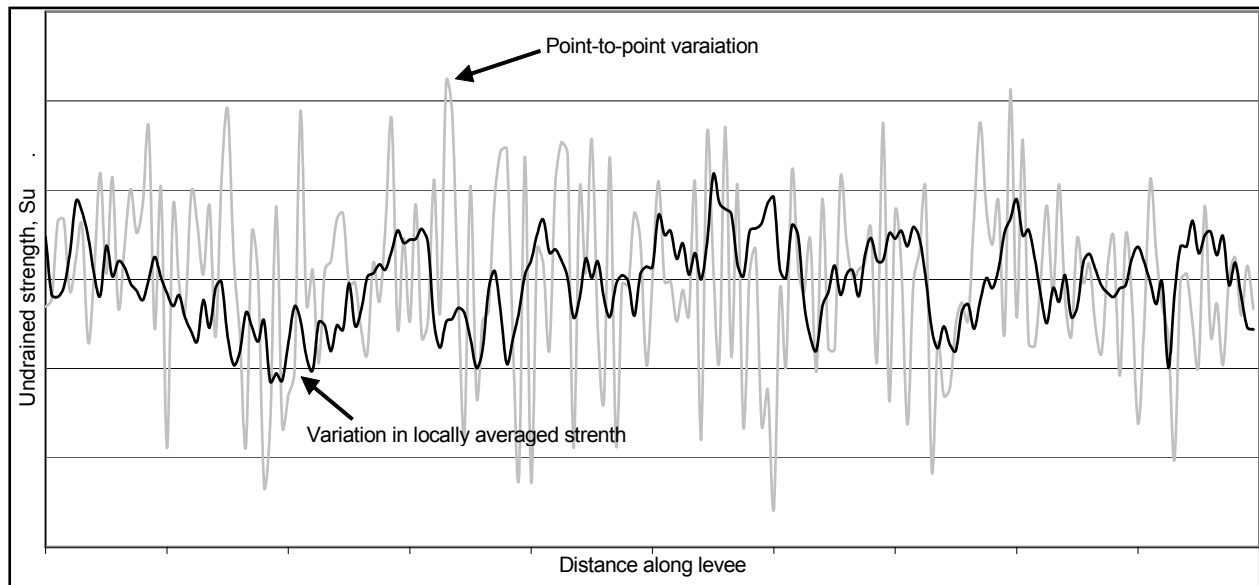


Figure 10-13. Point variation in undrained strength and variation among locally averaged strength.

The Reliability Index for the specific levee reach of length b is the number of standard deviations separating the mean condition from the limiting state,

$$\beta_b = \frac{E[FS]-1}{\text{Var}(FS)} = \frac{E[FS]-1}{\Omega_{FS} E[FS]} \quad (10-2)$$

in which $E[FS]$ is the mean factor of safety, $\text{Var}(FS)$ is the variance, and Ω_{FS} is the COV.

Seepage

A number of seepage failure modes were considered for specific reaches of the HPS. These included:

1. Increases in pore pressures in foundation or levee soils, leading to decreases in effective stress and thus reduced shear strength;
2. Internal erosion (“piping”) caused by high seepage gradients in either foundation or levee soils, and either at the exit of the seepage or deep within the solid mass, leading to loss of material and the development of through-going channels; and
3. “Blowouts” caused by pore pressures on the protected side of a levee exceeding existing overburden pressures caused by the weight of overlying soils, leading to voids or sinkholes and thus failure.

Failures due to seepage pressures or erosion were observed during Katrina at the London Avenue Canal site and also present hazards at northern reaches of the IHNC. At London Avenue, “a line of sinkholes was observed at the inland side of the distressed east I-wall, and a sand boil at the inboard embankment toe indicate[d] that erosive seepage and piping had occurred beneath the levee” (IPET v.V 2006). In this area, the buried Pine Island Beach deposit, which is Holocene age (i.e., recent) sands, rises close to the present ground surface (Figure 10-5).

The fragility curves for any reach in which these sands rise to within the critical failure zone under a levee or wall were adjusted for seepage pressure effects. These affected reaches included not only those in the vicinity of the Pine Island Sand, but also those suspected of crossing untreated buried stream channels in other sections of the HPS. The adjustment of the fragility curves was accomplished by estimating potential pore pressure rise in the affected reaches, and reducing effective strengths in the sand layers accordingly. This lowers the predicted mean factor of safety, and correspondingly increases the probability of failure at given still water levels.

Length effect

The HPS of New Orleans includes long lengths of embankment or wall extending many miles across ground that is poorly characterized from an engineering perspective. Levees fail at locations where loads are high and strengths are low. If these critical locations are identified ahead of time, traditional methods can be used to analyze stability and calculate factors of safety. In such situations, the overall length of levee is immaterial, because the weakest spots have been identified and dealt with. The probability that the levee fails is that of these weakest spots.

The more common situation is that the levee system is not characterized with enough detail to know unambiguously where the weakest spots are. In this case, any reach of levee has some probability of experiencing higher than average loads or lower than average strengths, and as a result, of being a “weak spot.” Since this critical combination cannot be uniquely identified before a failure occurs, the longer the levee, the greater the chance that a critical combination exists somewhere, and thus the higher the probability of a failure somewhere.

For a long levee, the chance of at least one failure is equivalent to the chance that the variations of the mean soil strength across the failure surface shown schematically in Figure 10-13 drop below that required for stability at least once along the length. VanMarcke (1977a,b) has shown that this can be determined by considering the first crossings of a random process. The approximation to the probability of at least one failure as provided by VanMarcke (1977) was used in the calculations.

VanMarcke's derivation is approximately as follows: For a given loading condition, that is, height of water, uncertainty in the realized factor of safety against sliding depends principally on the average soil strength, S_u , across the area of the failure surface. This average strength varies from cross-section to cross-section because the soil properties themselves vary from spot to spot (Figure 10-13). The variability in the average is less than the variability in the point-to-point properties, because to some extent the highs and lows of strength balance out each other over the failure surface. The larger the failure surface relative to the autocorrelation of the soil properties, the more the variance of the local averages is reduced.

VanMarcke has shown that the variance of the spatial average for a unit-width plain strain cross section decreases approximately in proportion to (L/r_L) , for $L > r_L$, in which L is the cross-sectional length of the failure surface, and r_L is an equivalent autocovariance distance of the soil properties across the failure surface weighted for the relative proportion of horizontal and vertical segments of the surface. The variance across the full failure surface of width b along the axis of the levee is further reduced by averaging in the horizontal direction by an additional factor (b/r_H) , for $b > r_H$, in which r_H is the horizontal autocovariance distance. At the same time that the variance of the average strength on the failure surface is reduced by the averaging process, so, too, the autocovariance function of this averaged process stretches out from that of the point-to-point variation.

The primary level of analysis of levee reliability is the two-dimensional levee section. The presumption is that this 2D section applies over a unit length of levee, defined approximately as the horizontal autocorrelation distance, and treated as a probabilistically independent characteristic length. As the total length of levee increases, the probability of systems failure rises in proportion to length, and soon displays a classic exponential saturation shape trending asymptotically toward 1.0, according to the formula,

$$P_f = 1 - (1 - p)^n \quad (10-3)$$

in which, $P_f = 1 - (1 - p)^n$ is the probability of system failure, p is the 2D probability of failure, and n is the number of characteristic lengths within the reach.

Wave run-up¹

Wave run-up for each reach was calculated by the approach summarized in TAW (2002).

The average wave run-up and overtopping for levees was calculated according to the formula,

$$\frac{q}{\sqrt{gH_{m0}^3}} = \frac{0.067}{\sqrt{\tan \alpha}} \gamma_b \xi_0 \exp\left(-4.75 \frac{R_c}{H_{m0}} \frac{1}{\xi_0 \gamma_b \gamma_f \gamma_\beta \gamma_v}\right)$$

with maximum: $\frac{q}{\sqrt{gH_{m0}^3}} = 0.2 \exp\left(-2.6 \frac{R_c}{H_{m0}} \frac{1}{\gamma_f \gamma_\beta}\right)$

(10-4)

in which,

- q = overtopping rate [cft/s per ft]
- g = gravitational acceleration [= 32.18 ft/s²]
- H_{m0} = significant wave height at toe of the structure [ft] surf similarity parameter [-]
- α = slope [-]
- R_c = free crest height above still water line [ft]
- γ = influence factors for presence of berm (b), friction (f), wave incidence (β), vertical wall (v)

The coefficients 4.75 and 2.6 are empirical mean values. The standard deviations are 0.5 and 0.35, respectively and Normally distributed.

Equation (10-6) is valid for $\xi_0 < 5$ and slopes steeper than 1:8. For values of $\xi_0 > 7$ the corresponding relationship is,

$$\frac{q}{\sqrt{gH_{m0}^3}} = 10^{-0.92} \exp\left(-\frac{R_c}{\gamma_f \gamma_\beta H_{m0} (0.33 + 0.022 \xi_0)}\right)$$
(10-5)

The coefficient -0.92 is the empirical mean value, with standard deviation 0.24 and Normally distributed. The overtopping rate in the range $5 < \xi_0 < 7$ is obtained by linear interpolation of Equations (10-6) and (10-7) using the logarithmic value of the overtopping rates. The surf similarity parameter is defined as:

$$\xi_0 = \frac{\tan \alpha}{\sqrt{s_0}} \quad \text{with} \quad s_0 = \frac{2\pi H_{m0}}{g(T_{m-1,0})^2}$$
(10-6)

¹ This section draws heavily on the internal USACE memorandum, van Ledden (2007), “Wave overtopping IPET,” dated 21 June.

in which,

$$s_0 = \text{wave steepness [-]}$$

$$T_{m-1,0} = \text{mean period [s]}$$

Eq. (1) - (3) contain levee parameters such as the slope and the crest height and several influence factors for angle of wave incidence, friction, the presence of a berm and a vertical wall. The hydraulic levee designs in the New Orleans area generally have two steep sloping sections of 1:3 – 1:5 and a wave berm in between. The wave berm is located at the design still water line. A common wave berm factor for these levee designs is $\gamma_b = 0.65 - 0.75$. Apart from specific cases, a *grass-covered levees without floodwalls on top and perpendicular wave attack* is assumed. Hence, there is no reduction of the overtopping rate due to friction, wave attack and vertical walls. Based on this, we suggest to use in the risk model the following settings: slope $\alpha = 1/4$, a berm factor $\gamma_b = 0.7$ and $\gamma_f = \gamma_\beta = \gamma_v = 1$ (“no effect”).

The average wave overtopping over floodwalls is correspondingly,

$$\frac{q}{\sqrt{gH_{m0}^3}} = 0.082 \exp\left(-3.0 \frac{R_c}{H_{m0}} \frac{1}{\gamma_\beta \gamma_s}\right) \quad (10-7)$$

in which,

$$q = \text{overtopping rate [cft/s per ft]}$$

$$H_{m0} = \text{significant wave height at toe of the structure [ft]}$$

$$R_c = \text{free crest height above still water line [ft]}$$

$$\gamma = \text{influence factors for wave incidence } (\beta) \text{ and type of geometry } (s)$$

The coefficient 3.0 is the empirical mean value, with standard deviation 0.26, and a normal distribution assumed. The influence factors are: $\gamma_s = 1$ and $\gamma_\beta = 0.83$ for plain impermeable floodwalls with perpendicular wave attack of short-crested waves.

For both levees and floodwalls, the average wave overtopping can be computed using the still water level from ADCIRC and the wave information from STWAVE. The mean wave period $T_{m-1,0}$ is derived directly from the STWAVE results at 600 ft in front of the levees/floodwalls¹. The significant wave height at the toe of the structure (H_{m0}) is also derived from the STWAVE results, but is adapted because of depth-limited breaking in front the structure. The significant wave height based on the STWAVE results is limited to the maximum significant wave height according to: $H_{m0,max} = \gamma(\zeta - z_{toe})$; in which, γ : breaker parameter [-], ζ : still water level [ft], and z_{toe} : bottom level at toe of structure [ft].

The breaker parameter in Eq. (5) is set at $\gamma = 0.4$ in the design study. The bed level at the toe of most of the structures is assumed to be at $z_{toe} = 0$ ft. The standard deviation for the significant wave height is assumed to be 10% of the value based on STWAVE (or after reduction due to

¹ Note that only the peak period T_p is available for the 152 storm suite of the 2007 situation. The peak period T_p can be converted easily into the mean period $T_{m-1,0}$ using $T_{m-1,0} = T_p/1.1$.

depth-limited breaking according to Eq. (5)). The error in the wave period is set at 20% of the STWAVE result. The error is assumed to Normally distributed. Both errors are based on expert judgment due to lack of field data.

I-Wall fragility, no overtopping

The reliability analysis for I-walls was similarly based on limiting equilibrium calculations of factor of safety against instability. For I-walls, the analysis is based on the Performance Team’s mechanism of cracks developing in the soil immediately behind the wall and sheetpile, allowing hydrostatic pressure on the sheetpile. The equilibrium of a soil wedge to the protected side of the wall (Figure 10-14) was calculated for this condition. The calculations were based on undrained ($\phi=0$) failure conditions. Undrained strengths of soils underlying the levees and walls were based on “Q-test” results. The design consideration of balancing forces and moments on the sheet pile to determine depth of penetration was considered immaterial to the reliability analysis of the wall sections.

Based on the results of the Performance Team’s analyses, it was assumed that cracking initiated at 5 feet of water elevation on an I-wall. Thus, for water elevations lower than 5 feet, the factor of safety was that calculated in the GDMs. But at 5 feet, when a crack formed in the soil, the factor of safety underwent a step change to a forward (protected side) wedge failure.

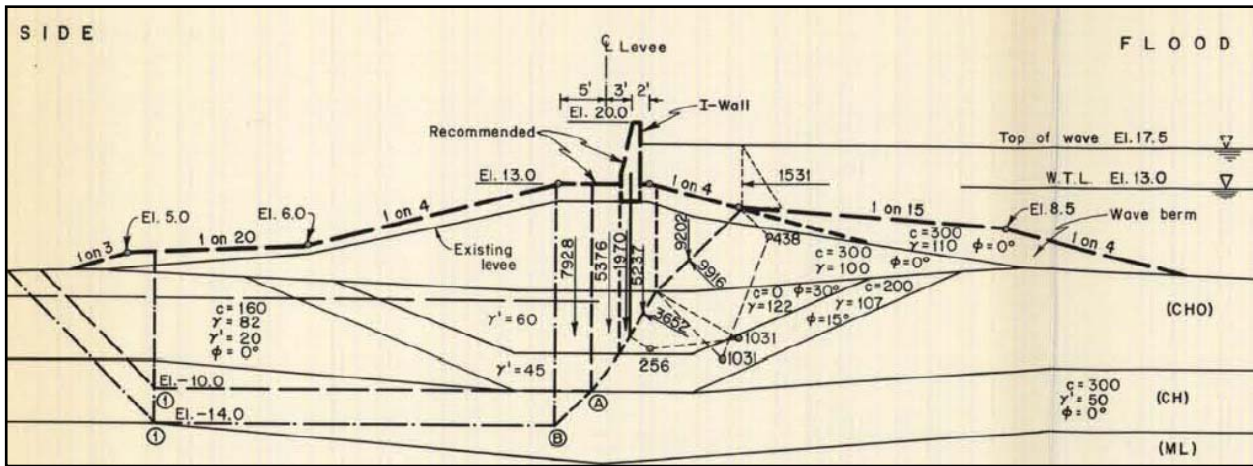


Figure 10-14. Sheet pile failure by deep wedge instability.

If soil separations developed in front of the sheetpile or the levee, the condition resulted in increased hydrostatic forces on the flood side of the I-wall and the levee. If the separation was of sufficient depth, the hydrostatic forces on the wall may exceed the shear strength of the supporting soil and cause failure along wedge lines of least resistance behind the sheetpile. Reliability calculations were based on the probability that shear resistance of a wedge was exceeded by the loads on the levee and floodwall for a given hurricane.

Levee and I-Wall fragility, with overtopping

Reliability calculations were based on the probability of overtopping causing erosion of the protected side of a levee that led to a breach. Two approaches were considered. The first approach considered flow velocities over the levee. The second approach considered water elevation, which is estimated by the storm surge modeling, as an indirect parameter of flow velocity.

Based on the Performance Team's results, the probability of erosion breaching was considered to be negligible for floodwall sections, and related to the presence of significant depth of hydraulic fill for levee sections. The fragility curve for levee sections was assumed to be that of the static failure analysis (above) up to the point of overtopping, and then a step function to $P_f=1.0$ for those sections with significant depths of hydraulic fill. For levee sections without significant hydraulic fill, the fragility curve remained flat at the top of wall fragility for overtopping.

Figure 10-14 shows fragility curves developed for reaches defined in the Jefferson drainage basin. The fragilities values were developed as described in the preceding sections for conditions of no overtopping (water elevations up to the top of the wall or levee) and overtopping.

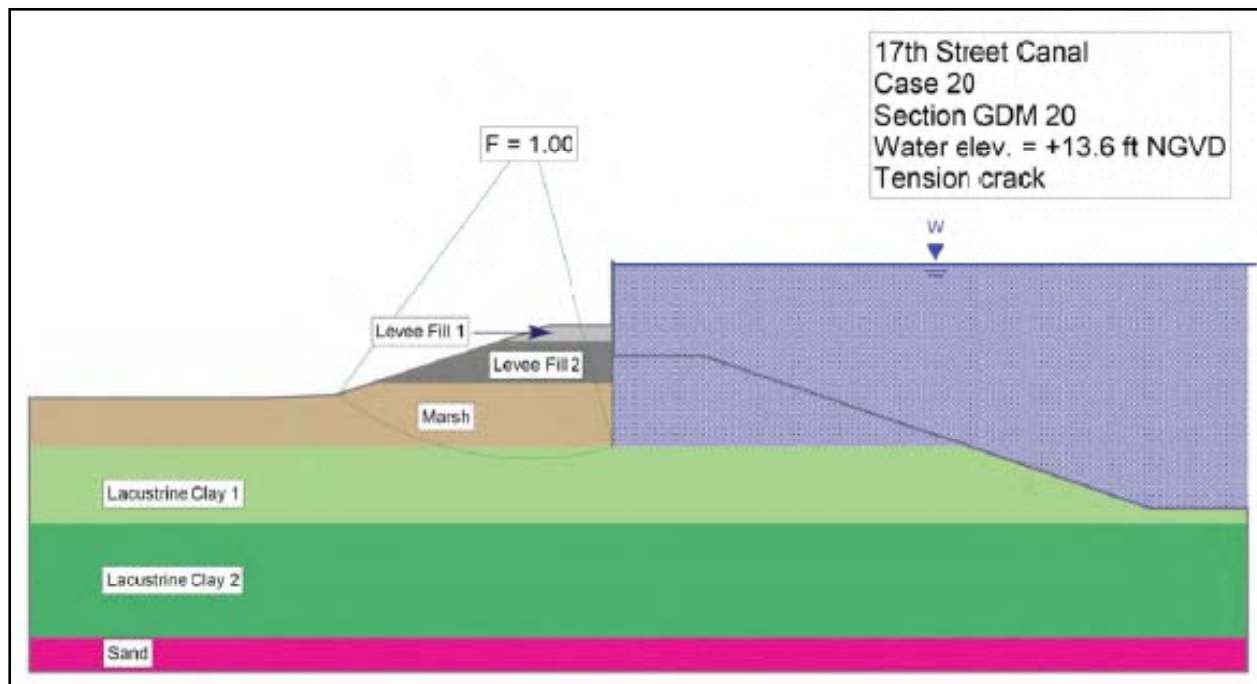


Figure 10-15. Failure by rotation of I-wall, reducing I-wall elevation

Scour and erosion

The probability of overtopping of levees or floodwalls leading to scour and consequent failure was directly estimated based on empirically observed rates of failure during Katrina and

documented in IPET Volume V (2006), and as shown in Table 10-8. These are consistent with later analyses by Briaud, et al. (2006).

Table 10-8. Empirical frequency of overtopping scour failure of levees and walls as observed in Katrina, as a function of the velocity of overtopping flow (correlated to depth of overtopping) and soil type.				
LEVEES	≤0.5 FOOT	≤1.0 FOOT	≤2.0 FEET	3 FEET
Hydraulic Fill	0	0	1	1
Clay	0	0	0.25	0.5
Protected	0	0	0	0.1
WALLS	≤0.5 FOOT	≤1.0 FOOT	≤2.0 FEET	3 FEET
Hydraulic Fill	0	0	0.5	1
Clay	0	0	0.25	0.5
Protected	0	0	0	0.1

Transitions and Point Structures

A number of HPS breaches were observed at transitions between HPS components. These breaches were typically at levee to I-wall, levee to T-wall or I-wall to T-wall transitions. Many of the HPS breaches were at point structures such as gates (road and railroad), pump stations, or around drainage control structures. These transitions indicate a weak link in the HPS due to the differing stiffness of the components which permit them to become areas of significant erosion during a hurricane event.

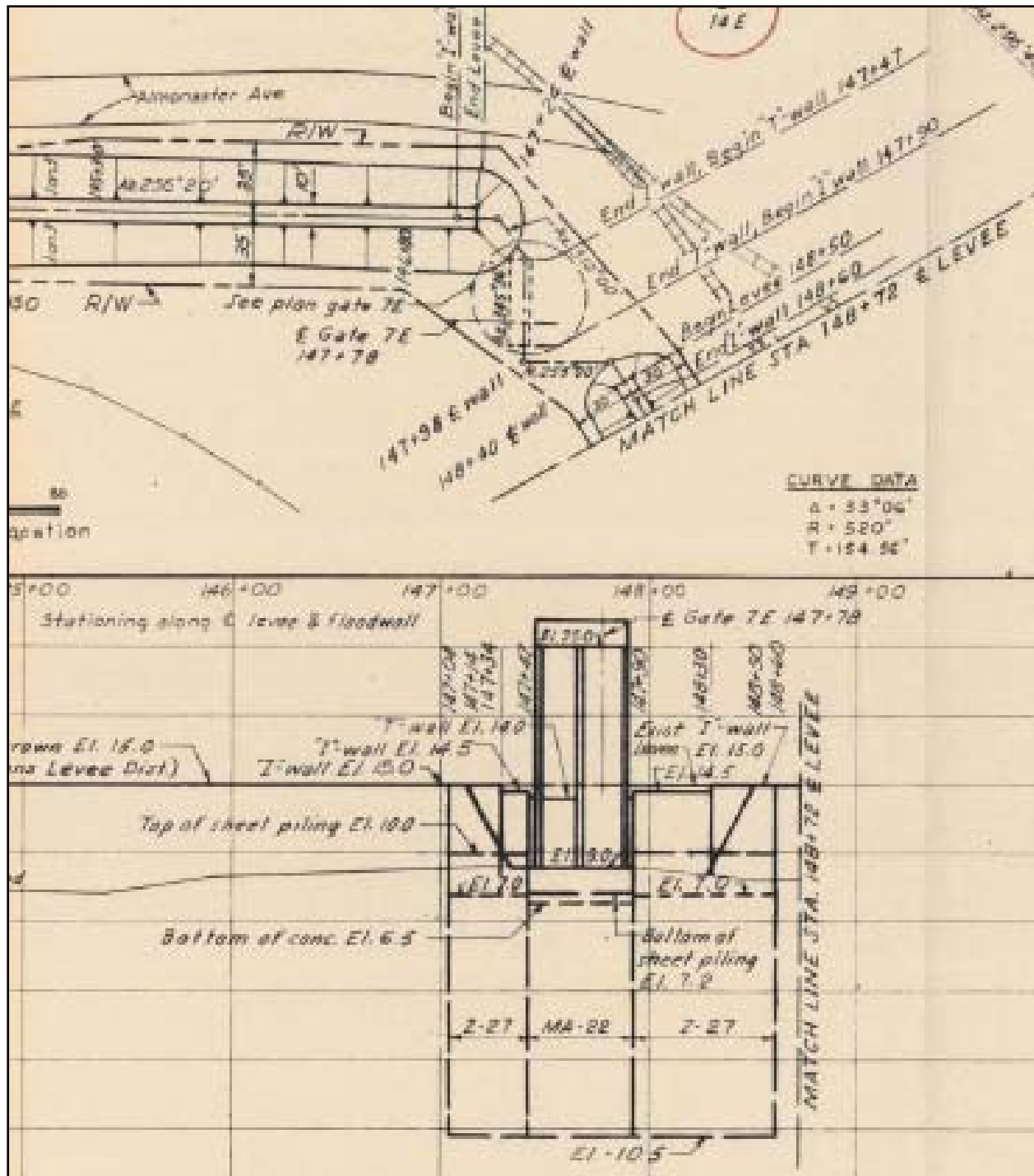


Figure 10-16. Example of Transition Zone for East Bank of INHC

Many of these transition zones failed to use a “wrap-in” levee section to a more rigid wall structure. Instead, the levee sections sloped quickly away from the transition to expose the I- or T-wall. The steep slopes permitted a concentrated zone for the erosion of the levee that eventually exposed the I-wall or T-wall structure to additional loading and continued eroding. This dynamic process could lead to instability and collapse or damage to end sections of the

wall. An example of a levee transition for a gate section on the east bank of the INHC is shown in Figure 10-15.

The failure modes for these transition zones are complex and dynamic. The failure modes use the qualitative erosion parameters developed by the Performance Team as the basis for change in the stability of components at the transition zones. That is, the fragility of the transitions was taken to be similar to that of overtopped levee sections, and to depend on the combination of height of overtopping water and the presence of hydraulic fill enlargement to the levee section. Reliability for point structures (gates, control structures, pump stations) was taken as a point probability of failure for design loading.

Failure Mode 1—Scour and erosion caused point structure (i.e. drainage pipe) instability. A levee breach may occur due to loss of the I- or T-walls at a point structure and scour could create instability and collapse of the structure, resulting in a breached area.

Failure Mode 2—Breach occurs at the water stop between the I-wall and T-wall panel junction. This failure mode may be caused by differential displacement between panels and may develop tensile and shear forces in the water stop and panels. This may be due to levee erosion on the flood side or different rotation point between panels, or to lateral displacement of the levee from a foundation shear failure. This failure mode was not explicitly included in the risk calculations.

Failure Mode 3—Breach at the levee and I-wall transition. This failure mode occurs due to levee erosion on the protected side, where the erosion starts at the end of the levee transition and progresses back toward the I-wall, until the I-wall rotates toward the protected side. This was treated as Failure Mode 1.

Pumping Stations

The adverse performance of mechanical, electrical, and human elements of the HPS, such as pumps, the availability of power, and the closure of gates, is treated as random point (i.e., aleatory) events with discrete probabilities of failure based on the statistical record during Katrina and on information provided by other IPET teams.

The pumping stations are critical HPS system components because they maintain the flood levels on the protected side. Unfortunately, many of the pumping stations during Katrina reached and exceeded their pumping capacity shortly into the storm. Their reliability during Katrina was not exceedingly high as the stations primarily failed due to rising waters at the plants, a lack of external or backup power source, or were shut down due to inefficient pumping. These systems are designed to handle specific level of rainfall and are easily overwhelmed when the levees are overtopped by a hurricane event. The following failure modes were possible for the pumping stations: no commercial power, back up generator failed, mechanical fuel unavailable, pumps not functioning at time of incident, mechanical failure of components, operator unavailability, debris blocking intakes, or reversed or back flow through outfall pipes.

The reliability of the pumping stations was included in the risk model as point sources. The reliability is based on data collected by the Pumping Team, performance data maintained by Task Force Hope, and information from the dewatering plan for New Orleans developed by the New Orleans District. The fragility curves for each pumping station are limited to a specific elevation or volume of water within the drainage basin. These fragility curves vary for each pumping station and reflect the interior drainage areas and back flow potential as determined by the Interior Drainage Team.

References

- Briaud J.-L., Chen H.-C., Govindasamy A.V., Storesund R. (2007), "Erosion tests on samples from the New Orleans levees", proceedings of the Geo-Denver national conference, edited by Harold Olsen, ASCE, Reston, Virginia, USA.
- DeGroot, D. (2006). "Analyzing spatial variability of in situ soil properties," *Uncertainty In The Geological Environment*, ASCE Congress, Madison v2, pp. 21-238.
- IPET (2006). *Performance Evaluation of the New Orleans and Southeast Louisiana Hurricane Protection Systems*, Final Report of the Interagency Performance Evaluation Task Force, Vol. V, "Performance—Levees and Floodwalls, Appendix 13, Levee erosion and scour from overtopping storm surge," US Army Corps of Engineers, Washington, DC.
- IPET (2006). *Performance Evaluation of the New Orleans and Southeast Louisiana Hurricane Protection Systems*, Final Report of the Interagency Performance Evaluation Task Force, Vol. V, "Performance—Levees and Floodwalls, Appendix 21, Regional geology and history overview," US Army Corps of Engineers, Washington, DC.
- IPET (2006). *Performance Evaluation of the New Orleans and Southeast Louisiana Hurricane Protection Systems*, Final Report of the Interagency Performance Evaluation Task Force, Vol. VI, "Interior Drainage and Pumping," US Army Corps of Engineers, Washington, DC.
- IPET (2006). *Performance Evaluation of the New Orleans and Southeast Louisiana Hurricane Protection Systems*, Final Report of the Interagency Performance Evaluation Task Force, Vol. V, "Performance—Levees and Floodwalls, Appendix 21, Regional geology and history overview," US Army Corps of Engineers, Washington, DC.
- Jack R. Benjamin & Associates (2006). "Initial technical framework paper—levee stability," Delta Risk Management Strategy, Prepared for [the California] Department of Water Resources, September 6, 18pp.
- Matheron, G. (1989). *Estimating and Choosing*, A. M. Hasofer, Translator, Springer Verlag, Berlin.
- McDonald, L. (2002). "Probabilities—discussion on considerations," *Working Paper*, Dam Safety Interest Group.
- TAW (2002). "Technical report wave run-up and wave overtopping at dikes," Technical Advisory Committee on Flood Defence, The Netherlands.

USACE (1972). "New Orleans East Lakefront Levee Paris Road to South Point, Lake Pontchartrain," Barrier Plan, DM 2 Supplement 5B, New Orleans District, June.

USACE (1999). "Risk-Based Analysis in Geotechnical Engineering for Support of Planning Studies," ETL 1110-2-556, US Army Corps of Engineers, CECW-EG, Washington, DC, 28 May.

USACE (1998). "Risk-based analysis for flood damage reduction studies," EM 1110-2-1619, US Army Corps of Engineers, Washington, DC.

VanMarcke, E. H. (1977a). "Probabilistic modeling of soil profiles." *J. Geotech. Engrg. Div.*, ASCE, 103(11), 1227-1246.

VanMarcke, E.H. (1977b). "Reliability of earth slopes," *Journal of the Geotechnical Engineering Division, ASCE*, v.103(GT11): 1247-1265.

Appendix 11

Uncertainty Analysis

Introduction

One of the objectives of the risk analysis was to quantitatively assess the uncertainties associated with the estimated levels of flooding for possible hurricane events, which included assessing the uncertainties associated with the occurrence rate of hurricane events, estimated surge and wave elevations, and the performance of the HPS (its reliability).

There are two types of uncertainty: aleatory and epistemic uncertainty. Aleatory uncertainty is attributed to the inherent randomness of events in nature, manifesting as variability over time for phenomena that take place at a single location (temporal variability), or variability over space for phenomena that take place at different locations at a single time (spatial variability), or as variability over both time and space. These events are predicted in terms of their likelihood of occurring (e.g., the chance of heads in a coin flip). Aleatory uncertainty is, in principle, irreducible. Epistemic uncertainty is attributed to our lack of knowledge or information about events and processes, or our lack of understanding of physical laws that limits our ability to model the real world. For example, the ability to determine the likelihood of an event (i.e., its rate of occurrence) requires that certain data be available. If limited data are available, the estimated rate may be quite uncertain (i.e., statistical confidence intervals on parameter estimates would be large). A second type of knowledge uncertainty is attributed to a lack of understanding or knowledge about physical processes that must be modeled (e.g., the meteorological processes that generate hurricane events). In these instances expert evaluations are often required to assess the current state of knowledge and to quantitatively evaluate the level of uncertainty. Knowledge-based uncertainty is referred to as epistemic uncertainty.

Aleatory and epistemic uncertainty affect the outcomes of a reliability analysis in different ways. Aleatory uncertainty manifests as variations, or frequencies of occurrence, over space or time. Epistemic uncertainties manifest as statistical error and systematic biases in probability estimates, and may introduce correlations among aleatory frequencies.

The distinction between aleatory and epistemic uncertainty can often seem arbitrary. For example, the distinction depends on the models that are used in a particular analysis. Nonetheless, making a distinction between the sources of uncertainty in a logical manner helps insure that all uncertainties are quantified and identified. In principle, epistemic uncertainties are

reducible with the collection of additional data or the use/development of improved models. However, in a given project, it is typically not possible to reduce these uncertainties. Uncertainties identified as aleatory were included in the risk analysis. Aleatory uncertainty values were identified for the surge and wave setup elevations, rainfall, and weir coefficients. Epistemic uncertainties were evaluated separately from the risk analysis.

Aleatory Uncertainties

Surge and Wave Setup Elevation Uncertainty. The estimated surge and wave set up elevations were the result of wind, surge, and wave analyses conducted with PBL, ADCIRC, WAM, and a Boussinesq wave setup model for local effects near levees and floodwalls. These analyses were quite detailed, but could not include all factors that affected surge and wave setup elevations.

Two types of uncertainty in the estimated water elevations provided by the hydrographs were:

- random variations from location to location for a given storm
- perfectly correlated variations for each storm, where all the hydrographs increased or decreased together

The idealized characterization of hurricanes in the PBL model led to variability between the predicted and actual results (e.g., surge elevations). That is, if there were a set of ‘real’ hurricanes with the same characteristics (e.g., central pressure, etc.), the recorded hydrographs for each hurricane at a given location would not be exactly the same. The variability between modeled and actual events due to PBL modeling limitations was spatially systemic in that the estimated characteristics of a particular hurricane has a common effect (higher or lower surge elevations) at all locations.

Factors that contributed to the uncertainty in the ADCIRC, WAM, and Boussinesq analyses included time-varying tides, time-varying local topography (e.g., if trees were swept away, the local surface resistance to water flow would change), finite model resolution, and variations in the wind fields and the air/sea interaction that were not captured by the idealized PBL wind model.

The detailed topography entered into the ADCIRC, WAM, and Boussinesq models calculated varying water elevations from location to location for each storm. The water elevations were dependent on the topography leading up to each location of interest on the HPS. Correlated variations in the water elevations for each storm were primarily due to tidal effects, local changes in topography over time during the event, and uncertainty in the wind modeling for each storm. Random variations in water elevations from location to location have a much smaller effect on basin flooding than do a uniform increase or decrease of the water elevation over the entire HPS. For this reason, local random variations in water elevations were ignored in Forte. Forte computed the effect of perfectly correlated variations in water elevation, as such variations

can have a significant effect on HPS reach failure, basin flooding, and the associated consequences of flooding.

Forte has two input parameters for estimating the uncertainty in the surge and wave setup elevations (see App 17). However, since the surge and wave setup elevations were combined in the hydrographs, a single combined uncertainty value was input for the surge and wave setup standard. The coefficient of variation (COV) for the uncertainty in amplitude (both surge and wave effects) was estimated to be about 0.15, which was based on expert judgment by IPET team members knowledgeable about hurricane events and modeling and was applied to the entire duration of each hydrograph.

Levee and Floodwall Fragility Uncertainty. Four categories of uncertainty were included in the HPS reliability analysis:

1. Geological and geotechnical uncertainties, involving the spatial distribution of soils and soil properties within and beneath the HPS and geotechnical parameters.
2. Structural uncertainties, involving the performance of man-made systems such as levees, floodwalls, and point features such as drainage pipes; and the engineering modeling of that performance, including geotechnical performance modeling.
3. Erosion uncertainties, involving the performance of levees and fills around floodwalls during overtopping, and at points of transition between levees and floodwall, in some cases leading to loss of grade or loss of structural support, and consequently to breaching.
4. Mechanical equipment uncertainties, including gates, pumps, and other operating systems, and human operator factors affecting the performance of mechanical equipment.

The HPS reliability analysis calculated fragilities (conditional probabilities of failure) for defined reaches of each basin, where surge and wave setup elevation was the conditional parameter. Thus, uncertainties associated with hurricane effects, wind loads, water heights, and other factors of loading conditions were not considered in the reliability analysis.

To determine the probability of failure of a given reach, uncertainties in hydrograph elevations were convoluted with the HPS fragilities to generate marginal (i.e., unconditional) probabilities of HPS failure that resulted in flooding of a basin. Fragility curves for levees and floodwalls were calculated for two conditions:

1. global stability without overtopping, for which reliability was calculated at the design elevation and top of levee, and a smooth curve was approximated to the lower water elevation at sea level
2. overtopping with subsequent erosion, for which reliability was estimated at four water elevations of overtopping: ½ foot, 1 foot, 2 feet, and 3 feet above the top of levee or flood wall, based on empirical data from Katrina.

Reliability assessments were performed for individual reaches of approximately homogeneous structural type, elevation, geotechnical conditions, and water elevations. This resulted in fragility curves for each reach by mode of failure which were input to Forte (see Appendix 15). Such fragility curves represented the aleatory (i.e., random) uncertainties from one hurricane to another.

The risk model (Appendix 9) used water elevations from the hurricane hazard and the HPS fragilities to calculate probability of volume and duration of flooding within each drainage basin. The risk model separately tracked uncertainties from both the hurricane hazard and the structural and geotechnical response, to give a best estimate of frequency and duration of flooding, along with measures of uncertainty in those frequencies.

Forte input parameters for estimating the uncertainty in the HPS reliability included COVs for breach with overtopping, breach without overtopping, and closure structures (e.g. open gates). A fragility factor was added to Forte that allowed adjustment of the position of the fragility curve along the x-axis for epistemic uncertainty analysis, but this factor was not used in the final risk analyses. The default value of zero corresponded to no shift in the fragility curve.

The COV for breach with and without overtopping events was based on the COV for the weir coefficient, which is described in the next section. Breach without overtopping events had a COV of 0.3 and breach with overtopping events had a COV of 0.2. The COV for Closure structures (gates) being left open was set to 0.2, based on empirical data from Katrina.

Weir Coefficient Uncertainty

For overtopping events, Forte computed the volume of water that flowed over a reach into a sub-basin using a weir equation and the height of the water above the top of the levee or floodwall. The weir equation uses an empirical coefficient, known as the weir coefficient C_w ,

$$Q = C_w LH^{3/2}$$

where Q is the flow rate over a weir, L is the weir length, and H is the weir depth.

The weir coefficient has an uncertainty to account for the highly complex and variable nature of flow over a levee or floodwall. Each time the weir equation was accessed in Forte for volume computations, a random coefficient was computed that modified the mean flow into the sub-basin.

The risk analysis subdivided the New Orleans HPS into approximately 135 reaches, based on similar construction features and elevations. A random realization of the weir coefficient was used over the entire length of a defined reach. This approach resulted in random variations in overtopping flow rates between different reaches, but assumed a uniform value within a given reach (i.e., the weir coefficient was perfectly correlated along any given reach). The COV of the weir coefficient was taken as 0.2, based on expert judgment by IPET Team members.

Rainfall Uncertainty

For each hurricane event, Forte computed an additional volume of water due to rainfall that was added to each sub-basin after the flooding from HPS overtopping or reach failures was computed. A simplified model of rainfall inside the basins was developed, as described in Appendix 8. The rainfall components evaluated were the mean rainfall contribution from the symmetric component of the mean rain field and the asymmetric component of the rain field.

For hurricanes that passed to the right or near a given basin, the azimuthal dependence of the rainfall field was conservatively neglected. For hurricanes that passed to the left of a basin, the asymmetric component was accounted for by multiplying the above symmetric mean rainfall values by 1.5. This factor includes intensification due to land effects.

Rainfall uncertainty in Forte was estimated with a lognormal random variable with mean value 1 and log standard deviation 0.697. This random factor was applied to the entire mean rainfall time history. In reality, rainfall intensity inside a given basin would display significant fluctuations in time and space, which locally could far exceed a factor of 2. However, the above random factor is considered adequate to reflect uncertainty of the total precipitation volume in a basin during the passage of a hurricane.

Epistemic Uncertainties

Only the aleatory uncertainties defined above were included in the Forte analyses. Epistemic uncertainties were considered separately from the Forte analyses. Sources of epistemic uncertainty are described below.

Hurricane Frequency Uncertainty. The uncertainty in the rates of hurricane occurrence is primarily due to the limited historical sample size. Other sources of uncertainty include possible errors in the assumed form of marginal and conditional distributions (especially in the tail regions), and the uncertain near-future hurricane activity due to fluctuations and trends associated with climate changes and multi-decadal cycles.

There is an epistemic uncertainty in the rate of hurricane occurrence associated with any particular hydrograph. This is primarily due to the relatively small strong-storm sample size.

Future Climatic Effects Uncertainty. Uncertainty on the hurricane statistics in the Gulf of Mexico during the next 50 to 100 years is dominated by multi-decadal oscillations. Specifically, considering that the North Atlantic is now experiencing a 50 percent higher-than normal activity and that this elevated activity may persist over a number of years and possibly for decades, it is reasonable for the next 50 to 100 years to increase the average historical rate of hurricanes for the next 50 to 100 years by 20 percent and to allow for an additional 25 percent uncertainty factor around this corrected rate. The latter factor includes uncertainty on the historical rate due to the finite observation period (16%) as well as uncertainty on the future evolution of the hurricane frequency (judgmentally assessed).

Considering the general consensus and dissenting views on the effect of global warming on hurricane intensity, the historical mean pressure deficit is increased by 3 percent and an uncertainty factor of 5 percent is applied to the increased mean value. Since the effects of different factors on hurricane frequency and intensity are poorly correlated, these components of epistemic uncertainty were treated as independent.

Table C1 in Appendix 8 (copied below) estimates that an upper bound for wave height and surge increases due to a doubling of high activity periods over a nominal 30-year cycle would be approximately 9 percent for a 500-year return period to 18 percent for a 25-year return period.

Table C1. Estimated changes in extreme waves heights and surges for selected return periods, given a doubling of years with high hurricane activity (from App 8).		
Return Period (years)	Change in Wave Height (percent)	Change in surge (percent)
25	+15	+18
50	+13	+16
100	+12	+15
250	+11	+12
500	+10	+9

Hurricane Duration Uncertainty. There is uncertainty associated with the duration of each hydrograph, which is primarily related to uncertainties in the two factors that primarily control the storm duration, the storm radii and forward speed. The COV in both the storm radii and forward speed was estimated to be 0.15. The COV of the hydrograph duration was estimated to be the square root of the sum of the squares ($\sqrt{0.15^2 + 0.15^2}$), or about 0.2.

The effect of duration uncertainty would be to lengthen or shorten the hydrograph and the duration of overtopping, and so increase or decrease the volume of inundation. Since the time for a breach to occur was not been included in the risk model, the effect of this factor was not considered.

High Water Mark (HWM) Data Uncertainty. Care was taken when FEMA evaluated the quality of the high water mark data from Katrina. All HWM recorded throughout the Katrina flood region were rated on a scale that indicated whether the data was considered to be of high quality (more likely to be accurate) or a lower quality. Many of the high quality data points were documented with photos and/or video taken during the storm.

Katrina Hydrograph Uncertainty. The Katrina storm hydrographs used in the risk analysis were provided by the IPET Storm Team. The hydrograph peak elevations were verified to be within 0.5 to 1.0 ft of measured HWM data at locations where HWM data was available outside of the basins.

Katrina Inundation Uncertainty. High quality HWM data was selected to evaluate the estimated basin flood elevations. However, it was recognized that there were other contributing factors when comparing HWM and Forte elevations:

1. The HWMs were sample measurements based on one realization (i.e., Katrina). Sampling variability would be expected if another storm similar to Katrina was repeated many times. Such variability could be significant.
2. The HWMs are not necessarily the maximum water levels after the water settled in an entire subbasin, but more likely a level which remained long enough to level stains.
3. The HWMs were measured while the drainage and pumping systems were active.
4. The HWMs were measured while backflow to the water bodies occurred at breaches.

Hurricane Protection System and Inundation Uncertainty

The HPS risk and reliability analysis evaluates the frequency of flooding as a result of rainfall, levee overtopping, and levee failure. As part of the risk and reliability analysis, the uncertainty in the analysis results will be estimated.

- the uncertainty in the frequency that a basin will be flooded (due to any cause; overtopping, non-overtopping)
- the uncertainty in the frequency of flood levels in each basin (i.e., the uncertainty in flood elevations for the 50, 100, and 500-year flood levels)

Appendix 12

Consequences

Overview

One of the primary outputs of the risk and reliability modeling of the IPET Risk Team are estimates of the probability distributions of life loss and direct physical damage relating to the performance of the Hurricane Protection System (HPS) in the Greater New Orleans area. The risk was estimated for the following two scenarios:

1. Pre-Katrina (August 28, 2005)
2. The Current HPS (June 1, 2007).

The Risk Team worked in close collaboration with Consequence Team to obtain estimates of life loss and property loss as a function of maximum inundation elevation in the 27 sub-basins that comprise the following 10 basins of the New Orleans HPS:

East Bank

1. New Orleans Metro - Orleans East Bank
2. New Orleans East
3. St. Bernard Parish
4. Jefferson Parish
5. St. Charles Parish
6. Plaquemines

West Bank

1. Cataouache
2. Westwego to Harvey Canal

3. Harvey Canal to Algiers Canal
4. Algiers Canal to Hero Canal

The numbers of sub-basins that are contained within portions of the following parishes are indicated in parentheses: Jefferson (7), Orleans (12), Plaquemines (1), St. Bernard (5), and St. Charles (2) Parishes (See Figure 12-1).

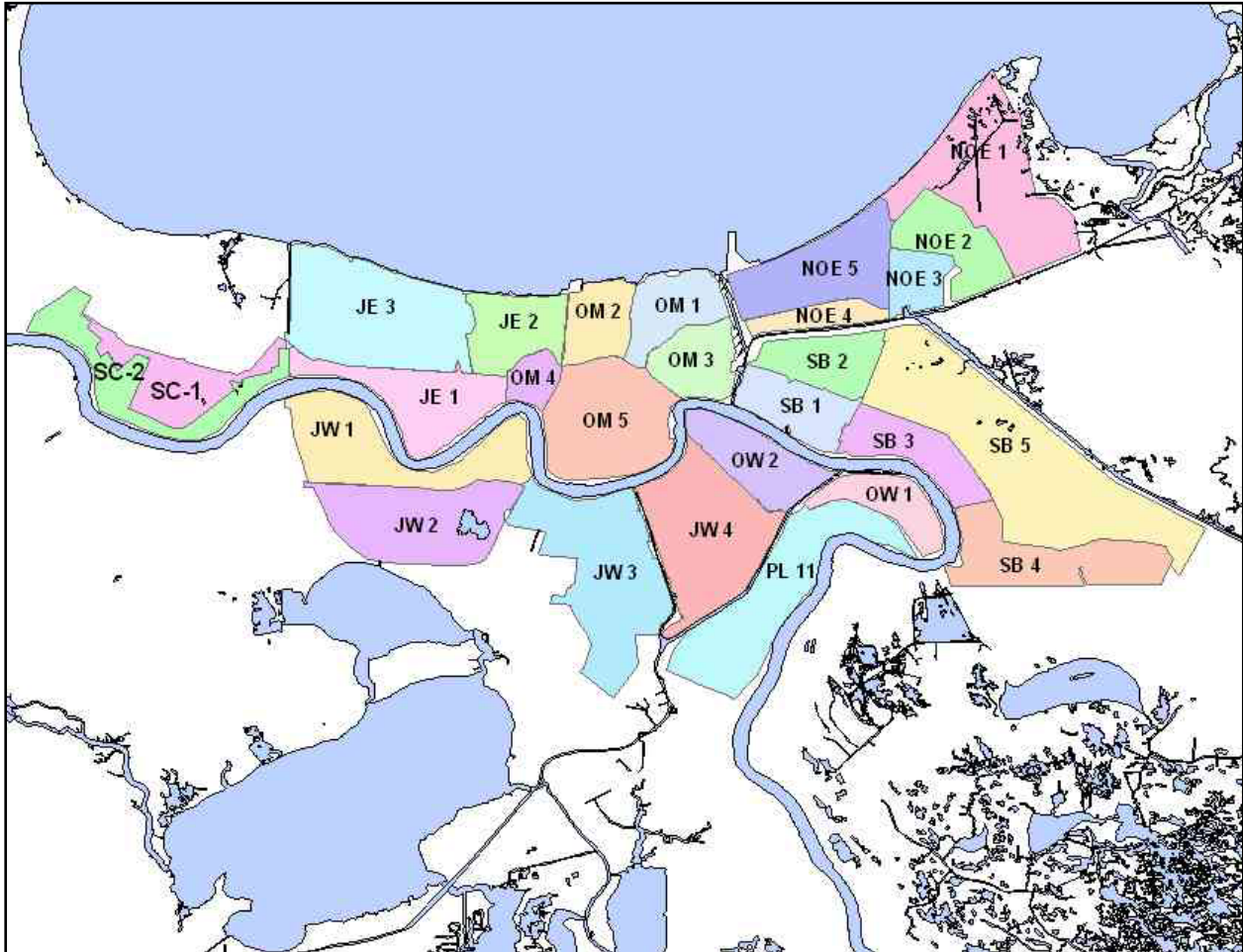


Figure12-1: Sub-basin Map

The Risk Model was run for different hurricane realizations that represent a wide range of hurricane events with different severities, directions, points of landfall, etc. For each of these hurricane realizations, the Risk Model represented the performance of the HPS and estimated the probability that inundation would result from insufficient internal drainage, overtopping of the levees, and levee breaching. The resulting estimates of maximum inundation depths were used as a basis for interpolation of life loss and property loss estimates using the relationships provided by the Consequence Team. Estimates were made for each of the 27 sub-basins and for the pre-Katrina and current scenarios. Thus, it was necessary for the life loss and property loss estimates to cover a range of elevations associated with a range of hurricane events that could impact New Orleans from minor inundation to an elevation 36 ft above sea level.

The estimates of life loss were developed as probability distributions and the estimates of property loss were developed as best estimates with an associated 90 percent confidence interval rather than single-value or point estimates. The probability distributions for life loss and confidence intervals for property losses represent various types of uncertainties in the estimates, which are described below.

Life Loss Estimation

Life loss was estimated by the Consequence Team using two computer models as follows:

- LIFESim Modeling System¹ was developed: a) to estimate how the population in the flooded sub-basins would redistribute vertically in relation to the depth of inundation; and b) to classify population into one of three flood lethality zones, which are defined in the LIFESim model and by McClelland and Bowles (2002), and an additional sub-zone for people who would be expected to be able to walk away from the inundation area following inundation. Thus, LIFESim was run without evacuation.
- A Monte Carlo Uncertainty Model, which was developed to take the vertically re-distributed estimates of population in the three flood lethality zones from LIFESim, estimated: a) the immediate loss of life using fatality rate probability distributions from LIFESim and McClelland (2000) accounting for evacuation effectiveness as a random variable that varied according to a triangular probability distribution (65 percent, 80 percent, 95 percent); and b) delayed fatalities amongst those who survived the initial inundation but were not rescued, where the rescue effectiveness was accounted for a random variable that varied according to a uniform probability distribution between 99.5 percent and 100 percent in the Safe Flood Lethality Zone and between 95 percent and 100 percent in the Compromised and Chance Flood Lethality Zones.

The entire process is described in a report by Abt Associates, Inc. (2006) and involved the following steps:

- 1) Calibration of LIFESim to the Hurricane Katrina event.
- 2) Use of LIFESim and the Monte Carlo Uncertainty Model to estimate immediate and delayed life loss associated with the entire range of maximum inundation levels, given the population and housing stock that existed prior to Hurricane Katrina.
- 3) Use of LIFESim and the Monte Carlo Uncertainty Model to estimate immediate and delayed life loss associated with the entire range of maximum inundation levels, given the population and housing stock that were expected to exist June 1, 2006.

Various limitations in this approach and some potential future improvements are described in the report by Abt Associates, Inc. (2006). The distributions of life-loss estimates for each

¹ Institute for Dam Safety Risk Management at Utah State University (Aboelata and Bowles 2005) LIFESim includes a simulation module for warning and evacuation, which was not used in this study.

sub-basin currently combine aleatory uncertainty associated with the fatality rates in each Flood Lethality Zone and epistemic uncertainties associated with evacuation and rescue effectivenesses. It is desired to treat the epistemic and aleatory uncertainties separately in future work.

Direct Economic Loss Estimation

The objective of the direct economic damage analysis was to develop potential stage-damage curves that might represent the flood damage potential as of June 1, 2007. This required accounting for the severity of the Katrina damage and the amount of property loss recovery since Katrina. In some areas flooded by Katrina, where water depths were low, recovery has been almost complete. In other areas, where water depths were high, little recovery or reinvestment has taken place. It is extremely difficult and at the peril of the analyst to make general estimates about the amount of recovery. None the less, some guidance exists in terms of what others have assumed about recovery. The analysis conducted followed the basic parameters provided in the RAND Gulf States Policy Institute published a report titled “The Repopulation of New Orleans after Hurricane Katrina” (2006). In developing estimates of repopulation over time, the authors relied on the depth of flooding as the basic determinant of the rate of population recovery.

Table 12-1 shows the depth categories and damage recovery rates assumed in developing the June 2006 stage-damage. A RAND category of <2 foot was subdivided into two categories: <1 foot and 1 to 2 feet. Additionally, the >4 feet category was subdivided into three categories: 4 to 6 feet; 6 to 8 feet; and >8 feet. These categories are consistent with those used in social, cultural and historic analysis of the impacts of Katrina the post-Katrina recovery. However, the values of recovery rates are to some degree arbitrary and other rates may be justified. For the estimate of the post-Katrina stage-damage functions shown in this section, these rates were used. The use of these values resulted in an estimate of the March 2006 population of New Orleans of approximately 155,000 people. This is within the range of other estimates.

The June 2006 estimate of potential stage-property damage started with these assumptions. However, the range of depths of flooding was expanded to include more depth of flooding categories while preserving the basic concept.

Table 12-1: Estimated Repopulation Rates for New Orleans		
Period	Depth of Flooding	Repopulation Rate (%)
December 2005	No flooding	65
	<2 feet	20
	2–4 feet	5
	>4 feet	1
March 2006	No flooding	100
	<2 feet	35
	2–4 feet	15
	>4 feet	5
September 2006	No flooding	110
	<2 feet	75
	2–4 feet	25
	>4 feet	10
Source: RAND (2006), "The Repopulation of New Orleans after Hurricane Katrina."		

Approach

The post-Katrina stage-damage tables and curves were estimated using the same sub-basin definitions as for the pre-Katrina values. Additionally, the estimation started with the same census block approach. The Katrina depth grid was used to estimate the depth of flooding for each census block. These depths were then used to select the census blocks that incurred damages within each of the categories shown in Table 12-1. For instance, within the Orleans Metro 5 sub-basin, 1,535 census blocks had flooding of 1 foot or less while a total of 4,400 census blocks were flooded. Table 12-2 shows the complete estimate of the number of the census blocks flooded by Katrina by depth category.

From these selected census blocks, damages at each stage were aggregated to the sub-basin level for each of the recovery category. This calculation determined the amount of the Katrina damage within each depth category. This was repeated for each of the Katrina flood depth categories.

For each resulting sub-basin stage-damage, the recovery factors from Table 12-1 were applied. The recovered potential damage value was then aggregated at each stage. This provides an estimate of the Current HPS potential property damage at each stage for all property damaged estimated to have occurred from Katrina. The last step in the process was to adjust the potential pre-Katrina stage-damages by first subtracting the Katrina damage at each stage and then adding the potential recovered damage at each stage. This was necessary because the Katrina flood levels were not high enough to damage all the property in a sub-basin, at least for some sub-basins.

Therefore, for some property, recovery from flooding was not necessary, so it contributed its full damage potential to the post-Katrina, Current HPS, stage-damage. Table 12-5 provides the

pre-Katrina damage potential and the Current HPS damage potential by stage for all sub-basins flooded by Katrina. Stage-damage for all other sub-basins retained the pre-Katrina stage-damages. All stages are in NAVD88 (2004.65).

Tables 12-3 and 12-4 provide the pre-Katrina fatality potential and the Current HPS fatality potential by stage for all sub-basins flooded by Katrina. Note these tables reflect the post-Katrina repopulation as 1 June 2006. Stage-fatality for all other sub-basins retained the pre-Katrina stage-fatalities. All stages are in NAVD88 (2004.65).

Table 12-2: Number of Census Blocks within Each Subbasin Flooded by Katrina by Depth Category						
Subbasin Name	Count Of Census Blocks within Katrina Flood Depth Category					
	0-1 feet	1 to 2 feet	2 to 4 feet	4 to 6 feet	6 to 8 feet	> 8 feet
JE2	5	6	8	1	1	1
NOE2	1	2	2	10	19	7
NOE3	7	8	12	8	59	7
NOE4	18	3	0	0	0	0
NOE5	27	31	156	173	371	99
OM1	37	37	107	126	163	361
OM2	24	24	46	56	121	321
OM3	301	136	387	358	219	61
OM4	63	51	72	50	9	1
OM5	1535	346	871	957	640	35
SB1	31	25	91	153	200	375
SB3	62	32	49	117	173	44
SB4	5	37	62	50	13	0

Table 12-3 Pre-Katrina – Stage-Fatality

Elevation (ft)	OW1			OW2		
	5%	95%	Mean	5%	95%	Mean
-1.200E+01	0.000E+00	0.000E+00	0.000E+00	0.000E+00	0.000E+00	0.000E+00
-1.100E+01	0.000E+00	0.000E+00	0.000E+00	0.000E+00	0.000E+00	0.000E+00
-1.000E+01	0.000E+00	0.000E+00	0.000E+00	0.000E+00	0.000E+00	0.000E+00
-9.000E+00	0.000E+00	0.000E+00	0.000E+00	0.000E+00	0.000E+00	0.000E+00
-8.000E+00	0.000E+00	0.000E+00	0.000E+00	8.720E-03	2.237E-01	1.010E-01
-7.000E+00	0.000E+00	0.000E+00	0.000E+00	1.744E-02	4.473E-01	2.021E-01
-6.000E+00	0.000E+00	0.000E+00	0.000E+00	1.188E-01	1.940E+00	8.842E-01
-5.000E+00	0.000E+00	0.000E+00	0.000E+00	2.202E-01	3.433E+00	1.566E+00
-4.000E+00	0.000E+00	0.000E+00	0.000E+00	1.176E+00	6.997E+00	3.671E+00
-3.000E+00	6.353E-05	1.630E-03	7.361E-04	2.132E+00	1.056E+01	5.776E+00
-2.000E+00	1.271E-04	3.259E-03	1.472E-03	3.266E+00	1.810E+01	9.616E+00
-1.000E+00	5.400E-04	1.385E-02	6.257E-03	4.399E+00	2.565E+01	1.346E+01
0.000E+00	9.529E-04	2.444E-02	1.104E-02	6.662E+00	3.478E+01	1.871E+01
1.000E+00	1.348E-03	3.458E-02	1.562E-02	8.925E+00	4.392E+01	2.397E+01
2.000E+00	1.744E-03	4.472E-02	2.020E-02	1.431E+01	7.348E+01	3.785E+01
3.000E+00	6.153E-03	1.485E-01	6.724E-02	1.969E+01	1.030E+02	5.173E+01
4.000E+00	1.056E-02	2.523E-01	1.143E-01	4.150E+01	1.878E+02	1.009E+02
5.000E+00	3.526E-02	7.662E-01	3.486E-01	6.332E+01	2.726E+02	1.500E+02
6.000E+00	5.996E-02	1.280E+00	5.829E-01	1.080E+02	4.066E+02	2.434E+02
7.000E+00	8.664E-02	1.399E+00	6.363E-01	1.526E+02	5.406E+02	3.367E+02
8.000E+00	1.133E-01	1.519E+00	6.896E-01	1.909E+02	6.699E+02	4.200E+02
9.000E+00	2.877E-01	2.529E+00	1.137E+00	2.292E+02	7.992E+02	5.032E+02
1.000E+01	4.620E-01	3.540E+00	1.584E+00	2.819E+02	9.969E+02	6.231E+02
1.100E+01	1.359E+00	6.906E+00	3.515E+00	3.347E+02	1.195E+03	7.429E+02
1.200E+01	2.256E+00	1.027E+01	5.447E+00	4.499E+02	1.670E+03	1.015E+03
1.300E+01	3.810E+00	1.438E+01	8.587E+00	5.652E+02	2.145E+03	1.287E+03
1.400E+01	5.364E+00	1.849E+01	1.173E+01	8.275E+02	2.997E+03	1.850E+03
1.500E+01	5.855E+00	2.018E+01	1.280E+01	1.090E+03	3.849E+03	2.413E+03
1.600E+01	6.346E+00	2.188E+01	1.388E+01	1.337E+03	4.678E+03	2.948E+03
1.700E+01	7.170E+00	2.823E+01	1.640E+01	1.584E+03	5.507E+03	3.483E+03
1.800E+01	7.993E+00	3.457E+01	1.893E+01	1.806E+03	6.274E+03	3.970E+03
1.900E+01	1.336E+01	6.909E+01	3.400E+01	2.027E+03	7.041E+03	4.458E+03
2.000E+01	1.873E+01	1.036E+02	4.908E+01	2.272E+03	7.895E+03	4.998E+03
2.100E+01	3.813E+01	1.518E+02	8.787E+01	2.516E+03	8.748E+03	5.538E+03
2.200E+01	5.753E+01	2.000E+02	1.267E+02	2.779E+03	9.660E+03	6.118E+03
2.300E+01	6.151E+01	2.139E+02	1.356E+02	3.042E+03	1.057E+04	6.698E+03
2.400E+01	6.550E+01	2.278E+02	1.445E+02	3.276E+03	1.138E+04	7.214E+03

Table 12-3 Pre-Katrina – Stage-Fatality (Continued)

Elevation (ft)	NOE1			NOE2		
	5%	95%	Mean	5%	95%	Mean
-1.200E+01	0.000E+00	0.000E+00	0.000E+00	0.000E+00	0.000E+00	0.000E+00
-1.100E+01	0.000E+00	0.000E+00	0.000E+00	0.000E+00	0.000E+00	0.000E+00
-1.000E+01	0.000E+00	0.000E+00	0.000E+00	0.000E+00	0.000E+00	0.000E+00
-9.000E+00	0.000E+00	0.000E+00	0.000E+00	0.000E+00	0.000E+00	0.000E+00
-8.000E+00	0.000E+00	0.000E+00	0.000E+00	0.000E+00	0.000E+00	0.000E+00
-7.000E+00	0.000E+00	0.000E+00	0.000E+00	1.816E-03	4.659E-02	2.105E-02
-6.000E+00	0.000E+00	0.000E+00	0.000E+00	3.633E-03	9.319E-02	4.210E-02
-5.000E+00	0.000E+00	0.000E+00	0.000E+00	1.653E-02	4.239E-01	1.915E-01
-4.000E+00	0.000E+00	0.000E+00	0.000E+00	2.942E-02	7.547E-01	3.409E-01
-3.000E+00	0.000E+00	0.000E+00	0.000E+00	5.422E-02	1.386E+00	6.259E-01
-2.000E+00	0.000E+00	0.000E+00	0.000E+00	7.902E-02	2.016E+00	9.110E-01
-1.000E+00	0.000E+00	0.000E+00	0.000E+00	9.187E-02	2.236E+00	1.012E+00
0.000E+00	8.338E-05	1.008E-03	4.802E-04	1.047E-01	2.456E+00	1.113E+00
1.000E+00	1.668E-04	2.016E-03	9.604E-04	1.445E-01	2.545E+00	1.172E+00
2.000E+00	1.089E-03	1.141E-02	5.518E-03	1.843E-01	2.635E+00	1.230E+00
3.000E+00	2.011E-03	2.081E-02	1.008E-02	3.056E-01	2.941E+00	1.425E+00
4.000E+00	3.734E-03	2.748E-02	1.324E-02	4.269E-01	3.247E+00	1.620E+00
5.000E+00	5.456E-03	3.415E-02	1.640E-02	5.362E-01	3.503E+00	1.793E+00
6.000E+00	1.003E-02	7.461E-02	3.152E-02	6.455E-01	3.760E+00	1.966E+00
7.000E+00	1.461E-02	1.151E-01	4.664E-02	9.045E-01	6.650E+00	2.922E+00
8.000E+00	4.229E-02	1.779E-01	9.972E-02	1.163E+00	9.541E+00	3.878E+00
9.000E+00	6.997E-02	2.407E-01	1.528E-01	4.001E+00	3.060E+01	1.236E+01
1.000E+01	7.640E-02	2.632E-01	1.669E-01	6.839E+00	5.165E+01	2.085E+01
1.100E+01	8.282E-02	2.857E-01	1.811E-01	2.188E+01	1.127E+02	5.578E+01
1.200E+01	9.133E-02	3.313E-01	2.032E-01	3.692E+01	1.738E+02	9.071E+01
1.300E+01	9.985E-02	3.769E-01	2.253E-01	6.715E+01	2.604E+02	1.538E+02
1.400E+01	1.302E-01	6.143E-01	3.196E-01	9.738E+01	3.471E+02	2.168E+02
1.500E+01	1.605E-01	8.517E-01	4.138E-01	1.170E+02	4.113E+02	2.592E+02
1.600E+01	3.306E-01	1.305E+00	7.606E-01	1.367E+02	4.756E+02	3.015E+02
1.700E+01	5.007E-01	1.759E+00	1.107E+00	1.388E+02	4.829E+02	3.061E+02
1.800E+01	5.832E-01	2.037E+00	1.288E+00	1.409E+02	4.902E+02	3.107E+02
1.900E+01	6.658E-01	2.316E+00	1.468E+00	1.436E+02	4.992E+02	3.164E+02
2.000E+01	6.735E-01	2.343E+00	1.485E+00	1.463E+02	5.083E+02	3.221E+02
2.100E+01	6.812E-01	2.369E+00	1.502E+00	1.523E+02	5.291E+02	3.353E+02
2.200E+01	6.847E-01	2.382E+00	1.510E+00	1.583E+02	5.499E+02	3.486E+02
2.300E+01	6.883E-01	2.395E+00	1.518E+00	1.646E+02	5.725E+02	3.629E+02
2.400E+01	6.984E-01	2.427E+00	1.538E+00	1.710E+02	5.951E+02	3.772E+02

Table 12-3 Pre-Katrina – Stage-Fatality (Continued)

Elevation (ft)	NOE3			NOE4		
	5%	95%	Mean	5%	95%	Mean
-1.200E+01	0.000E+00	0.000E+00	0.000E+00	0.000E+00	0.000E+00	0.000E+00
-1.100E+01	0.000E+00	0.000E+00	0.000E+00	0.000E+00	0.000E+00	0.000E+00
-1.000E+01	0.000E+00	0.000E+00	0.000E+00	0.000E+00	0.000E+00	0.000E+00
-9.000E+00	0.000E+00	0.000E+00	0.000E+00	0.000E+00	0.000E+00	0.000E+00
-8.000E+00	0.000E+00	0.000E+00	0.000E+00	0.000E+00	0.000E+00	0.000E+00
-7.000E+00	0.000E+00	0.000E+00	0.000E+00	0.000E+00	0.000E+00	0.000E+00
-6.000E+00	0.000E+00	0.000E+00	0.000E+00	0.000E+00	0.000E+00	0.000E+00
-5.000E+00	0.000E+00	0.000E+00	0.000E+00	1.412E-04	3.621E-03	1.636E-03
-4.000E+00	3.402E-02	8.725E-01	3.942E-01	1.412E-04	3.621E-03	1.636E-03
-3.000E+00	1.369E-01	3.512E+00	1.587E+00	1.412E-04	3.621E-03	1.636E-03
-2.000E+00	2.399E-01	6.152E+00	2.779E+00	1.412E-04	3.621E-03	1.636E-03
-1.000E+00	5.787E-01	8.104E+00	3.811E+00	1.421E-03	3.645E-02	1.647E-02
0.000E+00	9.176E-01	1.006E+01	4.843E+00	1.826E-03	4.604E-02	2.081E-02
1.000E+00	2.986E+00	1.772E+01	9.158E+00	2.230E-03	5.562E-02	2.515E-02
2.000E+00	5.055E+00	2.538E+01	1.347E+01	4.176E-03	9.278E-02	4.220E-02
3.000E+00	8.539E+00	4.074E+01	2.153E+01	6.122E-03	1.299E-01	5.925E-02
4.000E+00	1.202E+01	5.610E+01	2.960E+01	1.084E-02	1.533E-01	7.060E-02
5.000E+00	2.164E+01	8.393E+01	4.940E+01	1.556E-02	1.766E-01	8.194E-02
6.000E+00	3.125E+01	1.118E+02	6.920E+01	4.666E-02	3.673E-01	1.663E-01
7.000E+00	4.053E+01	1.426E+02	8.923E+01	7.775E-02	5.580E-01	2.506E-01
8.000E+00	4.980E+01	1.734E+02	1.093E+02	2.179E-01	1.157E+00	5.718E-01
9.000E+00	6.013E+01	2.177E+02	1.336E+02	3.580E-01	1.755E+00	8.929E-01
1.000E+01	7.045E+01	2.619E+02	1.580E+02	6.284E-01	2.425E+00	1.429E+00
1.100E+01	9.705E+01	4.081E+02	2.282E+02	8.987E-01	3.094E+00	1.964E+00
1.200E+01	1.236E+02	5.543E+02	2.983E+02	9.438E-01	3.251E+00	2.064E+00
1.300E+01	2.255E+02	9.105E+02	5.242E+02	9.888E-01	3.408E+00	2.163E+00
1.400E+01	3.273E+02	1.267E+03	7.502E+02	1.081E+00	4.033E+00	2.428E+00
1.500E+01	4.597E+02	1.662E+03	1.027E+03	1.174E+00	4.657E+00	2.694E+00
1.600E+01	5.921E+02	2.057E+03	1.304E+03	1.714E+00	7.458E+00	4.077E+00
1.700E+01	6.265E+02	2.178E+03	1.381E+03	2.255E+00	1.026E+01	5.459E+00
1.800E+01	6.608E+02	2.299E+03	1.457E+03	3.858E+00	1.467E+01	8.754E+00
1.900E+01	6.730E+02	2.341E+03	1.484E+03	5.460E+00	1.908E+01	1.205E+01
2.000E+01	6.851E+02	2.383E+03	1.511E+03	6.148E+00	2.143E+01	1.356E+01
2.100E+01	7.032E+02	2.444E+03	1.549E+03	6.835E+00	2.377E+01	1.507E+01
2.200E+01	7.213E+02	2.505E+03	1.588E+03	6.912E+00	2.403E+01	1.524E+01
2.300E+01	7.537E+02	2.620E+03	1.660E+03	6.988E+00	2.430E+01	1.540E+01
2.400E+01	7.861E+02	2.734E+03	1.733E+03	7.096E+00	2.466E+01	1.564E+01

Table 12-3 Pre-Katrina – Stage-Fatality (Continued)

Elevation (ft)	NOE5		
	5%	95%	Mean
-1.200E+01	0.000E+00	0.000E+00	0.000E+00
-1.100E+01	0.000E+00	0.000E+00	0.000E+00
-1.000E+01	0.000E+00	0.000E+00	0.000E+00
-9.000E+00	1.494E-01	3.832E+00	1.731E+00
-8.000E+00	3.232E-01	8.289E+00	3.744E+00
-7.000E+00	4.969E-01	1.275E+01	5.758E+00
-6.000E+00	8.620E-01	2.163E+01	9.776E+00
-5.000E+00	1.227E+00	3.052E+01	1.379E+01
-4.000E+00	2.650E+00	4.470E+01	2.071E+01
-3.000E+00	4.073E+00	5.888E+01	2.762E+01
-2.000E+00	1.262E+01	9.192E+01	4.507E+01
-1.000E+00	2.118E+01	1.250E+02	6.253E+01
0.000E+00	5.627E+01	2.518E+02	1.382E+02
1.000E+00	9.136E+01	3.786E+02	2.139E+02
2.000E+00	1.762E+02	6.590E+02	3.968E+02
3.000E+00	2.610E+02	9.394E+02	5.797E+02
4.000E+00	3.461E+02	1.217E+03	7.623E+02
5.000E+00	4.312E+02	1.496E+03	9.449E+02
6.000E+00	5.048E+02	1.779E+03	1.114E+03
7.000E+00	5.783E+02	2.062E+03	1.284E+03
8.000E+00	7.841E+02	3.100E+03	1.806E+03
9.000E+00	9.899E+02	4.138E+03	2.328E+03
1.000E+01	1.638E+03	6.196E+03	3.719E+03
1.100E+01	2.286E+03	8.255E+03	5.111E+03
1.200E+01	2.946E+03	1.041E+04	6.528E+03
1.300E+01	3.605E+03	1.256E+04	7.945E+03
1.400E+01	3.990E+03	1.387E+04	8.786E+03
1.500E+01	4.374E+03	1.519E+04	9.628E+03
1.600E+01	4.604E+03	1.600E+04	1.014E+04
1.700E+01	4.835E+03	1.681E+04	1.065E+04
1.800E+01	4.999E+03	1.738E+04	1.101E+04
1.900E+01	5.162E+03	1.794E+04	1.137E+04
2.000E+01	5.354E+03	1.861E+04	1.180E+04
2.100E+01	5.546E+03	1.929E+04	1.223E+04
2.200E+01	5.676E+03	1.974E+04	1.252E+04
2.300E+01	5.806E+03	2.020E+04	1.280E+04
2.400E+01	5.891E+03	2.050E+04	1.299E+04

Table 12-3 Pre-Katrina – Stage-Fatality (Continued)

Elevation (ft)	OM1			OM2		
	5%	95%	Mean	5%	95%	Mean
-1.200E+01	0.000E+00	0.000E+00	0.000E+00	7.508E-01	1.315E+01	6.061E+00
-1.100E+01	0.000E+00	0.000E+00	0.000E+00	1.064E+00	1.680E+01	7.794E+00
-1.000E+01	0.000E+00	0.000E+00	0.000E+00	2.865E+00	4.129E+01	1.549E+01
-9.000E+00	8.096E-02	2.986E-01	1.824E-01	4.666E+00	6.579E+01	2.318E+01
-8.000E+00	1.619E-01	5.972E-01	3.649E-01	2.644E+01	1.332E+02	6.798E+01
-7.000E+00	2.143E-01	8.507E-01	5.017E-01	4.822E+01	2.007E+02	1.128E+02
-6.000E+00	2.668E-01	1.104E+00	6.385E-01	7.812E+01	2.879E+02	1.747E+02
-5.000E+00	4.931E-01	3.167E+00	1.633E+00	1.080E+02	3.751E+02	2.367E+02
-4.000E+00	7.194E-01	5.229E+00	2.627E+00	1.227E+02	4.244E+02	2.687E+02
-3.000E+00	1.034E+00	1.004E+01	4.855E+00	1.374E+02	4.737E+02	3.006E+02
-2.000E+00	1.348E+00	1.486E+01	7.084E+00	1.500E+02	5.207E+02	3.292E+02
-1.000E+00	1.348E+00	1.486E+01	7.084E+00	1.627E+02	5.678E+02	3.578E+02
0.000E+00	1.348E+00	1.486E+01	7.084E+00	2.053E+02	8.081E+02	4.717E+02
1.000E+00	8.128E+00	5.889E+01	2.862E+01	2.480E+02	1.048E+03	5.856E+02
2.000E+00	1.990E+01	1.046E+02	5.426E+01	4.147E+02	1.552E+03	9.372E+02
3.000E+00	3.168E+01	1.504E+02	7.990E+01	5.814E+02	2.055E+03	1.289E+03
4.000E+00	5.795E+01	2.323E+02	1.346E+02	7.098E+02	2.486E+03	1.567E+03
5.000E+00	8.422E+01	3.142E+02	1.893E+02	8.382E+02	2.916E+03	1.845E+03
6.000E+00	1.173E+02	4.216E+02	2.602E+02	9.228E+02	3.207E+03	2.032E+03
7.000E+00	1.504E+02	5.290E+02	3.311E+02	1.007E+03	3.498E+03	2.218E+03
8.000E+00	1.894E+02	6.735E+02	4.189E+02	1.057E+03	3.670E+03	2.327E+03
9.000E+00	2.283E+02	8.179E+02	5.068E+02	1.106E+03	3.842E+03	2.436E+03
1.000E+01	3.027E+02	1.115E+03	6.803E+02	1.162E+03	4.037E+03	2.560E+03
1.100E+01	3.770E+02	1.412E+03	8.538E+02	1.218E+03	4.231E+03	2.683E+03
1.200E+01	5.509E+02	2.030E+03	1.241E+03	1.295E+03	4.498E+03	2.852E+03
1.300E+01	7.248E+02	2.648E+03	1.629E+03	1.372E+03	4.765E+03	3.021E+03
1.400E+01	9.938E+02	3.563E+03	2.217E+03	1.444E+03	5.015E+03	3.179E+03
1.500E+01	1.263E+03	4.479E+03	2.805E+03	1.515E+03	5.266E+03	3.338E+03
1.600E+01	1.574E+03	5.527E+03	3.480E+03	1.563E+03	5.434E+03	3.445E+03
1.700E+01	1.885E+03	6.576E+03	4.156E+03	1.610E+03	5.602E+03	3.551E+03
1.800E+01	2.141E+03	7.452E+03	4.718E+03	1.631E+03	5.675E+03	3.598E+03
1.900E+01	2.397E+03	8.327E+03	5.279E+03	1.652E+03	5.747E+03	3.644E+03
2.000E+01	2.553E+03	8.868E+03	5.622E+03	1.671E+03	5.814E+03	3.686E+03
2.100E+01	2.709E+03	9.409E+03	5.965E+03	1.690E+03	5.880E+03	3.727E+03
2.200E+01	2.830E+03	9.834E+03	6.233E+03	1.708E+03	5.944E+03	3.768E+03
2.300E+01	2.951E+03	1.026E+04	6.502E+03	1.727E+03	6.008E+03	3.809E+03
2.400E+01	3.046E+03	1.059E+04	6.712E+03	1.745E+03	6.075E+03	3.851E+03

Table 12-3 Pre-Katrina – Stage-Fatality (Continued)

Elevation (ft)	OM3			OM4		
	5%	95%	Mean	5%	95%	Mean
-1.200E+01	0.000E+00	0.000E+00	0.000E+00	0.000E+00	0.000E+00	0.000E+00
-1.100E+01	0.000E+00	0.000E+00	0.000E+00	1.007E-03	2.583E-02	1.167E-02
-1.000E+01	0.000E+00	0.000E+00	0.000E+00	2.014E-03	5.166E-02	2.334E-02
-9.000E+00	0.000E+00	0.000E+00	0.000E+00	1.252E-02	3.492E-01	1.214E-01
-8.000E+00	0.000E+00	0.000E+00	0.000E+00	2.302E-02	6.467E-01	2.194E-01
-7.000E+00	0.000E+00	0.000E+00	0.000E+00	2.178E-01	1.814E+00	7.472E-01
-6.000E+00	0.000E+00	0.000E+00	0.000E+00	4.127E-01	2.982E+00	1.275E+00
-5.000E+00	4.004E-02	5.220E-01	2.429E-01	1.170E+00	4.837E+00	2.746E+00
-4.000E+00	8.009E-02	1.044E+00	4.858E-01	1.928E+00	6.692E+00	4.216E+00
-3.000E+00	5.456E-01	5.165E+00	2.499E+00	2.362E+00	8.299E+00	5.197E+00
-2.000E+00	1.011E+00	9.287E+00	4.511E+00	2.797E+00	9.907E+00	6.177E+00
-1.000E+00	1.907E+00	2.050E+01	9.799E+00	3.471E+00	1.327E+01	7.884E+00
0.000E+00	2.802E+00	3.172E+01	1.509E+01	4.145E+00	1.663E+01	9.590E+00
1.000E+00	5.188E+00	4.896E+01	2.373E+01	6.205E+00	2.702E+01	1.478E+01
2.000E+00	7.574E+00	6.621E+01	3.237E+01	8.265E+00	3.740E+01	1.996E+01
3.000E+00	1.976E+01	1.280E+02	6.116E+01	1.507E+01	6.099E+01	3.488E+01
4.000E+00	3.194E+01	1.899E+02	8.995E+01	2.187E+01	8.458E+01	4.979E+01
5.000E+00	7.468E+01	3.231E+02	1.791E+02	3.390E+01	1.232E+02	7.557E+01
6.000E+00	1.174E+02	4.563E+02	2.683E+02	4.593E+01	1.618E+02	1.013E+02
7.000E+00	1.748E+02	6.341E+02	3.891E+02	5.789E+01	2.034E+02	1.276E+02
8.000E+00	2.323E+02	8.119E+02	5.100E+02	6.985E+01	2.449E+02	1.539E+02
9.000E+00	2.809E+02	9.771E+02	6.158E+02	8.648E+01	3.039E+02	1.908E+02
1.000E+01	3.295E+02	1.142E+03	7.216E+02	1.031E+02	3.630E+02	2.277E+02
1.100E+01	3.970E+02	1.450E+03	8.881E+02	1.294E+02	4.581E+02	2.866E+02
1.200E+01	4.645E+02	1.757E+03	1.055E+03	1.557E+02	5.533E+02	3.455E+02
1.300E+01	6.922E+02	2.586E+03	1.567E+03	1.980E+02	6.962E+02	4.376E+02
1.400E+01	9.199E+02	3.415E+03	2.079E+03	2.403E+02	8.391E+02	5.296E+02
1.500E+01	1.308E+03	4.718E+03	2.923E+03	2.847E+02	9.930E+02	6.271E+02
1.600E+01	1.696E+03	6.020E+03	3.767E+03	3.291E+02	1.147E+03	7.247E+02
1.700E+01	2.119E+03	7.431E+03	4.680E+03	3.807E+02	1.325E+03	8.379E+02
1.800E+01	2.542E+03	8.842E+03	5.593E+03	4.323E+02	1.503E+03	9.512E+02
1.900E+01	2.867E+03	9.965E+03	6.309E+03	4.849E+02	1.685E+03	1.067E+03
2.000E+01	3.192E+03	1.109E+04	7.025E+03	5.375E+02	1.868E+03	1.183E+03
2.100E+01	3.467E+03	1.204E+04	7.632E+03	5.827E+02	2.024E+03	1.283E+03
2.200E+01	3.742E+03	1.300E+04	8.239E+03	6.279E+02	2.180E+03	1.382E+03
2.300E+01	3.986E+03	1.385E+04	8.778E+03	6.567E+02	2.282E+03	1.446E+03
2.400E+01	4.231E+03	1.469E+04	9.316E+03	6.855E+02	2.383E+03	1.510E+03

Table 12-3 Pre-Katrina – Stage-Fatality (Continued)

Elevation (ft)	OM5		
	5%	95%	Mean
-1.200E+01	0.000E+00	0.000E+00	0.000E+00
-1.100E+01	0.000E+00	0.000E+00	0.000E+00
-1.000E+01	0.000E+00	0.000E+00	0.000E+00
-9.000E+00	0.000E+00	0.000E+00	0.000E+00
-8.000E+00	0.000E+00	0.000E+00	0.000E+00
-7.000E+00	0.000E+00	0.000E+00	0.000E+00
-6.000E+00	0.000E+00	0.000E+00	0.000E+00
-5.000E+00	0.000E+00	0.000E+00	0.000E+00
-4.000E+00	8.259E-01	3.053E+00	1.861E+00
-3.000E+00	1.652E+00	6.106E+00	3.721E+00
-2.000E+00	3.532E+00	2.417E+01	1.235E+01
-1.000E+00	5.412E+00	4.222E+01	2.097E+01
0.000E+00	7.129E+00	6.399E+01	3.118E+01
1.000E+00	8.845E+00	8.575E+01	4.140E+01
2.000E+00	1.223E+01	1.145E+02	5.566E+01
3.000E+00	1.562E+01	1.433E+02	6.992E+01
4.000E+00	3.979E+01	2.925E+02	1.325E+02
5.000E+00	6.397E+01	4.417E+02	1.950E+02
6.000E+00	1.752E+02	7.693E+02	4.227E+02
7.000E+00	2.865E+02	1.097E+03	6.504E+02
8.000E+00	4.201E+02	1.520E+03	9.339E+02
9.000E+00	5.537E+02	1.943E+03	1.217E+03
1.000E+01	6.791E+02	2.364E+03	1.490E+03
1.100E+01	8.045E+02	2.786E+03	1.762E+03
1.200E+01	9.419E+02	3.305E+03	2.075E+03
1.300E+01	1.079E+03	3.825E+03	2.389E+03
1.400E+01	1.436E+03	5.444E+03	3.262E+03
1.500E+01	1.794E+03	7.063E+03	4.134E+03
1.600E+01	2.786E+03	1.028E+04	6.275E+03
1.700E+01	3.777E+03	1.350E+04	8.415E+03
1.800E+01	4.850E+03	1.707E+04	1.073E+04
1.900E+01	5.923E+03	2.064E+04	1.305E+04
2.000E+01	6.808E+03	2.369E+04	1.499E+04
2.100E+01	7.694E+03	2.673E+04	1.694E+04
2.200E+01	8.312E+03	2.888E+04	1.831E+04
2.300E+01	8.930E+03	3.102E+04	1.967E+04
2.400E+01	9.564E+03	3.322E+04	2.106E+04

Table 12-3 Pre-Katrina – Stage-Fatality (Continued)

Elevation (ft)	SB1			SB3		
	5%	95%	Mean	5%	95%	Mean
-1.200E+01	0.000E+00	0.000E+00	0.000E+00	0.000E+00	0.000E+00	0.000E+00
-1.100E+01	0.000E+00	0.000E+00	0.000E+00	0.000E+00	0.000E+00	0.000E+00
-1.000E+01	0.000E+00	0.000E+00	0.000E+00	0.000E+00	0.000E+00	0.000E+00
-9.000E+00	0.000E+00	0.000E+00	0.000E+00	0.000E+00	0.000E+00	0.000E+00
-8.000E+00	0.000E+00	0.000E+00	0.000E+00	0.000E+00	0.000E+00	0.000E+00
-7.000E+00	0.000E+00	0.000E+00	0.000E+00	0.000E+00	0.000E+00	0.000E+00
-6.000E+00	0.000E+00	0.000E+00	0.000E+00	0.000E+00	0.000E+00	0.000E+00
-5.000E+00	0.000E+00	0.000E+00	0.000E+00	0.000E+00	0.000E+00	0.000E+00
-4.000E+00	0.000E+00	0.000E+00	0.000E+00	0.000E+00	0.000E+00	0.000E+00
-3.000E+00	0.000E+00	0.000E+00	0.000E+00	0.000E+00	0.000E+00	0.000E+00
-2.000E+00	0.000E+00	0.000E+00	0.000E+00	0.000E+00	0.000E+00	0.000E+00
-1.000E+00	0.000E+00	0.000E+00	0.000E+00	0.000E+00	0.000E+00	0.000E+00
0.000E+00	0.000E+00	0.000E+00	0.000E+00	0.000E+00	0.000E+00	0.000E+00
1.000E+00	1.226E+00	2.429E+01	1.111E+01	5.927E-01	4.089E+00	2.070E+00
2.000E+00	2.453E+00	4.859E+01	2.222E+01	1.185E+00	8.178E+00	4.141E+00
3.000E+00	2.597E+00	4.999E+01	2.290E+01	3.716E+00	2.489E+01	1.267E+01
4.000E+00	2.742E+00	5.139E+01	2.358E+01	6.246E+00	4.159E+01	2.120E+01
5.000E+00	6.060E+00	1.307E+02	4.488E+01	7.259E+00	4.414E+01	2.292E+01
6.000E+00	9.377E+00	2.099E+02	6.618E+01	8.272E+00	4.668E+01	2.464E+01
7.000E+00	8.578E+01	4.743E+02	2.294E+02	3.417E+01	1.340E+02	8.054E+01
8.000E+00	1.622E+02	7.387E+02	3.926E+02	6.006E+01	2.213E+02	1.364E+02
9.000E+00	2.826E+02	1.072E+03	6.403E+02	1.576E+02	5.524E+02	3.486E+02
1.000E+01	4.031E+02	1.405E+03	8.879E+02	2.552E+02	8.836E+02	5.607E+02
1.100E+01	4.096E+02	1.424E+03	9.015E+02	2.552E+02	8.836E+02	5.607E+02
1.200E+01	4.162E+02	1.442E+03	9.151E+02	2.552E+02	8.836E+02	5.607E+02
1.300E+01	4.162E+02	1.442E+03	9.151E+02	2.624E+02	1.040E+03	6.035E+02
1.400E+01	4.162E+02	1.442E+03	9.152E+02	2.696E+02	1.197E+03	6.462E+02
1.500E+01	4.586E+02	2.103E+03	1.114E+03	4.215E+02	2.120E+03	1.061E+03
1.600E+01	5.009E+02	2.764E+03	1.312E+03	5.735E+02	3.043E+03	1.477E+03
1.700E+01	1.117E+03	4.493E+03	2.590E+03	1.077E+03	4.266E+03	2.479E+03
1.800E+01	1.733E+03	6.223E+03	3.867E+03	1.580E+03	5.490E+03	3.481E+03
1.900E+01	2.161E+03	7.627E+03	4.793E+03	1.624E+03	5.649E+03	3.580E+03
2.000E+01	2.590E+03	9.031E+03	5.718E+03	1.667E+03	5.808E+03	3.679E+03
2.100E+01	2.611E+03	9.101E+03	5.764E+03	1.667E+03	5.808E+03	3.679E+03
2.200E+01	2.632E+03	9.170E+03	5.809E+03	1.667E+03	5.808E+03	3.680E+03
2.300E+01	2.656E+03	9.237E+03	5.854E+03	1.675E+03	5.833E+03	3.695E+03
2.400E+01	2.679E+03	9.304E+03	5.899E+03	1.683E+03	5.859E+03	3.711E+03

Table 12-3 Pre-Katrina – Stage-Fatality (Continued)

Elevation (ft)	SB4			SB5		
	5%	95%	Mean	5%	95%	Mean
-1.200E+01	0.000E+00	0.000E+00	0.000E+00	0.000E+00	0.000E+00	0.000E+00
-1.100E+01	0.000E+00	0.000E+00	0.000E+00	0.000E+00	0.000E+00	0.000E+00
-1.000E+01	0.000E+00	0.000E+00	0.000E+00	0.000E+00	0.000E+00	0.000E+00
-9.000E+00	0.000E+00	0.000E+00	0.000E+00	0.000E+00	0.000E+00	0.000E+00
-8.000E+00	0.000E+00	0.000E+00	0.000E+00	0.000E+00	0.000E+00	0.000E+00
-7.000E+00	0.000E+00	0.000E+00	0.000E+00	0.000E+00	0.000E+00	0.000E+00
-6.000E+00	0.000E+00	0.000E+00	0.000E+00	0.000E+00	0.000E+00	0.000E+00
-5.000E+00	0.000E+00	0.000E+00	0.000E+00	0.000E+00	0.000E+00	0.000E+00
-4.000E+00	0.000E+00	0.000E+00	0.000E+00	0.000E+00	0.000E+00	0.000E+00
-3.000E+00	0.000E+00	0.000E+00	0.000E+00	0.000E+00	0.000E+00	0.000E+00
-2.000E+00	0.000E+00	0.000E+00	0.000E+00	0.000E+00	0.000E+00	0.000E+00
-1.000E+00	0.000E+00	0.000E+00	0.000E+00	0.000E+00	0.000E+00	0.000E+00
0.000E+00	0.000E+00	0.000E+00	0.000E+00	0.000E+00	0.000E+00	0.000E+00
1.000E+00	1.997E-02	3.719E-01	1.711E-01	0.000E+00	0.000E+00	0.000E+00
2.000E+00	3.994E-02	7.439E-01	3.423E-01	0.000E+00	0.000E+00	0.000E+00
3.000E+00	2.766E-01	4.299E+00	1.992E+00	1.666E-05	6.477E-05	3.834E-05
4.000E+00	5.134E-01	7.855E+00	3.641E+00	3.333E-05	1.295E-04	7.668E-05
5.000E+00	1.277E+00	1.081E+01	5.174E+00	2.959E-03	7.356E-02	3.327E-02
6.000E+00	2.041E+00	1.376E+01	6.707E+00	5.884E-03	1.470E-01	6.647E-02
7.000E+00	4.988E+00	2.563E+01	1.312E+01	1.039E-02	1.924E-01	8.391E-02
8.000E+00	7.936E+00	3.749E+01	1.954E+01	1.490E-02	2.378E-01	1.014E-01
9.000E+00	1.495E+01	5.921E+01	3.437E+01	5.916E-01	2.146E+00	1.336E+00
1.000E+01	2.197E+01	8.092E+01	4.921E+01	1.168E+00	4.055E+00	2.571E+00
1.100E+01	2.976E+01	1.054E+02	6.568E+01	1.199E+00	4.157E+00	2.637E+00
1.200E+01	3.756E+01	1.298E+02	8.215E+01	1.229E+00	4.259E+00	2.703E+00
1.300E+01	4.235E+01	1.550E+02	9.445E+01	1.229E+00	4.259E+00	2.703E+00
1.400E+01	4.715E+01	1.801E+02	1.068E+02	1.229E+00	4.259E+00	2.703E+00
1.500E+01	4.965E+01	2.663E+02	1.282E+02	1.230E+00	4.260E+00	2.703E+00
1.600E+01	5.216E+01	3.525E+02	1.497E+02	1.230E+00	4.260E+00	2.703E+00
1.700E+01	6.059E+01	3.733E+02	1.666E+02	1.405E+00	8.264E+00	3.781E+00
1.800E+01	6.902E+01	3.941E+02	1.834E+02	1.580E+00	1.227E+01	4.859E+00
1.900E+01	1.457E+02	5.831E+02	3.365E+02	4.637E+00	1.971E+01	1.096E+01
2.000E+01	2.224E+02	7.721E+02	4.896E+02	7.694E+00	2.716E+01	1.705E+01
2.100E+01	2.299E+02	7.993E+02	5.066E+02	7.854E+00	2.754E+01	1.737E+01
2.200E+01	2.374E+02	8.265E+02	5.237E+02	8.014E+00	2.792E+01	1.769E+01
2.300E+01	2.381E+02	8.288E+02	5.251E+02	8.014E+00	2.792E+01	1.769E+01
2.400E+01	2.388E+02	8.311E+02	5.265E+02	8.014E+00	2.792E+01	1.769E+01

Table 12-3 Pre-Katrina – Stage-Fatality (Continued)

Elevation (ft)	JE1			JE2		
	5%	95%	Mean	5%	95%	Mean
-1.200E+01	0.000E+00	0.000E+00	0.000E+00	0.000E+00	0.000E+00	0.000E+00
-1.100E+01	0.000E+00	0.000E+00	0.000E+00	5.896E-02	1.512E+00	6.831E-01
-1.000E+01	0.000E+00	0.000E+00	0.000E+00	6.633E-02	1.701E+00	7.685E-01
-9.000E+00	0.000E+00	0.000E+00	0.000E+00	7.369E-02	1.890E+00	8.539E-01
-8.000E+00	0.000E+00	0.000E+00	0.000E+00	5.672E-01	6.410E+00	2.458E+00
-7.000E+00	0.000E+00	0.000E+00	0.000E+00	1.061E+00	1.093E+01	4.062E+00
-6.000E+00	0.000E+00	0.000E+00	0.000E+00	5.702E+00	2.459E+01	1.362E+01
-5.000E+00	0.000E+00	0.000E+00	0.000E+00	1.034E+01	3.825E+01	2.317E+01
-4.000E+00	0.000E+00	0.000E+00	0.000E+00	1.636E+01	5.973E+01	3.658E+01
-3.000E+00	0.000E+00	0.000E+00	0.000E+00	2.237E+01	8.121E+01	4.998E+01
-2.000E+00	0.000E+00	0.000E+00	0.000E+00	2.781E+01	1.045E+02	6.323E+01
-1.000E+00	0.000E+00	0.000E+00	0.000E+00	3.326E+01	1.278E+02	7.647E+01
0.000E+00	0.000E+00	0.000E+00	0.000E+00	4.322E+01	2.323E+02	1.129E+02
1.000E+00	0.000E+00	0.000E+00	0.000E+00	5.319E+01	3.368E+02	1.493E+02
2.000E+00	0.000E+00	0.000E+00	0.000E+00	1.432E+02	6.527E+02	3.477E+02
3.000E+00	1.666E-05	6.477E-05	3.834E-05	2.332E+02	9.686E+02	5.461E+02
4.000E+00	3.333E-05	1.295E-04	7.668E-05	3.702E+02	1.380E+03	8.331E+02
5.000E+00	2.959E-03	7.356E-02	3.327E-02	5.073E+02	1.792E+03	1.120E+03
6.000E+00	5.884E-03	1.470E-01	6.647E-02	6.136E+02	2.142E+03	1.350E+03
7.000E+00	1.039E-02	1.924E-01	8.391E-02	7.200E+02	2.491E+03	1.579E+03
8.000E+00	1.490E-02	2.378E-01	1.014E-01	7.843E+02	2.715E+03	1.720E+03
9.000E+00	5.916E-01	2.146E+00	1.336E+00	8.486E+02	2.939E+03	1.861E+03
1.000E+01	1.168E+00	4.055E+00	2.571E+00	9.899E+02	3.639E+03	2.223E+03
1.100E+01	1.199E+00	4.157E+00	2.637E+00	1.131E+03	4.339E+03	2.584E+03
1.200E+01	1.229E+00	4.259E+00	2.703E+00	1.658E+03	6.045E+03	3.716E+03
1.300E+01	1.229E+00	4.259E+00	2.703E+00	2.185E+03	7.752E+03	4.848E+03
1.400E+01	1.229E+00	4.259E+00	2.703E+00	2.664E+03	9.342E+03	5.886E+03
1.500E+01	1.230E+00	4.260E+00	2.703E+00	3.143E+03	1.093E+04	6.924E+03
1.600E+01	1.230E+00	4.260E+00	2.703E+00	3.416E+03	1.188E+04	7.524E+03
1.700E+01	1.405E+00	8.264E+00	3.781E+00	3.688E+03	1.282E+04	8.124E+03
1.800E+01	1.580E+00	1.227E+01	4.859E+00	3.845E+03	1.336E+04	8.469E+03
1.900E+01	4.637E+00	1.971E+01	1.096E+01	4.001E+03	1.390E+04	8.813E+03
2.000E+01	7.694E+00	2.716E+01	1.705E+01	4.164E+03	1.447E+04	9.171E+03
2.100E+01	7.854E+00	2.754E+01	1.737E+01	4.327E+03	1.503E+04	9.529E+03
2.200E+01	8.014E+00	2.792E+01	1.769E+01	4.504E+03	1.565E+04	9.923E+03
2.300E+01	8.014E+00	2.792E+01	1.769E+01	4.680E+03	1.627E+04	1.032E+04
2.400E+01	8.014E+00	2.792E+01	1.769E+01	4.779E+03	1.662E+04	1.054E+04

Table 12-3 Pre-Katrina – Stage-Fatality (Continued)

Elevation (ft)	JE3		
	5%	95%	Mean
-1.200E+01	0.000E+00	0.000E+00	0.000E+00
-1.100E+01	0.000E+00	0.000E+00	0.000E+00
-1.000E+01	0.000E+00	0.000E+00	0.000E+00
-9.000E+00	4.069E-02	7.390E-01	3.409E-01
-8.000E+00	8.138E-02	1.478E+00	6.818E-01
-7.000E+00	1.340E+00	1.135E+01	4.916E+00
-6.000E+00	2.599E+00	2.122E+01	9.151E+00
-5.000E+00	1.248E+01	5.682E+01	3.127E+01
-4.000E+00	2.235E+01	9.243E+01	5.338E+01
-3.000E+00	3.686E+01	1.641E+02	9.256E+01
-2.000E+00	5.137E+01	2.358E+02	1.317E+02
-1.000E+00	6.634E+01	3.098E+02	1.691E+02
0.000E+00	8.132E+01	3.838E+02	2.065E+02
1.000E+00	1.568E+02	8.388E+02	4.084E+02
2.000E+00	2.322E+02	1.294E+03	6.102E+02
3.000E+00	4.716E+02	1.963E+03	1.105E+03
4.000E+00	7.110E+02	2.631E+03	1.599E+03
5.000E+00	9.994E+02	3.541E+03	2.210E+03
6.000E+00	1.288E+03	4.450E+03	2.821E+03
7.000E+00	1.380E+03	4.775E+03	3.026E+03
8.000E+00	1.472E+03	5.100E+03	3.230E+03
9.000E+00	1.715E+03	6.406E+03	3.874E+03
1.000E+01	1.958E+03	7.712E+03	4.518E+03
1.100E+01	3.102E+03	1.189E+04	7.098E+03
1.200E+01	4.246E+03	1.607E+04	9.678E+03
1.300E+01	6.014E+03	2.155E+04	1.341E+04
1.400E+01	7.782E+03	2.703E+04	1.714E+04
1.500E+01	8.261E+03	2.872E+04	1.820E+04
1.600E+01	8.740E+03	3.040E+04	1.927E+04
1.700E+01	8.931E+03	3.106E+04	1.969E+04
1.800E+01	9.121E+03	3.173E+04	2.011E+04
1.900E+01	9.362E+03	3.254E+04	2.063E+04
2.000E+01	9.602E+03	3.335E+04	2.114E+04
2.100E+01	1.008E+04	3.504E+04	2.221E+04
2.200E+01	1.056E+04	3.673E+04	2.328E+04
2.300E+01	1.085E+04	3.773E+04	2.391E+04
2.400E+01	1.113E+04	3.872E+04	2.455E+04

Table 12-3 Pre-Katrina – Stage-Fatality (Continued)

Elevation (ft)	JW1			JW2		
	5%	95%	Mean	5%	25%	Mean
-1.200E+01	0.000E+00	0.000E+00	0.000E+00	0.000E+00	0.000E+00	0.000E+00
-1.100E+01	0.000E+00	0.000E+00	0.000E+00	0.000E+00	0.000E+00	0.000E+00
-1.000E+01	0.000E+00	0.000E+00	0.000E+00	0.000E+00	0.000E+00	0.000E+00
-9.000E+00	0.000E+00	0.000E+00	0.000E+00	0.000E+00	0.000E+00	0.000E+00
-8.000E+00	8.314E-03	1.987E-01	8.998E-02	0.000E+00	0.000E+00	0.000E+00
-7.000E+00	1.663E-02	3.974E-01	1.800E-01	0.000E+00	0.000E+00	0.000E+00
-6.000E+00	2.193E-02	4.154E-01	1.903E-01	4.000E-05	1.936E-04	4.635E-04
-5.000E+00	2.722E-02	4.334E-01	2.007E-01	8.000E-05	3.872E-04	9.270E-04
-4.000E+00	9.473E-02	1.509E+00	6.987E-01	2.157E-03	9.819E-03	2.334E-02
-3.000E+00	1.622E-01	2.584E+00	1.197E+00	4.233E-03	1.925E-02	4.574E-02
-2.000E+00	2.833E-01	3.087E+00	1.476E+00	3.649E-02	1.518E-01	3.557E-01
-1.000E+00	4.044E-01	3.589E+00	1.754E+00	6.875E-02	2.843E-01	6.656E-01
0.000E+00	1.151E+00	8.715E+00	3.769E+00	2.192E-01	7.510E-01	1.694E+00
1.000E+00	1.897E+00	1.384E+01	5.783E+00	3.696E-01	1.218E+00	2.722E+00
2.000E+00	5.192E+00	2.445E+01	1.278E+01	6.380E-01	1.754E+00	3.725E+00
3.000E+00	8.486E+00	3.506E+01	1.978E+01	9.063E-01	2.290E+00	4.728E+00
4.000E+00	1.410E+01	5.164E+01	3.146E+01	1.538E+00	3.342E+00	6.310E+00
5.000E+00	1.971E+01	6.821E+01	4.315E+01	2.169E+00	4.395E+00	7.893E+00
6.000E+00	2.150E+01	7.447E+01	4.706E+01	5.709E+00	9.938E+00	1.586E+01
7.000E+00	2.330E+01	8.072E+01	5.097E+01	9.249E+00	1.548E+01	2.384E+01
8.000E+00	2.795E+01	1.052E+02	6.298E+01	1.742E+01	2.873E+01	4.037E+01
9.000E+00	3.260E+01	1.296E+02	7.499E+01	2.560E+01	4.198E+01	5.691E+01
1.000E+01	5.370E+01	2.170E+02	1.244E+02	3.374E+01	5.531E+01	7.424E+01
1.100E+01	7.481E+01	3.044E+02	1.739E+02	4.187E+01	6.864E+01	9.156E+01
1.200E+01	1.176E+02	4.309E+02	2.631E+02	4.548E+01	7.461E+01	1.002E+02
1.300E+01	1.605E+02	5.575E+02	3.524E+02	4.908E+01	8.058E+01	1.088E+02
1.400E+01	1.755E+02	6.083E+02	3.853E+02	6.463E+01	1.077E+02	1.555E+02
1.500E+01	1.905E+02	6.591E+02	4.183E+02	8.019E+01	1.348E+02	2.021E+02
1.600E+01	2.026E+02	7.021E+02	4.448E+02	1.652E+02	2.746E+02	3.846E+02
1.700E+01	2.147E+02	7.451E+02	4.713E+02	2.503E+02	4.144E+02	5.671E+02
1.800E+01	2.517E+02	8.863E+02	5.567E+02	3.424E+02	5.656E+02	7.617E+02
1.900E+01	2.888E+02	1.028E+03	6.421E+02	4.345E+02	7.167E+02	9.563E+02
2.000E+01	3.675E+02	1.291E+03	8.120E+02	4.547E+02	7.506E+02	1.002E+03
2.100E+01	4.462E+02	1.554E+03	9.820E+02	4.749E+02	7.844E+02	1.048E+03
2.200E+01	5.117E+02	1.779E+03	1.126E+03	4.803E+02	7.935E+02	1.059E+03
2.300E+01	5.772E+02	2.003E+03	1.270E+03	4.858E+02	8.026E+02	1.071E+03
2.400E+01	6.138E+02	2.132E+03	1.351E+03	4.989E+02	8.235E+02	1.099E+03

Table 12-3 Pre-Katrina – Stage-Fatality (Continued)

Elevation (ft)	JW3			JW4		
	5%	95%	Mean	5%	95%	Mean
-1.200E+01	0.000E+00	0.000E+00	0.000E+00	0.000E+00	0.000E+00	0.000E+00
-1.100E+01	0.000E+00	0.000E+00	0.000E+00	0.000E+00	0.000E+00	0.000E+00
-1.000E+01	0.000E+00	0.000E+00	0.000E+00	4.917E-04	7.954E-03	3.705E-03
-9.000E+00	0.000E+00	0.000E+00	0.000E+00	9.834E-04	1.591E-02	7.410E-03
-8.000E+00	0.000E+00	0.000E+00	0.000E+00	1.237E-02	1.622E-01	7.666E-02
-7.000E+00	3.717E-04	9.533E-03	4.306E-03	2.376E-02	3.086E-01	1.459E-01
-6.000E+00	7.433E-04	1.907E-02	8.613E-03	1.144E-01	1.235E+00	5.928E-01
-5.000E+00	9.020E-03	1.982E-01	7.939E-02	2.050E-01	2.160E+00	1.040E+00
-4.000E+00	1.730E-02	3.774E-01	1.502E-01	6.534E-01	5.894E+00	2.883E+00
-3.000E+00	1.981E-01	1.797E+00	7.772E-01	1.102E+00	9.628E+00	4.727E+00
-2.000E+00	3.789E-01	3.217E+00	1.404E+00	3.240E+00	2.481E+01	1.240E+01
-1.000E+00	1.843E+00	9.844E+00	5.188E+00	5.377E+00	4.000E+01	2.006E+01
0.000E+00	3.307E+00	1.647E+01	8.973E+00	9.448E+00	6.187E+01	3.172E+01
1.000E+00	5.694E+00	3.084E+01	1.644E+01	1.352E+01	8.373E+01	4.337E+01
2.000E+00	8.081E+00	4.520E+01	2.390E+01	2.237E+01	1.188E+02	6.325E+01
3.000E+00	1.092E+01	6.322E+01	3.313E+01	3.122E+01	1.539E+02	8.313E+01
4.000E+00	1.376E+01	8.123E+01	4.237E+01	5.328E+01	2.417E+02	1.322E+02
5.000E+00	2.080E+01	1.179E+02	6.145E+01	7.534E+01	3.294E+02	1.813E+02
6.000E+00	2.785E+01	1.547E+02	8.053E+01	1.292E+02	5.222E+02	2.997E+02
7.000E+00	5.421E+01	2.563E+02	1.378E+02	1.830E+02	7.149E+02	4.181E+02
8.000E+00	8.058E+01	3.580E+02	1.951E+02	2.729E+02	9.888E+02	6.066E+02
9.000E+00	1.381E+02	5.400E+02	3.166E+02	3.627E+02	1.263E+03	7.952E+02
1.000E+01	1.957E+02	7.221E+02	4.381E+02	4.401E+02	1.547E+03	9.695E+02
1.100E+01	2.709E+02	9.742E+02	6.016E+02	5.174E+02	1.831E+03	1.144E+03
1.200E+01	3.461E+02	1.226E+03	7.650E+02	6.727E+02	2.430E+03	1.500E+03
1.300E+01	4.495E+02	1.604E+03	9.975E+02	8.281E+02	3.028E+03	1.856E+03
1.400E+01	5.529E+02	1.982E+03	1.230E+03	1.167E+03	4.479E+03	2.663E+03
1.500E+01	7.401E+02	2.653E+03	1.647E+03	1.506E+03	5.929E+03	3.470E+03
1.600E+01	9.274E+02	3.323E+03	2.064E+03	2.267E+03	8.265E+03	5.078E+03
1.700E+01	1.243E+03	4.558E+03	2.793E+03	3.029E+03	1.060E+04	6.687E+03
1.800E+01	1.558E+03	5.794E+03	3.523E+03	3.575E+03	1.246E+04	7.877E+03
1.900E+01	2.189E+03	7.862E+03	4.883E+03	4.121E+03	1.432E+04	9.067E+03
2.000E+01	2.821E+03	9.930E+03	6.243E+03	4.552E+03	1.581E+04	1.002E+04
2.100E+01	3.415E+03	1.194E+04	7.534E+03	4.982E+03	1.729E+04	1.096E+04
2.200E+01	4.009E+03	1.395E+04	8.825E+03	5.255E+03	1.824E+04	1.156E+04
2.300E+01	4.477E+03	1.556E+04	9.856E+03	5.528E+03	1.919E+04	1.217E+04
2.400E+01	4.945E+03	1.717E+04	1.089E+04	5.821E+03	2.022E+04	1.282E+04

Table 12-3 Pre-Katrina – Stage-Fatality (Continued)

Elevation (ft)	PL11		
	5%	95%	Mean
-1.200E+01	2.767E-01	1.212E+00	6.872E-01
-1.100E+01	3.432E-01	1.776E+00	9.593E-01
-1.000E+01	4.097E-01	2.341E+00	1.231E+00
-9.000E+00	4.555E-01	2.541E+00	1.345E+00
-8.000E+00	5.013E-01	2.740E+00	1.458E+00
-7.000E+00	7.744E-01	6.113E+00	2.544E+00
-6.000E+00	1.048E+00	9.487E+00	3.631E+00
-5.000E+00	4.072E+00	1.803E+01	9.811E+00
-4.000E+00	7.097E+00	2.657E+01	1.599E+01
-3.000E+00	1.002E+01	3.558E+01	2.214E+01
-2.000E+00	1.294E+01	4.459E+01	2.829E+01
-1.000E+00	1.413E+01	4.865E+01	3.089E+01
0.000E+00	1.532E+01	5.272E+01	3.349E+01
1.000E+00	1.690E+01	5.953E+01	3.729E+01
2.000E+00	1.848E+01	6.633E+01	4.109E+01
3.000E+00	2.597E+01	1.064E+02	6.045E+01
4.000E+00	3.346E+01	1.465E+02	7.980E+01
5.000E+00	5.770E+01	2.152E+02	1.298E+02
6.000E+00	8.193E+01	2.839E+02	1.798E+02
7.000E+00	9.195E+01	3.184E+02	2.017E+02
8.000E+00	1.020E+02	3.530E+02	2.237E+02
9.000E+00	1.127E+02	3.905E+02	2.474E+02
1.000E+01	1.235E+02	4.280E+02	2.710E+02
1.100E+01	1.384E+02	4.797E+02	3.037E+02
1.200E+01	1.533E+02	5.314E+02	3.364E+02
1.300E+01	1.744E+02	6.062E+02	3.833E+02
1.400E+01	1.955E+02	6.809E+02	4.301E+02
1.500E+01	2.253E+02	7.829E+02	4.956E+02
1.600E+01	2.551E+02	8.849E+02	5.611E+02
1.700E+01	2.709E+02	9.403E+02	5.959E+02
1.800E+01	2.868E+02	9.957E+02	6.307E+02
1.900E+01	3.195E+02	1.113E+03	7.038E+02
2.000E+01	3.523E+02	1.231E+03	7.770E+02
2.100E+01	4.088E+02	1.424E+03	9.008E+02
2.200E+01	4.653E+02	1.616E+03	1.025E+03
2.300E+01	4.964E+02	1.724E+03	1.093E+03
2.400E+01	5.275E+02	1.832E+03	1.162E+03

Table 12-3 Pre-Katrina – Stage-Fatality (Concluded)

Elevation (ft)	SC1			SC2		
	5%	95%	Mean	5%	95%	Mean
-1.200E+01	0.000E+00	0.000E+00	0.000E+00	0.000E+00	0.000E+00	0.000E+00
-1.100E+01	0.000E+00	0.000E+00	0.000E+00	0.000E+00	0.000E+00	0.000E+00
-1.000E+01	0.000E+00	0.000E+00	0.000E+00	0.000E+00	0.000E+00	0.000E+00
-9.000E+00	0.000E+00	0.000E+00	0.000E+00	0.000E+00	0.000E+00	0.000E+00
-8.000E+00	0.000E+00	0.000E+00	0.000E+00	0.000E+00	0.000E+00	0.000E+00
-7.000E+00	0.000E+00	0.000E+00	0.000E+00	0.000E+00	0.000E+00	0.000E+00
-6.000E+00	0.000E+00	0.000E+00	0.000E+00	0.000E+00	0.000E+00	0.000E+00
-5.000E+00	0.000E+00	0.000E+00	0.000E+00	0.000E+00	0.000E+00	0.000E+00
-4.000E+00	0.000E+00	0.000E+00	0.000E+00	0.000E+00	0.000E+00	0.000E+00
-3.000E+00	0.000E+00	0.000E+00	0.000E+00	0.000E+00	0.000E+00	0.000E+00
-2.000E+00	0.000E+00	0.000E+00	0.000E+00	0.000E+00	0.000E+00	0.000E+00
-1.000E+00	0.000E+00	0.000E+00	0.000E+00	0.000E+00	0.000E+00	0.000E+00
0.000E+00	0.000E+00	0.000E+00	0.000E+00	0.000E+00	0.000E+00	0.000E+00
1.000E+00	0.000E+00	0.000E+00	0.000E+00	0.000E+00	0.000E+00	0.000E+00
2.000E+00	0.000E+00	0.000E+00	0.000E+00	3.671E-03	9.415E-02	4.253E-02
3.000E+00	0.000E+00	0.000E+00	0.000E+00	7.341E-03	1.883E-01	8.506E-02
4.000E+00	0.000E+00	0.000E+00	0.000E+00	5.968E-02	1.521E+00	6.874E-01
5.000E+00	0.000E+00	0.000E+00	0.000E+00	1.120E-01	2.854E+00	1.290E+00
6.000E+00	9.412E-06	2.414E-04	1.091E-04	4.273E-01	4.618E+00	2.210E+00
7.000E+00	1.882E-05	4.828E-04	2.181E-04	7.426E-01	6.381E+00	3.130E+00
8.000E+00	1.604E-02	5.968E-02	3.687E-02	1.863E+00	1.486E+01	6.670E+00
9.000E+00	3.207E-02	1.189E-01	7.353E-02	2.984E+00	2.334E+01	1.021E+01
1.000E+01	3.867E-01	1.340E+00	8.474E-01	9.355E+00	4.333E+01	2.330E+01
1.100E+01	7.413E-01	2.561E+00	1.621E+00	1.573E+01	6.332E+01	3.638E+01
1.200E+01	1.766E+00	6.074E+00	3.856E+00	2.634E+01	1.005E+02	5.967E+01
1.300E+01	2.790E+00	9.587E+00	6.091E+00	3.695E+01	1.377E+02	8.296E+01
1.400E+01	2.940E+00	1.011E+01	6.419E+00	5.326E+01	1.896E+02	1.176E+02
1.500E+01	3.089E+00	1.063E+01	6.748E+00	6.957E+01	2.415E+02	1.523E+02
1.600E+01	3.298E+00	1.233E+01	7.408E+00	8.632E+01	3.043E+02	1.904E+02
1.700E+01	3.506E+00	1.404E+01	8.068E+00	1.031E+02	3.670E+02	2.285E+02
1.800E+01	5.428E+00	3.787E+01	1.583E+01	1.462E+02	5.658E+02	3.341E+02
1.900E+01	7.349E+00	6.170E+01	2.359E+01	1.893E+02	7.645E+02	4.398E+02
2.000E+01	2.279E+01	9.731E+01	5.392E+01	3.020E+02	1.115E+03	6.796E+02
2.100E+01	3.823E+01	1.329E+02	8.425E+01	4.147E+02	1.466E+03	9.194E+02
2.200E+01	3.917E+01	1.362E+02	8.636E+01	5.214E+02	1.840E+03	1.155E+03
2.300E+01	4.011E+01	1.396E+02	8.848E+01	6.281E+02	2.215E+03	1.391E+03
2.400E+01	4.044E+01	1.407E+02	8.918E+01	7.713E+02	2.696E+03	1.701E+03

Table 12-4 Current HPS – Stage-Fatality

Elevation (ft)	OW1			OW2		
	5%	95%	Mean	5%	95%	Mean
-1.200E+01	0.000E+00	0.000E+00	0.000E+00	0.000E+00	0.000E+00	0.000E+00
-1.100E+01	0.000E+00	0.000E+00	0.000E+00	0.000E+00	0.000E+00	0.000E+00
-1.000E+01	0.000E+00	0.000E+00	0.000E+00	0.000E+00	0.000E+00	0.000E+00
-9.000E+00	0.000E+00	0.000E+00	0.000E+00	0.000E+00	0.000E+00	0.000E+00
-8.000E+00	0.000E+00	0.000E+00	0.000E+00	8.780E-03	2.252E-01	1.017E-01
-7.000E+00	0.000E+00	0.000E+00	0.000E+00	1.756E-02	4.504E-01	2.035E-01
-6.000E+00	0.000E+00	0.000E+00	0.000E+00	1.201E-01	1.960E+00	8.930E-01
-5.000E+00	0.000E+00	0.000E+00	0.000E+00	2.227E-01	3.469E+00	1.583E+00
-4.000E+00	0.000E+00	0.000E+00	0.000E+00	1.190E+00	7.069E+00	3.710E+00
-3.000E+00	5.647E-05	1.448E-03	6.543E-04	2.158E+00	1.067E+01	5.838E+00
-2.000E+00	1.129E-04	2.897E-03	1.309E-03	3.304E+00	1.828E+01	9.716E+00
-1.000E+00	4.753E-04	1.219E-02	5.507E-03	4.449E+00	2.590E+01	1.359E+01
0.000E+00	8.376E-04	2.149E-02	9.705E-03	6.732E+00	3.512E+01	1.890E+01
1.000E+00	1.176E-03	3.018E-02	1.363E-02	9.015E+00	4.435E+01	2.420E+01
2.000E+00	1.515E-03	3.887E-02	1.756E-02	1.444E+01	7.418E+01	3.821E+01
3.000E+00	5.990E-03	1.442E-01	6.528E-02	1.987E+01	1.040E+02	5.222E+01
4.000E+00	1.046E-02	2.495E-01	1.130E-01	4.191E+01	1.896E+02	1.019E+02
5.000E+00	3.548E-02	7.692E-01	3.500E-01	6.394E+01	2.753E+02	1.515E+02
6.000E+00	6.049E-02	1.289E+00	5.870E-01	1.091E+02	4.107E+02	2.458E+02
7.000E+00	8.772E-02	1.410E+00	6.413E-01	1.542E+02	5.461E+02	3.401E+02
8.000E+00	1.150E-01	1.531E+00	6.956E-01	1.929E+02	6.767E+02	4.242E+02
9.000E+00	2.917E-01	2.555E+00	1.149E+00	2.315E+02	8.073E+02	5.083E+02
1.000E+01	4.685E-01	3.579E+00	1.602E+00	2.847E+02	1.007E+03	6.292E+02
1.100E+01	1.375E+00	6.980E+00	3.554E+00	3.380E+02	1.206E+03	7.502E+02
1.200E+01	2.281E+00	1.038E+01	5.506E+00	4.542E+02	1.686E+03	1.025E+03
1.300E+01	3.838E+00	1.448E+01	8.647E+00	5.705E+02	2.165E+03	1.299E+03
1.400E+01	5.395E+00	1.857E+01	1.179E+01	8.353E+02	3.025E+03	1.867E+03
1.500E+01	5.829E+00	2.009E+01	1.275E+01	1.100E+03	3.886E+03	2.436E+03
1.600E+01	6.263E+00	2.161E+01	1.371E+01	1.350E+03	4.722E+03	2.976E+03
1.700E+01	7.047E+00	2.789E+01	1.616E+01	1.599E+03	5.559E+03	3.516E+03
1.800E+01	7.832E+00	3.416E+01	1.860E+01	1.823E+03	6.333E+03	4.008E+03
1.900E+01	1.322E+01	6.911E+01	3.380E+01	2.046E+03	7.107E+03	4.499E+03
2.000E+01	1.862E+01	1.041E+02	4.900E+01	2.293E+03	7.967E+03	5.043E+03
2.100E+01	3.827E+01	1.527E+02	8.827E+01	2.539E+03	8.828E+03	5.588E+03
2.200E+01	5.792E+01	2.013E+02	1.275E+02	2.804E+03	9.747E+03	6.173E+03
2.300E+01	6.193E+01	2.153E+02	1.365E+02	3.070E+03	1.067E+04	6.758E+03
2.400E+01	6.594E+01	2.293E+02	1.454E+02	3.305E+03	1.149E+04	7.278E+03

Table 12-4 Current HPS – Stage-Fatality (Continued)

Elevation (ft)	NOE1			NOE2		
	5%	95%	Mean	5%	95%	Mean
-1.200E+01	0.000E+00	0.000E+00	0.000E+00	0.000E+00	0.000E+00	0.000E+00
-1.100E+01	0.000E+00	0.000E+00	0.000E+00	0.000E+00	0.000E+00	0.000E+00
-1.000E+01	0.000E+00	0.000E+00	0.000E+00	0.000E+00	0.000E+00	0.000E+00
-9.000E+00	0.000E+00	0.000E+00	0.000E+00	0.000E+00	0.000E+00	0.000E+00
-8.000E+00	0.000E+00	0.000E+00	0.000E+00	0.000E+00	0.000E+00	0.000E+00
-7.000E+00	0.000E+00	0.000E+00	0.000E+00	8.941E-05	2.293E-03	1.036E-03
-6.000E+00	0.000E+00	0.000E+00	0.000E+00	1.788E-04	4.587E-03	2.072E-03
-5.000E+00	0.000E+00	0.000E+00	0.000E+00	8.188E-04	2.100E-02	9.488E-03
-4.000E+00	0.000E+00	0.000E+00	0.000E+00	1.459E-03	3.742E-02	1.690E-02
-3.000E+00	0.000E+00	0.000E+00	0.000E+00	2.717E-03	6.908E-02	3.121E-02
-2.000E+00	0.000E+00	0.000E+00	0.000E+00	3.975E-03	1.007E-01	4.553E-02
-1.000E+00	0.000E+00	0.000E+00	0.000E+00	4.883E-03	1.124E-01	5.103E-02
0.000E+00	2.353E-06	6.035E-05	2.726E-05	5.792E-03	1.240E-01	5.653E-02
1.000E+00	4.706E-06	1.207E-04	5.453E-05	1.014E-02	1.374E-01	6.438E-02
2.000E+00	2.588E-05	6.639E-04	2.999E-04	1.449E-02	1.508E-01	7.223E-02
3.000E+00	4.706E-05	1.207E-03	5.453E-04	3.319E-02	2.091E-01	1.077E-01
4.000E+00	4.835E-05	1.210E-03	5.473E-04	5.190E-02	2.673E-01	1.433E-01
5.000E+00	4.963E-05	1.213E-03	5.494E-04	8.603E-02	3.542E-01	2.065E-01
6.000E+00	7.061E-05	1.256E-03	5.799E-04	1.202E-01	4.411E-01	2.697E-01
7.000E+00	9.158E-05	1.299E-03	6.104E-04	1.459E-01	6.190E-01	3.436E-01
8.000E+00	1.823E-04	1.510E-03	7.403E-04	1.717E-01	7.968E-01	4.176E-01
9.000E+00	2.730E-04	1.720E-03	8.702E-04	3.248E-01	1.848E+00	8.613E-01
1.000E+01	3.911E-04	2.432E-03	1.186E-03	4.778E-01	2.900E+00	1.305E+00
1.100E+01	5.092E-04	3.144E-03	1.502E-03	1.231E+00	5.957E+00	3.058E+00
1.200E+01	1.138E-03	6.180E-03	3.008E-03	1.983E+00	9.015E+00	4.811E+00
1.300E+01	1.767E-03	9.217E-03	4.514E-03	3.476E+00	1.335E+01	7.934E+00
1.400E+01	3.628E-03	2.787E-02	1.115E-02	4.969E+00	1.768E+01	1.106E+01
1.500E+01	5.489E-03	4.652E-02	1.778E-02	5.939E+00	2.086E+01	1.315E+01
1.600E+01	1.779E-02	7.653E-02	4.228E-02	6.909E+00	2.404E+01	1.524E+01
1.700E+01	3.009E-02	1.065E-01	6.678E-02	7.008E+00	2.438E+01	1.546E+01
1.800E+01	3.608E-02	1.264E-01	7.978E-02	7.107E+00	2.472E+01	1.567E+01
1.900E+01	4.207E-02	1.463E-01	9.277E-02	7.235E+00	2.516E+01	1.594E+01
2.000E+01	4.248E-02	1.477E-01	9.367E-02	7.362E+00	2.559E+01	1.622E+01
2.100E+01	4.289E-02	1.492E-01	9.456E-02	7.660E+00	2.662E+01	1.687E+01
2.200E+01	4.314E-02	1.501E-01	9.512E-02	7.958E+00	2.765E+01	1.753E+01
2.300E+01	4.339E-02	1.510E-01	9.567E-02	8.271E+00	2.876E+01	1.823E+01
2.400E+01	4.410E-02	1.532E-01	9.714E-02	8.584E+00	2.987E+01	1.894E+01

Table 12-4 Current HPS – Stage-Fatality (Continued)

Elevation (ft)	NOE3			NOE4		
	5%	95%	Mean	5%	95%	Mean
-1.200E+01	0.000E+00	0.000E+00	0.000E+00	0.000E+00	0.000E+00	0.000E+00
-1.100E+01	0.000E+00	0.000E+00	0.000E+00	0.000E+00	0.000E+00	0.000E+00
-1.000E+01	0.000E+00	0.000E+00	0.000E+00	0.000E+00	0.000E+00	0.000E+00
-9.000E+00	0.000E+00	0.000E+00	0.000E+00	0.000E+00	0.000E+00	0.000E+00
-8.000E+00	0.000E+00	0.000E+00	0.000E+00	0.000E+00	0.000E+00	0.000E+00
-7.000E+00	0.000E+00	0.000E+00	0.000E+00	0.000E+00	0.000E+00	0.000E+00
-6.000E+00	0.000E+00	0.000E+00	0.000E+00	0.000E+00	0.000E+00	0.000E+00
-5.000E+00	0.000E+00	0.000E+00	0.000E+00	4.706E-05	1.207E-03	5.453E-04
-4.000E+00	1.701E-03	4.364E-02	1.971E-02	4.706E-05	1.207E-03	5.453E-04
-3.000E+00	6.909E-03	1.772E-01	8.006E-02	4.706E-05	1.207E-03	5.453E-04
-2.000E+00	1.212E-02	3.108E-01	1.404E-01	4.706E-05	1.207E-03	5.453E-04
-1.000E+00	2.853E-02	4.161E-01	1.948E-01	4.706E-04	1.207E-02	5.453E-03
0.000E+00	4.494E-02	5.213E-01	2.492E-01	5.929E-04	1.521E-02	6.870E-03
1.000E+00	1.469E-01	9.374E-01	4.709E-01	7.153E-04	1.835E-02	8.288E-03
2.000E+00	2.490E-01	1.353E+00	6.926E-01	1.205E-03	3.090E-02	1.396E-02
3.000E+00	4.734E-01	2.427E+00	1.230E+00	1.694E-03	4.346E-02	1.963E-02
4.000E+00	6.978E-01	3.501E+00	1.768E+00	2.542E-03	6.140E-02	2.496E-02
5.000E+00	1.372E+00	5.405E+00	3.149E+00	3.389E-03	7.935E-02	3.029E-02
6.000E+00	2.045E+00	7.308E+00	4.531E+00	3.340E-02	2.905E-01	1.184E-01
7.000E+00	2.648E+00	9.288E+00	5.825E+00	6.340E-02	5.016E-01	2.066E-01
8.000E+00	3.250E+00	1.127E+01	7.118E+00	2.399E-01	1.236E+00	6.146E-01
9.000E+00	3.835E+00	1.367E+01	8.484E+00	4.163E-01	1.970E+00	1.023E+00
1.000E+01	4.420E+00	1.606E+01	9.850E+00	7.026E-01	2.700E+00	1.599E+00
1.100E+01	5.803E+00	2.320E+01	1.341E+01	9.889E-01	3.430E+00	2.176E+00
1.200E+01	7.187E+00	3.034E+01	1.696E+01	1.017E+00	3.531E+00	2.240E+00
1.300E+01	1.224E+01	4.814E+01	2.821E+01	1.046E+00	3.632E+00	2.304E+00
1.400E+01	1.730E+01	6.594E+01	3.945E+01	1.078E+00	3.777E+00	2.383E+00
1.500E+01	2.389E+01	8.593E+01	5.329E+01	1.111E+00	3.923E+00	2.463E+00
1.600E+01	3.047E+01	1.059E+02	6.713E+01	1.285E+00	4.632E+00	2.870E+00
1.700E+01	3.231E+01	1.124E+02	7.121E+01	1.459E+00	5.341E+00	3.278E+00
1.800E+01	3.414E+01	1.188E+02	7.529E+01	1.919E+00	6.806E+00	4.257E+00
1.900E+01	3.481E+01	1.211E+02	7.676E+01	2.380E+00	8.271E+00	5.236E+00
2.000E+01	3.547E+01	1.234E+02	7.823E+01	2.581E+00	8.974E+00	5.686E+00
2.100E+01	3.640E+01	1.265E+02	8.023E+01	2.783E+00	9.678E+00	6.137E+00
2.200E+01	3.733E+01	1.297E+02	8.223E+01	2.808E+00	9.764E+00	6.191E+00
2.300E+01	3.894E+01	1.354E+02	8.581E+01	2.833E+00	9.851E+00	6.245E+00
2.400E+01	4.054E+01	1.410E+02	8.939E+01	2.866E+00	9.965E+00	6.317E+00

Table 12-4 Current HPS – Stage-Fatality (Continued)

Elevation (ft)	NOE5		
	5%	95%	Mean
-1.200E+01	0.000E+00	0.000E+00	0.000E+00
-1.100E+01	0.000E+00	0.000E+00	0.000E+00
-1.000E+01	0.000E+00	0.000E+00	0.000E+00
-9.000E+00	5.058E-02	1.297E+00	5.861E-01
-8.000E+00	7.701E-02	1.975E+00	8.923E-01
-7.000E+00	1.034E-01	2.653E+00	1.199E+00
-6.000E+00	1.383E-01	3.539E+00	1.599E+00
-5.000E+00	1.731E-01	4.424E+00	1.998E+00
-4.000E+00	2.592E-01	5.395E+00	2.466E+00
-3.000E+00	3.453E-01	6.367E+00	2.934E+00
-2.000E+00	8.712E-01	8.046E+00	3.905E+00
-1.000E+00	1.397E+00	9.724E+00	4.875E+00
0.000E+00	4.062E+00	1.869E+01	1.034E+01
1.000E+00	6.726E+00	2.765E+01	1.580E+01
2.000E+00	1.219E+01	4.612E+01	2.762E+01
3.000E+00	1.765E+01	6.458E+01	3.944E+01
4.000E+00	2.417E+01	8.573E+01	5.337E+01
5.000E+00	3.069E+01	1.069E+02	6.729E+01
6.000E+00	3.720E+01	1.318E+02	8.222E+01
7.000E+00	4.370E+01	1.567E+02	9.715E+01
8.000E+00	5.982E+01	2.285E+02	1.362E+02
9.000E+00	7.593E+01	3.003E+02	1.752E+02
1.000E+01	1.179E+02	4.373E+02	2.659E+02
1.100E+01	1.598E+02	5.742E+02	3.566E+02
1.200E+01	2.071E+02	7.314E+02	4.587E+02
1.300E+01	2.544E+02	8.886E+02	5.608E+02
1.400E+01	2.965E+02	1.033E+03	6.531E+02
1.500E+01	3.387E+02	1.177E+03	7.453E+02
1.600E+01	3.716E+02	1.291E+03	8.180E+02
1.700E+01	4.046E+02	1.405E+03	8.907E+02
1.800E+01	4.247E+02	1.475E+03	9.352E+02
1.900E+01	4.447E+02	1.545E+03	9.797E+02
2.000E+01	4.595E+02	1.597E+03	1.012E+03
2.100E+01	4.742E+02	1.649E+03	1.045E+03
2.200E+01	4.859E+02	1.689E+03	1.071E+03
2.300E+01	4.976E+02	1.730E+03	1.097E+03
2.400E+01	5.084E+02	1.768E+03	1.121E+03

Table 12-4 Current HPS – Stage-Fatality (Continued)

Elevation (ft)	OM1			OM2		
	5%	95%	Mean	5%	95%	Mean
-1.200E+01	0.000E+00	0.000E+00	0.000E+00	4.014E-02	7.398E-01	3.407E-01
-1.100E+01	1.648E-05	1.286E-03	3.144E-04	5.766E-02	9.349E-01	4.348E-01
-1.000E+01	3.295E-05	2.572E-03	6.288E-04	2.091E-01	3.059E+00	1.091E+00
-9.000E+00	2.424E-02	8.533E-02	5.353E-02	3.606E-01	5.184E+00	1.747E+00
-8.000E+00	4.845E-02	1.681E-01	1.064E-01	2.156E+00	1.065E+01	5.460E+00
-7.000E+00	6.112E-02	2.206E-01	1.360E-01	3.952E+00	1.611E+01	9.173E+00
-6.000E+00	7.379E-02	2.732E-01	1.656E-01	6.342E+00	2.331E+01	1.418E+01
-5.000E+00	1.209E-01	4.813E-01	2.835E-01	8.732E+00	3.051E+01	1.919E+01
-4.000E+00	1.681E-01	6.895E-01	4.014E-01	1.053E+01	3.660E+01	2.310E+01
-3.000E+00	2.134E-01	1.044E+00	5.740E-01	1.234E+01	4.270E+01	2.702E+01
-2.000E+00	2.588E-01	1.398E+00	7.466E-01	1.424E+01	4.934E+01	3.122E+01
-1.000E+00	2.588E-01	1.398E+00	7.466E-01	1.615E+01	5.599E+01	3.543E+01
0.000E+00	2.588E-01	1.398E+00	7.466E-01	1.927E+01	7.023E+01	4.316E+01
1.000E+00	1.071E+00	6.949E+00	3.228E+00	2.240E+01	8.447E+01	5.090E+01
2.000E+00	2.796E+00	1.382E+01	7.100E+00	3.241E+01	1.171E+02	7.242E+01
3.000E+00	4.520E+00	2.070E+01	1.097E+01	4.243E+01	1.496E+02	9.395E+01
4.000E+00	7.901E+00	3.010E+01	1.788E+01	5.211E+01	1.824E+02	1.150E+02
5.000E+00	1.128E+01	3.951E+01	2.479E+01	6.180E+01	2.152E+02	1.361E+02
6.000E+00	1.394E+01	4.866E+01	3.060E+01	7.093E+01	2.466E+02	1.561E+02
7.000E+00	1.659E+01	5.781E+01	3.641E+01	8.005E+01	2.779E+02	1.762E+02
8.000E+00	2.000E+01	6.983E+01	4.396E+01	8.631E+01	2.997E+02	1.900E+02
9.000E+00	2.341E+01	8.185E+01	5.150E+01	9.256E+01	3.214E+02	2.038E+02
1.000E+01	2.875E+01	1.019E+02	6.367E+01	9.722E+01	3.375E+02	2.140E+02
1.100E+01	3.408E+01	1.219E+02	7.584E+01	1.019E+02	3.536E+02	2.242E+02
1.200E+01	4.513E+01	1.618E+02	1.006E+02	1.082E+02	3.758E+02	2.383E+02
1.300E+01	5.618E+01	2.018E+02	1.254E+02	1.146E+02	3.980E+02	2.523E+02
1.400E+01	7.389E+01	2.626E+02	1.642E+02	1.221E+02	4.242E+02	2.689E+02
1.500E+01	9.161E+01	3.234E+02	2.030E+02	1.296E+02	4.505E+02	2.855E+02
1.600E+01	1.127E+02	3.952E+02	2.490E+02	1.338E+02	4.654E+02	2.950E+02
1.700E+01	1.337E+02	4.670E+02	2.950E+02	1.380E+02	4.803E+02	3.044E+02
1.800E+01	1.536E+02	5.347E+02	3.384E+02	1.400E+02	4.872E+02	3.089E+02
1.900E+01	1.734E+02	6.025E+02	3.818E+02	1.420E+02	4.942E+02	3.133E+02
2.000E+01	1.867E+02	6.483E+02	4.109E+02	1.437E+02	4.999E+02	3.169E+02
2.100E+01	1.999E+02	6.942E+02	4.401E+02	1.453E+02	5.055E+02	3.205E+02
2.200E+01	2.093E+02	7.272E+02	4.609E+02	1.472E+02	5.122E+02	3.247E+02
2.300E+01	2.187E+02	7.601E+02	4.818E+02	1.491E+02	5.189E+02	3.290E+02
2.400E+01	2.261E+02	7.858E+02	4.981E+02	1.507E+02	5.246E+02	3.325E+02

Table 12-4 Current HPS – Stage-Fatality (Continued)

Elevation (ft)	OM3			OM4		
	5%	95%	Mean	5%	95%	Mean
-1.200E+01	0.000E+00	0.000E+00	0.000E+00	0.000E+00	0.000E+00	0.000E+00
-1.100E+01	0.000E+00	0.000E+00	0.000E+00	3.576E-04	9.174E-03	4.144E-03
-1.000E+01	0.000E+00	0.000E+00	0.000E+00	7.153E-04	1.835E-02	8.288E-03
-9.000E+00	0.000E+00	0.000E+00	0.000E+00	4.071E-03	1.126E-01	3.988E-02
-8.000E+00	0.000E+00	0.000E+00	0.000E+00	7.426E-03	2.068E-01	7.147E-02
-7.000E+00	0.000E+00	0.000E+00	0.000E+00	6.749E-02	5.597E-01	2.318E-01
-6.000E+00	0.000E+00	0.000E+00	0.000E+00	1.276E-01	9.127E-01	3.921E-01
-5.000E+00	4.656E-03	9.461E-02	3.208E-02	3.614E-01	1.490E+00	8.471E-01
-4.000E+00	9.312E-03	1.892E-01	6.416E-02	5.952E-01	2.067E+00	1.302E+00
-3.000E+00	1.052E-01	6.077E-01	3.092E-01	7.235E-01	2.533E+00	1.589E+00
-2.000E+00	2.010E-01	1.026E+00	5.542E-01	8.517E-01	3.000E+00	1.876E+00
-1.000E+00	3.333E-01	2.665E+00	1.322E+00	1.049E+00	3.983E+00	2.373E+00
0.000E+00	4.656E-01	4.304E+00	2.090E+00	1.246E+00	4.967E+00	2.869E+00
1.000E+00	7.944E-01	8.308E+00	3.697E+00	1.874E+00	8.033E+00	4.430E+00
2.000E+00	1.123E+00	1.231E+01	5.305E+00	2.502E+00	1.110E+01	5.992E+00
3.000E+00	4.897E+00	2.978E+01	1.405E+01	4.446E+00	1.745E+01	1.018E+01
4.000E+00	8.670E+00	4.725E+01	2.279E+01	6.390E+00	2.381E+01	1.436E+01
5.000E+00	1.896E+01	7.549E+01	4.359E+01	9.482E+00	3.406E+01	2.106E+01
6.000E+00	2.925E+01	1.037E+02	6.439E+01	1.257E+01	4.431E+01	2.775E+01
7.000E+00	3.680E+01	1.294E+02	8.087E+01	1.579E+01	5.526E+01	3.476E+01
8.000E+00	4.435E+01	1.550E+02	9.735E+01	1.901E+01	6.621E+01	4.177E+01
9.000E+00	5.438E+01	1.901E+02	1.194E+02	2.298E+01	8.057E+01	5.066E+01
1.000E+01	6.441E+01	2.253E+02	1.415E+02	2.695E+01	9.493E+01	5.955E+01
1.100E+01	8.052E+01	2.907E+02	1.794E+02	3.383E+01	1.197E+02	7.492E+01
1.200E+01	9.664E+01	3.561E+02	2.174E+02	4.071E+01	1.445E+02	9.030E+01
1.300E+01	1.369E+02	4.955E+02	3.059E+02	5.140E+01	1.804E+02	1.135E+02
1.400E+01	1.771E+02	6.349E+02	3.945E+02	6.209E+01	2.163E+02	1.366E+02
1.500E+01	2.322E+02	8.198E+02	5.141E+02	7.253E+01	2.524E+02	1.596E+02
1.600E+01	2.873E+02	1.005E+03	6.338E+02	8.296E+01	2.886E+02	1.825E+02
1.700E+01	3.419E+02	1.192E+03	7.529E+02	9.452E+01	3.286E+02	2.080E+02
1.800E+01	3.966E+02	1.378E+03	8.721E+02	1.061E+02	3.686E+02	2.334E+02
1.900E+01	4.554E+02	1.585E+03	1.002E+03	1.170E+02	4.065E+02	2.574E+02
2.000E+01	5.143E+02	1.791E+03	1.132E+03	1.279E+02	4.444E+02	2.815E+02
2.100E+01	5.927E+02	2.062E+03	1.305E+03	1.394E+02	4.842E+02	3.068E+02
2.200E+01	6.711E+02	2.333E+03	1.477E+03	1.509E+02	5.240E+02	3.322E+02
2.300E+01	7.454E+02	2.590E+03	1.640E+03	1.585E+02	5.504E+02	3.489E+02
2.400E+01	8.197E+02	2.846E+03	1.804E+03	1.660E+02	5.768E+02	3.657E+02

Table 12-4 Current HPS – Stage-Fatality (Continued)

Elevation (ft)	OM5		
	5%	95%	Mean
-1.200E+01	0.000E+00	0.000E+00	0.000E+00
-1.100E+01	0.000E+00	0.000E+00	0.000E+00
-1.000E+01	0.000E+00	0.000E+00	0.000E+00
-9.000E+00	0.000E+00	0.000E+00	0.000E+00
-8.000E+00	0.000E+00	0.000E+00	0.000E+00
-7.000E+00	0.000E+00	0.000E+00	0.000E+00
-6.000E+00	0.000E+00	0.000E+00	0.000E+00
-5.000E+00	0.000E+00	0.000E+00	0.000E+00
-4.000E+00	4.621E-02	2.368E-01	1.281E-01
-3.000E+00	9.242E-02	4.735E-01	2.561E-01
-2.000E+00	3.024E-01	3.900E+00	1.837E+00
-1.000E+00	5.124E-01	7.326E+00	3.418E+00
0.000E+00	8.923E-01	1.230E+01	5.751E+00
1.000E+00	1.272E+00	1.727E+01	8.085E+00
2.000E+00	2.051E+00	2.555E+01	1.210E+01
3.000E+00	2.830E+00	3.384E+01	1.611E+01
4.000E+00	7.114E+00	6.206E+01	2.813E+01
5.000E+00	1.140E+01	9.028E+01	4.014E+01
6.000E+00	3.477E+01	1.669E+02	8.835E+01
7.000E+00	5.814E+01	2.435E+02	1.365E+02
8.000E+00	9.600E+01	3.695E+02	2.184E+02
9.000E+00	1.339E+02	4.956E+02	3.002E+02
1.000E+01	1.875E+02	6.704E+02	4.153E+02
1.100E+01	2.412E+02	8.452E+02	5.303E+02
1.200E+01	2.983E+02	1.046E+03	6.565E+02
1.300E+01	3.554E+02	1.246E+03	7.828E+02
1.400E+01	4.512E+02	1.646E+03	1.011E+03
1.500E+01	5.470E+02	2.047E+03	1.239E+03
1.600E+01	7.893E+02	2.861E+03	1.767E+03
1.700E+01	1.032E+03	3.676E+03	2.295E+03
1.800E+01	1.323E+03	4.669E+03	2.931E+03
1.900E+01	1.615E+03	5.661E+03	3.568E+03
2.000E+01	1.928E+03	6.729E+03	4.252E+03
2.100E+01	2.241E+03	7.797E+03	4.935E+03
2.200E+01	2.488E+03	8.650E+03	5.478E+03
2.300E+01	2.736E+03	9.503E+03	6.021E+03
2.400E+01	2.972E+03	1.032E+04	6.543E+03

Table 12-4 Current HPS – Stage-Fatality (Continued)

Elevation (ft)	SB1			SB3		
	5%	95%	Mean	5%	95%	Mean
-1.200E+01	0.000E+00	0.000E+00	0.000E+00	0.000E+00	0.000E+00	0.000E+00
-1.100E+01	0.000E+00	0.000E+00	0.000E+00	0.000E+00	0.000E+00	0.000E+00
-1.000E+01	0.000E+00	0.000E+00	0.000E+00	0.000E+00	0.000E+00	0.000E+00
-9.000E+00	0.000E+00	0.000E+00	0.000E+00	0.000E+00	0.000E+00	0.000E+00
-8.000E+00	0.000E+00	0.000E+00	0.000E+00	0.000E+00	0.000E+00	0.000E+00
-7.000E+00	0.000E+00	0.000E+00	0.000E+00	0.000E+00	0.000E+00	0.000E+00
-6.000E+00	0.000E+00	0.000E+00	0.000E+00	0.000E+00	0.000E+00	0.000E+00
-5.000E+00	0.000E+00	0.000E+00	0.000E+00	0.000E+00	0.000E+00	0.000E+00
-4.000E+00	0.000E+00	0.000E+00	0.000E+00	0.000E+00	0.000E+00	0.000E+00
-3.000E+00	0.000E+00	0.000E+00	0.000E+00	0.000E+00	0.000E+00	0.000E+00
-2.000E+00	0.000E+00	0.000E+00	0.000E+00	0.000E+00	0.000E+00	0.000E+00
-1.000E+00	0.000E+00	0.000E+00	0.000E+00	0.000E+00	0.000E+00	0.000E+00
0.000E+00	0.000E+00	0.000E+00	0.000E+00	0.000E+00	0.000E+00	0.000E+00
1.000E+00	1.538E-01	2.010E+00	9.435E-01	3.095E-02	4.228E-01	1.978E-01
2.000E+00	3.075E-01	4.020E+00	1.887E+00	6.190E-02	8.456E-01	3.957E-01
3.000E+00	3.249E-01	4.141E+00	1.948E+00	1.954E-01	2.552E+00	1.199E+00
4.000E+00	3.422E-01	4.262E+00	2.008E+00	3.289E-01	4.259E+00	2.001E+00
5.000E+00	6.525E-01	1.331E+01	4.361E+00	3.924E-01	4.376E+00	2.085E+00
6.000E+00	9.628E-01	2.236E+01	6.713E+00	4.559E-01	4.493E+00	2.169E+00
7.000E+00	9.138E+00	4.768E+01	2.373E+01	3.702E+00	1.535E+01	9.133E+00
8.000E+00	1.731E+01	7.300E+01	4.075E+01	6.948E+00	2.620E+01	1.610E+01
9.000E+00	2.770E+01	1.029E+02	6.238E+01	1.953E+01	6.875E+01	4.335E+01
1.000E+01	3.809E+01	1.329E+02	8.401E+01	3.212E+01	1.113E+02	7.061E+01
1.100E+01	3.864E+01	1.344E+02	8.514E+01	3.212E+01	1.113E+02	7.061E+01
1.200E+01	3.918E+01	1.360E+02	8.627E+01	3.212E+01	1.113E+02	7.061E+01
1.300E+01	3.918E+01	1.360E+02	8.628E+01	3.297E+01	1.285E+02	7.539E+01
1.400E+01	3.918E+01	1.360E+02	8.628E+01	3.382E+01	1.457E+02	8.017E+01
1.500E+01	4.295E+01	1.905E+02	1.031E+02	5.103E+01	2.482E+02	1.268E+02
1.600E+01	4.671E+01	2.449E+02	1.199E+02	6.824E+01	3.508E+02	1.734E+02
1.700E+01	9.819E+01	3.885E+02	2.261E+02	1.252E+02	4.919E+02	2.873E+02
1.800E+01	1.497E+02	5.322E+02	3.324E+02	1.822E+02	6.330E+02	4.012E+02
1.900E+01	1.809E+02	6.359E+02	4.004E+02	1.890E+02	6.577E+02	4.168E+02
2.000E+01	2.122E+02	7.397E+02	4.685E+02	1.959E+02	6.824E+02	4.323E+02
2.100E+01	2.137E+02	7.448E+02	4.718E+02	1.959E+02	6.824E+02	4.323E+02
2.200E+01	2.152E+02	7.499E+02	4.751E+02	1.959E+02	6.824E+02	4.323E+02
2.300E+01	2.165E+02	7.535E+02	4.774E+02	1.967E+02	6.852E+02	4.341E+02
2.400E+01	2.178E+02	7.572E+02	4.798E+02	1.976E+02	6.880E+02	4.358E+02

Table 12-4 Current HPS – Stage-Fatality (Continued)

Elevation (ft)	SB4		
	5%	95%	Mean
-1.200E+01	0.000E+00	0.000E+00	0.000E+00
-1.100E+01	0.000E+00	0.000E+00	0.000E+00
-1.000E+01	0.000E+00	0.000E+00	0.000E+00
-9.000E+00	0.000E+00	0.000E+00	0.000E+00
-8.000E+00	0.000E+00	0.000E+00	0.000E+00
-7.000E+00	0.000E+00	0.000E+00	0.000E+00
-6.000E+00	0.000E+00	0.000E+00	0.000E+00
-5.000E+00	0.000E+00	0.000E+00	0.000E+00
-4.000E+00	0.000E+00	0.000E+00	0.000E+00
-3.000E+00	0.000E+00	0.000E+00	0.000E+00
-2.000E+00	0.000E+00	0.000E+00	0.000E+00
-1.000E+00	0.000E+00	0.000E+00	0.000E+00
0.000E+00	0.000E+00	0.000E+00	0.000E+00
1.000E+00	4.429E-03	9.593E-02	4.364E-02
2.000E+00	8.859E-03	1.919E-01	8.728E-02
3.000E+00	5.590E-02	1.075E+00	4.924E-01
4.000E+00	1.029E-01	1.958E+00	8.975E-01
5.000E+00	2.036E-01	2.272E+00	1.079E+00
6.000E+00	3.043E-01	2.586E+00	1.261E+00
7.000E+00	7.299E-01	4.183E+00	2.123E+00
8.000E+00	1.156E+00	5.779E+00	2.984E+00
9.000E+00	2.260E+00	9.830E+00	5.411E+00
1.000E+01	3.365E+00	1.388E+01	7.838E+00
1.100E+01	5.317E+00	1.970E+01	1.192E+01
1.200E+01	7.269E+00	2.552E+01	1.601E+01
1.300E+01	8.792E+00	3.376E+01	1.995E+01
1.400E+01	1.031E+01	4.200E+01	2.389E+01
1.500E+01	1.113E+01	7.379E+01	3.162E+01
1.600E+01	1.194E+01	1.056E+02	3.936E+01
1.700E+01	1.478E+01	1.122E+02	4.495E+01
1.800E+01	1.761E+01	1.189E+02	5.055E+01
1.900E+01	4.328E+01	1.793E+02	1.012E+02
2.000E+01	6.895E+01	2.397E+02	1.519E+02
2.100E+01	7.069E+01	2.459E+02	1.558E+02
2.200E+01	7.242E+01	2.522E+02	1.598E+02
2.300E+01	7.261E+01	2.528E+02	1.602E+02
2.400E+01	7.280E+01	2.535E+02	1.606E+02

Table 12-4 Current HPS – Stage-Fatality (Continued)

Elevation (ft)	JE1			JE2		
	5%	95%	Mean	5%	95%	Mean
-1.200E+01	0.000E+00	0.000E+00	0.000E+00	0.000E+00	0.000E+00	0.000E+00
-1.100E+01	0.000E+00	0.000E+00	0.000E+00	5.956E-02	1.528E+00	6.901E-01
-1.000E+01	0.000E+00	0.000E+00	0.000E+00	6.700E-02	1.719E+00	7.764E-01
-9.000E+00	0.000E+00	0.000E+00	0.000E+00	7.445E-02	1.910E+00	8.626E-01
-8.000E+00	0.000E+00	0.000E+00	0.000E+00	5.770E-01	6.503E+00	2.494E+00
-7.000E+00	0.000E+00	0.000E+00	0.000E+00	1.080E+00	1.110E+01	4.126E+00
-6.000E+00	0.000E+00	0.000E+00	0.000E+00	5.812E+00	2.505E+01	1.387E+01
-5.000E+00	0.000E+00	0.000E+00	0.000E+00	1.055E+01	3.899E+01	2.362E+01
-4.000E+00	1.334E-01	5.056E-01	3.016E-01	1.669E+01	6.096E+01	3.732E+01
-3.000E+00	2.668E-01	1.011E+00	6.031E-01	2.284E+01	8.292E+01	5.103E+01
-2.000E+00	7.894E-01	2.776E+00	1.737E+00	2.842E+01	1.068E+02	6.460E+01
-1.000E+00	1.312E+00	4.540E+00	2.870E+00	3.400E+01	1.306E+02	7.816E+01
0.000E+00	1.820E+00	6.716E+00	4.109E+00	4.417E+01	2.372E+02	1.153E+02
1.000E+00	2.329E+00	8.892E+00	5.347E+00	5.435E+01	3.438E+02	1.525E+02
2.000E+00	3.048E+00	1.215E+01	7.170E+00	1.463E+02	6.670E+02	3.552E+02
3.000E+00	3.768E+00	1.541E+01	8.993E+00	2.382E+02	9.903E+02	5.580E+02
4.000E+00	5.941E+00	3.590E+01	1.696E+01	3.787E+02	1.412E+03	8.521E+02
5.000E+00	8.114E+00	5.639E+01	2.493E+01	5.191E+02	1.834E+03	1.146E+03
6.000E+00	2.066E+01	9.780E+01	5.153E+01	6.277E+02	2.191E+03	1.381E+03
7.000E+00	3.320E+01	1.392E+02	7.813E+01	7.363E+02	2.548E+03	1.616E+03
8.000E+00	5.805E+01	2.252E+02	1.324E+02	8.013E+02	2.774E+03	1.758E+03
9.000E+00	8.290E+01	3.111E+02	1.866E+02	8.663E+02	3.000E+03	1.900E+03
1.000E+01	1.204E+02	4.358E+02	2.679E+02	1.009E+03	3.710E+03	2.266E+03
1.100E+01	1.578E+02	5.606E+02	3.492E+02	1.153E+03	4.420E+03	2.632E+03
1.200E+01	2.035E+02	7.207E+02	4.499E+02	1.689E+03	6.157E+03	3.785E+03
1.300E+01	2.492E+02	8.808E+02	5.506E+02	2.225E+03	7.894E+03	4.937E+03
1.400E+01	3.216E+02	1.148E+03	7.141E+02	2.713E+03	9.515E+03	5.995E+03
1.500E+01	3.941E+02	1.416E+03	8.775E+02	3.202E+03	1.114E+04	7.053E+03
1.600E+01	5.299E+02	1.895E+03	1.179E+03	3.479E+03	1.210E+04	7.663E+03
1.700E+01	6.656E+02	2.375E+03	1.480E+03	3.756E+03	1.306E+04	8.274E+03
1.800E+01	8.657E+02	3.066E+03	1.920E+03	3.914E+03	1.360E+04	8.622E+03
1.900E+01	1.066E+03	3.757E+03	2.360E+03	4.073E+03	1.415E+04	8.971E+03
2.000E+01	1.308E+03	4.581E+03	2.888E+03	4.238E+03	1.472E+04	9.333E+03
2.100E+01	1.551E+03	5.404E+03	3.416E+03	4.403E+03	1.529E+04	9.696E+03
2.200E+01	1.791E+03	6.234E+03	3.944E+03	4.581E+03	1.592E+04	1.009E+04
2.300E+01	2.031E+03	7.064E+03	4.472E+03	4.760E+03	1.655E+04	1.049E+04
2.400E+01	2.249E+03	7.813E+03	4.950E+03	4.861E+03	1.691E+04	1.072E+04

Table 12-4 Current HPS – Stage-Fatality (Continued)

Elevation (ft)	JE3		
	5%	95%	Mean
-1.200E+01	0.000E+00	0.000E+00	0.000E+00
-1.100E+01	0.000E+00	0.000E+00	0.000E+00
-1.000E+01	0.000E+00	0.000E+00	0.000E+00
-9.000E+00	4.116E-02	7.489E-01	3.454E-01
-8.000E+00	8.231E-02	1.498E+00	6.907E-01
-7.000E+00	1.362E+00	1.153E+01	4.992E+00
-6.000E+00	2.641E+00	2.155E+01	9.293E+00
-5.000E+00	1.268E+01	5.775E+01	3.178E+01
-4.000E+00	2.272E+01	9.395E+01	5.426E+01
-3.000E+00	3.748E+01	1.668E+02	9.411E+01
-2.000E+00	5.224E+01	2.397E+02	1.340E+02
-1.000E+00	6.749E+01	3.150E+02	1.720E+02
0.000E+00	8.274E+01	3.903E+02	2.100E+02
1.000E+00	1.594E+02	8.534E+02	4.154E+02
2.000E+00	2.362E+02	1.316E+03	6.207E+02
3.000E+00	4.798E+02	1.997E+03	1.124E+03
4.000E+00	7.235E+02	2.678E+03	1.627E+03
5.000E+00	1.018E+03	3.605E+03	2.250E+03
6.000E+00	1.312E+03	4.532E+03	2.873E+03
7.000E+00	1.405E+03	4.863E+03	3.081E+03
8.000E+00	1.499E+03	5.193E+03	3.289E+03
9.000E+00	1.746E+03	6.515E+03	3.942E+03
1.000E+01	1.992E+03	7.837E+03	4.595E+03
1.100E+01	3.152E+03	1.208E+04	7.212E+03
1.200E+01	4.312E+03	1.632E+04	9.829E+03
1.300E+01	6.108E+03	2.189E+04	1.362E+04
1.400E+01	7.904E+03	2.745E+04	1.740E+04
1.500E+01	8.391E+03	2.917E+04	1.849E+04
1.600E+01	8.878E+03	3.088E+04	1.958E+04
1.700E+01	9.071E+03	3.155E+04	2.000E+04
1.800E+01	9.264E+03	3.222E+04	2.043E+04
1.900E+01	9.508E+03	3.305E+04	2.095E+04
2.000E+01	9.752E+03	3.387E+04	2.147E+04
2.100E+01	1.024E+04	3.559E+04	2.256E+04
2.200E+01	1.073E+04	3.730E+04	2.364E+04
2.300E+01	1.102E+04	3.832E+04	2.429E+04
2.400E+01	1.130E+04	3.933E+04	2.493E+04

Table 12-4 Current HPS – Stage-Fatality (Continued)

Elevation (ft)	JW1			JW2		
	5%	95%	Mean	5%	95%	Mean
-1.200E+01	0.000E+00	0.000E+00	0.000E+00	0.000E+00	0.000E+00	0.000E+00
-1.100E+01	0.000E+00	0.000E+00	0.000E+00	0.000E+00	0.000E+00	0.000E+00
-1.000E+01	0.000E+00	0.000E+00	0.000E+00	0.000E+00	0.000E+00	0.000E+00
-9.000E+00	0.000E+00	0.000E+00	0.000E+00	0.000E+00	0.000E+00	0.000E+00
-8.000E+00	8.278E-03	1.981E-01	8.970E-02	0.000E+00	0.000E+00	0.000E+00
-7.000E+00	1.656E-02	3.962E-01	1.794E-01	0.000E+00	0.000E+00	0.000E+00
-6.000E+00	2.174E-02	4.140E-01	1.896E-01	3.882E-05	9.958E-04	4.499E-04
-5.000E+00	2.692E-02	4.318E-01	1.999E-01	7.765E-05	1.992E-03	8.997E-04
-4.000E+00	9.405E-02	1.512E+00	6.996E-01	2.114E-03	5.033E-02	2.280E-02
-3.000E+00	1.612E-01	2.592E+00	1.199E+00	4.150E-03	9.866E-02	4.471E-02
-2.000E+00	2.814E-01	3.096E+00	1.478E+00	3.605E-02	7.686E-01	3.500E-01
-1.000E+00	4.017E-01	3.599E+00	1.757E+00	6.796E-02	1.438E+00	6.554E-01
0.000E+00	1.156E+00	8.771E+00	3.791E+00	2.180E-01	3.649E+00	1.684E+00
1.000E+00	1.911E+00	1.394E+01	5.824E+00	3.681E-01	5.860E+00	2.713E+00
2.000E+00	5.236E+00	2.462E+01	1.288E+01	6.348E-01	7.903E+00	3.723E+00
3.000E+00	8.561E+00	3.531E+01	1.994E+01	9.015E-01	9.946E+00	4.733E+00
4.000E+00	1.419E+01	5.197E+01	3.167E+01	1.537E+00	1.318E+01	6.328E+00
5.000E+00	1.983E+01	6.863E+01	4.341E+01	2.172E+00	1.641E+01	7.923E+00
6.000E+00	2.162E+01	7.487E+01	4.732E+01	5.744E+00	3.265E+01	1.596E+01
7.000E+00	2.342E+01	8.112E+01	5.123E+01	9.316E+00	4.888E+01	2.400E+01
8.000E+00	2.808E+01	1.058E+02	6.330E+01	1.755E+01	7.099E+01	4.066E+01
9.000E+00	3.275E+01	1.304E+02	7.537E+01	2.578E+01	9.310E+01	5.732E+01
1.000E+01	5.405E+01	2.185E+02	1.252E+02	3.399E+01	1.192E+02	7.480E+01
1.100E+01	7.536E+01	3.065E+02	1.751E+02	4.220E+01	1.453E+02	9.228E+01
1.200E+01	1.185E+02	4.340E+02	2.650E+02	4.580E+01	1.614E+02	1.009E+02
1.300E+01	1.616E+02	5.614E+02	3.549E+02	4.940E+01	1.775E+02	1.095E+02
1.400E+01	1.768E+02	6.127E+02	3.881E+02	6.504E+01	2.909E+02	1.564E+02
1.500E+01	1.919E+02	6.639E+02	4.213E+02	8.068E+01	4.043E+02	2.032E+02
1.600E+01	2.041E+02	7.073E+02	4.481E+02	1.661E+02	6.714E+02	3.865E+02
1.700E+01	2.163E+02	7.507E+02	4.749E+02	2.515E+02	9.386E+02	5.698E+02
1.800E+01	2.537E+02	8.933E+02	5.610E+02	3.440E+02	1.227E+03	7.652E+02
1.900E+01	2.911E+02	1.036E+03	6.471E+02	4.365E+02	1.515E+03	9.606E+02
2.000E+01	3.706E+02	1.302E+03	8.188E+02	4.569E+02	1.588E+03	1.007E+03
2.100E+01	4.500E+02	1.568E+03	9.905E+02	4.773E+02	1.660E+03	1.053E+03
2.200E+01	5.161E+02	1.794E+03	1.136E+03	4.828E+02	1.680E+03	1.065E+03
2.300E+01	5.822E+02	2.021E+03	1.281E+03	4.883E+02	1.699E+03	1.077E+03
2.400E+01	6.192E+02	2.150E+03	1.363E+03	5.016E+02	1.743E+03	1.105E+03

Table 12-4 Current HPS – Stage-Fatality (Continued)

Elevation (ft)	JW3			JW4		
	5%	95%	Mean	5%	95%	Mean
-1.200E+01	0.000E+00	0.000E+00	0.000E+00	0.000E+00	0.000E+00	0.000E+00
-1.100E+01	0.000E+00	0.000E+00	0.000E+00	0.000E+00	0.000E+00	0.000E+00
-1.000E+01	0.000E+00	0.000E+00	0.000E+00	5.118E-04	8.286E-03	3.860E-03
-9.000E+00	0.000E+00	0.000E+00	0.000E+00	1.024E-03	1.657E-02	7.719E-03
-8.000E+00	0.000E+00	0.000E+00	0.000E+00	1.270E-02	1.662E-01	7.856E-02
-7.000E+00	3.859E-04	9.898E-03	4.471E-03	2.438E-02	3.159E-01	1.494E-01
-6.000E+00	7.717E-04	1.980E-02	8.942E-03	1.162E-01	1.247E+00	5.992E-01
-5.000E+00	9.314E-03	2.051E-01	8.210E-02	2.080E-01	2.179E+00	1.049E+00
-4.000E+00	1.786E-02	3.904E-01	1.553E-01	6.595E-01	5.946E+00	2.909E+00
-3.000E+00	2.028E-01	1.843E+00	7.957E-01	1.111E+00	9.714E+00	4.769E+00
-2.000E+00	3.878E-01	3.295E+00	1.436E+00	3.270E+00	2.504E+01	1.251E+01
-1.000E+00	1.882E+00	9.998E+00	5.275E+00	5.428E+00	4.037E+01	2.025E+01
0.000E+00	3.376E+00	1.670E+01	9.114E+00	9.568E+00	6.253E+01	3.207E+01
1.000E+00	5.791E+00	3.119E+01	1.665E+01	1.371E+01	8.469E+01	4.388E+01
2.000E+00	8.207E+00	4.568E+01	2.418E+01	2.268E+01	1.203E+02	6.404E+01
3.000E+00	1.107E+01	6.386E+01	3.350E+01	3.165E+01	1.559E+02	8.420E+01
4.000E+00	1.393E+01	8.204E+01	4.282E+01	5.403E+01	2.448E+02	1.340E+02
5.000E+00	2.108E+01	1.193E+02	6.217E+01	7.640E+01	3.337E+02	1.837E+02
6.000E+00	2.823E+01	1.566E+02	8.153E+01	1.309E+02	5.288E+02	3.035E+02
7.000E+00	5.501E+01	2.599E+02	1.398E+02	1.854E+02	7.239E+02	4.233E+02
8.000E+00	8.180E+01	3.632E+02	1.980E+02	2.764E+02	1.001E+03	6.143E+02
9.000E+00	1.402E+02	5.479E+02	3.213E+02	3.673E+02	1.279E+03	8.052E+02
1.000E+01	1.987E+02	7.326E+02	4.447E+02	4.455E+02	1.566E+03	9.815E+02
1.100E+01	2.749E+02	9.885E+02	6.104E+02	5.237E+02	1.854E+03	1.158E+03
1.200E+01	3.511E+02	1.244E+03	7.761E+02	6.807E+02	2.458E+03	1.518E+03
1.300E+01	4.560E+02	1.627E+03	1.012E+03	8.378E+02	3.062E+03	1.877E+03
1.400E+01	5.610E+02	2.010E+03	1.248E+03	1.179E+03	4.524E+03	2.691E+03
1.500E+01	7.497E+02	2.686E+03	1.668E+03	1.521E+03	5.986E+03	3.505E+03
1.600E+01	9.384E+02	3.362E+03	2.088E+03	2.289E+03	8.342E+03	5.127E+03
1.700E+01	1.257E+03	4.606E+03	2.824E+03	3.057E+03	1.070E+04	6.748E+03
1.800E+01	1.575E+03	5.851E+03	3.560E+03	3.608E+03	1.257E+04	7.948E+03
1.900E+01	2.211E+03	7.935E+03	4.930E+03	4.158E+03	1.445E+04	9.149E+03
2.000E+01	2.846E+03	1.002E+04	6.299E+03	4.592E+03	1.595E+04	1.010E+04
2.100E+01	3.445E+03	1.204E+04	7.601E+03	5.025E+03	1.744E+04	1.106E+04
2.200E+01	4.044E+03	1.407E+04	8.902E+03	5.301E+03	1.840E+04	1.167E+04
2.300E+01	4.517E+03	1.570E+04	9.943E+03	5.577E+03	1.936E+04	1.227E+04
2.400E+01	4.990E+03	1.733E+04	1.098E+04	5.872E+03	2.039E+04	1.293E+04

Table 12-4 Current HPS – Stage-Fatality (Continued)

Elevation (ft)	PL11		
	5%	95%	Mean
-1.200E+01	2.828E-01	1.235E+00	7.010E-01
-1.100E+01	3.505E-01	1.808E+00	9.773E-01
-1.000E+01	4.181E-01	2.382E+00	1.254E+00
-9.000E+00	4.645E-01	2.584E+00	1.368E+00
-8.000E+00	5.109E-01	2.786E+00	1.483E+00
-7.000E+00	7.870E-01	6.230E+00	2.589E+00
-6.000E+00	1.063E+00	9.673E+00	3.695E+00
-5.000E+00	4.147E+00	1.836E+01	9.993E+00
-4.000E+00	7.231E+00	2.705E+01	1.629E+01
-3.000E+00	1.020E+01	3.621E+01	2.254E+01
-2.000E+00	1.316E+01	4.536E+01	2.878E+01
-1.000E+00	1.438E+01	4.950E+01	3.143E+01
0.000E+00	1.559E+01	5.364E+01	3.408E+01
1.000E+00	1.720E+01	6.055E+01	3.794E+01
2.000E+00	1.880E+01	6.746E+01	4.180E+01
3.000E+00	2.640E+01	1.082E+02	6.146E+01
4.000E+00	3.401E+01	1.489E+02	8.112E+01
5.000E+00	5.866E+01	2.188E+02	1.320E+02
6.000E+00	8.332E+01	2.887E+02	1.828E+02
7.000E+00	9.352E+01	3.238E+02	2.052E+02
8.000E+00	1.037E+02	3.590E+02	2.275E+02
9.000E+00	1.147E+02	3.972E+02	2.516E+02
1.000E+01	1.257E+02	4.355E+02	2.758E+02
1.100E+01	1.408E+02	4.881E+02	3.090E+02
1.200E+01	1.560E+02	5.408E+02	3.423E+02
1.300E+01	1.774E+02	6.165E+02	3.898E+02
1.400E+01	1.988E+02	6.922E+02	4.373E+02
1.500E+01	2.290E+02	7.957E+02	5.038E+02
1.600E+01	2.592E+02	8.992E+02	5.702E+02
1.700E+01	2.754E+02	9.558E+02	6.057E+02
1.800E+01	2.916E+02	1.012E+03	6.412E+02
1.900E+01	3.250E+02	1.132E+03	7.157E+02
2.000E+01	3.583E+02	1.252E+03	7.902E+02
2.100E+01	4.152E+02	1.446E+03	9.149E+02
2.200E+01	4.721E+02	1.640E+03	1.040E+03
2.300E+01	5.036E+02	1.749E+03	1.109E+03
2.400E+01	5.351E+02	1.859E+03	1.179E+03

Table 12-4 Current HPS – Stage-Fatality (Concluded)

Elevation (ft)	SC1			SC2		
	5%	95%	Mean	5%	95%	Mean
-1.200E+01	0.000E+00	0.000E+00	0.000E+00	0.000E+00	0.000E+00	0.000E+00
-1.100E+01	0.000E+00	0.000E+00	0.000E+00	0.000E+00	0.000E+00	0.000E+00
-1.000E+01	0.000E+00	0.000E+00	0.000E+00	0.000E+00	0.000E+00	0.000E+00
-9.000E+00	0.000E+00	0.000E+00	0.000E+00	0.000E+00	0.000E+00	0.000E+00
-8.000E+00	0.000E+00	0.000E+00	0.000E+00	0.000E+00	0.000E+00	0.000E+00
-7.000E+00	0.000E+00	0.000E+00	0.000E+00	0.000E+00	0.000E+00	0.000E+00
-6.000E+00	0.000E+00	0.000E+00	0.000E+00	0.000E+00	0.000E+00	0.000E+00
-5.000E+00	0.000E+00	0.000E+00	0.000E+00	0.000E+00	0.000E+00	0.000E+00
-4.000E+00	0.000E+00	0.000E+00	0.000E+00	0.000E+00	0.000E+00	0.000E+00
-3.000E+00	0.000E+00	0.000E+00	0.000E+00	0.000E+00	0.000E+00	0.000E+00
-2.000E+00	0.000E+00	0.000E+00	0.000E+00	0.000E+00	0.000E+00	0.000E+00
-1.000E+00	0.000E+00	0.000E+00	0.000E+00	0.000E+00	0.000E+00	0.000E+00
0.000E+00	0.000E+00	0.000E+00	0.000E+00	0.000E+00	0.000E+00	0.000E+00
1.000E+00	0.000E+00	0.000E+00	0.000E+00	0.000E+00	0.000E+00	0.000E+00
2.000E+00	0.000E+00	0.000E+00	0.000E+00	3.718E-03	9.536E-02	4.308E-02
3.000E+00	0.000E+00	0.000E+00	0.000E+00	7.435E-03	1.907E-01	8.615E-02
4.000E+00	0.000E+00	0.000E+00	0.000E+00	6.044E-02	1.541E+00	6.961E-01
5.000E+00	0.000E+00	0.000E+00	0.000E+00	1.135E-01	2.891E+00	1.306E+00
6.000E+00	1.059E-05	2.716E-04	1.227E-04	4.328E-01	4.675E+00	2.238E+00
7.000E+00	2.118E-05	5.432E-04	2.454E-04	7.521E-01	6.460E+00	3.169E+00
8.000E+00	1.589E-02	5.967E-02	3.676E-02	1.890E+00	1.507E+01	6.764E+00
9.000E+00	3.177E-02	1.188E-01	7.327E-02	3.027E+00	2.368E+01	1.036E+01
1.000E+01	3.837E-01	1.330E+00	8.410E-01	9.488E+00	4.392E+01	2.362E+01
1.100E+01	7.356E-01	2.541E+00	1.609E+00	1.595E+01	6.416E+01	3.689E+01
1.200E+01	1.772E+00	6.096E+00	3.871E+00	2.669E+01	1.019E+02	6.047E+01
1.300E+01	2.809E+00	9.652E+00	6.133E+00	3.742E+01	1.396E+02	8.405E+01
1.400E+01	2.961E+00	1.018E+01	6.465E+00	5.407E+01	1.925E+02	1.194E+02
1.500E+01	3.113E+00	1.071E+01	6.798E+00	7.071E+01	2.454E+02	1.548E+02
1.600E+01	3.323E+00	1.243E+01	7.466E+00	8.778E+01	3.094E+02	1.936E+02
1.700E+01	3.533E+00	1.416E+01	8.133E+00	1.048E+02	3.734E+02	2.325E+02
1.800E+01	5.476E+00	3.828E+01	1.598E+01	1.486E+02	5.749E+02	3.396E+02
1.900E+01	7.419E+00	6.240E+01	2.384E+01	1.924E+02	7.764E+02	4.468E+02
2.000E+01	2.305E+01	9.842E+01	5.453E+01	3.065E+02	1.131E+03	6.896E+02
2.100E+01	3.867E+01	1.345E+02	8.522E+01	4.206E+02	1.486E+03	9.324E+02
2.200E+01	3.963E+01	1.378E+02	8.737E+01	5.287E+02	1.866E+03	1.172E+03
2.300E+01	4.058E+01	1.412E+02	8.951E+01	6.369E+02	2.246E+03	1.411E+03
2.400E+01	4.090E+01	1.423E+02	9.020E+01	7.825E+02	2.735E+03	1.726E+03

Table 12-5: Stage-Damage for All Sub-basins			
Subbasin Name	Water Elevation	Pre-Katrina Stage-Damage	Post-Katrina Stage-Damage June 2006
JE2	-12	0.0	0.0
JE2	-11	0.0	0.0
JE2	-10	0.0	0.0
JE2	-9	0.9	0.9
JE2	-8	1.0	1.0
JE2	-7	2.4	2.4
JE2	-6	8.1	8.1
JE2	-5	52.0	52.0
JE2	-4	470.7	470.7
JE2	-3	2,190.3	2,190.3
JE2	-2	3,394.0	3,394.0
JE2	-1	3,857.5	3,857.5
JE2	0	4,228.2	4,228.2
JE2	1	4,506.3	4,504.7
JE2	2	4,752.0	4,747.6
JE2	3	4,994.2	4,985.7
JE2	4	5,237.5	5,224.7
JE2	5	5,499.4	5,485.1
JE2	6	5,736.9	5,722.4
JE2	7	5,864.8	5,850.0
JE2	8	5,943.8	5,928.9
JE2	9	6,079.7	6,064.5
JE2	10	6,175.8	6,160.3
JE2	11	6,215.7	6,199.9
JE2	12	6,243.1	6,227.0
JE2	13	6,262.7	6,246.4
JE2	14	6,277.7	6,261.2
JE2	15	6,286.6	6,269.9
JE2	16	6,292.0	6,275.2
JE2	17	6,295.9	6,279.0
JE2	18	6,298.8	6,281.9
JE2	19	6,300.2	6,283.3
JE2	20	6,300.6	6,283.7
JE2	21	6,300.7	6,283.8
JE2	22	6,300.7	6,283.9
JE2	23	6,300.7	6,283.9
JE2	24	6,300.7	6,283.9

Table 12-5: Stage-Damage for All Sub-basins (continued)			
Subbasin Name	Water Elevation	Pre-Katrina Stage-Damage	Post-Katrina Stage-Damage June 2006
NOE1	-3	0.0	0.0
NOE1	-2	0.0	0.0
NOE1	-1	0.0	0.0
NOE1	0	0.1	0.0
NOE1	1	6.0	0.1
NOE1	2	8.0	0.1
NOE1	3	9.1	0.1
NOE1	4	10.5	0.1
NOE1	5	10.9	0.1
NOE1	6	10.9	0.1
NOE1	7	10.9	0.1
NOE1	8	11.3	0.1
NOE1	9	11.7	0.1
NOE1	10	12.0	0.1
NOE1	11	12.1	0.1
NOE1	12	12.1	0.1
NOE1	13	12.3	0.1
NOE1	14	12.4	0.1
NOE1	15	12.4	0.1
NOE1	16	12.4	0.1
NOE1	17	12.4	0.1
NOE1	18	12.4	0.1
NOE1	19	12.4	0.1
NOE1	20	12.4	0.1
NOE1	21	12.4	0.1
NOE1	22	12.4	0.1
NOE1	23	12.4	0.1
NOE1	24	12.4	0.1

Table 12-5: Stage-Damage for All Sub-basins (continued)			
Subbasin Name	Water Elevation	Pre-Katrina Stage-Damage	Post-Katrina Stage-Damage June 2006
NOE2	-8	0.0	0.0
NOE2	-7	0.0	0.0
NOE2	-6	0.0	0.0
NOE2	-5	0.5	0.0
NOE2	-4	19.3	0.0
NOE2	-3	29.0	0.0
NOE2	-2	98.3	0.7
NOE2	-1	114.5	0.9
NOE2	0	116.3	0.9
NOE2	1	120.6	1.0
NOE2	2	123.3	1.0
NOE2	3	124.1	1.1
NOE2	4	126.1	1.1
NOE2	5	127.6	1.1
NOE2	6	134.5	1.1
NOE2	7	138.6	1.2
NOE2	8	139.8	1.2
NOE2	9	140.8	1.2
NOE2	10	142.0	1.2
NOE2	11	142.5	1.2
NOE2	12	142.5	1.2
NOE2	13	142.6	1.2
NOE2	14	142.6	1.2
NOE2	15	142.7	1.2
NOE2	16	142.7	1.2
NOE2	17	142.7	1.2
NOE2	18	142.7	1.2
NOE2	19	142.7	1.2
NOE2	20	142.7	1.2
NOE2	21	142.7	1.2
NOE2	22	142.7	1.2
NOE2	23	142.7	1.2
NOE2	24	142.7	1.2

Table 12-5: Stage-Damage for All Sub-basins (continued)			
Subbasin Name	Water Elevation	Pre-Katrina Stage-Damage	Post-Katrina Stage-Damage June 2006
NOE3	-6	0.0	0.0
NOE3	-5	0.3	0.0
NOE3	-4	8.0	0.0
NOE3	-3	39.6	0.1
NOE3	-2	189.0	1.6
NOE3	-1	365.8	3.6
NOE3	0	399.8	4.5
NOE3	1	416.2	5.6
NOE3	2	510.1	22.3
NOE3	3	528.7	25.0
NOE3	4	563.7	31.5
NOE3	5	577.3	33.3
NOE3	6	594.1	33.8
NOE3	7	618.7	34.4
NOE3	8	629.6	35.2
NOE3	9	636.6	35.9
NOE3	10	649.1	37.6
NOE3	11	666.7	40.3
NOE3	12	668.4	40.4
NOE3	13	671.0	40.9
NOE3	14	677.1	42.2
NOE3	15	678.8	42.5
NOE3	16	680.2	42.8
NOE3	17	680.3	42.8
NOE3	18	680.3	42.8
NOE3	19	680.3	42.8
NOE3	20	680.3	42.8
NOE3	21	680.3	42.8
NOE3	22	680.3	42.8
NOE3	23	680.3	42.8
NOE3	24	680.3	42.8
NOE3	25	680.3	42.8

Table 12-5: Stage-Damage for All Sub-basins (continued)			
Subbasin Name	Water Elevation	Pre-Katrina Stage-Damage	Post-Katrina Stage-Damage June 2006
NOE4	-1	0.0	0.0
NOE4	0	0.1	0.1
NOE4	1	24.9	12.7
NOE4	2	32.6	19.4
NOE4	3	34.6	20.7
NOE4	4	49.1	33.9
NOE4	5	54.3	38.7
NOE4	6	55.7	40.0
NOE4	7	56.6	40.7
NOE4	8	57.4	41.2
NOE4	9	58.0	41.7
NOE4	10	59.5	42.9
NOE4	11	60.1	43.3
NOE4	12	60.5	43.7
NOE4	13	61.9	44.4
NOE4	14	62.9	45.1
NOE4	15	63.6	45.6
NOE4	16	65.4	47.4
NOE4	17	65.8	47.7
NOE4	18	65.9	47.9
NOE4	19	66.0	47.9
NOE4	20	66.0	47.9
NOE4	21	66.0	47.9
NOE4	22	66.0	47.9
NOE4	23	66.0	47.9
NOE4	24	66.0	47.9

Table 12-5: Stage-Damage for All Sub-basins (continued)			
Subbasin Name	Water Elevation	Pre-Katrina Stage-Damage	Post-Katrina Stage-Damage June 2006
NOE5	-12	0.0	0.0
NOE5	-11	0.1	0.0
NOE5	-10	1.2	0.0
NOE5	-9	5.2	0.0
NOE5	-8	42.7	0.0
NOE5	-7	241.5	1.8
NOE5	-6	962.3	9.9
NOE5	-5	2,316.5	25.4
NOE5	-4	3,083.4	42.5
NOE5	-3	3,484.4	63.4
NOE5	-2	4,121.0	146.5
NOE5	-1	4,560.7	225.3
NOE5	0	4,940.0	325.0
NOE5	1	5,066.5	359.3
NOE5	2	5,183.0	378.0
NOE5	3	5,430.1	467.7
NOE5	4	5,594.9	508.4
NOE5	5	5,674.0	517.9
NOE5	6	5,778.1	529.9
NOE5	7	5,878.2	540.8
NOE5	8	5,945.3	553.9
NOE5	9	5,974.5	563.8
NOE5	10	5,993.7	569.3
NOE5	11	6,007.4	575.7
NOE5	12	6,021.6	584.6
NOE5	13	6,025.7	587.1
NOE5	14	6,028.0	589.0
NOE5	15	6,034.6	595.2
NOE5	16	6,036.7	597.1
NOE5	17	6,037.3	597.7
NOE5	18	6,037.5	597.9
NOE5	19	6,037.5	597.9
NOE5	20	6,037.5	597.9
NOE5	21	6,037.5	597.9
NOE5	22	6,037.5	597.9
NOE5	23	6,037.5	597.9
NOE5	24	6,037.5	597.9

Table 12-5: Stage-Damage for All Sub-basins (continued)			
Subbasin Name	Water Elevation	Pre-Katrina Stage-Damage	Post-Katrina Stage-Damage June 2006
OM1	-12	0.0	0.0
OM1	-11	0.0	0.0
OM1	-10	0.0	0.0
OM1	-9	0.0	0.0
OM1	-8	0.0	0.0
OM1	-7	8.4	0.0
OM1	-6	102.8	0.0
OM1	-5	401.7	0.0
OM1	-4	782.6	0.0
OM1	-3	1,008.1	0.7
OM1	-2	1,269.7	3.3
OM1	-1	1,531.3	9.3
OM1	0	1,713.2	16.7
OM1	1	1,864.2	29.1
OM1	2	2,012.0	51.5
OM1	3	2,208.9	89.3
OM1	4	2,339.4	131.2
OM1	5	2,458.6	188.1
OM1	6	2,526.4	221.6
OM1	7	2,574.8	234.9
OM1	8	2,603.0	238.7
OM1	9	2,625.3	242.1
OM1	10	2,650.3	245.8
OM1	11	2,675.0	251.1
OM1	12	2,689.4	255.4
OM1	13	2,702.4	261.0
OM1	14	2,717.7	268.7
OM1	15	2,725.8	272.8
OM1	16	2,731.7	276.2
OM1	17	2,737.6	279.5
OM1	18	2,738.9	280.3
OM1	19	2,739.7	280.9
OM1	20	2,739.9	281.1
OM1	21	2,739.9	281.1
OM1	22	2,739.9	281.1
OM1	23	2,739.9	281.1
OM1	24	2,739.9	281.1

Table 12-5: Stage-Damage for All Sub-basins (continued)			
Subbasin Name	Water Elevation	Pre-Katrina Stage-Damage	Post-Katrina Stage-Damage June 2006
OM2	-11	0.0	0.0
OM2	-10	0.0	0.0
OM2	-9	0.0	0.0
OM2	-8	0.0	0.0
OM2	-7	2.0	0.0
OM2	-6	69.9	0.0
OM2	-5	347.6	0.0
OM2	-4	677.1	0.0
OM2	-3	884.1	0.2
OM2	-2	1,040.1	1.8
OM2	-1	1,196.3	4.1
OM2	0	1,260.9	6.9
OM2	1	1,376.7	26.7
OM2	2	1,482.4	44.3
OM2	3	1,573.3	64.0
OM2	4	1,685.3	103.2
OM2	5	1,763.0	142.9
OM2	6	1,835.0	188.5
OM2	7	1,858.6	191.5
OM2	8	1,877.2	194.5
OM2	9	1,893.8	197.9
OM2	10	1,909.8	201.1
OM2	11	1,922.1	203.6
OM2	12	1,930.7	207.6
OM2	13	1,938.9	212.8
OM2	14	1,945.5	218.0
OM2	15	1,948.6	220.5
OM2	16	1,949.5	221.2
OM2	17	1,950.0	221.5
OM2	18	1,950.9	222.4
OM2	19	1,951.1	222.5
OM2	20	1,951.1	222.6
OM2	21	1,951.1	222.6
OM2	22	1,951.1	222.6
OM2	23	1,951.1	222.6
OM2	24	1,951.1	222.6

Table 12-5: Stage-Damage for All Sub-basins (continued)			
Subbasin Name	Water Elevation	Pre-Katrina Stage-Damage	Post-Katrina Stage-Damage June 2006
OM3	-10	0.0	0.0
OM3	-9	0.0	0.0
OM3	-8	0.0	0.0
OM3	-7	0.0	0.0
OM3	-6	0.8	0.0
OM3	-5	8.7	0.0
OM3	-4	29.8	0.0
OM3	-3	65.9	0.1
OM3	-2	154.4	1.1
OM3	-1	376.1	4.7
OM3	0	661.8	16.0
OM3	1	1,030.8	40.5
OM3	2	1,364.6	87.0
OM3	3	1,708.7	166.7
OM3	4	2,030.1	287.9
OM3	5	2,281.0	456.3
OM3	6	2,436.6	582.1
OM3	7	2,581.6	691.5
OM3	8	2,696.6	774.4
OM3	9	2,793.1	832.9
OM3	10	2,859.7	866.2
OM3	11	2,910.0	887.7
OM3	12	2,952.5	903.5
OM3	13	2,984.3	919.7
OM3	14	3,010.0	936.8
OM3	15	3,029.5	950.5
OM3	16	3,045.5	963.0
OM3	17	3,060.7	976.3
OM3	18	3,069.1	984.1
OM3	19	3,073.2	987.9
OM3	20	3,075.8	990.3
OM3	21	3,077.0	991.5
OM3	22	3,077.3	991.8
OM3	23	3,077.7	992.1
OM3	24	3,077.7	992.2
OM3	25	3,077.7	992.2

Table 12-5: Stage-Damage for All Sub-basins (continued)			
Subbasin Name	Water Elevation	Pre-Katrina Stage-Damage	Post-Katrina Stage-Damage June 2006
OM4	-6	0.0	0.0
OM4	-5	2.9	0.0
OM4	-4	5.8	0.0
OM4	-3	8.8	0.1
OM4	-2	27.7	0.7
OM4	-1	68.5	1.8
OM4	0	142.1	7.2
OM4	1	219.1	13.7
OM4	2	308.1	28.6
OM4	3	420.5	59.1
OM4	4	618.1	158.1
OM4	5	790.4	288.4
OM4	6	880.0	366.3
OM4	7	954.5	430.0
OM4	8	982.0	449.4
OM4	9	1,013.4	470.1
OM4	10	1,034.5	480.0
OM4	11	1,055.3	490.9
OM4	12	1,075.7	500.7
OM4	13	1,096.4	514.2
OM4	14	1,110.8	525.7
OM4	15	1,119.4	531.8
OM4	16	1,131.1	539.9
OM4	17	1,139.5	547.2
OM4	18	1,145.6	552.7
OM4	19	1,151.2	557.9
OM4	20	1,153.5	560.1
OM4	21	1,155.0	561.6
OM4	22	1,155.3	561.9
OM4	23	1,155.6	562.1
OM4	24	1,155.6	562.2

Table 12-5: Stage-Damage for All Sub-basins (continued)			
Subbasin Name	Water Elevation	Pre-Katrina Stage-Damage	Post-Katrina Stage-Damage June 2006
OM5	-9	0.0	0.0
OM5	-8	0.0	0.0
OM5	-7	0.0	0.0
OM5	-6	0.7	0.0
OM5	-5	0.8	0.0
OM5	-4	6.8	0.1
OM5	-3	37.9	0.4
OM5	-2	200.5	2.3
OM5	-1	785.0	10.6
OM5	0	1,483.2	34.8
OM5	1	2,167.0	79.3
OM5	2	2,859.8	177.1
OM5	3	3,721.4	358.5
OM5	4	4,837.3	827.4
OM5	5	5,522.0	1,296.7
OM5	6	6,034.1	1,701.3
OM5	7	6,834.7	2,387.0
OM5	8	7,538.2	2,966.8
OM5	9	8,112.3	3,415.2
OM5	10	8,574.3	3,758.4
OM5	11	8,920.2	4,012.9
OM5	12	9,305.7	4,303.0
OM5	13	9,511.7	4,449.5
OM5	14	9,679.7	4,572.3
OM5	15	9,846.8	4,675.5
OM5	16	10,031.8	4,800.2
OM5	17	10,144.1	4,897.0
OM5	18	10,260.3	5,003.6
OM5	19	10,353.9	5,092.2
OM5	20	10,401.1	5,137.0
OM5	21	10,436.4	5,170.6
OM5	22	10,457.9	5,191.1
OM5	23	10,488.4	5,220.1
OM5	24	10,512.5	5,242.9
OM5	25	10,517.8	5,247.9
OM5	26	10,520.0	5,250.0
OM5	27	10,520.5	5,250.5
OM5	28	10,520.6	5,250.6
OM5	29	10,520.6	5,250.6
OM5	30	10,520.6	5,250.6
OM5	31	10,520.6	5,250.6
OM5	32	10,520.6	5,250.6
SB1	-5	0.0	0.0
SB1	-4	0.3	0.0
SB1	-3	8.7	0.0
SB1	-2	53.7	0.0
SB1	-1	196.4	0.0

Table 12-5: Stage-Damage for All Sub-basins (continued)			
Subbasin Name	Water Elevation	Pre-Katrina Stage-Damage	Post-Katrina Stage-Damage June 2006
SB1	0	476.7	0.3
SB1	1	876.7	4.7
SB1	2	1,262.7	8.3
SB1	3	1,496.9	11.5
SB1	4	1,722.8	17.3
SB1	5	1,983.3	32.6
SB1	6	2,159.9	53.1
SB1	7	2,306.0	78.2
SB1	8	2,403.4	98.9
SB1	9	2,480.3	116.1
SB1	10	2,542.2	124.8
SB1	11	2,582.0	129.2
SB1	12	2,617.0	133.5
SB1	13	2,650.5	138.2
SB1	14	2,676.6	141.4
SB1	15	2,694.2	144.2
SB1	16	2,707.6	147.1
SB1	17	2,717.6	149.3
SB1	18	2,725.5	150.9
SB1	19	2,729.7	152.2
SB1	20	2,731.4	152.8
SB1	21	2,732.3	153.3
SB1	22	2,732.8	153.7
SB1	23	2,733.3	154.2
SB1	24	2,733.3	154.2
SB1	25	2,733.4	154.3
SB1	26	2,733.5	154.4

Table 12-5: Stage-Damage for All Sub-basins (continued)			
Subbasin Name	Water Elevation	Pre-Katrina Stage-Damage	Post-Katrina Stage-Damage June 2006
SB3	-5	0.0	0.0
SB3	-4	0.0	0.0
SB3	-3	0.1	0.0
SB3	-2	0.3	0.0
SB3	-1	3.7	0.0
SB3	0	70.6	0.0
SB3	1	217.6	0.3
SB3	2	633.5	3.7
SB3	3	1,149.7	10.4
SB3	4	1,524.6	23.5
SB3	5	1,723.6	33.4
SB3	6	1,836.2	44.2
SB3	7	1,938.8	63.5
SB3	8	2,077.3	117.4
SB3	9	2,190.4	185.2
SB3	10	2,298.0	239.2
SB3	11	2,393.5	270.9
SB3	12	2,455.8	286.1
SB3	13	2,490.8	294.3
SB3	14	2,509.6	297.9
SB3	15	2,524.3	301.4
SB3	16	2,540.0	306.9
SB3	17	2,554.3	314.6
SB3	18	2,563.1	320.5
SB3	19	2,568.0	323.9
SB3	20	2,573.5	327.3
SB3	21	2,576.7	329.7
SB3	22	2,578.6	331.2
SB3	23	2,580.0	332.6
SB3	24	2,580.4	333.0
SB3	25	2,580.6	333.1

Table 12-5: Stage-Damage for All Sub-basins (Concluded)			
Subbasin Name	Water Elevation	Pre-Katrina Stage-Damage	Post-Katrina Stage-Damage June 2006
SB4	1	0.0	0.0
SB4	2	0.4	0.0
SB4	3	7.3	0.1
SB4	4	32.7	1.3
SB4	5	89.7	6.4
SB4	6	190.2	21.7
SB4	7	295.3	48.0
SB4	8	387.5	81.1
SB4	9	438.6	100.6
SB4	10	465.4	106.5
SB4	11	491.2	112.5
SB4	12	497.1	113.9
SB4	13	503.4	114.8
SB4	14	515.7	116.6
SB4	15	527.7	119.1
SB4	16	537.8	122.5
SB4	17	544.7	124.8
SB4	18	549.4	126.0
SB4	19	552.6	126.7
SB4	20	553.7	127.2
SB4	21	554.3	127.5
SB4	22	554.5	127.5
SB4	23	554.5	127.6
SB4	24	554.5	127.6
SB4	25	554.5	127.6
SB4	26	554.5	127.6
SB4	27	554.5	127.6
SB4	28	554.5	127.6
SB4	29	554.5	127.6
SB4	30	554.5	127.6
SB4	31	554.5	127.6
SB4	32	554.5	127.6
SB4	33	554.5	127.6
SB4	34	554.5	127.6
SB4	35	554.5	127.6
SB4	36	554.5	127.6

References

- Kevin McCarthy, D.J. Peterson, Narayan Sastry, and Michael Pollard. (2006) “The Repopulation of New Orleans after Hurricane Katrina.” RAND Gulf States Policy Institute. RAND URL: <http://www.rand.org/>
- Aboelata, M. and D.S. Bowles. 2005. LIFESim: A Model for Estimating Dam Failure Life Loss. Draft report to the Institute for Water Resources, US Army Corps of Engineers by the Institute for Dam Safety Risk Management, Utah State University, Logan, Utah.
- Aboelata, M., D.S. Bowles, and D.M. McClelland. 2003. ‘Life-loss Estimation for Floods including Dam Failure.’ GIS Model for Estimating Dam Failure Life Loss. In Y.Y. Haines and D.A. Moser, (eds.), American Society of Civil Engineers.
- Aboelata, M., D.S. Bowles, and D.M. McClelland. 2004a. ‘A Model for Estimating Dam Failure Life Loss.’ ANCOLD Bulletin 127:43-62. August.
- Aboelata, M., D.S. Bowles, and A. Chen. 2004b. ‘Transportation model for evacuation in estimating dam failure life loss.’ Proceedings of the Australian National Committee on Large Dams Conference, Melbourne, Victoria, Australia.
- Abt Associates, Inc. 2006. Estimating Loss of Life from Hurricane-Related Flooding in the Greater New Orleans Area. Loss-of-Life Modeling Report. Prepared for U.S. Army Corps of Engineers, Institute for Water Resources, Alexandria, VA.
- McClelland, D.M. 2000. Personal Communication of Updated Probability Distributions for Fatality Rates for Each Flood Zone. November 30.
- McClelland, D. M. 2002. “A team approach to improving dam-safety emergency action plans, flood maps, and emergency response plans using life-loss risk assessment.” EAP 2002: International Workshop for Emergency Preparedness at Dams, sponsored by FERC and ASDSO.
- McClelland, D.M. and Bowles, D.S. 2002. ‘Estimating Life Loss for Dam Safety Risk Assessment - a Review and New Approach.’ Institute for Water Resources, U.S. Army Corps of Engineers, Alexandria, VA.

Appendix 13

Risk Analysis Results

Introduction

The results of the risk analysis of the New Orleans Hurricane Protection System (HPS) are presented in this appendix. The purpose of the analysis was to evaluate the risk of inundation and the corresponding risks to life and property posed by the HPS prior to the arrival of hurricane Katrina and as it existed on 1 June 2007. These points in time studied are referred to as the “Pre-Katrina (or Pre-K)” and “Current” conditions, respectively. The spreadsheet computer program FoRTE (presented in Appendix 15) developed by the risk team was used as the basis for establishing elevation-exceedence curves for these conditions for three states of pumping system effectiveness. Analyses were run for no pumping, pumping at 50% of capacity and at 100% of capacity. The computer runs included pumping by modifying the sub-basin rainfall by the amount of pumping volume expected for each storm. Pumping volumes were estimated deterministically and subtracted from the rainfall volume calculated for each storm.

Elevations used to produce inundation mapping were selected using several factors to modify the computer generated elevation-exceedence curves. The computer runs did not include overtopping water volumes due to wave run-up so this item was added to the runs using deterministic models. The risk program conducted interflow analyses between sub-basins at the basin level by individual storms but did not do interflow analyses for the basins when the storms were aggregated. Therefore, the program results at the 50-, 100-, and 500-year exceedence rates were examined and balanced by looking at the water volumes produced at each exceedence level using the stage-storage relationships for the sub-basins. If the interflow elevations between sub-basins were exceeded, water volumes were redistributed and new water surface elevations determined. Note that the exceedence rates are conditional on the storm set provided to the risk team with frequencies as shown in Appendix 8, which do not consider tropical storms and lower intensity, more frequent hurricanes.

Measuring System Performance

The primary measure used to evaluate the risks associated with the New Orleans HPS is water elevations within the system based on the amount of inflow water volume from overtopping, breaching, rainfall and closure structures left open. These elevations were used to

determine the rate of overtopping of the reaches, construct inundation maps, and to determine life and economic risks.

Overtopping Rates

One measure of the effectiveness of the HPS is how often the system can be expected to be overtopped by the storms predicted to strike the New Orleans area. This measure, while not risk based, provided decision makers with additional information about system performance. The rates of overtopping were determined for the Pre-K and Current HPS for the total 152 storm set provided by the IPET/LaCPR storm team. Note that while the entire 152 storm set was used to determine overtopping rates, only the 77 storms with frequencies provided by the storm team were used in the actual risk analysis. The number of times that each reach within the basins was overtopped was calculated by counting the storm events whose peak surge exceeded the reach elevation. The overtopping rate was then determined by dividing the total number of times that a reach was overtopped by the number of storms (152). Basin and HPS overtopping rates were also determined and are presented in Table 13-1. The rates are also graphically shown in Figures 13-10 and 13-11 for the Pre-K and Current HPS, respectively, with color coding to rank areas by the overtopping rate.

As shown in Table 13-1, the number of overtopping events in the Current HPS is reduced somewhat from those of Pre-K levels in most basins and at many reaches. This is due to restoring damaged levees to the Pre-Katrina authorized elevation, which in many cases is higher than the actual Pre-K elevation because of subsidence and datum changes. Areas that show high rates of overtopping, greater than 25% of the storms, in the Pre-Katrina HPS are in New Orleans East along the IHNC and MRGO, all of the southern portions of Jefferson West Bank and most of Plaquemines. The overall rates of overtopping, however, are very similar in both HPS.

Table 13-1 Overtopping Rates for Reaches and Sub-basins									
Station No.	Reach Name	Sub-basin	Pre-K			Current			Color Legend
			No of OT	% of storms OT	Color	No of OT	% of storms OT	Color	
1	NOE 1	NOE5	5.0	0.033		6.0	0.039		0=Dark Green
2	NOE 2	NOE5	5.0	0.033		6.0	0.039		0-.1 = Lt Green
3	NOE 3	NOE5	5.0	0.033		6.0	0.039		.1-.2 = Lt Blue
4	NOE 4	NOE5	5.0	0.033		6.0	0.039		.2-.3 = Yellow
5	NOE 5	NOE5	5.0	0.033		6.0	0.039		.3-.4 = Orange
6	NOE 6	NOE5	1.0	0.007		2.0	0.013		.4-.5 = Red
7	NOE 7	NOE5	1.0	0.007		2.0	0.013		
8	NOE 8	NOE5	2.0	0.013		3.0	0.020		
9	NOE 9	NOE1	0.0	0.000		0.0	0.000		
10	NOE 10	NOE1	2.0	0.013		3.0	0.020		
11	NOE 11	NOE1	3.0	0.020		4.0	0.026		
12	NOE 12	NOE1	3.0	0.020		4.0	0.026		
13	NOE 13	NOE1	3.0	0.020		4.0	0.026		
14	NOE 14	NOE1	13.0	0.086		14.0	0.092		
15	NOE 15	NOE1	18.0	0.118		10.0	0.066		

Table 13-1 Overtopping Rates for Reaches and Sub-basins

Station No.	Reach Name	Sub-basin	Pre-K			Current			Color Legend	
			No of OT	% of storms OT	Color	No of OT	% of storms OT	Color		
16	NOE 16	NOE1	27.0	0.178		14.0	0.092			
17	NOE 17	NOE2	34.0	0.224		18.0	0.118			
18	NOE 18	NOE2	27.0	0.178		27.0	0.178			
19	NOE 19	NOE3	28.0	0.184		28.0	0.184			
20	NOE 20	NOE3	39.0	0.257		38.0	0.250			
21	NOE 21	NOE3	39.0	0.257		38.0	0.250			
22	NOE 22	NOE3	34.0	0.224		33.0	0.217			
23	NOE 23	NOE4	56.0	0.368		55.0	0.362			
24	NOE 24	NOE4	56.0	0.368		55.0	0.362			
25	NOE 25	NOE4	54.0	0.355		53.0	0.349			
26	NOE 26	NOE4	52.0	0.342		51.0	0.336			
27	NOE 27	NOE4	51.0	0.336		50.0	0.329			
28	NOE 28	NOE4	69.0	0.454		54.0	0.355			
29	NOE 29	NOE5	3.0	0.020		4.0	0.026			
Total NOE			640.0	0.145		594.0	0.135			
30	JE1	JE3	12.0	0.079		13.0	0.086			
31	JE2	JE3	6.0	0.039		7.0	0.046			
32	JE3	JE3	1.0	0.007		2.0	0.013			
33	JE4	JE3	0.0	0.000		0.0	0.000			
34	JE5	JE2	0.0	0.000		0.0	0.000			
35	JE6	JE2	0.0	0.000		0.0	0.000			
37	JE8	JE1	0.0	0.000		0.0	0.000			
38	JE9	JE3	38.0	0.250		38.0	0.250			
Total JE			57.0	0.013		60.0	0.014			
39	SC1	SC1	32.0	0.211		31.0	0.204			
40	SC2	SC1	44.0	0.289		17.0	0.112			
41	SC3	SC1	37.0	0.243		36.0	0.237			
42	SC4	SC2	0.0	0.000		0.0	0.000			
43	SC5	SC2	0.0	0.000		0.0	0.000			
44	SC6	SC2	0.0	0.000		0.0	0.000			
Total SC			113.0	0.124		84.0	0.092			
45	OM1	OM2	0.0	0.000		0.0	0.000			
46	OM2	OM2	0.0	0.000		0.0	0.000			
47	OM3	OM2	0.0	0.000		0.0	0.000			
48	OM4	OM2	0.0	0.000		0.0	0.000			
49	OM5	OM2	0.0	0.000		0.0	0.000			
50	OM6	OM1	0.0	0.000		0.0	0.000			
51	OM7	OM1	0.0	0.000		0.0	0.000			
52	OM8	OM1	0.0	0.000		0.0	0.000			
53	OM9	OM1	0.0	0.000		0.0	0.000			
54	OM10	OM2	3.0	0.020		4.0	0.026			
55	OM11	OM2	0.0	0.000		0.0	0.000			
56	OM12	OM1	0.0	0.000		0.0	0.000			
57	OM13	OM1	0.0	0.000		0.0	0.000			

Table 13-1 Overtopping Rates for Reaches and Sub-basins

Station No.	Reach Name	Sub-basin	Pre-K			Current			Color Legend	
			No of OT	% of storms OT	Color	No of OT	% of storms OT	Color		
58	OM14	OM1	0.0	0.000		0.0	0.000			
59	OM15	OM1	0.0	0.000		0.0	0.000			
60	OM16	OM1	0.0	0.000		0.0	0.000			
61	OM17	OM1	2.0	0.013		3.0	0.020			
62	OM18	OM3	33.0	0.217		32.0	0.211			
63	OM19	OM3	49.0	0.322		20.0	0.132			
64	OM20	OM3	51.0	0.336		50.0	0.329			
65	OM21	OM3	0.0	0.000		0.0	0.000			
66	OM22	OM3	0.0	0.000		0.0	0.000			
67	OM23	OM3	0.0	0.000		0.0	0.000			
68	OM24	OM5	0.0	0.000		0.0	0.000			
69	OM25	OM5	0.0	0.000		0.0	0.000			
70	OM26	OM5	0.0	0.000		0.0	0.000			
71	OM27	OM4	0.0	0.000		0.0	0.000			
36	JE7	OM4	0.0	0.000		0.0	0.000			
Total OM			138.0	0.032		109.0	0.026			
72	SB1	SB1	50.0	0.329		20.0	0.132			
73	SB2	SB2	12.0	0.079		13.0	0.086			
74	SB3	SB2	20.0	0.132		21.0	0.138			
75	SB4	SB5	2.0	0.013		0.0	0.000			
76	SB5	SB4	0.0	0.000		0.0	0.000			
77	SB6	SB4	0.0	0.000		0.0	0.000			
78	SB7	SB3	0.0	0.000		0.0	0.000			
79	SB8	SB1	0.0	0.000		0.0	0.000			
80	SB9	SB1	0.0	0.000		0.0	0.000			
Total SB			84.0	0.061		54.0	0.039			
81	PL1	PL1	140.0	0.921		133.0	0.875			
82	PL2	PL1	48.0	0.316		48.0	0.316			
83	PL3	PL1	0.0	0.000		0.0	0.000			
84	PL4	PL2	39.0	0.257		39.0	0.257			
85	PL5	PL2	2.0	0.013		3.0	0.020			
86	PL6	PL3	136.0	0.895		130.0	0.855			
87	PL7	PL3	0.0	0.000		0.0	0.000			
88	PL8	PL7	31.0	0.204		30.0	0.197			
89	PL9	PL7	3.0	0.020		4.0	0.026			
90	PL10	PL7	20.0	0.132		21.0	0.138			
91	PL11	PL8	21.0	0.138		22.0	0.145			
92	PL12	PL8	1.0	0.007		2.0	0.013			
94	PL13	PL8	44.0	0.289		45.0	0.296			
95	PL14	PL8	2.0	0.013		3.0	0.020			
96	PL15	PL8	0.0	0.000		0.0	0.000			
96	PL16	PL9	13.0	0.086		14.0	0.092			
97	PL17	PL10	22.0	0.145		23.0	0.151			
98	PL18	PL10	26.0	0.171		27.0	0.178			
99	PL19	PL9	44.0	0.289		45.0	0.296			

Table 13-1 Overtopping Rates for Reaches and Sub-basins

Station No.	Reach Name	Sub-basin	Pre-K			Current			Color Legend	
			No of OT	% of storms OT	Color	No of OT	% of storms OT	Color		
100	PL20	PL4	0.0	0.000		0.0	0.000			
101	PL21	PL5	0.0	0.000		0.0	0.000			
102	PL22	PL4	0.0	0.000		0.0	0.000			
103	PL23	PL5	0.0	0.000		0.0	0.000			
104	PL24	PL1	3.0	0.020		4.0	0.026			
105	PL25	PL6	1.0	0.007		2.0	0.013			
106	PL26	PL1	0.0	0.000		0.0	0.000			
107	PL27	PL6	0.0	0.000		0.0	0.000			
Total PL			596.0	0.145		595.0	0.145			
108	CW1	JW1	133.0	0.875		128.0	0.842			
109	CW2	JW2	122.0	0.803		118.0	0.776			
110	CW3	JW2	127.0	0.836		115.0	0.757			
111	CW4	JW2	127.0	0.836		122.0	0.803			
112	CW5	JW2	136.0	0.895		130.0	0.855			
113	CW6	JW2	115.0	0.757		111.0	0.730			
114	CW7	JW3	26.0	0.171		26.0	0.171			
115	CW8	JW1	0.0	0.000		0.0	0.000			
116	WH1	JW3	19.0	0.125		19.0	0.125			
117	WH2	JW3	97.0	0.638		68.0	0.447			
118	WH3	JW3	48.0	0.316		47.0	0.309			
119	WH4	JW3	1.0	0.007		2.0	0.013			
120	WH5	JW3	4.0	0.026		2.0	0.013			
121	WH6	JW3	26.0	0.171		26.0	0.171			
122	WH7	JW3	96.0	0.632		71.0	0.467			
123	WH8	JW3	48.0	0.316		6.0	0.039			
124	WH9	JW3	0.0	0.000		0.0	0.000			
125	WH10	JW3	0.0	0.000		0.0	0.000			
127	HA2	JW4	0.0	0.000		0.0	0.000			
128	HA3	JW4	122.0	0.803		47.0	0.309			
129	HA4	JW4	60.0	0.395		59.0	0.388			
135	HA10	JW4	0.0	0.000		0.0	0.000			
Total JW			1307.0	0.391		1097.0	0.328			
126	HA1	OW2	0.0	0.000		0.0	0.000			
130	HA5	OW2	17.0	0.112		18.0	0.118			
131	HA6	OW1	0.0	0.000		0.0	0.000			
132	HA7	OW1	3.0	0.020		4.0	0.026			
133	HA8	OW1	145.0	0.954		138.0	0.908			
134	HA9	OW2	94.0	0.618		91.0	0.599			
Total OW			259.0	0.284		251.0	0.275			
Total All Basins			3194.00	0.157		2844.00	0.140			

Expected Water Surface Elevations

The results of the risk analysis are presented in terms of the water surface elevations expected in each sub-basin for the “no pumping,” “50% pumping,” and “100% pumping” scenarios in Tables 13-2 to 13-4 and the three exceedence (50, 100 and 500-Year) rates used to construct the inundation maps. Inundation maps are provided in the figures at the end of this Appendix.

Results without pumping – Table 13-2 shows the water elevations within each sub-basin for the Pre-K and Current HPS if the pumping system is considered to not be operating. This pumping scenario most closely approximates the actual performance of the system during hurricanes with intensities and frequencies similar to Katrina. The 50-year water volumes and resulting elevations (Figures 13-2 and 13-3) are primarily hurricane rainfall in the basins, while the 100-year elevations (Figures 13-4, 13-5 and 13-6) show the impact of the large amount of overtopping, levee or wall breaching and open closure structures.

Reductions in water surface elevations expected for the Current HPS were noted in the OM and SB basins, but were largely unchanged in all other basins. SB showed the most reduction in water elevation due to the improvements made in the Current HPS with reductions of 2 to 2.5 feet. All basins fill during 500-year events in both the Pre-Katrina and Current HPS (Figures 13-7, 13-8 and 13-9).

Results with 50% pumping – Table 13-3 shows the water elevations within each sub-basin for the Pre-K and Current HPS if the pumping system is considered to be operating at 50% capacity. The 50-year water inflow volumes and resulting elevations are primarily hurricane rainfall in the basins. This pumping scenario most closely approximates the possible performance of the system during a 50-year event for both Pre-K and Current HPS when the pumps would only have to evacuate hurricane rains, which would be expected to be less than the design rainfall for the pumps (about a 10-year tropical storm). Therefore, the differences in water elevations between the no pumping and 50% pumping scenarios, for both the Pre-K and Current HPS, are small for the 50-year event.

Results with 100% pumping – Table 13-4 shows the water elevations within each sub-basin for the Pre-K and Current HPS if the pumping system is considered to be operating at 100% of capacity. This scenario is presented for comparison purposes with the other scenarios only since the New Orleans pumping system, or any other pumping system, cannot realistically be expected to perform at this level. The significant impact is the reduction of interior flooding. Water elevations could be reduced by as much as 4 feet in show areas for the 50 year event, while the 100-Year show the impact of the large amount of overtopping, levee or wall breaching and open closure structures. During hurricanes with intensities and frequencies similar to Katrina, the Pre-K pumping system would be expected to perform as shown, as it did during Katrina, and not be able to handle flooding from overtopping or breaching inflows. Reductions in water surface elevations expected for the Current HPS were noted in the OM and SB basins, but were largely unchanged in all other basins. All basins fill during 500-year events in both the Pre-Katrina and Current HPS.

**Table 13-2 Risk Analysis Results Without Pumping
Elevations NAVD88 2004.65**

Sub-basin	50-year elevations		100-year elevations		500-year elevations	
	Pre-k	Current	Pre-k	Current	Pre-k	Current
OW1	-1	-1	1	1	6	6
OW2	-3	-3	4	4	8	8
NOE1	0	0	2	1	12	13
NOE2	-4	-4	2	2	12	13
NOE3	-4	-4	2	2	12	13
NOE4	-1	-1	4	4	12	13
NOE5	-8	-8	-1	-1	12	13
OM1	-5	-5	3	3	14	14
OM2	-5	-5	3	-2	14	14
OM3	-1	-1	3	3	14	14
OM4	-1	-1	3	-2	14	14
OM5	-1	-1	3	2	14	14
SB1	-1	-1	12	10	14	14
SB2	1	1	12	10	14	14
SB3	0	0	12	10	14	14
SB4	2	2	12	10	14	14
SB5	3	3	12	10	14	14
JE1	3	3	4	4	14	14
JE2	-4	-4	-3	-3	14	14
JE3	-5	-5	-3	-3	1	14
JW1	0	0	4	4	8	8
JW2	-4	-4	4	4	8	8
JW3	-2	-2	4	4	8	8
JW4	-5	-5	4	4	8	8
PL11	-2	-2	0	-1	6	9
SC1	2	2	4	5	10	10
SC2	4	4	5	5	10	10

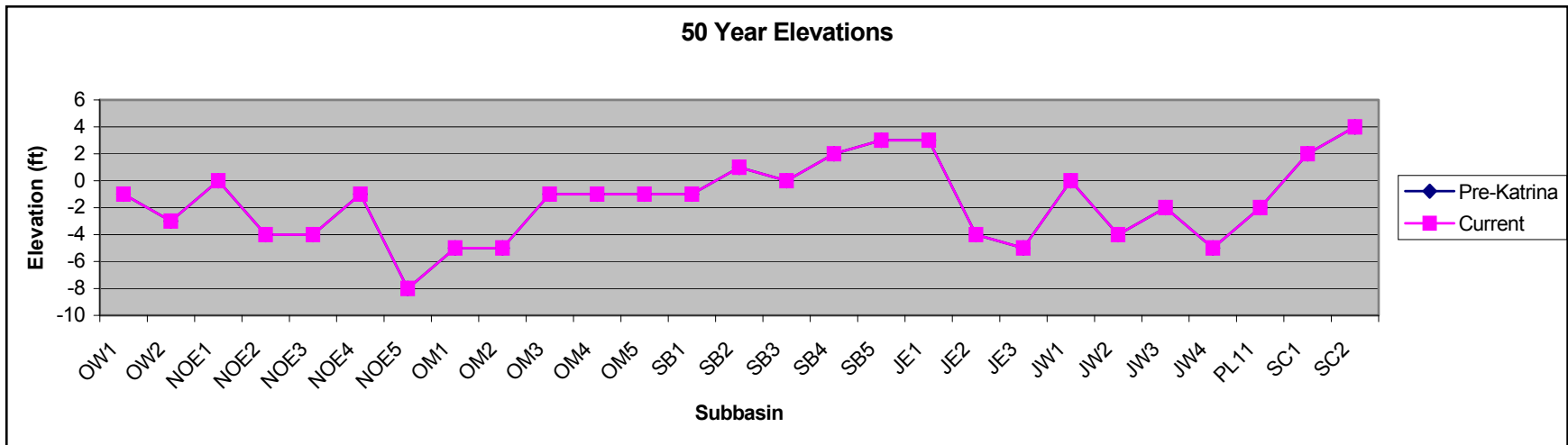


Figure 13-1 – 50-Year Inundation Elevations for Pre-K and Current HPS

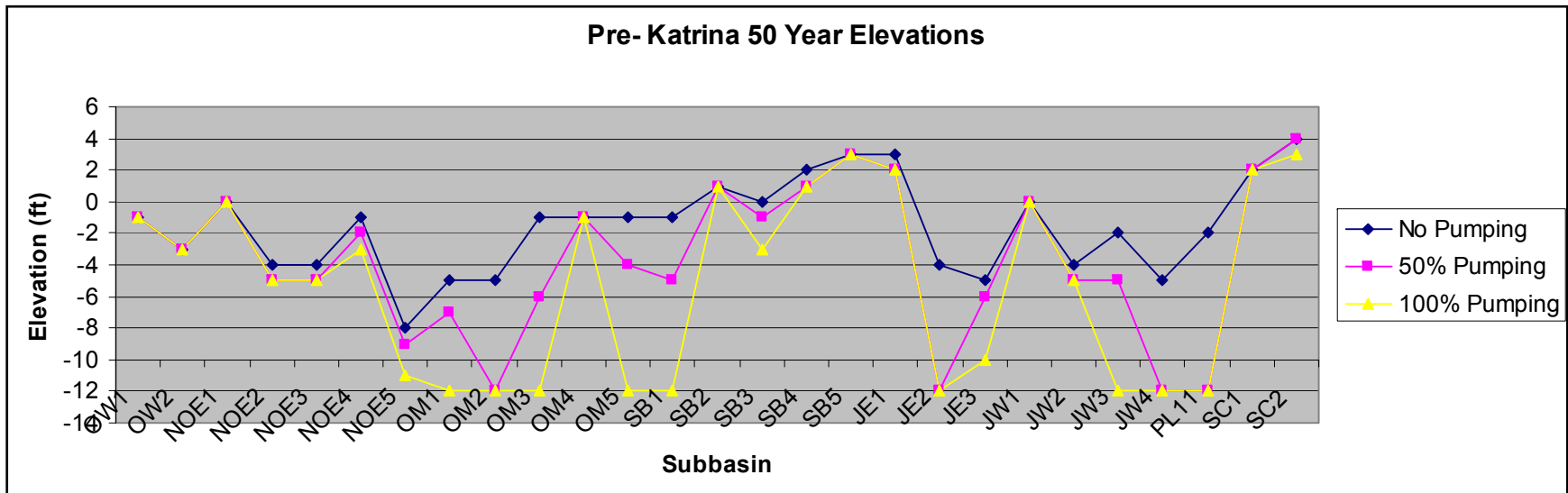


Figure 13-2 – 50-Year Inundation Elevations for Pre-K HPS with Pumping Scenarios

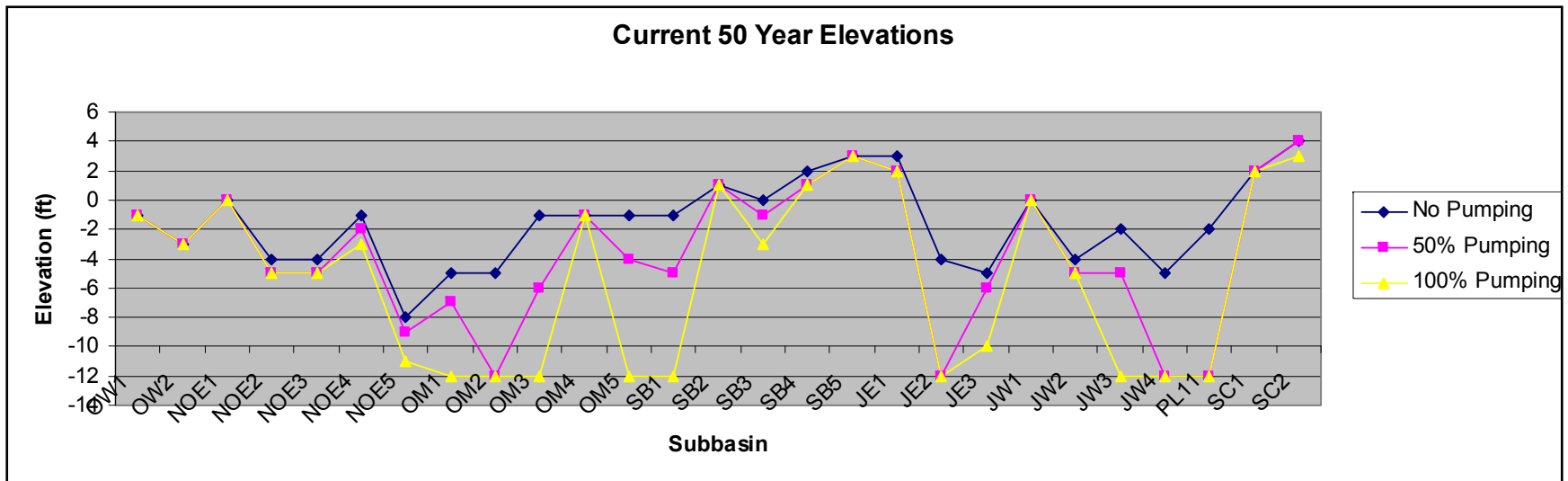


Figure 13-3 – 50-Year Inundation Elevations for Current HPS with Pumping Scenarios

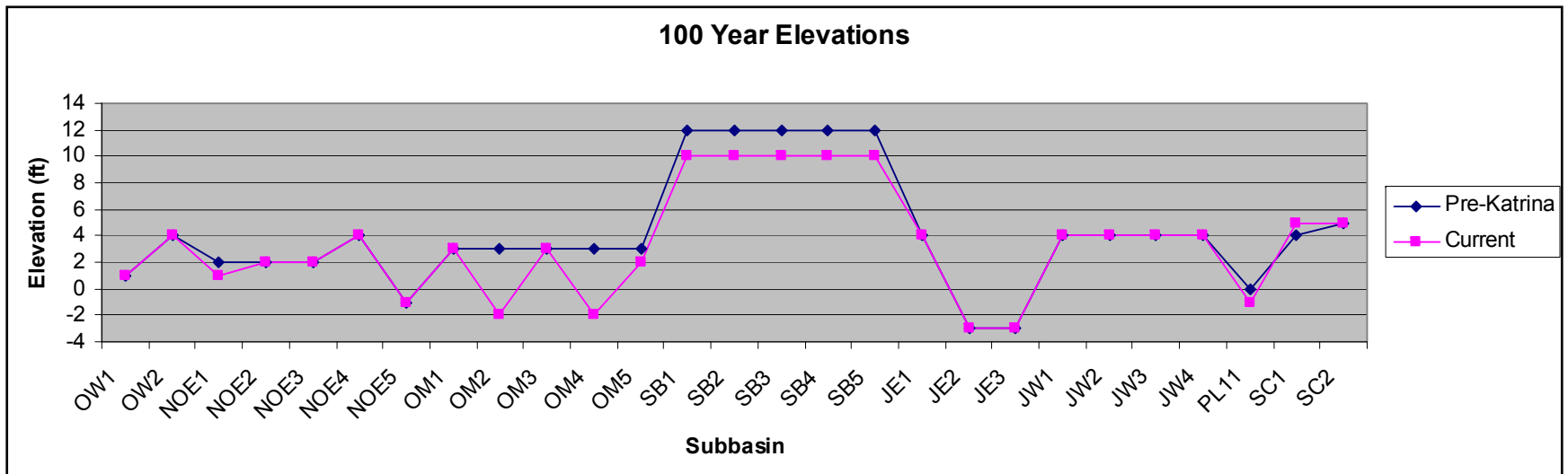


Figure 13-4 – 100-Year Inundation Elevations for Pre-K and Current HPS

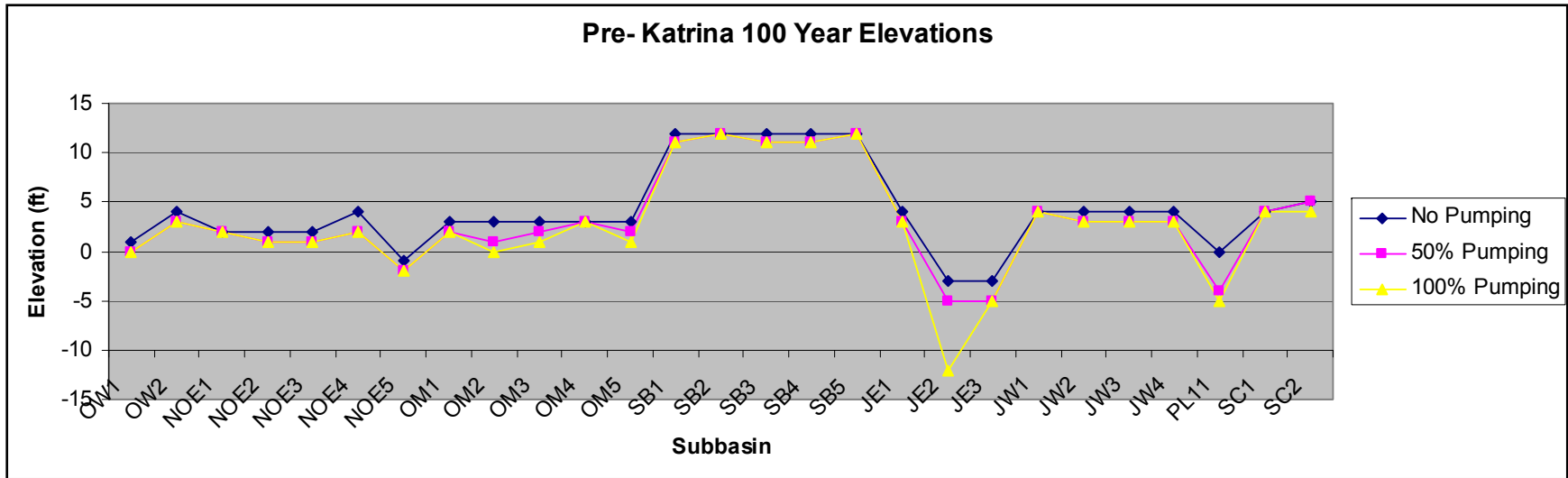


Figure 13-5 – 100-Year Inundation Elevations for Pre-K HPS with Pumping Scenarios

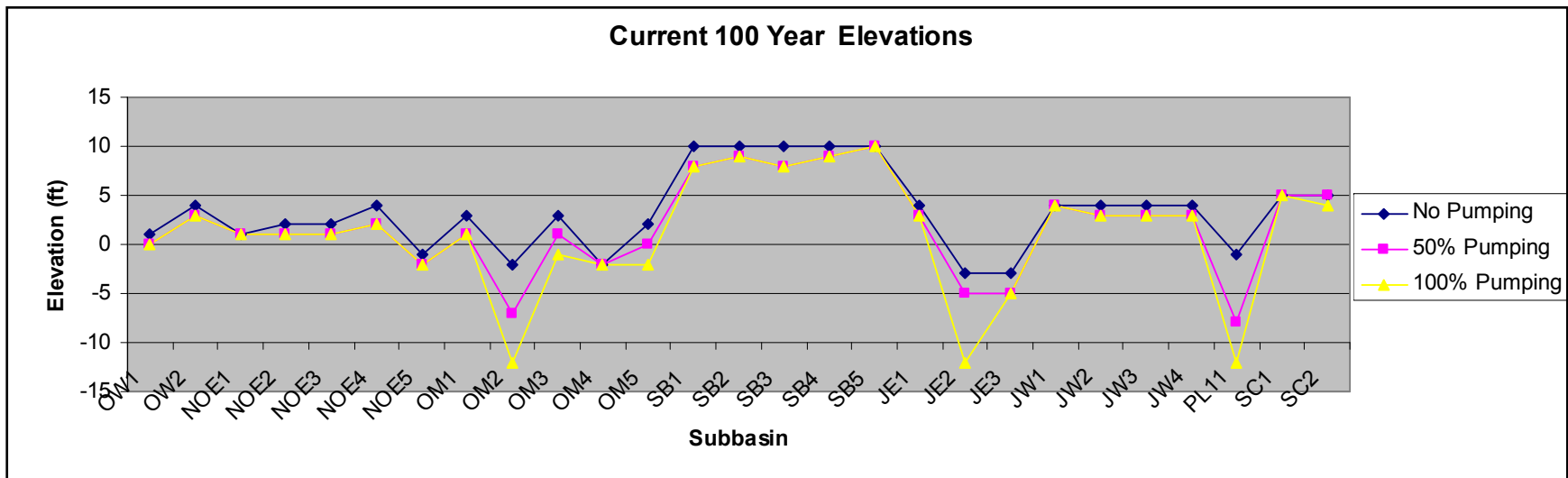


Figure 13-6 – 100-Year Inundation Elevations for Current HPS with Pumping Scenarios

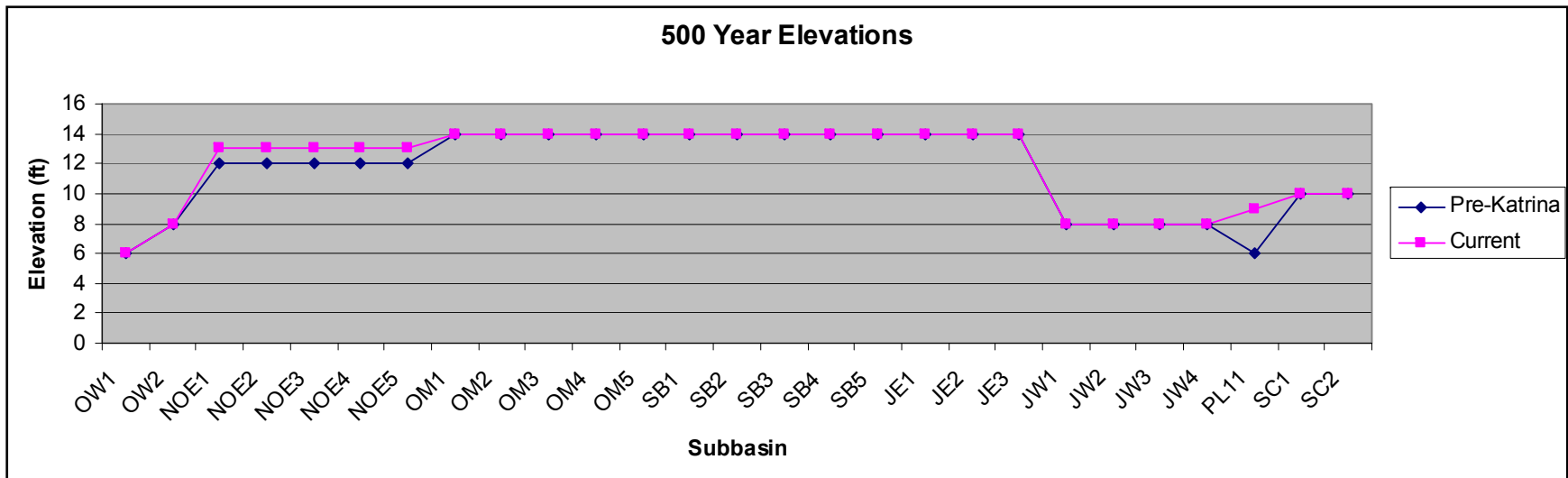


Figure 13-7 – 500-Year Inundation Elevations for Pre-K and Current HPS

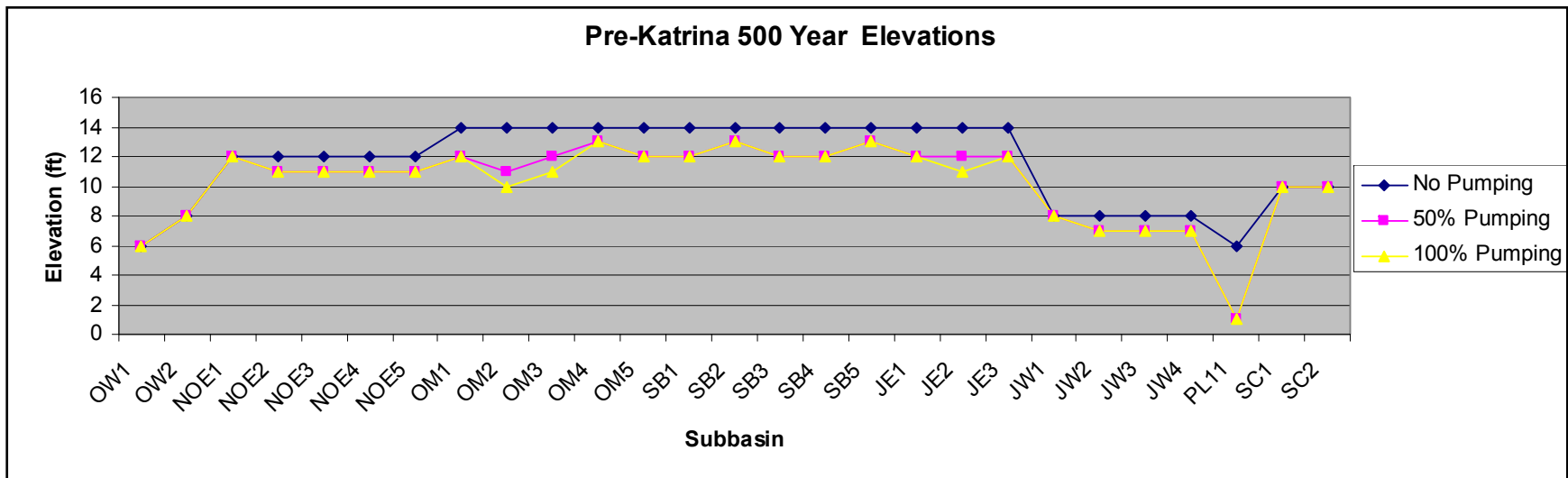


Figure 13-8 – 500-Year Inundation Elevations for Pre-K with Pumping Scenarios

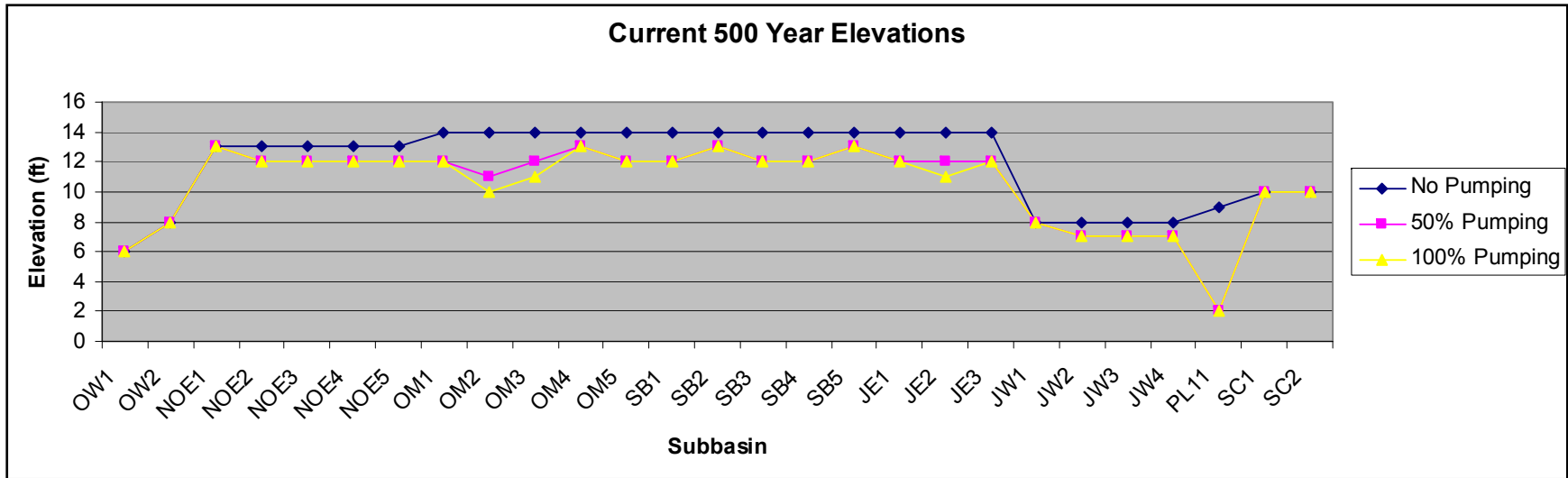


Figure 13-9 – 500-Year Inundation Elevations for Current HPS with Pumping Scenarios

**Table 13-3 Risk Analysis Results With 50% Pumping
Elevations NAVD88 2004.65**

Sub-basin	50-Year elevations		100-Year elevations		500-Year elevations	
	Pre-k	Current	Pre-k	Current	Pre-k	Current
OW1	-1	-1	0	0	6	6
OW2	-3	-3	3	3	8	8
NOE1	0	0	2	1	12	13
NOE2	-5	-5	1	1	11	12
NOE3	-5	-5	1	1	11	12
NOE4	-2	-2	2	2	11	12
NOE5	-9	-9	-2	-2	11	12
OM1	-7	-7	2	1	12	12
OM2	-12	-12	1	-7	11	11
OM3	-6	-6	2	1	12	12
OM4	-1	-1	3	-2	13	13
OM5	-4	-4	2	0	12	12
SB1	-5	-5	11	8	12	12
SB2	1	1	12	9	13	13
SB3	-1	-1	11	8	12	12
SB4	1	1	11	9	12	12
SB5	3	3	12	10	13	13
JE1	2	2	3	3	12	12
JE2	-12	-12	-5	-5	12	12
JE3	-6	-6	-5	-5	12	12
JW1	0	0	4	4	8	8
JW2	-5	-5	3	3	7	7
JW3	-5	-5	3	3	7	7
JW4	-12	-12	3	3	7	7
PL11	-12	-12	-4	-8	1	2
SC1	2	2	4	5	10	10
SC2	4	4	5	5	10	10

Table 13-4 Risk Analysis Results With 100% Pumping Elevations NAVD88 2004.65						
Sub-basin	50-Year elevations		100-Year elevations		500-Year elevations	
	Pre-k	Current	Pre-k	Current	Pre-k	Current
OW1	-1	-1	0	0	6	6
OW2	-3	-3	3	3	8	8
NOE1	0	0	2	1	12	13
NOE2	-5	-5	1	1	11	12
NOE3	-5	-5	1	1	11	12
NOE4	-3	-3	2	2	11	12
NOE5	-11	-11	-2	-2	11	12
OM1	-12	-12	2	1	12	12
OM2	-12	-12	0	-12	10	10
OM3	-12	-12	1	-1	11	11
OM4	-1	-1	3	-2	13	13
OM5	-12	-12	1	-2	12	12
SB1	-12	-12	11	8	12	12
SB2	1	1	12	9	13	13
SB3	-3	-3	11	8	12	12
SB4	1	1	11	9	12	12
SB5	3	3	12	10	13	13
JE1	2	2	3	3	12	12
JE2	-12	-12	-12	-12	11	11
JE3	-10	-10	-5	-5	12	12
JW1	0	0	4	4	8	8
JW2	-5	-5	3	3	7	7
JW3	-12	-12	3	3	7	7
JW4	-12	-12	3	3	7	7
PL11	-12	-12	-5	-12	1	2
SC1	2	2	4	5	10	10
SC2	3	3	4	4	9	9

Human and Economic Risks

The water elevations and exceedence rate presented in the foregoing sections were combined with the stage-damage and stage-fatality relationships developed by the IPET Consequence Team to determine the risks to life and property under the scenarios studied. Reference is made to the IPET Volume 7 for a complete explanation of the analyses conducted in support of loss relationships used herein.

Economic Risks - The economic consequences considered by the Consequence Team included: 1) direct property damages, and 2) indirect economic impacts on local and regional economies. Direct property damages were monetary damages to property at risk such as residential, commercial, industrial, public buildings, vehicles and infrastructure. For the risk scenarios, both pre- and post-Katrina stage-damage functions for properties, are based on base

property conditions that existed prior to Katrina. Only the direct economic damages were used in the risk assessment.

The potential economic damages for the Pre-K and Current HPS without pumping (Table 13-5) are equal at about \$11.3 Billion for the 50-Year event. The 100-Year potential damages are \$42.5 Billion for the Pre-K HPS and are reduced by more than \$2 Billion to about \$40.1 Billion for the Current HPS. For the 500-Year event, the sub-basins in both scenarios are expected to fill so the potential damages are equal at about \$73.3 Billion.

The potential economic damages for the Pre-K and Current HPS with 50% pumping (Table 13-6) are equal at about \$3.1 Billion for the 50-Year event. This represents a significant \$8 Billion reduction from the no pumping scenario and demonstrates the importance of maintaining pumping operations during the more frequent events. The 100-Year potential damages are \$34.1 Billion for the Pre-K HPS and are reduced by almost \$10 Billion to about \$30.3 Billion for the Current HPS, again demonstrating the effectiveness of the pumping system at reducing potential damages. For the 500-Year event, the sub-basins in both scenarios are expected to fill so the potential damages are equal at about \$72.0 Billion.

The potential economic damages for the Pre-K and Current HPS with 100% pumping (Table 13-7) are equal at about \$2.4 Billion for the 50-Year event. The 100-Year potential damages are \$32.5 Billion for the Pre-K HPS and are reduced to about \$28.7 Billion for the Current HPS. For the 500-Year event, the sub-basins in both scenarios are expected to fill so the potential damages are equal at about \$72.0 Billion. As may be expected, these values are all less than for the 50% pumping scenarios, however, the 100 % pumping scenario is presented for comparison purpose only to show how increased efficiency of the pumping system can reduce damages. Note that the most significant reductions were attained by the 50% pumping scenario.

Human Risks - The Consequence Team also examined the human health and safety consequences for a variety of event scenarios. For the actual Katrina scenario, the effects considered include recorded mortality as well as actual and potential morbidity, including both physical and mental health impacts. For the risk scenarios, both pre- and post-Katrina stage-fatality functions were developed and provided to the Risk Team for modeling residual risks in greater New Orleans. The post-Katrina stage-fatality functions, which are based on population and structure conditions that existed prior to Katrina. The mortality risk estimates do NOT consider the effects of evacuation on the rate of fatalities within the population at risk. Therefore, the fatalities shown in Tables 13-8, 13-9 and 13-10 are potential fatalities only and are not intended to be predictions of actual loss of life.

The potential fatalities for the Pre-K and Current HPS without pumping are equal at about 492 for the 50-Year event. The 100-Year potential fatalities are 3,708 for the Pre-K HPS and are reduced to about 2,388 for the Current HPS. For the 500-Year event, the potential fatalities are 40,877 for the Pre-K HPS and increase to 42,665 for the Current HPS. The increase in potential fatalities for the Current HPS is due to higher levee elevations in some sub-basins, which allow more water to collect in the basins.

The potential fatalities for the Pre-K and Current HPS with 50% pumping are equal at about 75 for the 50-Year event. This represents a reduction of more than 400 potential fatalities from

the no pumping scenario and demonstrates the importance of maintaining pumping operations during the more frequent events. The 100-Year potential fatalities are 2,706 for the Pre-K HPS and are reduced to about 1,237 for the Current HPS, again demonstrating the effectiveness of the pumping system at reducing potential damages by showing a reduction of 1,000 in potential fatalities. For the 500-Year event, the potential fatalities are 29,100 for the Pre-K HPS and increase to 30,600 for the Current HPS. The increase in potential fatalities for the Current HPS is due to higher levee elevations in some sub-basins, which allow more water to collect in the basins.

The potential fatalities for the Pre-K and Current HPS with 100% pumping are equal at about 35 for the 50-Year event. The 100-Year potential fatalities are 2,526 for the Pre-K HPS and are reduced to about 982 for the Current HPS. For the 500-Year event, the potential fatalities are 27,700 for the Pre-K HPS and increase to 29,200 for the Current HPS. The increase in potential fatalities for the Current HPS is due to higher levee elevations in some sub-basins, which allow more water to collect in the basins. As was shown in the economic damages, the potential fatalities in the 100% pumping scenario are all less than for the 50% pumping scenarios, but the most significant reductions were attained by the 50% pumping scenario.

Conclusions

The experience of Katrina proved that the risk to life and property in the New Orleans area was high and the results of the risk analysis quantifies the extent of that risk to the Pre-Katrina economy and population. The actual direct damages incurred due to the hurricane exceeded \$28 Billion and the loss of life was more than 700. The corresponding potential damages and life loss values obtained by the risk analysis are considerably higher, which points to the severity of the risk and attests to the effectiveness of the evacuation prior to the hurricane in reducing the loss of life. Examination of the three pumping scenarios shows the importance of the pumping system in reducing damages during the more frequent events, but also shows that the system is not capable of handling large inflow water volumes from overtopping or breaching during extreme events.

While the HPS has been repaired and improved dramatically over the Pre- Katrina HPS, the risk associated with the Current HPS to the area is still considered to be high for extreme events if the pre-Katrina potential consequences are used in the analysis. The risks to life and property would be expected to be reduced if existing demographics and redevelopment values were used, however the reduction would be due entirely to the reduced consequences of system failure and not due to the improvements to the system. In any case, the human and economic risks to New Orleans would be considered high during extreme events.

Table 13-5 – Potential Damages – No Pumping						
Sub-basin	Potential Damages Without Pumping					
	In Millions of 2005 Dollars					
	50-Year elevations		100-Year elevations		500-Year elevations	
	Pre-k	Current	Pre-k	Current	Pre-k	Current
OW1	23	23	34	34	170	170
OW2	412	412	2,305	2,305	3,105	3,105
NOE1	0	0	8	6	12	12
NOE2	19	19	123	123	143	143
NOE3	8	8	510	510	668	671
NOE4	0	0	42	42	61	62
NOE5	43	43	4,561	4,561	6,022	6,026
OM1	402	402	2,209	2,110	2,710	2,710
OM2	348	348	1,573	962	1,942	1,942
OM3	376	376	1,709	1,537	2,997	2,997
OM4	68	68	420	364	1,104	1,104
OM5	785	785	3,721	2,513	9,596	9,596
SB1	196	196	2,617	2,511	2,658	2,666
SB2	-	-	25	24	26	26
SB3	71	71	2,456	2,244	2,496	2,502
SB4	0	0	497	465	507	511
SB5	2	2	43	41	44	44
JE1	420	420	1,093	1,093	5,617	5,617
JE2	471	471	2,190	2,190	6,270	6,270
JE3	515	515	4,255	4,255	12,078	12,078
JW1	0	0	230	230	542	542
JW2	5	5	393	393	426	426
JW3	122	122	3,660	3,660	5,625	5,625
JW4	23	23	5,551	5,551	6,437	6,437
PL11	33	33	152	90	481	578
SC1	-	-	113	117	132	132
SC2	390	390	485	485	1,355	1,355
Totals	4,732	4,732	40,976	38,417	73,224	73,347

Table 13-6 – Potential Damages – 50% Pumping						
Sub-basin	Potential Damages With 50% Pumping					
	In Millions of 2005 Dollars					
	50-Year elevations		100-Year elevations		500-Year elevations	
	Pre-k	Current	Pre-k	Current	Pre-k	Current
OW1	23	23	28	28	170	170
OW2	412	412	2,205	2,205	3,105	3,105
NOE1	0	0	8	6	12	12
NOE2	1	1	121	121	143	143
NOE3	0	0	416	416	667	668
NOE4	0	0	33	33	60	61
NOE5	5	5	4,121	4,121	6,007	6,022
OM1	8	8	2,012	1,864	2,689	2,689
OM2	-	-	1,377	2	1,922	1,922
OM3	1	1	1,365	1,031	2,953	2,953
OM4	68	68	420	308	1,096	1,096
OM5	7	7	2,860	1,483	9,306	9,306
SB1	-	-	2,582	2,403	2,617	2,617
SB2	-	-	25	24	25	25
SB3	4	4	2,393	2,077	2,456	2,456
SB4	-	-	491	439	497	497
SB5	2	2	43	41	44	44
JE1	218	218	420	420	5,122	5,122
JE2	-	-	52	52	6,243	6,243
JE3	116	116	515	515	12,062	12,062
JW1	0	0	230	230	542	542
JW2	1	1	383	383	416	416
JW3	0	0	2,750	2,750	5,466	5,466
JW4	-	-	5,236	5,236	6,272	6,272
PL11	-	-	0	-	217	245
SC1	-	-	19	19	121	121
SC2	1,151	1,151	1,355	1,355	1,787	1,787
Totals	2,017	2,017	31,460	27,563	72,016	72,061

Table 13-7 – Potential Damages – 50% Pumping						
Sub-basin	Potential Damages With 100% Pumping					
	In Millions of 2005 Dollars					
	50-Year elevations		100-Year elevations		500-Year elevations	
	Pre-k	Current	Pre-k	Current	Pre-k	Current
OW1	23	23	28	28	170	170
OW2	412	412	2,205	2,205	3,105	3,105
NOE1	0	0	8	6	12	12
NOE2	1	1	121	121	143	143
NOE3	0	0	416	416	667	668
NOE4	0	0	33	33	60	61
NOE5	0	0	4,121	4,121	6,007	6,022
OM1	-	-	2,012	1,864	2,689	2,689
OM2	-	-	1,261	-	1,910	1,910
OM3	-	-	1,031	376	2,910	2,910
OM4	68	68	420	308	1,096	1,096
OM5	-	-	2,167	200	9,306	9,306
SB1	-	-	2,582	2,403	2,617	2,617
SB2	-	-	25	24	25	25
SB3	0	0	2,393	2,077	2,456	2,456
SB4	-	-	491	439	497	497
SB5	2	2	43	41	44	44
JE1	218	218	420	420	5,122	5,122
JE2	-	-	-	-	6,216	6,216
JE3	0	0	515	515	12,062	12,062
JW1	0	0	230	230	542	542
JW2	1	1	383	383	416	416
JW3	-	-	2,750	2,750	5,466	5,466
JW4	-	-	5,236	5,236	6,272	6,272
PL11	-	-	-	-	217	245
SC1	-	-	19	19	121	121
SC2	1,151	1,151	1,355	1,355	1,787	1,787
Totals	1,876	1,876	30,266	25,571	71,934	71,979

Table 13-8 – Potential Fatalities – No Pumping						
Sub-basin	Risk Analysis Results Without Pumping					
	50-Year elevations		100-Year elevations		500-Year elevations	
	Pre-k	Current	Pre-k	Current	Pre-k	Current
OW1	0	0	0	0	1	1
OW2	6	6	76	76	420	420
NOE1	0	0	0	0	0	0
NOE2	0	0	1	1	91	154
NOE3	0	0	13	13	298	524
NOE4	0	0	0	0	2	2
NOE5	4	4	63	63	6,528	7,945
OM1	2	2	80	67	1,923	1,923
OM2	237	237	1,289	315	3,100	3,100
OM3	10	10	61	47	1,823	1,823
OM4	8	8	35	27	484	484
OM5	21	21	70	49	2,825	2,825
SB1	-	-	915	764	915	915
SB2	-	-	-	-	-	-
SB3	-	-	561	455	616	629
SB4	0	0	82	49	98	102
SB5	0	0	3	3	3	3
JE1	0	0	0	0	3	3
JE2	37	37	50	50	5,367	5,367
JE3	31	31	73	73	15,271	15,271
JW1	4	4	31	31	63	63
JW2	0	0	6	6	40	40
JW3	1	1	42	42	195	195
JW4	1	1	132	132	607	607
PL11	28	28	33	31	180	236
SC1	-	-	-	-	1	1
SC2	1	1	1	1	23	23
Totals	391	391	3,619	2,296	40,877	42,655

Table 13-9 – Potential Fatalities – 50% Pumping						
Sub-basin	Risk Analysis Results with 50% pumping					
	50-Year elevations		100-Year elevations		500-Year elevations	
	Pre-k	Current	Pre-k	Current	Pre-k	Current
OW1	0	0	0	0	1	1
OW2	6	6	52	52	420	420
NOE1	0	0	0	0	0	0
NOE2	0	0	1	1	56	91
NOE3	-	-	9	9	228	298
NOE4	0	0	0	0	2	2
NOE5	2	2	45	45	5,111	6,528
OM1	1	1	54	29	1,241	1,241
OM2	-	-	586	113	2,683	2,683
OM3	-	-	32	24	1,055	1,055
OM4	8	8	35	20	438	438
OM5	2	2	56	31	2,075	2,075
SB1	-	-	901	393	915	915
SB2	-	-	-	-	-	-
SB3	-	-	561	136	561	561
SB4	0	0	66	34	82	82
SB5	0	0	3	3	3	3
JE1	-	-	0	0	3	3
JE2	-	-	23	23	3,716	3,716
JE3	9	9	31	31	9,678	9,678
JW1	4	4	31	31	63	63
JW2	0	0	5	5	24	24
JW3	0	0	33	33	138	138
JW4	-	-	83	83	418	418
PL11	0	0	16	1	37	41
SC1	-	-	-	-	-	-
SC2	10	10	23	23	152	152
Totals	42	42	2,647	1,121	29,099	30,625

Table 13-10 – Potential Fatalities – 100% Pumping						
Sub-basin	Risk Analysis Results with 100% pumping					
	50-Year elevations		100-Year elevations		500-Year elevations	
	Pre-k	Current	Pre-k	Current	Pre-k	Current
OW1	0	0	0	0	1	1
OW2	6	6	52	52	420	420
NOE1	0	0	0	0	0	0
NOE2	0	0	1	1	56	91
NOE3	-	-	9	9	228	298
NOE4	0	0	0	0	2	2
NOE5	-	-	45	45	5,111	6,528
OM1	-	-	54	29	1,241	1,241
OM2	-	-	472	-	2,560	2,560
OM3	-	-	24	10	888	888
OM4	8	8	35	20	438	438
OM5	-	-	41	12	2,075	2,075
SB1	-	-	901	393	915	915
SB2	-	-	-	-	-	-
SB3	-	-	561	136	561	561
SB4	0	0	66	34	82	82
SB5	0	0	3	3	3	3
JE1	-	-	0	0	3	3
JE2	-	-	-	-	2,584	2,584
JE3	-	-	31	31	9,678	9,678
JW1	4	4	31	31	63	63
JW2	0	0	5	5	24	24
JW3	-	-	33	33	138	138
JW4	-	-	83	83	418	418
PL11	0	0	10	0	37	41
SC1	-	-	-	-	-	-
SC2	10	10	23	23	152	152
Totals	28	28	2,481	951	27,678	29,204

Inundation Maps



Figure 13-10. Pre-K Overtopping Rates

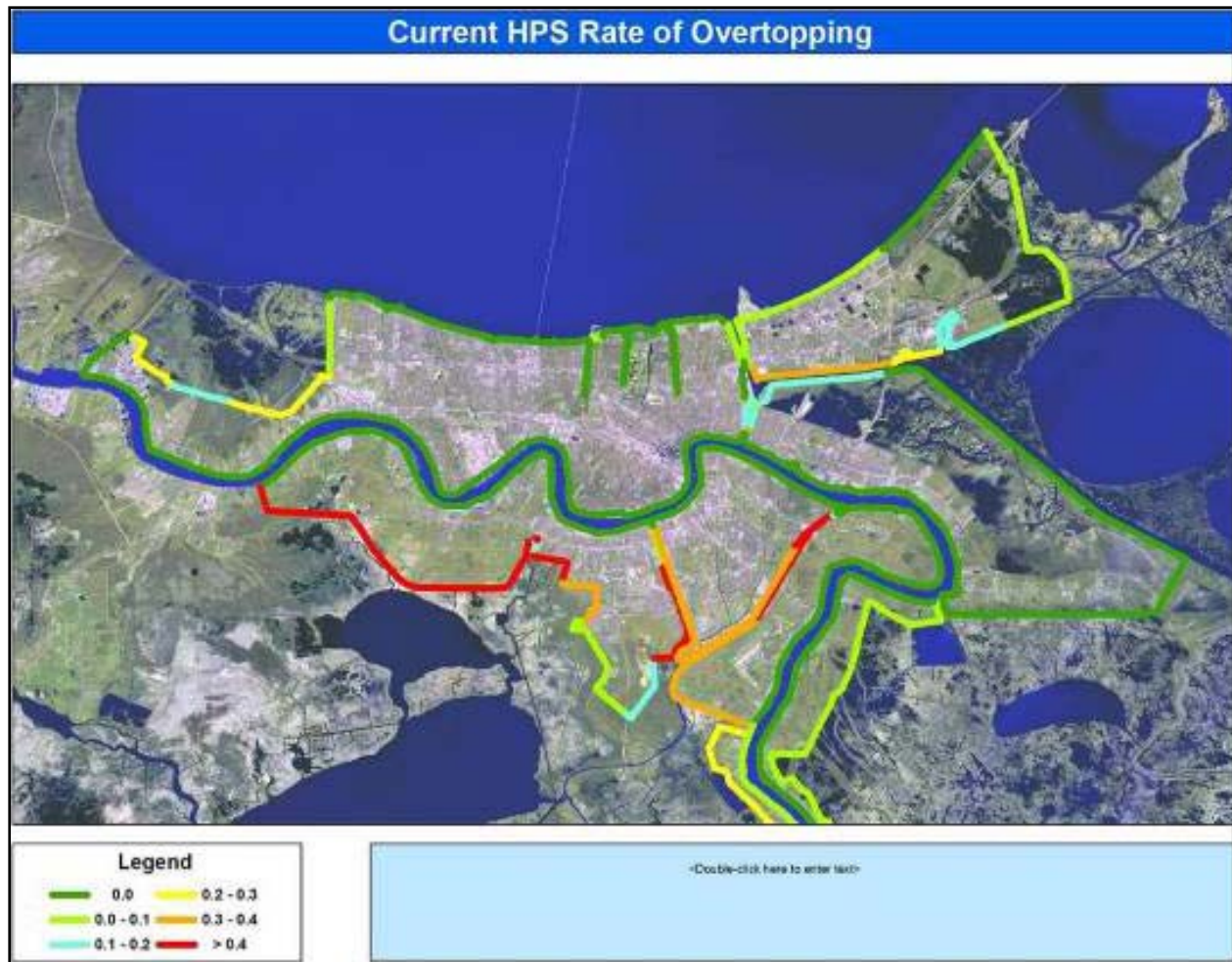


Figure 13-11 Current Overtopping Rates

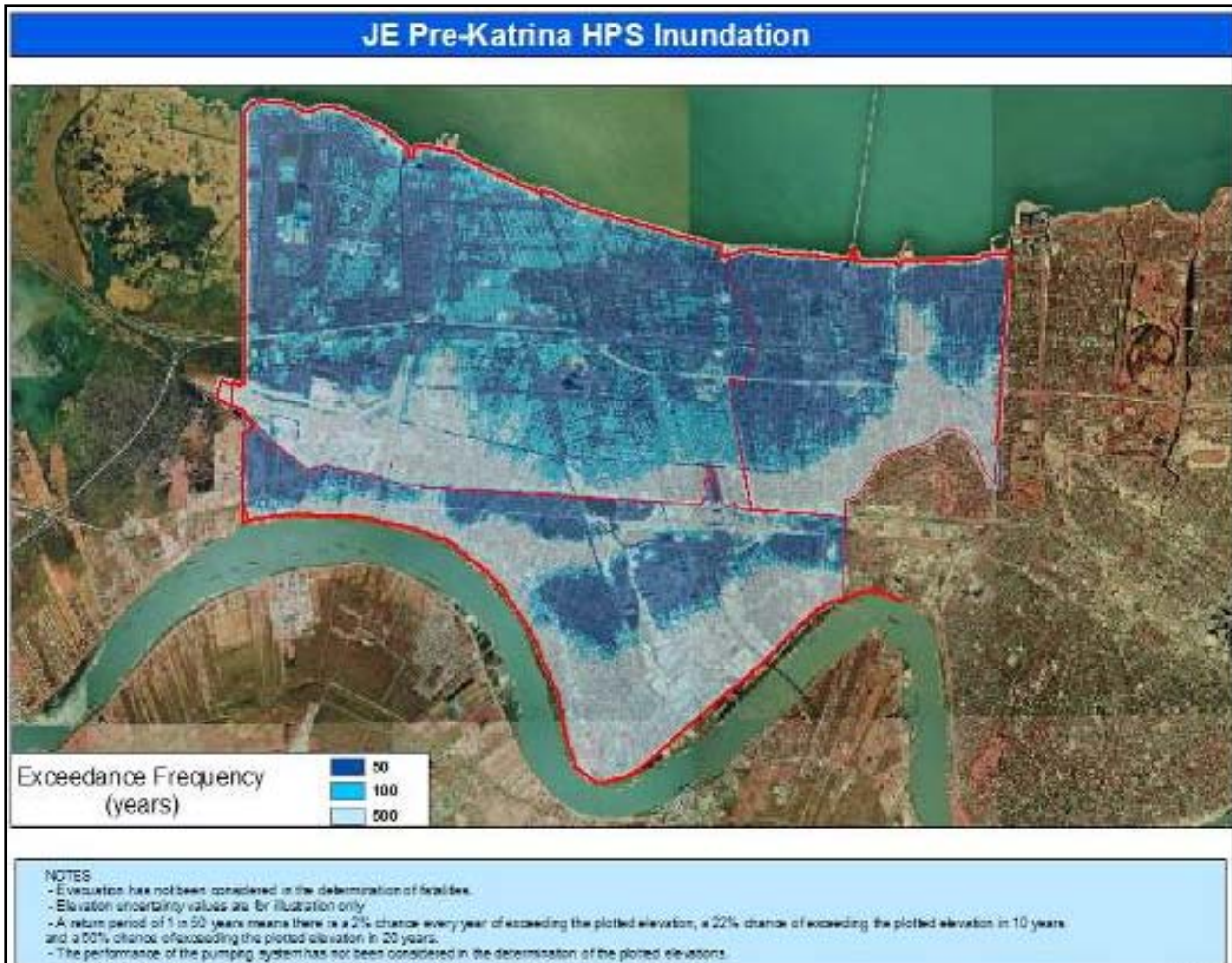


Figure 13-12 – Jefferson East Bank – Pre-Katrina Inundation Risk – No Pumping

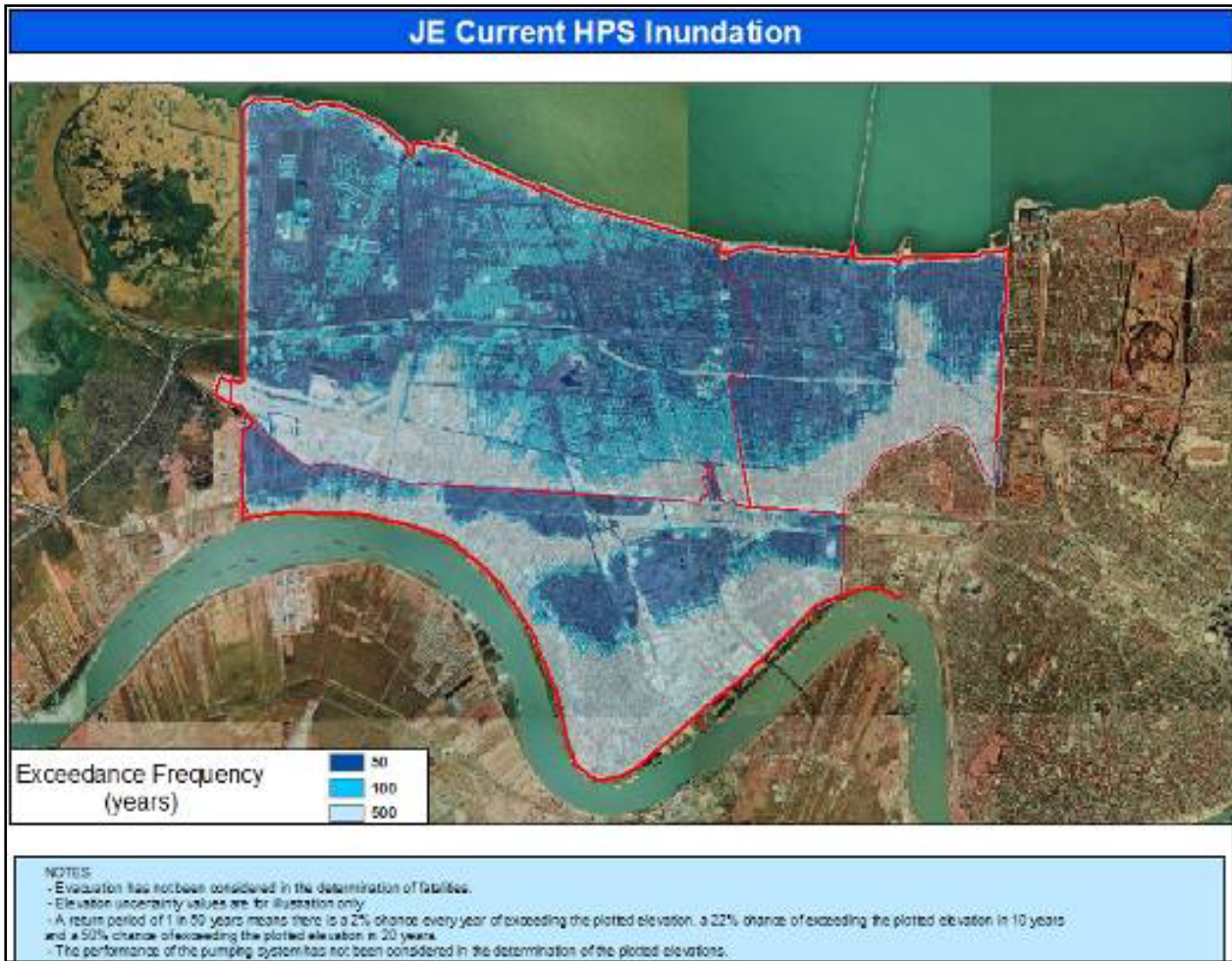


Figure 13-13 – Jefferson East Bank – Current Inundation Risk – No Pumping

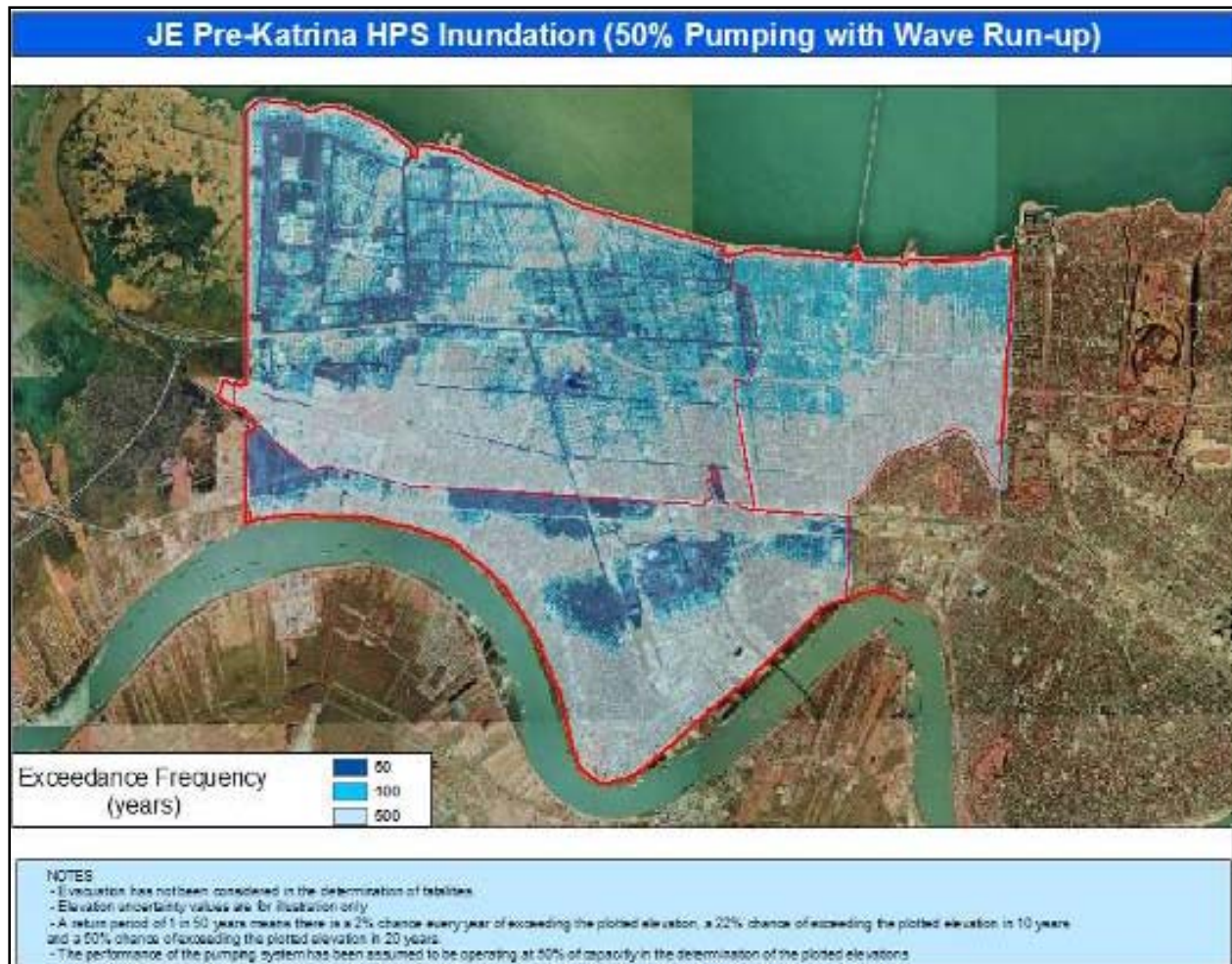


Figure 13-14 – Jefferson East Bank – Pre-Katrina Inundation Risk – 50% Pumping

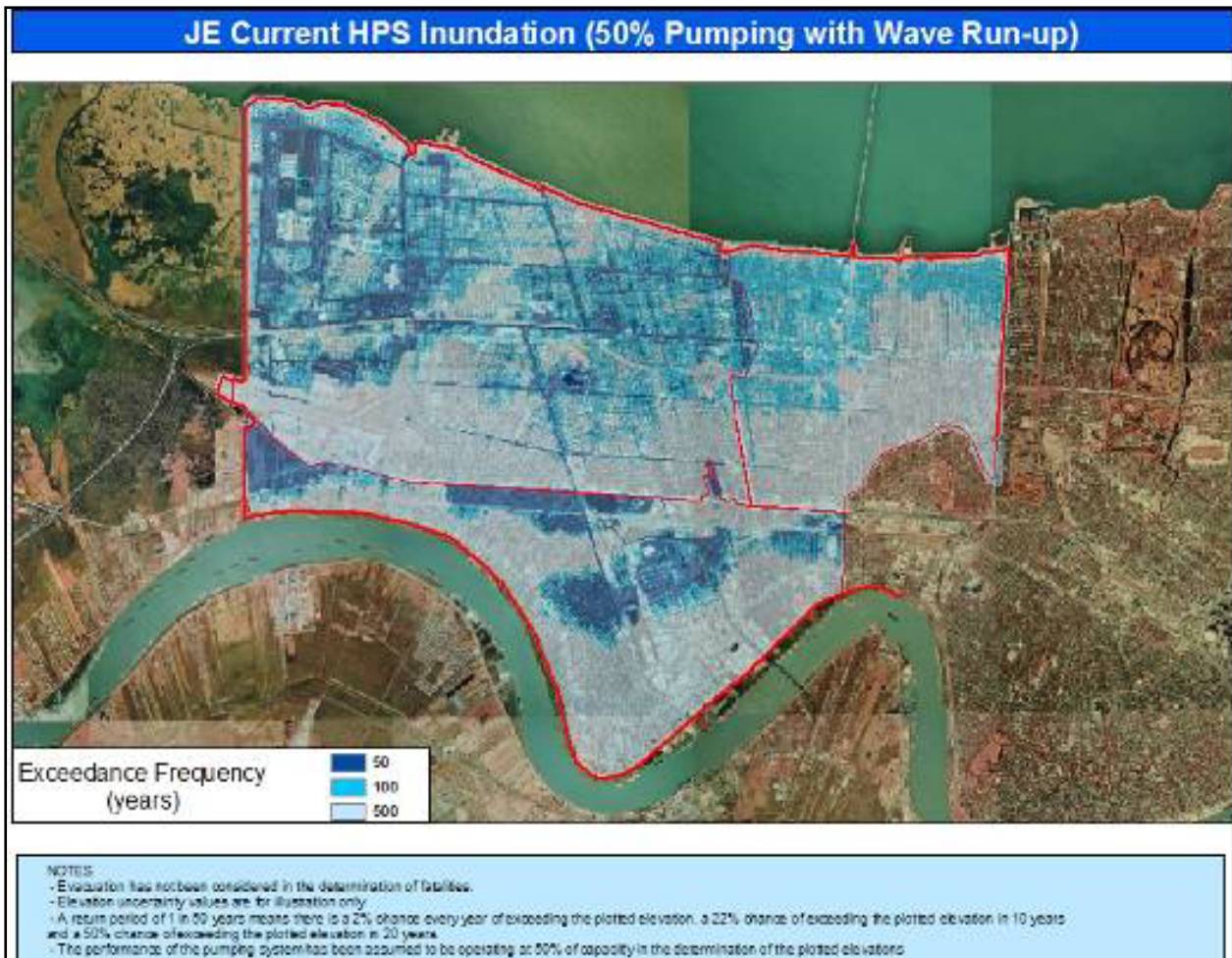


Figure 13-15 – Jefferson East Bank – Current Inundation Risk – 50% Pumping

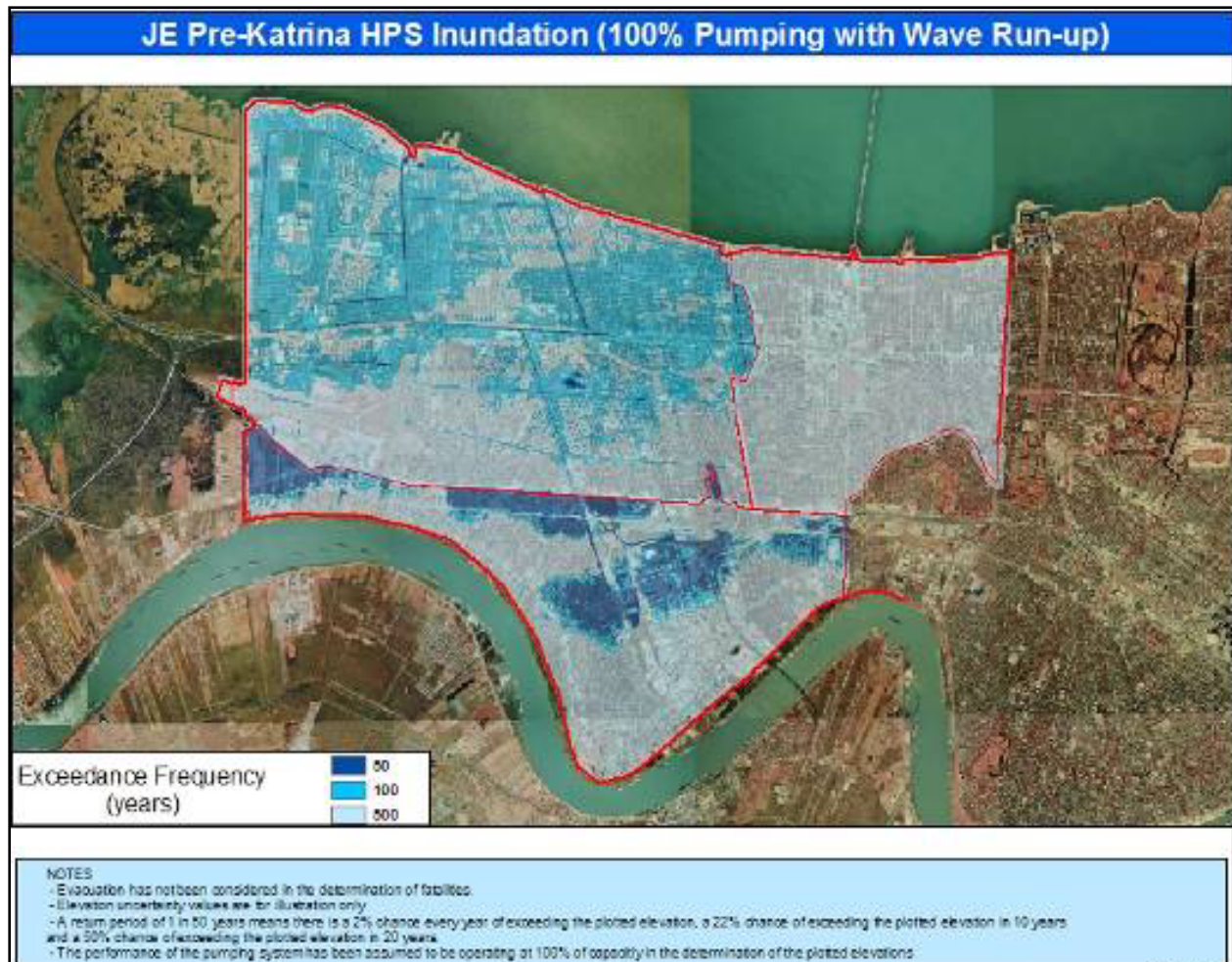


Figure 13-16 – Jefferson East Bank – Pre-Katrina Inundation Risk – 100% Pumping

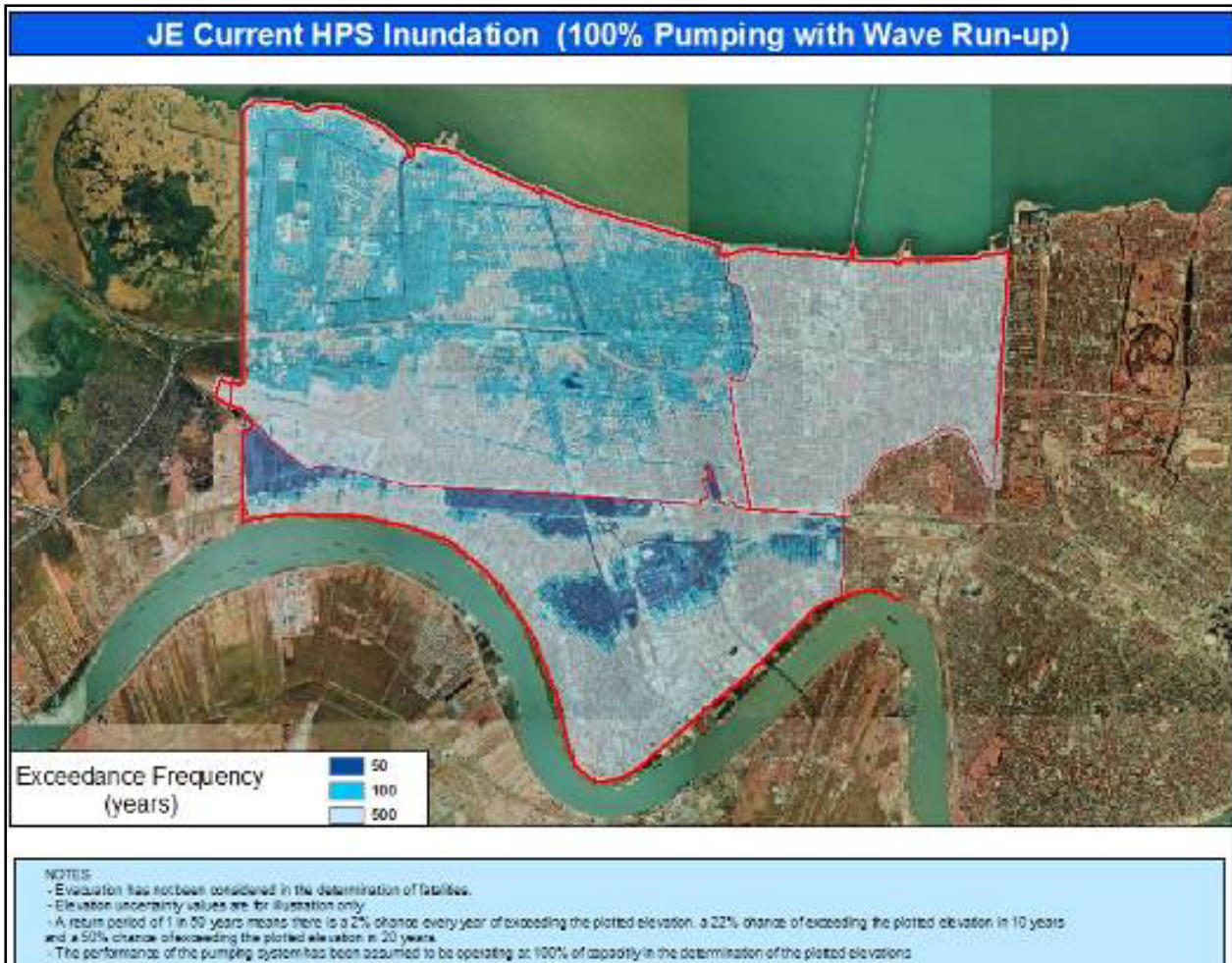


Figure 13-17 – Jefferson East Bank – Current Inundation Risk – 100% Pumping

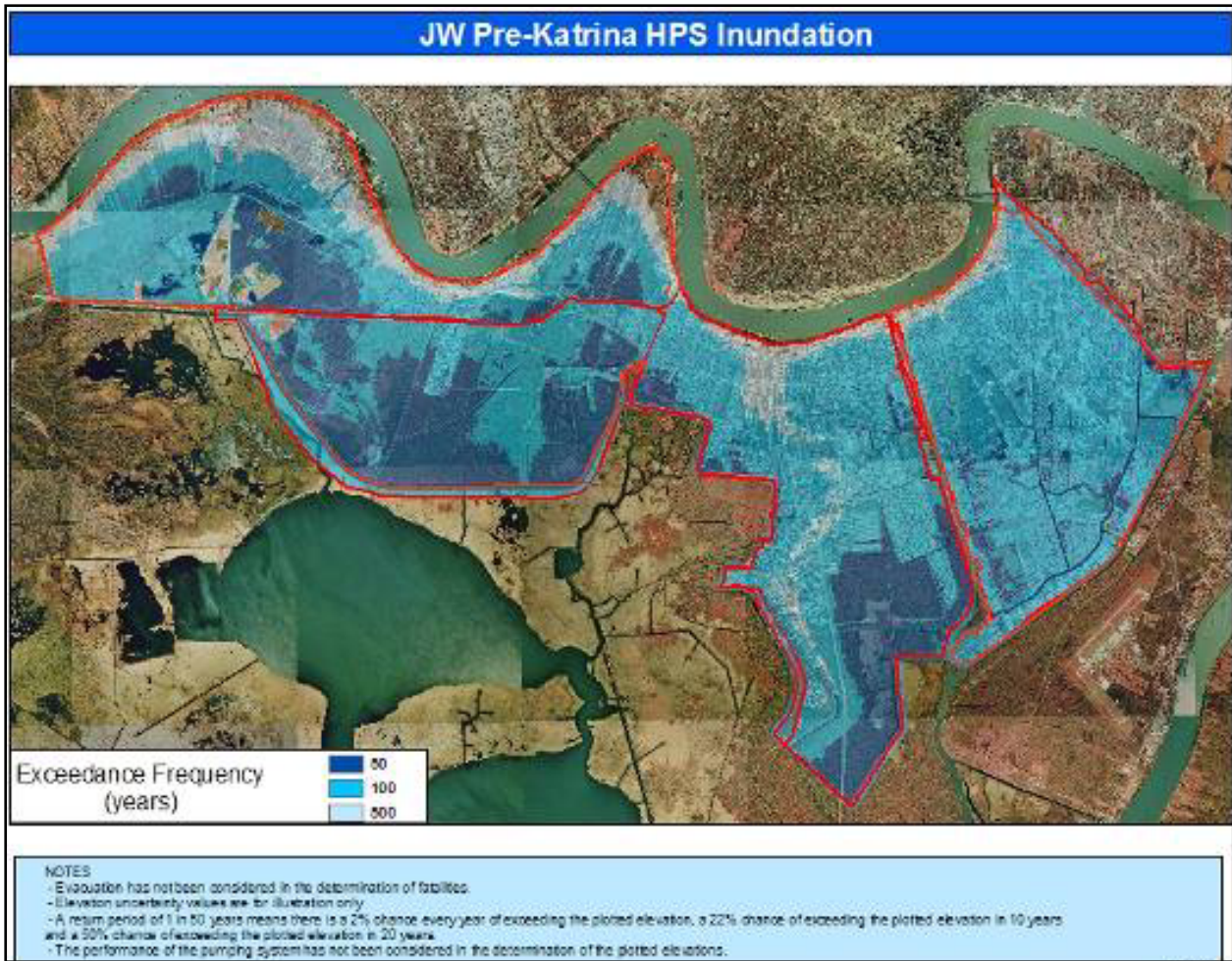


Figure 13-18 – Jefferson West Bank – Pre-Katrina Inundation Risk – No Pumping

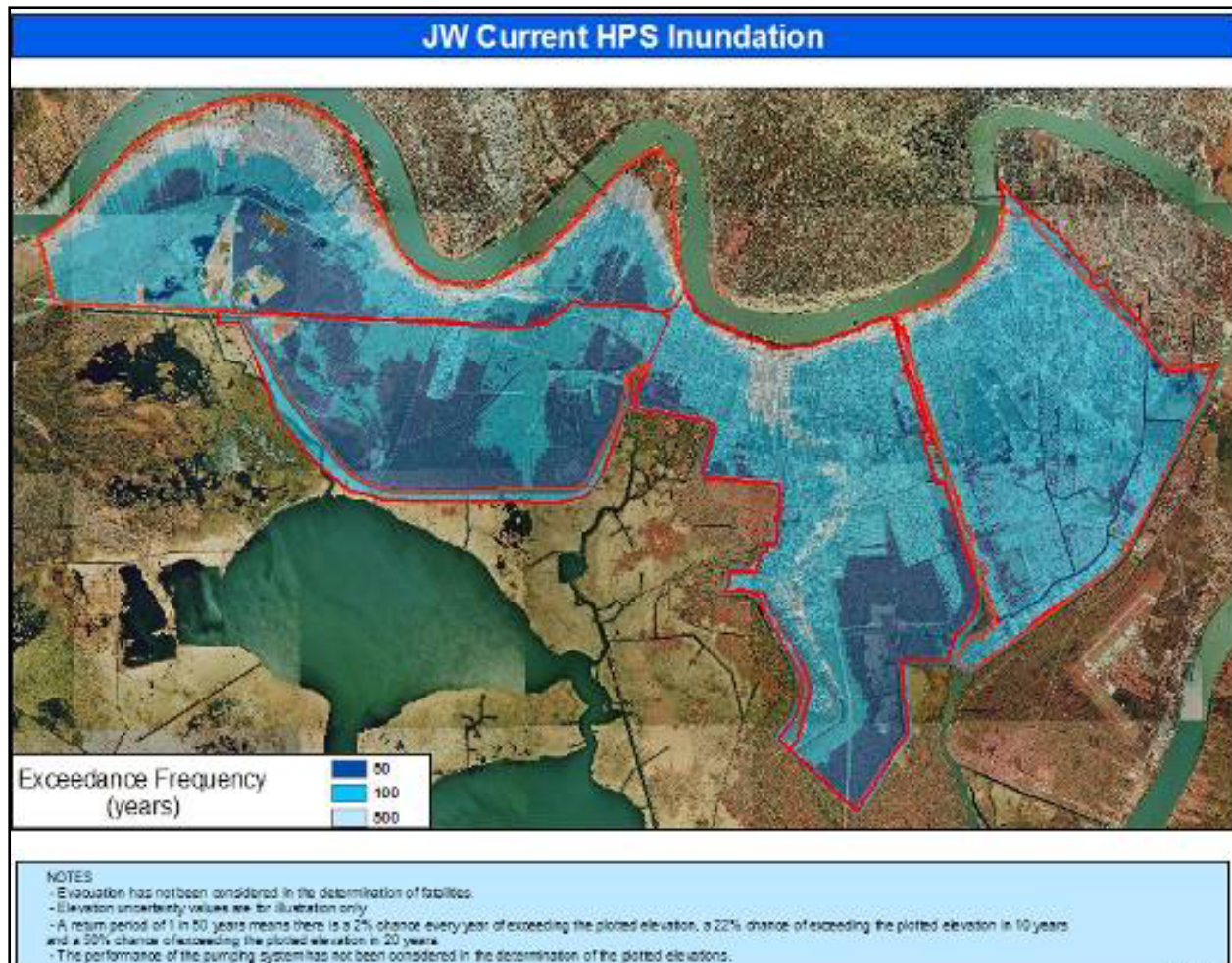


Figure 13-19 – Jefferson West Bank – Current Inundation Risk- No Pumping

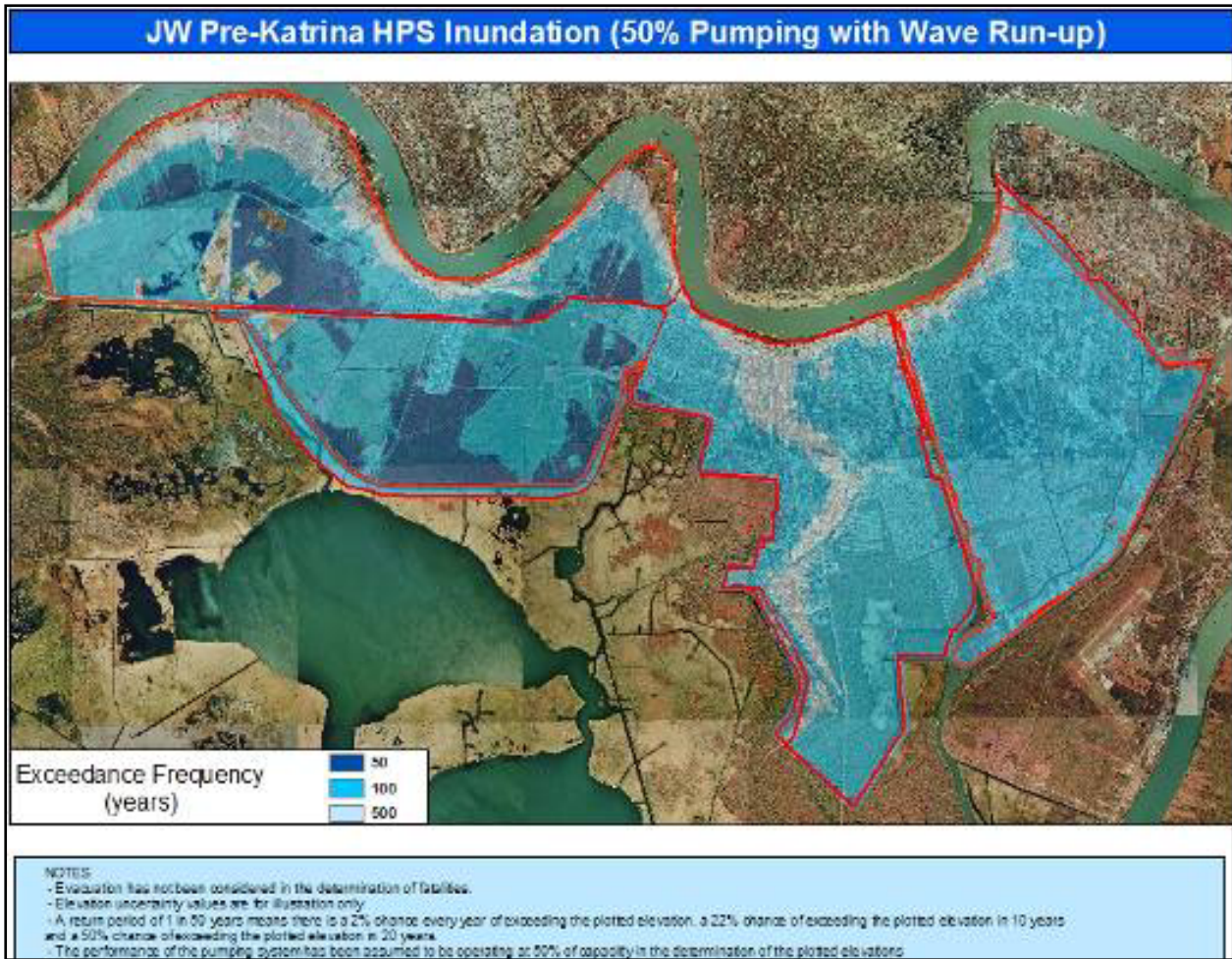


Figure 13-20 – Jefferson West Bank – Pre-Katrina Inundation Risk – 50% Pumping

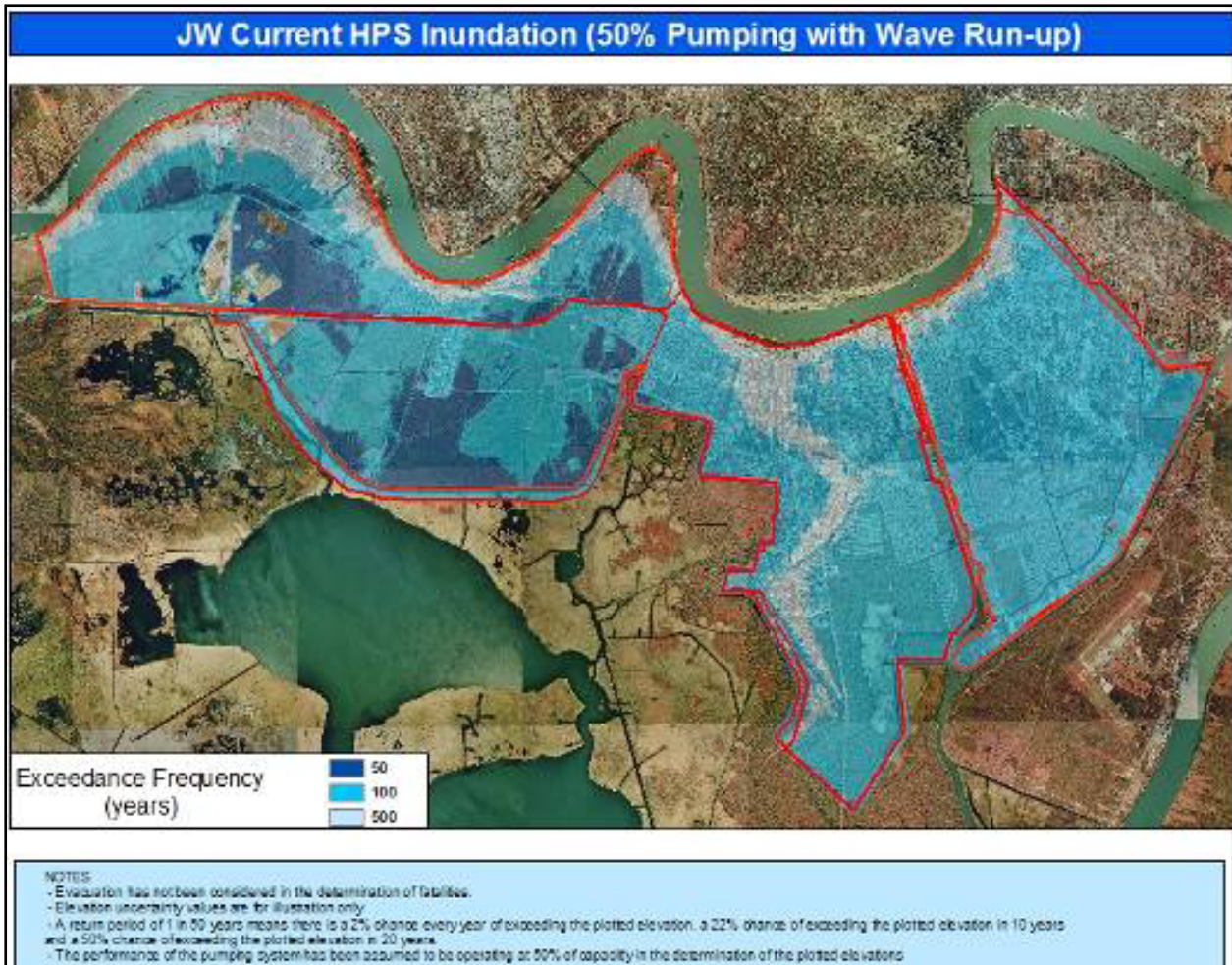


Figure 13-21 – Jefferson West Bank – Current Inundation Risk- 50% Pumping

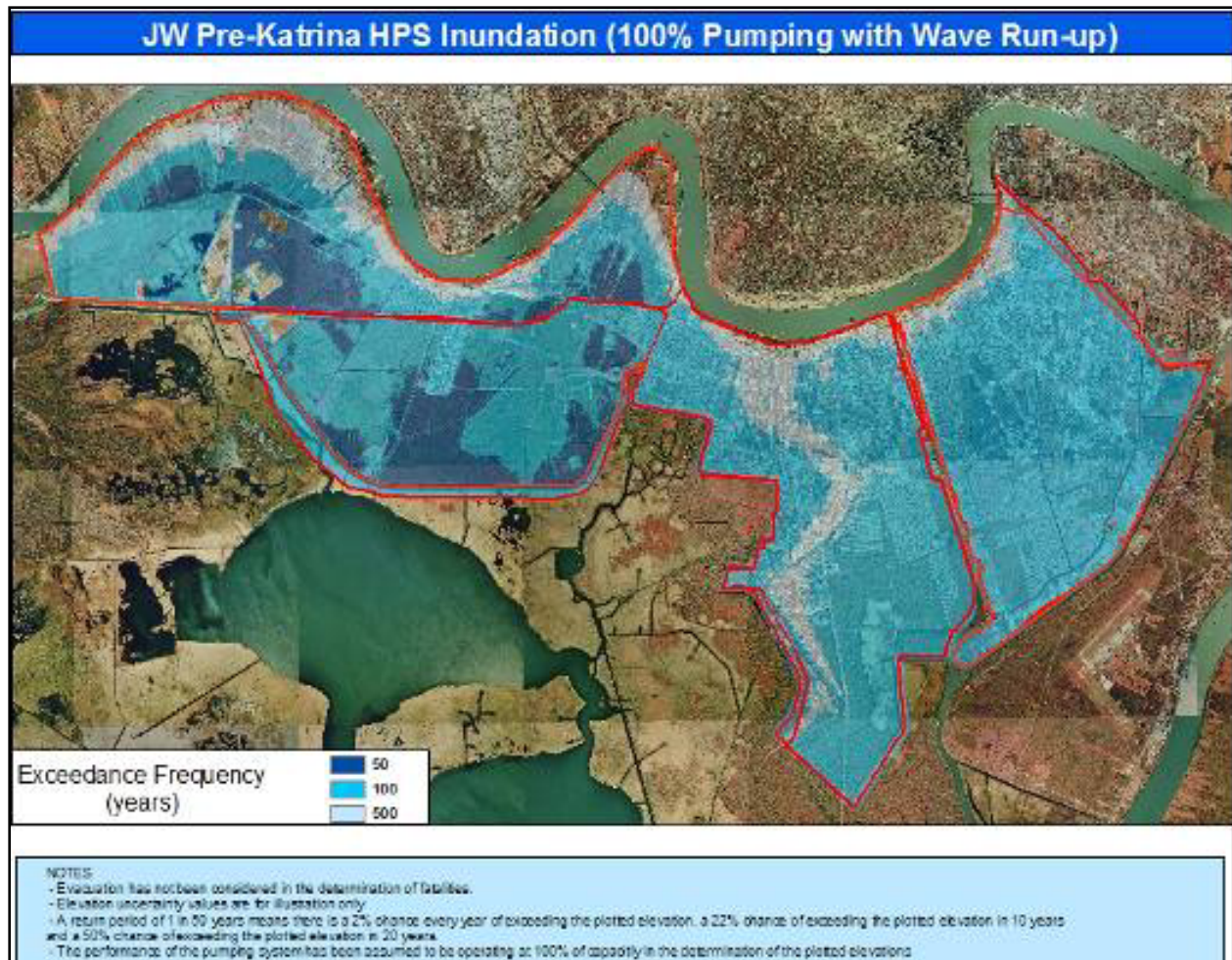


Figure 13-22 – Jefferson West Bank – Pre-Katrina Inundation Risk – 100% Pumping

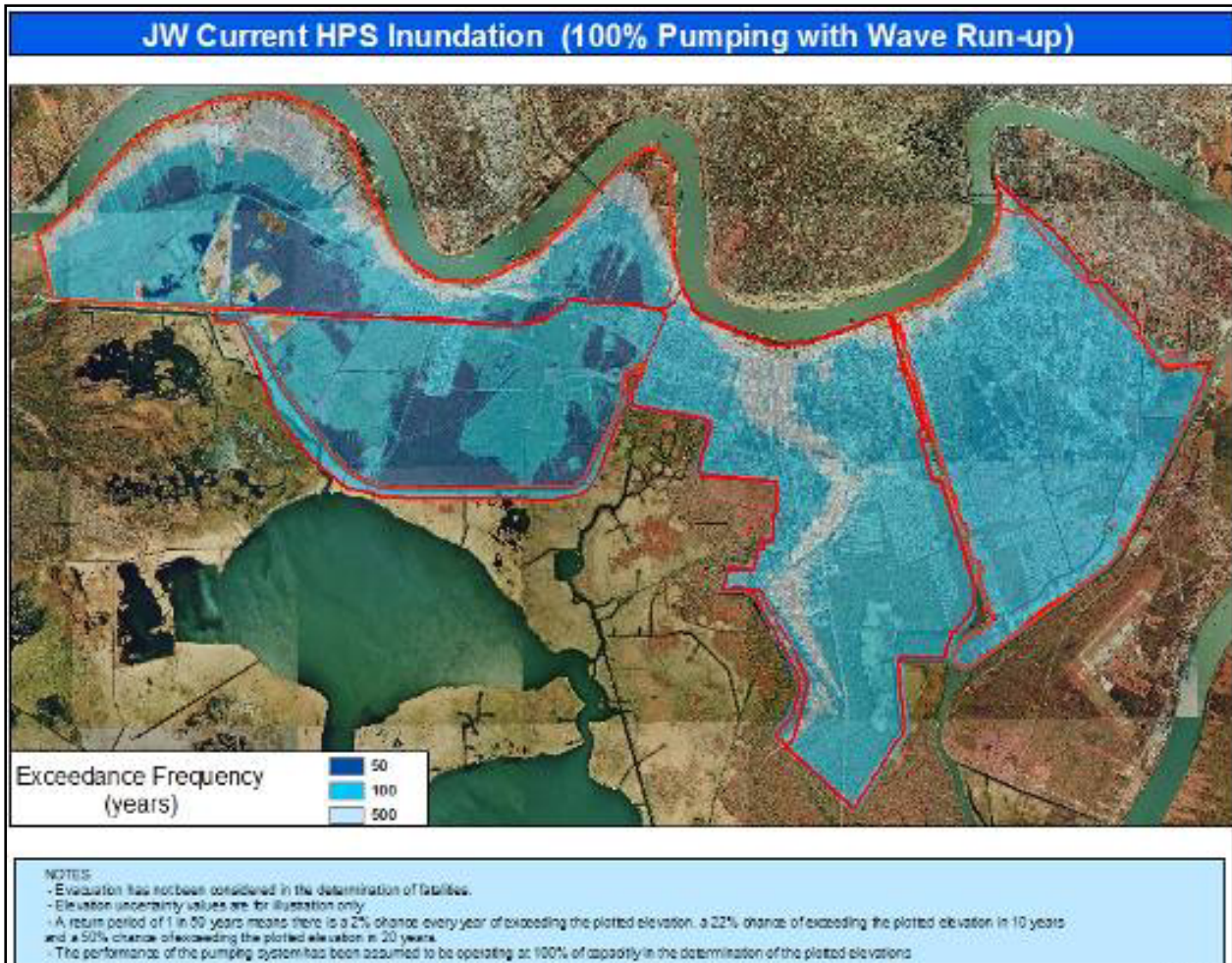


Figure 13-23 – Jefferson West Bank – Current Inundation Risk- 100% Pumping

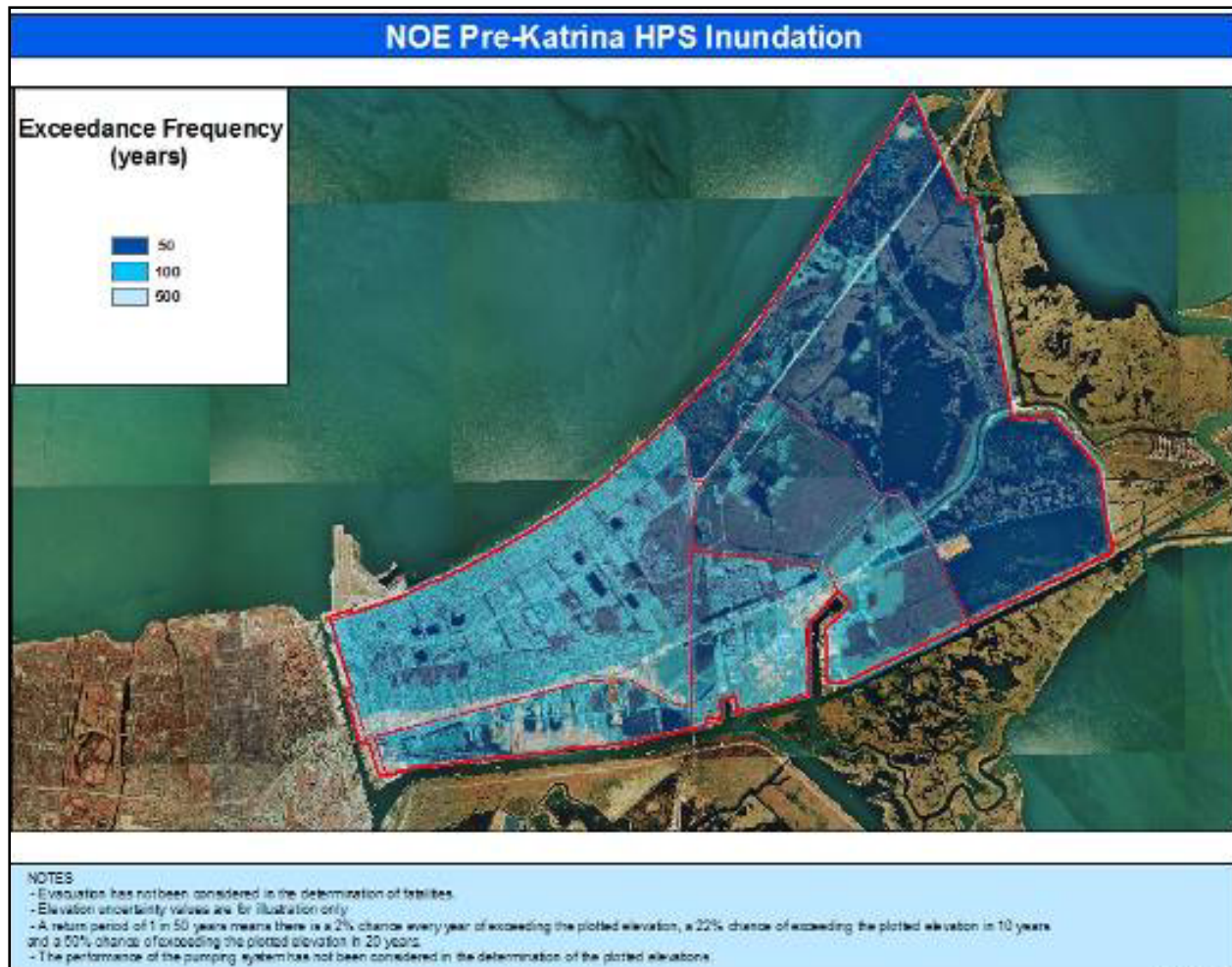


Figure 13-24 – New Orleans East – Pre-Katrina Inundation Risk- No Pumping

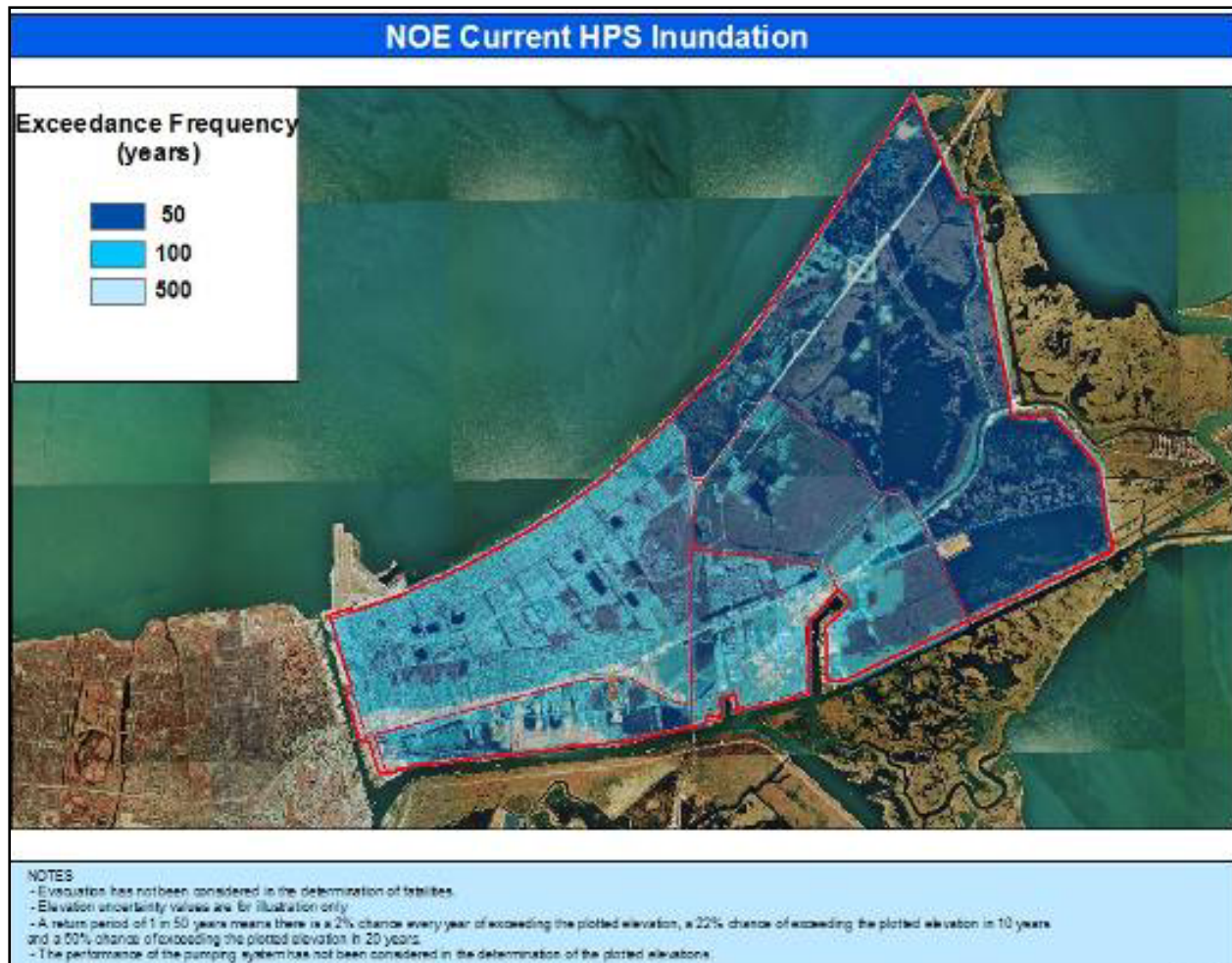


Figure 13-25 – New Orleans East – Current Inundation Risk – No Pumping

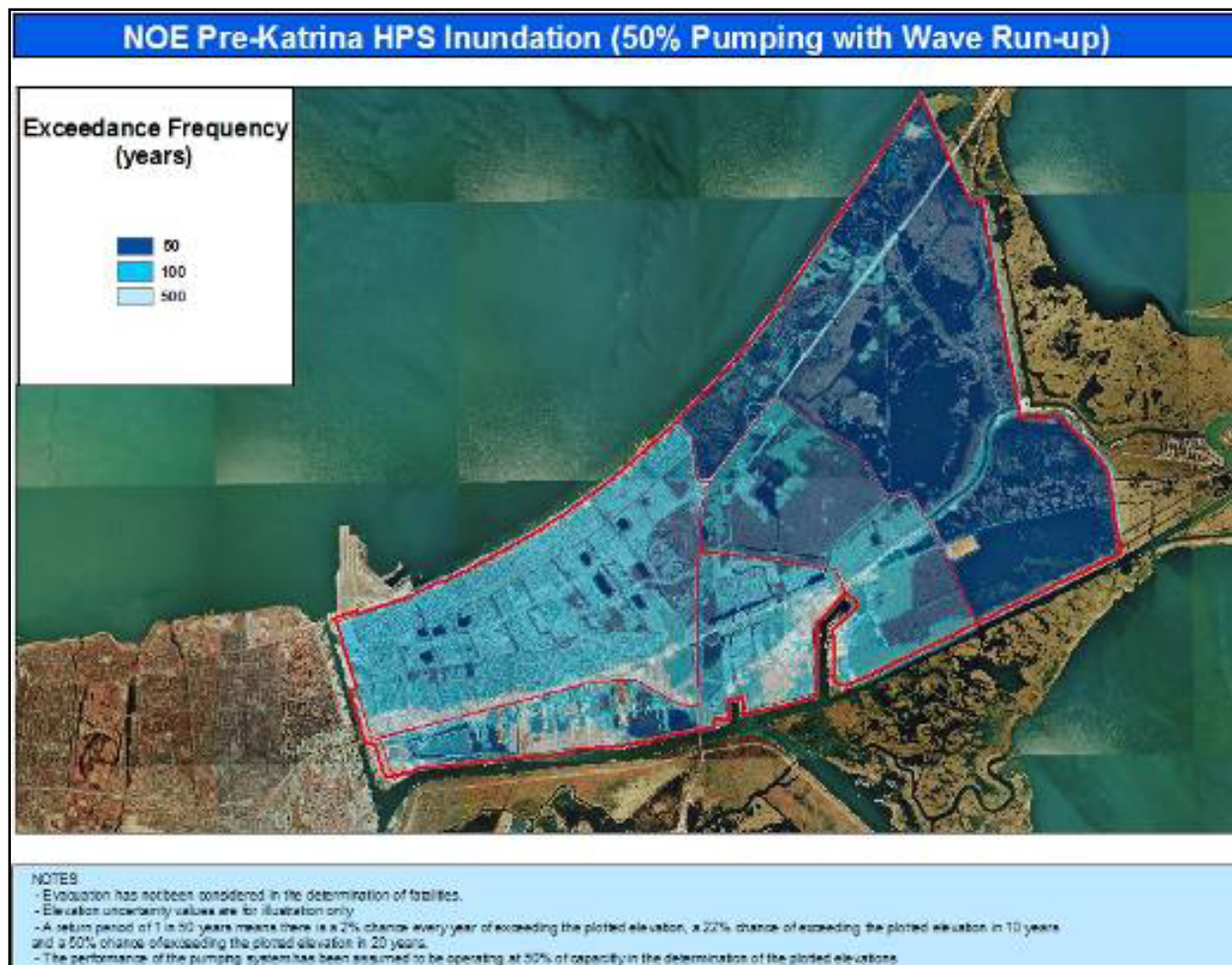


Figure 13-26 – New Orleans East – Pre-Katrina Inundation Risk- 50% Pumping

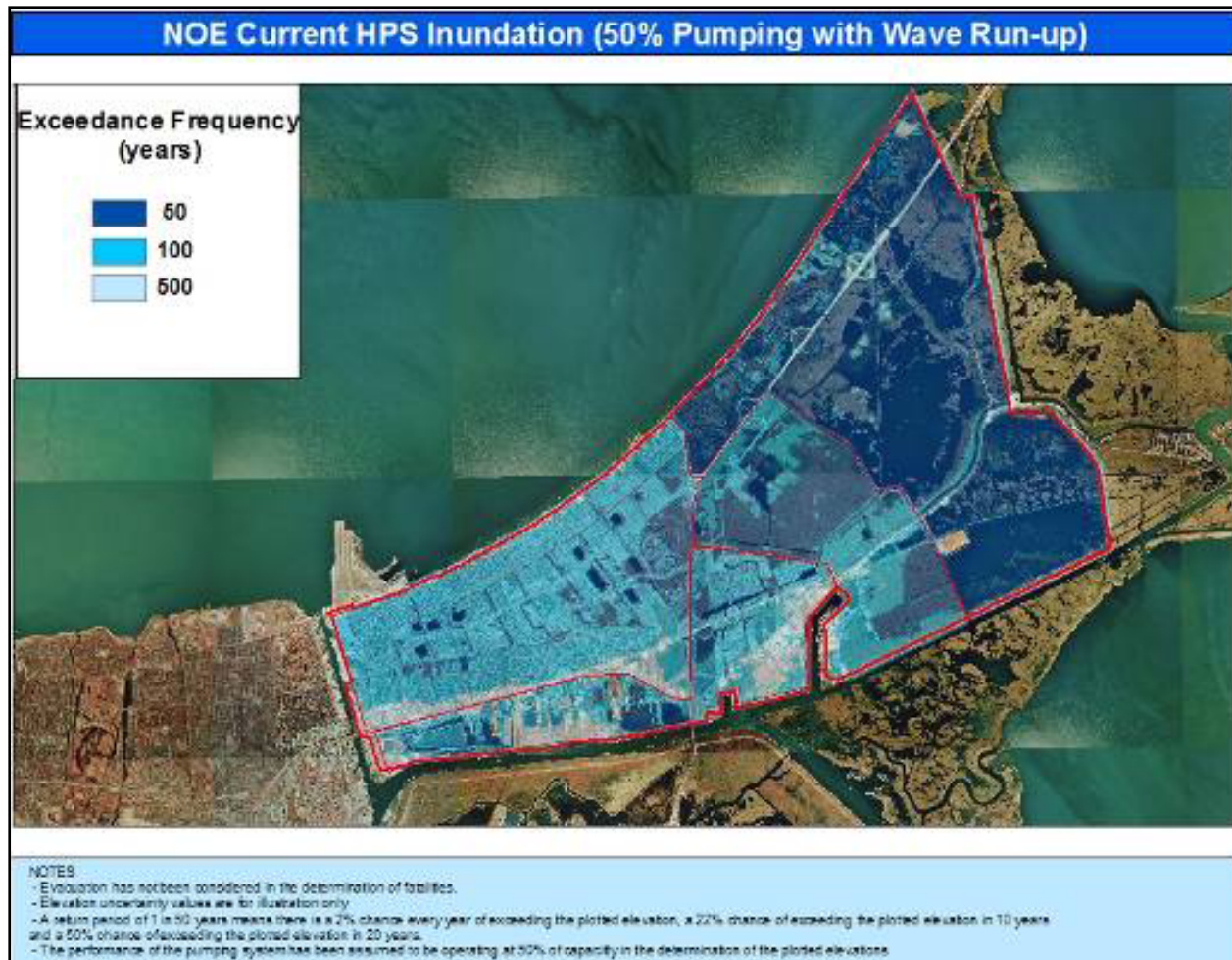


Figure 13-27 – New Orleans East – Current Inundation Risk – 50% Pumping

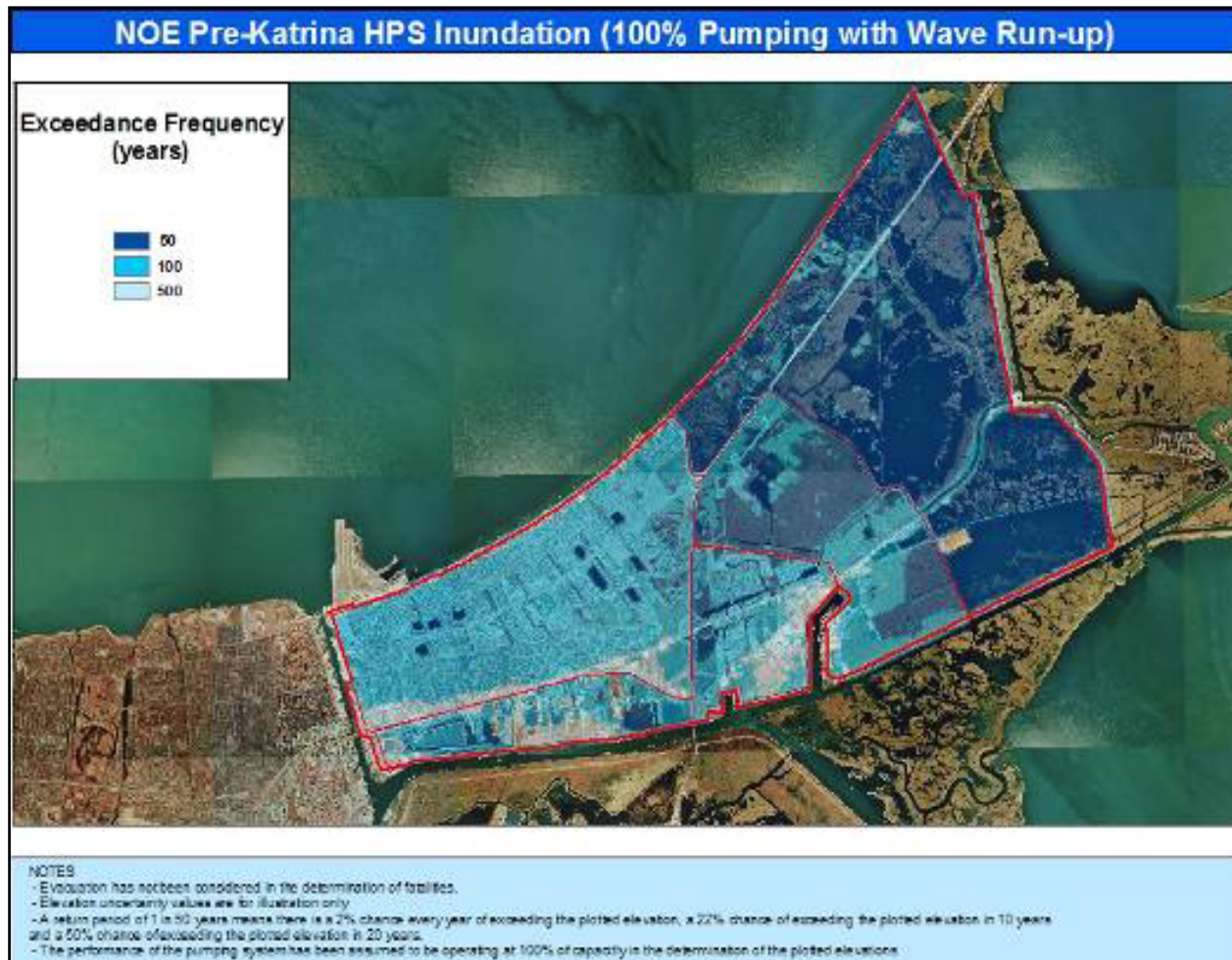


Figure 13-28 – New Orleans East – Pre-Katrina Inundation Risk- 100% Pumping

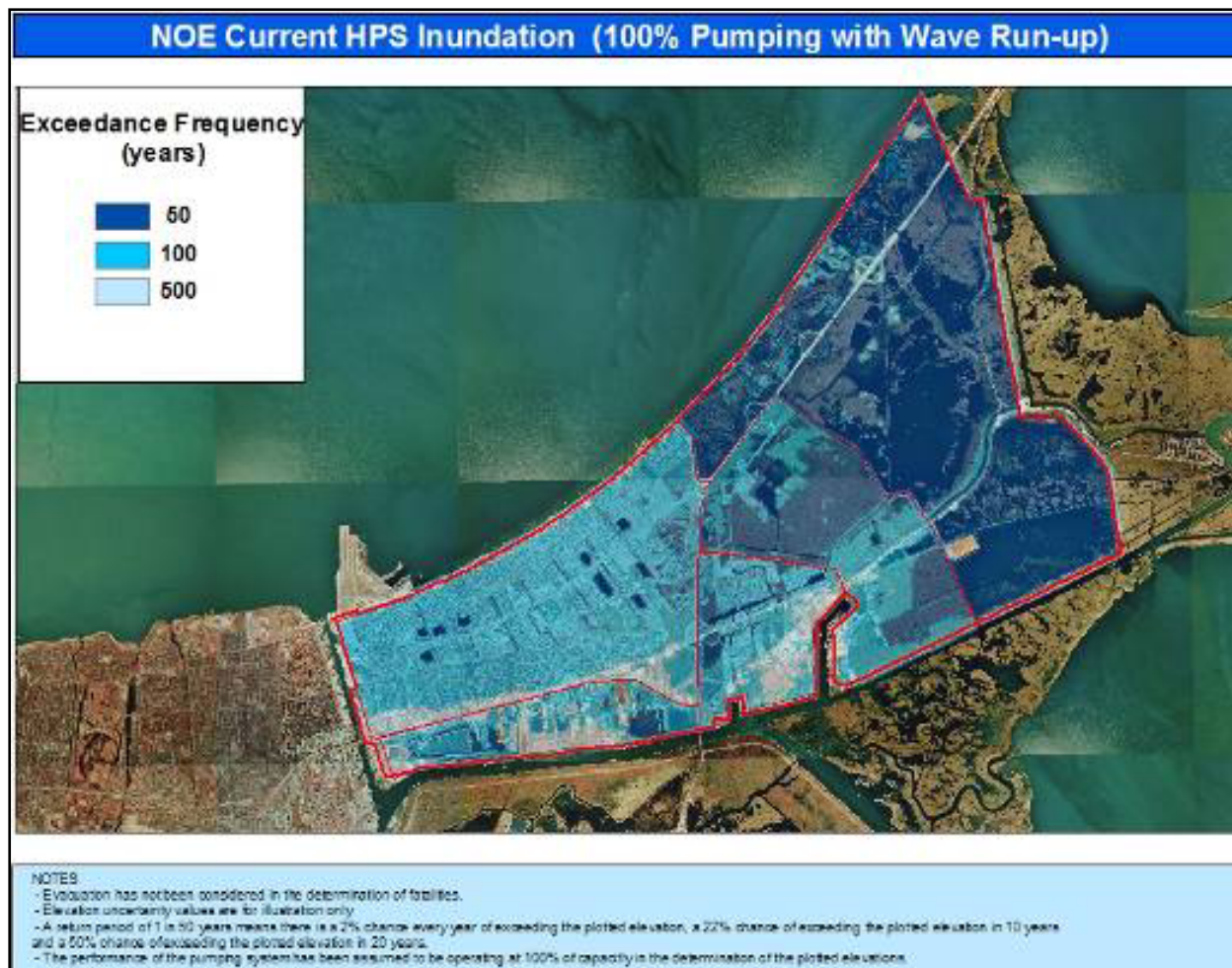


Figure 13-29 – New Orleans East – Current Inundation Risk – 100% Pumping

OM Pre-Katrina HPS Inundation (No Pumping with Wave Run-up)

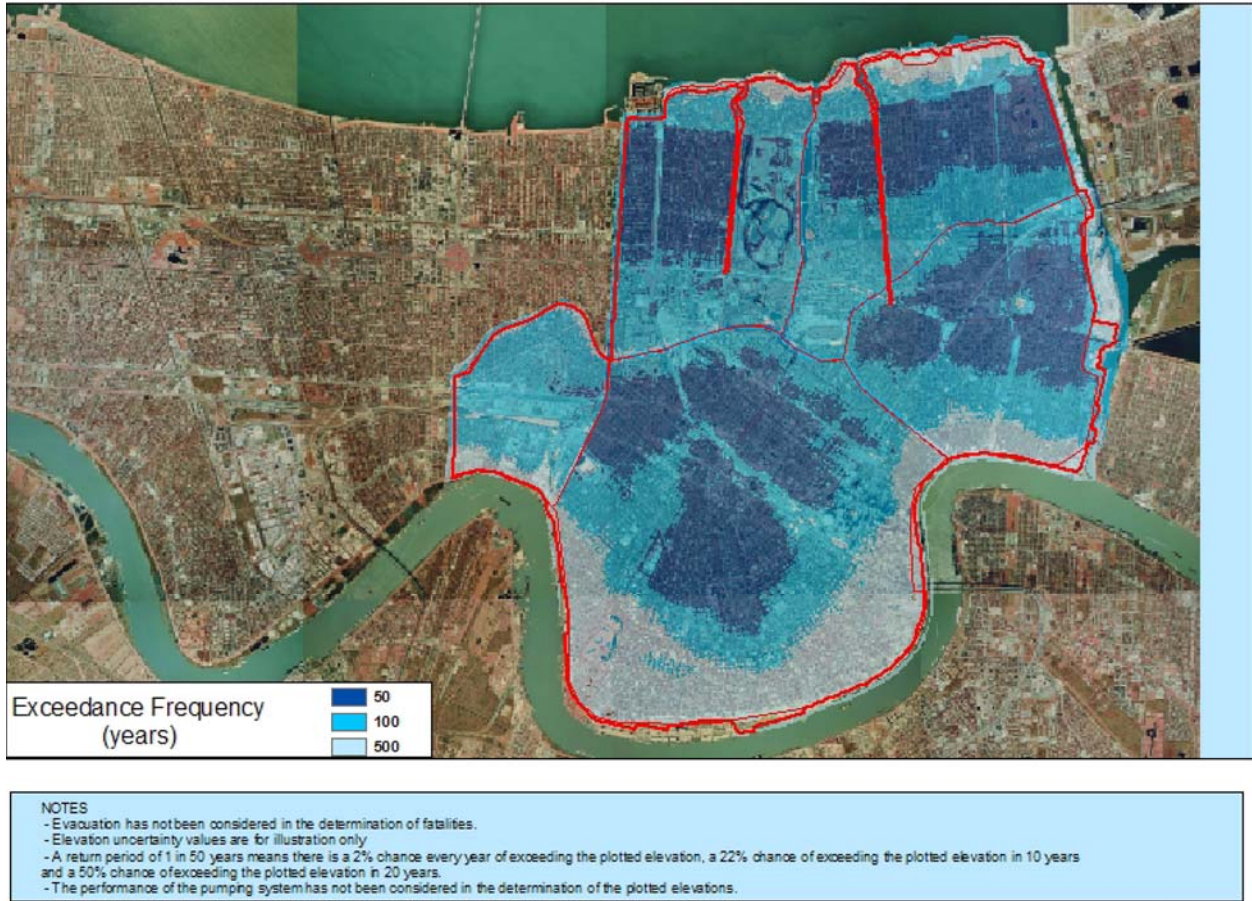
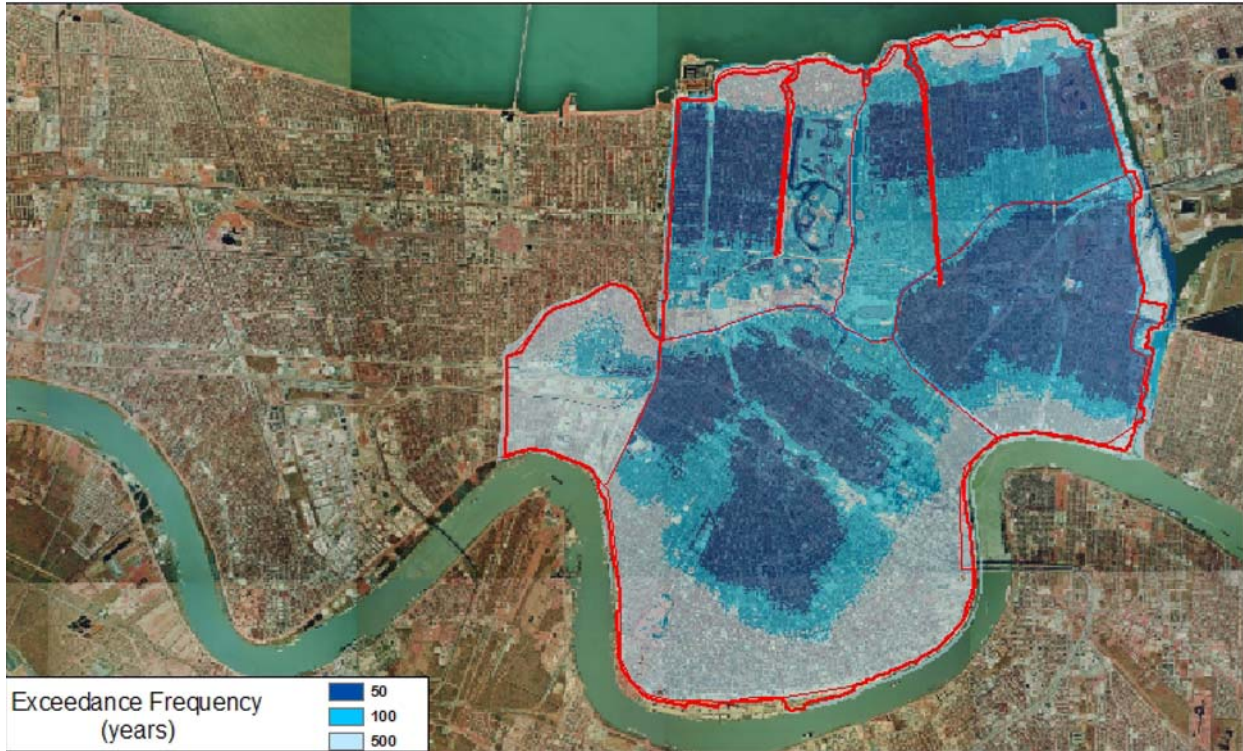


Figure 13-30 – Orleans East Bank – Pre-Katrina Inundation Risk – No Pumping

OM Current HPS Inundation (No Pumping with Wave Run-up)



NOTES
- Evacuation has not been considered in the determination of fatalities.
- Elevation uncertainty values are for illustration only
- A return period of 1 in 50 years means there is a 2% chance every year of exceeding the plotted elevation, a 22% chance of exceeding the plotted elevation in 10 years and a 50% chance of exceeding the plotted elevation in 20 years.
- The performance of the pumping system has not been considered in the determination of the plotted elevations.

11/29/2007

Figure 13-31 – Orleans East Bank – Current Inundation Risk – No Pumping

OM Pre-Katrina HPS Inundation (50% Pumping with Wave Run-up)

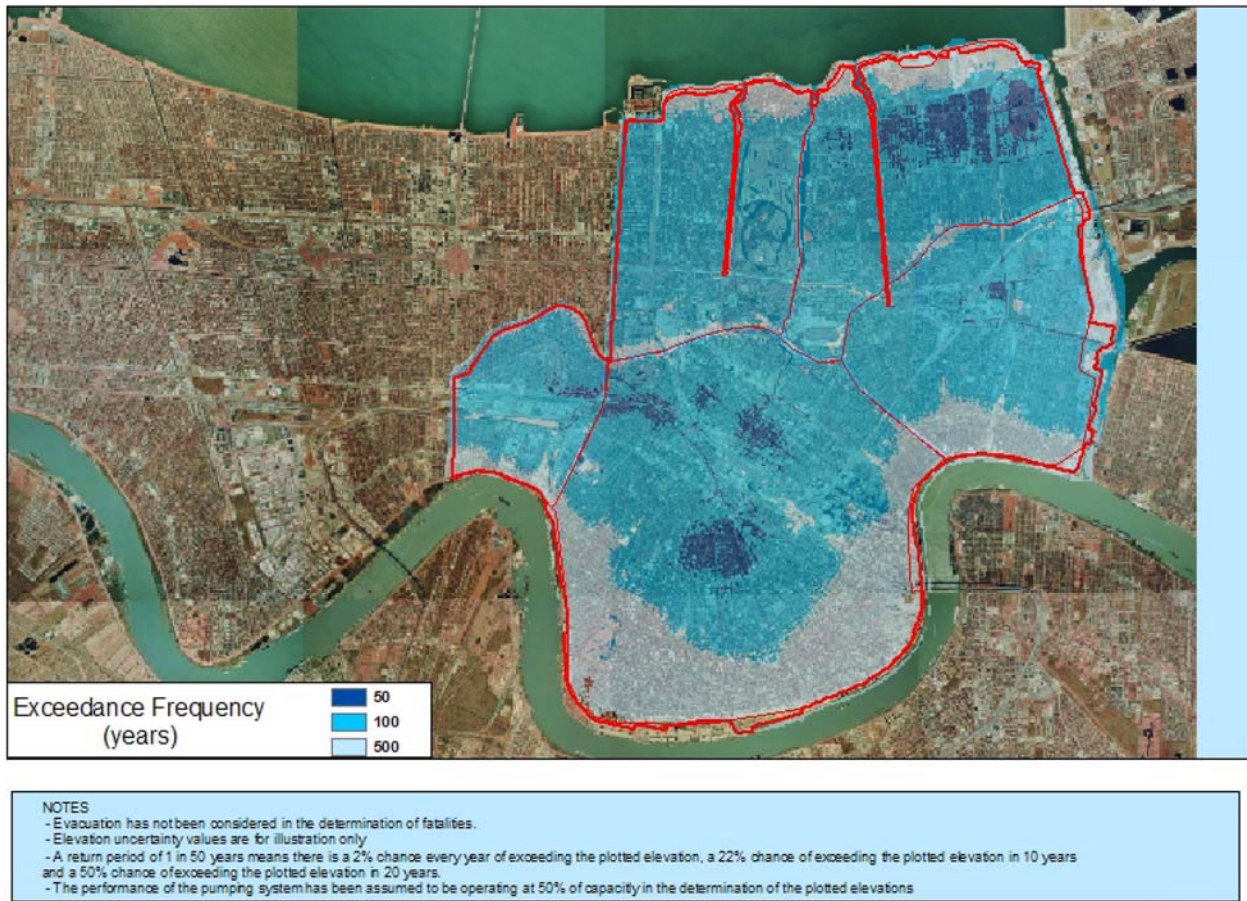
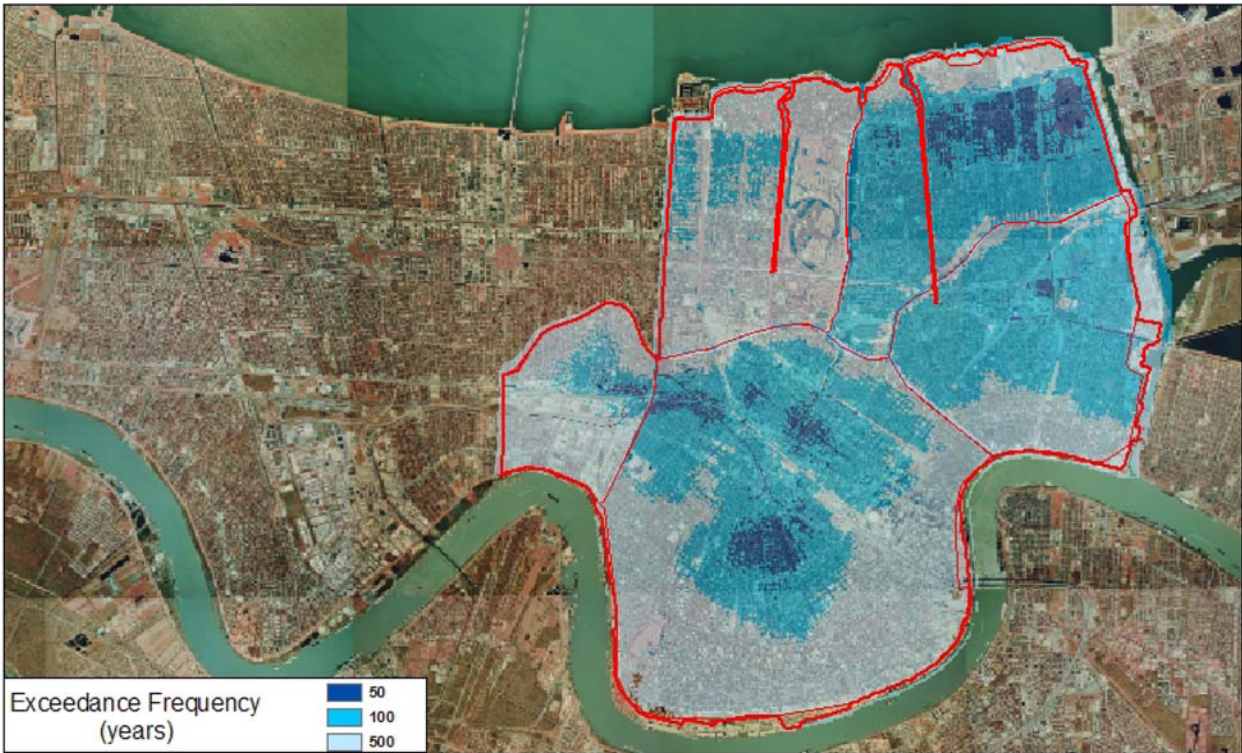


Figure 13-32 – Orleans East Bank – Pre-Katrina Inundation Risk – 50% Pumping

OM Current HPS Inundation (50% Pumping with Wave Run-up)



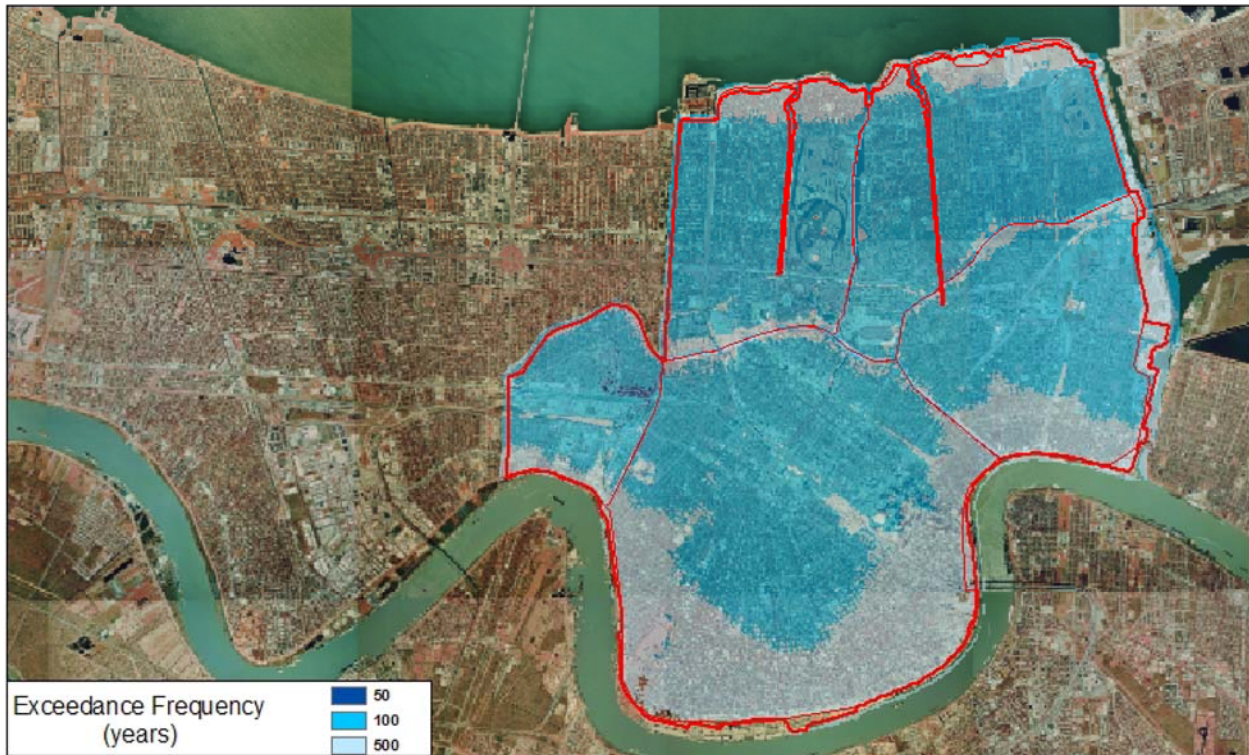
NOTES

- Evacuation has not been considered in the determination of fatalities.
- Elevation uncertainty values are for illustration only
- A return period of 1 in 50 years means there is a 2% chance every year of exceeding the plotted elevation, a 22% chance of exceeding the plotted elevation in 10 years and a 50% chance of exceeding the plotted elevation in 20 years.
- The performance of the pumping system has been assumed to be operating at 50% of capacity in the determination of the plotted elevations

11/29/2007

Figure 13-33 – Orleans East Bank – Current Inundation Risk – 50% Pumping

OM Pre-Katrina HPS Inundation (100% Pumping with Wave Run-up)



NOTES

- Evacuation has not been considered in the determination of fatalities.
- Elevation uncertainty values are for illustration only.
- A return period of 1 in 50 years means there is a 2% chance every year of exceeding the plotted elevation, a 22% chance of exceeding the plotted elevation in 10 years and a 50% chance of exceeding the plotted elevation in 20 years.
- The performance of the pumping system has been assumed to be operating at 100% of capacity in the determination of the plotted elevations.

11/29/2007

Figure 13-34 – Orleans East Bank – Pre-Katrina Inundation Risk – 100% Pumping

OM Current HPS Inundation (100% Pumping with Wave Run-up)

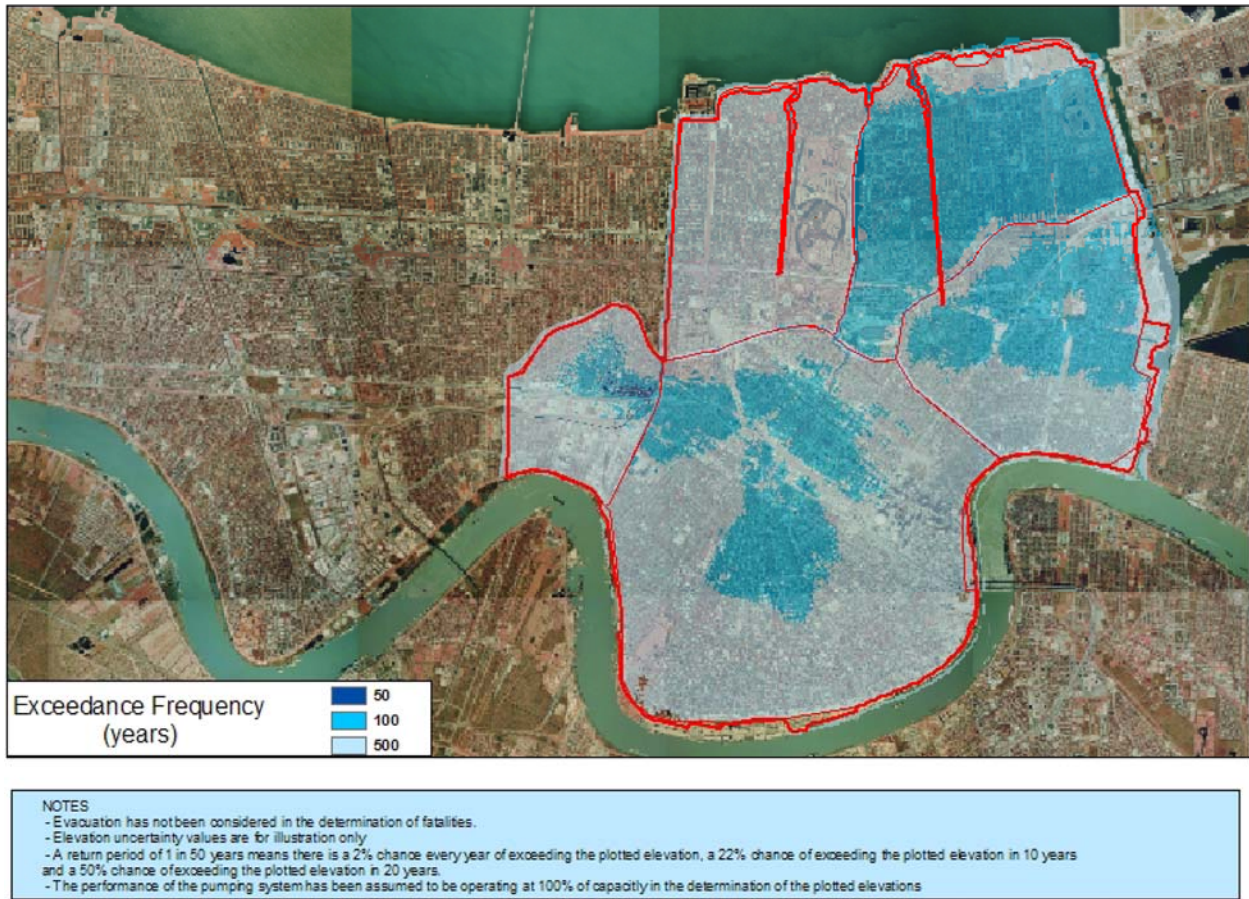


Figure 13-35 – Orleans East Bank – Current Inundation Risk – 100% Pumping

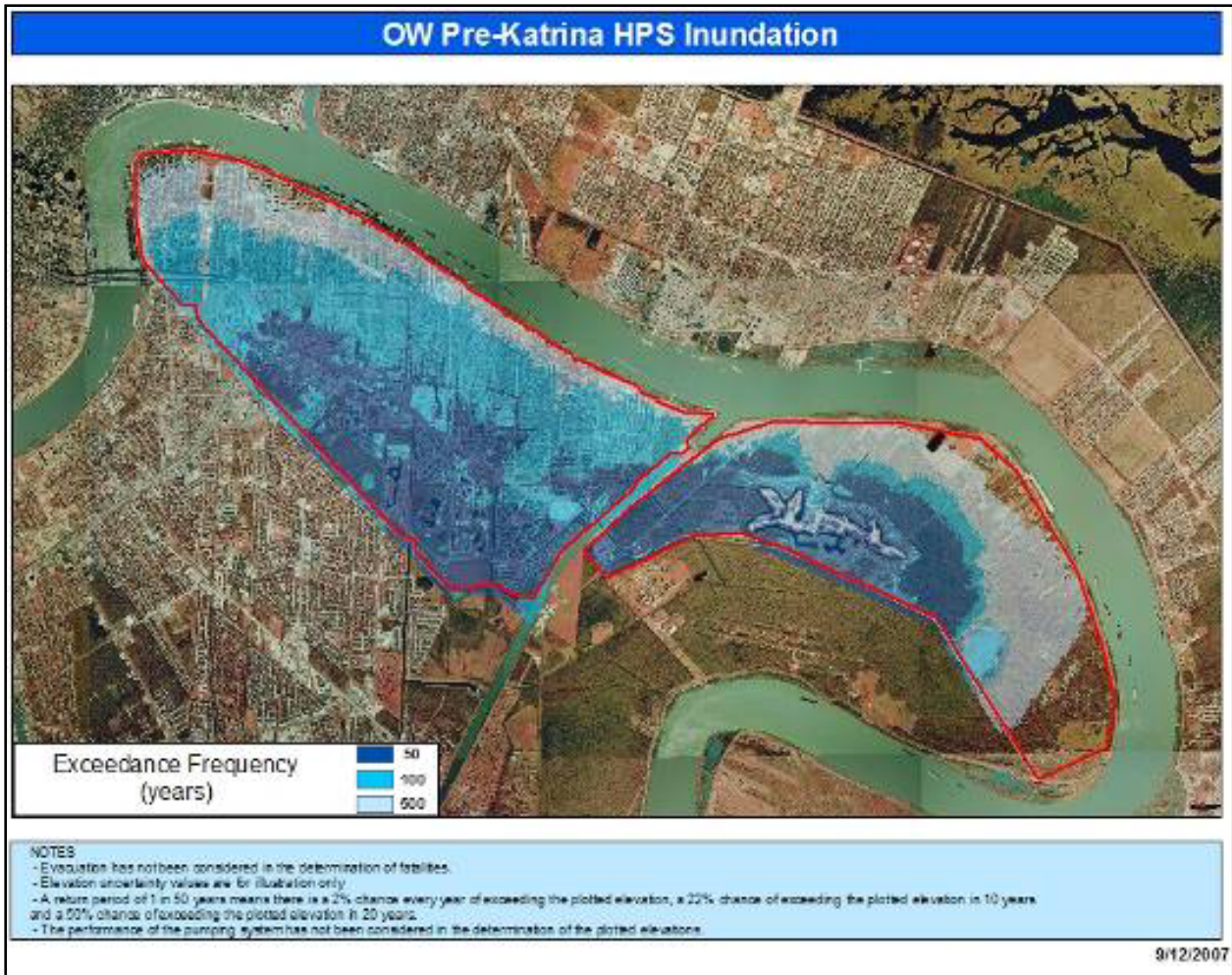


Figure13-36 – Orleans West Bank – Pre-Katrina Inundation Risk – No Pumping

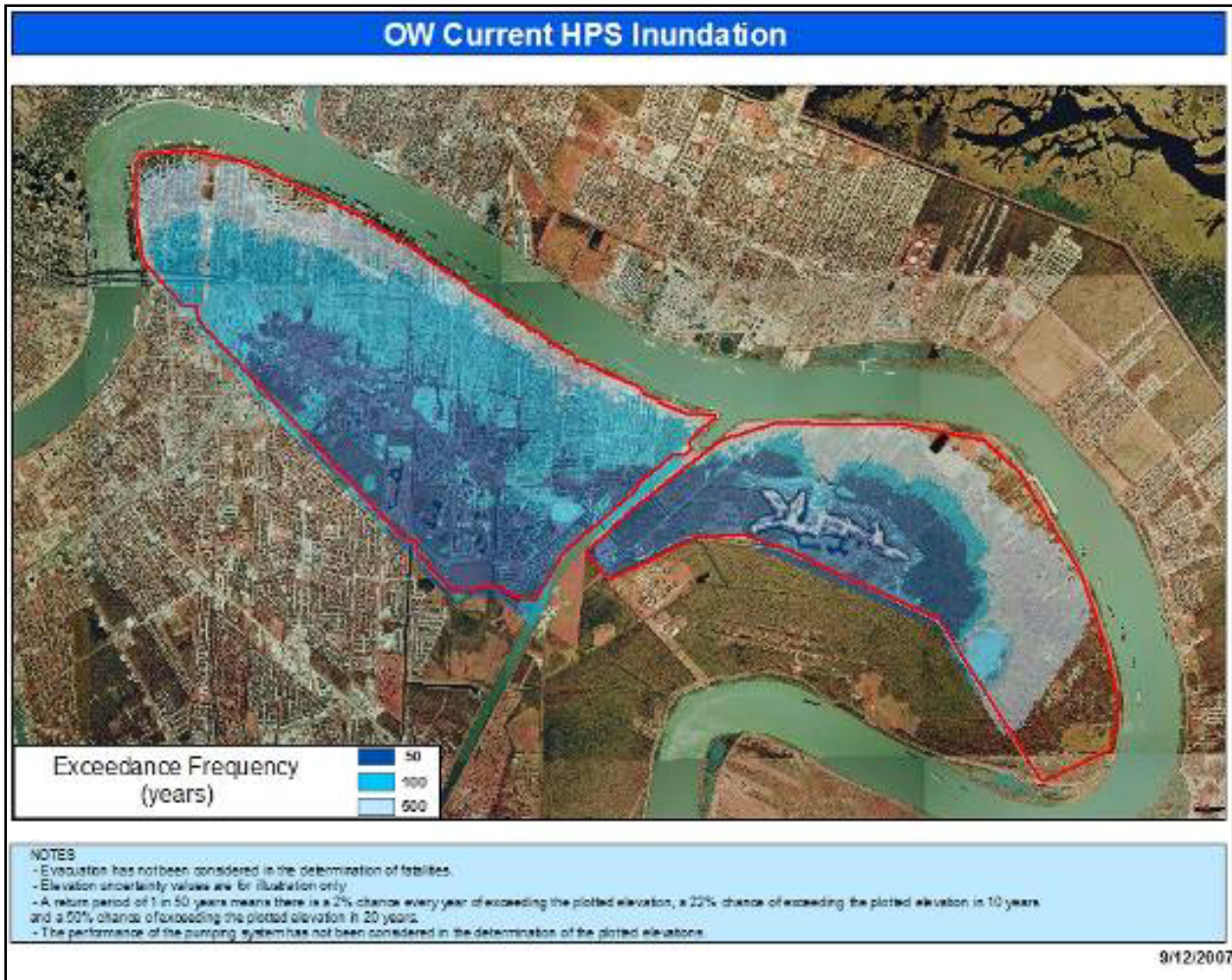
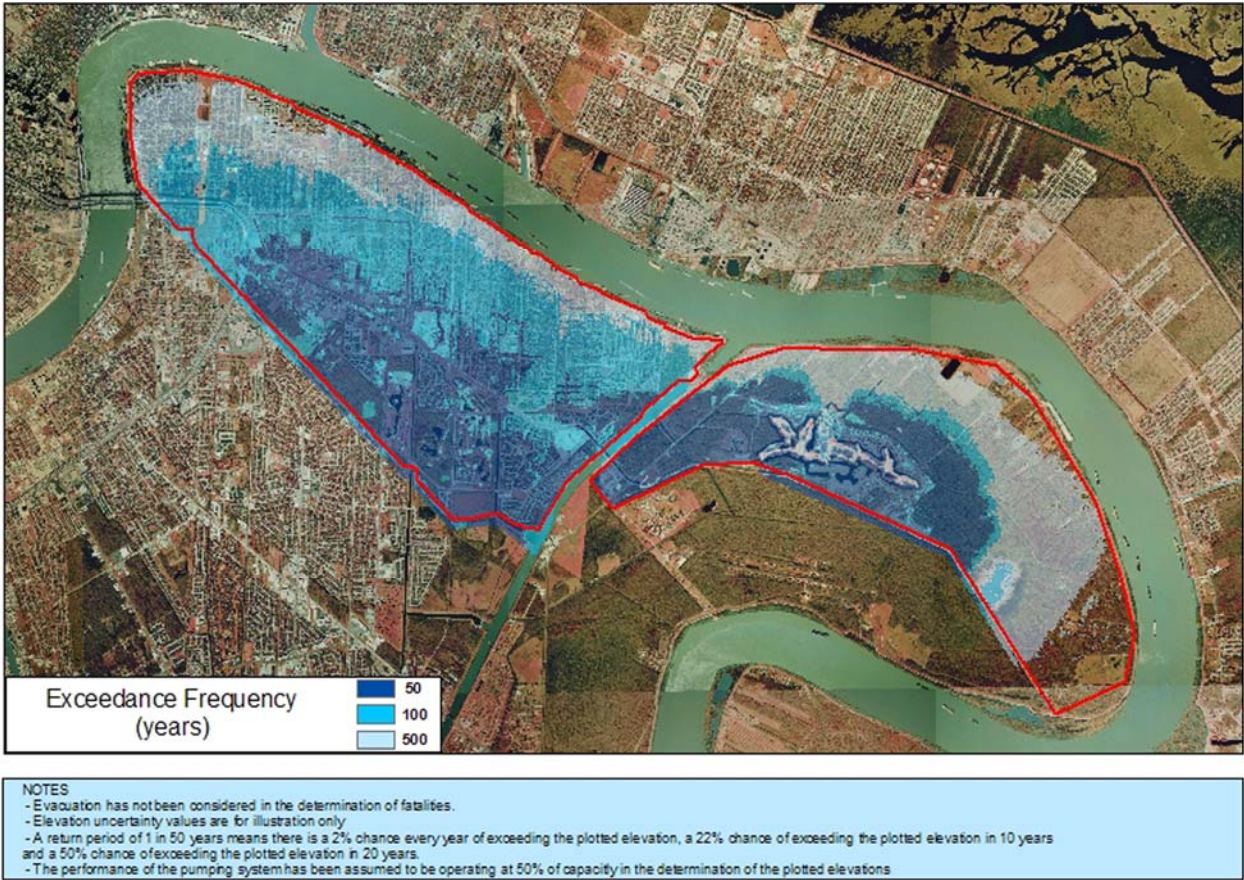


Figure13-37 – Orleans West Bank – Current Inundation Risk – No Pumping

OW Pre-Katrina HPS Inundation - 50% Pumping with Wave Run-up



11/29/200

Figure13-38 – Orleans West Bank – Pre-Katrina Inundation Risk – 50% Pumping

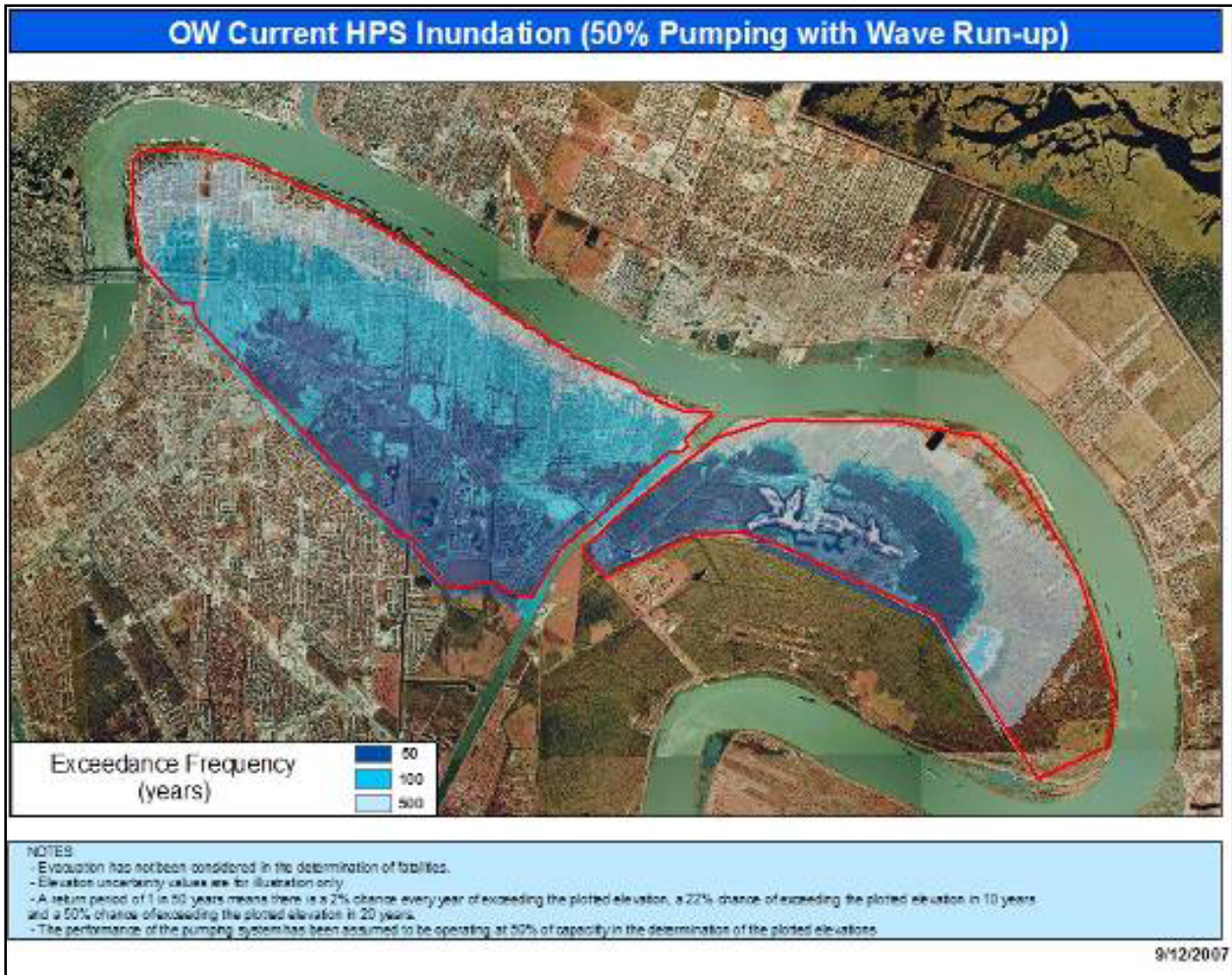


Figure13-39 – Orleans West Bank – Current Inundation Risk – 50% Pumping

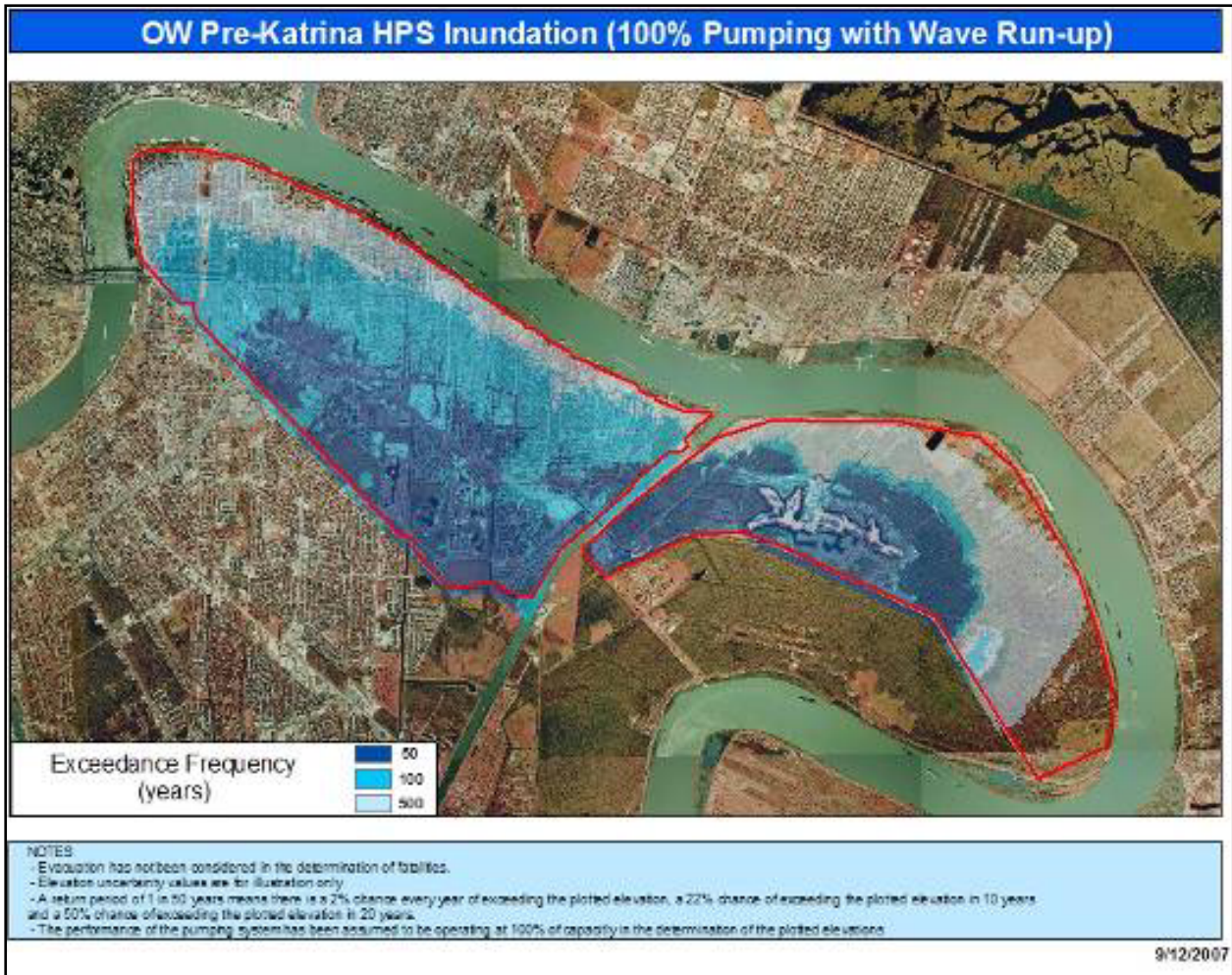


Figure13-40 – Orleans West Bank – Pre-Katrina Inundation Risk – 100% Pumping

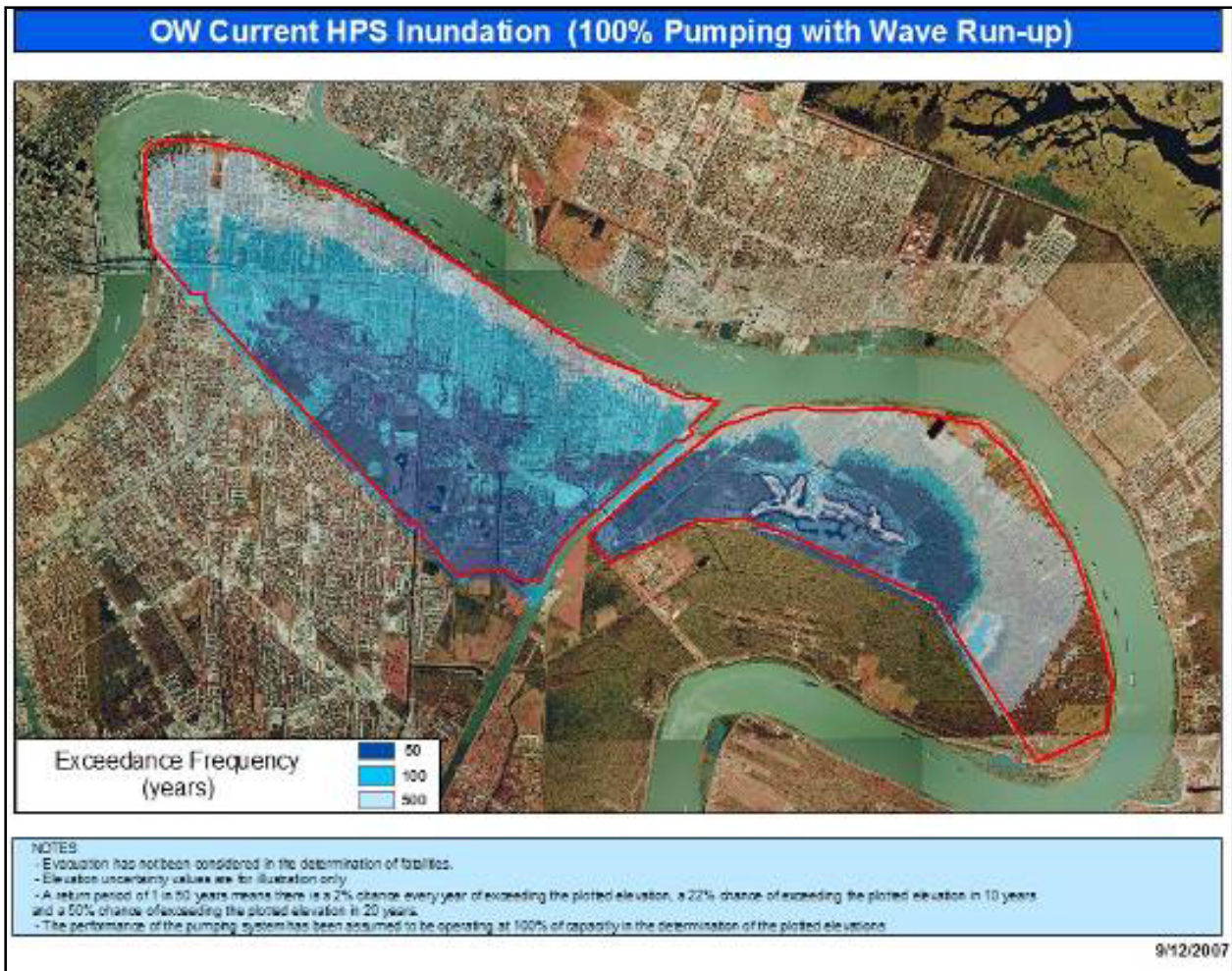


Figure13-41 – Orleans West Bank – Current Inundation Risk – 100% Pumping

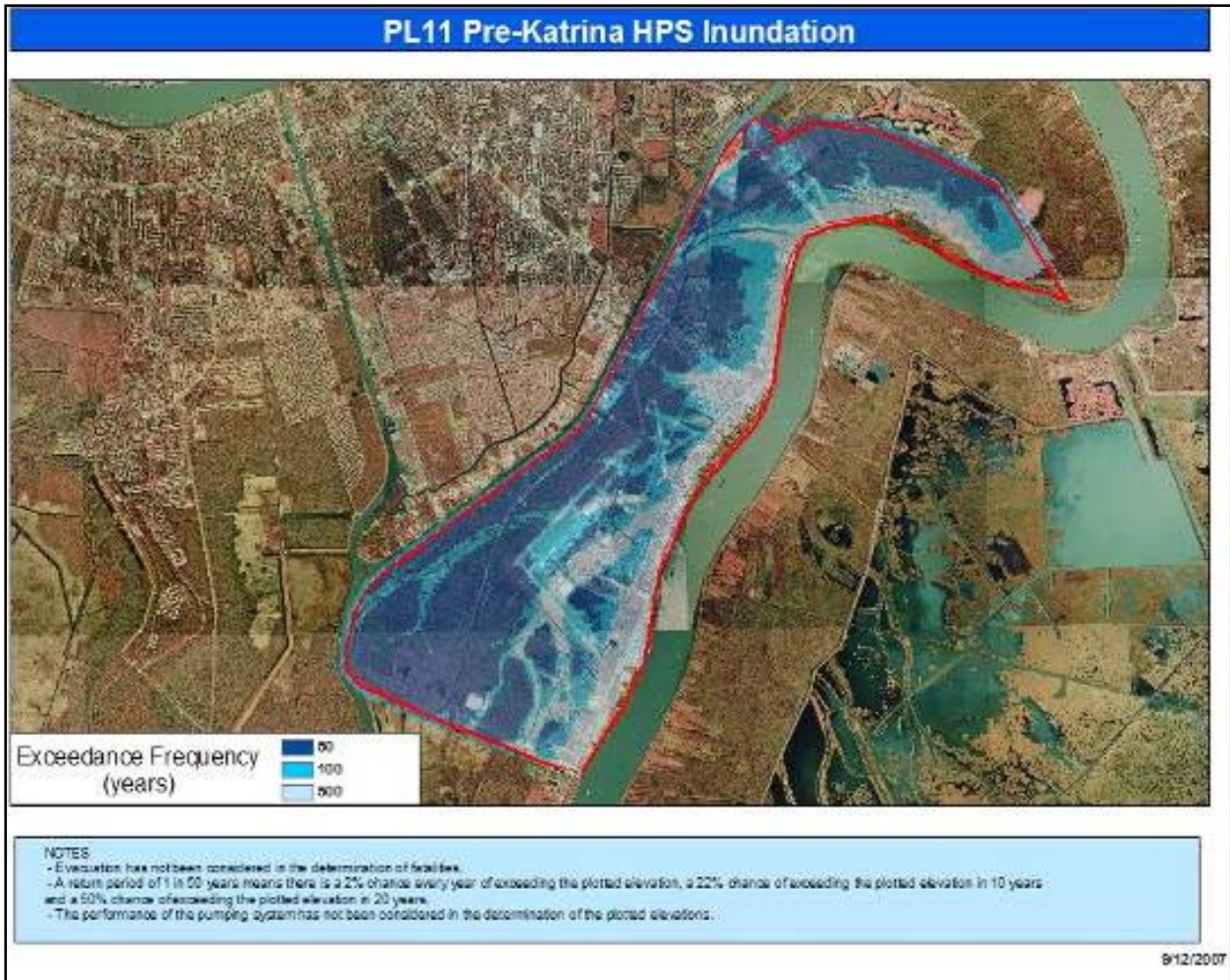


Figure 13-42 – Plaquemines (PL 11) – Pre-Katrina Inundation Risk – No Pumping

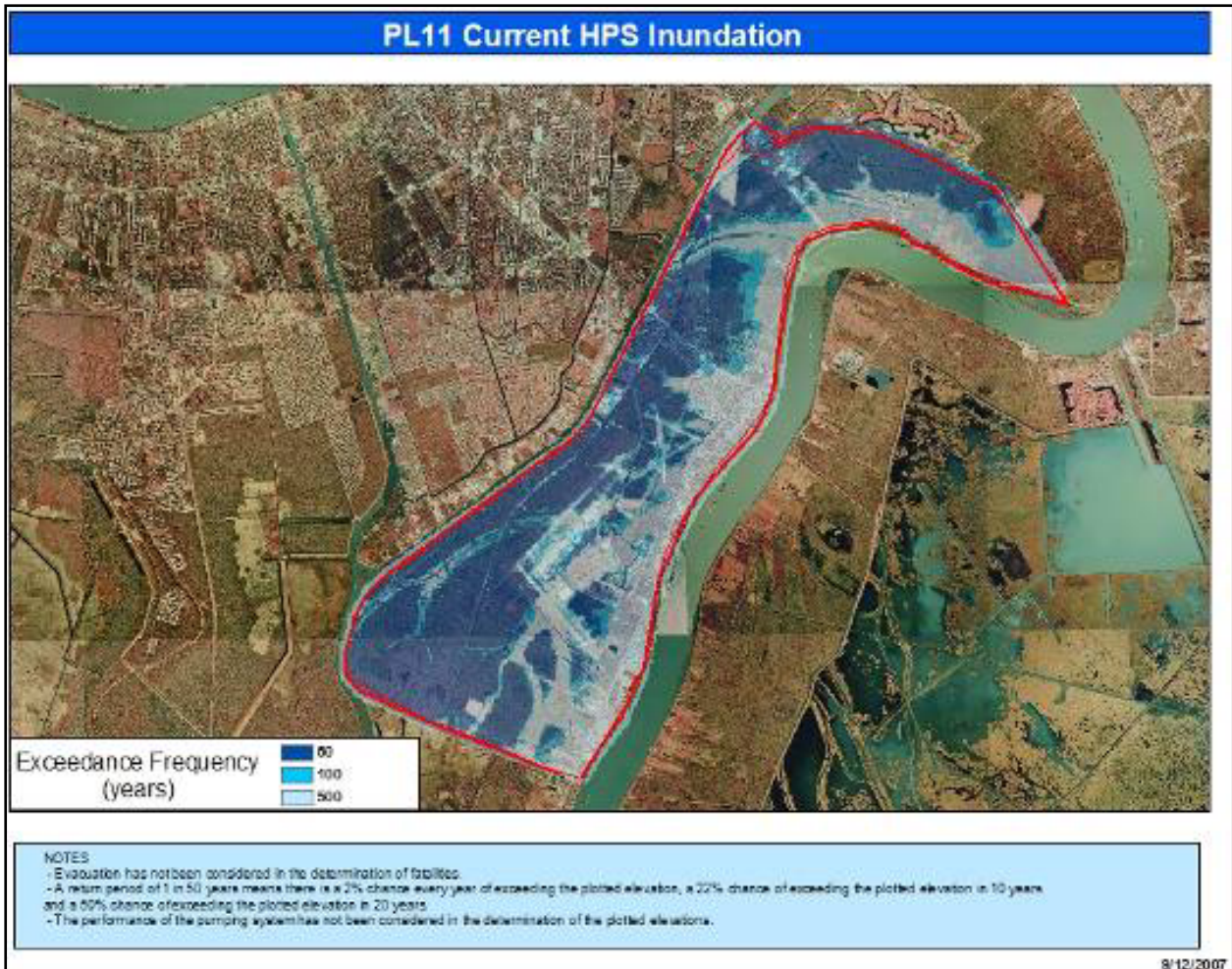


Figure 13-43 – Plaquemines (PL 11)– Current Inundation Risk – No Pumping

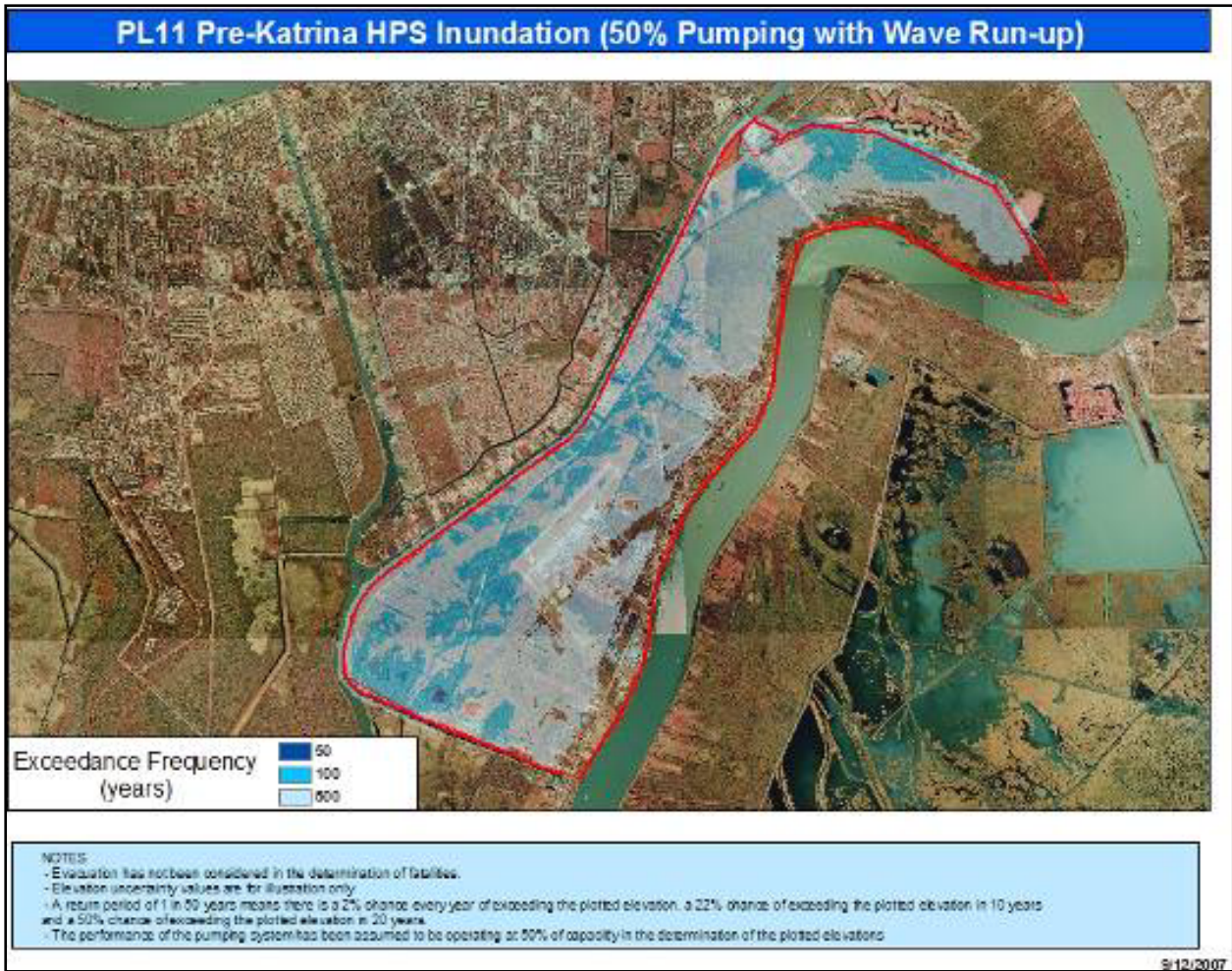


Figure 13-44 – Plaquemines (PL 11) – Pre-Katrina Inundation Risk – 50% Pumping

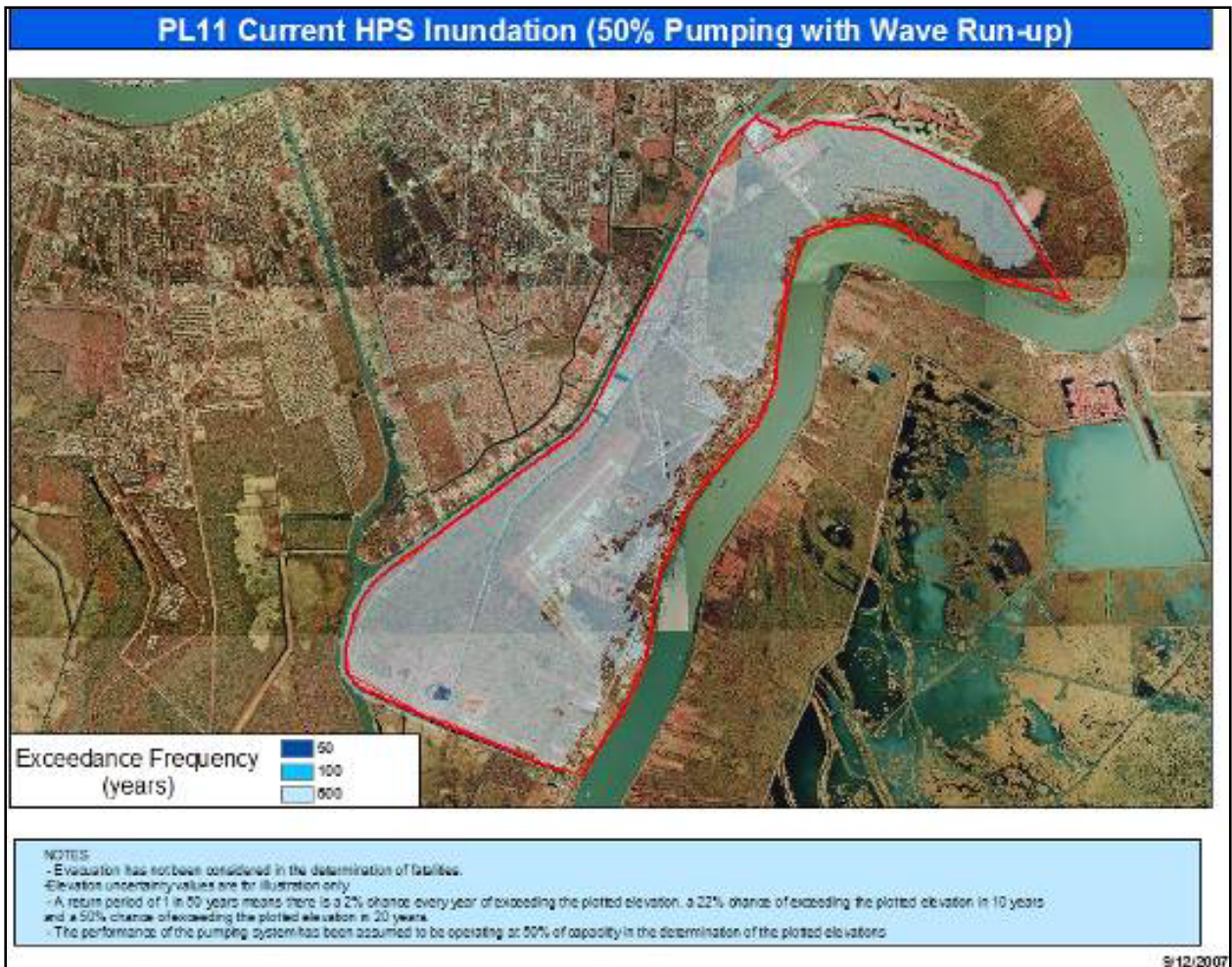


Figure 13-45 – Plaquemines (PL 11) – Current Inundation Risk – 50% Pumping

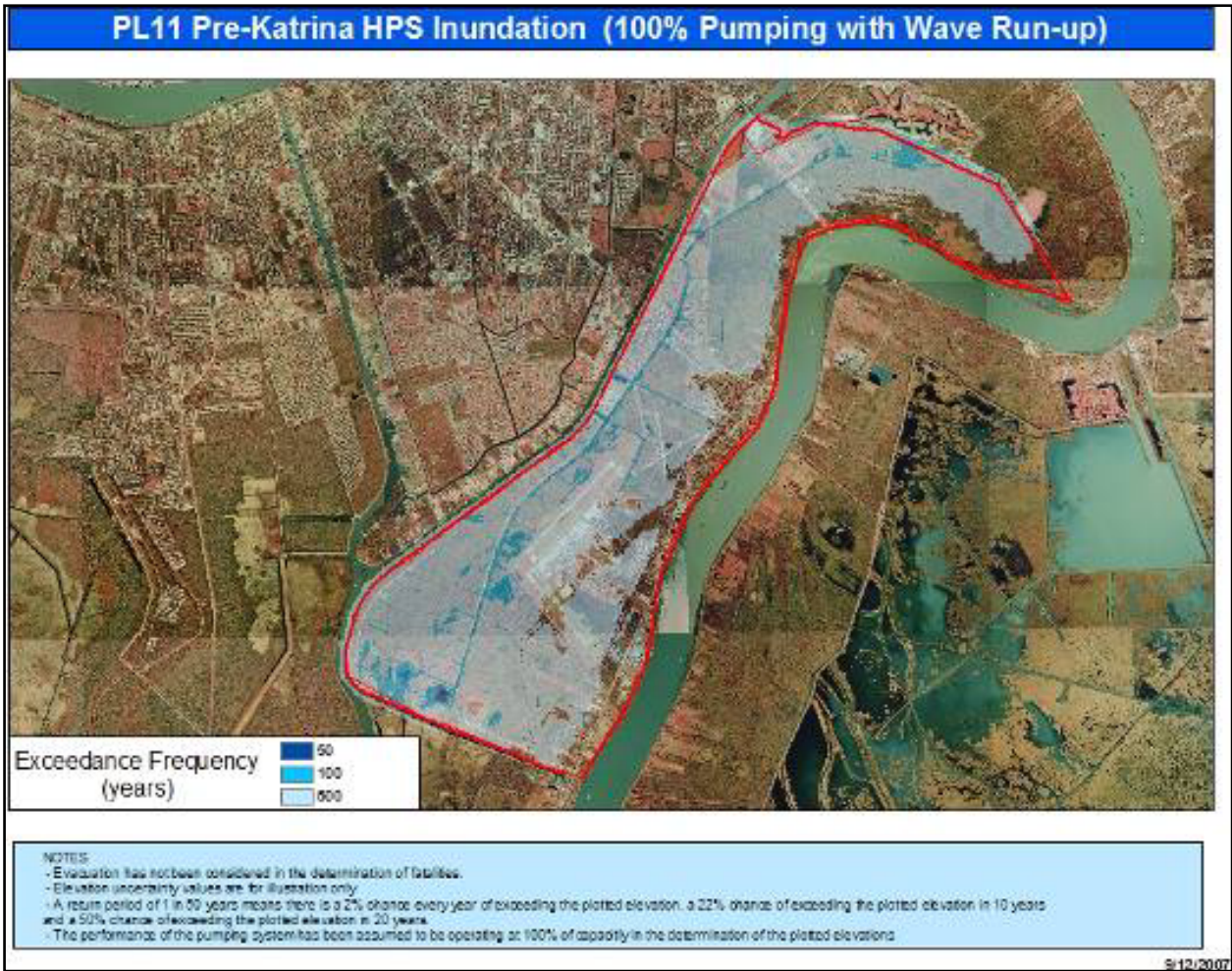


Figure 13-46 – Plaquemines (PL 11) – Pre-Katrina Inundation Risk – 100% Pumping

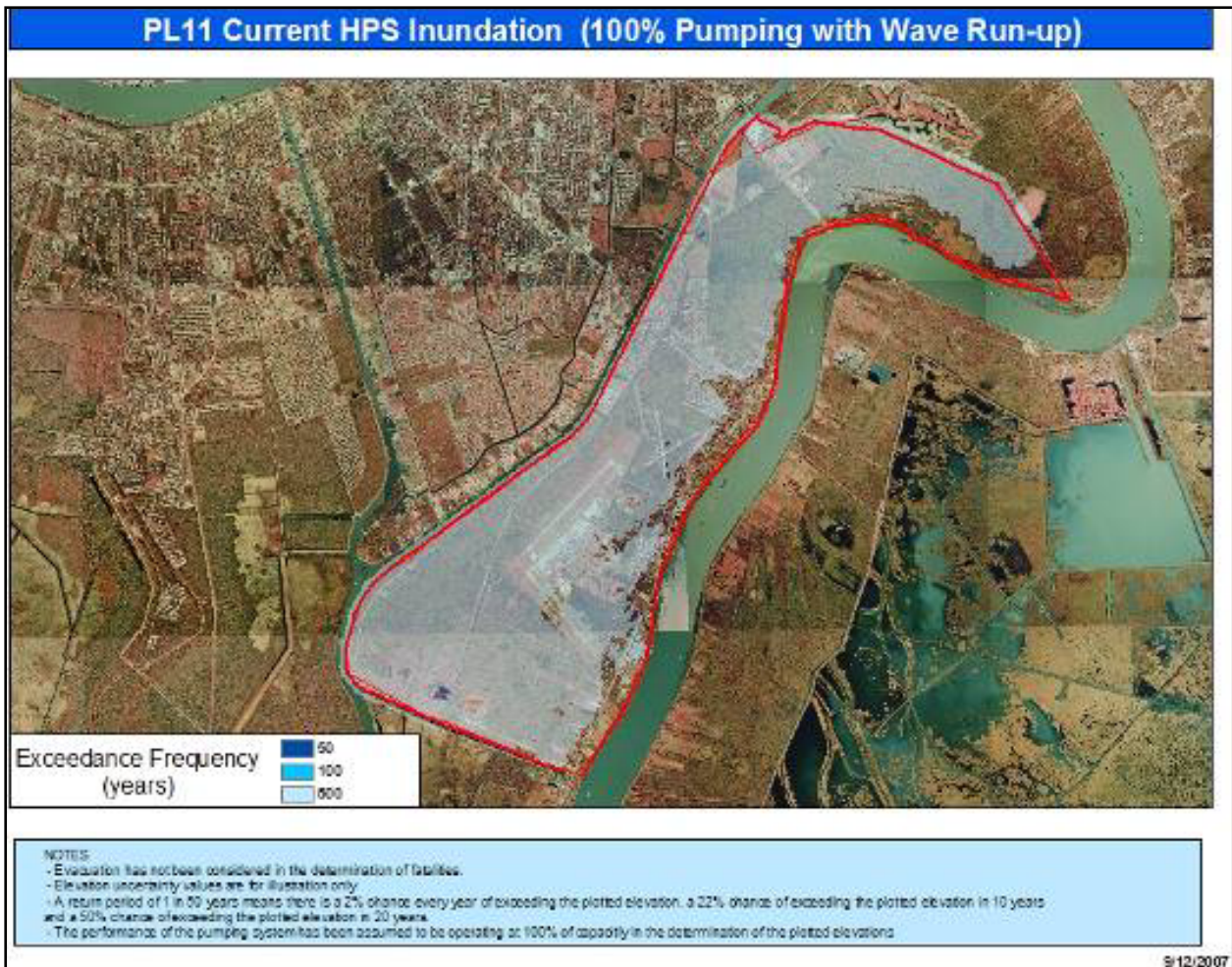


Figure 13-47 – Plaquemines (PL 11) – Current Inundation Risk – 100% Pumping

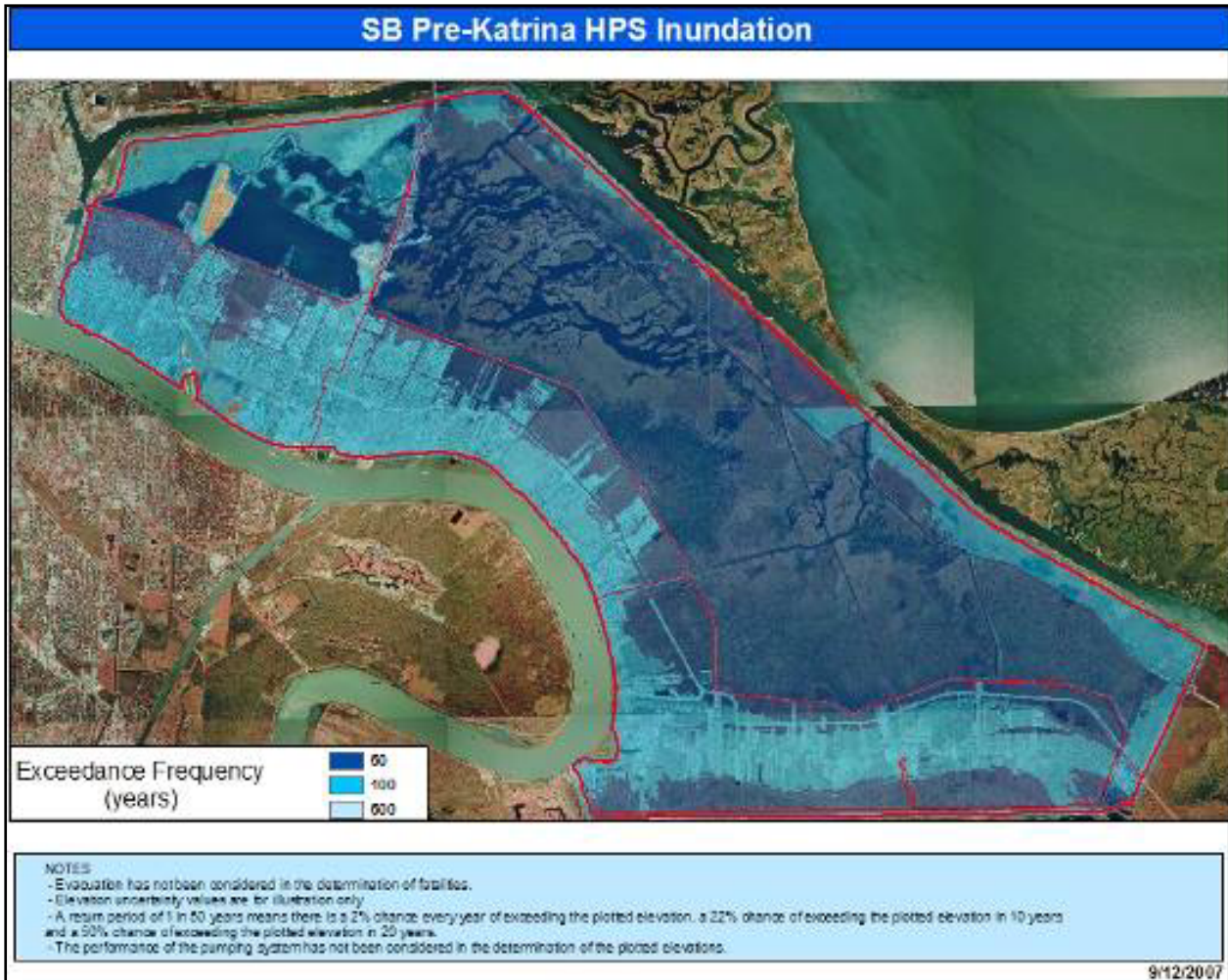


Figure 13-48 – St. Bernard – Pre-Katrina Inundation Risk – No Pumping

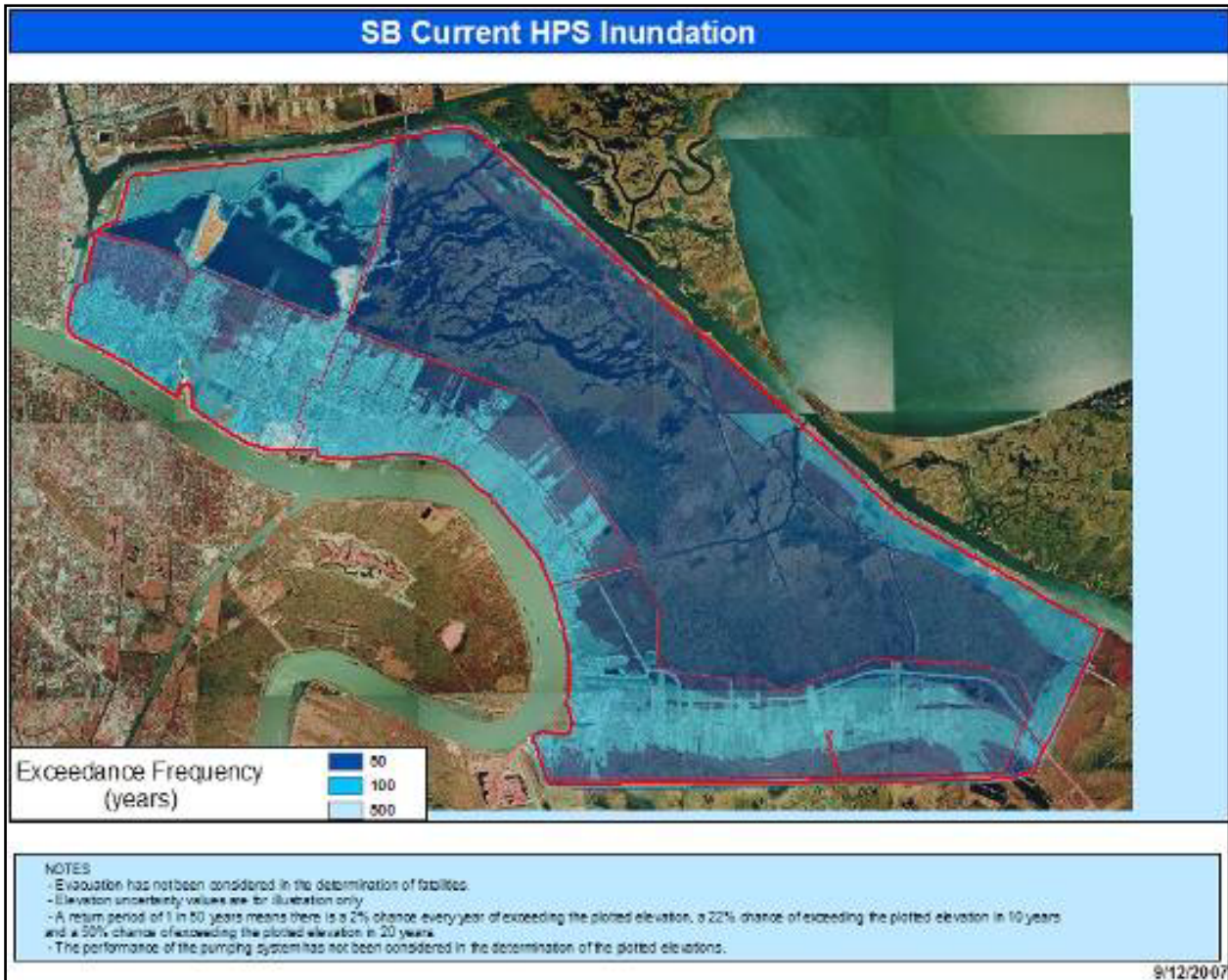


Figure 13-49 – St. Bernard – Current Inundation Risk – No Pumping

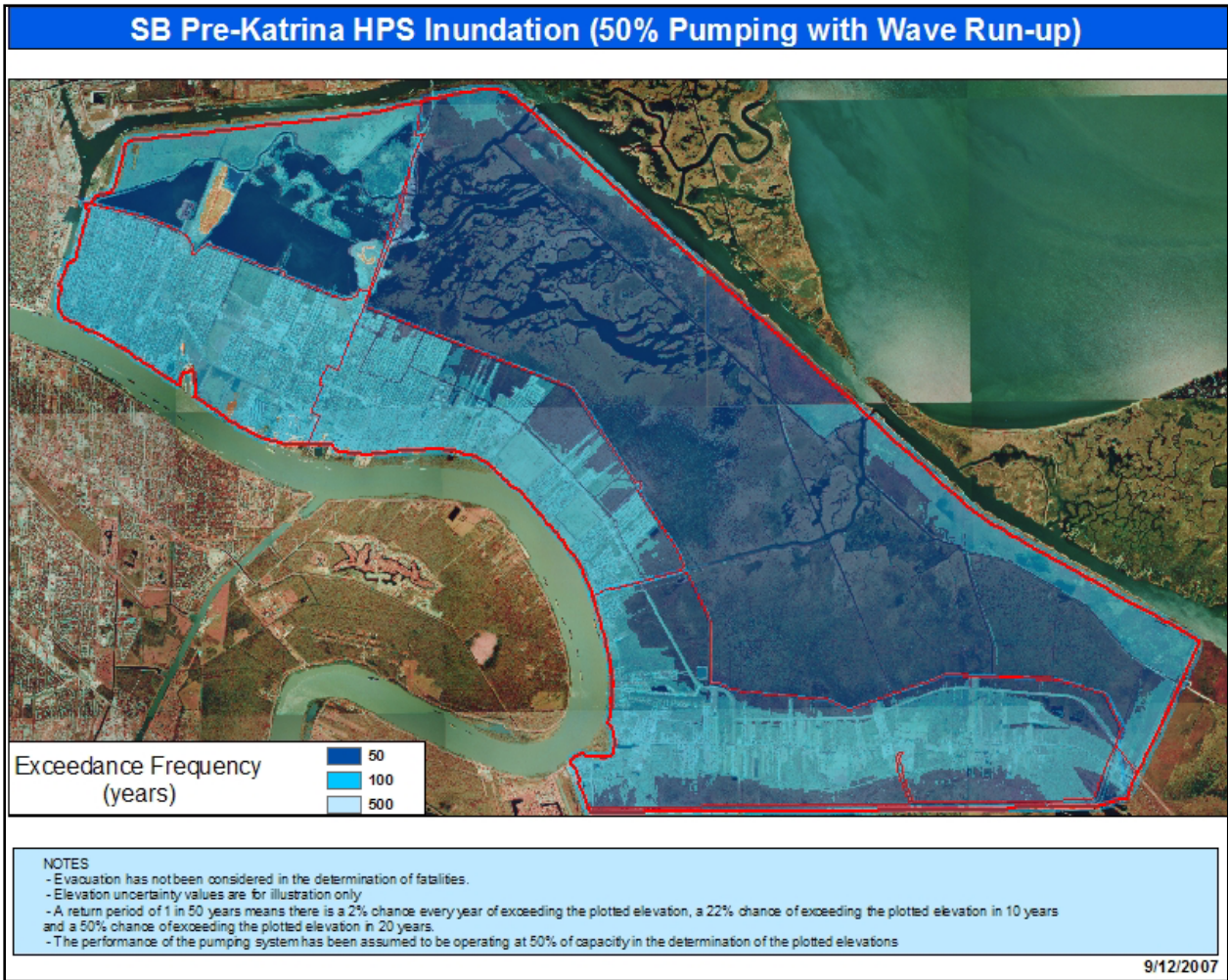


Figure 13-50 – St. Bernard – Pre-Katrina Inundation Risk – 50% Pumping

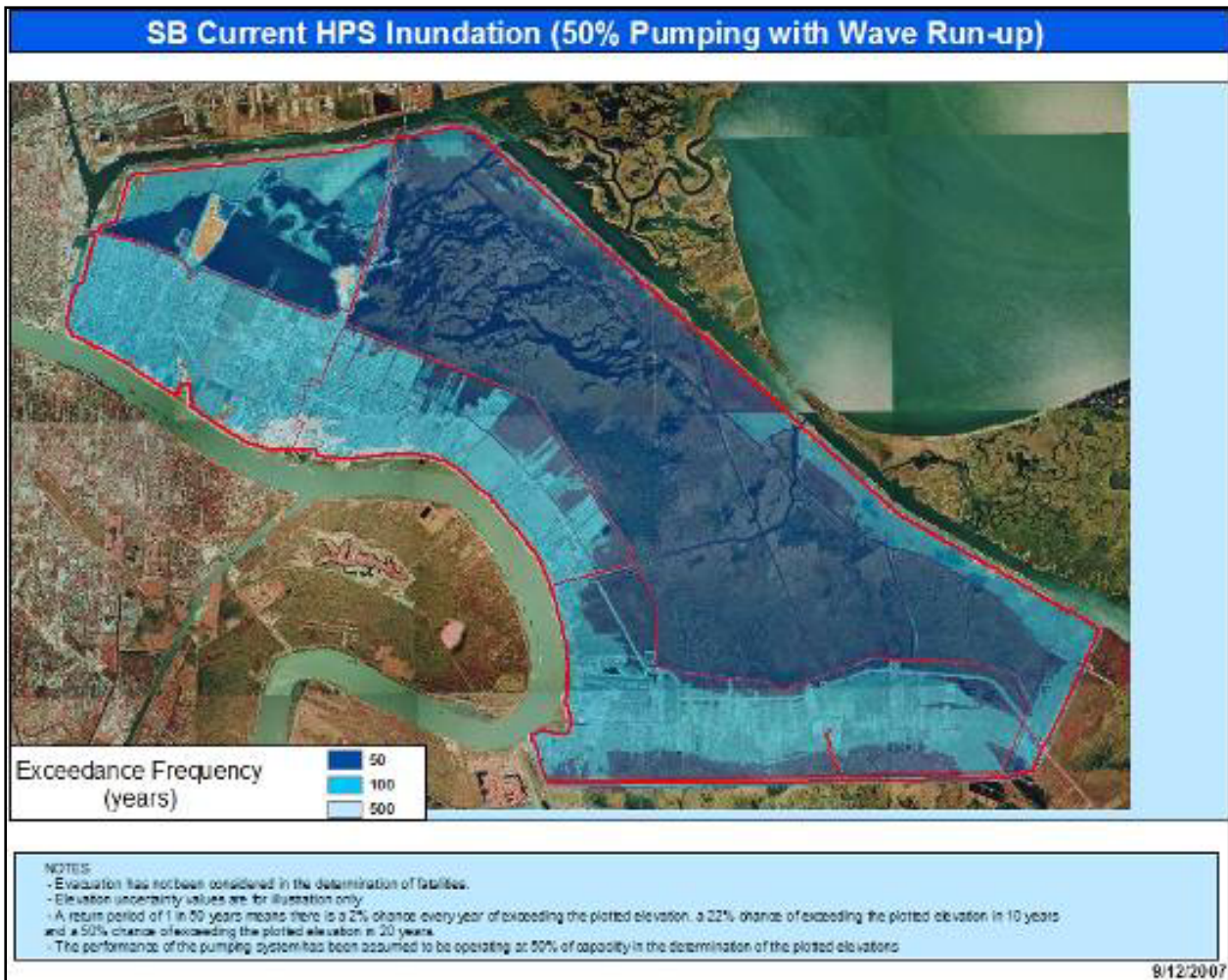


Figure 13-51 – St. Bernard – Current Inundation Risk – 50% Pumping

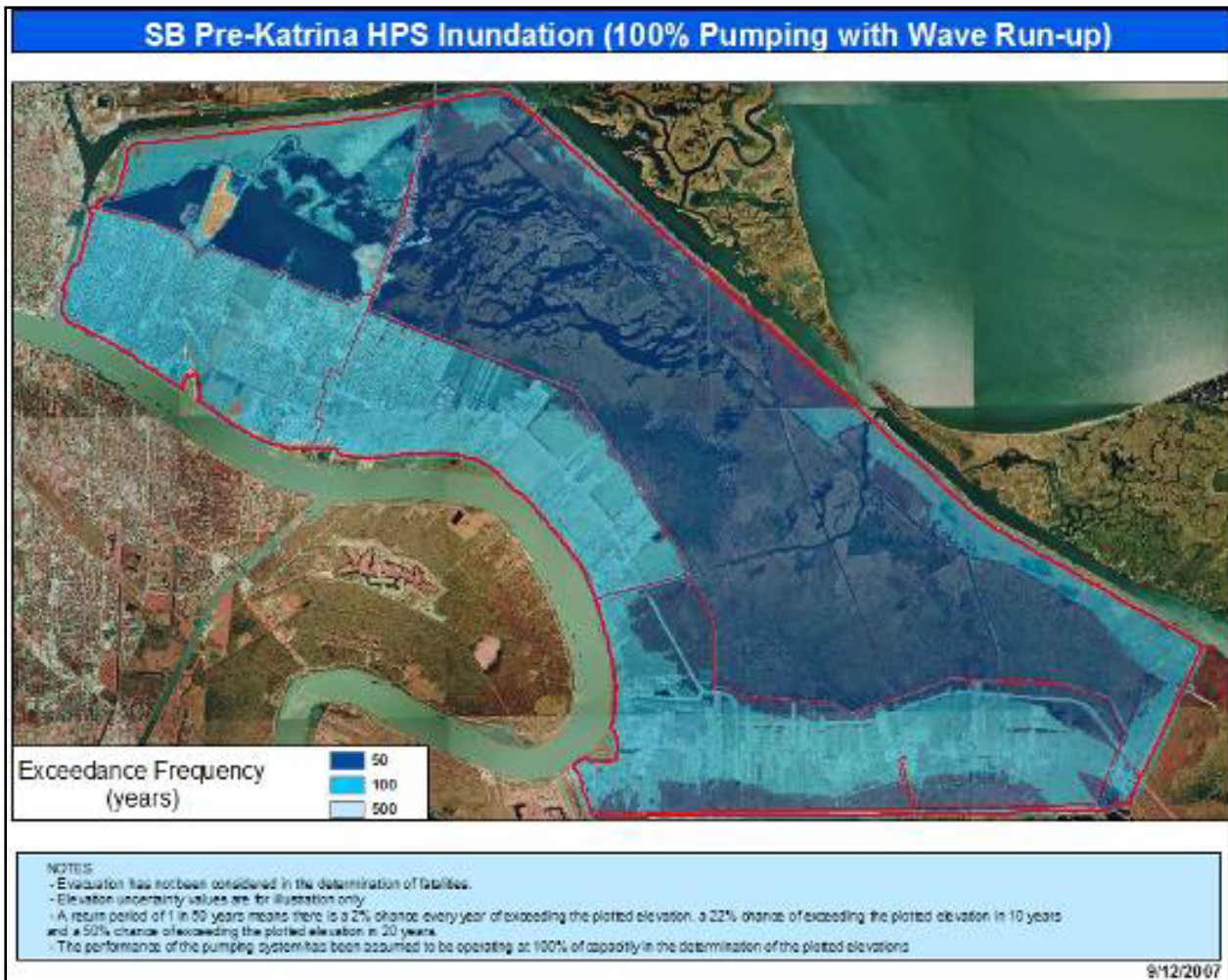


Figure 13-52 – St. Bernard – Pre-Katrina Inundation Risk – 100% Pumping

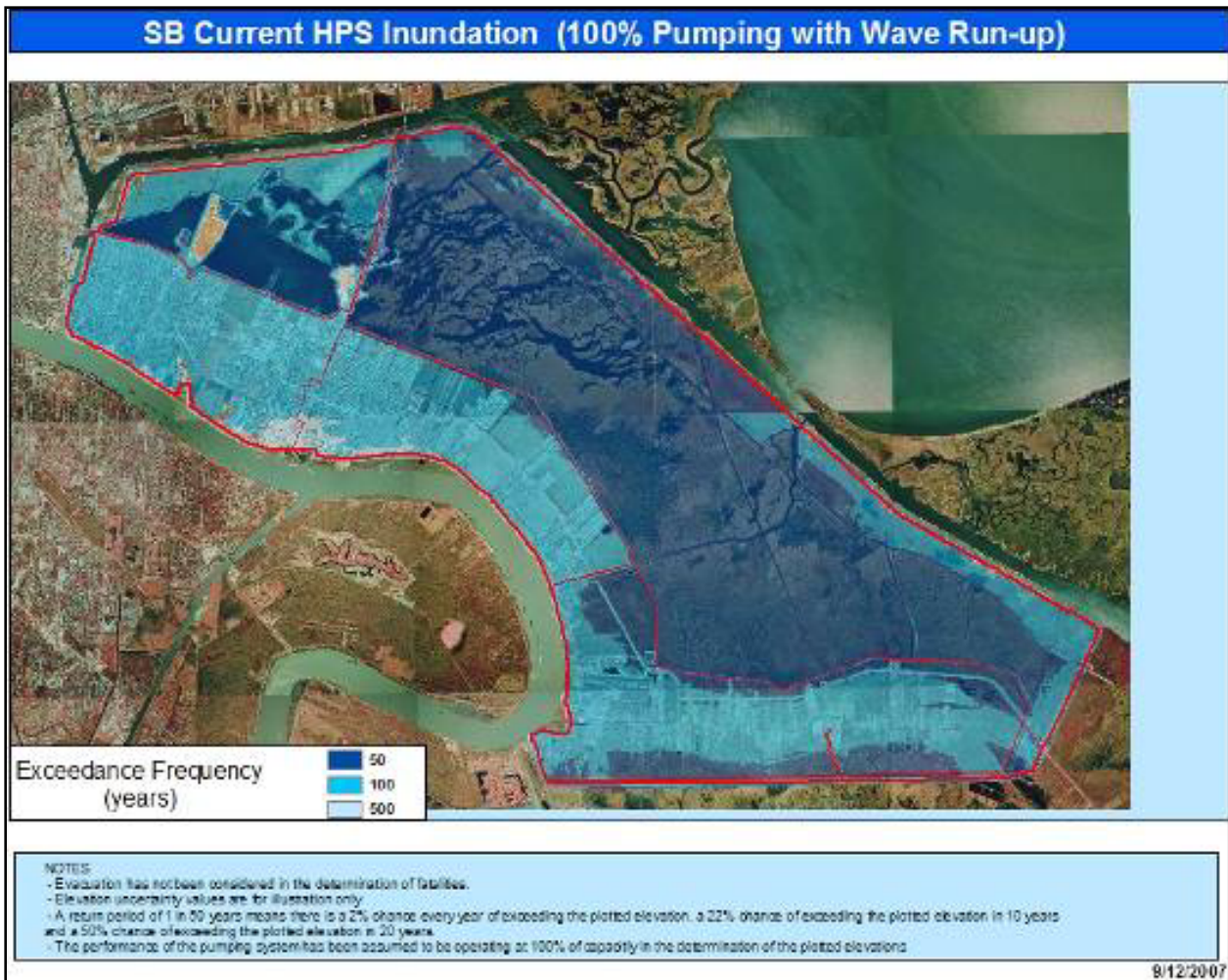


Figure 13-53 – St. Bernard – Current Inundation Risk – 100% Pumping

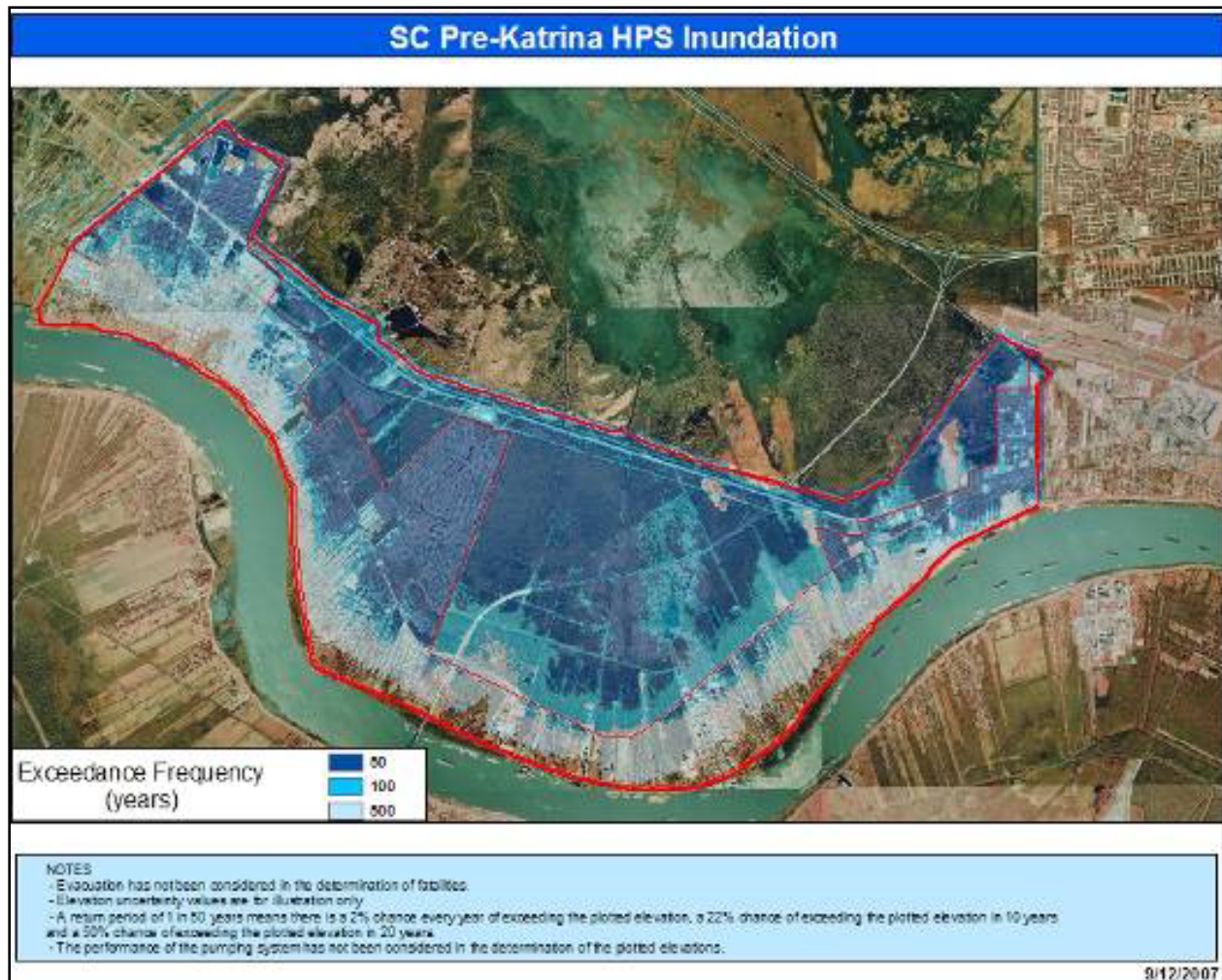


Figure 13-54 – St. Charles – Pre-Katrina Inundation Risk – No Pumping

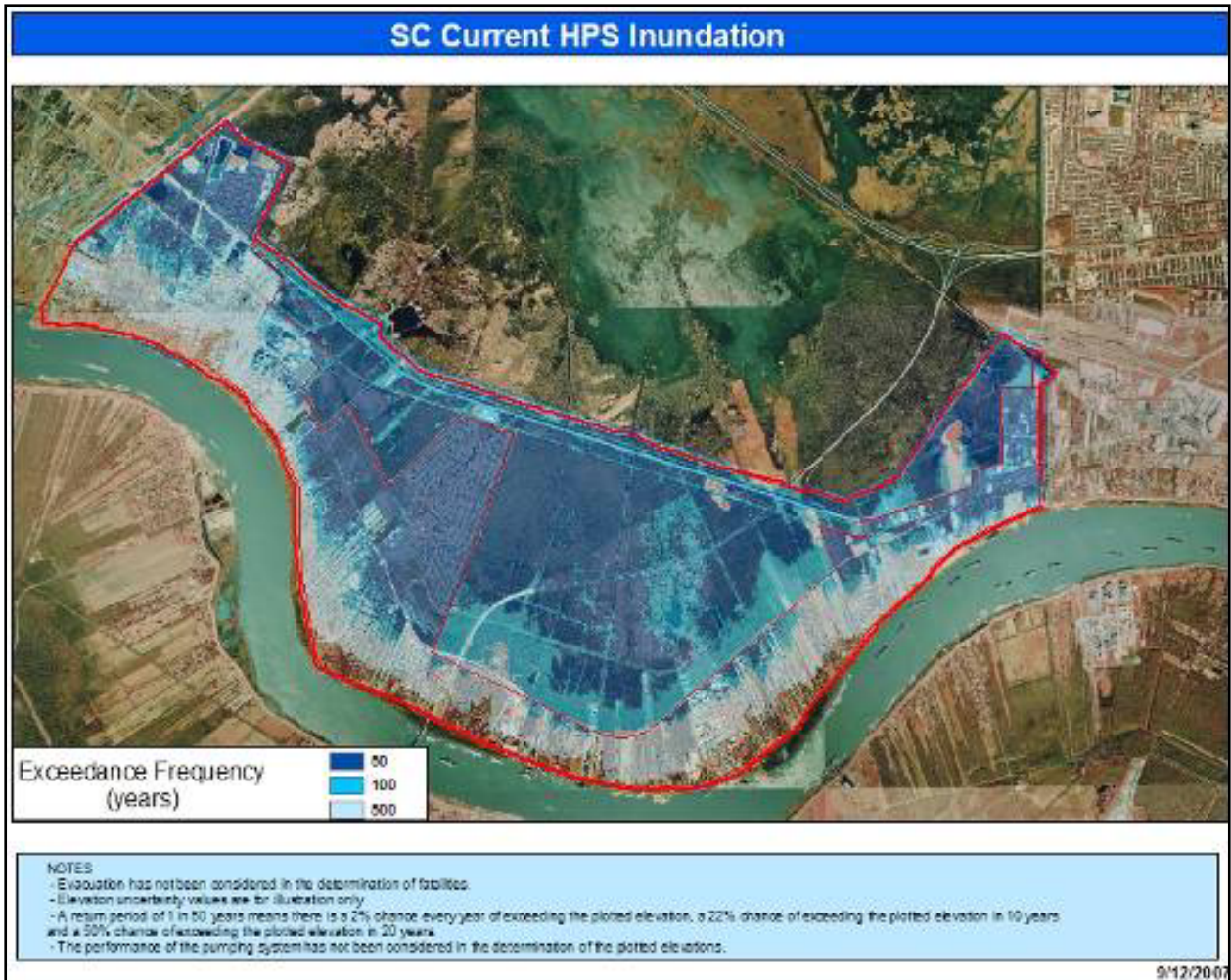


Figure 13-55 – St. Charles – Current Inundation Risk – No Pumping

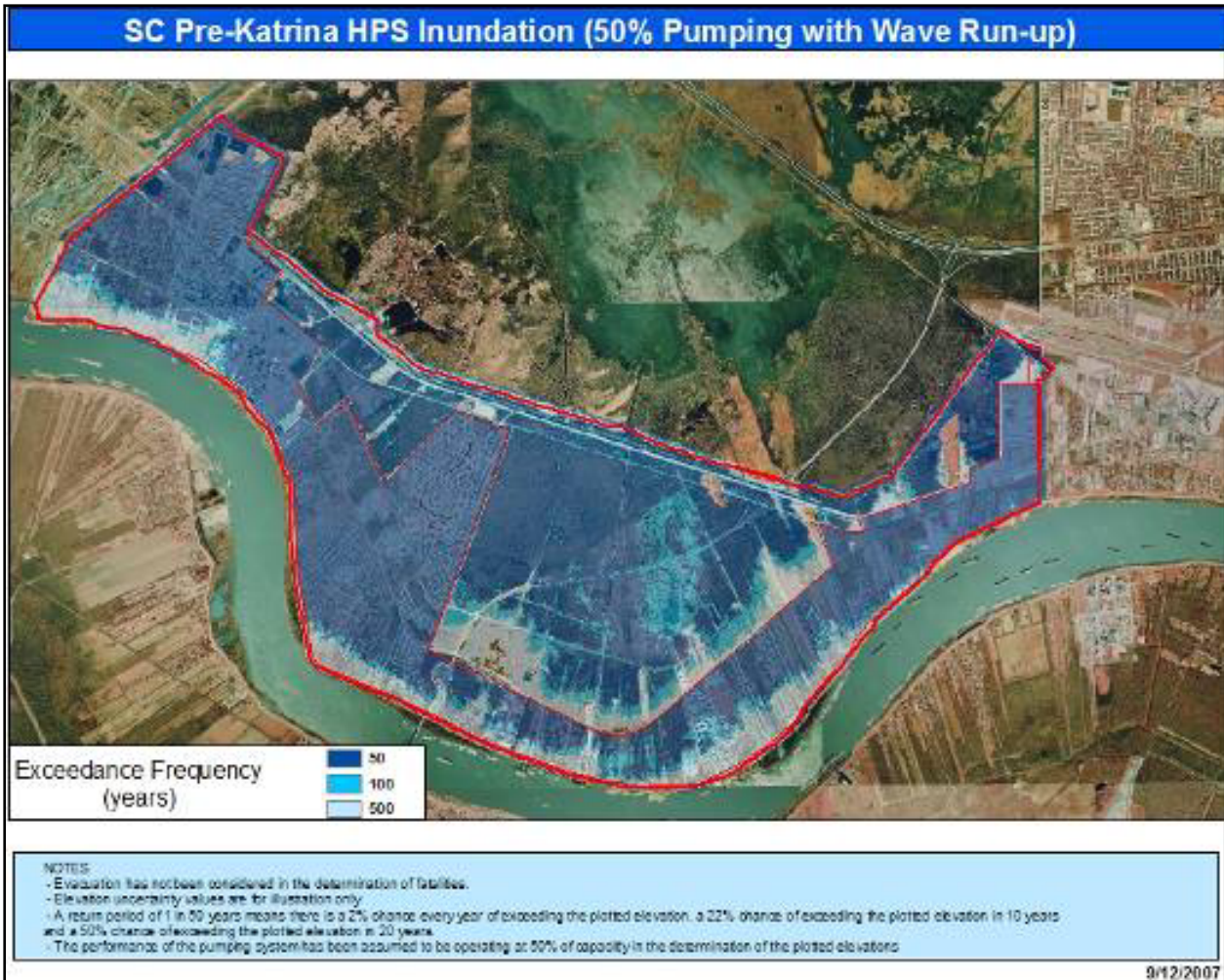


Figure 13-56 – St. Charles – Pre-Katrina Inundation Risk – 50% Pumping

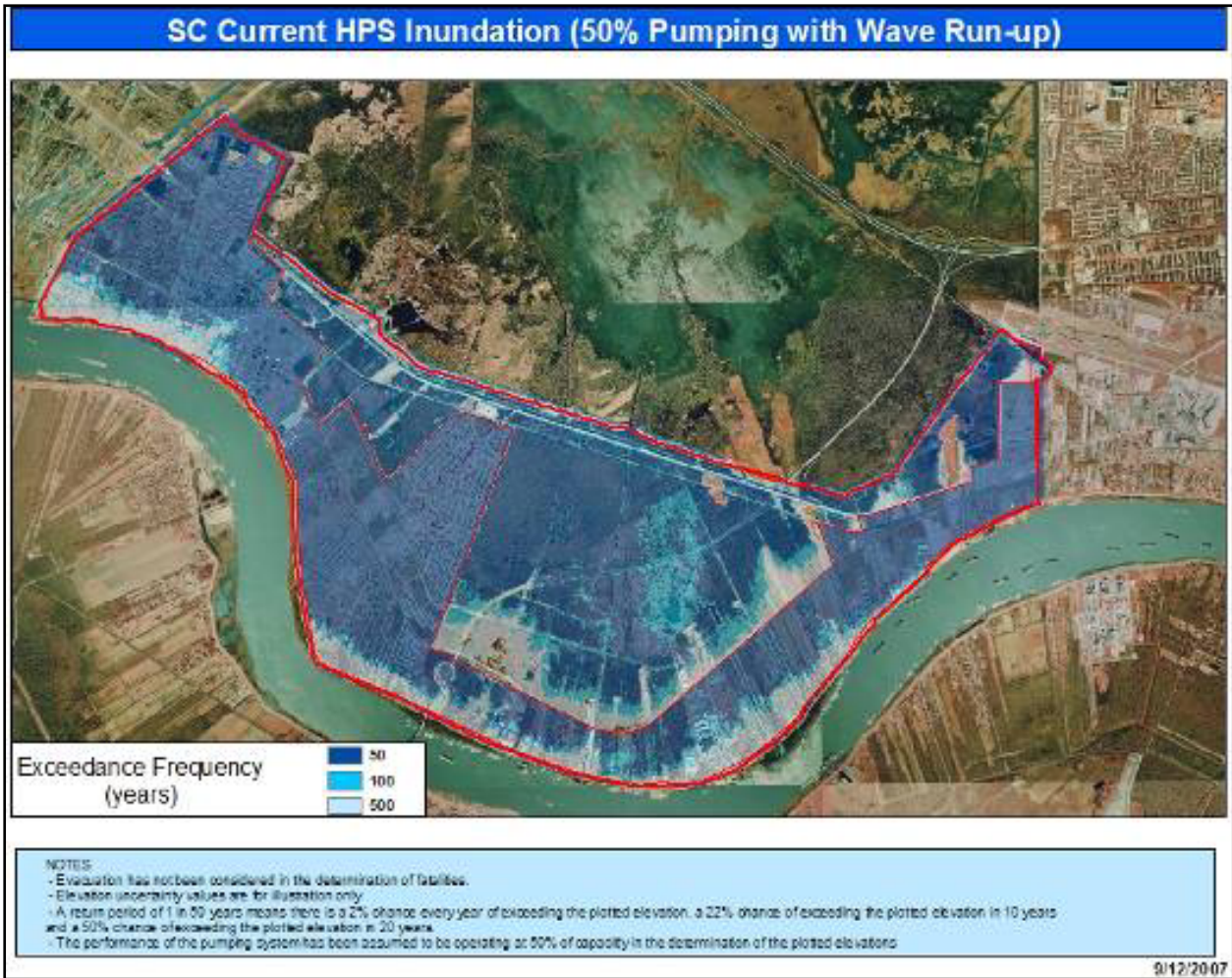


Figure 13-57 – St. Charles – Current Inundation Risk – 50% Pumping

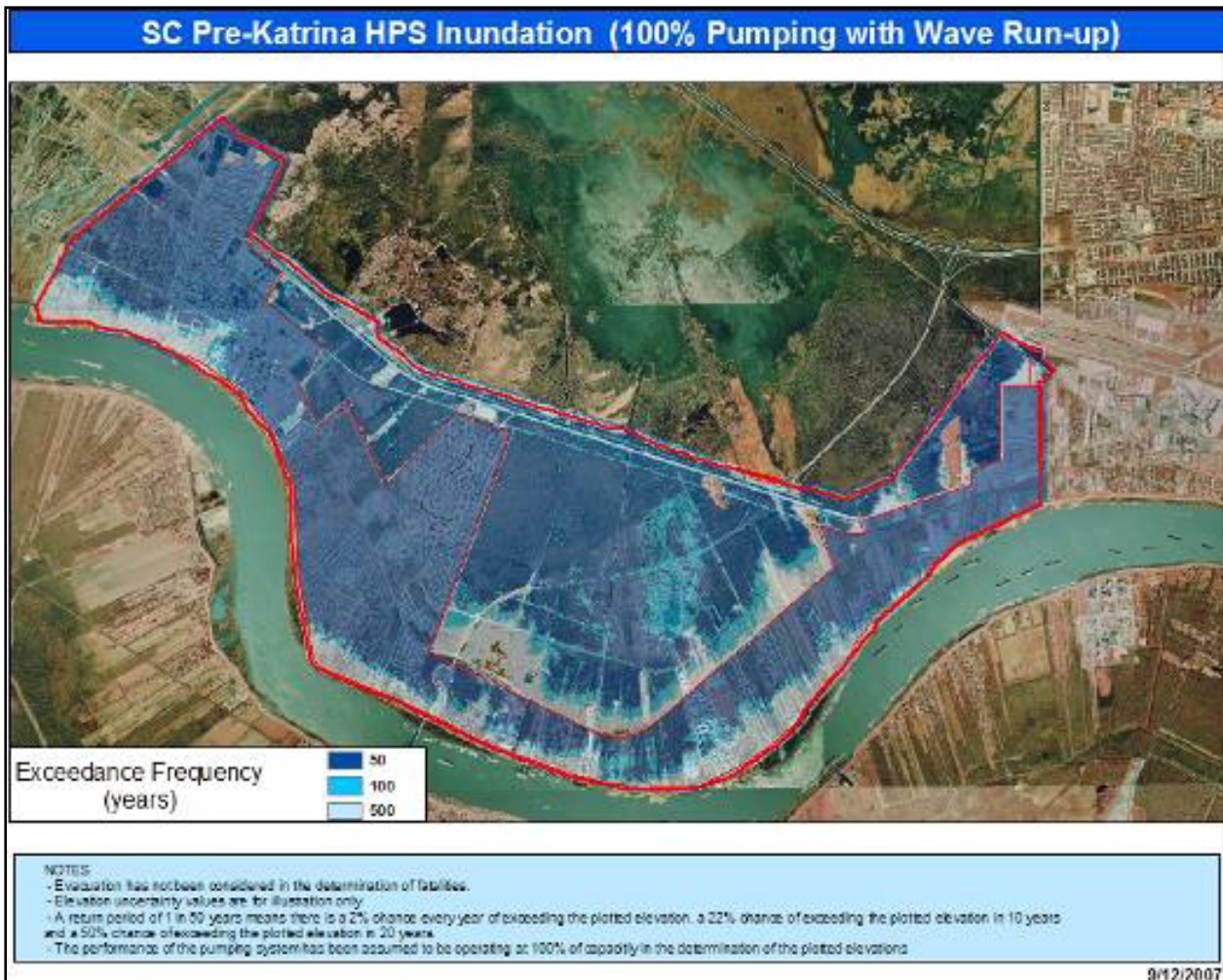


Figure 13-58 – St. Charles – Pre-Katrina Inundation Risk – 100% Pumping

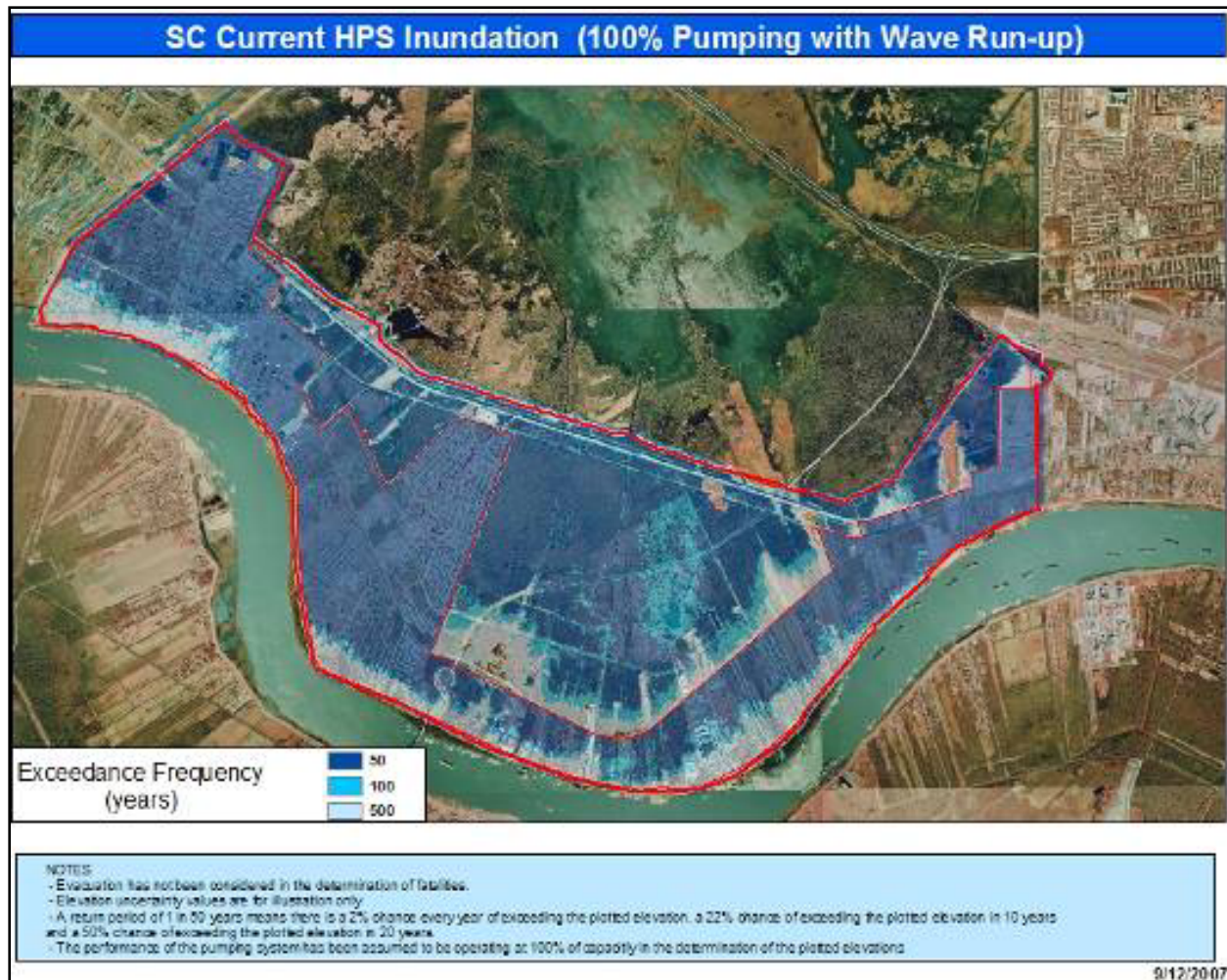


Figure 13-59 – St. Charles – Current Inundation Risk – 100% Pumping

Appendix 14

Hurricane Protection System

The Pre-Katrina and Current hurricane protections system (HPS) have been defined in the risk analysis using information from USACE design documents, Task Force Guardian, other IPET teams and extensive field surveys conducted by the IPET Risk Team. The Pre-Katrina analysis is intended to examine the actual risks based on the HPS that existed in New Orleans prior to the storm. It is not intended to recreate the “as-designed” HPS and therefore considers the failure modes that have been studied by IPET, the actual elevations of walls and levees, the in-place engineering properties of the system components and the foundation conditions that existed before Katrina struck.

The current hurricane protections system (HPS) was defined as the system that existed on 1 June 2007 using information from the New Orleans District, USACE design documents for improvements made to the HPS since hurricane Katrina, Task Force Guardian, Task Force Hope other IPET teams and the extensive field surveys conducted by the Risk Team. The Pre-Katrina HPS risk model was modified to reflect the changes made to the system to repair damage and make critical improvements. The revised model is intended to examine the current risks based on the HPS that now exists in New Orleans. It considers the failure modes that have been studied by IPET, the actual elevations of walls and levees, the in-place engineering properties of the system components and the foundation conditions that were found to exist on 1 June 2007.

Parish Basins and Sub-basins

The Pre-Katrina and Current HPS limits follow the six main parish boundaries, and each parish is subdivided into drainage sub-basins that define how water is collected within the parish. Figure 14-1 depicts the parish and sub-basin boundaries that make up the HPS. Boundaries between adjacent sub-basins are modeled to allow interflow between them based on the elevations of physical features that separate the sub-basins. Sub-basin definitions and interflow elevations were provided by the IPET Interior Drainage and Pumping Team. The physical features of each parish included in the Pre-Katrina and Current HPS used in the risk model are discussed in this appendix, and detailed information for each parish is provided in subsequent appendices.

Reaches

The boundaries of the basins that provide hurricane protection are divided into reaches that have similar engineering properties including structure type, failure modes, materials of construction and foundation type. These reaches are shown in tables for each basin that provide:

- Reach length
- Reach elevation in NAVD88 2004.65
- Structure type (W=Wall, L = Levee)
- Foundation type (H=Hydraulic fill, C=Clay, P=Pile)
- Sub-basin reference was water from the reach will flow into.

Three reaches were added to the Current HPS to model the canal closure gates at the end of the 17th Street, London Avenue and Orleans Avenue drainage canals. These reaches are numbers 136, 137 and 138 in the Current HPS. Table 14-18 compares the Pre-Katrina and Current HPS crest elevations. All other reach physical characteristics are identical in both HPS. Note differences in the fragility of reaches are discussed in Appendix 10.

Transitions

HPS components that form part of the flood barrier such as: structural transitions from levee to concrete wall, drainage structures, ramps that must be sandbagged during a flood event, closure gates and pump stations are included in the risk model. Tables are provided for each sub-basin that show:

- Type of component (T= transition, D=Drainage structure, R=Ramp, G=gate and P=Pump station)
- Reach where the component is located
- Width of the potential opening
- Invert elevation for water flowing through the component
- Sub-basin reference was water from the component will flow into.
- A description of the component.

The physical characteristics of transitions are identical in the Pre-Katrina and Current HPS.

Features

Additional gate and other features of the HPS are included in the risk model and tables are provided that show:

- Type of component (G= gate and O=Other type of structure)
- Reach where the component is located
- Other feature that the component is correlated with.
- Width of the potential opening
- Invert elevation for water flowing through the component
- Sub-basin reference where water from the feature will flow into.
- A description of the component.

The physical characteristics of features are identical in the Pre-Katrina and Current HPS.

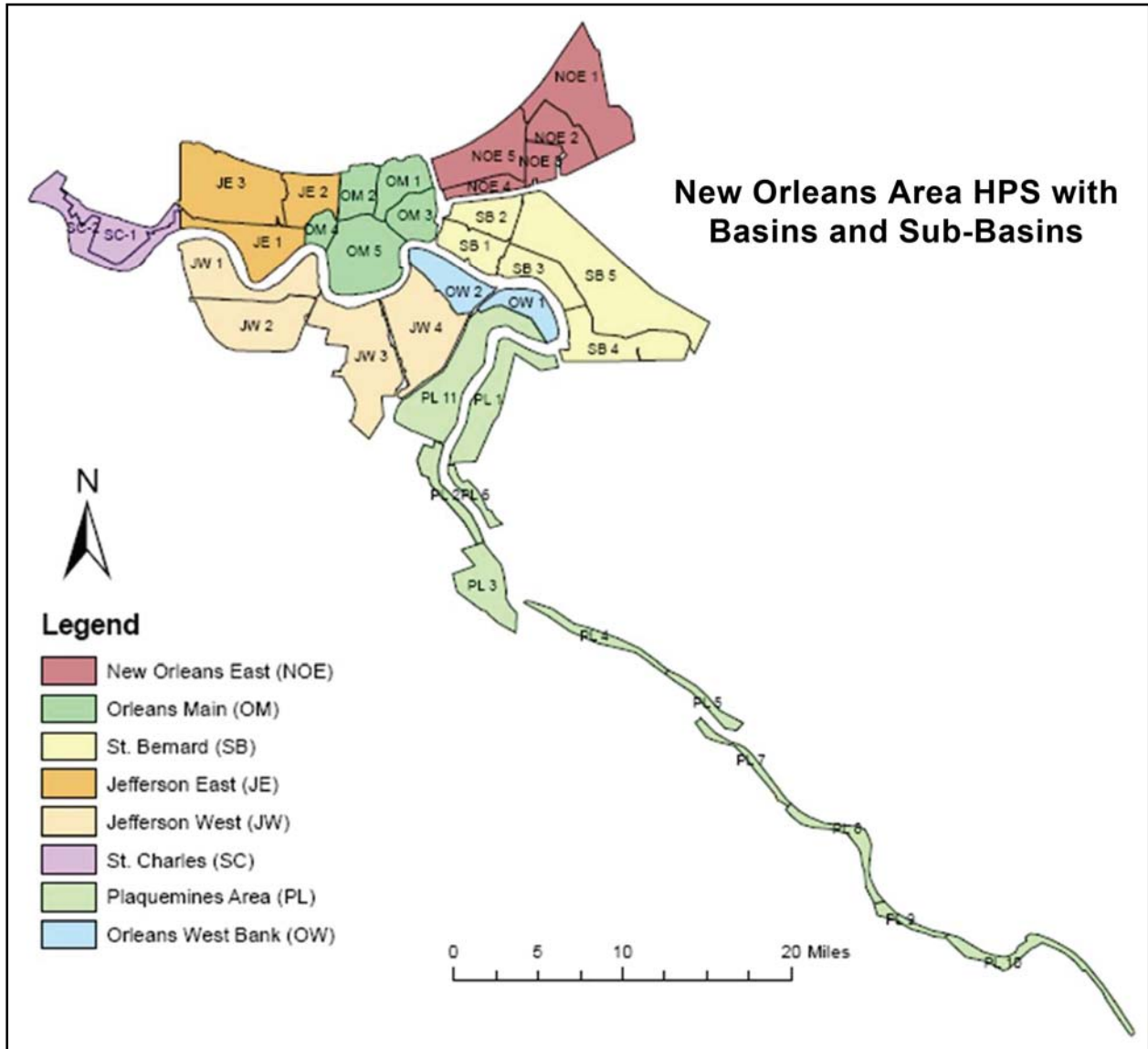


Figure 14-1. Pre-Katrina HPS Basins and Sub-basins

New Orleans East

The reaches that make up the New Orleans East risk model are shown in Figure 14-2, and data are provided in Tables 14-1, 14-2 and 14-3 for reaches, transitions and features, respectively.

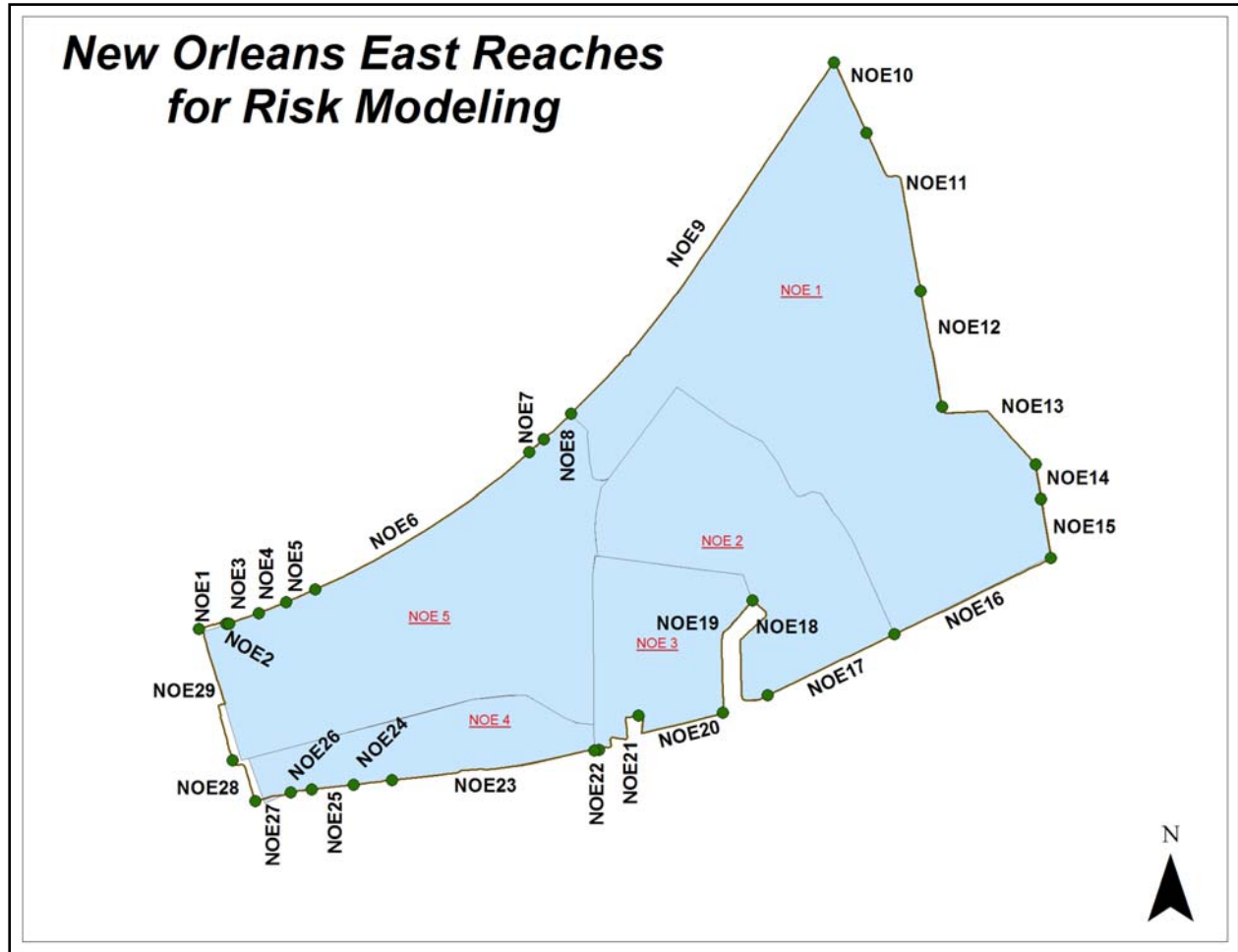


Figure 14-2. New Orleans East Reaches

Table 14-1 New Orleans East Reaches					
Risk Model Reach No.	Reach Length (ft)	Pre-Katrina Elevation (NAVD88 2004.65)	Reach Type	Foundation Material Type (H, C, P)	Subpolder Reference (3)
1	2,405	10.80	W	H	NOE5
2	250	10.80	L	H	NOE5
3	2,325	10.80	W	H	NOE5
4	2,330	10.80	L	H	NOE5
5	2,270	10.80	W	H	NOE5
6	19,110	13.00	L	H	NOE5
7	1,475	13.00	W	H	NOE5
8	2,725	13.00	L	H	NOE5
9	32900	18.20	L	H	NOE1
10	5,830	13.80	L	H	NOE1
11	13,325	14.00	L	H	NOE1
12	8,910	15.00	L	H	NOE1
13	9,185	15.80	L	H	NOE1
14	2,615	16.00	L	H	NOE1
15	4,470	16.00	L	H	NOE1
16	13,045	16.00	L	H	NOE1
17	10,570	16.00	L	H	NOE2
18	10,760	17.90	W	H	NOE2
19	9,320	17.90	W	H	NOE3
20	7,905	16.00	L	H	NOE3
21	5520	16.00	W	H	NOE3
22	385	16.00	L	H	NOE3
23	15,320	13.90	L	H	NOE4
24	2,910	13.80	W	H	NOE4
25	3,230	13.80	L	H	NOE4
26	1,640	13.80	W	H	NOE4
27	2,750	13.80	L	H	NOE4
28	4,100	12.00	L	H	NOE4
29	11,185	13.50	W	H	NOE5

Table 14-2 New Orleans East Transitions

Feature Number	Transition Type	Reach	Width (ft)	Elevation (ft) (NAVD88 2004.65)	Sub-Basin	Description of Feature
1	R	NOE1	25	9	NOE5	Ramp between RR track and bridge
2	T	NOE3	125	5.0	NOE5	LWT NOE 2/3
3	T	NOE3	80	5.0	NOE5	WLT NOE 3/4
4	T	NOE5	155	5.0	NOE5	LWT NOE 4/5
5	T	NOE5	95	5.0	NOE5	WLT NOE 5/6
6	T	NOE7	140	5.0	NOE5	LWT NOE 6/7
7	T	NOE7	130	5.0	NOE5	WLT NOE 7/8
8	D	NOE9	450	16.5	NOE1	Drainage Structure through levee
9	D	NOE9	830	17.5	NOE1	Drainage Structure through levee
10	D	NOE10	65	14.0	NOE1	Drainage Structure through levee
11	R	NOE10	215	8.0	NOE1	I-10 SB ramps
12	R	NOE11	145	7.0	NOE1	I-10 NB ramps
13	G	NOE11	255	6.0	NOE1	Hwy 11 Gate
14	D	NOE11	75	11.0	NOE1	Drainage Structure
15	D	NOE12	55	15.0	NOE1	Drainage Structure
16	G	NOE12	330	15.0	NOE1	Hwy 90 Gate
17	D	NOE14	120	17.0	NOE1	Drainage Structure
18	G	NOE15	95	14.0	NOE1	CSX RR Transition
19	P	NOE17	870	17.3	NOE2	Pump Station #15
20	T	NOE18	135	5.0	NOE2	LWT NOE 17/18
21	T	NOE19	60	5.0	NOE3	WLT NOE 19/20
22	R	NOE20	75	13.0	NOE3	Saturn Blvd Ramp
23	T	NOE21	140	17.0	NOE3	LWT NOE 20/21
24	T	NOE21	25	5.0	NOE3	WLT NOE 21/22
25	P	NOE23	50	5.0	NOE4	Grant Street PS
26	R	NOE23	40	13.0	NOE4	Ramp in levee at steel plant
27	R	NOE23	40	14.0	NOE4	Ramp in levee at steel plant
28	T	NOE24	75	13.0	NOE4	LWT NOE 23/24 - sheet pile transition
29	T	NOE24	80	14.0	NOE4	WLT NOE 24/25
30	T	NOE26	75	13.0	NOE4	LWT NOE 25/26 - sheet pile transition
31	T	NOE26	60	13.0	NOE4	WLT NOE 26/27
32	P	NOE26	150	13.0	NOE4	Amid PS - PS #20
33	R	NOE27	70	12.0	NOE4	Ramp to Offload Facility
34	R	NOE27	70	9.0	NOE4	Jourdan Rd Ramp
35	G	NOE27	90	5.0	NOE4	RR spur gate closure adjacent to Jourdan Road
36	G	NOE28	100	11.0	NOE4	Gate E-4
37	G	NOE28	100	6.0	NOE4	Gate E-5
38	G	NOE28	195	12.0	NOE4	Gate E-6
39	G	NOE28	135	12	NOE4	Gate E-7
40	R	NOE28	35	12	NOE4	Almonaster Ave Ramp from bridge
41	G	NOE 28	80	13	NOE4	Gate E-8
42	G	NOE28	90	13	NOE4	Gate E-9
43	T	NOE29	95	13	NOE5	LWT NOE 28/29
44	R	NOE29	50	13	NOE5	Jourdan Rd Ramp at Dwyer Road
45	G	NOE29	30	6	NOE5	RR Gate near Hayne Blvd

Table 14-3 New Orleans East Features

Feature Number	Gate (G) or Other Point Feature (O)	Reach	Correlated Features	Width (ft)	Elevation (ft) (NAVD88 2004.65) - Sill Elevation	Subbasin	Description of Feature	Notes
1	G	NOE1	1	35	1	NOE5	L-13 Swing gate into Lakefront airport by IHNC (under bridge)	
2	G	NOE1	2	22.0	1.75	NOE5	Gate L14	
3	G	NOE1	3	63.0	-0.5	NOE5	Gate L15	
4	G	NOE7	4	32.0	-1.5	NOE5	Lincoln Beach FW Gate	
5	G	NOE11	5	30.0	6	NOE1	Hwy 11 Gate	
6	G	NOE12	6	80.0	10	NOE1	Hwy 90 Gate	
7	G	NOE15	7	20.0	5.7	NOE1	CSX Gate	
8	G	NOE18	8	20.0	9.75	NOE2	Michoud Gate 1	Not used
9	G	NOE18	9	20.0	9.75	NOE2	Michoud Gate 2	Not used
10	G	NOE18	10	20.0	9.75	NOE2	Michoud Gate 3	Open
11	G	NOE18	11	20.0	9.75	NOE2	Michoud Gate 4	Open
12	G	NOE18	12	20.0	9.75	NOE2	Michoud Gate 5	Not used
13	G	NOE18	13	20.0	9.75	NOE2	Michoud Gate 6	Open
14	G	NOE18	14	20.0	9.75	NOE2	Michoud Gate 7	Open
15	G	NOE18	15	20.0	9.75	NOE2	Michoud Gate 8	Not used
16	G	NOE18	16	20.0	9.75	NOE2	Michoud Gate 9	Open
17	G	NOE18	17	20.0	9.75	NOE2	Michoud Gate 10	Open
18	G	NOE18	18	20.0	9.75	NOE2	Michoud Gate 11	Open
19	G	NOE18	19	20.0	9.75	NOE2	Michoud Gate 12	Open
20	G	NOE18	20	20.0	9.75	NOE2	Michoud Gate 13	Open
21	G	NOE18	21	20.0	9.75	NOE2	Michoud Gate 14	Open
22	G	NOE18	22	20.0	9.75	NOE2	Michoud Gate 15	Open
23	G	NOE18	23	20.0	9.75	NOE2	Michoud Gate 16	Open
24	G	NOE18	24	20.0	9.75	NOE2	Michoud Gate 17	Open
25	G	NOE18	25	20.0	9.75	NOE2	Michoud Gate 18	Not used
26	G	NOE19	26	20.0	12.8	NOE3	NASA Gate 1 to power plant	Open
27	G	NOE21	27	20.0	12.8	NOE3	NASA Gate 2 to power plant	Open
28	G	NOE21	28	20.5	6.5	NOE3	Gate closure N-1 for Bulk Loading Facility	Open
29	G	NOE27	29	20.0	7.8	NOE4	RR spur gate closure adjacent to Jourdan Road	Open
30	G	NOE28	30	20.0	6.5	NOE4	Gate E-4	Closed
31	G	NOE28	31	20.0	6.5	NOE4	Gate E-5	Open
32	G	NOE28	32	17.0	6.5	NOE4	Gate E-6	Closed - RR spur
33	G	NOE28	33	20.0	7.2	NOE4	Gate E-7	Closed
34	G	NOE28	34	37.0	6.5	NOE4	Gate E-8	Open RR
35	G	NOE29	35	35.0	6.5	NOE4	Gate E-9	Closed road
36	G	NOE29	36	15.0	7.2	NOE5	Gate E-10	Open to docks

37	G	NOE29	37	17.0	4.7	NOE5	Gate E-11	Open, RR, heavily damaged
38	G	NOE29	38	20.0	5.2	NOE5	Gate E-12	Open road
39	G	NOE29	39	17.0	2.2	NOE5	Gate E-13	Open RR
40	G	NOE29	40	30.0	-0.8	NOE5	Gate E-14	Open road Hayne Blvd
41	G	NOE29	41	33.0	9.2	NOE5	Gate E-15	RR gate
42	G	NOE29	42	32.0	5.7	NOE5	Gate L-12	Open road

Jefferson

The reaches that make up the Jefferson risk model are shown in Figure 14-3, and data are provided in Tables 14-4, 14-5 and 14-6 for reaches, transitions and features, respectively.

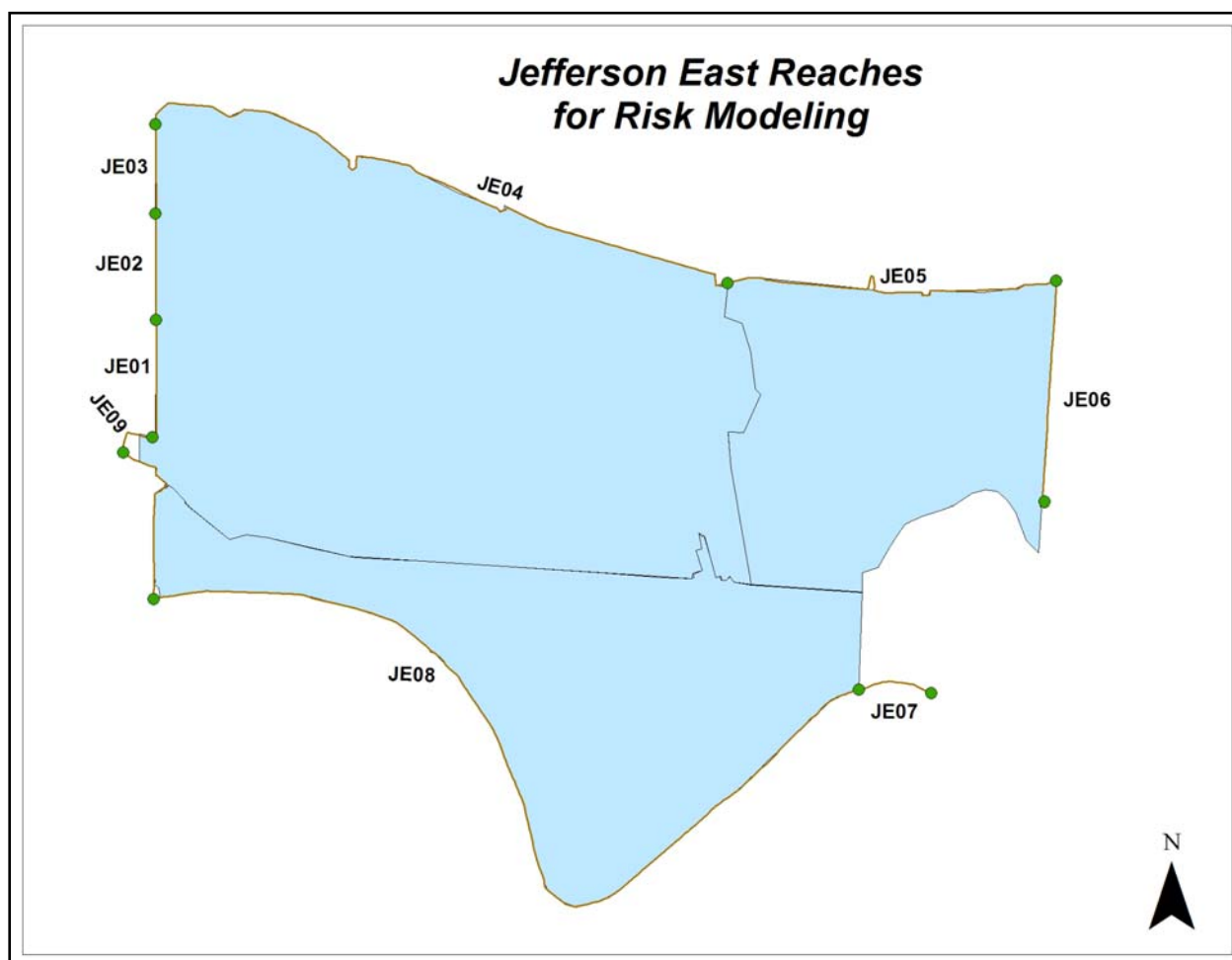


Figure 14-3. Jefferson East Bank Reaches

Table 14-4 Jefferson East Reaches					
Reach No.	Length (ft)	Pre-Katrina Elevation (NAVD88 2004.65)	Reach Type (1)	Foundation Material Type (H, C, P) (2)	Subbasin Reference (3)
30	6,745	12.80	W	C	JE3
31	5,915	13.90	W	C	JE3
32	4,945	13.90	W	C	JE3
33	36,430	14.40	L	C	JE3
34	19,925	15.50	L	C	JE2
35	12,300	15.50	W	H	JE2
36	4,205	25.30	L	C	OM4
37	53090	25.40	L	C	JE1
38	2,595	9.60	L	C	JE3
Table 14-4 Jefferson West Reaches					
108	21496	6.5	L	H	JW1
109	13947	7.8	L	H	JW2
110	24047	7.0	L	H	JW2
111	8180	6.5	W	C	JW2
112	1730	4.0	L	C	JW2
113	320	8.0	W	C	JW2
114	1495	9.0	W	C	JW3
115	85639	26.3	L	C	JW1
116	3060	9.0	W	C	JW3
117	11240	8.0	L	C	JW3
118	16370	9.8	L	C	JW3
119	22135	12.5	L	C	JW3
120	6690	12.0	W	C	JW3
121	16120	9.0	L	C	JW3
122	26700	8.0	L	C	JW3
123	9510	5.0	L	C	JW3
124	1165	24.8	W	C	JW3
125	20710	24.2	L	C	JW3
126	40198	22.0	L	C	OW2
127	14550	23.2	L	C	JW4
128	28337	5.0	L	C	JW4
129	44000	8.3	L	H	JW4
135	990	24.8	L	H	JW4

St. Charles

The reaches that make up the St. Charles risk model are shown in Figure 14-4, and data are provided in Tables 14-7, 14-8 and 14-9 for reaches, transitions and features, respectively.

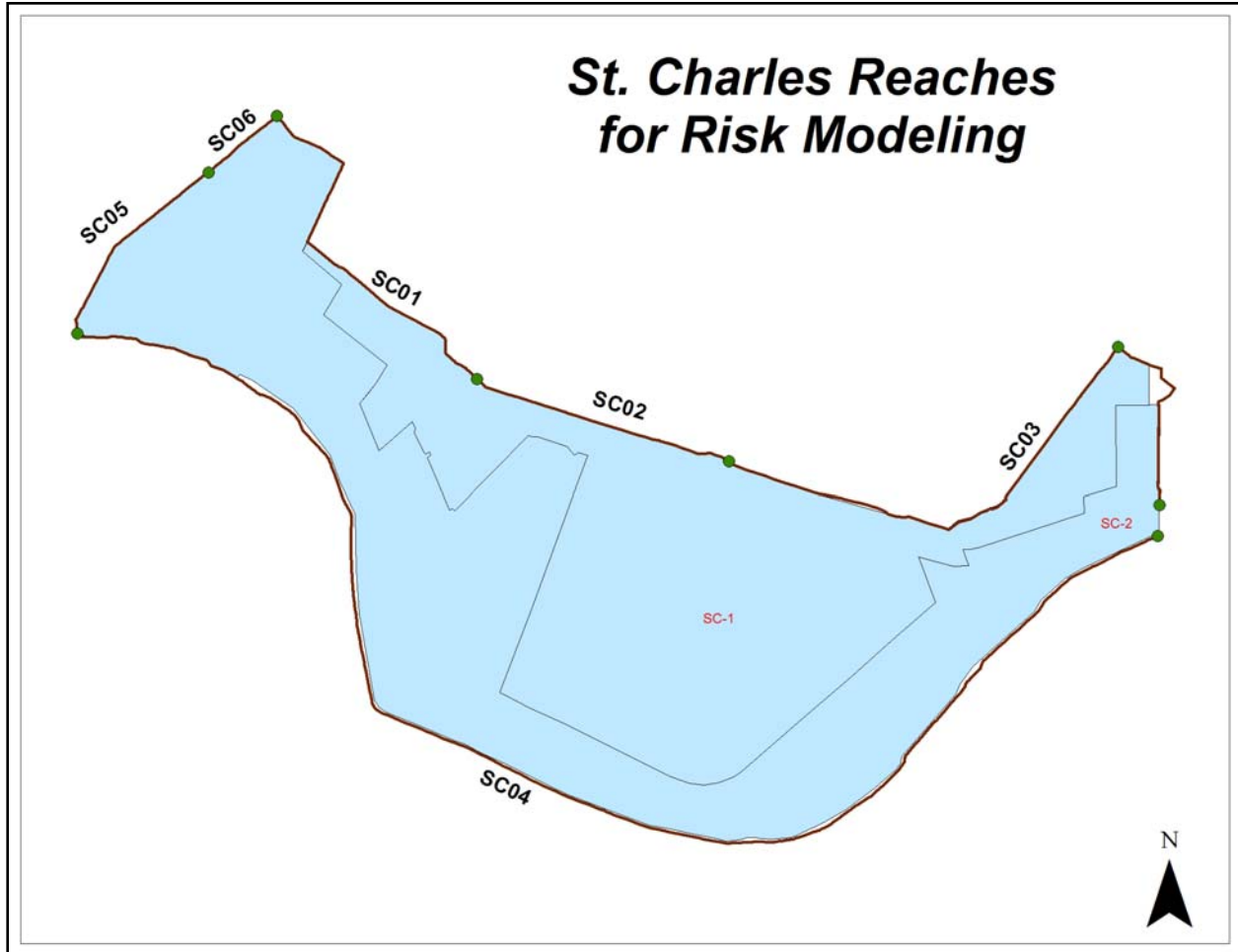


Figure 14-4. St. Charles Reaches

Table 14-7 St. Charles Reaches					
Reach No.	Length (ft)	Pre-Katrina Elevation (NAVD88 2004.65)	Reach Type (1)	Foundation Material Type (H, C, P) (2)	Subbasin Reference (3)
40	11710	10.0	L	C	SC1
41	23190	10.0	L	C	SC1
42	70465	27.9	L	C	SC2
43	9280	20.5	L	C	SC2
44	3795	20.3	L	C	SC2

Table 14-8 St. Charles Transitions						
Feature Number	Transition Type	Reach	Width (ft)	Elevation (ft) (NAVD88 2004.65)	Sub-Basin	Description of Feature
62	P	SC1	415.0	10.5	SC2	Bayou Trepagneir DS
63	G	SC1	145.0	10.5	SC1	Gate in levee - no road
64	G	SC1	530.0	10.5	SC1	Gate and sheetpile transion at Swept Road
65	R	SC1	30.0	10.5	SC1	Road off Airline Hwy
66	R	SC1	25.0	10.5	SC1	Road off Airline Hwy
67	T	SC2	455.0	12.3	SC1	Goodhope DS
68	D	SC2	543.0	11.8	SC1	Cross Bayou DS
69	D	SC2	510.0	11.3	SC1	St. Rose DS
70	G	SC3	28.0	11.8	SC1	Swing Gate at I-310
71	T	SC3	100.0	11.5	SC1	LWT I-310 FW
72	T	SC3	100.0	11.5	SC1	WLT I-310 FW
73	D	SC3	450.0	11.3	SC1	Almedia Canal Drainage
74	D	SC3	450	11.3	SC1	Walker Canal DS
75	G	SC3	450	11.3	SC1	RR Closure Structure

Table 14-9 St. Charles Features								
Feature Number	Gate (G) or Other Point Feature (O)	Reach	Correlated Features	Width (ft)	Elevation (ft) (NAVD88 2004.65) - Sill Elevation	Subbasin	Description of Feature	Notes
Jefferson East								
55	G	SC1	55	35	10.5	SC3	Gate in levee - no road	
56	G	SC3	56	28	6	SC3	Swing Gate at I-310	

Orleans Metro

The reaches that make up the Orleans Metro risk model are shown in Figure 14-5, and data are provided in Tables 14-10, 14-11 and 14-12 for reaches, transitions and features, respectively.

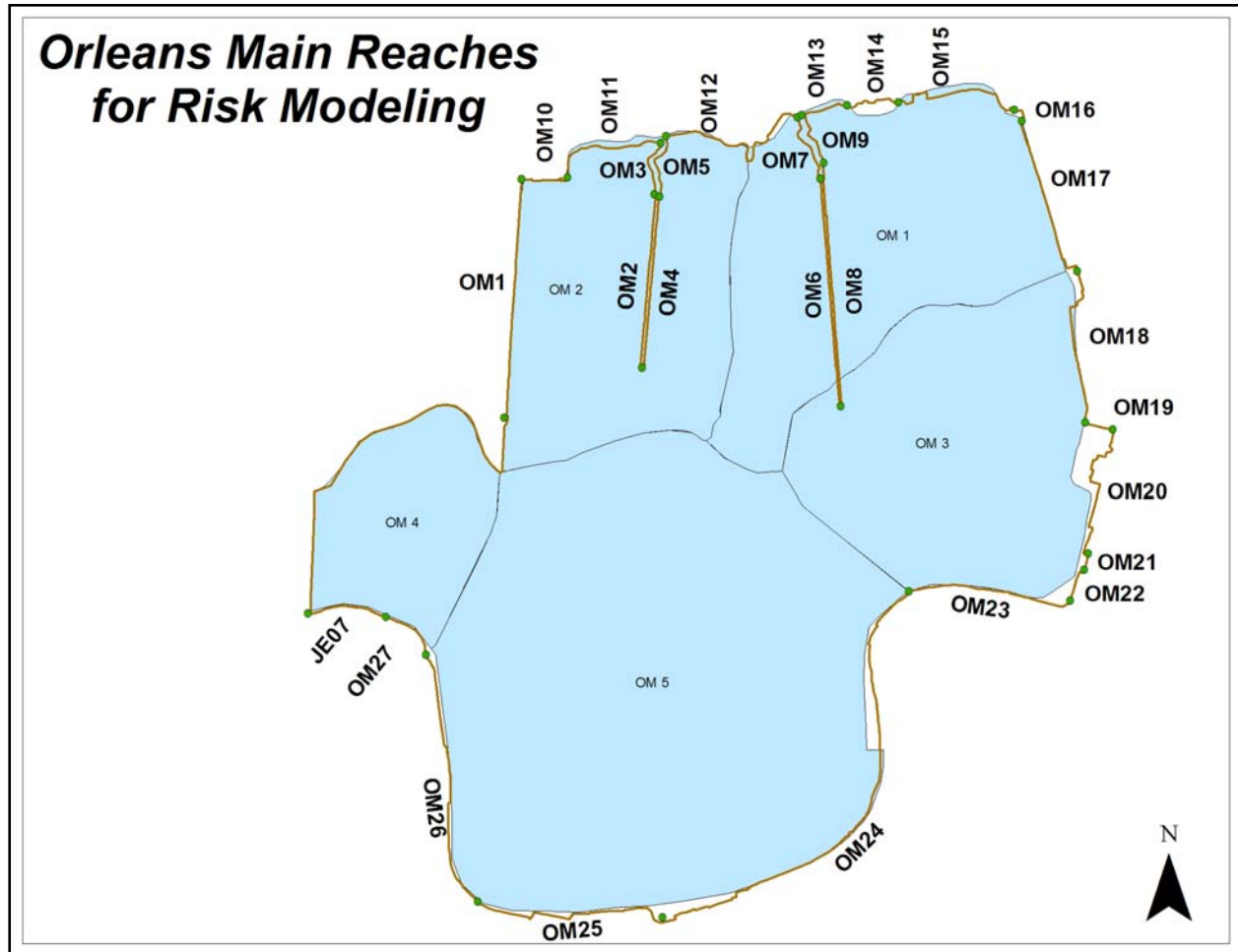


Figure 14-5. Orleans East Bank Reaches

Table 14-10 Orleans East Bank Reaches					
Reach No.	Length (ft)	Pre-Katrina Elevation (NAVD88 2004.65)	Reach Type (1)	Foundation Material Type (H, C, P) (2)	Subbasin Reference (3)
45	12,740	15.50	W	H	OM2
46	9,280	14.00	W	H	OM2
47	3,155	14.00	L	H	OM2
48	9,110	14.00	W	H	OM2
49	3,610	14.70	L	H	OM2
50	12,130	13.50	W	H	OM1
51	3,880	13.50	L	H	OM1
52	12,765	13.50	W	H	OM1
53	3,030	13.50	L	H	OM1
54	2,925	12.00	W	C	OM2
55	6,310	18.00	L	C	OM2
56	9,940	17.00	L	C	OM1
57	2,380	16.50	L	C	OM1
58	3,220	16.50	W	C	OM1
59	7,605	16.50	L	C	OM1
60	1,155	14.40	W	H	OM1
61	9,095	13.50	W	H	OM1
62	9,170	13.80	W	H	OM3
63	1,490	13.80	L	H	OM3
64	8,390	13.80	W	H	OM3
65	875	20.10	W	H	OM3
66	1,980	21.50	L	H	OM3
67	8,915	22.50	W	H	OM3
68	25,450	23.60	W	H	OM5
69	10,780	24.30	L	H	OM5
70	14,180	24.80	L	C	OM5
71	3,350	25.80	L	C	OM4

Table 14-11 Orleans East Bank Transitions

Feature Number	Transition Type	Reach	Width (ft)	Elevation (ft) (NAVD88 2004.65)	Sub-Basin	Description of Feature
Orleans East Bank						
76	P	OM1	355	15	OM2	Pump Station #6 - End of 17th Street Canal
77	P	OM1	180	15	OM2	Pump Station OP#10
78	P	OM4	170	15	OM2	Pump Station OP#7 FW - End of Orleans Canal
79	U	OM6	165	9.0	OM1	Unprotected area adjacent Pump Station #3
80	P	OM6	285	14.6	OM1	Pump Station #4 West FW - Middle of London Canal
81	P	OM8	179	13.6	OM1	Pump Station #3 FW - End of London Canal
82	P	OM8	355	17.3	OM1	Pump Station #4 East FW - Middle of London Canal
83	G	OM10	50	13.8	OM2	Gate at W. Roadway Street
84	T	OM10	180	14	OM2	WLT - OM 10/11
85	G	OM11	62	7.55	OM2	Gate 10 - Topaz Dr
86	R	OM11	58	13.8	OM2	NB Ramp at Canal Blvd
87	R	OM11	62	13.8	OM2	SB Ramp at Canal Blvd
88	T	OM12	50	12.05	OM2	Gate 9 - Marconi Dr.
89	R	OM12	160	16	OM2	Ramp 6 - Lakeshore Dr.
90	R	OM12	55	16	OM1	Ramp Lake Terrace Dr.
91	R	OM12	100	16	OM1	Ramp 5 - Lakeshore Dr.
92	R	OM14	150	16.8	OM1	Ramp 4 - Lakeshore Dr.
93	R	OM15	150	16.8	OM1	Ramp 3 - Lakeshore Dr.
94	R	OM15	150	16.3	OM1	Ramp 2 - Franklin Ave - double wide ramp
95	R	OM15	80	14.5	OM1	Ramp 1 - Leroy Johnson Drive
96	G	OM15	60	11.8	OM1	Gate 5 - Navy Reserve
97	G	OM15	145	11.55	OM1	Gate 4 - Navy Reserve
98	T	OM15	100	14	OM1	WLT O 16/15
99	G	OM16	28	10.05	OM1	Road Gate 3
100	G	OM16	33	7.3	OM1	RR - Gate 2
101	R	OM16	30	13.25	OM1	Ramp east of France Road near Hickey Bridge
102	R	OM17	30	14.75	OM1	France Road Ramp near Chef Mentuer Hwy
103	G	OM18	79	6.25	OM3	Road Gate 7W
104	G	OM18	67.5	7.4	OM3	RR Gate 8W
105	R	OM18	40	9	OM3	Ramp to Bridge
106	G	OM18	47	4.75	OM3	RR Gate 9W
107	R	OM18	35	14.75	OM3	France Rd Ramp
108	G	OM19	30	4.25	OM3	Gate 10W - RR open
109	R	OM19	80	14.75	OM3	France Road Ramp
110	G	OM19	75	2.25	OM3	Gate in Levee at Port of NO
111	G	OM19	75	2.25	OM3	Gate in Levee at Port of NO
112	P	OM20	330	6	OM3	Pump Station near Florida Ave Bridge

113	T	OM23	25	14	OM3	LWT OM 22/23
Orleans West Bank						
168	R	HA1	50	17	OW2	Chalmette - Lower Algiers Ferry Ramp
169	R	HA1	50	17	OW2	Chalmette - Lower Algiers Ferry Ramp
170	R	HA1	50	17	OW2	Chalmette - Lower Algiers Ferry Ramp
171	R	HA1	35	18	OW2	Ramp to Piers
172	R	HA1	125	15	OW2	Ramp to park area at point
173	T	HA1	420	17	OW2	Flood wall and gates around parking area
178	P	HA8	360	18.0	OW1	Pump Station #11

Table 14-12 Orleans Metro Features

Feature Number	Gate (G) or Other Point Feature (O)	Reach	Correlated Features	Width (ft)	Elevation (ft) (NAVD88 2004.65) - Sill Elevation	Subbasin	Description of Feature	Notes
Orleans East Features								
57	G	OM1	57	22	10.6	OM2	Gate E9 - Southern RR	In I-wall
58	G	OM1	58	10	7	OM2	Gate at OP#10 Pump Station	In I-wall
59	G	OM1	59	10	7	OM2	Gate north of I-10	In I-wall
60	G	OM1	60	8	7.3	OM2	Gate E4 - Veterans Blvd.	In I-wall
61	G	OM1	61	8	7.3	OM2	Gate E5 - Veterans Blvd	In I-wall
62	G	OM4	62	8.0	7	OM2	Gate at Harrison Ave	In I-wall
63	G	OM4	63	8.0	7	OM2	Gate at Harrison Ave	In I-wall
64	G	OM4	64	8.0	7	OM2	Gate at Filmore Ave	In I-wall
65	G	OM4	65	8.0	7	OM2	Gate at Filmore Ave	In I-wall
66	G	OM6	66	30	10	OM1	West CSX RR gate near Pump Station #3	RR tracks
67	G	OM6	67	8	7	OM1	Gate at Filmore Ave	In I-wall
68	G	OM6	68	8	7	OM1	Gate at Filmore Ave	In I-wall
69	G	OM8	69	30	10	OM1	East CSX RR gate near Pump Station #3	RR tracks
70	G	OM8	70	8	7	OM1	Gate at Filmore Ave	In I-wall
71	G	OM8	71	8	7	OM1	Gate at Filmore Ave	In I-wall
72	G	OM8	72	8	7	OM1	Gate at Leon C Simon Blvd	In I-wall
73	G	OM10	73	25	8.8	OM2	W. Roadway St	With ramp
74	G	OM10	74	25	8.8	OM2	Gate 15 - Into Marina Parking	
75	G	OM10	75	25	8.8	OM2	Gate 14 - Into Marina Parking	
76	G	OM10	76	25	8.8	OM2	Gate 13 - Into Marina Parking	
77	G	OM10	77	30	8.8	OM2	Gate 12 - Entrance to Marina	
78	G	OM10	78	60	6.05	OM2	Gate 11 - Lakeshore Dr.	
79	G	OM11	79	62	7.55	OM2	Gate 10 - Topaz Dr	
80	G	OM12	80	50	12.05	OM2	Gate 9 - Marconi Dr.	
81	G	OM12	81	60.0	-5	OM1	Bayou St John Floodgate	

Feature Number	Gate (G) or Other Point Feature (O)	Reach	Correlated Features	Width (ft)	Elevation (ft) (NAVD88 2004.65) - Sill Elevation	Subbasin	Description of Feature	Notes
82	G	OM14	82	25	10	OM1	Gate 3 UNO	
83	G	OM14	83	25	10	OM1	Gate 2 UNO	
84	G	OM14	84	25	10	OM1	Gate 1 UNO	
85	G	OM15	85	22	11.8	OM1	Gate 5 - Navy Reserve	
86	G	OM15	86	34	11.55	OM1	Gate 4 - Navy Reserve	
87	G	OM16	87	28	10.05	OM1	Road Gate 3	
88	G	OM16	88	33	7.3	OM1	RR - Gate 2	
89	G	OM17	89	30	5	OM1	Gate in France Road	
90	G	OM17	90	20	7.25	OM1	Gate 1W road closed	
91	G	OM17	91	20	7.55	OM1	Gate 2W RR open	
92	G	OM18	92	30	9.5	OM3	Gate 3W access open	
93	G	OM18	93	30	11.25	OM3	Gate 4W access open	
94	G	OM18	94	30	11.25	OM3	Gate 5W access open	
95	G	OM18	95	30	11.25	OM3	Gate 6W access open	
96	G	OM18	96	79	6.25	OM3	Gate 7W road closed	damaged
97	G	OM18	97	67.5	7.4	OM3	Gate 8W RR open	Failed during Katrina
98	G	OM18	98	47	4.75	OM3	Gate 9W RR open	damaged
99	G	OM18	99	80	4.25	OM3	Double Gates - France Rd Parkway	damaged
100	G	OM19	100	30	4.25	OM3	Gate 10W - RR open	damaged
101	G	OM19	101	25	4.25	OM3	Gate in levee at Port of NO	Failed during Katrina
102	G	OM19	102	25	4.25	OM3	Gate in levee at Port of NO	Failed during Katrina
103	G	OM20	103	45	2.5	OM3	Gate in pier access	no damage
104	G	OM20	104	45	2.5	OM3	Gate in pier access	no damage
105	G	OM20	105	25	6	OM3	Gate next to pump station	
106	G	OM20	106	30	2.25	OM3	Road closed	Florida Avenue Bridge Gate W20
107		OM20	107	20	2	OM3	RR closed	
108	G	OM20	108	30	2.25	OM3	RR open	Gate W21
109	G	OM20	109	40	2.75	OM3	Road open	Florida Ave Bridge
110	G	OM20	110	30	7.45	OM3	Road open	Florida Avenue Wharf

Feature Number	Gate (G) or Other Point Feature (O)	Reach	Correlated Features	Width (ft)	Elevation (ft) (NAVD88 2004.65) - Sill Elevation	Subbasin	Description of Feature	Notes
111	G	OM20	111	25	4.45	OM3	RR open	Florida Avenue Wharf
112	G	OM20	112	30	7.25	OM3	Road open	Florida Avenue Wharf
113	G	OM20	113	30	8	OM3	Road open	
114	G	OM20	114	30	8.25	OM3	Road open	
115	G	OM20	115	30	7.5	OM3	Road open	
116	G	OM20	116	30	1.75	OM3	Road open	Gate W6
117	G	OM20	117	30	2.35	OM3	RR closed	Gate W5
118	G	OM20	118	30	5.35	OM3	Road open	Gate W4
119	G	OM20	119	30	5.35	OM3	RR Access closed	Gate W3
120	G	OM20	120	30	3.5	OM3	Road open	Gate W2
121	G	OM20	121	30	2.25	OM3	Road open	Gate W1
122	G	OM23	122	30	7.5	OM3	Road Access	Off Poland Ave - Navy Complex
123	G	OM23	123	20	7.5	OM3	Road Access	Off Poland Ave - Navy Complex
124	G	OM23	124	20	7.5	OM3	RR Gate	Pauline St Wharf
125	G	OM23	125	35	7.5	OM3	Road Access	Pauline St Wharf
126	G	OM23	126	20	7.5	OM3	RR Gate	Pauline St Wharf
127	G	OM23	127	20	7.5	OM3	RR Gate	Off Charles St. - photo
128	G	OM23	128	30	7.5	OM3	Road Access	Off Charles St.
129	G	OM23	129	30	7.5	OM3	Road Access	Off Charles St.
130	G	OM24	130	20	7.5	OM5	RR Gate	Press St. Wharf
131	G	OM24	131	50	7.5	OM5	Road Access	Esplande St and Wharf
132	G	OM24	132	25	7.5	OM5	Road Access	To riverfront parking off N Peters
133	G	OM24	133	25	7.5	OM5	Road Access	To riverfront parking - St Peters
134	G	OM24	134	25	7.5	OM5	Road Access	To riverfront parking - Toulouse
135	G	OM24	135	25	7.5	OM5	Road Access	To riverfront parking - St. Louis
136	G	OM24	136	25	7.5	OM5	Road Access	To riverfront parking - Conti St
137	G	OM24	137	25	7.5	OM5	Road Access	To riverfront parking - Bienville
138	G	OM24	138	15	7.5	OM5	Pedestrian Crossing	North end of Riverwalk
139	G	OM24	139	25	7.5	OM5	Road Access	Convention Center openings

Feature Number	Gate (G) or Other Point Feature (O)	Reach	Correlated Features	Width (ft)	Elevation (ft) (NAVD88 2004.65) - Sill Elevation	Subbasin	Description of Feature	Notes
140	G	OM24	140	25	5	OM5	Road Access	Henderson Street
141	G	OM24	141	25	5	OM5	Road Access	Race Street
142	G	OM24	142	25	5	OM5	Road Access	Orange Street
143	G	OM24	143	50	5	OM5	Road Access	Celeste St - photo
144	G	OM24	144	50	5	OM5	Road Access	Port of NO - near Felicity St
145	G	OM24	145	30	5	OM5	Road Access	Port of NO - 3rd St
146	G	OM24	146	30	5	OM5	Road Access	Port of NO - Washington St
147	G	OM24	147	30	5	OM5	RR Gate	Port of NO - across from 9th ST
148	G	OM24	148	25	5	OM5	Road Access	Port of NO
149	G	OM24	149	20	5	OM5	RR Gate	Port of NO
150	G	OM24	150	25	7.5	OM5	Road Access	Port of NO - Louisiana Ave
151	G	OM24	151	25	7.5	OM5	Road Access	Port of NO
152	G	OM24	152	20	7.5	OM5	RR Gate	Port of NO - Napoleon Ave
153	G	OM24	153	30	7.5	OM5	Road Access	Port of NO - Warehouse Rd
154	G	OM24	154	30	7.5	OM5	Road Access	Port of NO
155	G	OM24	155	30	7.5	OM5	Road Access	Port of NO - Coffee Dr
156	G	OM24	156	30	7.5	OM5	Road Access	Port of NO - Leake Ave
157	G	OM24	157	30	7.5	OM5	Road Access	Port of NO - Henry Clay Dr
Orleans West Bank Features								
191	G	HA1	191	30	17	OW2	Gate WB1 - Canal Street Ferry	Canal Street Ferry
192	G	HA1	192	30	17	OW2	Gate WB2 - Canal Street Ferry	Canal Street Ferry

St. Bernard

The reaches that make up the St. Bernard risk model are shown in Figure 14-6, and data are provided in Tables 14-13, 14-14 and 14-15 for reaches, transitions and features, respectively.

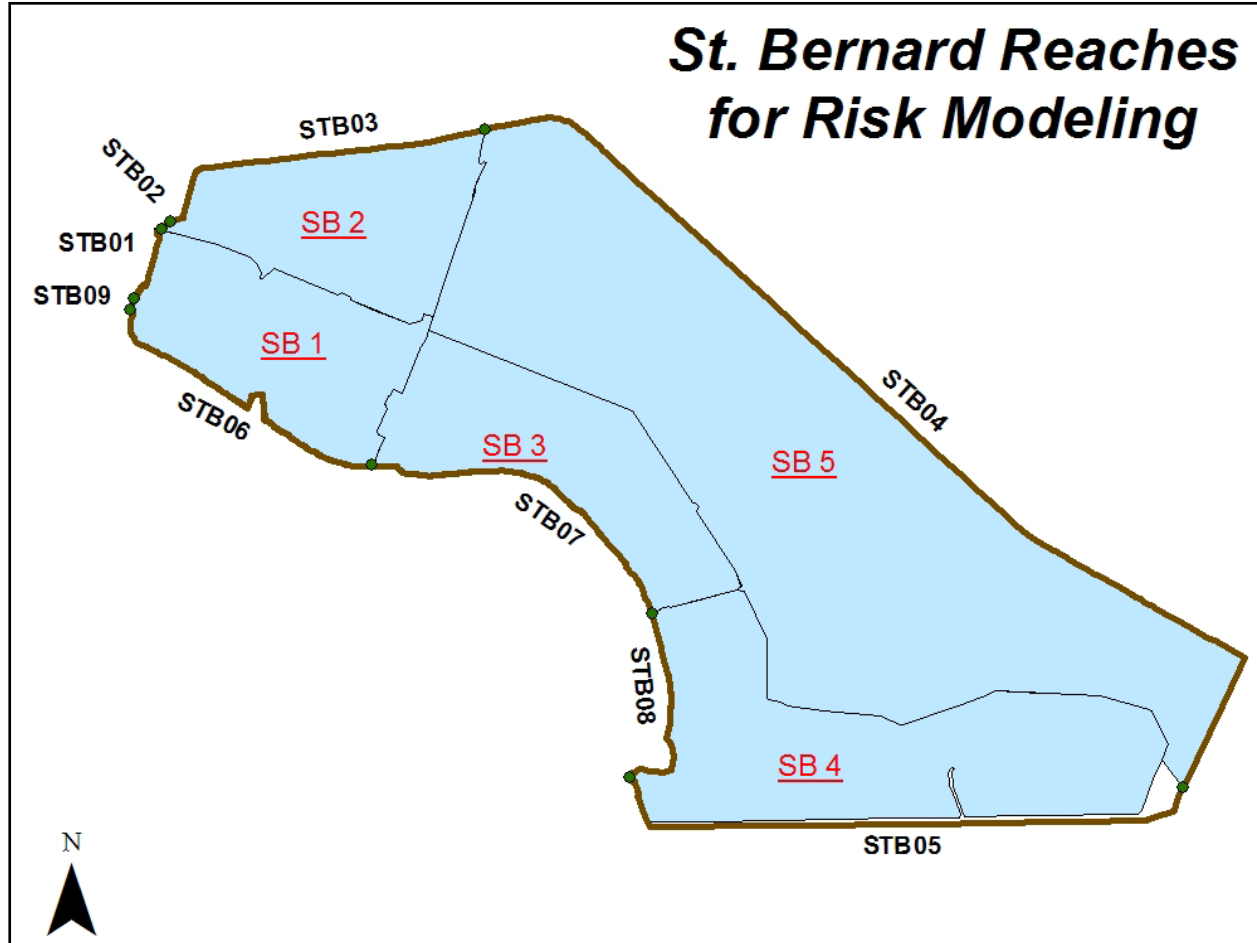


Figure 14-6. St. Bernard Reaches

Table 14-13. St. Bernard Reaches					
Reach No.	Length (ft)	Pre-Katrina Elevation (NAVD88 2004.65)	Reach Type (1)	Foundation Material Type (H, C, P) (2)	Subbasin Reference (3)
72	6,570	13.80	W	H	SB1
73	1,115	13.30	W	H	SB2
74	26,995	13.60	L	H	SB2
75	84,195	15.50	L	H	SB5
76	44,650	15.70	L	H	SB4
77	25,545	22.00	L	H	SB4
78	26,950	21.20	L	H	SB3
79	15,885	20.50	L	H	SB1
80	870	22.00	W	H	SB1

Table 14-14. St. Bernard Transitions

Feature Number	Transition Type	Reach	Width (ft)	Elevation (ft) (NAVD88 2004.65)	Sub-Basin	Description of Feature
114	R	SB1	30.0	9	SB1	Ramp for Surekote Rd
115	P	SB2	150.0	14	SB1	Pump Station #5
116	G	SB3	275.0	6	SB2	Gate in levee near Treasure Street
117	G	SB4	255.0	6	SB5	Transition Gate - near Bienvenue CS
118	D	SB4	430.0	-3	SB5	Transition Control Structure - Bayou Bienvenue
119	D	SB4	455.0	-3	SB5	Transition Control Structure - Bayou Dupre
120	R	SB5	170.0	6	SB4	Paris Road (Route 46) ramp
121	G	SB5	155.0	6	SB4	Bayou Road gate transition
122	P	SB5	230.0	15	SB4	Transition Pump Station #8 - St. Mary's
123	R	SB5	20.0	6	SB4	Ramp - Dean Road
124	R	SB8	30.0	10	SB4	Ramp at end of River Road
125	G	SB8	195.0	16.5	SB4	Road Gate Closure - canal
126	G	SB8	90	16	SB4	RR Gate Closure - canal
127	R	SB8	30	15	SB4	Ramp for Lumberyard Rd
128	G	SB8	160	16	SB4	RR Gate Closure - canal - 2 RR gates
129	G	SB8	40	14.5	SB4	Gate Closure - Domino Sugar Plant
130	G	SB8	45	14	SB4	Gate Closure - Port Ship Service Dock
131	G	SB8	65	13.5	SB4	Gate Closure - Near Mehle Ave

Table 14-15. St. Bernard Features

Feature Number	Gate (G) or Other Point Feature (O)	Reach	Correlated Features	Width (ft)	Elevation (ft) (NAVD88 2004.65) - Sill Elevation	Subbasin	Description of Feature	Notes
158	G	SB1	158	40	6.5	SB1	Gate Closure E-1	damaged
159	G	SB1	159	21	6.5	SB1	RR Gate Closure E-2	damaged
160	G	SB1	160	40	6.5	SB2	Gate Closure S-1	damaged
161	G	SB3	161	25	6.5	SB2	Gate near Treasure Street	no damage
162	G	SB4	162	40	6.5	SB2	Gate near Paris Road Bridge	severly damaged
163	G	SB4	163	50.0	6.5	SB5	Gate before Bayou Bienvenue Structure	damaged
164	G	SB4	164	56.0	-10.8	SB5	Bayou Bienvenue Sector Gate	damaged
165	G	SB4	165	56.0	-10.8	SB5	Bayou Dupre Sector Gate	damaged
166	G	SB5	166	34.0	10.9	SB4	Bayou Road swing gate	damaged
167	G	SB5	167	20	7.4	SB4	RR gate open	damaged
168	G	SB5	168	45	6.7	SB4	Highway 39 closure gate	damaged
169	G	SB8	169	4	17	SB4	Gate Closure - military park	no damage
170	G	SB8	170	32	16.5	SB4	Road Gate Closure - canal	no damage
171	G	SB8	171	20	16	SB4	RR gate - canal	no damage
172	G	SB8	172	24	16	SB4	RR Gate Closure - canal	no damage
173	G	SB8	173	24	16	SB4	RR Gate Closure - canal	no damage
174	G	SB8	174	20	14.5	SB4	Gate Closure - Domino Sugar Plant	no damage
175	G	SB8	175	45	14	SB4	Gate Closure - Port Ship Service Dock	no damage
176	G	SB8	176	35	13.5	SB4	Gate Closure - Near Mehle Ave	no damage

Plaquemines

The reaches that make up the Plaquemines risk model are shown in Figure 14-7a and Figure 14-7b, and data are provided in Tables 14-16 and 14-17 for reaches and transitions, respectively. There are no point features in the risk model for Plaquemines.

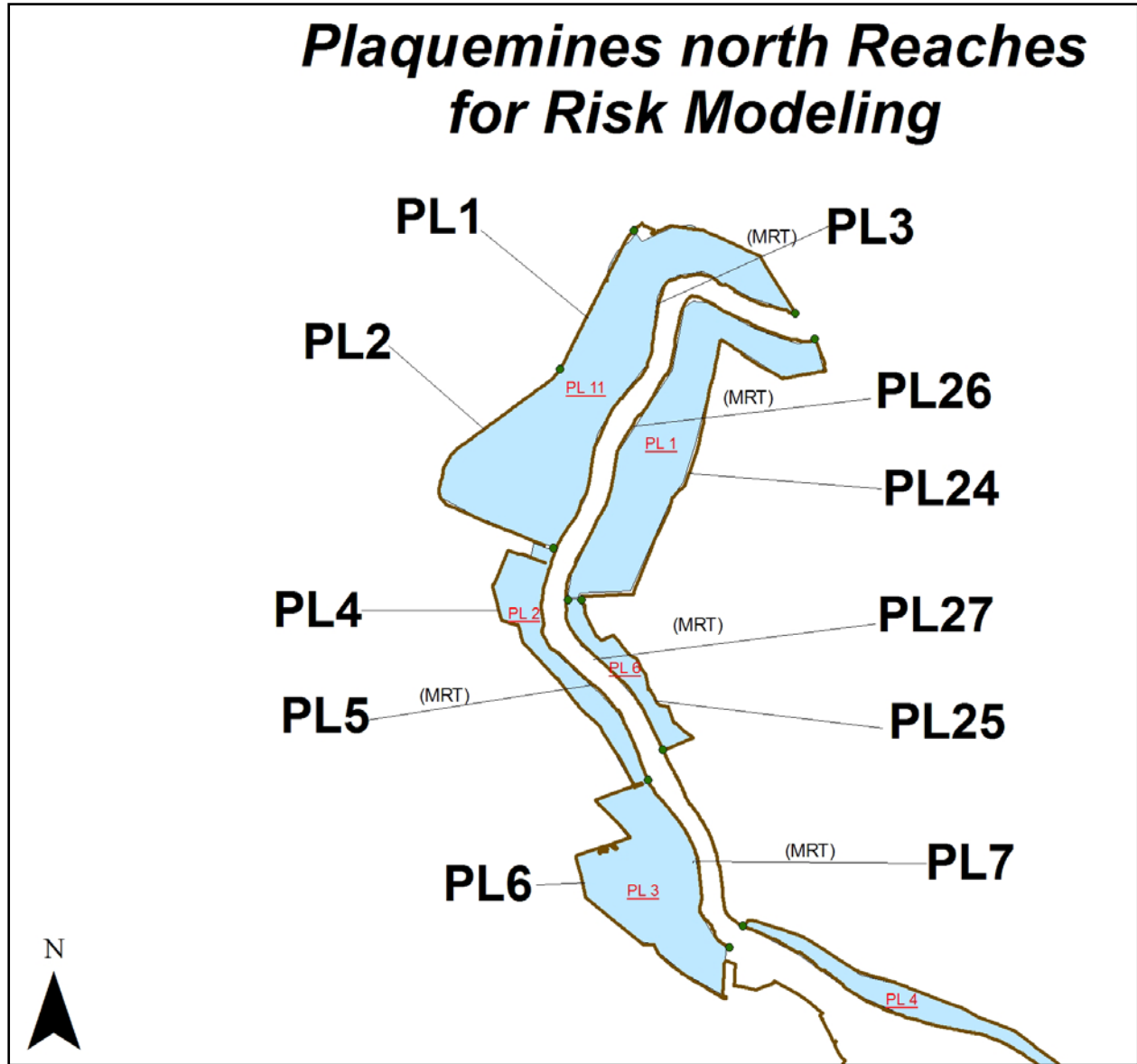


Figure 14-7a. Plaquemines North Reaches

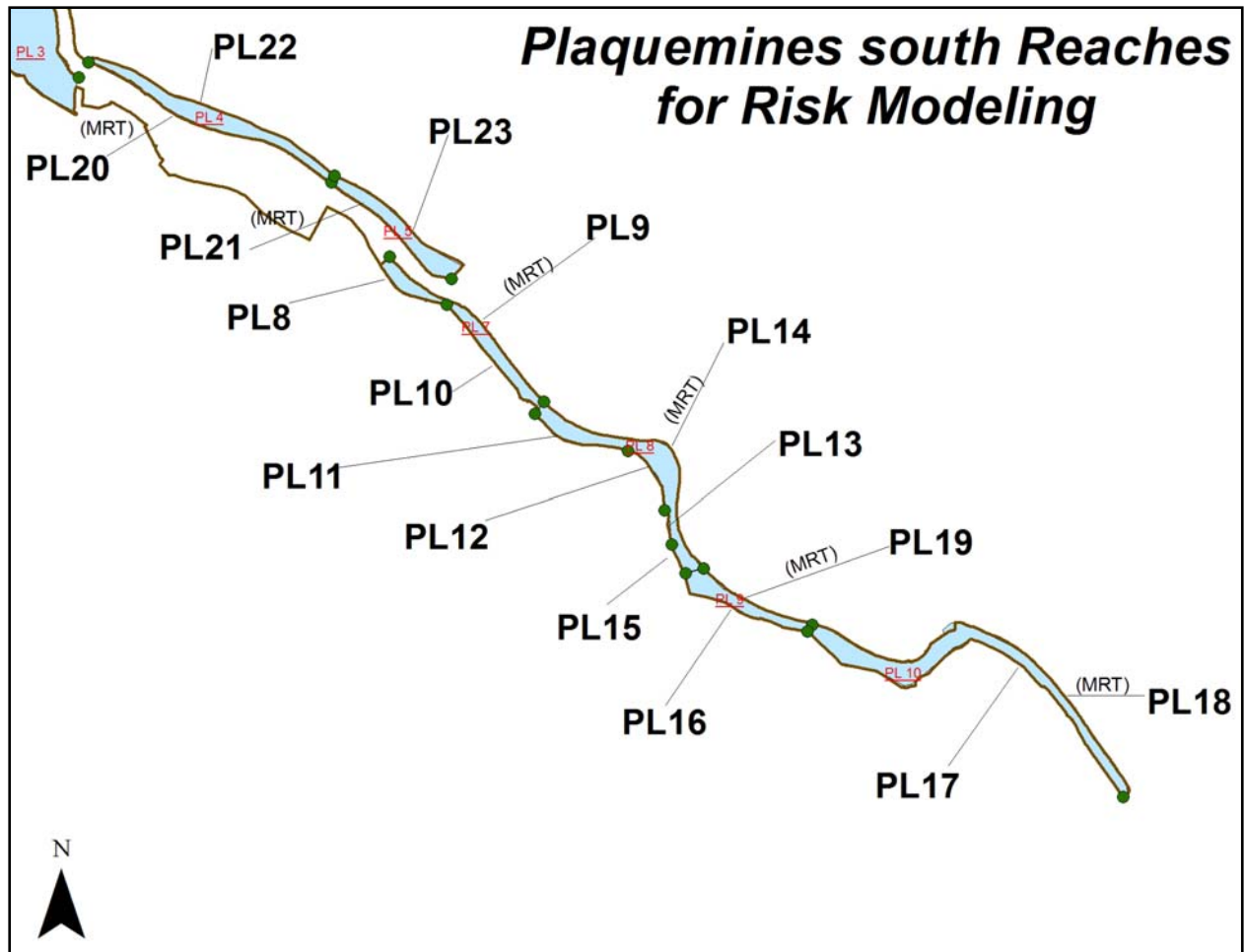


Figure 14-7b. Plaquemines South Reaches

Table 14-16 - Plaquemines Reaches					
Reach No.	Length (ft)	Pre-Katrina Elevation (NAVD88 2004.65)	Reach Type (1)	Foundation Material Type (H, C, P) (2)	Subbasin Reference (3)
81	22,000	6.00	L	H	PL11
82	41,525	8.50	L	H	PL11
83	57,470	18.10	L	C	PL11
84	50,610	8.50	L	H	PL2
85	36,605	16.40	L	C	PL2
86	60,615	6.40	L	H	PL3
87	25,865	15.70	L	C	PL3
88	17,170	11.20	L	H	PL7
89	39,195	16.20	L	C	PL7
90	27,100	13.50	L	H	PL7
91	19,120	13.60	L	H	PL8
92	13,774	12.70	L	H	PL8
93	6,635	13.80	L	H	PL8
94	49,470	16.30	L	C	PL8
95	6,160	14.90	L	H	PL8
96	26,710	15.00	L	H	PL9
97	78,500	14.70	L	H	PL10
98	79,100	15.00	L	C	PL10
99	22,740	13.90	L	C	PL9
100	51,200	16.60	L	C	PL4
101	32,235	15.60	L	C	PL5
102	50,475	17.30	L	H	PL4
103	29,050	17.50	L	H	PL5
104	62,810	12.00	L	H	PL1
105	30,940	12.40	L	H	PL6
106	61,710	18.60	L	C	PL1
107	25,225	17.00	L	C	PL6

Table 14-17 Plaquemines Transitions						
Feature Number	Transition Type	Reach	Width (ft)	Elevation (ft) (NAVD88 2004.65)	Sub-Basin	Description of Feature
132	P	PL1	400.0	8	PL12	Pump Station - Belle Chase #2
133	P	PL1	175.0	10	PL12	Pump Station - Belle Chase #1
134	P	PL4	280.0	10	PL2	Pump Station - Upper Ollie
135	P	PL6	100.0	8	PL3	Pump Station - Wilkerson Canal
136	P	PL8	120.0	18	PL8	Pointe A Lache West Pump Station
137	P	PL8	170.0	10	PL7	Diamond Pump Station
138	P	PL10	342.0	16	PL11	Hayes Pumping Station
139	P	PL11	550.0	17	PL8	Gainard Woods Pump Station
140	P	PL16	1010.0	20	PL9	Sunrise Pumping Station
141	G	PL16	635.0	19.5	PL9	Empire Flood Gate
142	P	PL17	627.0	19	PL10	Venice Pumping Station
143	P	PL17	975.0	19	PL10	Grand Liard (Buras) PS
144	P	PL22	100	18	PL4	Bellevue Pumping Station
145	P	PL27	175	20	PL5	Pointe A La Hache East Pumping Station
146	P	PL25	100	10.5	PL6	Belair Pump Station
147	P	PL25	200	14	PL1	Scarsdale Pump Station
148	P	PL24	80	9	PL1	Braitwaithe Pump Station
149	U	PL2	2200	8	PL2	Unprotected area between PL11 and PL2
150	U	PL1	1650	5	PL1	Unprotected area between PLAQ and STB
151	U	PL1	1730	18	PL1	MRT between PLAQ and STB

**Table 14-18
Pre-K and Current Reach Elevations**

Station No.	Reach Name	Subbasin Reference (2)	Levee Heights [ft] (1)		Station No.	Reach Name	Subbasin Reference (2)	Levee Heights [ft] (1)	
			Pre-K	Current				Pre-K	Current
1	NOE 1	NOE5	10.80	10.80	33	JE4	JE3	14.40	16.50
2	NOE 2	NOE5	10.80	10.80	34	JE5	JE2	15.50	16.50
3	NOE 3	NOE5	10.80	10.80	35	JE6	JE2	15.50	16.50
4	NOE 4	NOE5	10.80	10.80	36	JE7	OM4	25.30	26.60
5	NOE 5	NOE5	10.80	10.80	37	JE8	JE1	25.40	27.00
6	NOE 6	NOE5	13.00	13.00	38	JE9	JE3	9.60	14.00
7	NOE 7	NOE5	13.00	13.00	39	SC1	SC1	11.00	13.50
8	NOE 8	NOE5	13.00	13.00	40	SC2	SC1	10.00	13.00
9	NOE 9	NOE1	18.20	18.20	41	SC3	SC1	10.00	12.50
10	NOE 10	NOE1	13.80	13.80	42	SC4	SC2	27.90	28.40
11	NOE 11	NOE1	14.60	14.00	43	SC5	SC2	20.50	20.60
12	NOE 12	NOE1	15.00	15.00	44	SC6	SC2	20.30	20.70
13	NOE 13	NOE1	15.80	15.80	45	OM1	OM2	15.50	16.50
14	NOE 14	NOE1	17.00	16.00	46	OM2	OM2	14.00	18.00
15	NOE 15	NOE1	17.30	18.00	47	OM3	OM2	14.00	18.00
16	NOE 16	NOE1	15.80	18.00	48	OM4	OM2	14.00	18.00
17	NOE 17	NOE2	17.30	18.00	49	OM5	OM2	14.70	18.00
18	NOE 18	NOE2	17.90	17.90	50	OM6	OM1	13.50	18.00
19	NOE 19	NOE3	17.90	17.90	51	OM7	OM1	13.50	18.00
20	NOE 20	NOE3	17.90	16.00	52	OM8	OM1	13.50	18.00
21	NOE 21	NOE3	18.50	16.00	53	OM9	OM1	13.50	18.00
22	NOE 22	NOE3	18.50	16.00	54	OM10	OM2	14.00	14.00
23	NOE 23	NOE4	13.90	13.90	55	OM11	OM2	18.50	18.50
24	NOE 24	NOE4	13.80	13.80	56	OM12	OM1	17.00	18.00
25	NOE 25	NOE4	13.80	13.80	57	OM13	OM1	16.50	18.00
26	NOE 26	NOE4	13.80	13.80	58	OM14	OM1	16.50	20.50
27	NOE 27	NOE4	13.80	13.80	59	OM15	OM1	16.50	18.50
28	NOE 28	NOE4	13.80	13.00	60	OM16	OM1	14.40	18.00
29	NOE 29	NOE5	13.50	13.50	61	OM17	OM1	13.50	13.50
30	JE1	JE3	12.80	12.80	62	OM18	OM3	13.80	14.50
31	JE2	JE3	13.90	13.90	63	OM19	OM3	13.80	14.50
32	JE3	JE3	13.90	13.90	64	OM20	OM3	13.80	14.50
					65	OM21	OM3	20.10	22.00

Station No.	Reach Name	Subbasin Reference (2)	Levee Heights [ft] (1)		Station No.	Reach Name	Subbasin Reference (2)	Levee Heights [ft] (1)	
			Pre-K	Current				Pre-K	Current
66	OM22	OM3	21.50	21.50	103	PL23	PL5	17.50	17.50
67	OM23	OM3	22.50	23.70	104	PL24	PL1	12.00	14.50
68	OM24	OM5	23.60	24.40	105	PL25	PL6	12.40	14.50
69	OM25	OM5	24.30	25.50	106	PL26	PL1	18.60	18.70
70	OM26	OM5	24.80	26.00	107	PL27	PL6	17.00	17.60
71	OM27	OM4	25.80	26.60	108	CW1	JW1	6.5	10.0
72	SB1	SB1	13.80	15.50	109	CW2	JW2	7.8	10.0
73	SB2	SB2	13.30	16.50	110	CW3	JW2	7.9	11.0
74	SB3	SB2	13.60	14.60	111	CW4	JW2	6.5	11.0
75	SB4	SB5	17.20	18.00	112	CW5	JW2	4.0	11.0
76	SB5	SB4	15.70	17.20	113	CW6	JW2	8.0	10.0
77	SB6	SB4	22.00	22.50	114	CW7	JW3	9.0	9.5
78	SB7	SB3	21.20	21.30	115	CW8	JW1	26.3	27.0
79	SB8	SB1	20.50	20.50	116	WH1	JW3	9.0	9.5
80	SB9	SB1	22.00	22.00	117	WH2	JW3	9.5	10.5
81	PL1	PL1	6.00	10.00	118	WH3	JW3	9.8	11.5
82	PL2	PL1	8.50	10.00	119	WH4	JW3	12.5	12.5
83	PL3	PL1	18.10	19.00	120	WH5	JW3	12.5	12.5
84	PL4	PL2	8.50	8.50	121	WH6	JW3	9.0	10.0
85	PL5	PL2	16.40	17.50	122	WH7	JW3	9.0	10.0
86	PL6	PL3	6.40	8.30	123	WH8	JW3	10.0	10.0
87	PL7	PL3	15.70	17.20	124	WH9	JW3	24.8	24.8
88	PL8	PL7	11.20	12.80	125	WH10	JW3	24.2	25.0
89	PL9	PL7	16.20	17.50	126	HA1	OW2	22.0	22.0
90	PL10	PL7	13.50	13.50	127	HA2	JW4	23.2	24.3
91	PL11	PL8	13.60	14.00	128	HA3	JW4	9.6	10.0
92	PL12	PL8	12.70	14.50	129	HA4	JW4	8.3	10.0
94	PL13	PL8	13.80	15.10	130	HA5	OW2	16.0	21.7
95	PL14	PL8	16.30	17.50	131	HA6	OW1	20.1	20.8
96	PL15	PL8	14.90	15.50	132	HA7	OW1	16.0	21.7
96	PL16	PL9	15.00	15.50	133	HA8	OW1	5.70	10.00
97	PL17	PL10	14.70	15.50	134	HA9	OW2	8.0	10.0
98	PL18	PL10	15.00	16.80	135	HA10	JW4	24.80	24.80
99	PL19	PL9	13.90	17.50	136	CL1	OM2	N/A	16.5
100	PL20	PL4	16.60	16.70	137	CL2	OM2	N/A	18.0
101	PL21	PL5	15.60	16.50	138	CL3	OM1	N/A	18.0
102	PL22	PL4	17.30	17.50					

Notes: (1) Elevation Datum NAVD88-2004.65 ; (2) Subbasin where water from overtopping or breaching of reach will collect

Appendix 15

Risk Computer Model -Flood Risk Analysis for Tropical Storm Environments (FORTE)

Introduction

This section describes the Flood Risk Analysis for Tropical Storm Environments (FoRTE) tool used to obtain hurricane inundation elevation-exceedence profiles for the New Orleans area. FoRTE provides the analytical engine underlying the Interagency Performance Evaluation Task Force (IPET) study of the risks associated with the New Orleans hurricane protection system. FoRTE was designed to be accessible on most personal computers by leveraging the common Microsoft Excel interface. Currently, FoRTE is compatible with Microsoft Excel XP and 2007.

General Overview and User Interface

The standard FoRTE user interface is shown in Figure 1 with inputs labeled and described in Table 1. In general, execution of the FoRTE tool requires the following three steps:

1. **Input system definition:** this step defines the stage-storage relationships for the sub-basins, conditions for interflow between adjacent sub-basins, reach, transition, and feature definitions, and storm data.
2. **Specify analysis parameters:** this step specifies the parameters for analysis, to include uncertainty inputs, stratification inputs, and the hydrograph start time.
3. **Specify output options:** this step chooses the output and calculation options.

Input File Controls			
Time Increment		Seconds	START ANALYSIS
Start Time	0	Seconds	
Stratification Controls			
Number of Stratifications (A)	10	<input checked="" type="checkbox"/> ON	Maximum Storms 574
Surge Deviation Log Mean (B)	0.00	<input checked="" type="checkbox"/> ON	Total Deviation Log Mean 0.00
Surge Deviation StDev (C)	0.15	<input checked="" type="checkbox"/> ON	Total Deviation StDev 0.15
Wave Deviation Log Mean (D)	0.00		
Wave Deviation StDev (E)	0.00		
Data File Output Controls			
Stratified Water Output per Storm (F)	FORTE_PreKatrina_System_Volumes_Nominal_	<input checked="" type="checkbox"/> ON	
Reach and Basin Calculations (G)	FORTE_PreKatrina_System_Details_Nominal_	<input type="checkbox"/> ON	
Detailed Branch Output per Storm (H)	FORTE_PreKatrina_System_Branches_Nominal_	<input checked="" type="checkbox"/> ON	
Aggregate Loss Exceedance (I)	FORTE_PreKatrina_System_LossExceedance_Nominal_	<input type="checkbox"/> ON	
Storm Frequencies: (J)	<input type="checkbox"/> ON		
Date-Time Tag:	39222.7385	39222	7384
Loss-Exceedance Output Controls			
Start Elevation (ft) (K)	-14.0	Number of Increments	51
Stop Elevation (ft) (L)	36.0	Elevation Increment (ft) (M)	1.0
Start Time			Total Time
End Time			
CLEAR ANALYSIS SHEETS		Release 17-9H, Updated 05/21/2007	
		2005 System	
CASE DESCRIPTION			
This version includes updated 2005 NOEHPS system definition HPS System 2005 Final plus MVN - 25 March 07.xls			(N)

Uncertainty Inputs	
Rainfall - Log StDev (O)	0.69
Rainfall - Computed COV	0.78
Breach (NOT) Volume - CO (P)	0.30
Overtopping (OT) Volume - CO (Q)	0.20
Breach (OT) Volume - CO (R)	0.20
Open Gate Volume - CO (S)	0.20
Hydrograph Elev. Factor (T)	1.00
Fragility Factor (U)	0.00
Weir Factor (V)	1.00

Instructions

Step 1. Input System Definition

- Subbasin Data (Stage-Storage)
- Interflow Data
- Reach Data
- Transition Data
- Feature Data
- Storm Data

Step 2. Specify Analysis Parameters

- Hydrograph Start Time (Default 0-s)
- Stratification Inputs (Default 10; Max 60)
- Uncertainty Inputs

Step 3. Specify Output Options

- Filenames
- Rate Option
- Starting and Stopping Elevation (-14 to 36-ft)

Step 4. Click **START ANALYSIS**




Figure 15-1. FoRTE User Interface

Table 15-1. Description of FoRTE Inputs	
Item	Description
A	Number of evenly-spaced stratifications of the distribution on surges and waves. The check box to the right of this input field turns stratifications on (checked) and off (unchecked). An unchecked box sets the default number of stratifications to 1 regardless of the value entered in this cell.
B	Log-mean on the uncertainty distribution for surge height. The check box to the right of this input field toggles the consideration of uncertainty in surge height, where on (checked) accounts for uncertainty, and off (unchecked) assumes no uncertainty.
C	Log-standard deviation on the uncertainty distribution for surge height. This field is ignored if the check box in item B is set to off.
D	Log-mean on the uncertainty distribution for wave height. The check box to the right of this input field toggles the consideration of uncertainty in wave height, where on (checked) accounts for uncertainty, and off (unchecked) assumes no uncertainty.
E	Log-standard deviation on the uncertainty distribution for wave height. This field is ignored if the check box in item D is set to off.
F	Prefix for the output file containing surge heights and water volumes for each stratification. The check box to the right of this input field determines whether this type of output file will be generated by the FoRTE system (on is checked, and off is unchecked).
G	Prefix for the output files containing detailed calculations for each stratification. A separate file is generated for each stratification. The check box to the right of this input field determines whether this type of output file will be generated by the FoRTE system (on is checked, and off is unchecked).
H	Prefix for the output file containing detailed branch output per storm. This file is required for use with the FoRTE storm aggregator tool. The check box to the right of this input field determines whether this type of output file will be generated by the FoRTE system (on is checked, and off is unchecked).
I	Prefix for the output file containing the aggregate loss exceedance curves for each subbasin based on the number of storms studies in a given run. The check box to the right of this input field determines whether results will be aggregated to produce loss-exceedance curves, and whether this type of output file will be generated by the FoRTE system (on is checked, and off is unchecked).
J	This box turns on storm frequencies. Checked means that frequencies will be used as described in the storm frequencies sheet. Unchecked means that the rate is set to one. This latter option is the one needed for aggregating results using the FoRTE storm aggregator tool.
K	The starting elevation for generating loss exceedance curves. This input field is ignored if the check box in item I is unchecked.
L	The ending elevation for generating loss exceedance curves. This input field is ignored if the check box in item I is unchecked.
M	The elevation increment for generating loss exceedance curves. This input field is ignored if the check box in item I is unchecked.
N	This is a notes field used to describe the case and system under study.
O	Log standard deviation on the rainfall. This value assumes that rainfall is a lognormally distributed random variable with a log mean of 1.
P	Coefficient of variation on the volume of water due to breach for non-overtopping breach failures. This uncertainty is due to uncertainty in the Weir coefficient used for calculating water volume.
Q	Coefficient of variation on the volume of water due to overtopping. This uncertainty is due to uncertainty in the Weir coefficient used for calculating water volume.
R	Coefficient of variation on the volume of water due to breach for overtopping breach failures. This uncertainty is due to uncertainty in the Weir coefficient used for calculating water volume.
S	Coefficient of variation on the volume of water due to open closures and gates. This uncertainty is due to uncertainty in the Weir coefficient used for calculating water volume.
T	This is a modification factor used to adjust the height of the hydrographs. This factor is used for epistemic uncertainty analysis. The default value of one corresponds to no adjustment of the hydrographs.
U	This is a modification factor used to adjust the position of the fragility curve along the x-axis. This value shifts the entire fragility curve along the x-axis. This factor is used for epistemic uncertainty analysis. The default value of zero corresponds to no shift in the fragility curve.
V	This is a modification factor used to adjust the value of the Weir coefficients used for calculating volume. This factor is used for epistemic uncertainty analysis. The default value of one corresponds to no adjustment to the Weir coefficients.

System Definition

The definition of the hurricane protection system spans several spreadsheets as described in the following sections. In particular, the definition of the hurricane protection system includes the following elements:

- High-level basin information that includes the name of the basin and number of associated sub-basins; and
- Stage-storage relationships for each sub-basin that specifies the volume of water held in a sub-basin as a function of water elevation; and
- Interflow mapping matrix that specifies the elevation at which a sub-basin would begin to overflow into an adjacent sub-basin; and
- Reach, transition, and feature data that includes heights, widths, materials, probability of gate open for closures, fragility curve for reaches and transitions, and mapping to associated reaches (for transitions and closures), sub-basins, and basins.

Basin Information

Basic high-level basin information is provided in the “Basin Data” worksheet of the FoRTE tool. An annotated snapshot of the “Basin Data” worksheet is provided in Figure 15-2. The “Basin Data” worksheet stores the following information:

- Name of basin
- Number of sub-basins associated with a basin
- Prefix for mapping sub-basins and lower-level features to basins

Code	Name	Num Basin
OW	Orleans West Bank	2
NOE	New Orleans East	5
OM	Orleans Main	5
SB	St. Bernard	5
JE	Jefferson East	3
JW	Jefferson West	4
PL	Plaquemines Area	11
SC	St. Charles	2

Value specifies the number of subbasins associated with a basin

Prefix used for associated reaches and subbasins with a basin

Name of the basin

Note: This sheet is for reference only, and is not used for any calculations.

Figure 15-2. Worksheet showing count of sub-basins in each basin.

Sub-basin Stage-Storage Relationships

The stage-storage relationships for each sub-basin is provided in the “Sub-basin Data” worksheet of the FoRTE tool. An annotated snapshot of the “Sub-basin Data” worksheet is provided in Figure 15-3. The “Sub-basin Data” worksheet stores the following information:

- Vector of water elevations or stage (in feet) for which a corresponding water volume or storage is assigned
- Vector of corresponding water volumes (in cubic feet) for each sub-basin

1	A	B	C	D	E	F	G	H	I	J	K	L
2	Subbasin	Subbasins are across columns			aggregate from NOHPS sys def, then linearized via straight interpolation from low to high							
3	Note: Cell entries give storage (volume) at the corresponding stage (elevation) in the first column. Volume is given in units of cubic feet (cu-ft or ft ³)											
4	Stage (ft)	OW1	OW2	NOE1	NOE2	NOE3	NOE4	NOE5	OM1	OM2	OM3	OM4
5	-30	0.000E+00	0.000E+00	0.000E+00	0.000E+00	0.000E+00	0.000E+00	0.000E+00	0.000E+00	0.000E+00	0.000E+00	0.000E+00
6	-29	0.000E+00	0.000E+00	0.000E+00	0.000E+00	0.000E+00	0.000E+00	0.000E+00	0.000E+00	0.000E+00	0.000E+00	0.000E+00
7	-28	0.000E+00	0.000E+00	0.000E+00	0.000E+00	0.000E+00	0.000E+00	0.000E+00	0.000E+00	0.000E+00	0.000E+00	0.000E+00
8	-27	0.000E+00	0.000E+00	0.000E+00	0.000E+00	0.000E+00	0.000E+00	0.000E+00	0.000E+00	0.000E+00	0.000E+00	0.000E+00
9	-26	0.000E+00	0.000E+00	0.000E+00	0.000E+00	0.000E+00	0.000E+00	0.000E+00	0.000E+00	0.000E+00	0.000E+00	0.000E+00
10	-25	0.000E+00	0.000E+00	0.000E+00	0.000E+00	0.000E+00	0.000E+00	0.000E+00	0.000E+00	0.000E+00	0.000E+00	0.000E+00
11	-24	0.000E+00	0.000E+00	0.000E+00	0.000E+00	0.000E+00	0.000E+00	0.000E+00	0.000E+00	0.000E+00	0.000E+00	0.000E+00
12	-23	0.000E+00	0.000E+00	0.000E+00	0.000E+00	0.000E+00	0.000E+00	0.000E+00	0.000E+00	0.000E+00	0.000E+00	0.000E+00
13	-22	0.000E+00	0.000E+00	0.000E+00	0.000E+00	0.000E+00	0.000E+00	0.000E+00	0.000E+00	0.000E+00	0.000E+00	0.000E+00
14	-21	0.000E+00	0.000E+00	0.000E+00	0.000E+00	0.000E+00	0.000E+00	0.000E+00	0.000E+00	0.000E+00	0.000E+00	0.000E+00
15	-20	0.000E+00	0.000E+00	0.000E+00	0.000E+00	0.000E+00	0.000E+00	0.000E+00	0.000E+00	0.000E+00	0.000E+00	0.000E+00
16	-19	0.000E+00	0.000E+00	0.000E+00	0.000E+00	0.000E+00	0.000E+00	0.000E+00	0.000E+00	0.000E+00	0.000E+00	0.000E+00
17	-18	0.000E+00	0.000E+00	0.000E+00	0.000E+00	0.000E+00	0.000E+00	0.000E+00	0.000E+00	0.000E+00	0.000E+00	0.000E+00
18	-17	0.000E+00	0.000E+00	0.000E+00	0.000E+00	0.000E+00	0.000E+00	0.000E+00	0.000E+00	0.000E+00	0.000E+00	0.000E+00
19	-16	0.000E+00	0.000E+00	0.000E+00	0.000E+00	0.000E+00	0.000E+00	0.000E+00	0.000E+00	0.000E+00	0.000E+00	0.000E+00
20	-15	0.000E+00	0.000E+00	0.000E+00	0.000E+00	0.000E+00	0.000E+00	0.000E+00	0.000E+00	0.000E+00	0.000E+00	0.000E+00
21	-14	0.000E+00	7.040E+04	0.000E+00	0.000E+00	0.000E+00	0.000E+00	1.152E+06	8.430E+04	1.286E+05	1.244E+04	4.152E+04
22	-13	0.000E+00	7.812E+05	0.000E+00	0.000E+00	0.000E+00	0.000E+00	9.563E+06	1.343E+05	1.743E+05	2.809E+04	1.115E+05
23	-12	0.000E+00	1.710E+06	0.000E+00	0.000E+00	0.000E+00	0.000E+00	2.429E+07	1.975E+05	2.625E+05	1.520E+05	2.527E+05
24	-11	0.000E+00	2.889E+06	0.000E+00	0.000E+00	0.000E+00	0.000E+00	4.484E+07	2.814E+05	3.939E+05	3.773E+05	4.489E+05
25	-10	0.000E+00	4.384E+06	0.000E+00	1.120E+03	8.340E+02	0.000E+00	7.466E+07	4.087E+05	5.621E+05	6.880E+05	6.915E+05
26	-9	0.000E+00	6.325E+06	0.000E+00	5.652E+03	1.392E+06	0.000E+00	1.210E+08	1.031E+06	7.761E+05	1.067E+06	9.831E+05
27	-8	6.187E+01	8.916E+06	3.310E+04	7.551E+06	5.406E+06	3.100E+01	1.873E+08	2.614E+06	1.632E+06	1.638E+06	1.329E+06
28	-7	9.716E+05	1.254E+07	1.239E+05	2.239E+07	1.036E+07	2.571E+03	2.940E+08	1.163E+07	8.925E+06	2.466E+06	1.739E+06
29	-6	4.525E+06	1.827E+07	2.751E+05	5.085E+07	1.804E+07	5.907E+05	4.687E+08	4.285E+07	3.408E+07	4.044E+06	2.287E+06
30	-5	9.995E+06	2.644E+07	5.180E+05	1.320E+08	3.282E+07	1.483E+06	7.107E+08	9.992E+07	8.040E+07	7.549E+06	3.315E+06
31	-4	1.999E+07	3.937E+07	9.137E+05	2.690E+08	5.734E+07	4.120E+06	9.952E+08	1.782E+08	1.480E+08	1.701E+07	5.499E+06
32	-3	3.283E+08	7.787E+08	1.462E+09	1.530E+09	4.756E+08	1.805E+08	3.170E+09	1.020E+09	9.165E+08	4.851E+08	1.519E+08
33	-2	4.325E+08	9.641E+08	2.059E+09	1.770E+09	5.882E+08	2.502E+08	3.569E+09	1.210E+09	1.082E+09	6.462E+08	2.147E+08
34	-1	5.471E+08	1.164E+09	2.662E+09	2.011E+09	7.082E+08	3.291E+08	3.968E+09	1.409E+09	1.254E+09	8.212E+08	2.865E+08
35	0	6.720E+08	1.379E+09	3.268E+09	2.254E+09	8.315E+08	4.134E+08	4.370E+09	1.614E+09	1.432E+09	1.005E+09	3.652E+08
36	1	8.092E+08	1.605E+09	3.878E+09	2.498E+09	9.559E+08	5.026E+08	4.771E+09	1.827E+09	1.611E+09	1.195E+09	4.477E+08
37	2	9.564E+08	1.842E+09	4.488E+09	2.742E+09	1.081E+09	5.955E+08	5.172E+09	2.043E+09	1.792E+09	1.388E+09	5.326E+08
38	3	1.116E+09	2.090E+09	5.100E+09	2.986E+09	1.205E+09	6.904E+08	5.573E+09	2.261E+09	1.974E+09	1.584E+09	6.183E+08
39	4	1.289E+09	2.344E+09	5.711E+09	3.231E+09	1.331E+09	7.871E+08	5.974E+09	2.479E+09	2.156E+09	1.781E+09	7.044E+08
40	5	1.465E+09	2.604E+09	6.323E+09	3.476E+09	1.456E+09	8.858E+08	6.376E+09	2.697E+09	2.338E+09	1.980E+09	7.908E+08
41	6	1.642E+09	2.866E+09	6.935E+09	3.721E+09	1.582E+09	9.861E+08	6.777E+09	2.916E+09	2.520E+09	2.178E+09	8.774E+08
42	7	1.819E+09	3.129E+09	7.547E+09	3.966E+09	1.707E+09	1.088E+09	7.178E+09	3.134E+09	2.703E+09	2.377E+09	9.639E+08
43	8	1.996E+09	3.392E+09	8.160E+09	4.212E+09	1.833E+09	1.190E+09	7.579E+09	3.353E+09	2.885E+09	2.575E+09	1.050E+09
44	9	2.173E+09	3.656E+09	8.774E+09	4.457E+09	1.959E+09	1.294E+09	7.980E+09	3.572E+09	3.068E+09	2.774E+09	1.137E+09
45	10	2.350E+09	3.920E+09	9.388E+09	4.703E+09	2.084E+09	1.398E+09	8.381E+09	3.791E+09	3.251E+09	2.973E+09	1.224E+09
46	11	2.528E+09	4.184E+09	1.000E+10	4.948E+09	2.210E+09	1.502E+09	8.783E+09	4.010E+09	3.433E+09	3.171E+09	1.310E+09
47	12	2.705E+09	4.448E+09	1.061E+10	5.194E+09	2.336E+09	1.606E+09	9.184E+09	4.229E+09	3.616E+09	3.370E+09	1.397E+09
48	13	2.882E+09	4.712E+09	1.123E+10	5.440E+09	2.462E+09	1.711E+09	9.585E+09	4.448E+09	3.799E+09	3.569E+09	1.484E+09
49	14	3.060E+09	4.976E+09	1.184E+10	5.685E+09	2.588E+09	1.816E+09	9.986E+09	4.667E+09	3.982E+09	3.767E+09	1.570E+09
50	15	3.237E+09	5.241E+09	1.246E+10	5.931E+09	2.714E+09	1.920E+09	1.039E+10	4.887E+09	4.165E+09	3.966E+09	1.657E+09
51	16	3.414E+09	5.505E+09	1.307E+10	6.177E+09	2.840E+09	2.025E+09	1.079E+10	5.106E+09	4.348E+09	4.165E+09	1.743E+09
52	17	3.592E+09	5.770E+09	1.369E+10	6.425E+09	2.966E+09	2.130E+09	1.119E+10	5.325E+09	4.531E+09	4.363E+09	1.830E+09

Figure 15-3. Data input sheet for sub-basin stage-storage relationships.

Interflow Mapping

The interflow relationships for each sub-basin is provided in the “Interflow Mapping” worksheet of the FoRTE tool. An annotated snapshot of the “Interflow Mapping” worksheet is provided in Figure 15-4. The “Interflow Mapping” worksheet stores the following information:

- Water elevation at which a sub-basin (noted in a row) begins to overflow into an adjacent sub-basin (noted in a column).

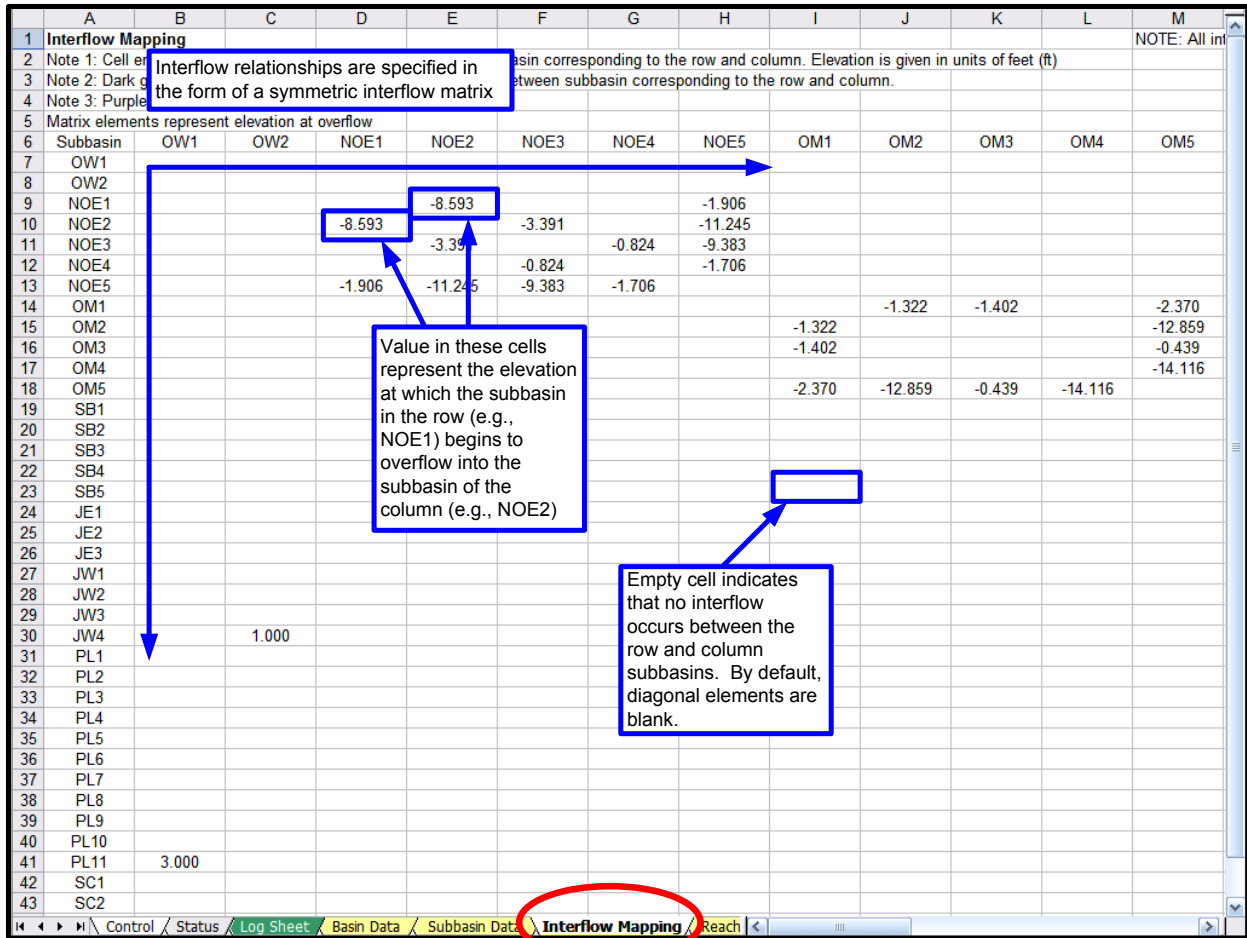


Figure 15-4. Sub-basin interflow matrix.

Reach Definition

Data that defines the reaches comprising the hurricane protection system is provided in the “Reach Data” worksheet of the FoRTE tool. An annotated snapshot of the “Reach Data” worksheet is provided in Figure 15-5. Descriptions of the inputs to the “Reach Data” worksheet are provided in Table 15-2.

Reach Data		Reach Data Start Row				Breach Fragility Curve										Breach Material		Official ID
Reach	Length (Feet)	Elevation (Feet)	Design Water Elevation (ft)	Reach Type	Reach Weir Coefficient	Basin Reference	Subbasin Reference	Erosion Modifier	Low Limit	Design	Top	0.5-ft OT	1.0-ft OT	2.0-ft OT	3.0-ft OT	6.0-ft OT		
1	2,405	10.8	10.0	W	3.0	NOE	NOE5	1.0	1.000E-12	1.169E-02	1.897E-02	1.897E-02	1.897E-02	2.835E-01	1.000E+00	1.000E+00	H3	NOE1
2	250	10.8	7.0	L	2.6	NOE	NOE5	1.0	1.000E-12	5.674E-03	1.006E-02	1.006E-02	1.006E-02	1.000E+00	1.000E+00	1.000E+00	H1	NOE2
3	2,325	10.8	10.0	W	3.0	NOE	NOE5	1.0	1.000E-12	1.130E-02	1.835E-02	1.835E-02	1.835E-02	2.755E-01	1.000E+00	1.000E+00	H3	NOE3
4	2,330	10.8	10.0	L	2.6	NOE	NOE5	1.0	1.000E-12	5.165E-02	8.993E-02	8.993E-02	8.993E-02	1.000E+00	1.000E+00	1.000E+00	H3	NOE4
5	2,270	10.8	12.0	W	3.0	NOE	NOE5	1.0	1.000E-12	1.103E-02	1.792E-02	1.792E-02	1.792E-02	2.700E-01	1.000E+00	1.000E+00	H3	NOE5
6	19,110	13.0	10.0	L	2.6	NOE	NOE5	1.0	1.000E-12	3.527E-01	5.383E-01	5.383E-01	5.383E-01	1.000E+00	1.000E+00	1.000E+00	H7	NOE6
7	1,475	13.0	11.0	W	3.0	NOE	NOE5	1.0	1.000E-12	7.183E-03	1.168E-02	1.168E-02	1.168E-02	1.849E-01	1.000E+00	1.000E+00	H2	NOE7
8	8,910	15.0	10.0	L	2.6	NOE	NOE5	1.0	1.000E-12	6.014E-02	1.043E-01	1.043E-01	1.043E-01	1.000E+00	1.000E+00	1.000E+00	H3	NOE8
9	9,185	15.8	13.0	L	2.6	NOE	NOE1	1.0	1.000E-12	5.271E-01	7.357E-01	7.357E-01	7.357E-01	1.000E+00	1.000E+00	1.000E+00	H9	NOE9
10	2,615	16.0	14.0	L	2.6	NOE	NOE1	1.0	1.000E-12	1.243E-01	2.100E-01	2.100E-01	2.100E-01	1.000E+00	1.000E+00	1.000E+00	H6	NOE10
11	13,045	16.0	12.5	L	2.6	NOE	NOE1	1.0	1.000E-12	2.616E-01	4.166E-01	4.166E-01	4.166E-01	1.000E+00	1.000E+00	1.000E+00	H7	NOE11
12	10,570	16.0	13.8	L	2.6	NOE	NOE2	1.0	1.000E-12	2.138E-01	3.478E-01	3.478E-01	3.478E-01	1.000E+00	1.000E+00	1.000E+00	H7	NOE12
13	10,760	17.9	16.0	W	3.0	NOE	NOE2	1.0	1.000E-12	5.123E-02	8.212E-02	8.212E-02	8.212E-02	7.750E-01	1.000E+00	1.000E+00	H7	NOE13
14	9,320	17.9	15.9	W	3.0	NOE	NOE3	1.0	1.000E-12	4.453E-02	7.154E-02	7.154E-02	7.154E-02	7.253E-01	1.000E+00	1.000E+00	H6	NOE14
15	7,905	16.0	14.0	L	2.6	NOE	NOE3	1.0	1.000E-12	1.647E-01	2.736E-01	2.736E-01	2.736E-01	1.000E+00	1.000E+00	1.000E+00	H6	NOE15
16	5,520	16.0	15.0	W	3.0	NOE	NOE3	1.0	1.000E-12	2.662E-02	4.301E-02	4.301E-02	4.301E-02	5.348E-01	1.000E+00	1.000E+00	H6	NOE16
17	385	16.0	11.0	L	2.6	NOE	NOE3	1.0	1.000E-12	8.725E-03	1.545E-02	1.545E-02	1.545E-02	1.000E+00	1.000E+00	1.000E+00	H1	NOE17
18	15,320	13.9	11.0	L	2.6	NOE	NOE4	1.0	1.000E-12	2.944E-01	4.618E-01	4.618E-01	4.618E-01	1.000E+00	1.000E+00	1.000E+00	H7	NOE18
19	2,910	13.8	10.5	W	3.0	NOE	NOE4	1.0	1.000E-12	1.412E-02	2.291E-02	2.291E-02	2.291E-02	3.320E-01	1.000E+00	1.000E+00	H3	NOE19
20	3,230	13.8	10.5	L	2.6	NOE	NOE4	1.0	1.000E-12	7.089E-02	1.225E-01	1.225E-01	1.225E-01	1.000E+00	1.000E+00	1.000E+00	H4	NOE20
21	1,640	13.8	12.0	W	3.0	NOE	NOE4	1.0	1.000E-12	7.983E-03	1.298E-02	1.298E-02	1.298E-02	2.034E-01	1.000E+00	1.000E+00	H2	NOE21
22	2,750	13.8	11.0	L	2.6	NOE	NOE4	1.0	1.000E-12	6.068E-02	1.053E-01	1.053E-01	1.053E-01	1.000E+00	1.000E+00	1.000E+00	H3	NOE22
23	4,100	12.0	9.5	L	2.6	NOE	NOE4	1.0	1.000E-12	8.910E-02	1.528E-01	1.528E-01	1.528E-01	1.000E+00	1.000E+00	1.000E+00	H5	NOE23
24	11,185	13.5	11.0	W	3.0	NOE	NOE5	1.0	1.000E-12	5.320E-02	8.523E-02	8.523E-02	8.523E-02	7.879E-01	1.000E+00	1.000E+00	H7	NOE24
25	6,745	12.8	10.5	W	3.0	JE	JE3	1.0	1.000E-12	1.000E-12	1.000E-12	1.000E-12	1.000E-12	3.216E-01	6.074E-01	1.000E+00	C6	JE1
26	5,915	13.9	11.0	W	3.0	JE	JE3	1.0	1.000E-12	1.000E-12	1.000E-12	1.000E-12	1.000E-12	2.885E-01	5.596E-01	1.000E+00	C6	JE2
27	4,945	13.9	10.5	W	3.0	JE	JE3	1.0	1.000E-12	1.000E-12	1.000E-12	1.000E-12	1.000E-12	2.476E-01	4.962E-01	1.000E+00	C5	JE3
28	36,430	14.4	12.0	L	2.6	JE	JE3	1.0	1.000E-12	7.186E-01	8.742E-01	8.742E-01	8.742E-01	8.771E-01	9.936E-01	1.000E+00	C9	JE4
29	19,925	15.5	13.0	L	2.6	JE	JE2	1.0	1.000E-12	5.001E-01	6.782E-01	6.782E-01	6.782E-01	6.822E-01	9.368E-01	1.000E+00	C7	JE5
30	12,300	15.5	11.0	W	3.0	JE	JE2	1.0	1.000E-12	1.096E-01	1.609E-01	1.609E-01	1.609E-01	8.183E-01	1.000E+00	1.000E+00	H7	JE6
31	4,205	25.3	21.5	L	2.6	OM	OM4	1.0	1.000E-12	1.000E-12	1.000E-12	1.000E-12	1.000E-12	2.149E-01	4.417E-01	1.000E+00	C5	JE7
32	53,090	25.4	22.5	L	2.6	JE	JE1	1.0	1.000E-12	1.000E-12	1.000E-12	1.000E-12	1.000E-12	9.529E-01	9.994E-01	1.000E+00	CB	JE8
33	2,595	9.6	3.0	L	2.6	JE	JE3	1.0	1.000E-12	8.635E-02	1.373E-01	1.373E-01	1.373E-01	1.387E-01	3.021E-01	1.000E+00	C3	JE9

Figure 15-5. Reach definition worksheet.

Table 15-2. Description of Reach Data inputs	
Item	Description
A	Reach ID. Each reach is assigned a unique integer ID corresponding to the IDs used to define hydrograph data.
B	Length of the reach section measured in feet.
C	Nominal top elevation of the reach section measured in feet. This is the value used to calculate the volume of water due to reach overtopping.
D	Nominal design elevation of the reach section measured in feet. This value is used for specifying failure probabilities on the fragility curve.
E	Reach type. "W" corresponds to "Wall" and "L" corresponds to "Levee." This value is used to determine the appropriate Weir coefficient.
F	Reach Weir coefficient. A nominal value of 2.6 is used for levees, and a nominal value of 3.0 is used for walls.
G	This is the ID of the associated basin containing the reach.
H	This is the ID of the associated subbasin containing the reach.
I	Erosion modifier. This value is not currently used for any calculations.
J	Breach fragility curve that specifies the probability of breach as a function of peak water elevation. The low limit corresponds to an elevation of 0-feet. The high-limit corresponds to an elevation of 6-feet above the nominal top elevation of the reach. Data points specified in between include probability of breach failure at the design and top elevations, and 0.5-feet, 1.0-feet, 2.0-feet, and 3.0-feet above the nominal top elevation of the reach.
K	Breach material specifies the composition of the reach as a two-character ID. The first character corresponds to the material composition (e.g., "H" for "hydraulic fill") and the second character corresponds to the length class (e.g., "5" for "4000-4999 feet"). This ID is used to determine the breach depth and breach width for use in calculating water volumes due to failure.
L	This is the official reach ID as specified by the IPET team. The first set of characters corresponds to the associated basin, and the number is a unique ID for reaches in that basin.

Transition Data

Data that defines the transitions within the hurricane protection system is provided in the "Transition Data" worksheet of the FoRTE tool. An annotated snapshot of the "Transition Data" worksheet is provided in Figure 15-6. Descriptions of the inputs to the "Transition Data" worksheet are provided in Table 15-3.

A	B	C	D	E	F	G	H	I	J	K	L	M	N	O	P	Q	R	
1	Transition Data	Transition Data Start Row				6												
2		Maximum number of transitions = 400																
3																		
4	(A) Transition	(B) Length (ft)	(C) Weighted Elevation (ft)	(D) Design Water Elevation (ft)	(E) Transition Type	(F) Transition Weir	(G) Reach Reference	(H) Subbasin Reference	(I) Reach Reference	(J) Breach Fragility Curve						(K) Breach Material		
5									Low Limit	Design	Top	0.5-ft OT	1.0-ft OT	2.0-ft OT	3.0-ft OT	6.0-ft OT		
6	1	25	9.0	9.0	R	3.0	NOE1	NOE5	1	1.00E-12	1.00E-12	1.000E-12	3.162E-07	1.000E-01	5.000E-01	1.000E+00	1.000E+00	R
7	2	125	5.0	5.0	T	3.0	NOE3	NOE5	3	1.00E-12	1.00E-12	1.000E-12	4.472E-07	2.000E-01	7.000E-01	1.000E+00	1.000E+00	T
8	3	80	5.0	5.0	T	3.0	NOE3	NOE5	3	1.00E-12	1.00E-12	1.000E-12	4.472E-07	2.000E-01	7.000E-01	1.000E+00	1.000E+00	T
9	4	155	5.0	5.0	T	3.0	NOE5	NOE5	5	1.00E-12	1.00E-12	1.000E-12	4.472E-07	2.000E-01	7.000E-01	1.000E+00	1.000E+00	T
10	5	95	5.0	5.0	T	3.0	NOE5	NOE5	5	1.00E-12	1.00E-12	1.000E-12	4.472E-07	2.000E-01	7.000E-01	1.000E+00	1.000E+00	T
11	6	140	5.0	5.0	T	3.0	NOE7	NOE5	7	1.00E-12	1.00E-12	1.000E-12	4.472E-07	2.000E-01	7.000E-01	1.000E+00	1.000E+00	T
12	7	130	5.0	5.0	T	3.0	NOE7	NOE5	7	1.00E-12	1.00E-12	1.000E-12	4.472E-07	2.000E-01	7.000E-01	1.000E+00	1.000E+00	T
13	8	450	16.5	16.5	D	3.0	NOE9	NOE1	9	1.00E-12	1.00E-12	1.000E-12	3.162E-07	1.000E-01	3.000E-01	1.000E+00	1.000E+00	D
14	9		17.5	17.5	D	3.0	NOE9	NOE1	9	1.00E-12	1.00E-12	1.000E-12	3.162E-07	1.000E-01	3.000E-01	1.000E+00	1.000E+00	D
15	10		14.0	14.0	D	3.0	NOE10	NOE1	10	1.00E-12	1.00E-12	1.000E-12	3.162E-07	1.000E-01	3.000E-01	1.000E+00	1.000E+00	D
16	11		8.0	8.0	R	3.0	NOE10	NOE1	10	1.00E-12	1.00E-12	1.000E-12	3.162E-07	1.000E-01	5.000E-01	1.000E+00	1.000E+00	R
17	12	145	7.0	7.0	R	3.0	NOE11	NOE1	11	1.00E-12	1.00E-12	1.000E-12	3.162E-07	1.000E-01	5.000E-01	1.000E+00	1.000E+00	R
18	13	255	6.0	6.0	G	3.0	NOE11	NOE1	11	1.00E-12	1.00E-12	1.000E-12	4.472E-07	2.000E-01	9.000E-01	1.000E+00	1.000E+00	G
19	14	75	11.0	11.0	D	3.0	NOE11	NOE1	11	1.00E-12	1.00E-12	1.000E-12	3.162E-07	1.000E-01	3.000E-01	1.000E+00	1.000E+00	D
20	15	55	15.0	15.0	D	3.0	NOE12	NOE1	12	1.00E-12	1.00E-12	1.000E-12	3.162E-07	1.000E-01	3.000E-01	1.000E+00	1.000E+00	D
21	16	330	15.0	15.0	G	3.0	NOE12	NOE1	12	1.00E-12	1.00E-12	1.000E-12	4.472E-07	2.000E-01	9.000E-01	1.000E+00	1.000E+00	G
22	17	120	17.0	17.0	D	3.0	NOE14	NOE1	14	1.00E-12	1.00E-12	1.000E-12	3.162E-07	1.000E-01	3.000E-01	1.000E+00	1.000E+00	D
23	18	95	14.0	14.0	G	3.0	NOE15	NOE1	15	1.00E-12	1.00E-12	1.000E-12	4.472E-07	2.000E-01	9.000E-01	1.000E+00	1.000E+00	G
24	19	870	17.3	17.3	P	3.0	NOE17	NOE2	17	1.00E-12	1.00E-12	1.000E-12	4.472E-07	2.000E-01	6.000E-01	1.000E+00	1.000E+00	P
25	20	135	5.0	5.0	T	3.0	NOE18	NOE2	18	1.00E-12	1.00E-12	1.000E-12	4.472E-07	2.000E-01	7.000E-01	1.000E+00	1.000E+00	T
26	21	60	5.0	5.0	T	3.0	NOE19	NOE3	19	1.00E-12	1.00E-12	1.000E-12	4.472E-07	2.000E-01	7.000E-01	1.000E+00	1.000E+00	T
27	22	75	13.0	13.0	R	3.0	NOE20	NOE3	20	1.00E-12	1.00E-12	1.000E-12	3.162E-07	1.000E-01	5.000E-01	1.000E+00	1.000E+00	R
28	23	140	17.0	17.0	T	3.0	NOE21	NOE3	21	1.00E-12	1.00E-12	1.000E-12	4.472E-07	2.000E-01	7.000E-01	1.000E+00	1.000E+00	T
29	24	25	5.0	5.0	T	3.0	NOE21	NOE3	21	1.00E-12	1.00E-12	1.000E-12	4.472E-07	2.000E-01	7.000E-01	1.000E+00	1.000E+00	T
30	25	50	5.0	5.0	P	3.0	NOE23	NOE4	23	1.00E-12	1.00E-12	1.000E-12	4.472E-07	2.000E-01	6.000E-01	1.000E+00	1.000E+00	P
31	26	40	13.0	13.0	R	3.0	NOE23	NOE4	23	1.00E-12	1.00E-12	1.000E-12	3.162E-07	1.000E-01	5.000E-01	1.000E+00	1.000E+00	R
32	27	40	14.0	14.0	R	3.0	NOE23	NOE4	23	1.00E-12	1.00E-12	1.000E-12	3.162E-07	1.000E-01	5.000E-01	1.000E+00	1.000E+00	R
33	28	75	13.0	13.0	T	3.0	NOE24	NOE4	24	1.00E-12	1.00E-12	1.000E-12	4.472E-07	2.000E-01	7.000E-01	1.000E+00	1.000E+00	T
34	29	80	14.0	14.0	T	3.0	NOE24	NOE4	24	1.00E-12	1.00E-12	1.000E-12	4.472E-07	2.000E-01	7.000E-01	1.000E+00	1.000E+00	T
35	30	75	13.0	13.0	T	3.0	NOE26	NOE4	26	1.00E-12	1.00E-12	1.000E-12	4.472E-07	2.000E-01	7.000E-01	1.000E+00	1.000E+00	T
36	31	60	13.0	13.0	T	3.0	NOE26	NOE4	26	1.00E-12	1.00E-12	1.000E-12	4.472E-07	2.000E-01	7.000E-01	1.000E+00	1.000E+00	T
37	32	150	13.0	13.0	P	3.0	NOE26	NOE4	26	1.00E-12	1.00E-12	1.000E-12	4.472E-07	2.000E-01	6.000E-01	1.000E+00	1.000E+00	P
38	33	70	12.0	12.0	R	3.0	NOE27	NOE4	27	1.00E-12	1.00E-12	1.000E-12	3.162E-07	1.000E-01	5.000E-01	1.000E+00	1.000E+00	R
39	34	70	9.0	9.0	R	3.0	NOE27	NOE4	27	1.00E-12	1.00E-12	1.000E-12	3.162E-07	1.000E-01	5.000E-01	1.000E+00	1.000E+00	R
40	35	90	5.0	5.0	G	3.0	NOE27	NOE4	27	1.00E-12	1.00E-12	1.000E-12	4.472E-07	2.000E-01	9.000E-01	1.000E+00	1.000E+00	G
41	36	100	11.0	11.0	G	3.0	NOE28	NOE4	28	1.00E-12	1.00E-12	1.000E-12	4.472E-07	2.000E-01	9.000E-01	1.000E+00	1.000E+00	G
42	37	100	6.0	6.0	G	3.0	NOE28	NOE4	28	1.00E-12	1.00E-12	1.000E-12	4.472E-07	2.000E-01	9.000E-01	1.000E+00	1.000E+00	G
43	38	195	12.0	12.0	G	3.0	NOE28	NOE4	28	1.00E-12	1.00E-12	1.000E-12	4.472E-07	2.000E-01	9.000E-01	1.000E+00	1.000E+00	G

Figure 15-6. Transition definition worksheet.

Table 15-3. Description of Transition Data inputs	
Item	Description
A	Transition ID. Each transition is assigned a unique integer ID.
B	Length of the transition section measured in feet.
C	Nominal top elevation of the transition section measured in feet. This value is used for specifying failure probabilities on the fragility curve.
D	Nominal design elevation of the transition section measured in feet. This value is used for specifying failure probabilities on the fragility curve.
E	Reach type. "R" corresponds to "Ramp," "T" corresponds to "Wall-levee," "D" corresponds to "Drainage Structure," "P" corresponds to "Pumping Stations," "G" corresponds to "Gates," and "U" corresponds to "Unknown." This value is used to determine the appropriate breach parameters.
F	Reach weir coefficient. A default value of 2.0 is used for all transitions.
G	This is the IPET ID of the reach containing the transition. This ID is used to map to the appropriate hydrograph.
H	This is the ID of the associated sub-basin containing the transition.
I	This is the FoRTE ID of the reach containing the transition.
J	Breach fragility curve that specifies the probability of breach as a function of peak water elevation. The low limit corresponds to an elevation of 0-feet. The high-limit corresponds to an elevation of 6-feet above the nominal top elevation of the reach. Data points specified in between include probability of breach failure at the design and top elevations, and 0.5-feet, 1.0-feet, 2.0-feet, and 3.0-feet above the nominal top elevation of the reach.
K	Transition material is equivalent to reach type in item E above.

Breach Failure

Data that define the width and depth of a breach within the hurricane protection system are provided in the "Breach Data" worksheet of the FoRTE tool. An annotated snapshot of the "Breach Data" worksheet is provided in Figure 15-7. Descriptions of the inputs to the "Breach Data" worksheet are provided in Table 15-4.

Breach Failure Data										
A	B	C	D						E	
			0 to 1ft			1ft to 3ft		>3 ft		
			Depth (ft)	Width (ft)	Depth (ft)	Width (ft)	Depth (ft)	Width (ft)		
Material	Symbol									
Hydraulic Fill, <1000 ft	H1	0	0	9	400	18	430	18	500	
Hydraulic Fill, 1001 ft	H2	0	0	9	400.4	18	430	18	500	
Hydraulic Fill, 2000 ft	H3	0	0	9	800	18	800	18	500	
Hydraulic Fill, 3000 ft	H4	0	0	9	1200	18	1200	18	500	
Hydraulic Fill, 4000 ft	H5	0	0	9	1600	18	1600	18	600	
Hydraulic Fill, 5000 ft	H6	0	0	9	2000	18	2000	18	750	
Hydraulic Fill, 10000 ft	H7	0	0	9	4000	18	4000	18	1500	
Hydraulic Fill, 20000 ft	H8	0	0	9	8000	18	8000	18	3000	
Hydraulic Fill, 30000 ft	H9	0	0	9	12000	18	12000	18	4500	
Hydraulic Fill, 40000 ft	HA	0	0	9	16000	18	16000	18	6000	
Hydraulic Fill, 50000 ft	HB	0	0	9	20000	18	20000	18	7500	
Clay, <1000 ft	C1	0	0	3	135	13	135	13	500	
Clay, 1001 ft	C2	0	0	3	135	13	135	13	500	
Clay, 2000 ft	C3	0	0	3	200	13	200	13	500	
Clay, 3000 ft	C4	0	0	3	300	13	300	13	500	
Clay, 4000 ft	C5	0	0	3	400	13	400	13	500	
Clay, 5000 ft	C6	0	0	3	500	13	500	13	500	
Clay, 10000 ft	C7	0	0	3	1000	13	1000	13	1000	
Clay, 20000 ft	C8	0	0	3	2000	13	2000	13	2000	
Clay, 30000 ft	C9	0	0	3	3000	13	3000	13	3000	
Clay, 40000 ft	CA	0	0	3	4000	13	4000	13	4000	
Clay, 50000 ft	CB	0	0	3	5000	13	5000	13	5000	
Unknown (Average), <1	U1	0	0	6	290	17	315	17	500	
Unknown (Average), 10	U2	0	0	6	300.3	17	315	17	500	
Unknown (Average), 20	U3	0	0	6	600	17	600	17	500	
Unknown (Average), 30	U4	0	0	6	900	17	900	17	500	
Unknown (Average), 40	U5	0	0	6	1200	17	1200	17	500	
Unknown (Average), 50	U6	0	0	6	1500	17	1500	17	625	
Unknown (Average), 10	U7	0	0	6	3000	17	3000	17	1250	
Unknown (Average), 20	U8	0	0	6	6000	17	6000	17	2500	
Unknown (Average), 30	U9	0	0	6	9000	17	9000	17	3750	
Unknown (Average), 40	UA	0	0	6	12000	17	12000	17	5000	
Unknown (Average), 50	UB	0	0	6	15000	17	15000	17	6250	
Wall, <1000 ft	W1	0	0	0	0	17	315	17	500	
Wall, 1001 ft	W2	0	0	0	0	17	315	17	500	
Wall, 2000 ft	W3	0	0	0	0	17	315	17	500	
Wall, 3000 ft	W4	0	0	0	0	17	315	17	500	
Wall, 4000 ft	W5	0	0	0	0	17	400	17	500	
Wall, 5000 ft	W6	0	0	0	0	17	500	17	500	
Wall, 10000 ft	W7	0	0	0	0	17	1000	17	750	
Wall, 20000 ft	W8	0	0	0	0	17	2000	17	1500	
Wall, 30000 ft	W9	0	0	0	0	17	3000	17	2250	
Wall, 40000 ft	WA	0	0	0	0	17	4000	17	3000	
Wall, 50000 ft	WB	0	0	0	0	17	5000	17	3750	
Wall-Levee	T	3	50	3	50	3	50	0	0	
Drainage Structures	D	5.5	65	5.5	65	5.5	65	0	0	
Pump Stations	P	5	100	5	100	5	100	0	0	
Ramps	R	3	Full Breach	3	Full Breach	3	Full Breach	0	0	
Gates	G	5	25	5	25	5	25	0	0	
Unknown	U	0	0	0	0	0	0	0	0	

Figure 15-7. Breach data definition worksheet.

Item	Description
A	Material and length description.
B	Symbol used for associating different breach materials and lengths to system levees and transitions
C	Breach depths measured from the top of reach or transition (in feet) and breach widths (in feet) for several overtopping conditions: (1) 0 to 1-ft overtopping, (2) 1 to 3-ft overtopping, and (3) > 3-ft overtopping.
D	Breach depths measured from the top of reach or transition (in feet) and breach widths (in feet) for non-overtopping conditions. Note that these inputs do not apply to transitions.

Features

Data that define the closures within the hurricane protection system are provided in the “Features” worksheet of the FoRTE tool. An annotated snapshot of the “Features” worksheet is provided in Figure 15-8. Descriptions of the inputs to the “Features” worksheet are provided in Table 15-5.

1	A	B	C	D	E	F	G	H	I
2	Gate Data		Maximum features		395				
3									
4	(A) Feature Number	(B) Type	(C) Category	(D) Reach	(E) Correlated Features	(F) Length (ft)	(G) Bottom Elevation (ft)	(H) Prob Open	(I) Reach
5	1	G	G	1	1	35.0	1.0	0.010	NOE1
6	2	G	G	1	2	22.0	1.8	0.010	NOE1
7	3	G	G	1	3	63.0	-0.5	0.010	NOE1
8	4	G	G	7	4	32.0	-1.5	0.010	NOE7
9	5	G	G	11	5	30.0	6.0	0.010	NOE11
10	6	G	G	12	6	80.0	10.0	0.010	NOE12
11	7	G	G	15	7	20.0	5.7	0.010	NOE15
12	8	G	G	18	8	20.0	9.8	0.000	NOE18
13	9	G	G	18	9	20.0	9.8	0.000	NOE18
14	10	G	G	18	10	20.0	9.8	0.010	NOE18
15	11	G	G	18	11	20.0	9.8	0.010	NOE18
16	12	G	G	18	12	20.0	9.8	0.000	NOE18
17	13	G	G	18	13	20.0	9.8	0.010	NOE18
18	14	G	G	18	14	20.0	9.8	0.010	NOE18
19	15	G	G	18	15	20.0	9.8	0.000	NOE18
20	16	G	G	18	16	20.0	9.8	0.010	NOE18
21	17	G	G	18	17	20.0	9.8	0.010	NOE18
22	18	G	G	18	18	20.0	9.8	0.010	NOE18
23	19	G	G	18	19	20.0	9.8	0.010	NOE18
24	20	G	G	18	20	20.0	9.8	0.010	NOE18
25	21	G	G	18	21	20.0	9.8	0.010	NOE18
26	22	G	G	18	22	20.0	9.8	0.010	NOE18
27	23	G	G	18	23	20.0	9.8	0.010	NOE18
28	24	G	G	18	24	20.0	9.8	0.010	NOE18
29	25	G	G	18	25	20.0	9.8	0.000	NOE18
30	26	G	G	19	26	20.0	12.8	0.010	NOE19
31	27	G	G	21	27	20.0	12.8	0.010	NOE21
32	28	G	G	21	28	20.5	6.5	0.010	NOE21
33	29	G	G	27	29	20.0	7.8	0.010	NOE27
34	30	G	G	28	30	20.0	6.5	0.000	NOE28
35	31	G	G	28	31	20.0	6.5	0.010	NOE28
36	32	G	G	28	32	17.0	6.5	0.000	NOE28
37	33	G	G	28	33	20.0	7.2	0.000	NOE28
38	34	G	G	28	34	37.0	6.5	0.010	NOE28
39	35	G	G	29	35	35.0	6.5	0.000	NOE29
40	36	G	G	29	36	15.0	7.2	0.010	NOE29
41	37	G	G	29	37	17.0	4.7	0.010	NOE29
42	38	G	G	29	38	20.0	5.2	0.010	NOE29
43	39	G	G	29	39	17.0	2.2	0.010	NOE29
44	40	G	G	29	40	30.0	-0.8	0.010	NOE29
45	41	G	G	29	41	33.0	9.2	0.010	NOE29
46	42	G	G	29	42	32.0	5.7	0.010	NOE29
47	43	G	G	31	43	6.0	6.0	0.010	JE2
48	44	G	G	32	44	6.0	6.0	0.010	JE3
49	45	G	G	33	45	20.0	10.0	0.010	JE4
50	46	G	G	33	46	22.0	10.0	0.010	JE4
51	47	G	G	33	47	60.0	10.0	0.010	JE4
52	48	G	G	34	48	22.0	11.8	0.010	JE5
53	49	G	G	34	49	22.0	11.8	0.010	JE5
54	50	G	G	34	50	20.0	9.5	0.010	JE5
55	51	G	G	35	51	8.0	7.3	0.010	JE6

Each row defines a unique gate

Figure 15-8. Feature (closure) data definition worksheet.

Table 15-5. Description of Feature Data inputs	
Item	Description
A	Feature ID. Each closure is assigned a unique feature ID.
B	Type of feature. Options are "G" for "Gate" and "R" for "Ramp."
C	Feature category. The only option is "G" for "Gate." This field is not used for any calculations.
D	ID of associated reach. This value is used to map the gates to the corresponding reaches.
E	IDs of correlated features used for determining probability of open among a set of related features.
F	Length of closure opening when open (in feet). This value is used with the Wier formula to determine volume of water passing through the gate when left open.
G	Bottom elevation of closure when open (in feet). This value is used with the Wier formula to determine volume of water passing through the gate when left open.
H	Probability that the gate will be left open during a storm.
I	Associated IPET reach ID.

Storm Data

Data that define the storm parameters (not including hydrographs) affecting the hurricane protection system are provided in the "Storm Data" worksheet of the FoRTE tool. An annotated snapshot of the "Storm Data" worksheet is provided in Figure 15-9. Descriptions of the inputs to the "Storm Data" worksheet are provided in Table 15-6.

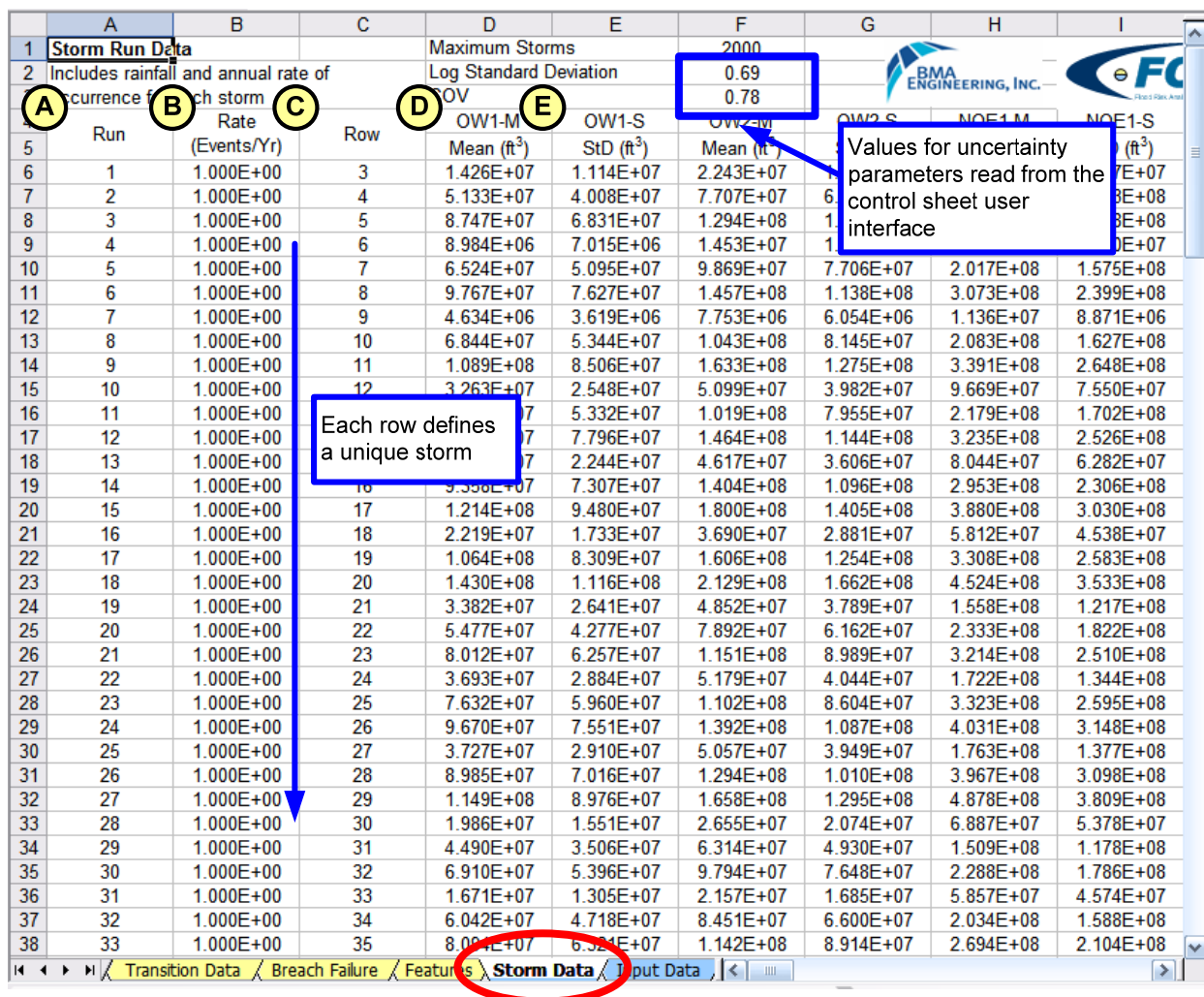


Figure 15-9. Storm data definition worksheet.

Item	Description
A	Run ID. This is the ID of the storm. This value is used to map storm parameters to input hydrographs.
B	Storm recurrence rate in events per year. By default this value is set to 1 to accommodate offline aggregation using the FoRTE Storm Aggregator.
C	Row ID. This is not a user defined input.
D	Mean volume of water due to precipitation for each storm. This column is repeated for each sub-basin.
E	Standard deviation of water volume due to precipitation for each storm. This value is calculated for each storm and sub-basin by multiplying the Rainfall COV by the mean precipitation water volume.

Hydrograph Processing and Calculation Worksheets

The FoRTE tool performs calculations on hydrograph data as illustrated in Figure 15-10.

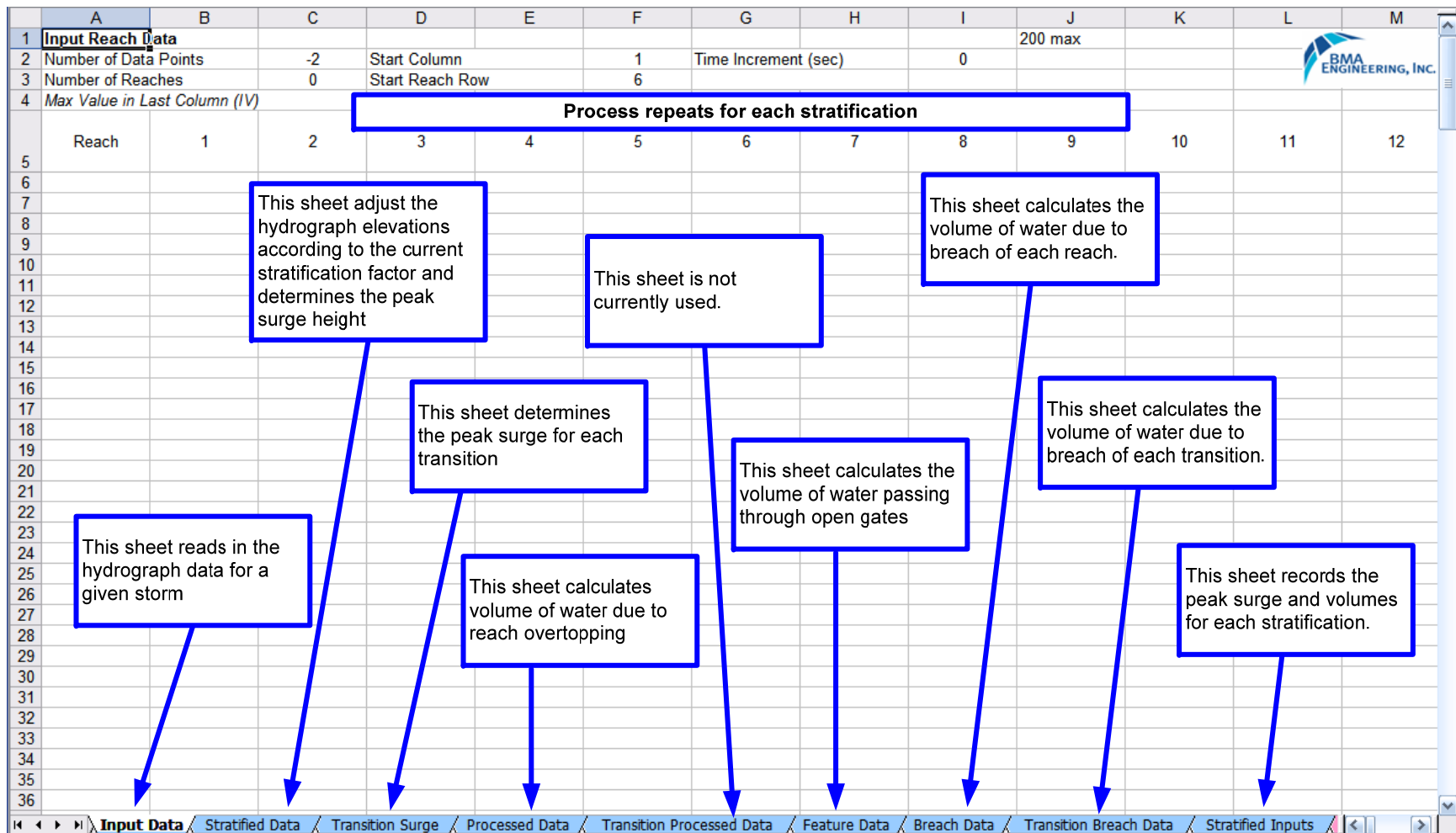


Figure 15-10. Hydrograph processing and calculation worksheets.

In particular, FoRTE begins by reading a hydrograph file for a given storm into the “Input Data” worksheet. Then, for each stratification, FoRTE does the following:

1. FoRTE applies a stratification factor to the hydrograph surge heights according to the current stratification and determines the peak surge for each reach (“Stratified Data” worksheet)
2. The peak surge is determined for each transition (“Transition Surge” worksheet)
3. The volume of water due to overtopping of each reach is calculated (“Processed Data” worksheet)
4. The volume of water passing through open gates is calculated (“Feature Data” worksheet”)
5. The volume of water due to breach of each reach and transition is calculated (“Breach Data” and “Transition Breach Data” worksheets)
6. The surge and volume data is then accumulated and stored in the “Stratified Inputs” worksheet.

If the option to output “Stratified Water Output per Storm” is selected, the FoRTE tool will output the “Stratified Inputs” sheet according to the filename specified on the control sheet user interface.

Branch Calculations and Analysis Results Worksheets

Following the hydrograph processing and calculation phase, the FoRTE tool processes the information for each stratification in turn to determine reach probabilities, and sub-basin water volumes, elevations, and probabilities (or rates) for each branch of the system event tree. The sheets are described in Figure 15-11. If “Detailed Branch Output per Storm” is desired, the FoRTE system will output the “Elevation Consequences” sheet according to the filename specified on the control sheet user interface.

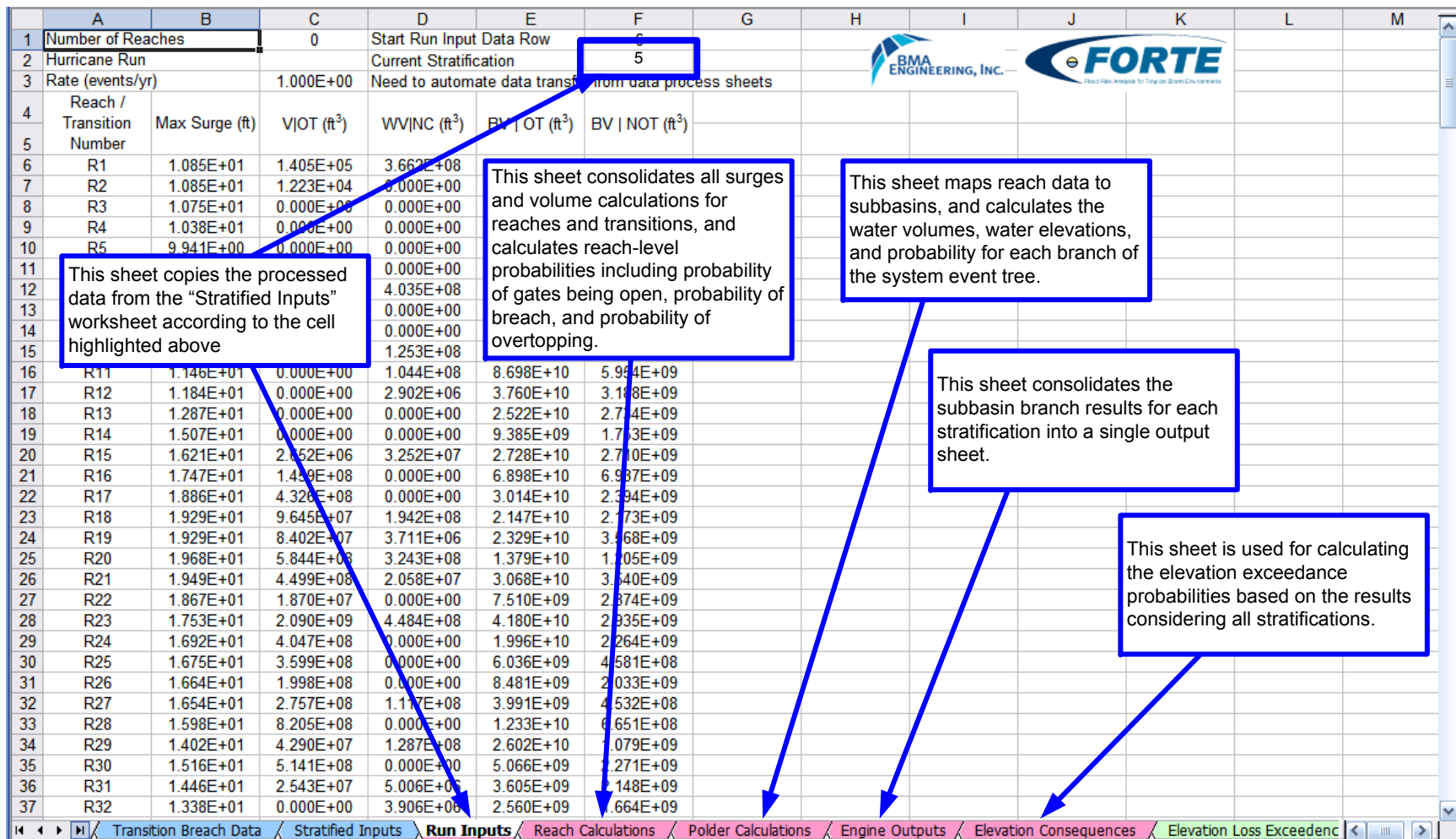


Figure 15-11. Branch calculations and results worksheets.

Performing a FoRTE Analysis

To perform a FoRTE analysis, perform the following steps:

1. Enter the appropriate system definition, including sub-basin stage storage and interflow relationships, reach data, transition data, breach failure data, and feature data, as was described in the previous sections.
2. Specify analysis parameters and output file options on the control sheet as specified in the “General Overview and User Interface” section of this document (Table 15-1).
3. Click on the “Start Analysis” button. When prompted, select the input hydrographs ending with a *.dat extension for calculations. The FoRTE tool accommodates selecting as many as 256 data files for batch processing. FoRTE will output files to the same directory containing the hydrographs.

(Note that it may take as long as 1-2 hours per storm depending on the capabilities of the host computer; the best performance was observed on a Intel Core 2 Duo processor (2 GHz), which resulted in an average run time of about 20 minutes per storm.)

4. To consolidate the results from multiple storms to produce loss-exceedance rate curves, use the FoRTE Storm Aggregator (Figure 15-12). To do this, proceed as follows:
 - a. Load “FoRTE Storm Aggregator”
 - b. Check to make sure all storms have the correct frequencies on the “Storm Data” worksheet
 - c. Click on the “Click Here to Build Loss Exceedance Curves from...” button and select the data files corresponding to the storms you wish to aggregate.
 - d. When complete, the results will be available on the “Elevation Loss Exceedance” worksheet.

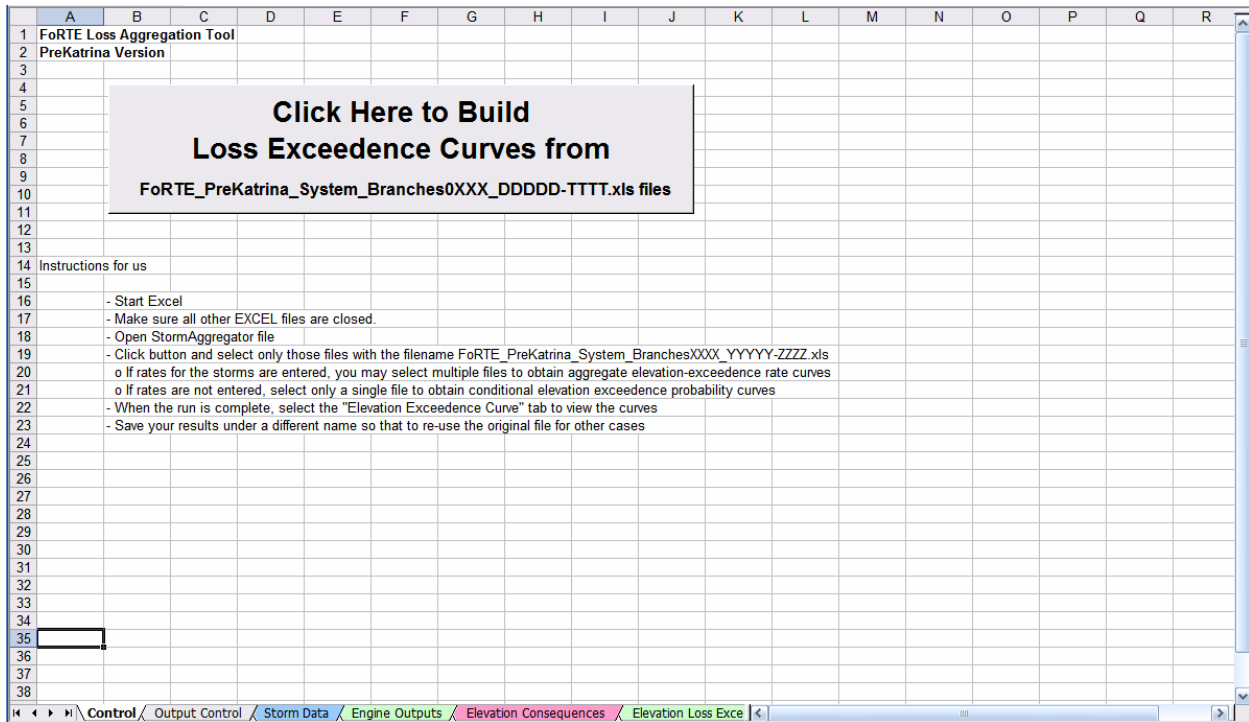


Figure 15-12. Screenshot of the FoRTE Storm Aggregator tool.